An Investigation of Privileged Substructural Motifs as Templates for the Discovery and Design of Chloroquine-Resistance Reversal Agents

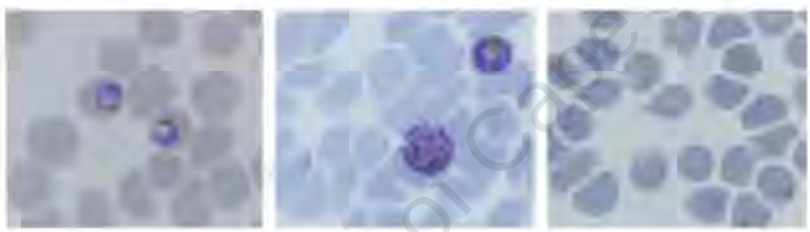

Susan Yeh

Thesis presented for the degree of

Doctor of Philosophy in Pharmacology

University of Cape Town

Supervisors: Assoc. Prof. P. J. Smith, Assoc. Prof. K. Chibale

2005

January

DECLARATION

An Investigation of Privileged Substructural Motifs as Templates for the Discovery and Design of Chloroquine-Resistance Reversal Agents

I, Susan Yeh hereby declare that the work on which this thesis is based is my original work (except where acknowledgements indicate otherwise) and that neither the work nor any part of this work has been, is being, or is to be submitted for another degree at this or any other University.

I grant the University of Cape Town free license to reproduce the thesis in whole or in part, for the purpose of research.

Signed:..... Signed by candidate .....

Date:..... 06 - Jan - 2005 .....

ACKNOWLEDGEMENTS

I am grateful to have had two wonderful supervisors. Without their guidance, support and patience, this work would not have been possible. I very much value the liberty and the scope they had entrusted me with for the project development. It was truly a privilege to work in your labs.

I would like to thank past and present Pharmacology postgraduate students Donelly van Schalkwyk, Malefa Tselanyane, Carmen Lategan, Denise Saravanakumar, Claire Tacon, Gary Gabriels, Dr. Justin Wilkins, Dr. Grant Langdon, Dr. Cailean Clarkson, Dr. Natalie Brine, Dr. Bongi Gumede, Dr. Chiku Mtegha and Dr. Jason Walden for their invaluable friendships, expertise and for making the working environment enjoyable. Special thanks are due to Dale Taylor for proofreading this manuscript. My gratitude also goes to Medicinal Chemistry students, Alex Chipeleme, Chitalu Musonda and Natasha October for making the chemistry non-mysterious.

Thank you to Pharmacology staff, Dr. Heinrich Hoppe, Sumaya Salie, Noor Salie, Noel Jordan and Jessica Peterson for their help throughout the research. Special thanks also go to Dr. William Campbell for proofreading the chemistry part of the manuscript.

My sincere gratitude goes to Dr. Pierre Falson of the Department de Biologie of Commissariat à L'Energie Atomique for providing the invaluable opportunity to work in France. Merci beaucoup to Prof. Philippe Champeil, Dr. Manuel Garrigos, Dr. Christine Jaxel, Dr. Milena Salerno-Philips, Dr. Zoltan Nagy, Cédric Montigny, Guillaume Lenoir, Florence Mousson and Marie Habets for having me, and helping me to understand yeasts better, other than their function in beers, putting up with my copious questions about everything and making my stay memorable. Merci à tous pour tout.

My affection goes to my family and friends for their unconditional support and love, and for asking about the well being of my parasite babies. It is greatly appreciated. I am deeply grateful to my best friend, Nile Hsu, who supported me with encouragement, patience, advice and even technical support, without you, this would not have been possible. I would like to dedicate this thesis to my grandfather who is watching and guiding me from heaven.

ABSTRACT

The emergence of chloroquine (CQ) resistance in *Plasmodium falciparum* throughout the malaria–endemic tropical world has necessitated alternative treatments for malaria. One approach is to restore CQ's efficacy by using it in combination with resistance reversers or chemosensitizers like verapamil and chloropheniramine. However, most of these chemosensitizers are effective only at concentrations toxic to humans. A series of novel compounds were designed, synthesized and tested with the aim of assessing their effect on CQ effectiveness in *Plasmodium falciparum* resistant strains.

In the initial exploratory drug discovery phase, a series of compounds were rationally designed based on known structure-activity relationship studies on multi-drug resistant chemosensitizers and synthesized via polymer-assisted synthesis in solution. *N'-[4-(Biphenyl-2-ylmethoxy)-benzyl]-N,N-dimethyl-propane*-1,3-*diamine* displayed the greatest potential as a dual-acting antiplasmodial agent (IC_{50}< 0.6 μM) and chemosensitizer (RMI_{K1}=0.67; RMI_{RSA11}=0.82), and low *in vitro* cytotoxicity against a mammalian cell line (CHO). The biphenyl moiety in the identified hit molecule was tentatively proposed as the potential pharmacophore. Subsequently a library of biphenyl compounds, which varied in the structural features of the aromatic ring system and the amine moiety, were synthesized in solution. The novel compounds were characterized by infrared spectroscopy, ^{1}H, ^{13}C NMR, mass spectroscopy and microanalysis and tested *in vitro* for antiplasmodial and chemoreversal activity as well as cytotoxicity and their effect on tritiated CQ uptake. Comparisons of the 17 bi- and tri-arylamines revealed several generalizations on structure-activity relationships for antiplasmodial and chemoreversal activity. A number of derivatives increased CQ accumulation and potentiating effects against resistant strains of *P. falciparum* (K1 and RSA11) with 1-*biphenyl-2-ylmethyl-4-methyl-piperazine* also displaying strong intrinsic antimalarial activity. In addition, one compound (1-[4-(3',4'-*dimethoxy-biphenyl-4-ylmethoxy)-benzyl*]-4-*methoxy-piperazine*) exhibited a strong resistance reversal effect (RMI_{RSA11}=0.31) without promoting the uptake of CQ within the resistant parasites. Three of the synthesized compounds showed considerable potential and warrant further investigation as leads. In terms of substrate specificity, it is the first time studies on the effect of antimalarial resistance reversers on drug transporters in yeast have been attempted. Although the drug transporter study did not shed light on the CQ resistance mechanism, it has provided a new possible means to study the structure and function of yeast or malaria transporter proteins.

TABLE OF CONTENTS

CHAPTER 2

Drug Discovery and Development & Rational Drug Design

CHAPTER 3

Materials and Methods

APPENDIX 1

^{1}H, ^{13}C NMR and Mass Spectra

APPENDIX 2

***In Vitro* Antiplasmodial and Resistance reversal Dose Response Curves (Phase I)**

APPENDIX 3

***In Vitro* Antiplasmodial, Resistance Reversal & Cytotoxicity Dose Response Curves (Phase II)**

LIST OF FIGURES AND SCHEMES

CHAPTER 3

CHAPTER 4

CHAPTER 5

CHAPTER 6

CHAPTER 7

APPENDIX 1

APPENDIX 2

APPENDIX 3

LIST OF TABLES

CHAPTER 6

CHAPTER 7

LIST OF ABBREVIATIONS

ABC	ATP-Binding Cassette
AChE	acetylcholinesterase
ADMET	adsorption, distribution, metabolism, excretion and toxicity
APAD	3-acetyl pyridine adenine dinucleotide
AQ	amodiaquine
BBIQ	bisbenzylisoquinoline
BCRP	breast cancer resistance protein
ca	approximately
CHO	Chinese hamster ovarian cells
CQ	chloroquine
CQ^R	CQ resistant
CQ^S	CQ sensitive
DDT	dicophane
DHFR	dihydrofolate reductase
DHPS	dihydropteroate synthetase
DMEM	Dulbecos Modified Eagles Medium
DMSO	dimethoxysulphoxide
DN	daunomycin
DV	digestive vacuole
EtOAc	ethey acetate
et al.	and all others
FCS	fetal calf serum
FPIX	ferriprotoporphrin IX
g	gram(s)
GSH	glutathione
Hb	haemoglobin
hr	hour(s)
Hz	hertz
IC_{50}	50% inhibitory concentration

IR	infra red
J	coupling constant
L	litre
LCA	liquid culture assay
MDR	multi-drug resistant
MeOH	methanol
mg	milligram(s)
min	minute(s)
ml	millilitre
mM	milli molar
MRP	multidrug resistance-associated proteins
MTT	3-(4,5-dimethylthiazol-2-yl)-2,5-diphenyltetrazoliumbromide
NAD	nicotinamide adenine dinucleotide
NBD	nucleotide-binding domains
NBT	nitroblue tetrazolium
ND	not determinable
nM	nanomolar
NMR	nuclear magnetic resonance
NO	nitric oxide
NTCP	sodium taurocholate cotransporting peptide
OAT	organic anion transporters
OATP	organic anion transporting polypeptides
OCT	organic cation transporters
OCTN	novel organic cation transporters
PBS	phosphate buffered saline
PDR	pleiotropic drug resistance
PEPT	oligopeptide transporters
PES	phenazine ethosulphate
PfCRT	*Plasmodium falciparum* CQ resistance transporter
PfPgh-1	*Plasmodium falciparum* P-glycoprotein homologue 1
Pgp	P-glycoprotein
pLDH	parasite lactate dehydrogenase

ppm	parts per million
pRBC	parasitized red blood cells
PTBD	1, 5, 7– triazabicyclo[4,4,0]dec-5-ene
QN	quinine
RBC	red blood cell
R & D	research and development
R_I	resistance index
RMI	resistance modification index
rpm	revolutions per minute
SAR	structure-activity relationship
SD	standard deviation
TLC	thin layer chromatography
TNF-α	tumor necrosis factor-alpha
VPL	verapamil
WHO	World Health Organization
WT	wild type
YCF1p	yeast cadmium factor protein
Yor1p	yeast oligomycine resistance protein
λ	wavelength (nm)
µg	microgram(s)
µg/ml	micrograms per millilitre
µl	microlitre

Chapter 1

Introduction: Malaria, Antimalarials and ABC transporters

1.1 Historical outlines of malaria

Malaria caused by protozoan parasites of the genus *Plasmodium* was traced back more than 4000 years ago as its characteristic symptom of enlarged spleens were found in Egyptian mummies. Elsewhere in the world, writers, poets and religious figures have recorded the affliction.

When unable to defend herself by the sword
Rome could defend herself by means of the fever.
— The poet Godfrey of Viterbo, 1167

In ancient Rome, outsiders were most vulnerable to the disease; the conditions were described as 'Roman fever' which later gave rise to the Italian word, *mal'aria* (bad air) to describe the cause of the disease (Sherman, 1998). It was only in the early 1880s that malarial gametocytes found in human blood were viewed under the microscope. Pioneering work by Dr. Giovanni Battista Grassi and Sir Ronald Ross established the parasite's life cycle, for which the latter was awarded the Nobel Prize for medicine and physiology in 1902. As the history unraveled, collective wisdom of discovery, development of antimalarial drugs and knowledge of mosquito vectors have helped to better understand malaria.

1.2 Malaria epidemics

The global picture of malaria is such that 300 million to 500 million people are infected and at least one million die each year, mostly children under the age of 5 (WHO, 2004). As the life-threatening infectious disease persists, it has occurred in tropical and subtropical developing countries on all continents (Fig. 1.2.A). Today, 90% of malaria cases and deaths are recorded in sub-Saharan Africa.

There are two main factors responsible for the high mortality in Africa, namely natural and man-made epidemics. These factors include climatic change, natural disasters,

conflict of war, mining and failure of control measures make the physical environment more suitable for the growth of the transmission vector – the female *Anopheles* mosquito. Other factors such as massive refugee movements, the emergence of multi-drug resistant parasites, mosquito resistance to antimosquito compounds and weak health care infrastructures have also contributed to the problem of eradicating the scourge of malaria. However, the World Health Organisation and other campaigns have committed to halve the deaths from malaria by 2010 whereas the current strategies focus upon prompt access to treatment, provision of clean water and use of insecticide treated bed nets.

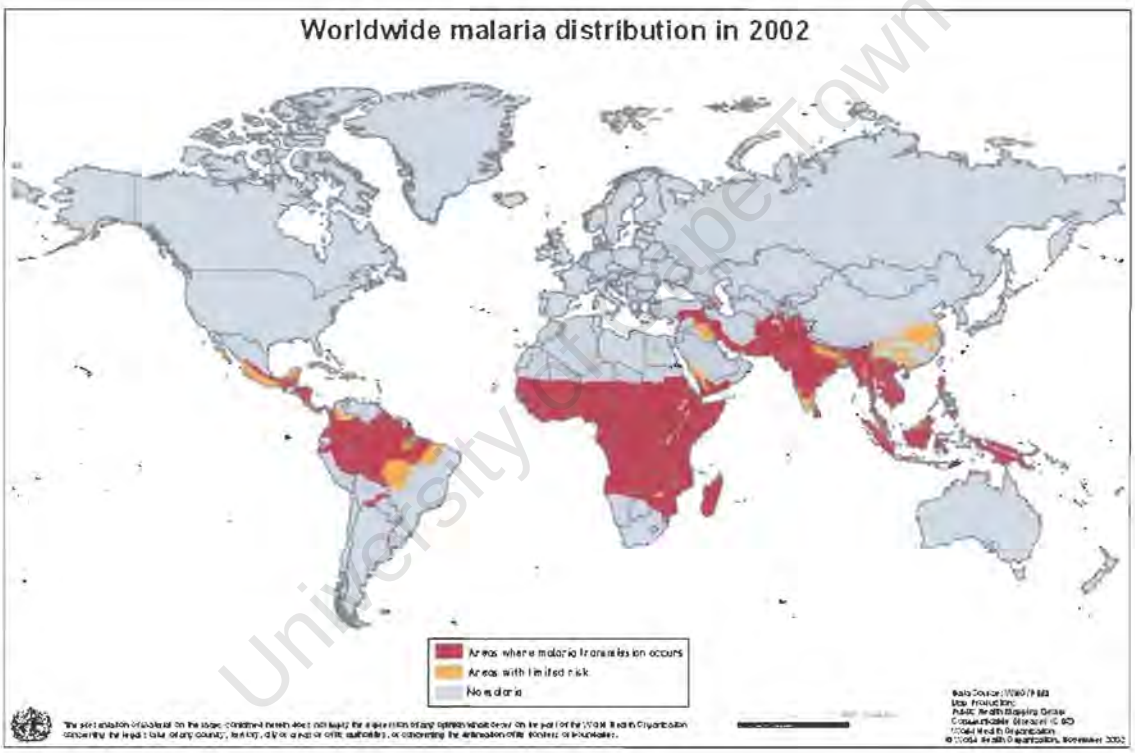

Fig. 1.2.A. Global distribution of Malaria. (Reproduced from http://www.gmap.net/oxford/image/malaria_2002.jpg)

The distribution of endemic malaria in South Africa is confined to the provinces of KwaZulu-Natal, Mpumalanga and Limpopo (Fig. 1.2.B) (Department of Health, 2003; http://www.malaria.org.za/Malaria_Risk/Update/update.html). In South Africa today, the highest risk areas are the international Mozambican border areas. The dangerous endemic disease is brought across mostly by infected travelers, who further transmit malaria to the female *Anopheles* by a blood meal; consequently mosquitoes infect other

non-immune human hosts.

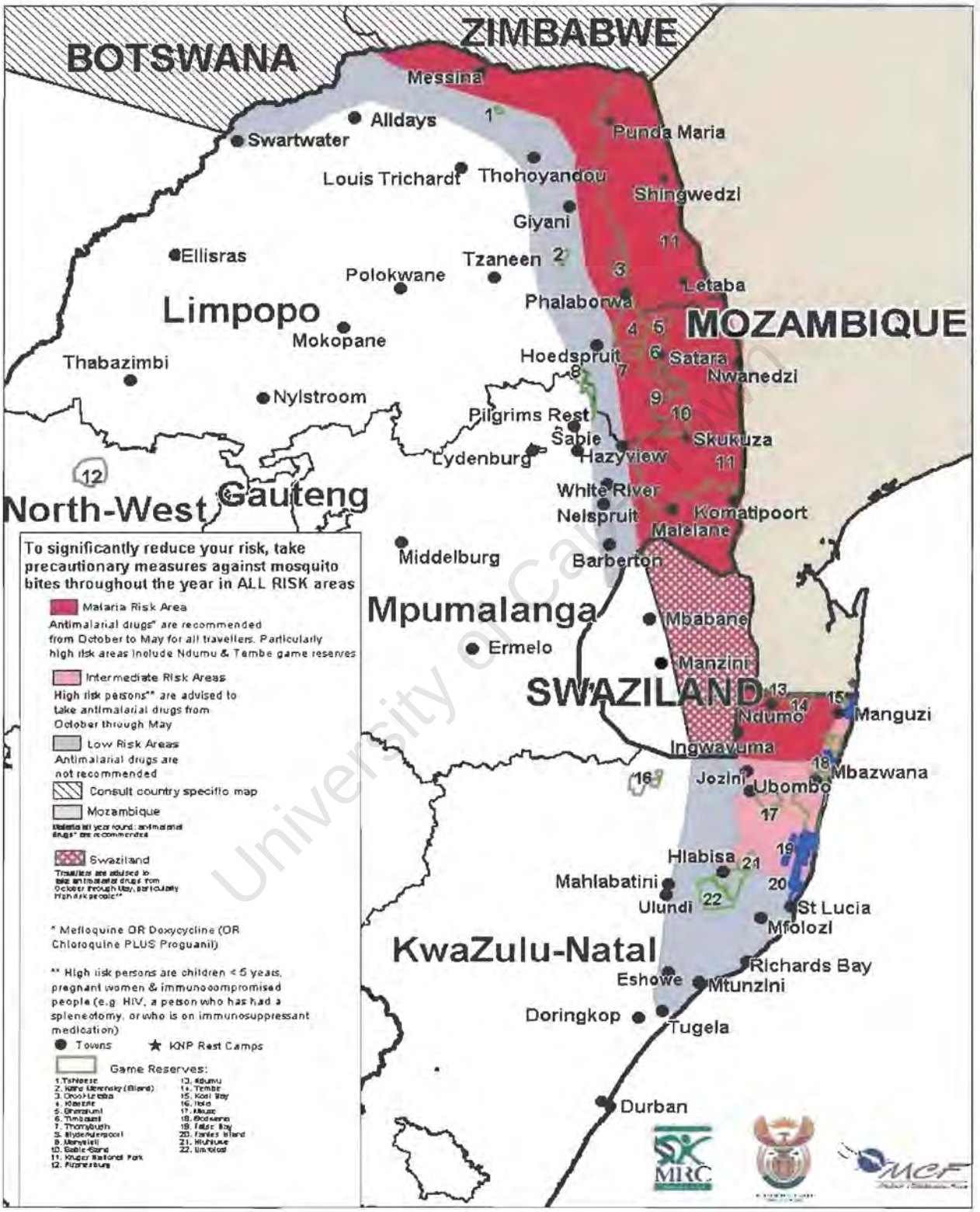

Fig. 1.2.B. Map of Malaria risk areas in South Africa. (Reproduced from http://www.malaria.org.za/Malaria_Risk/Risk_Maps/risk_maps.html)

1.3 The socioeconomic burden of malaria

Malaria is recognized not only as a health problem but also as a social and economic problem since it is closely associated with poverty. When highly exposed populations are attacked in malaria endemic areas, where the agriculture need is great, the number of working days will be reduced, and the monetary loss as a result of fewer working days will limit the human resources to contribute to social and economic development. It will also endanger children's education owing to low school attendance. Malaria is believed to be responsible for hindering economic growth up to 1.3% annually in some African countries (http://www.rbm.who.int/cmc_upload/0/000/015/370/RBMInfosheet_3.htm). It therefore affects the survival of the inhabitants and continues the marginalization.

In South Africa today, malaria is understood to be a disease of poverty and a cause of poverty as well. Despite the extensive effort by the Department of Health to prevent and control malaria by lowering the cost of insecticide-treated bed nets, chemoprophylaxis and vector control by intra-domiciliary spraying, the emergence of drug resistance remains one of the greatest challenges to eradicate malaria as it does worldwide (Department of Health, 2003). The prevalence of malaria will hamper international trade, foreign investments and tourism that is particularly essential for economic growth in our rainbow nation.

1.4 Parasite-host interactions

In 1880, scientists discovered a one-cell parasite, *Plasmodium*, as the real cause of malaria. Human malaria is caused by four species of the *Plasmodium* parasites including *P. falciparum, P. vivax, P. ovale* and *P. malariae* of which *falciparum* malaria is the most common infection and causes the greatest risk of complications and deaths (Sherman *et al.*, 1998). The life cycle of malaria parasites involves four stages and two hosts, human host and female *Anopheles* mosquito. *Plasmodium* parasites undergo asexual reproduction both in the tissue and in red blood cells of the vertebrate hosts and one sexual and asexual development phase in the mosquito vector (Fig. 1.4) (Gerena *et al.*, 1992).

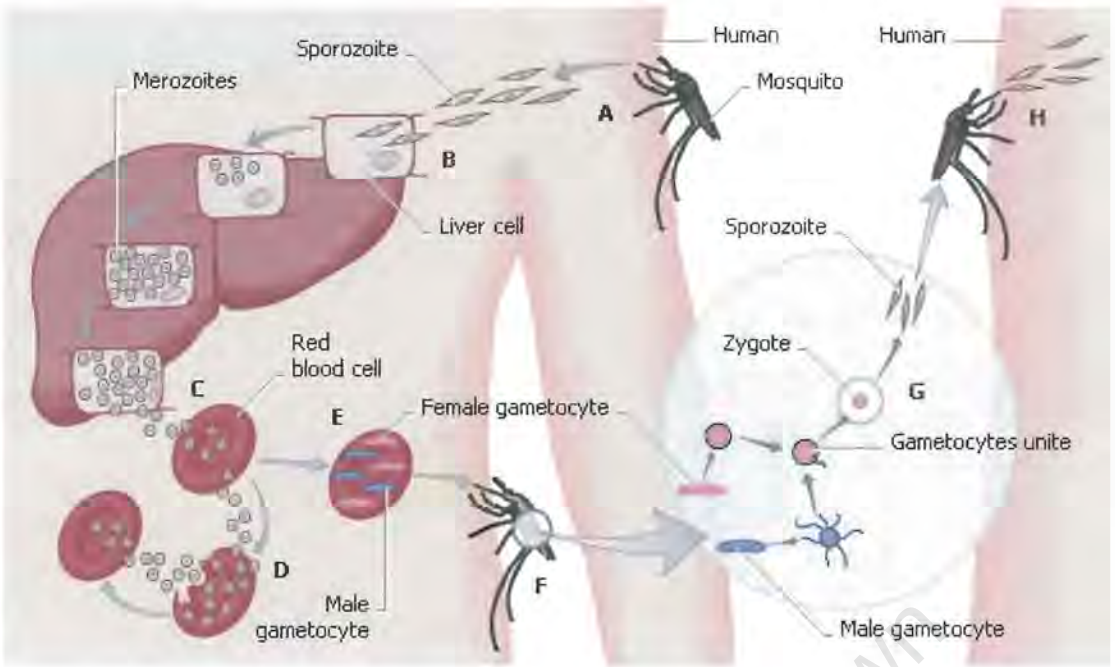

Fig. 1.4. The life cycle of malaria parasites.
(Reproduced from http://images.encarta.msn.com/xrefmedia/aencmed/targets/illus/ilt/T073615A.gif)

The infective forms of human malaria parasites, sporozoites, enter blood circulation by means of an infected *Anopheles* mosquito during a blood meal and travel rapidly to the liver cells where they grow and multiply to produce merozoites asexually (Bitonti *et al.*, 1988; Dieckmann-Schuppert *et al.*, 1993). Upon maturation, merozoites are released into the bloodstream to invade other erythrocytes or parenchymatous cells of the liver. During the intra-erythrocytic stage, merozoites undergo a process of asexual reproduction in human hosts by feeding on the erythrocytes, growing and multiplying cyclically from trophozoites to mature blood schizonts with a number of nuclei. Malaria symptoms such as chills, fevers and nausea only begin when the parasites start to divide asexually in the red blood cells. One schizont can divide to produce numerous merozoites which ingest the erythrocytes and are released back to the bloodstream to invade new red blood cells. This is referred to as the erythrocytic stage of the life cycle, and is repeated every 48 hours (Bitonti *et al.*, 1988). These multiplied parasites are now capable of developing into male and female gametocytes which will unite to form zygotes in the gut of the mosquito when taken up by a blood feed. In the sporogonic cycle in the mosquito body, a zygote then forms an oocyst which multiplies and divides asexually into sporozoites on the outer layer of the gut. A large number of sporozoites are produced

and make their way to the mosquito's salivary glands, which allow the transmission when saliva and anti-coagulants are injected into a non-immune human host to perpetuate the malaria cycle. Thus, it completes the life cycle of malaria – man to mosquito to man (Dieckmann-Schuppert *et al.,* 1993). At each transmission cycle, sexual exchange occurs and is believed to be one of the reasons for rapid spread of traits through parasite populations (Bitonti *et al.,* 1988).

1.5 Prevention and control

Prevention is better than cure! The current measures to prevent malaria are controversial as there are numerous developments taking place. Growing political commitment has taken action on the battle by making public awareness and constructing appropriate health infrastructures and resources. The key to preventing malaria is to correctly identify populations at risk and then give them prompt access to early diagnosis and effective treatment. Moreover, innovative controls need not only be efficient therapies but also cost-effective regimens, especially in the malaria prevalent African continent.

Measures to control the progression of malaria should be aimed at reducing contacts with the transmission vector, mosquitoes, by means of effective insecticides and larvicidies spraying at risk environments. For example, dicophane (DDT) is remarkably safe when used in small quantities (Smith *et al.,* 2000). One of the main reasons for the resurgence of malaria in South Africa is the discontinued use of DDT in 1996 resulting in malaria cases soaring in KwaZulu Natal (Yamey *et al.,* 2004). Personal preventive measures include the use of window screens, protective clothing, insect repellents, mosquito-proof bednets and appropriate chemoprophylactic agents to avoid the development of the disease.

Although *Plasmodium* possesses a multi-stage life cycle and diverse genetics has complicated vaccine developments for years, the treatment and control of malaria is still profoundly reliant on chemoprophylaxis and chemotherapy nowadays. Until a powerful wonder drug is developed in future, the current choice of therapies depends on scientific evidence and clinical experiences. The strategy involves accurate early diagnosis, timely

control and efficient, safe, cost-effective and up-to-date antimalarial agents. Nevertheless, the greatest current problem with drug prophylaxis is not only drug resistance but also compliance to drug regimens.

1.6 Antimalarial chemotherapy

The malaria burden is compounded by the relationship between human hosts and the complicated parasitic life cycle. Because of the 48 hour parasitic cycle, the reduction of parasitaemia *in vivo* can be used as a pharmacodynamic measure of antimalarial drug effect. Parasites persisting beyond 48 hours after starting antimalarial treatment (i.e. parasite clearance time) are a sensitive indication of drug resistance. Moreover, depending on the doses and patient factors, side effects are a common problem with any drug. A number of currently used antimalarial medications cause side effects, which are recorded (Table 1.6). Antimalarial agents, despite their difficulties, remain an essential means to prevent the infectious disease.

Table 1.6. Example of current antimalarials and their associated problems.

Therapeutic agents	Side Effects	Reference
Quinine Sulfate	Tinnitus	Sherman *et al.*, 1998
Mefloquine	Nausea, headache and diarrhea	Department of Health, 2003
Chloroquine	Oral aphthous, ulceration	Department of Health, 2003
Proguanil	Mouth ulcers	Sherman *et al.*, 1998
		Hyde *et al.*, 2002
Fansidar	Severe allergic reactions	Sherman *et al.*, 1998
		Ridley, 2002
Arternisinin	Recrudescence and neurotoxicity	Pasvol *et al.*, 1995
		Sherman *et al.*, 1998

Antimalarials are categorized by their mode of action at different parasitic stages that they affect (Schmatz and Schaeffer, 1991). The vast majority of the currently used antimalarial drugs are aimed at the intra-erythrocytic stage of the parasitic life cycle thus preventing disease development and further transmission. The first category comprises the most commonly used quinoline–based antimalarials, such as quinine and its

derivatives chloroquine (CQ), amodiaquine, mefloquine and halofantrine. Antifolate (sulfa) drugs as the second main group includes pyrimethamine, proguanil, sulfonamide and sulfadoxine which are representatives of dihydrofolate reductase (DHFR) and dihydropteroate synthetase (DHPS) inhibitors. Artemisinin and its analogues artesunate and arteether complete the third main class of antimalarials in the pipeline.

Although remarkable progress has been made towards vaccine development, an effective and affordable vaccine is not yet available. The genetically diverse *Plasmodium* and evolutionary parasite resistance to the therapeutic agents have complicated vaccine development. However, comprehension of the mode of action of the drug and resistance mechanism will provide invaluable insight into rational vaccine design and drug discovery to thwart and at last eradicate the scourge of malaria.

1.6.1 Quinine and its derivatives

The antimalarial properties of quinine (QN) (Fig. 1.6.1) were first discovered from the bark of the *Cinchona* tree in the early 17th century. In modern African history, QN also had a profound influence when Europeans attempted to explore Africa. Expeditions by non-immune travelers often ended up in disasters. As a result West Africa was once called the "white man's grave". At present, QN still plays an important role in the treatment of severe malaria and is administered intravenously (Foley and Tilley, 1997).

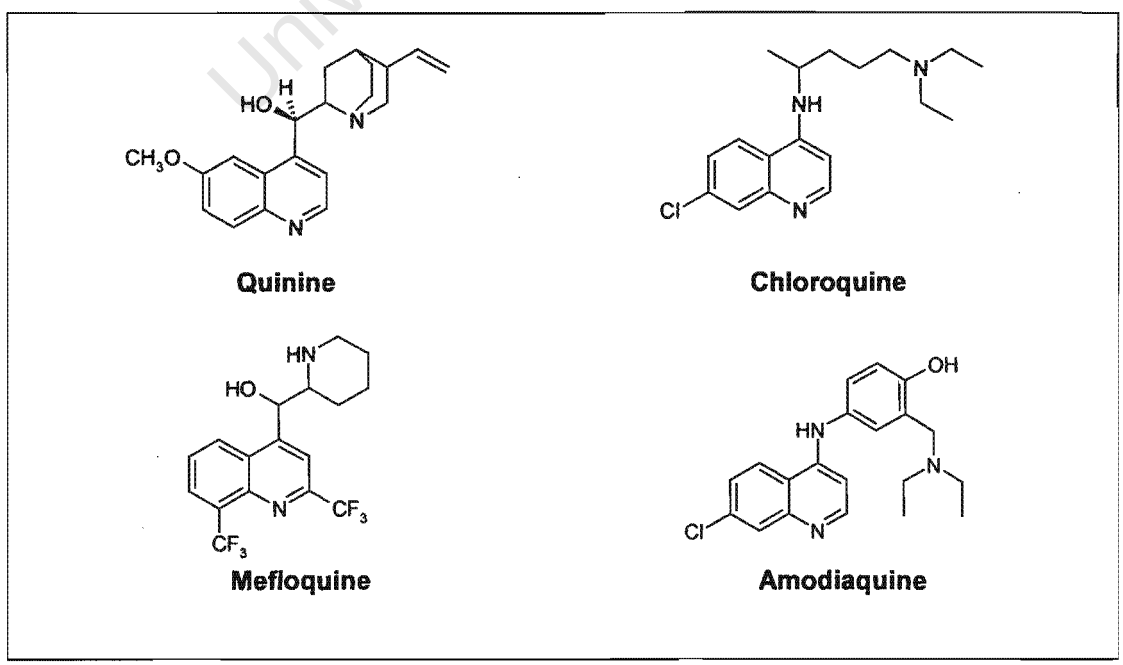

Fig. 1.6.1. Chemical structures of quinoline-based antimalarials.

QN was synthesized for the first time in 1944, but because of its complex structure, there is not an economically viable synthesis available and QN is still obtained from natural sources. The miraculous 'fever tree' plantations were in Java, which came under Japanese control in the Second World War, and QN was no longer available to the allied forces. In addition to this, setbacks such as parasite resistance to QN and it side effects – including sharp ringing in the ears – have driven research into alternative treatments. Ultimately it led to the development of chloroquine (CQ) – the most important antimalarial for almost half a century (Krogstad, 1996).

1.6.1.1 Chloroquine

CQ, 7-chloro-4-(4-diethylamino-1-methylbutylamino)quinoline, was synthesized as a less-toxic QN derivative by Bayer AG in 1934 (Krogstad *et al.*, 1987; Ward *et al.*, 1997;). It is relatively easy to make and hence very cheap. Conversely, novel drugs are very expensive – as much as 8 dollars a pill – compared to pennies for CQ. In addition, CQ was the only antimalarial known for its safety in therapy during pregnancy and in young children (Wolfe and Corders, 1985; Francis et al., 1997; Bray and Ward, 1998). Thousands of compounds have been screened for malaria treatment, however, none was found to be as powerful and as safe as CQ. Consequently, safety, affordability, rapid onset of action and minimal side effects attributed to the success of the most widely used therapeutic agent in the world.

The popularity of orally administered CQ, which became a prophylactic for travelers as well as a chemotherapeutic, inevitably led to widespread drug resistance; particularly in regions where table salts were chloroquinized in this endeavor to eliminate the risks in entire populations. This directed research to the development of its synthetic analogues mefloquine and amodiaquine. Many more 4-aminoquinoline and 8-aminoquinoline derivatives await approval for clinical use (WHO, 1981; Hawley *et al.*, 1998). Despite the prominent use of this class of antimalarials, its mechanisms of resistance and mode of action remain to be fully elucidated.

The advantages of CQ include well-established safety, cost-effectiveness and biological activity *in vivo*, which could provide insightful information on its mechanism of action. Its ease of synthesis has highlighted the importance of studying CQ since similar synthesis strategies may be used in drug development (De *et al.*, 1997). It is therefore hoped that CQ resistance will be reversed by better understanding of the drug and the molecular basis of drug-parasite interaction so that it can be reintroduced to treat complicated falciparum malaria.

1.6.1.2 CQ's mode of action

Evidence has shown that CQ is able to bind to DNA and inhibit DNA replication by intercalation (O'Brien and Hahn, 1965; Ciak and Hahn, 1966). It was therefore believed that this was the mode of action in *P. falciparum*. However, the specificity and concentration dependence of CQ with respect to non-specific DNA binding have questioned this hypothesis (Krogstad *et al.*, 1992). Currently there are various hypotheses to explain the mode of action of CQ (Ward *et al.*, 1997). Several common features were ascertained including that: (i) CQ is highly effective against the asexual blood stage of the parasite life cycle by interfering with the haemoglobin degradation process in the parasitic lysosomes, (ii) there is a high concentration of the weak base CQ in the acidic vacuole.

During the intra-erythrocytic stage of parasite development, *P. falciparum* ingests up to 80% of host-derived haemoglobin (Hb) as nutrient source (Yayon *et al.*, 1984; Zarchin *et al.*, 1986; Goldberg *et al.*, 1990; Slater and Cerami, 1992; Sullivan *et al.*, 1996). Hb is ingested via the cytosome, which is a mouth-like structure that engulfs the erythrocytes into the parasites in a process resembling endocytosis. Vesicles are then pinched off and Hb is carried to CQ's believed site of action, the acidic food vacuole, where proteolysis occurs (Goldberg *et al.*, 1990; Goldberg and Slater, 1992). Hb is broken down by aspartic (plasmepsins I and II) and cysteine (falcipain) proteases of which the primary degradation is considered to be the interaction of plasmepsin I with the native Hb. This Hb digestion process produces a byproduct of haem moiety, ferriprotoporphrin IX (FPIX) (Goldberg and Slater, 1992; Rosenthal *et al.*, 1996; Foley and Tilley, 1997). The potential lytic molecule attacks a variety of enzymes and damages biological membranes if

soluble (Slater and Cerami, 1992). Although lacking haem oxygenase, the parasite perfected the detoxification mechanism by dimerizing haem into non-toxic insoluble crystals, haemozoin (malaria pigment), which remain until infected erythrocytes burst. In light of the above, it is proposed that CQ's principle mode of action is to interfere with haem dimerization resulting in a build up of toxic free haem (haematin) and/or drug-haem complexes, leading to parasite death (Chou *et al.,* 1980; Dorn *et al.,* 1994; Orjih *et al.,* 1994). Egan and coworkers further support this hypothesis by providing compelling evidence that haemozoin is structurally identical to β-haematin, which can be made spontaneously under non-physiological conditions (Egan *et al.,* 1994). Under the physico-chemical process *in vitro*, CQ was found to perturb the dimerization equilibrium between monomeric (α-haematin) and dimeric (β-haematin) form of haematin by preferentially binding to haem dimers to form CQ-haematin complex (FPIX-CQ-FPIX) (Sullivan *et al.*, 1996b; Dorn *et al.,* 1998; Egan, 2001). Consequently, CQ reduces the availability of free haem to be integrated into haemazoin, leading to parasite lysis as a result of toxic free haem accumulating within the acidic food vacuole.

Although there is substantial evidence suggesting CQ acts through interaction with haem-derived compounds, the precise mechanism of action remains to be established. In addition, it has been proposed that CQ accumulation in the *Plasmodium* food vacuole is directed by its dibasic property and the pH gradient across the vacuolar membrane (Ferrari, *et al.,* 1991). The uncharged CQ is protonated once it diffuses passively into the acidic environment (pH 4.5 – 5.0). The diprotonated CQ cannot move across the hydrophobic vacuolar membrane, and is effectively trapped within the acidic food vacuole. The stage-specific CQ is thus proposed to inhibit haemoglobin proteolysis and/or alternatively inhibit the dimerization process. In contrast, CQ competitively inhibits haem degradation by glutathione thus increasing haem efflux out of the food vacuole (Ginsburg *et al.,* 1998; Deharo *et al.,* 2003), leading to haem accumulation within the parasite membrane. The damaging of the biological membrane leads to homeostasis disruption, causing parasites to burst. All these hypotheses are consistent with CQ's safety since the parasitic food vacuole does not exist in mammalian cells and is therefore a unique target or site of action.

1.6.1.3 CQ resistance

It is well accepted that CQ's antimalarial activity stems from the drug's uptake and accumulation into the parasites. However, evolved CQ resistant (CQ^R) strains accumulate less CQ than their susceptible ones, thereby reducing CQ uptake to prevent the incorporation of potentially toxic haematin into inert haemozoin within the food vacuole of the parasites (Fitch *et al.*, 1982). The molecular explanations remain subject to much debate. Several leading biochemical models proposed include (i) alteration of the digestive vacuole (DV) pH, (ii) changes in CQ flux across the cytoplasmic membrane of parasites or parasitic DV membrane (iii) reduced binding to an intracellular receptor, haematin and (iv) increased glutathione-mediated detoxification.

1.6.1.3.1 Alteration of digestive vacuolar pH

As a lipophilic basic drug, non-protonated CQ (pKa_1 = 8.1, pKa_2 = 10.2) enters the parasitic lysosome (DV) by passive diffusion, where it becomes protonated and remains 'trapped' (Foley and Tilley, 1997). The membrane-impermeable CQ accumulates at mM concentration levels, preventing parasite detoxification of its own waste. It is thought that the smaller the pH gradient, the smaller the CQ accumulation. According to this model, CQ^R *P. falciparum* achieves an increased lysosomal pH to limit pH gradient differences, thereby reducing the expected CQ accumulation by a weakened ATPase proton pump in the DV membrane (Bray *et al.*, 1992; Raynes *et al.*, 1999; Hyde, 2002).

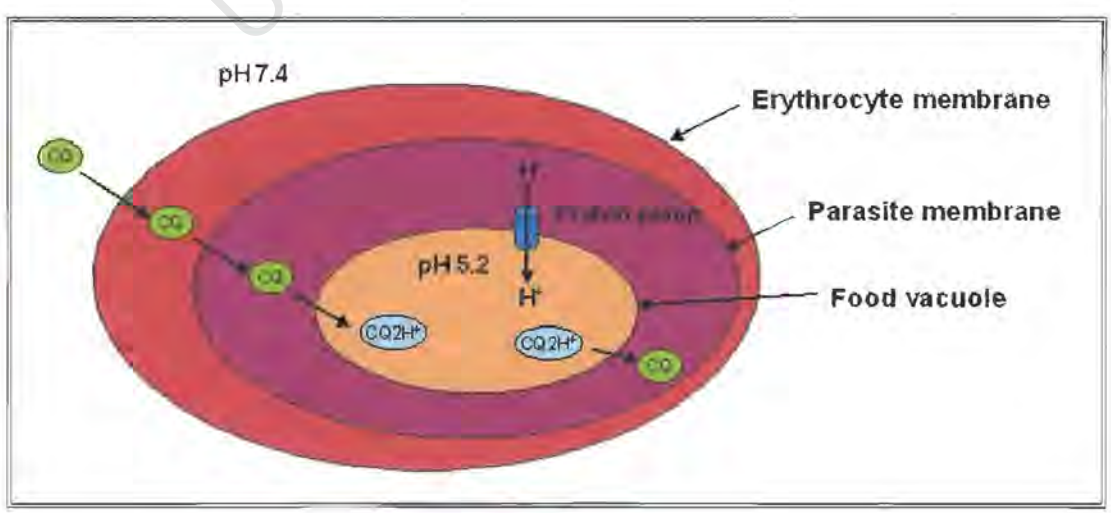

Fig. 1.6.1.3.1 Schematic diagram of the CQ transport.

1.6.1.3.2 Decreased CQ uptake and increased CQ efflux

Since haemaglobin is host-derived, it is thought that CQ resistance cannot arise from the structural change of the haematin target; in turn, a reduced uptake of CQ to lower the levels of CQ in resistant isolates has been proposed. Interesting results have shown that some inhibitors of the Na^+/H^+ exchanger competitively inhibit the transport of CQ, further supporting this notion (Sanchez et al., 1997; Wünsch *et al.,* 1998).

Alternatively, CQ resistant falciparum malaria has been proposed to possess an efflux process analogous to multi-drug resistant (MDR) cancer cells. One such distinguishing feature of MDR cancer cells is the overexpression of an ATP-dependent drug exporter, P-glycoprotein (Pgp) which is thought to be the characteristic transporter of a wide range of unrelated compounds out of the cells (Riordan *et al.,* 1985). Genetic evidence revealed a homologue of Pgp in *P. falciparum,* termed PfPgh-1, localizing to the DV membrane (Foote *et al.,* 1990; Ridley, 2002). Krogstad and his colleagues further support this proposal by the observation that the efflux rate of pre-accumulated CQ in CQ^R parasites is faster than in CQ^S parasites (Krogstad *et al.,* 1987; Martiney *et al.,* 1995). More recent investigations put forward suggest that the transfection of the Pgh-1 encoding gene, *Pfmdr1* on the chromosome 5, from CQ^R to CQ^S results in decreased CQ concentration in resistant parasites, also supports the involvement of Pgh-1 (Reed *et al.,* 2000). Furthermore, reversal of CQ resistance with verapamil and other resistance modulators provides additional evidence for the analogy to MDR cells as MDR phenotypes can be reversed by compounds inhibiting Pgp transport to increase their sensitivity to the drug (Martin *et al.,* 1987; Ford, 1996).

1.6.1.3.3 A molecular marker for CQ resistance – PfCRT

CQ resistance was very slow to develop, suggesting multiple mutations were required to produce the resistance phenotype. Laborious gene mapping efforts have been carried out by investigators worldwide and a CQ resistance candidate gene was eventually identified on chromosome 7 and thought to be responsible for the difference in CQ accumulation between CQ-sensitive and –resistant isolates (Wellems *et al.,* 1991; Su *et al.,* 1997; Wootton *et al.,* 2002). A milestone in CQ resistance was established by the discovery and absolute association with the lysosomal integral protein, PfCRT

(*Plasmodium falcparum* CQ resistance transporter) in genetic cross analysis *in vitro* (Fidock *et al.*, 2000).

Compelling evidence showed that sensitive parasites conferred a resistance phenotype with a mutant *pfcrt* gene transfection. In addition, transfected mutants were found to have a lower vacuolar pH, contradicting the hypothesis that resistant parasites possess elevated vacuolar pH. In a complementary study, Dzekunov and co-workers further demonstrated a lower pH in CQ^R parasites rather than in CQ^S clones (Dzekunov *et al.*, 2000). These observations put forward the hypothesis that a lower vacuolar pH favours the haemozoin formation (Fidock *et al.*, 2000; Hyde 2002). Moreover, it has been reported that verapamil reversibility was associated with a mutated chloride channel (Martiney *et al.*, 1995); recent empirical data showed that PfCRT expressed in yeasts exhibited some chloride channel features (Zhang *et al.*, 2002). This chloride channel could direct an increase in DV pH by varying the entrance and exit of chloride ions, thereby preventing access of basic drugs interacting with haematin (Zhang *et al.*, 2002).

Despite the fact that verapamil has little antimalarial effect, it is shown to restore CQ sensitivity in CQ^R *P. falciparum* (Martin *et al.*, 1987; Adovelande *et al.*, 1998). A recent study on the correlation of drug activity with residue hydrophobicity, side-chain volume and charge in mutant PfCRT CQ-sensitive and –resistant parasites showed verapamil chemosensitized the *pfcrt*-modified isolates to CQ (Sidhu *et al.*, 2002). The results provide additional evidence that PfCRT may function as a channel which, when mutated, permits efflux of CQ from DV, thereby decreasing the CQ concentration within the lysosomes of CQ resistant parasites. Evidence brought forward suggests that verapamil, as a known CQ^R reversal agent, interacts hydrophobically with the lysosomal intergral proteins and replaces the lost positive charge of PfCRT causing the protonated CQ to be trapped inside the parasitic DV, leading to parasite death (Sidhu *et al.*, 2002; Warhurst, 2003). It is thought that the more hydrophobic resistance reversers are more likely to bind to PfCRT proteins and block the efflux of protonated CQ, restoring CQ sensitivity. Although a number of hypotheses have been proposed to be possible mechanisms of CQ resistance, it is inevitable to conclude that the transmembrane protein may be involved in drug flux and/or pH regulation (Fidock *et al.*, 2002; Warhurst, 2003).

1.6.2 The antifolates

The antifolate antimalarials were generated through the knowledge of cell biology and synthetic medicinal chemistry (Ridley, 2002). This class of compounds is still commonly used as the first-line alternative to CQ in Africa since they are cheap and particularly effective against a mass scale of CQ-resistant African lines (Landgraf *et al.*, 1994). However, the long established parasite resistance to antifolates in parts outside Africa has threatened the use of this formulation (Sherman *et al.*, 1998). The principal antifolates are dihydrofolate reductase (DHFR) inhibitors, pyrimethamine and proguanil, and dihydropteroate synthetase (DHPS) inhibitors, sulfadoxine and dapsone (Fig. 1.6.2).

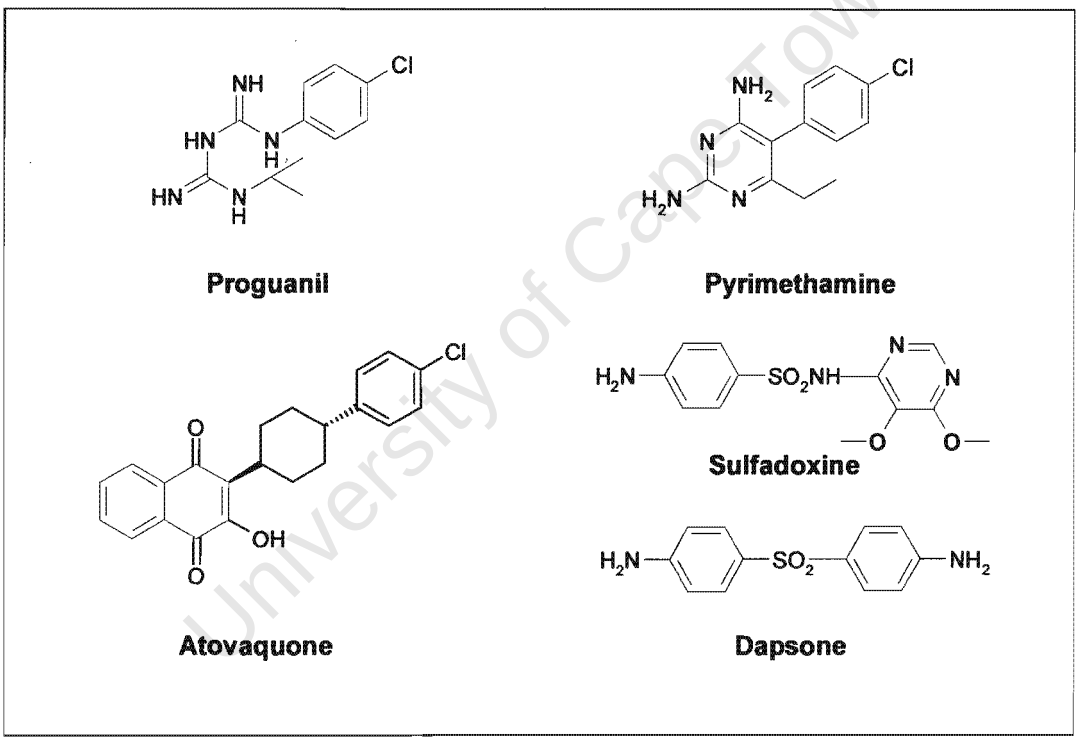

Fig. 1.6.2. Chemical structures of antifolate drugs.

1.6.2.1 Antifolate's mode of action

Most host tissues either synthesize purine and pyrimidine rings *de novo* from their precursors (CO_2, folic acid) or use exogenous uptake to produce nucleotides (Sherman *et al.*, 1998). Malaria parasites exhibit *de novo* folate biochemical pathways during asexual development. In contrast, red blood cells are incapable of synthesizing folic

acids. Instead, humans obtain the vital nutrients through dietary intake. The principal action of antifolates is the inhibition of plasmodial folate biosynthetic pathways consequently inhibiting DNA synthesis.

Fully reduced folate cofactors are essential for nucleotide and amino acid metabolism and are therefore essential for *Plasmodium* growth (Ridley, 2002). However, the multi-step folate synthesis involves various enzymes of which DHFR and DHPS are targeted by current antifolates. Cycloguanil, the active metabolite of both pyrimethamine and proguanil, inhibits DHFR activity which reduces dihydrofolate into the reduced functional form by competing with its natural substrates (Pasvol *et al.,* 1995). Similarly, sulfadoxine competitively inhibits the dihydrofolate precursor formation by mimicking the natural substrate of DHPS, *p*-aminobenzoic acid (Pasvol *et al.,* 1995; Hyde, 2002). Pyrimethamine and sulfadoxine combination, known as Fansidar, is the most significant formulation as both compounds act synergistically with each other and target the same biosynthetic pathway. Furthermore, long half-lives of the components highlights the practical use of treating sensitive falciparum particularly to out-patients as a single dose regimen (Pasvol *et al.,* 1995).

1.6.2.2 Antifolate resistance

Extensive use of Fansidar inevitably led to antifolate resistance which is now widespread. Resistance to antifolates is by far the best understood mechanism in all drug-resistance processes to date. The major resistance mechanism is mutations at the target enzymes (Wang *et al.,* 1997; Ridley, 2002). High-level pyrimethamine resistance results from the accumulation of mutations in the *dhfr* domain whereas the relationship of *dhps* mutations correlates with sulfadoxine resistance (Hyde, 2002). The acquired mutations alter the binding affinity of the inhibitors to the target enzymes, thereby enabling the parasites to tolerate elevated concentrations of antifolate antimalarials (Sherman *et al.,* 1998). Despite the combination of mutations in the target enzymes of *Plasmodium*, exogenous uptake of folate by human hosts also contributes to the clinical failure of this class of antimalarials by means of parasite's salvage of pre-formed folate, thus by-passing the blockage of *de novo* folate metabolism (Hyde, 2002).

In response to the emergence of antifolate resistance, another synergistic combination is proguanil with atovaquone, Malarone, was licensed for clinical use in 2002. It is currently used primarily as a prophylactic agent. This fixed-dose formulation of Malarone shows similarity to that of Fansidar though targeting mitochondrial electron transport (Ridley, 2002). However, drawbacks associated with high cost due to complex synthetic routes to atovaquone and the rapid development of atovaquone resistance prevent Malarone's widespread use, especially in malaria endemic areas of the African continent.

1.6.3 Artemisinin and its derivatives

The active antimalarial ingredient artemisinin originated from the Chinese herbal plant *qing hao* (*Artemisia annua*) in the early 1970s (Hyde, 2002). The isolated natural product artemisinin was used as a parent compound to generate several semi-synthetic analogues, sodium artesunate, arteether, artemether and dihydroartemisinin, in order to increase its solubility and antimalarial activity (Fig. 1.6.3). This class of drugs has a unique structural feature that lacks a nitrogen-containing heterocyclic ring, which is found in most antimalarials.

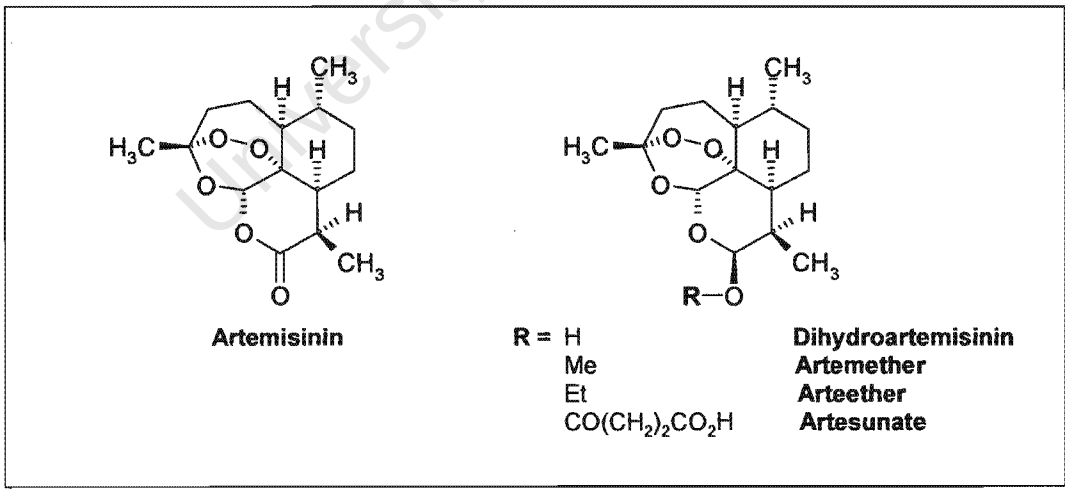

Fig. 1.6.3. Chemical structures of artemisinin and its derivatives.

These antimalarials are fast acting against gametocytes, the sexual stage of parasites that infect *Anopheles* vectors, thereby limiting the transmission to new hosts and circumvent the spread of resistant malaria (Ridley, 2002). At present, artemisinin and its

analogues play an invaluable role in the treatment of acute and uncomplicated malaria in South-East Asia (Pasvol *et al.,* 1995). In other parts of the world, artemether, arteether and artesunate are being used increasingly or being evaluated for use.

1.6.3.1 Artemisinin's mode of action

The precise mode of action of artemisinin is still to be settled, however, there is a consensus that the mechanism involves the unique structural feature of the endoperoxide bridge of artemisinin and its derived free radicals.

Peroxides are known to transform into free radicals, accordingly it has been suggested that free radicals cause oxidative stress in *Plasmodium*, resulting in parasite death. This model involves activation and alkylation (Meshnick *et al.,* 1996). The activation is thought to be initiated by an Fe(II)-mediated cleavage of the endoperoxide bridge (Fig. 1.6.3.1). Consequently, this process generates one or more types of highly reactive free radicals which are capable of alkylating or otherwise covalently modifying parasitic proteins (Meshnick *et al.,* 1996; Olliaro *et al.,* 2001; Hyde, 2002; Ridley, 2003). This theory thus suggests the oxido-reductive interaction with Fe(II)-haem in the parasitic digestive vacuole where carbon-centered free radicals inhibit several target proteins, damaging parasites.

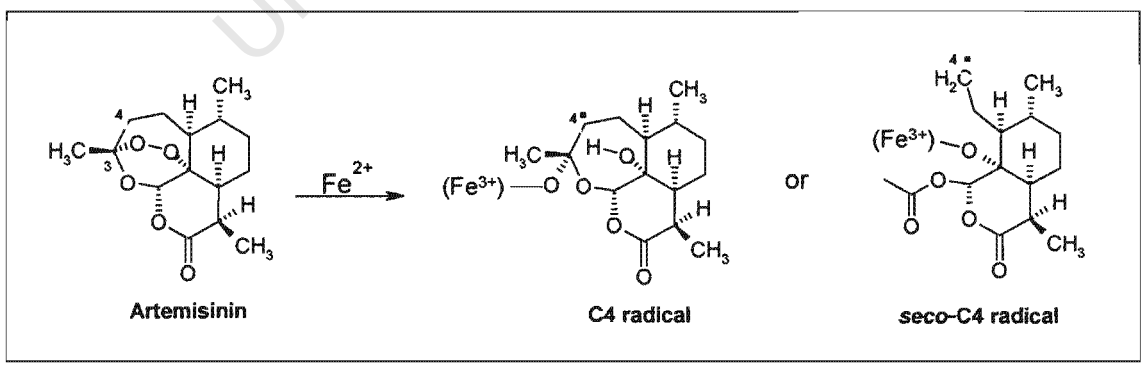

Fig. 1.6.3.1. Proposed interaction of artemisinin with iron (Reproduced from Dr. Robert G. Ridley, UNDP/WorldBank/WHO Special Programme for Research and Training in Tropical Disease, World Health Organization, CH-1211 Geneva 27, Switzerland). Ridley, 2003, *Nature*.

In contrast, Krishna and co-workers showed compelling evidence that artemisinins are found to spread throughout the cytoplasm, but specifically in the food vacuole of the parasites (Eckstein-Ludwig *et al.,* 2003). Moreover, the study demonstrated that the iron-dependent mechanism generates artemisinin-derived free radicals that are able to inhibit a malarial calcium-dependent ATPase, eventually resulting in parasite death (Eckstein-Ludwig *et al.,* 2003; Ridley, 2003). Meshnick and colleagues have shown artemisinin can bind to several different proteins; thus it is thought that the drug has other molecular targets, in addition to the Ca^{2+}– ATPase (Meshnick *et al.,* 1996).

Furthermore, the effect of artemisinin on nitric oxide (NO) synthase and transcriptional factor NF-kB activation in a human astrocytoma cell line was investigated (Aldieri *et al.,* 2003). Cerebral malaria is caused by parasite accumulation in the capillaries of the brain and/or excess tumor necrosis factor-alpha (TNF-α), which is regulated by the most upstream nuclear factor, NF-kB. TNF-α further correlates with the severity of *P. falciparum* since it can induce NO overproduction related to neuronal dysfunction in cerebral malaria. This study suggested another mechanism of action that arteminisin was able to modulate NO synthesis by suppressing the transcriptional factor, NF-kB, as well as its antiparasitic properties.

1.6.3.2 Artemisinin resistance

There have been no significant clinical reports of resistance to artemisinin and its derivatives even though these drugs are being used increasingly. However, *in vitro* investigations revealed artemisinin resistance has been achieved in *P. falciparum* by drug pressure, demonstrating the possibility of resistance (Inselburg, 1985). In a complementary study, some parasites were shown to respond to drug pressure by entering a dormant stage that is resistant to further inhibition (Hoshen *et al.,* 2000).

Short half-lives of these antimalarials necessitate a longer term regimen as monotherapy often leads to high recrudescence rates (Pasvol *et al.,* 1995). It is therefore recommended to be co-administered with drugs from different families with longer half-lives to decrease the possibility of inevitable drug resistance (Ridley, 2002). However, the fact that the more potent artemisinin derivatives are much more expensive

than the conventional antimalarials has hampered the practical use on a large scale, particularly in Africa where help is needed the most.

1.6.4 Urgent medical aid for malarial chemotherapy

The competence of parasites to evolve resistance has outpaced the strenuous efforts of investigators and heath officials worldwide to eradicate this global burden of malaria through vector control programs, preventive and curative measures. However, despite the weight of previous failures to combat malaria, and the variety of threats we endure, the fact that mosquito and parasitic genomes have been sequenced recently has raised hopes to control and treat this disease in the coming 7 – 15 years (Holt *et al.,* 2002; Gardener *et al.,* 2002). At present, since malaria control relies profoundly on chemotherapeutic agents, it is imperative to rapidly put in place strategic plans for the discovery and development of novel antimalarials and/or other alternatives if we are to avoid the ever-increasing drug resistance phenomenon. An alternative strategy to overcome this obstacle is drug combination. One approach to drug discovery and development is the investigation of new resistance modulators by combining the power of biology and medicinal chemistry.

1.7 The need for drug combinations

There is a growing consensus that fixed-dosed combinations are crucial to malaria control as drug combinations potentially offer several important advantages over monotherapy. Most importantly, drug combination would reduce the possibility of antimalarial drug resistance to evolve since at least one agent would have been clinically active. Second, they should provide improved efficacy because the appropriate combinations would have afforded additive potency, providing synergistic effects. Third, poor compliance with complex drug regimens could be significantly improved particularly in areas with poor health infrastructure and follow up supervision. Another probable additional advantage would be cost-effectiveness if the combinations would increase the potency of one drug to another, thereby reducing dosages of individual agents (Fidock, *et al.,* 2004). In Thailand, the combination of artesunate and mefloquine is a recommended policy and has already shown excellent efficacy and reduced the prevalence of mefloquine resistance (Ridley, 2002).

Ideally, combination regimens should incorporate two novel agents to limit the exposure of single agents to resistance. However, these are the major challenges in new antimalarial drug discovery and development. An alternative approach is to realize resistance modulators which potentiate the action of current existing antimalarials.

1.7.1 Chemosensitizers/ resistance modulators

Multi-drug resistance (MDR) in cancer is defined as the capability of tumor cells to survive continuous exposure to chemotherapeutic drugs. In MDR, inhibitors applied to drugs or compounds that are able to overcome MDR are called "overcoming agents", "reversers", "modulators", "modifiers" and "chemosensitizers". Work with MDR cells has shown the possibility to reverse anticancer agent resistance by using a combination of chemosensitizers or resistance modulators, which are agents able to antagonize multi-drug resistance, at safe therapeutic doses (Hwang *et al.*, 1996). In *P. falciparum*, it has been suggested that a phenomenon similar to the MDR phenotype in cancer cells may be a possible mechanism to explain the CQ resistance since the combination of the calcium channel blocker, verapamil, with CQ was able to sensitize malaria parasites to CQ *in vitro* (Martin *et al.*, 1987). Such a combination strategy has been adapted to overcome and/or delay multidrug resistance in malaria. It is based on the principle that drug resistance to antimalarial drugs occurs by an independent mechanism and that multidrug resistance will only occur when a single organism or cell develops mutations which leads to resistance to each independent drug (Bitonti *et al.*, 1988). This multidrug therapy has been investigated widely and comprehended. One major advantage of this tactic is the possibility of prolonging the life of CQ which provides invaluable advantages such as safety, efficiency, cost-effectiveness, and wide versatility for both prophylactic and curative purposes.

1.7.1.1 Synthetic chemosensitizers in malaria

Chemosensitizers in malaria are ideally drugs which do not exhibit intrinsic antimalarial activity when used alone but enhance the effect of antimalarial drugs. Furthermore, reversal of resistance is associated with an increase in drug accumulation in the drug resistant lines. A number of commonly used synthetic drugs such as calcium channel blockers like verapamil and fantofarone; antidepressants, imipramine and desipramine;

the antipsychotic trifluoperazine; antihistamines, chlorophenaramine and promethazine have been demonstrated to restore drug sensitivity in resistant cells by reducing the inhibitory concentration to that of the susceptible cells within tumor cells (Fig. 1.7.1.1-A). In parallel, initiated by the pioneering studies in cancer therapy, these cancer MDR chemosensitizers have been shown to restore CQ sensitivity in CQ^R isolates *in vitro* and in animal models (Martin *et al.,* 1987; Sherman *et al.,* 1998; Adovelande *et al.,* 1998). Unfortunately, unacceptably high concentrations of these resistance reversers are required for their effects in many cases. On the other hand, the inexpensive antihistamine chloropheniramine has been shown to restore CQ sensitivity at safe dosing levels. However, the adverse effect of drowsiness has limited the acceptance of this therapy (Sowunmi *et al.,* 1997). In a more recent study, the combination of a cocktail of structurally and functionally diverse MDR chemosensitizers in cancer cells at pharmacological concentrations has shown clinically relevant resistance reversal against CQ resistance strains (van Schalkwyk *et al.,* 2001). In view of the striking similarity with those observed in MDR anticancer agents, it has been postulated that a similar resistance reversal mechanism exists in malaria (Martin *et al.,* 1987; Rasoanaivo *et al.,* 1996). In cancer therapy, lines of evidence suggested that a decrease in drug accumulation within tumor cells is a mechanism of anticancer drug resistance. In the mechanism of CQ resistance, it has been reported that resistant malaria parasites accumulate less CQ than their sensitive counterparts so that CQ does not reach the required dose level to kill the resistant malaria parasites (Fitch, 1970; Krogstad *et al.,* 1987). More recently, there has been evidence supporting the mechanism that the active verapamil-sensitive efflux carrier (*via* either P-glycoprotein efflux pump and/or the transporter protein, PfCRT, and/or through vacuole proton leak) expels the incoming CQ from the parasites in resistant cells (Sanchez *et al.,* 2003). It showed that the efflux pump has a low affinity for ATP. In resistant cells, an ATP-dependent CQ efflux carrier moves CQ out of its intracellular compartment with the result that a small rise in the intracellular ATP level was not sufficient to activate the pump fully; compared to an increased extent in CQ accumulation with the addition of glucose in sensitive strains. Although the precise mechanism of CQ resistance and its reversal remain a subject of debate, it has prompted research into the mechanism of CQ resistance and its reversal and stimulated interest in other chemosensitizing agents.

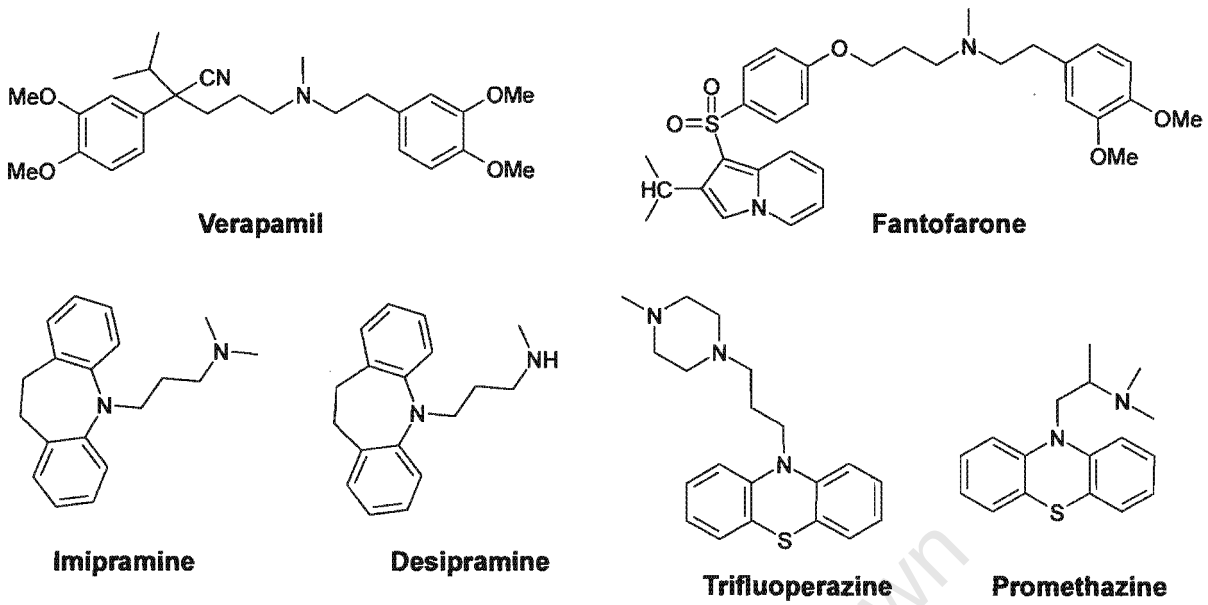

Figure 1.7.1.1-A. Chemical structures of commonly used drugs as modulating agents in cancer cells and in CQ^R *P. falciparum* isolates.

It has been proposed that studies on diversity-oriented chemical synthesis involving the generation of random mutations of resistance proteins/ proteins involved in resistance, and directing chemical libraries against these mutants can be used as the first step in a process to explore cellular and organismal pathways (Spring *et al.*, 2001; Chibale, 2002). The success of this approach would provide simultaneous identification of the protein target (therapeutic target validation) and chemosensitizers that modulate the functions of these proteins (chemical target validation). With respect to this, structure-activity relationships and molecular modeling studies should provide a pharmacophoric moiety for reversal agents and propose a model of drug interactions (Alibert *et al.*, 2002). Several synthetic potential CQ resistance reversers have shown some interesting results for *Plasmodia* (Fig. 1.7.1.1-B) (Rasoanaivo *et al.*, 1996; 1999; Batra *et al.*, 2000; Guan *et al.*, 2002; Osa *et al.*, 2003).

The calcium channel modulator, chloropromazine was found to act synergistically with CQ *in vitro* against the resistant strain from Indochina at concentrations much lower than therapeutically required doses (Kyle *et al.*, 1990; Rasoanaivo *et al.*, 1996). Compounds **1a** and **1b** (Fig. 1.7.1.1-B.) showed superior resistance modification index (RMI - see

Chapter 5, section 5.3.2) of 0.21 and 0.23 compared to that of verapamil (0.51) *in vitro* (Guan *et al.*, 2002). In the complementary studies, synthetic compounds CDRI-87/209 and **2a-c** were shown to be potent CQ resistance reversers (Batra *et al.*, 2000; Osa *et al.*, 2003).

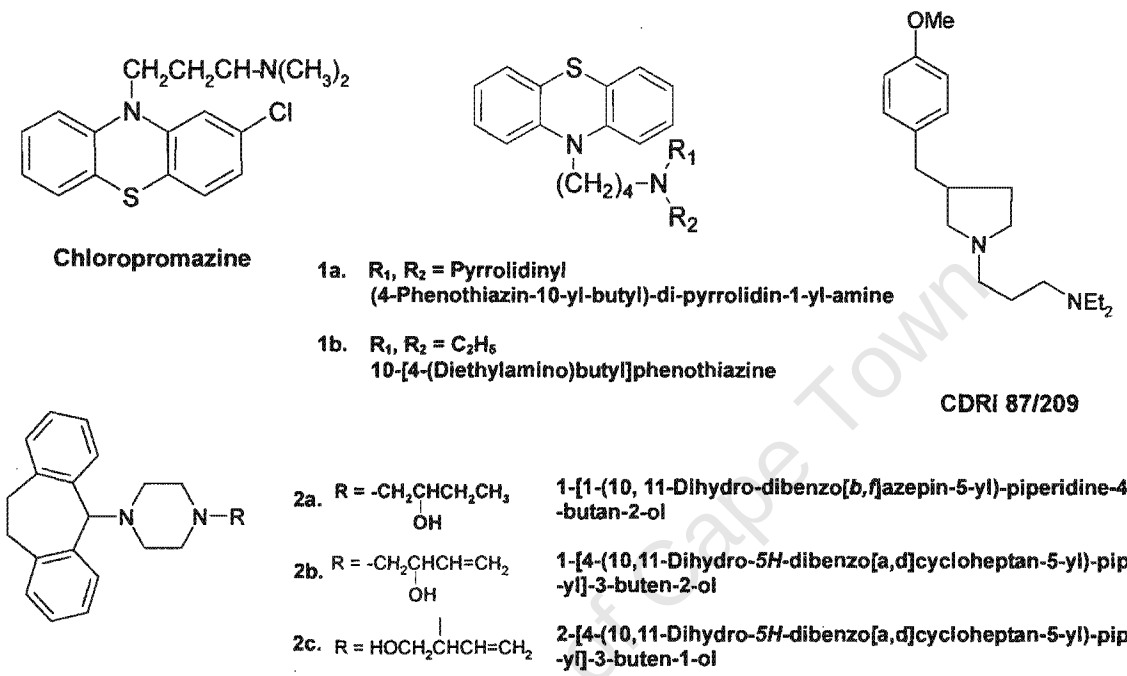

Figure 1.7.1.1-B. Chemical structures of some synthetic malaria chemosensitizers under investigations.

1.7.1.2 Naturally occurring chemosensitizers

In natural products, structurally related flavonoids castitin and artemitin were found to be capable of enhancing the growth inhibition of artemisinin selectively of *P. falciparum* (Fig. 1.7.1.2) (Rasoanaivo *et al.*, 1996). In addition, the structurally related isoquinoline dimers of herveline A, B and C, isolated from the stem barks of *Hernandiaceae* species from Madagascar and the indole alkaloids of strychnobrasiline were found to restore CQ resistance against Cameroon CQ resistant strains when used in combination with CQ.

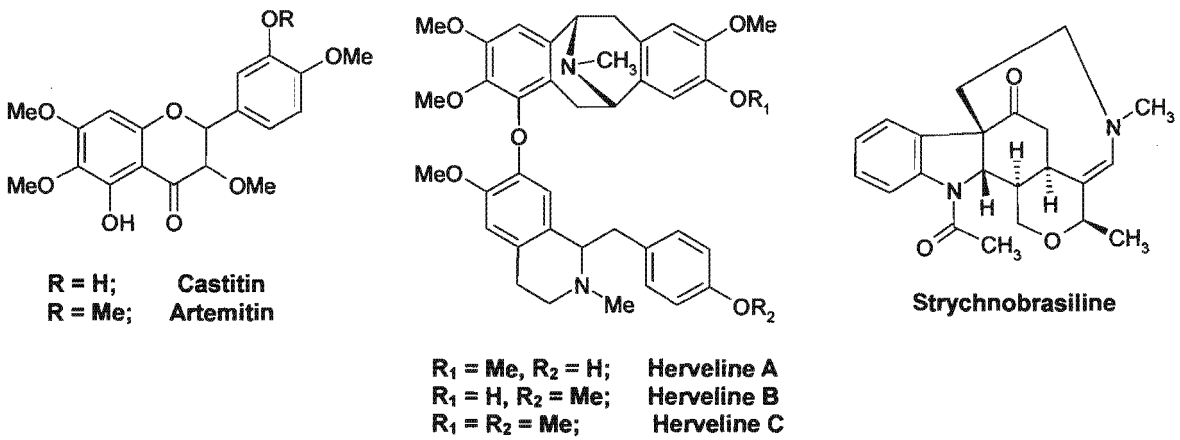

Figure 1.7.1.2. Structures of several naturally occurring products as chemosensitizers in malaria.

The circumvention of drug resistance in malaria by the use of resistance reversal agents in combination with standard antimalarial drugs may serve as a viable treatment to restore the efficacy of the latter in patients with malaria. However, even though these preliminary results of combination therapy in malaria have shown some potential in the treatment of complicated malaria, further details of pharmacological safety and efficacy studies are necessary to reveal clinical importance. In this regard, new resistance modulators with more selectivity in the mechanism of reversal are needed. Although CQ appears to have failed as a first-line antimalarial in most parts of the world, this well-tolerated antimalarial agent may be resurrected by combination therapy with effective resistance reversal agents (Rosenthal, 2003).

1.8 Impact of ABC drug transporter studies on drug discovery and development

Drug transporters also play a significant role in drug delivery, drug design, discovery and development processes. The important information on their functional characteristics such as substrate specificity and their localization provides imperative information about the mechanisms of drug disposition. In addition, knowledge about the resistance mechanism involved will allow the development of new drugs to minimize and circumvent drug resistance. Transporters of the ATP-Binding Cassette (ABC) family are known to provide the basis for drug resistance mechanisms from pathogenic yeasts, fungi and bacteria to mammalian cancer cells (Bauer *et al.*, 1999; Klokouzas *et al.*, 2003).

1.8.1 ATP-Binding Cassette (ABC) transporters

Transporters are categorized into primary, secondary or tertiary active transporters. Primary active transporters like ABC transporters are driven by ATP hydrolysis. The driving force for secondary or tertiary active transporters, such as organic anion transporters (OAT), organic anion transporting polypeptides (OATP), sodium taurocholate cotransporting peptide (NTCP), organic cation transporters (OCT), novel organic cation transporters (OCTN), and oligopeptide transporters (PEPT) is an exchange of intracellular and/or extracellular ions (Mizuno *et al.*, 2003; Burckhardt and Wolff, 2000; Lee *et al.*, 2001).

The ABC transporter proteins can be classified into two major subfamilies which are extensively involved in the tolerance to a wide diversity of cytotoxic agents (Cui *et al.*, 1996). One subgroup consists of human mediating multidrug resistance (MDR) of which MDR1 was the first discovered ABC transporter protein (Katzmann *et al.*, 1999). The other comprises of human multidrug resistance-associated proteins (MRP) that have more recently been found. Members of the ABC superfamily share similar molecular architecture with a repeating structure of a set of transmembrane domains followed by nucleotide-binding domains (NBD) (Cui *et al.*, 1996; Katzmann *et al.*, 1999). Nonetheless, MRP possesses several distinct features different from MDR1. First, MRP has an additional set of transmembranes at its N-terminus. Second, MRP proteins modify substrates such as glutathione (GSH) and glucuronide conjugates (Fig. 1.8.1) (Mizuno *et al.*, 2003; Katzmann *et al.*, 1999; Li *et al.*, 1997). Lastly, $NBD_1$of MRP has a characteristic spacing of functional motifs and high sequence similarity.

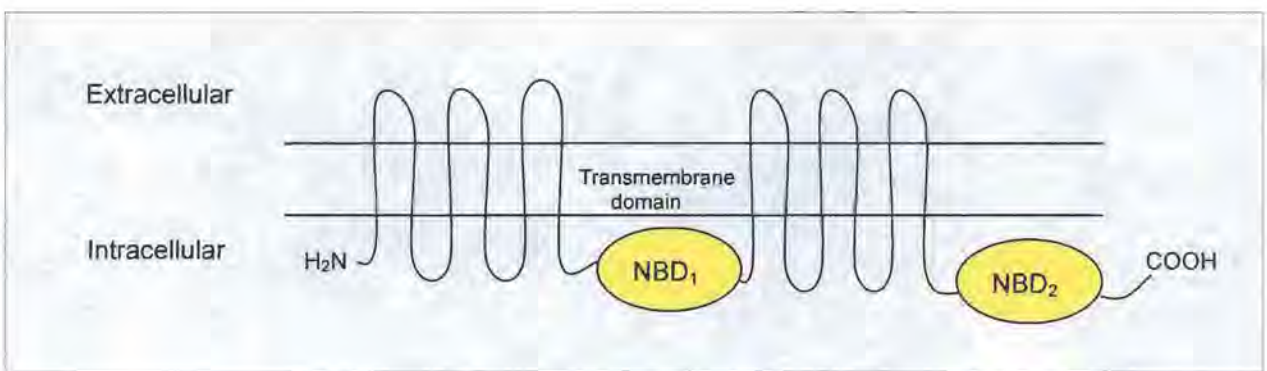

Figure 1.8.1. Schematic representation of the structure of a common ABC transporter.

Several well known ABC transporter proteins are medically associated with clinical drug resistance in humans, for instance, the *mdr1* gene product of Pgp, MRP1-8 proteins and more recently breast cancer resistance protein (BCRP) (Klokouzas *et al.,* 2003). These transporter proteins have been targeted for inhibition by resistance modulators to enhance the chemosensitivity of resistant tumors. Similarly, the *Pfmdr1* encoded PfPgh1 in *P. falciparum* adapted the human multidrug resistance phenomena and there is consistent evidence of its involvement in the resistance process (Martin *et al.,* 1987; Adovelande *et al.,* 1998; van Schalkwyk *et al.,* 2001). Such a drug targeting approach is one effective tactic to optimize pharmacological profiles of drug candidates.

1.8.2 ABC transporters in *Saccharomyces cerevisiae*

It is well accepted that PfPgh1 and PfCRT are involved in the drug resistance process in falciparum malaria. Even though PfCRT shares no homology to the ABC superfamily, its critical role in transport function has yet to be shown. In contrast, the knowledge and technology required for transport studies are well established in yeasts, it is thought that the study of drug transport in malaria will be greatly assisted by the information from yeast transport systems.

The baker's yeast, *Saccharomyces cerevisiae*, was the first eukaryotic organism found to possess a number of ABC transporter proteins (Bauer *et al.,* 1999). It is believed that mammalian MDR and *P. falciparum* multidrug resistance phenomenon are analogous to pleiotropic drug resistance (PDR) in yeasts. In addition, the fact that yeast has several orthologues of mammalian disease genes makes yeast an invaluable model system to unravel molecular mechanisms of transport function (Bauer *et al.,* 1999). In an attempt to better understand the function of PfCRT, a successful expression of a full-length malaria parasite integral membrane protein in yeast *Pichia pastoris* was achieved despite the very high AT content in malarial genes (Zhang *et al.,* 2002). The study concluded that mutant Pfcrt function in conferring CQ^R may include the effect on the H^+ pump system. The heterologous Pfcrt expression in yeast has undoubtedly assisted further understanding of its transport function.

Inspired by this successful manipulation in yeast transport systems, another attempt at transport protein study in yeast is of interest. A homologue of mammalian multidrug resistance protein, yeast cadmium factor protein (YCF1p), localized to the vacuolar membrane in yeast *S. cerevisiae* is investigated (Fig.1.8.2).

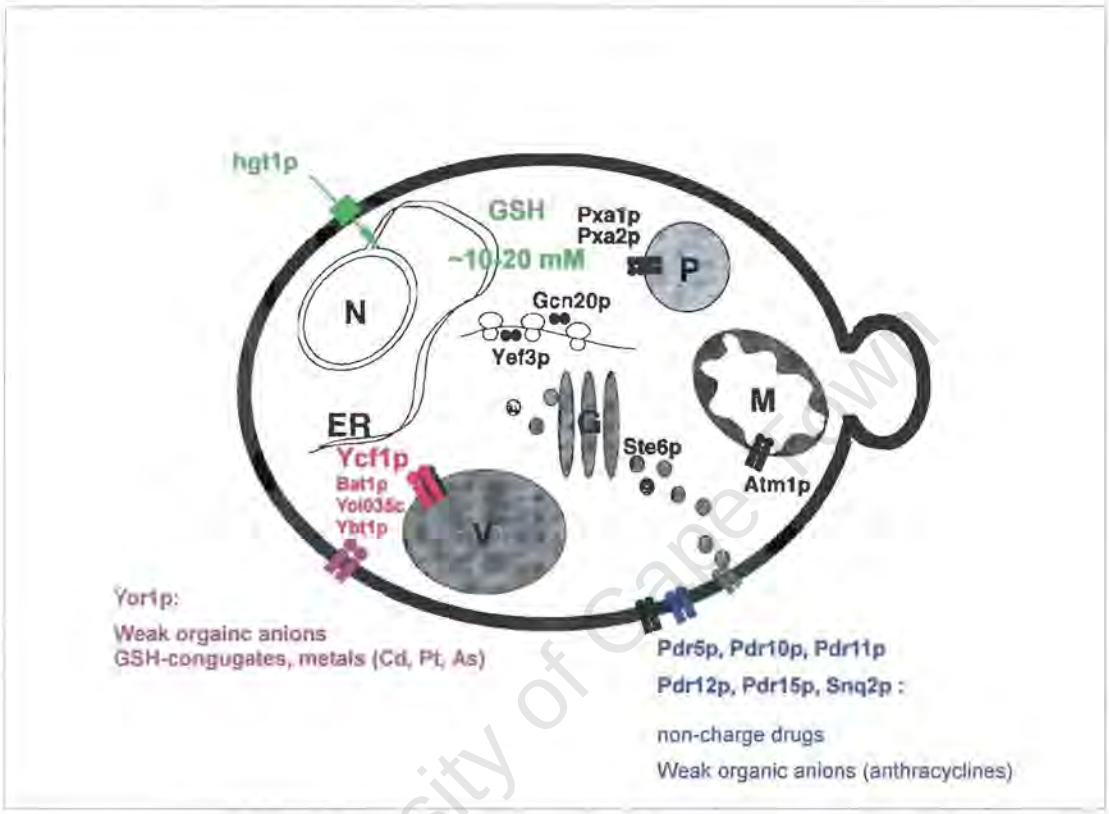

Figure 1.8.2. Schematic diagram of ABC transporters of yeast *S. Cerevisiae*. YCF1p is localized to the vacuolar membrane. ER, endoplasmic reticulum; G, Golgi apparatus; M, mitochondrion; N, nucleus; P, peroxisomes; and V, vacuole. (Adapted from Bauer *et al.*, 1999, *Biochimica et Biophysica Acta*)

1.8.3 The yeast cadmium factor protein (YCF1p)

The mammalian MRP homologue YCF1p coded by 1515 amino acids was the first ABC transporter protein identified in response to its ability to elevate Cd^{2+} tolerance. YCF1p shows a domain organization similarity to MRP (42.6% identity; 63.4% similar) and also to human MDR (Li *et al.*, 1996; Cui *et al.*, 1996; Kolaczkowski *et al.*, 1998). In addition, evidence revealed that YCF1p not only shares structural resemblance but also a functional homology to MRP (Li *et al.*, 1996). It plays an important role in vacuolar detoxification of heavy metals like arsenite, arsenate and antimony in addition to Cd^{2+}. YCF1p localizes to the membrane of the digestive vacuole which is the primary turnover site. In contrast, DV is also the site of CQ action in *P. falciparum* and PfCRT was found to

localize to the DV membrane. Thus, potentially important information derived from the drug interaction against YCF1p in *S. Cerevisiae* is likely to provide information into the function of the related eukaryotic proteins.

1.8.4 ABC transporters and their role in Chloroquine resistance in *P. falciparum*

ABC transporters have become the targets for inhibition by resistance modulators to enhance chemosensitivity in tumor cells, for example, the recently discovered breast cancer protein (Klokouzas *et al.,* 2003). Multiple cellular mechanisms in MDR involve cellular reaction and intracellular distribution, which involves the efflux transport and intracellular entrapment of the chemosensitizers (Wiese and Pajeva, 2001). The outword transport is associated with the transport protein, Pgp and to a lesser extent MRP. The idea that ABC transporters may be involved in CQ resistance in *P. falciparum* came from the initial finding that CQ resistance appears to be modulated by the human Pgp modulators verapamil and desipramine *in vitro*.

Some research has shown the involvement of *P. falciparum* MDR (*PfMDR1*) gene in antimalarial resistance by transfections of the polymorphic mutations of the *PfMDR1* gene into CQ-sensitive clones containing the wild-type *PfMDR1* gene (Foote *et al.,* 1990; Reed.*et al.,* 2000). The studies showed that although not the determinant of CQ resistance, the Pgp homologue in *P. falciparum* (Pgh-1) modulates resistance to quinine, to CQ (in a strain-specific manner) but not to mefloquine, halofantrine and the structurally unrelated artemisinin (Reed et *al.,* 2000; Duraisingh *et al.,* 2000). It can be tentatively concluded that the Pgh-1 substrates are chemically and structurally different compounds considering the fact that some reversers (verapamil, cyclosporine A, diltiazem) were found to be able to bind to Pgp and are transported by it, others (progesterone) block the efflux of the cytotoxic agents even though binding to it (Wiese and Pajeva, 2001).

More recent work has brought evidence for a drug efflux carrier as the mechanism of CQ resistance in falciparum (Sanchez *et al.,* 2003). The data suggests that CQ binds to intracellular binding sites; however, in CQ resistant cells the energy-dependent verapamil-sensitive efflux pump was able to expel CQ out of the intracellular

compartment so that there was not sufficient CQ accumulation to cause parasite death. Such efflux process can be inhibited by CQ resistance reversers like verapamil. Collectively, the very substantial studies on the accumulations of CQ in malaria-infected red blood cells have shown that ABC transporters are relevant to CQ resistance in *P. falciparum*. It is likely to act alongside other proteins (perhaps PfCRT) to bring about the drug resistance.

Chapter 2

Drug research and development

2.1 Drug discovery and development

To tackle the global burden of malaria, new treatments such as vaccines, antimalarial drugs and/or resistance modulators are desperately needed to meet the challenge of resistance as it arises. The current drug discovery and development process attempts to identify molecules not only easy to manufacture (affordability is crucial), stable, readily formulated but also in consideration of bioavailability ADMET (adsorption, distribution, metabolism, excretion and toxicity) properties. Worldwide, investigators have focused upon drug research and development (R&D) with enormous effort put into traditional medicinal plant discovery and more recently in medicinal chemistry approaches. However, only a limited number of potential molecules meet the criteria as drug candidates and even fewer are registered as medicines (Table 2.1). Drug design and discovery is envisioned as an extraordinary complex process. In the early discovery process, a hit molecule which gives a positive outcome in a bioassay in the exploratory screens has to be realized before being modified as a lead. A lead is the molecule optimized through pharmacokinetic, pharmacodynamic as well as efficacy studies into promising lead compounds that can be selected as pre-clinical candidates. In passing the need for a lead series of compounds, it is essential to show evidence of *in vivo* activity, structure-activity relationship (SAR) trends, known mechanism of action, selectivity, physical properties and chemical tractability. Physical properties are as referred by the Lipinski's rule of 5 (see section 2.1.1 for details) while chemical tractability deals with the presence of multiple functional groups at which the molecule can be modified to improve desirable properties. Followed by successful animal studies, the ultimate drug candidate(s) enter the human three–phase clinical development before registration. Major hurdles encountered are i) the potential molecules are toxic to humans even though they are highly active *in vitro* and ii) although meeting the requirements *in vitro*, fail to reveal activity *in vivo*. Drug efficacy, pharmacology and toxicity are all important parameters in the selection of compounds for development.

In this study, it is the intention to exploit the use of technologies of medicinal chemistry with the knowledge of basic biology and biochemistry of parasites to synthesize and screen a library of molecules in the search for potential CQ chemosensitizer lead compounds.

Table 2.1 Criteria for hit, lead and pre-clinical candidate compounds

	Hit	Lead series	Pre-clinical candidate
in vitro activity	√	√	√
in vivo activity		√	√
Structure-activity-relationship trends		√	√
Known mechanism of action		√	√
Pharmacokinetic profile		√	√
Acceptable estimated daily dose			√
Selectivity: related systems		√	√
Selectivity: wide range system			√
Acceptable cytochrome P450 profile			√
Physical properties: molecular weight, logP		√	√
Solubility			√
Chemically tractable			√
Synthetic routes			√
Clean in early toxicology (e.g. 7 day rat)			√

2.1.1 Lead identification and optimization

This transition phase before entering pre-clinical development undergoes extensive analyses with respect to improved pharmacological activities and minimized undesired properties of the hit molecules identified. This process is likely the most labor intensive and difficult to achieve as identified hits are to be developed into lead molecules which are often further modified into promising pre-clinical candidates.

Lead optimization includes identification of a pharmacophore. The pharmacophore of a compound is the minimum structural requirement for binding to a receptor. It is responsible for the observed pharmacological activities. It is normally identified prior to any modifications to the hits. This requires repetitive cycles of chemistry and biology in order to generate structure-activity relationships using medicinal chemistry, which can generate a vast chemical diversity of compounds simultaneously in a resource-effective manner (Terret *et al.*, 1995). Much effort has gone into rational drug design of new compounds to improve hit and lead targets (Erlanson *et al.*, 2004).

Much progress has been made to define adequate parameters to guide chemical synthesis producing molecules that possess the desired pharmacological properties and bioavailability. This is perhaps best embodied in 'Lipinski's rule of 5' (Lipinski *et al.*, 1997; Lipinski *et al.*, 1997; Ridley, 2002; Fidock *et al.*, 2004). These defined frontiers encompass low molecular weight (<500 Da), Log P (<5; where P is a lipophilicity measurement), the number of hydrogen-bond donors (<5) and the number of hydrogen-bond acceptors (<10) (Lipinski *et al.*, 1997). Therefore, the pharmacological properties (ADMET) of a compound can be estimated as a function of its physiochemical profiles. Implementation of these parameters is ultimately important to obtain leads that are likely to demonstrate activity in an *in vivo* model. In the drug development process, a lead compound is modified until its property profiles fulfill the required criteria (see Table 2.1) for pre-clinical candidates.

2.2 Rational drug design

There are different approaches in drug discovery to discover hit compounds: empirical screening, rational drug design, drug metabolism studies and clinical observations, of which, the rational approach is one of the major source of hits. Rational drug design is based on designing a compound to interact with an identified biological target. This approach is summarized in Table 2.2.

Table 2.2 Rational drug design

1. Identify gene or protein target → determine whether the target is amenable to the treatment
2. Obtain structural information on target protein → pharmacophore
3. Virtually screen chemical libraries using pharmacophore → SAR studies
4. Synthesize suitable compounds using chemical approach → Chemical synthesis
5. Perform *in vitro* biological evaluation → hits? leads?
6. Determine the effects of potential candidates on target protein function → antagonists?

To generate drugs targeting an identified protein, structural and functional information on the pharmacophore of the target is useful when available. Prior to synthesis of a structurally related library of compounds, the structure-activity relationships of potential

substrates to the pharmacophore are studied in order to identify new compounds. Subsequently, libraries of compounds with known structures are evaluated *in vitro* to find pharmacophore matches in order to discover hit and/or lead molecules. Those candidate compounds then undergo further investigations to reveal their clinical properties as agonists or antagonists.

2.2.1 Fragment – based drug discovery approach

In efforts to improve hit rates, investigators have analyzed the relationship between the structural configurations of leads and their corresponding pharmacological activities (Teague *et al.,* 1999; Hann *et al.,* 2001). This led to the conclusion that "the smaller the better". Fragment-based approaches are the strategies that low molecular weight chemical fragments are initially selected on the basis of their ability to bind to or inhibit the target of interest in a functional assay (Erlanson *et al.,* 2004). In other words, these small molecules are considered as building blocks of more complex molecules which are optimized further to meet the criteria as hits or leads. Fragment optimization, which is the process of converting fragments into hits and/or leads, generally involves combining a fragment with elements from a known substrates or inhibitor to create a hybrid molecule with improved pharmacological properties (ADMET). For example, the Alzheimer's disease target acetylcholinesterase (AChE) is the protein used to assemble its own inhibitor (Fig. 2.2.1). The dimeric molecule (**4**) enhanced the affinities compared to their monomeric components (**5**). In addition, AChE was chemically modified by linking with **6** using cycloaddition chemistry to produce the AChE inhibitor **7** with potent affinity for enzyme binding (Kd = 410 femtomolar) (Erlanson *et al.,* 2004).

"Fragment–based" approaches have been developed to generate a series of non-complex molecules which are built by combination or optimization of small fragments. The rationale behind fragment–based strategies is to produce simple lead-like molecules that can be further modified into better selective leads retaining drug-like properties. Lead-likeness and drug-likeness are best interpreted by Rishton; "drug-likeness serving to identify compounds suitable for drug development and product candidacy, and lead-likeness serving to identify compounds that are tractable for optimization by medicinal chemists" (Rishton, 2003).

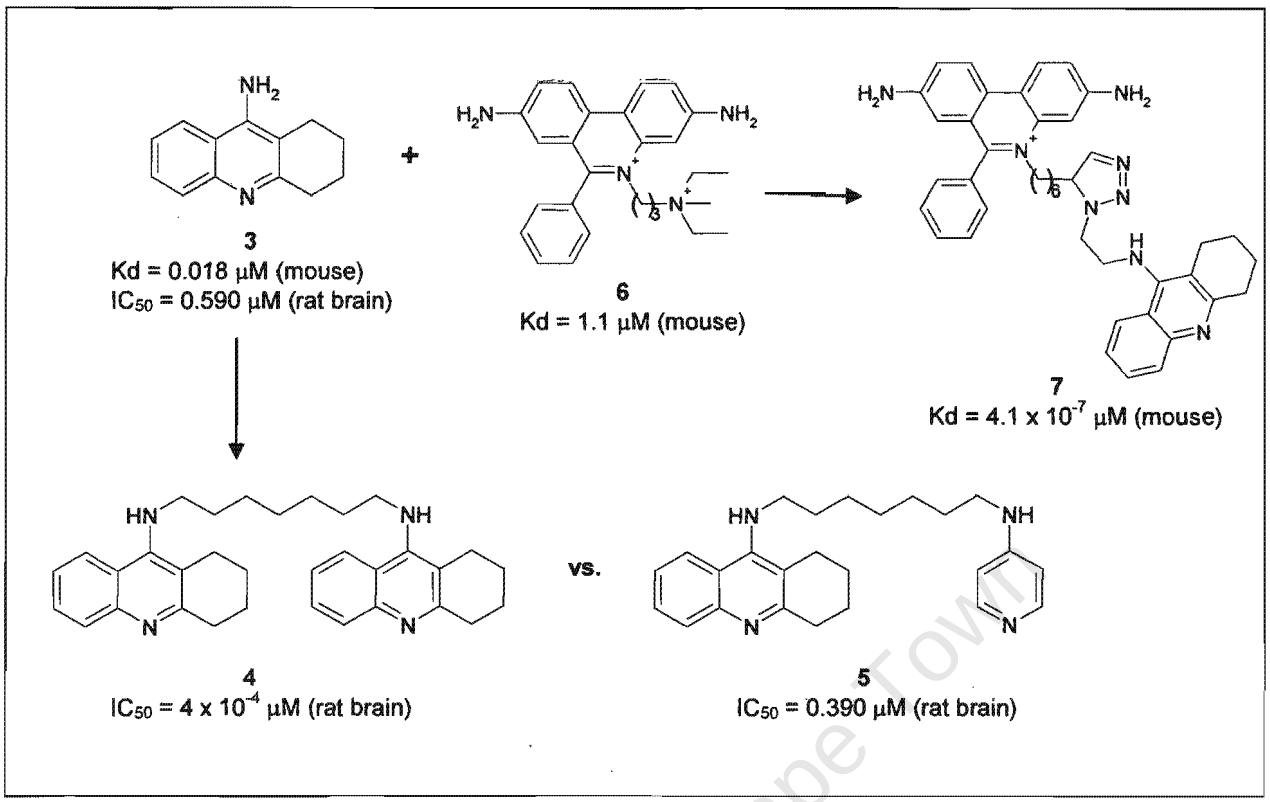

Figure 2.2.1. Fragment optimization of acetylcholinesterase. (Adapted from Erlanson *et al.*, 2004, *J. Med. Chem.*)

2.2.2 The privileged structure approach

Initially, the term "privileged structure" was first defined as "a single molecular framework able to provide ligands for diverse receptors" by Evans *et al.* in 1988. In the development of the benzodiazepine-based cholecystokinin-A antagonists, certain so called "privileged structures" or substructural motifs were shown to be capable of providing useful ligands for more than one receptor in the study and thereby concluded that "these structures appear to contain common features which facilitate binding to various proteinaceous receptor surfaces, perhaps through binding elements different from those employed for binding of the natural ligands". Since the privileged structure term was introduced, the selection and derivatization of these substructural motifs has become a working strategy. For example several pre-clinical or clinical candidates evolved from their corresponding leads were under investigations in Merck (Fattori, 2004) (Fig. 2.2.2). For example, the privileged spiropiperidine fragment (shown in red) was incorporated into the synthesis of pre-clinical or clinical candidates from the corresponding leads (left). The preferred substructural motif remained in the potent agonists with high affinity after the lead

optimization process in the development of growth hormone secretagogues, Somatostatin-2 receptor and Melanocortin-4 receptor agonists. Nevertheless, the strengths of the privileged structure approach are the potential to use less complex molecules and therefore more 'drug-like' and the possibility to easily enter the areas of biology and chemistry not previously explored.

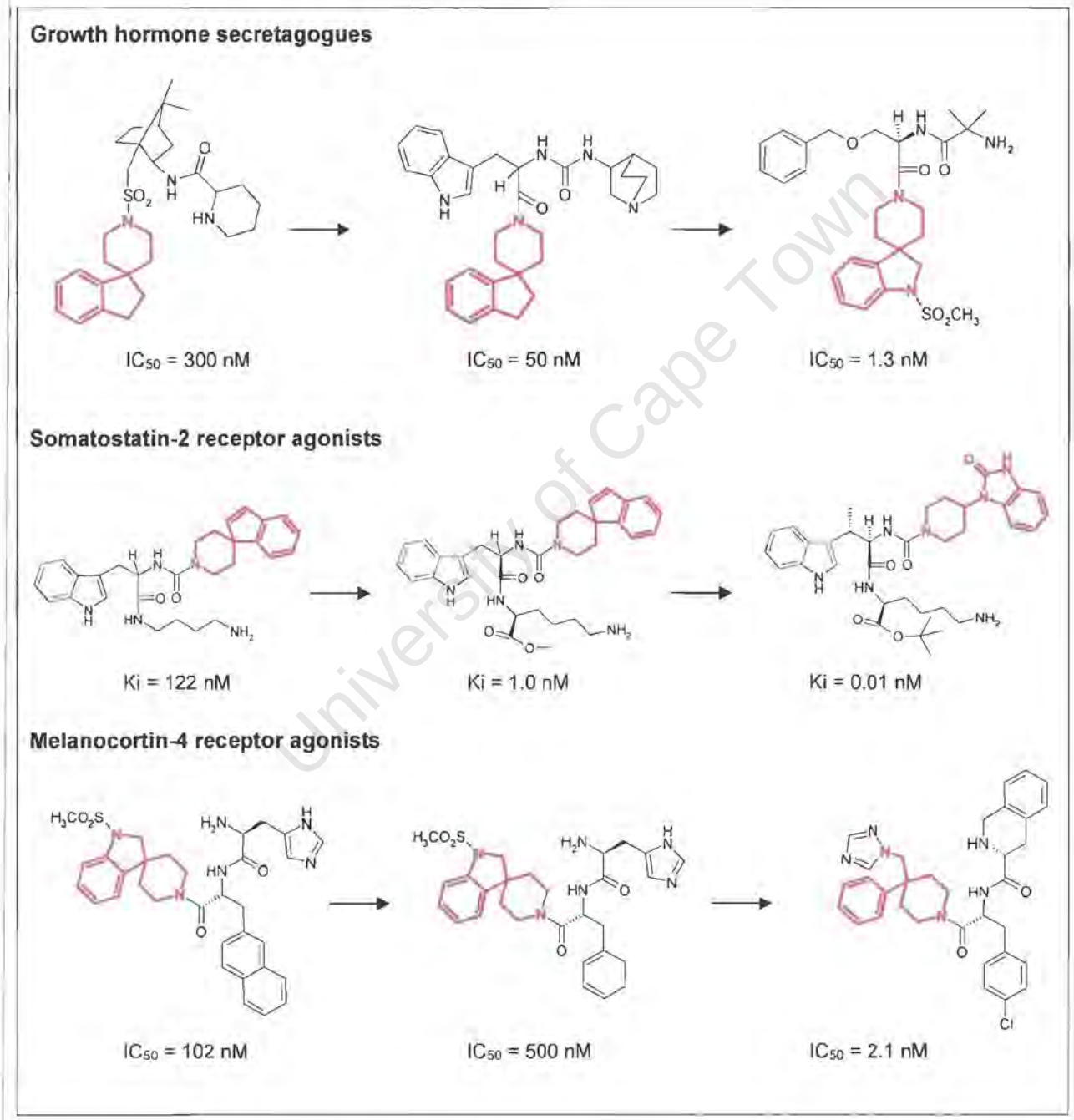

Figure 2.2.2. Several pre-clinical or clinical candidates obtained in Merck through derivatization of one among the privileged fragments, the spiropiperidine unit (red). Evolution from lead (left) to the corresponding pre-clinical or clinical candidates. (Adapted from Fattori, 2004, *DDT*)

2.2.2.1 Structure-activity relationships in chemosensitizers

Careful inspection of the structures of selected MDR chemosensitizers in malaria (Fig. 1.7.1.1-A) showed that two essential features of the molecules for resistance reversal activity are observed: a hydrophobic aromatic ring and an alkyl side chain with two amino groups separated by two or three carbons (Rasoanaivo *et al.,* 1996; Guan *et al.,* 2002). In a complementary study in cancer, it has been reported that a derivative of 4-quinolino-2-hydroxypiperazine(5-[3-{4-(10,11-dihydro-5*H*-dibenzo[a,d]cycloheptane-5-yl)piperazin-1-yl}-2-hydroxypropoxy]quinoline) (DSP) had high MDR reversal activities against resistant cancer cells without significant toxicity (Suzuki *et al.,* 1997). There were then attempts to synthesize and investigate a number of its derivatives for their reversal of MDR *P. falciparum* (Osa *et al.,* 2003). Similarly, a phenothiazine derivative **8**, which consists of a phenothiazine ring system and a pyrrolidinyl group joined by a 4-C alkyl linkage, displayed superior *in vitro* resistance reversal effect to verapamil in malaria (Fig. 2.2.2.1-A) (Guan *et al.,* 2002). These studies indicate the general structural features of the aromatic ring systems and a tertiary amine that are frequently observed in MDR modulators (Ferté *et al.,* 1999; Guan *et al.,* 2002). In line with the hydrophobicity requirement on the aromatic ring for good reversal effect, the introduction of a hydrophobic group in chalcones resulted in much more active compounds than the parent chalcones in cancer (Bois *et al.,* 1999; Rasoanaivo *et al,* submitted). In contrast, the uncharged polyethoxylated nonylphenol compound, NP30, was able to reverse mefloquine, QN, and quinidine resistance (> 80%) and, to a lesser extent, CQ resistance (Fig. 2.2.2.1-A) (Ciach *et al.,* 2003). The fact that the structure of NP30 does not contain nitrogen atoms leads to the suggestion that the protonable nitrogen in the chemical structures of resistance reversers is more important for CQ resistance reversal. Using the MDR Pgp inhibitor vinblastine as a probe, it was reported on the other hand that the two planar aromatic domains and the basic nitrogen were important features for cancer MDR reversal activities (Pearce *et al.,* 1990; Wiese and Pajeva, 2001).

In addition, the substitution patterns of the aromatic rings also play an important role in effecting CQ resistance reversal. Since veraparnil, fangchinoline (**9c**) and fantofarone were found to be very potent resistance modulators both in cancer and malaria, it was thought that they may be useful reference compounds. The presence of the methoxy

groups in the structures of verapamil, fangchinoline and fantofarone points to the importance of this substituent in the aromatic ring system for resistance reversal. It is noteworthy that the promising CQ resistance modulator 1-(3'-diethylaminopropyl)-3-((4-methoxyphenyl) methylene)pyrrolidine (**10** in Fig. 2.2.2.1-A) also possesses a methoxy group in addition to the lipophilic aromatic ring and two protonatable nitrogens in its structure.

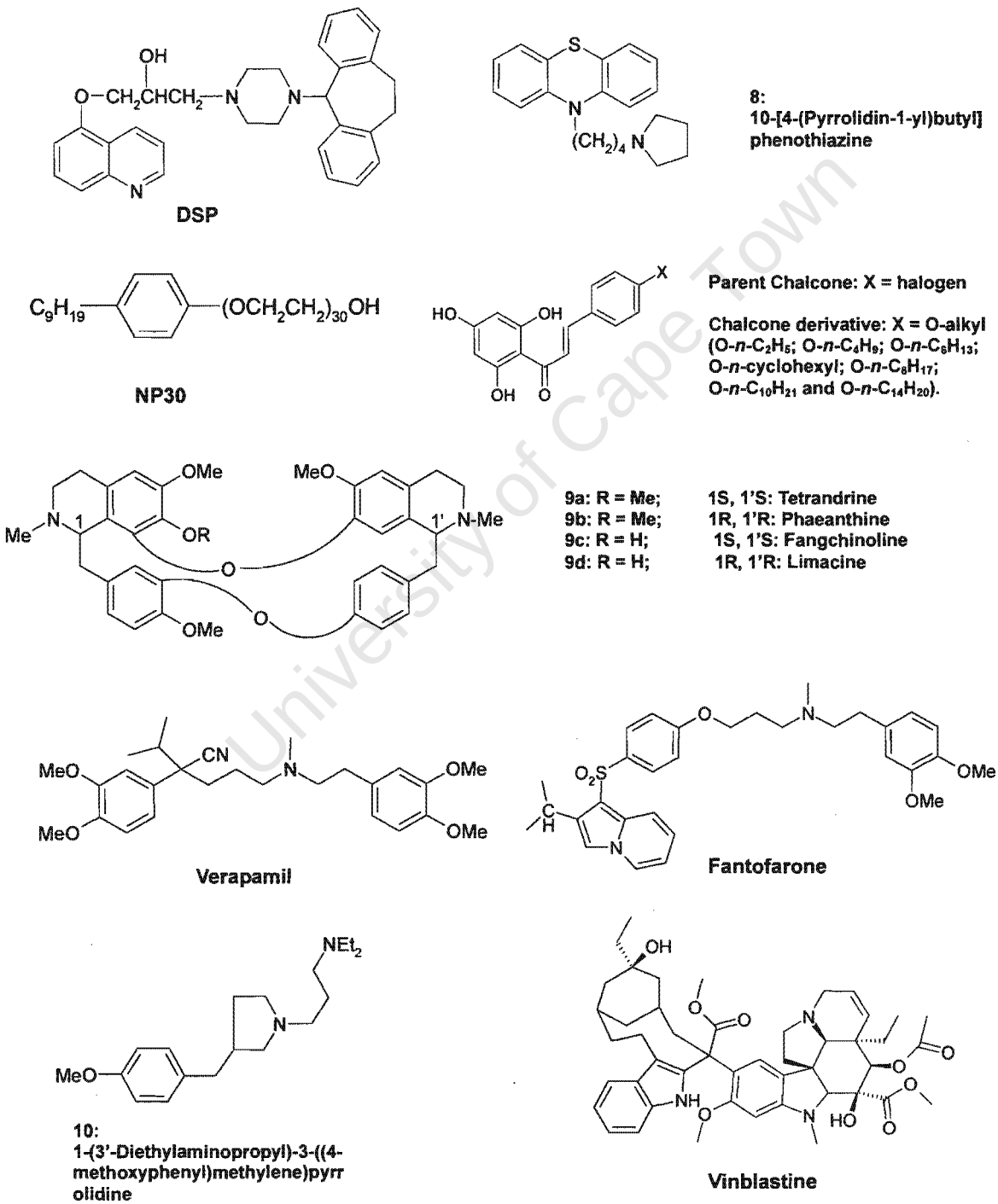

Figure 2.2.2.1-A. Chemical structures of various effective resistance modulators.

Besides the aromatic hydrophobic group, protonatable nitrogen and side chain substitutions, structural configurations are also an important factor. When compared within the bisbenzylisoquinoline (BBIQ) analogues, tetrandrine (**9a**) was found to act synergistically compared to its enantiomer phaeanthine (**9b**), which showed additive effects against CQ resistant parasites (Fig. 2.2.2.1-A). This suggests that the configurations at C-1 and C-1' have an effect on the reversal activity within the BBIQ family. Moreover, the other two alkaloids **9c** and **9d** differ only by their configurations at C-1 and C-1', Fangchinoline (**9c**) having the configuration of 1S, 1'S was a more effective CQ resistance reverser than its enantiomer limacine (**9d**) (Rasoanaivo *et al.*, 1996).

2.2.2.2 A basic chemosensitizing pharmacophore hypothesis

In connection with the MDR modulators, it was recently proposed that basic chemosensitizing pharmacophores may be present in most malaria reversers. Such basic pharmacophores were identified as -S-$(CH_2)_n$-S' (Fig. 2.2.2.2-A), in which S and S' could be nitrogen or phenyl groups and n = 3, 4, 5, 6, by careful inspections of some synthetic and naturally occurring chemosensitizers isolated from medicinal plants of *Strychnos myrtoides* and *Erythroxylum pervillei* (Rasoanaivo *et al.*, submitted). In the study, a common unit of *N*-phenyl-1,3-diamino-propane was identified from malagashanine, chloropromazine and desipramine (Fig. 2.2.2.2-B). In addition, a 1-phenyl-4-amino unit was also identified in the synthetic chemosensitizers cyproheptadine, amitriptyline and penfluridol. In another complementary study, the reduction of the benzene ring of the indoline group in malagashanine showed similar activity to that of the parent compound (Trigalo *et al.*, 2004), which suggests that this functional group (benzene ring) was not directly involved in the chemosensitization of the concerned indole *Strychnos* alkaloids (Rasoanaivo *et al.*, submitted). This led to the proposal that the 1,4-diamino fragment (red) is another bioactive unit which is also found embedded in a number of synthetic chemosensitizers, *Strychnos* alkaloids and chlorpheniramine (Fig. 2.2.2.2-B). Of those compounds studied, all showed resistance reversal activities *in vitro* and thus it was concluded that 1,n-diphenyl structure (n = 3, 4, 5, 6) might possess chemosensitizing activities.

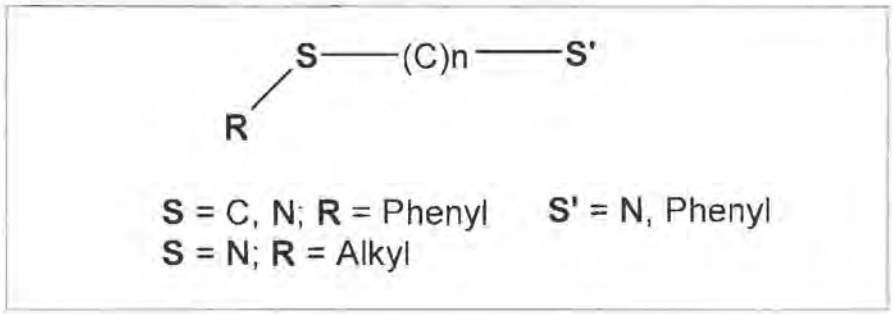

Figure 2.2.2.2-A. Proposed unifying chemosensitizing pharmacophore in malaria. (Reproduced from Rasoanaivo *et al.*, submitted).

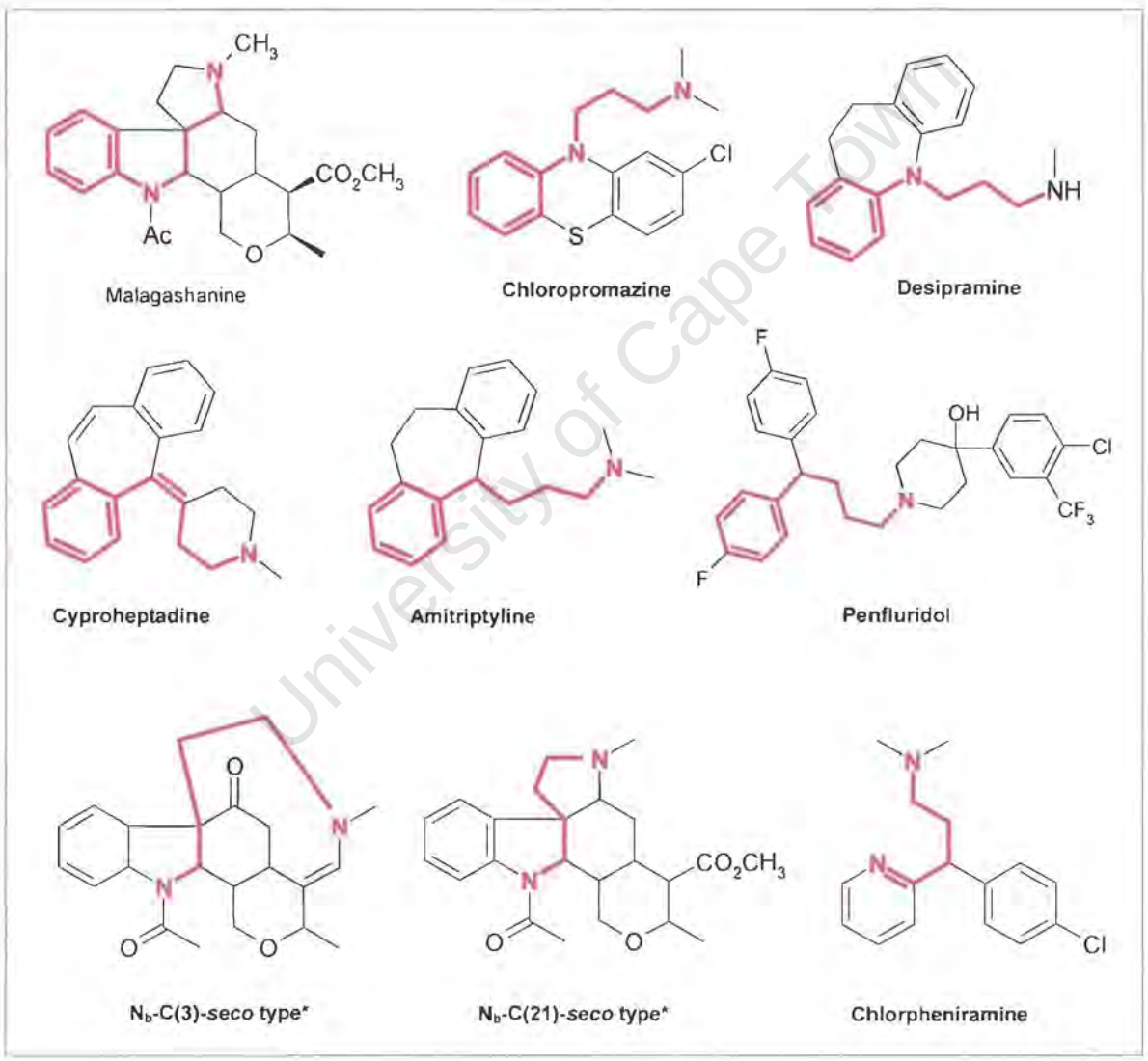

Figure 2.2.2.2-B. Chemical structures of diverse chemosensitizers. A common basic chemosensitizing fragment (shown in red) was proposed as the chemosensitizing pharmacophore.

*The *seco* derivatives were derived from *Strychnos* species.

2.2.2.3 Potential of biphenyl-based chemosensitizers

Statistical NMR-derived (nuclear magnetic resonance) binding data on 11 protein targets was analyzed in an effort to identify favoured protein binding molecular motifs (Hajduck *et al.,* 2000). It was found that the biphenyl substructure preferentially binds to nearly 50% of the proteins tested. This study confirmed that the biphenyl motif is a simple substructure, which can fit into a wide range of pockets that exist on protein surfaces (Table. 2.2.2.3). It has also been found to appear in 4.3% of all known drugs (Horton *et al.,* 2003).

Table 2.2.2.3. Identified privileged structures using NMR-Derived Binding data (Adapted from Hajduk *et al.,* 2000, *J. Med. Chem.*)

Name	Structure	Protein targets[a]	% Drugs[b]
COOH	CO_2H	6 (55%)	19.4
Biphenyl	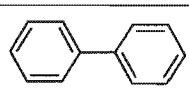	5 (45%)	4.3
Diphenylmethane	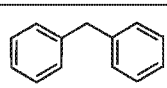	3 (27%)	8.6
Naphthyl	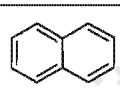	1 (9%)	3.3
Phenyl		1 (8%)	73.3
Cyclohexyl		1 (9%)	12.2
Bibenzyl	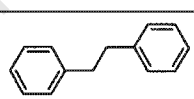	1 (9%)	5.9
Benzimidazole	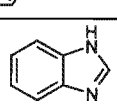	1 (9%)	0.8
Quinoline	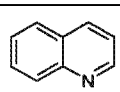	1 (9%)	4.2
Triazine		1 (9%)	0.2
Benzofuran	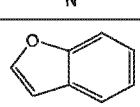	1 (9%)	0.8
Phenylphosphate	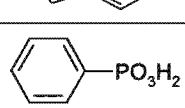	1 (9%)	0.03

[a]The number of projects (11) for which the substructure was represented.
[b]Percentage of 154 000 compounds from World Drug Index (Derwent) and Maccs Drug Data Report (MDL) that contain this substructure.

The privileged biphenyl framework offers a great degree of flexibility about the aromatic linkage as well as molecular rigidity and bioavailability; studies have revealed aromatics form favourable interactions with polar substituents and even positively charged groups (Hajduck *et al.,* 2000; Horton et *al.,* 2003; Fattori, 2004). With this degree of versatility, the biphenyl substructure (Fig. 2.2.2.3) is very popular in pharmaceutical industries and has produced a number of promising leads (Patchett, 2002; Fattori, 2004). For example, biphenyls are shown as potential anti-tumor, anti-hypertensive and anti-atherosclerotic agents (Horton *et al.,* 2003).

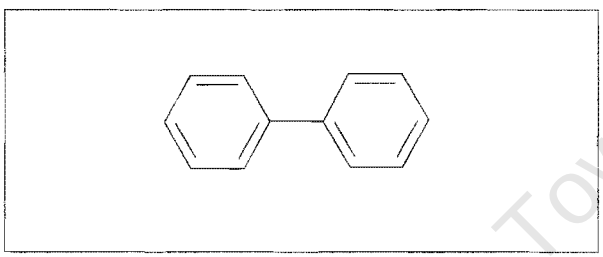

Figure 2.2.2.3. Chemical structure of biphenyl motif.

From a synthetic chemistry point of view, the biphenyl motif is an attractive template for chemical library generation. Several known reactions are utilized for biphenyl privileged fragments, including Ullmann synthesis, Stille, Kharasch, Negishi and Suzuki reactions (Horton *et al.,* 2003). Suzuki chemistry particularly lends itself to chemical diversity generation due to the commercial availability of boronic acid monomers, which can also be synthesized.

In this study, the rationale behind the drug design is to generate potential CQ resistance modulators consisting of a hydrophobic biphenyl moiety as a template or scaffold and incorporating amino groups based on previous SAR studies. It is hypothesized that the lipophilic character of the biphenyl moiety could result in attachment to the PfCRT channel and a positive charge possibly provided by the amino group could replace the lost positive charge on the mutated channel protein, PfCRT, subsequently restoring CQ sensitivity as suggested by Sidhu, Warhurst and co-workers (Sidhu et al., 2002; Warhurst et al., 2002). It is therefore of interest to investigate and examine the resistance reversal activity and toxicity of the novel compounds at an optimal concentration that would avoid or minimize toxicity to human hosts.

2.2.3 Efficacy screening models

Drug discovery involves several different stages in which selection of potential molecular targets is the primary process in the early investigation (Fig. 2.2.3). Initially, an improved understanding of the molecular basis of the pathogens, the drug's mode of action and resistance mechanism can provide potential targets. These targets can be selected from enzymes or pathways that are present in the pathogen, but absent from humans or those shared between two hosts with structural differences provided. Employing mutated organisms is an alternative means to measure the effect of an inhibitor. It will demonstrate the mutated form, which an enzyme or receptor loses its efficacy, is infact the target (Fidock *et al.*, 2004). In addition, new genomic and proteomic technologies have greatly improved our capabilities to characterize potential molecular targets.

In addition, it is equally important to develop an appropriate *in vitro* bioassay in initial screening to provide essential information on the activities of potential hit molecules. Generally, *in vitro* screens for compounds are often more rapid and less expensive than *in vivo* animal models since lower organisms or sub-cellular cultures are commonly used. Once appropriate laboratory tools are established, different compounds generated can be readily screened. Consequently, hits are identified when positive results are produced from the assay.

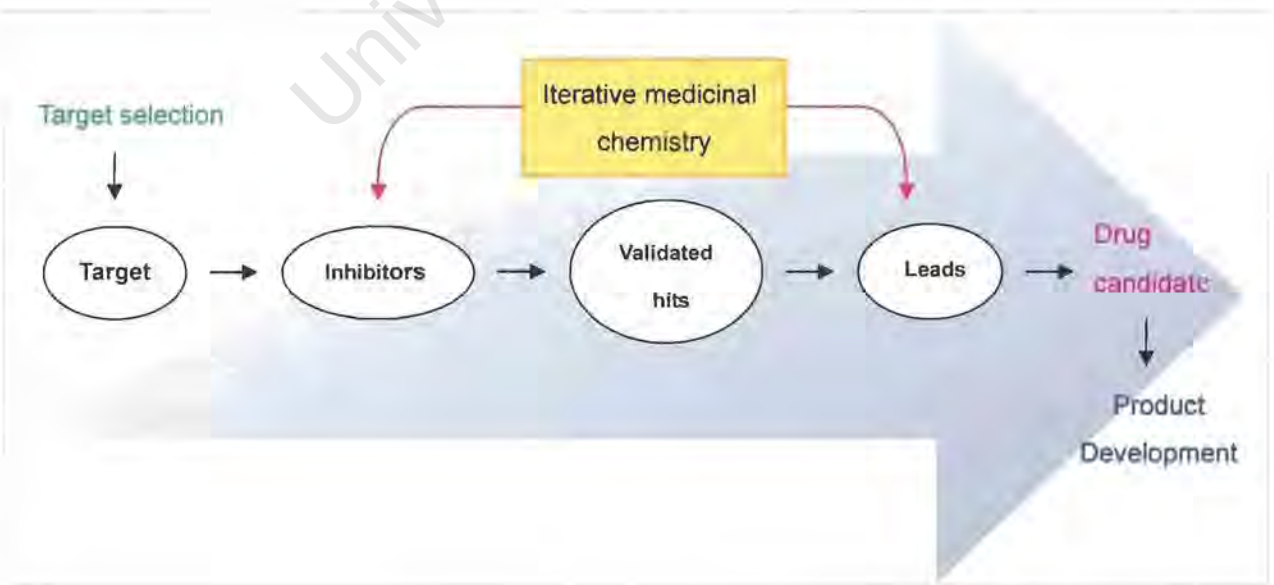

Figure 2.2.3. The process of drug discovery. (Adapted from Nwaka and Ridley, 2003, *Nature Rev.*)

In summary, once a target is selected, potential hit molecules which are rationally designed and synthesized are screened in the preliminary *in vitro* assay until a positive result is produced. This identified hit molecule can thus be further modified into potential leads. This process requires repetitive chemical modifications and biological evaluations until a potential lead molecule gives the confidence that a pre-clinical candidate can be found (see Table 2.1). At this stage the drug candidate will enter pre-clinical and clinical studies (Fig. 2.2.3).

2.2.4 Drug development

Broadly speaking, there are three main stages in the drug development process, 1) pre-clinical evaluation, 2) clinical validation and 3) registration (Fig. 2.2.4). When the lead molecule is identified during the drug discovery process, it will enter pre-clinical safety and efficacy studies. During pre-clinical development, extensive detailed pharmacological properties such as acute toxicity and pharmacokinetics (ADMET) are assessed from relevant animal models to generate a wide range of safety measures before entering human clinical trials. The first phase of clinical verification is aimed at safety, pharmacokinetics and tolerability in healthy volunteers whereas finding the dose-range, side-effect and clinical proof profiles occur during phase II (Fidock *et al.*, 2004). In the last phase of clinical trials, a large sample of subjects is examined to confirm a wide margin of safety profile and efficacy of the drug before submission for registration (Ridley, 2002). Together with the registration process, it is estimated that 10–15 years is required to complete the analyses of a drug.

Figure 2.2.4. The process of drug development.

The risks of taking the newly developed drug are reduced as the drug development progresses. However, this drug development process requires not only devoted manpower but also huge financial resources which currently rely upon pharmaceutical industries and donations from the private and public sectors.

2.3 Scope of the study

This study combines the knowledge of biology and medicinal chemistry to identify potential selective and non-toxic chloroquine–resistance reversal agents based upon the privileged biphenyl sub-structural motif as well as investigations into transport of cytotoxic compounds in a yeast membrane protein.

Objectives of this study are to:

1. Rationally design and synthesize novel potential CQ resistance reversal agents or chemosensitizers in malaria, based upon known structure–activity relationship studies
2. Generate preliminary structure-activity relationships within a series of biphenyl-based chemosensitizers
3. Investigate the *in vitro* antiplasmodial activity and resistance reversal effect of the potential hits in *P. falciparum*
4. Perform *in vitro* investigations into the function of specific transport of cytotoxic compounds in a membrane protein of yeast *Saccharomyces cerevisiae*.

Chapter 3

Materials and methods

3.1 Chemistry

3.1.1 General

1-Phenylpiperazine and *N*-methylpiperazine were obtained from Lancaster, Scientific, and Sigma-Aldrich South Africa, respectively while 1-benzylpiperazine was synthesized chemically. The remaining reagents and solvents were obtained from Sigma-Aldrich South Africa. Reactions were monitored by thin layer chromatography (TLC) on aluminium-backed silica gel 60 F_{254} coated sheets (Merck) and visualized with a combination of ultraviolet light (254 nm) and anisaldehyde spray (freshly prepared from a 2.5% solution of *p*-methoxybenzaldehyde (20 cm^3) and 18M sulfuric acid (1 cm^3)), followed by heating at 200 °C. Column chromatography was carried out using Merck Kieselgel 60: 70-230 mesh. Melting points were measured on a Reichert-Jung hot stage microscope and are uncorrected. Infrared (IR) spectra were recorded (NaCl) on a Thermo Mattson Satellite FTIR spectrometer connected to a desktop PC running EZ OMNIC software (version 6.0A). ^1H NMR and ^{13}C NMR spectra were recorded on either a Varian VXR-200 at 200 MHz, Varian Mercury 300 MHz or a Varian Unity spectrometer at 400 MHz instrument (Department of Chemistry, University of Cape Town) and are recorded in parts per million (ppm). All NMR spectra were measured in $CDCl_3$ and tetramethylsilane (TMS) was used as an internal reference. Mass spectra were recorded on LC-MS (Department of Pharmacology, University of Cape Town). (See Chapter 4 for further details).

3.2 Cultivation of *P. falciparum in vitro*

Different strains of *P. falciparum* were selected for this study: D10 (IC_{50}^{CQ} = 23 nM), a CQ-sensitive strain (provided by the Walter and Eliza Hall Institute of Medical Research in Melbourne, Australia), RSA11 (IC_{50}^{CQ} = 186 nM) and K1 (IC_{50}^{CQ} = 190 nM), CQ-resistant strains (provided by Dr. Janet Freese, Malaria Research Programme, Medical Research Council of South Africa, Durban, South Africa; and isolated at Kanchnaburi, Thailand, respectively).

Haematocrit

The proportion of the volume of a sample of blood represented by red blood cells.

Parasitaemia

A quantitative measure of the percentage of the erythrocytes that are parasitized.

Giemsa

A nucleic acid stain used to visually distinguish parasites from the surrounding cells.

The parasites were maintained at 5% haematocrit in continuous culture by a method modified from that of Trager and Jensen (Trager and Jensen, 1978). *P. falciparum* parasites were infected with type O–positive human erythrocytes (Western Province Blood Transfusion Service, Groote Schuur Hospital, Cape Town, South Africa) with 10% type A-positive human serum. The culture was suspended in RPMI 1640 (Biowhittaeker) culture medium supplemented with 25 mM HEPES buffer (Sigma), 1% sodium bicarbonate and gentamicin (40 mg/ml) and hypoxanthine (44mg/L). Medium was renewed daily and parasitaemia was determined using Giemsa stained blood smears of the cultures. The cultures were kept continuously at 37 °C under an atmosphere of 3% O_2, 4% CO_2 and 93% N_2. Cultures were synchronized by treatment with 5% D-sorbitol (Sigma) in the ring stage of development (Lambros and Vanderberg, 1979).

3.2.1 Dose response curve experiments

3.2.1.1 Drug preparations and dilutions

CQ (Sigma) was used as a positive control to determine *in vitro* susceptibility and the interactions of two drugs in both combination studies against the different clones of *P. falciparum*. CQ and verapamil stock solutions of 1mg/ml were made up in Millipore water and serially diluted with complete medium to the desired concentrations for use. The novel compounds generated were first dissolved in minimal DMSO and then Millipore water to achieve a 2mg/ml stock solution before sonication. The amount of DMSO added varied between 0% – 8.4% depending on the solubility of the compounds. The highest DMSO concentration reached in the wells of the microtitre plate is 1.7% which exerts non–detectable measurement on parasite survival on the system. The stock solutions of CQ and newly synthesized compounds (less than 2-weeks old) were aliquoted in multiple eppendorffs and stored at –4°C till use. However, the otherwise unstable verapamil solution was freshly prepared on the day of the experiments.

3.2.1.2 Plate design

The blank wells were prepared with 2% haematocrit of O^+ red blood cells (RBC) in complete medium whereas parasitized red blood cells (pRBC) of 2% haematocrit and 2% parasitaemia served as a control. Synchronized parasitic erythrocytes were harvested in the trophozoite stage of the growth development (2% haematocrit, 2% parasitaemia) and incubated in 96-well microtitration plates (Greiner) arranged in a matrix of eight rows (A to H) and 12 columns (1 to 12) (Fig. 3.2.1.2). The plates were incubated in an airtight gas chamber with a gas environment of 3% O_2, 4% CO_2 and 93% N_2 at 37 °C.

Figure 3.2.1.2. Visual presentation of a microtitration plate.

To start the dose response experiment, 200 µl of drug solution (typically 100 µg/ml) was added into each well in column 3 using a dispenser. To the rest of the wells, 100 µl of complete medium was added throughout the test plate by the dispenser. Two–fold serial dilutions were made from column 3 across the plate by removing 100 µl of the drug solution from column 3 and then added into column 4 and so on using a multi-channel dispenser. To the designed blank wells of column 1, 100 µl of prepared RBC was added. To the control wells of column 2 together with the rest of the test wells were topped up with 100 µl of previously prepared pRBC. Therefore, the final concentration for each well consisted of 1% haematocrit and 1% parasitaemia with respect to 1% haematocrit of the blanks. A large concentration range of 100 µg/ml to 0.20 µg/ml of the sample tested was achieved. The prepared test plates is therefore made up of a blank in column 1, control in column 2 and test wells from column 3 to 12.

The designed microtitre plates were covered with lids and incubated in an airtight gas chamber at 37 °C for 48 hours until further bioassay development after flushing with a gas mixture of 3% O_2, 4% CO_2 and 93% N_2.

3.2.2 Lactate dehydrogenase assay

Intrinsic antiplasmodial activities and the abilities of the synthesized compounds to reverse CQ resistance were evaluated in CQ-sensitive (D10) and CQ-resistant strains (K1 and RSA11) using the parasite lactate dehydrogenase (pLDH) assay described by Makler *et al*, 1993. This is a non-radioisotopic method used *in vitro* to study malaria drug susceptibility by an index of parasite growth.

The assay is based on the conversion that host lactate dehydrogenase (LDH) activity uses 3-acetyl pyridine adenine dinucleotide analogue (APAD) and nicotinamide adenine dinucleotide, NAD, as a coenzyme during the conversion of lactate to pyruvate (Fig. 3.2.2) (Makler *et al,* 1993). In other words, the parasitic LDH (pLDH) uses APAD as a coenzyme and reduces it to APADH during the conversion of pyruvate to lactate.

The formation of APADH can be colorimetrically measured using the yellow light–sensitive nitroblue tetrazolium (NBT)/ phenazine ethosulphate (PES) regent which is subsequently reduced into a blue formazan product. In addition, the amount of the blue formazan product formed is proportional to the pLDH activity.

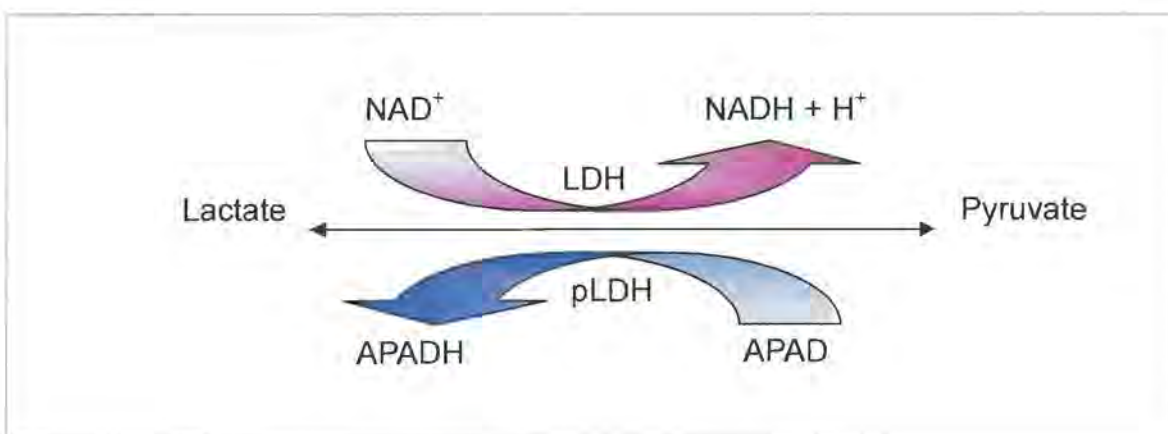

Figure 3.2.2. Conversion of lactate to pyruvate.

The pLDH activity can therefore be monitored using the Malstat reagent containing triton (1ml/L), APAD (0.33g/L) and TRIS buffer (3.3g/L) and 1.96 mM NBT with 0.24 mM PES (Sigma) solution in millipore water. At the completion of the 48 hour incubation period of the test plates, 100 μl of Malstat reagent and 25 μl of NBT/PES solution were added into each well of new microtitre plates. The test plates were removed from the incubation gas chamber and the parasites were re-suspended within the original test plates before transferring 15 μl of the parasites with a multi-channel dispenser into the corresponding well of the plates containing prepared Malstat reagents and NBT/PES solution. The absorbance of the formed formazan salts was then measured at a wavelength (λ) of 620 nm on a 7520 Microplate reader from Cambridge Technology Inc. Since the pLDH is proportional to the blue formazan products formed, the percentage parasite viability is determined on the basis of the formula below:

$$\% \text{ Parasite viability} = \left[\frac{A_{\lambda 620} \text{ test well (pRBC + drug)} - A_{\lambda 620} \text{ Blank well (PBC)}}{A_{\lambda 620} \text{ Control well (pRBC)} - A_{\lambda 620} \text{ Blank well (PBC)}} \right] \times 100$$

The resulting absorbance data were transformed into percentage viability and analyzed with calculated values of means and standard errors of the mean by Sigmaplot. Using a non–linear regression analysis in GraphPad Prism, fractional inhibitory concentrations (IC_{50}= 50% inhibitory concentration) of the synthesized compounds were determined graphically from semi-logarithmic plots.

3.2.3 *In vitro* drug interactions

3.2.3.1 Resistance reversal effect

The susceptibility of the *Plasmodium falciparum* to CQ, verapamil and synthesized compounds alone and in combination with sub-inhibitory concentrations were compared. Serial dilutions of CQ were prepared as above (Chapter 3.2.1.2) in a designed microtitre plate. This is followed by the addition of 10 μl of each individual sample at a selected sub-lethal dose, which was pre-determined from intrinsic antiplasmodial activity from dose response curves, into the test wells of column 3 to 12 across the plate. Similarly, the microtitre plates were prepared, incubated and developed as described above.

3.2.3.2 Fixed – ratio method

A fixed–ratio technique was adapted from Chawira and Warhurst, 1987 to investigate the drug interactions of CQ and the hit compound, **P7**, which showed the best positive results from the primary *in vitro* screens (Chapter 5), against both CQ^S and CQ^R isolates of *P. falciparum in vitro*. This graphical representation is called isobologram analysis which gives an indication of whether the interaction is additive, synergistic or antagonistic. This is to assist the clinical potential for the combination.

Prior to commencing this drug–interaction study, the acquired fractional inhibitory concentration values (IC_{50}, IC_{25}, IC_{10} and IC_1) of CQ and **P7** in D10 and RSA11 were predetermined from the aforementioned dose response curve experiments. Several inhibitory concentrations were chosen because variation between interaction studies is expected to produce different results (Gupta *et al.*, 2002).

RBC of 2% haematocrit and pRBC of 2% haematocrit and 2% parasitaemia were prepared as described previously. Dose response bioassays of CQ and compound **P7** were included as controls for this study in rows A-B and C-D, respectively, of a 96-well microtitre plate while column 1 served as a blank. For the IC_{50} drug-interaction, 100µl of 2 x IC_{50} concentration of CQ and **P7** prepared were added into wells E to H of column 2 and 12, respectively to achieve a final concentration of 50% inhibitory concentration in the corresponding wells (Fig. 3.2.3.2). Similarly, in the each well of E to H of column 3 to 11 across the plate received a total 100µl of 2 x IC_{50} concentration aliquots of CQ and **P7** in the ratio of 90:10, 80:20, 70:30, 60:40, 50:50, 40:60, 30:70, 20:80 and 10:90. In column 1, 100µl of RBC was added to complete the blanks whereas 100µl of pRBC was added into the rest of the wells on the plates to top up to a final volume of 200µl in each well. The designed test plate was covered with a lid and incubated in a gas chamber with a gas environment of 3% O_2, 4% CO_2 and 93% N_2 at 37°C. Likewise, this protocol was repeated with other drug-interaction studies of different fractional inhibitory concentrations against D10 and RSA11 strains of *P. falciparum*.

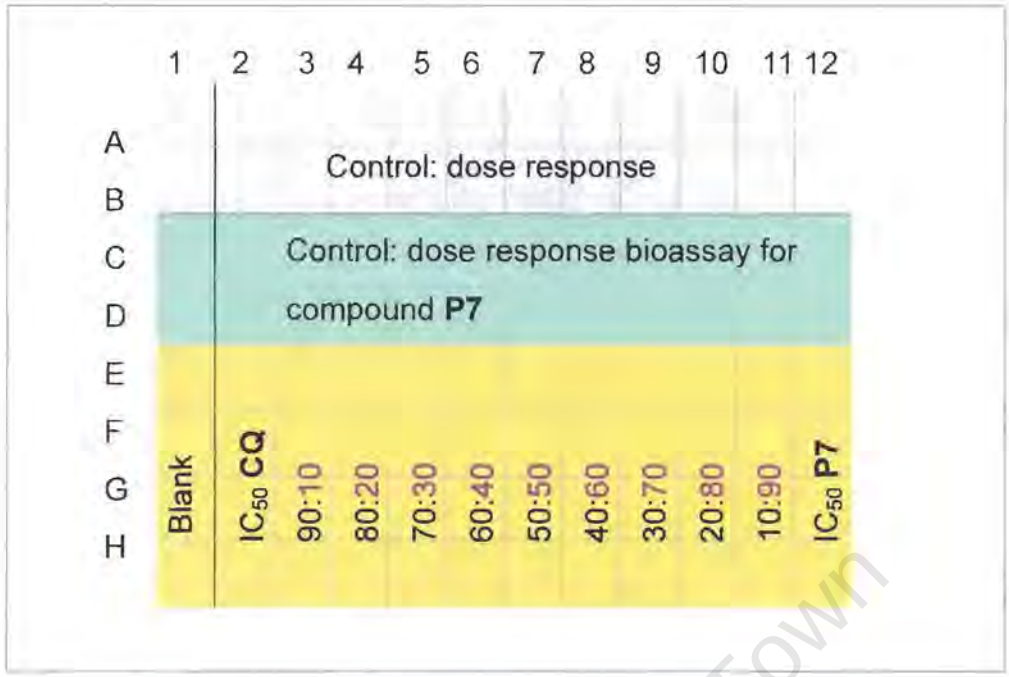

Figure 3.2.3.2. Graphical presentation of plate design for drug-interaction studies.

After 48 hr, the plate was developed using the pLDH assay and the resulting data were calculated and transformed into isobolograms by Sigmaplot and GraphPad Prism.

3.2.4 Radio–labeled CQ accumulation assay

Synchronous parasitized red blood cells were harvested in the trophozoite growth development (1% haematocrit, 5% parasitaemia) in microcentrifuge tubes. Together with solvent controls, the tubes were pre-incubated in a water bath at 37 °C for 15 min in the presence of a fixed concentration of the potential resistance reversers before being exposed to 20μl of pre-aliquoted 100nM ^{3}H-CQ (18.8 Ci/mmol; Amersham) to achieve a final concentration of 1nM ^{3}H-CQ in each tube. After 1h incubation, 100 μl of dibutyl phthalate DBP (Sigma) was added into each tube and centrifuged. The supernatant was then aspirated off leaving the parasitized/uninfected erythrocytes behind. The tip of each eppendorff was cut into labeled scintillation vials to which 2 ml of scintillation liquid was added in advance. It was followed by the addition of 25 μl EDTA into each vial to form a stable chelator complex before being lysed down with 100 μl of Solvable. Lastly, 100 μl of H_2O_2 (30%) was used to quench the colour effect of the red blood cells. The radioactivity within each vial was counted for 10 min in a Packard Tri-Carb 4060 liquid

scintillation spectrophotometer. The resulting experimental data obtained were calculated and transformed into comparable bar charts using GraphPad Prism software and Microsoft Excel.

3.3 Mammalian Cell Culture

The cytotoxicity tests of the novel compounds were evaluated against the mammalian Chinese Hamster Ovarian (CHO) cell line, which was maintained continuously. The CHO cells obtained were donated by S. Schwager, Department of Medical Biochemistry, University of Cape Town.

The cells were cultured as adherent monolayers in Dulbecos Modified Eagles Medium (DMEM) supplemented with 10% heat-inactivated fetal calf serum (FCS) and gentamycin (0.04 μg/ml). The cells were maintained in 5% CO_2 – 95% air humidified atmosphere at 37 °C. The medium was changed at frequent intervals to stabilize the pH as well as remove waste products and cell debris.

Medium renewal was done by washing twice with sterile, warm PBS (Phosphate Buffered Saline) buffer followed by 5 ml trypsin-EDTA (1%), which "lifted" the cells from adherent flasks for less than 2 min at 37 °C. Trypsin was inactivated by adding an equal amount of growth medium. The cell suspension was centrifuged at 750 rpm for 5 min with the supernatant discarded. The cell button was resuspended with a volume of medium relative to the size of the cell pellet, and aliquots of the cell suspension were transferred into new culture flasks (75 ml) with fresh medium. Culture flasks were then incubated in an incubator of 5% - 95% air humidified environment at 37 °C. The trypan blue colourimetric method was used to investigate the viability since viable cells have intact cell membranes, which prevent the blue dye entering the cells. Therefore, viable cells appeared bright in the field of view. Thus the percentage of viable cells can be determined. In addition, those cells that underwent less than 10 subcultures were used providing fresh cultures were thawed from stocks in liquid N_2.

3.3.1 Cell plating

Cells in the exponential phase of the growth development are required to perform cytotoxicity screening. Cell plating was performed when cells reached confluency. CHO cells were plated in 96-well flat-bottomed microtitre plates (Costar) at a cell density of $1x10^4$ cells per well, in which cells were ensured to be in the exponential growth.

A positive control of daunomycin (Sigma) was used in this cytotoxicity study. Dilution of daunomycin and synthesized compounds were made on the day experiments were commenced with cell culture medium. The stock solution of daunomycin was made up for 2mg/ml while the stock solutions were made as prepared in dose response assays. Similarly, the highest DMSO concentration reached in the well was 1.7%, which was insufficient to cause an effect in the system. This was followed by six stock dilutions raging from 100μg/ml to 1ng/ml.

Cells were harvested as previously described and cell density was estimated using the Trypan blue method on a haemocytometer. Cell dilutions were made accordingly before being plated in the microtitre plates, which were incubated at 5% – 95% CO_2 – air humidified atmosphere at 37 °C for 24h. After the incubation, the medium was carefully aspirated off from each well and appropriate drug concentrations accordingly added into the wells. Cell cultures were plated and allowed to incubate for a further 48h for cell attachment and flattening (Mosmann, 1983). A colorimetric (MTT) assay was then performed to determine the percentage of viable cells.

3.3.2 MTT assay

Selected synthesized compounds were assessed for cytotoxicity, in terms of mitochondrial impairment, using the Tetrazolium Salt assay (Mosmann, 1983). This method is based on the breakdown of the ring structure of the tetrazolium salt, 3-(4,5-dimethylthiazol-2-yl)-2,5-diphenyltetrazoliumbromide (MTT), by the mitochondrial dehydrogenase of the viable cells (Mosmann, 1983; Sieuwerts *et al.,* 1995). The amount of formazan crystals formed is directly proportional to the metabolic activity and the number of viable cells in the sample.

Light-sensitive water-soluble yellow MTT was reduced to a water insoluble dark purple coloured formazan product in viable cells. The amount of formazan formed was determined spectrophotometrically after dissolving the dark purple crystals in dimethyl sulphoxide (DMSO) (Stieuwerts *et al.*, 1995).

After incubating the plates for 48h, 25µl of a MTT stock solution of 5.0 mg/ml was added into each well of the plates, which were allowed to incubate for a further 4h. The plates were then centrifuged at 2050 rpm for 10 min and followed by medium removal from each well before DMSO was used to dissolve the formazan salts formed by viable cells. The plates were shaken cautiously on a microplate shaker for 5 min. Absorbance was monitored at a wavelength of 540 nm with a 7520 Microplate reader from Cambridge Technology Inc. The percentage of viable mammalian cells was thus calculated on the basis of the formula below:

$$\% \text{ Cell viability} = \left[\frac{A_{\lambda 540} \text{ test well (cells+ drug)} - A_{\lambda 540} \text{ Blank well (medium)}}{A_{\lambda 540} \text{ Control well (cells only)} - A_{\lambda 540} \text{ Blank well (medium)}} \right] \times 100$$

The experimental data was analyzed and transformed into percentage cell viability with calculated mean values and standard errors of the mean by Sigmaplot software. A non-linear regression analysis was established using GraphPad Prism software.

3.4 Cell proliferation/ Substrate specificity

Three isogenic strains of *Saccharomyces cerevisiae* were purchased from Euroscarf. The *S. cerevisiae* was cultured in YPD (1% Yeast Extract (Bacto) + 1% Bactopeptone (Bacto) +1% Dextrose (Sigma)) medium at 28 °C at 200 rpm (Table 3.4). Medium change was performed at frequent intervals by adequate dilutions of cells into fresh (less than two-week old) YPD (pH6.4).

Table 3.4. *S. cerevisiae* yeast strains used in this study.

Strain	Strain Code	Information of Cloned Strains
-	US50-18C	Wild Type[a]
-	AD1	Δ*YOR1*
-	AD1-3	Δ*YOR1*, Δ*SNQ2*, Δ*PDR5*
-	AD1,2,4-7	Δ*YOR1*, Δ*SNQ2*, Δ*PDR10*, Δ*PDR11*, Δ*YCF1*, Δ*PDR3*
-	Super Yor	Δ*YOR1*, Δ*SNQ2*, Δ*PDR5*, Δ*PDR10*, Δ*PDR11*, Δ*YCF1*, Δ*PDR3*
BY4742w	BY4742	Wild Type[b]
YGR281w	YOR1	Δ*YOR1*
YDR135c	YCF1	Δ*YCF1*

[a]Respective wild type strain for AD1, AD1-3, AD1,2,4-7 and Super Yor.
[b]Respective wild type strain for YOR1and YCF1.

Cell concentrations were determined spectrophotometrically at λ_{600} (absorbance between 3–5 units) and harvested the day before starting the experiment to ensure cells are at their exponential growth. Test compounds and drug concentrations were prepared as in dose response curve experiments.

3.4.1 Solid medium assay

Sterile YPD agar plates (1% Yeast Extract (Bacto) + 1% Bactopeptone (Bacto) + 1% Dextrose (Sigma) + 4% glycerol (Sigma, cell culture grade)) were freshly prepared (less than one-week old) and stored at -4°C. Yeast cells were harvested from continuous cultures and centrifuged at 5000 rpm for 5 min followed by pellet resuspension with 5 ml Y.Gly medium (1%Yeast Extract + 4% Glycerol) pre-warmed at 28°C. The harvested cells were then incubated at 28°C 200 rpm for 2h.

Optical densities at λ_{600} were monitored and 1OD/ml yeast cell concentration were prepared before serially diluted to 1/10, 1/100, 1/1000, 1/10, 000 and 1/100, 000. These yeast cells at various concentrations in YPD medium were suspended well before being applied onto the YPD agar plates. The agar plates were then incubated at 28°C for 3 days to allow cell growth. Upon maturation, cell colonies were determined visually and manually to determine the amount of acquired cells in one 96-well microtitre plate.

3.4.2 Drug susceptibility testing

Cadmium chloride ($CdCl_2 \cdot 2H_2O$) was used as a positive control for the assay. In addition to the cadmium chloride, various desired drug concentrations were prepared on the day before commencing the experiment. *S. cerevisiae* was harvested during the exponential growth development and incubated in YGly medium containing various compounds of interest at 28°C and 200 rpm. Microtitre plates were designed, adjusted and prepared in a similar manner to dose response curve experiments. The cell proliferation process (cell suspension) was monitored at regular intervals at λ_{620} on a 7520 Microplate reader from Cambridge Technology Inc. Data analysis of the experimental data was carried out using SigmaPlot and GraphPad Prism softwares to obtain the estimated inhibitory concentration of cells against compounds tested.

Chapter 4

Synthesis and characterization of target compounds

4. Synthesis and characterization of target compounds

4.1 Introduction

In attempts to exploit structural molecular diversity, the general methods of classical solution phase synthesis and polymer-assisted synthesis in solution were used to generate various classes of compounds. The traceable synthetic routes, isolations as well as the characterizations of the potential CQ resistance modulators are described in this chapter.

4.2 Polymer-assisted synthesis in solution

Pioneering work by Merrifield on the use of polymeric supports in organic synthesis has led to considerable interest in this technology. The need to rapidly generate libraries of compounds has driven a conceptual revolution into solid-phase synthesis (Fig. 4.2; method A). Solid phase organic synthesis (SPOS) involves attachment of a reactant (A) onto a polymeric (solid) support via a bifunctional protecting group (linker). The polymer-bound reactant A is then treated with a large excess of a second reactant (B) to produce polymer-bound product (A-B), which upon cleavage from the solid support delivers A-B in solution. Purification and isolation is often by simple washing and filtration, which is facilitated by the general lack of solubility of most polymers in common organic solvents. The optimization of solid-phase synthesis, coupled with the evolution of medicinal chemistry has resulted in the development of a new methodology of polymer-assisted solution-phase organic synthesis for expediting the drug discovery process (Fig. 4.2; methods B – D). In the process where functional polymers are used as reagents and catalysts (Fig. 4.2; method B), the substrates do not remain attached to the solid support during multi-step sequences in solution. Instead, the polymer-bound reagents and/or catalysts promote a chemical transformation of a substrate which is cleaved from the support in the final step. Other new functionalized polymers are polymer scavengers which are the resins added after a chemical reaction to remove the excess of reactants and/or by-products (method C). In addition, the molecule to be removed can also be "tagged" (i.e. derivatized and functionalized) to facilitate its removal by polymer-supported scavengers. Moreover, a subset of functionalized polymers is able to "capture" a small molecule as an activated polymer intermediate, upon washing to

remove the soluble by-products, the intermediate then "releases" the products back into the solution (method D). In multi-step syntheses, polymer-supported reagents and catalysts, along with the use of scavenging reagents and resin "capture-release" methods, can be combined to generate even more complex molecules (Kirschning *et al.*, 2001).

Polymer-assisted solution-phase synthesis provides several advantages over the conventional solution-phase chemistry, such as the improved methods of reaction workups and purifications by simple filtration and washing, the ability to use an excess of reagents to drive the reaction to completion without causing workup complications, the adaptation of continuous-flow processes (i.e. automated synthesis) and reuse of a catalyst or a supported reagent after regeneration (Kirschning *et al.*, 2001).

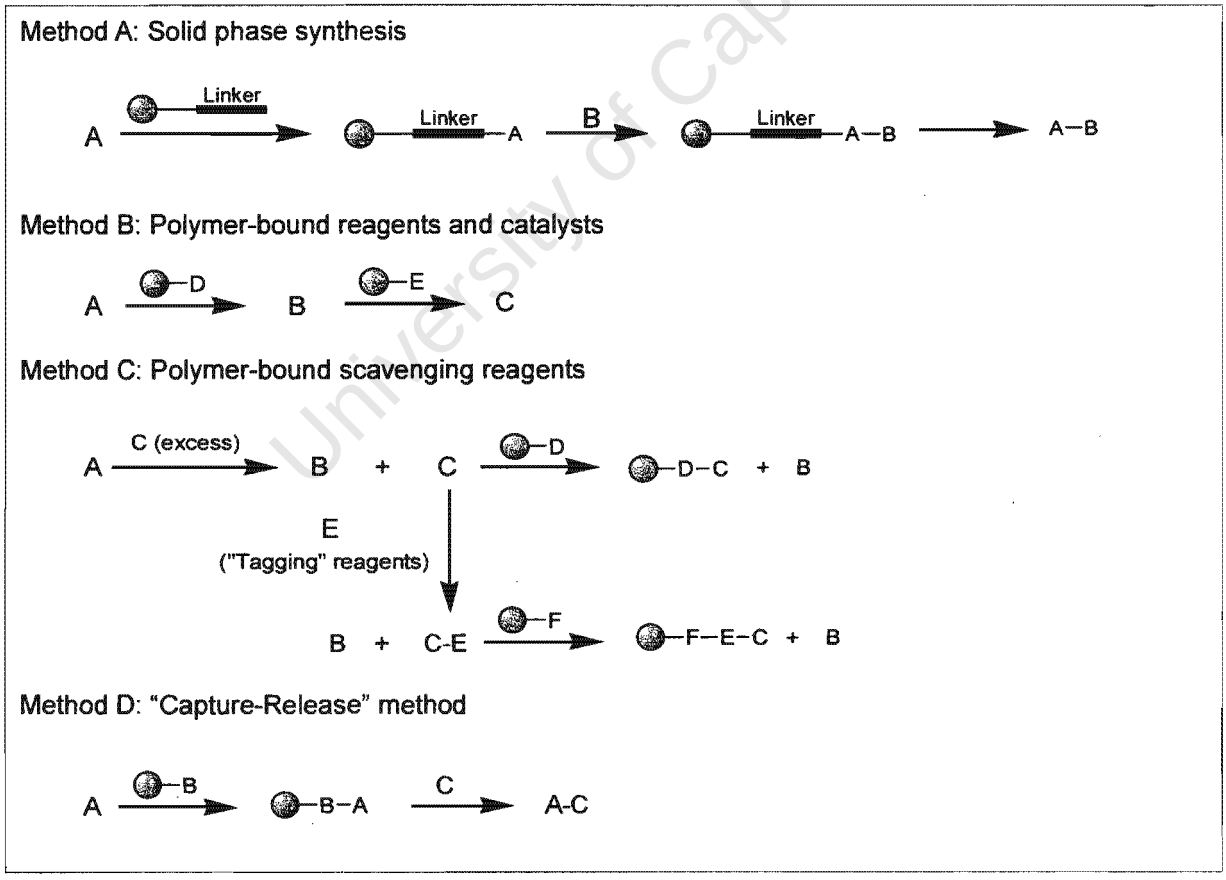

Figure 4.2. Various uses of polymer supports in organic synthesis. (Adapted from Kirschning *et al.*, 2001. *Angew. Chem, Int. Ed.*)

4.3 Polymer-assisted synthesis in solution of initial exploratory compounds P4-P7

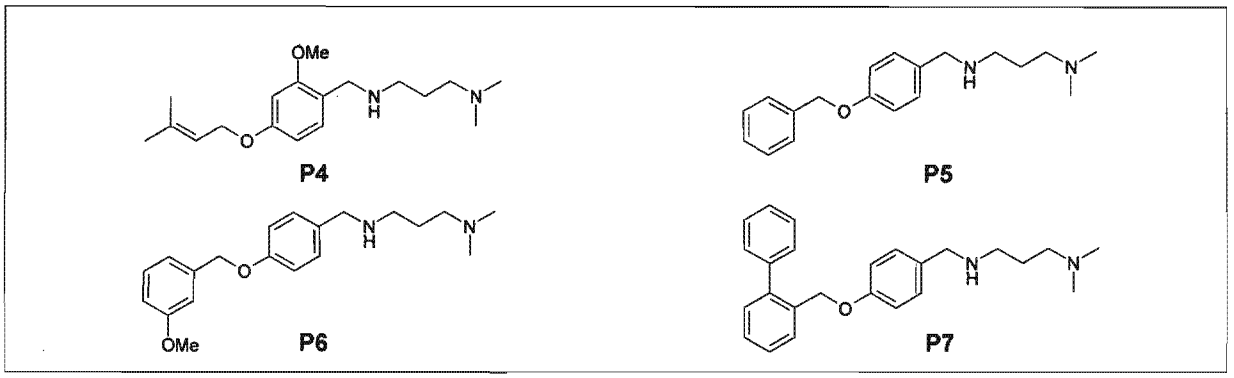

In the first step of the multi-step synthesis (Scheme 1), a polymer-assisted O-alkylation of the phenolic benzaldehyde (**I**) was carried out using a polystyrene-supported base PTBD (1, 5, 7– triazabicyclo[4,4,0]dec-5-ene) (Fig. 4.3). This polymer-bound reagent served as a base in the phenol deprotonation step as well as a scavenger to mop up the liberated HBr and the excess unreacted starting phenol. The resulting products (**II**) were isolated and purified in high yields by simple filtration and evaporation (Xu *et al.,* 1997).

The second step involved a borohydride resin-mediated reductive amination of the aromatic aldehydes. Excess amine relative to the carbonyl intermediate (**II**) was used and the subsequent imine adduct was formed readily in methanol. Reduction was then performed using polymer-bound borohydride while the polymer-supported aldehyde (Fig. 4.3) functioned to selectively separate the desired secondary product and the excess starting primary amine by imine formation (Kaldor *et al.,* 1996). Subsequent filtration and evaporation afforded the secondary amines (**P4-P7**) in excellent yields (Table 4.3). Since both polymer-supported reagents act at different sites, the on- and off- polymer reactions allow this convenient one pot experimental procedure. The mechanism of this reductive amination is depicted in scheme 2.

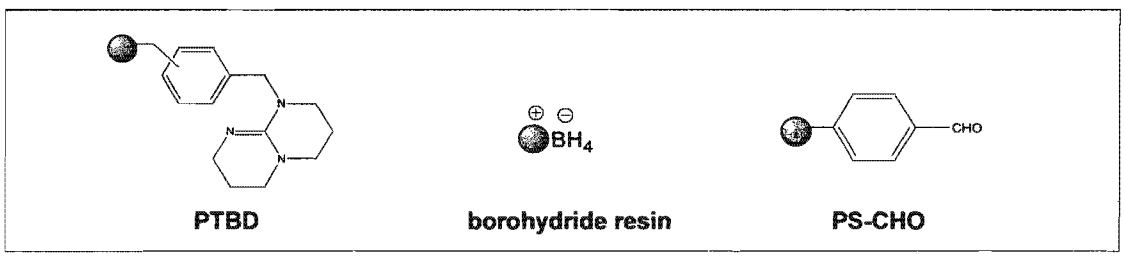

Figure 4.3. Representations of PTBD, borohydride resin and polymer-supported aldehyde (PS-CHO).

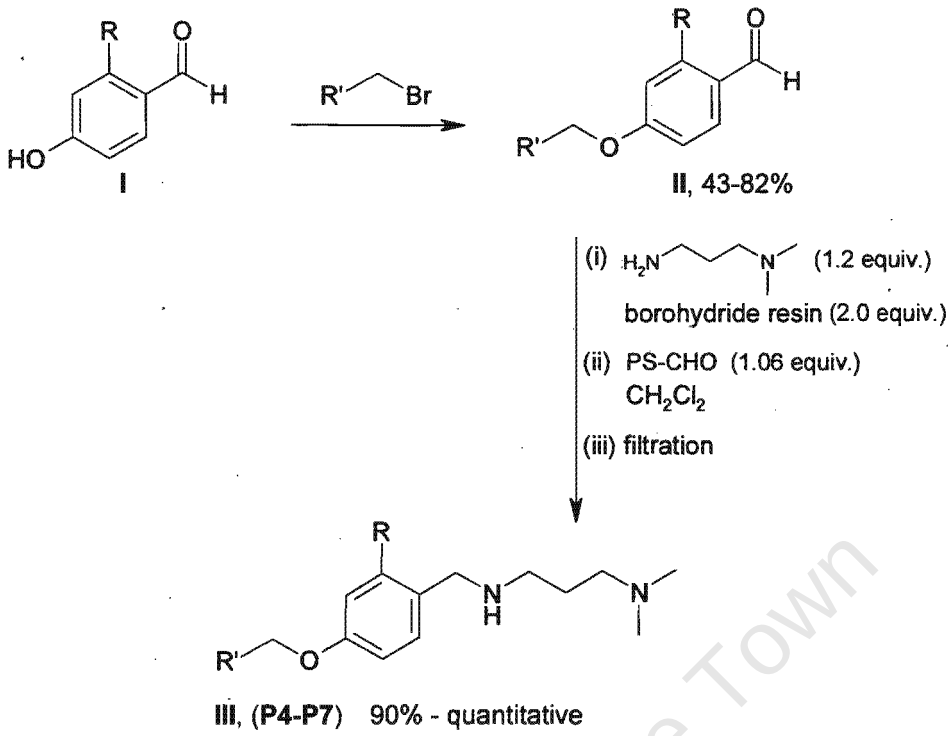

Scheme 1. Chemical synthesis of potential chemosensitizers.

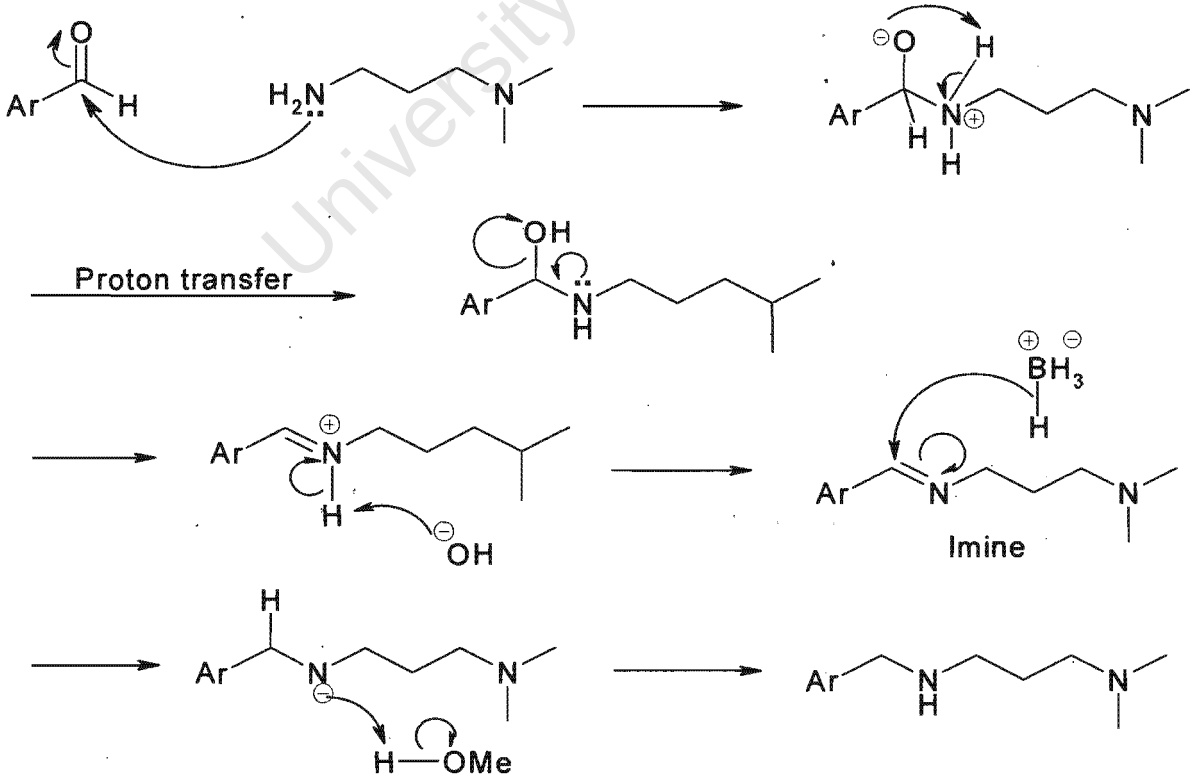

Scheme 2. Graphical presentation of the mechanism of reductive amination.

4.3.1 Synthesis of polyamines P4-P7

Synthesis of the polyamines **P4-P7** involved the generation of aldehyde intermediates by alkylation using polymer-supported reagents with appropriate bromides, followed by a reductive amination of the aldehyde intermediates with 3-dimethyaminopropylamine to give the corresponding products. The NMR spectra, IR measurements, mass spectra and melting points for compounds **P4-P7** are in section 4.5.

4.3.1.1 General procedure A: Alkylation using PTBD

4-Hydroxybenzaldehyde (86 mg, 1.2 eq.) and benzyl bromide (0.07 cm^3, 1.0 eq.) were added to a 20 cm^3 sealed glass vial containing the PTBD resins (0.10m equiv.) in 7 cm^3 acetonitrile. The reaction was vortexed vigorously at room temperature under nitrogen atmosphere until the halide was completely consumed. After 18h, the reaction was filtered free of polymeric material. The filtrate was purified by chromatography on silica gel.

Benzyl bromide → **Intermediate 1** (0.58 mmol scale), 64 mg, 43%
3-Methoxybenzyl bromide → **Intermediate 2** (0.75 mmol scale), 139 mg, 77%
2-Phenyl benzylbromide → **Intermediate 3** (0.61 mmol scale), 144 mg, 82%

4.3.1.2 General procedure B: Reductive amination using borohydride resin

3-Dimethylaminopropylamine (0.03 cm^3, 0.27 mmol) and benzaldehydes (0.23 mmol) were dissolved in 1 cm^3 MeOH in a medium screw-capped glass vial. The reaction vial was shaken on an orbital shaker for 4h to allow imine formation. The resulting reaction mixture was then treated with Amberlite® IRA-400 borohydride resin (2.5 mmol BH_4^- /g resin, 2.0 equiv.) (Aldrich). The slurry was then shaken for an additional 24h to effect the reduction to the secondary amine. Lastly, the polystyrene-linked benzaldehyde resin (2.5-3.0 mmol/ g resin, 1.06 equiv.) and 1 cm^3 CH_2Cl_2 was added to the reaction. After 18h, the reaction slurry was filtered through a cotton plug and the residual solids were rinsed with MeOH.

Compound P4 (0.23mmols scale), 76.2mg, 94%
*Intermediate **1*** (64 mg, 43%) → **Compound P5** (0.30mmols scale), 81.4mg, 90%
*Intermediate **2*** (139 mg, 77%) → **Compound P6** (0.46mmols scale), 178mg, quantitative yield
*Intermediate **3*** (144 mg, 82%) → **Compound P7** (0.38mmols scale), 139mg, 97%

Table 4.3 Synthesized intermediates **I1-I3** and compounds **P4-P7** during the initial exploratory phase.

Compd	R	R'	% yield
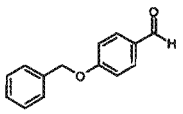 **II (I1)**	H	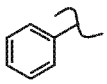	43
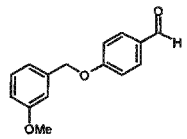 **II (I2)**	H	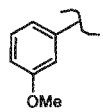	77
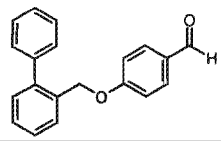 **II (I3)**	H	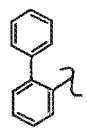	82
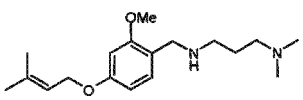 **III (P4)**	OMe		94
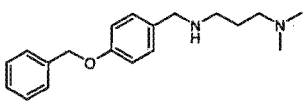 **III (P5)**	H	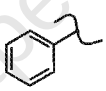	90
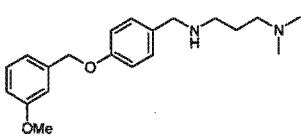 **III (P6)**	H	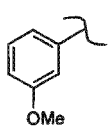	quantitative
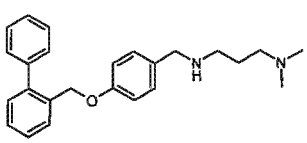 **III (P7)**	H	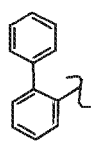	97

4.4 Synthesis of biphenyl piperazinyl analogues via the Suzuki cross coupling reaction

4.4.1 Suzuki cross coupling

In view of the tremendous importance of the biaryl subunit, several methods for generating these molecules have been developed over the past two decades. The most commonly used catalytic biaryl cross couplings are the Kharasch, Negishi, Stille and Suzuki reactions (Stanforth, 1997). These reactions utilize either nickel or palladium (Pd) catalysts to prepare symmetrical and unsymmetrical biaryls.

In the mid to late 1970's the Kharasch reaction achieved such cross-couplings when an aryl Grignard reagent reacted with an aryl halide while the Negishi reaction used arylzinc reagents and aryl halides. This was followed by the discovery of the more versatile Stille reaction which utilized arylstannanes and aryl halides as coupling partners. This reaction was more compatible and tolerant than the Kharasch and Negishi reactions. However, the major disadvantage of the Stille coupling is the toxicity of organotin reagents and their byproducts (Stanforth, 1997). In the early 1980's, the Suzuki reaction, in which boronic acids reacts with aryl halides, was developed and has since proved to be as extremely versatile as the Stille reaction.

The catalytic process of both modified Suzuki coupling protocols using Pd is presented in scheme 3. The biaryl synthesis starts with an oxidative addition of the catalyst to the aryl halide (Ar^2X, X = halogen) to afford the $Ar^2[Pd(II)]X$ intermediate before transmetallation to give a diarylated Pd moiety, $Ar^2[Pd]Ar^1$. Lastly, the biaryl product Ar^2Ar^1 and Pd(0) are formed by a reductive elimination reaction of the diarylated $Ar^2[Pd]Ar^1$ compound. The catalyst is recycled and re-enters the catalytic circle (Stanforth, 1997).

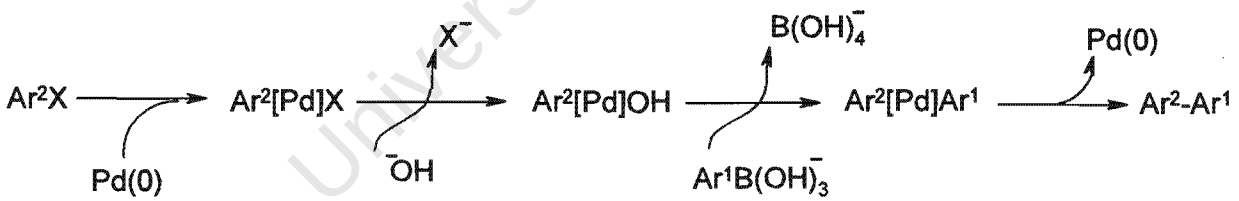

Scheme 3. Catalytic Suzuki reaction by palladium. Ar = aryl; X = halogen. (Adapted from Stanforth, 1997, *Tetrahedron*).

In this study, the synthesis of unsymmetrical biaryl motifs was carried out via the Suzuki reaction in three general reaction schemes (Scheme 4) to produce an analogous library. In the general reaction Scheme 4-A, 4-bromobenzaldehyde underwent Suzuki couplings with mono-, bi- and tri-methoxy boronic acids to produce the biphenyl intermediates **II** in high yields (80–94%). Formation of these intermediates was confirmed by ^1H NMR. The distinctive proton signals of the biaryls at δ 7-7.5 ppm and the methoxy signals at δ

3.8-3.9 ppm were cleanly identified. Reductive amination of the aldehydes afforded the biphenyl polyamine products **III** (**P11-P20**). The ^{1}H NMR revealed signals from the piperazinyl unit at δ 2-3 ppm, which differentiates the intermediates **II** (**I8-I10**) and polyamine products **III** (**P11-P20**) (details in section 4.5 experimental). Products were obtained in higher yields (63-95%) when dichloromethane was used in the reductive amination step compared to the corresponding reactions in methanol (23-35%).

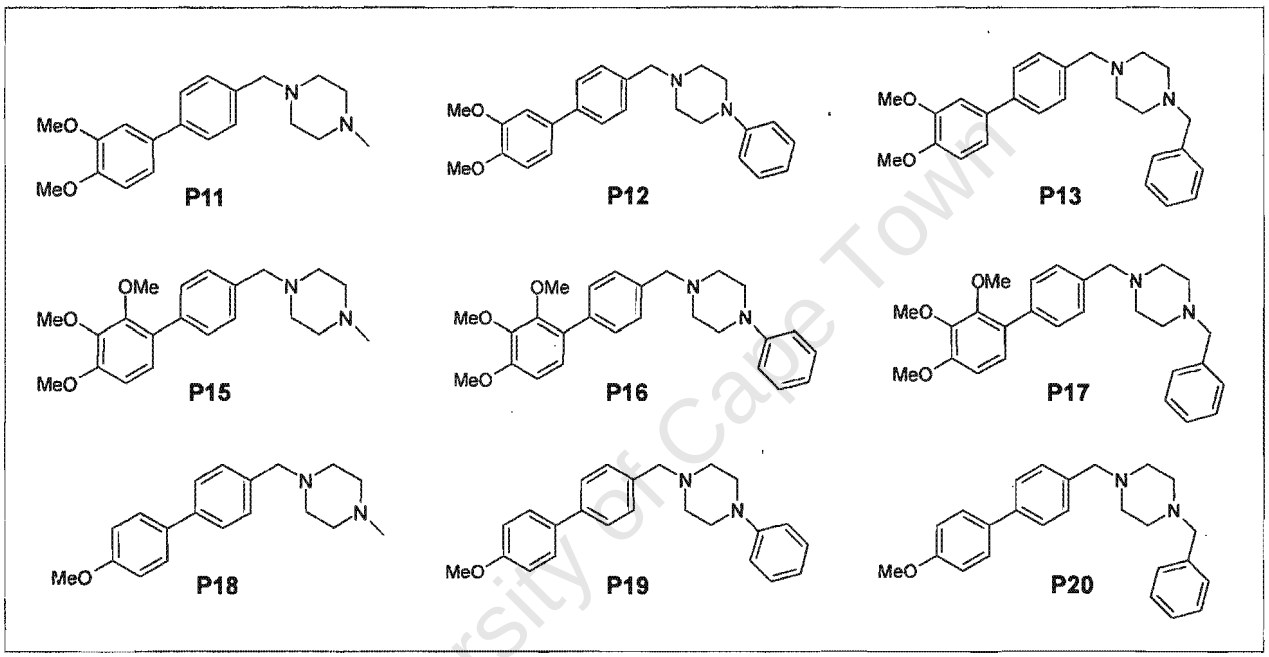

Figure 4.4.1-A. Target compounds for Scheme 4-A.

A.

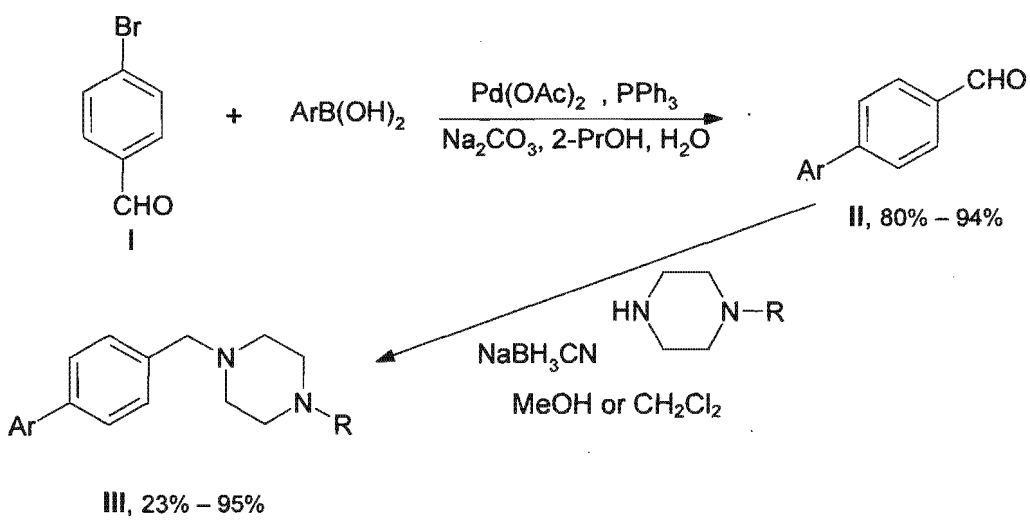

Scheme 4-A. Synthesis of biphenyl compounds.

4.4.2 Synthesis of biphenylamines P11-P20

Synthesis of biphenylamines **P11-P20** involved the generation of mono- bi-, tri-methoxy-biphenyl -4-carbaldehyde intermediates, which were derived from 4-bromobenzaldehyde with different boronic acids using Suzuki cross coupling reactions, followed by a reductive amination with appropriate piperazines to give the corresponding products. The NMR spectra, IR measurements, mass spectra and melting points for compounds **P11-P20** are in section 4.5.

4.4.2.1 General procedure C: Suzuki cross coupling reactions

A tube equipped with a magnetic stirring bar and nitrogen inlet was charged with 4-bromobenzaldehyde (300 mg, 1.62 mmol) and mono-, bi- or tri-methoxyphenylboronic acid (1.70 mmol) in 3.0 cm^3 isopropanol under a N_2 purge. The mixture was stirred at room temperature for 30 min, allowing solids to dissolve. The resulting solution was treated with palladium acetate (1.09 mg, 0.005 mmol), triphenylphosphine (3.83 mg, 0.015 mmol), 0.98 cm^3 of 2M $NaHCO_3$ and 0.6 cm^3 of water under N_2. The reaction was brought to reflux for 18h before the heat was removed. An additional 2.5 cm^3 of water was added to the reaction while hot followed by removal of N_2. The reaction was then allowed to stir open to the atmosphere for 2.5h while cooling to room temperature. The darkened mixture was then diluted with 5 cm^3 ethyl acetate and transferred to a separating funnel. The 2 phases were separated and the aqueous phase was washed with 2 x 5.0 cm^3 ethyl acetate. The combined organic layer was washed with 5.0 cm^3 of aqueous 5% $NaHCO_3$ followed by 2 x 5.0 cm^3 of saturated brine. The organic layer was placed in a flask with a magnetic stirring bar, treated with activated carbon (0.15 mg) and stirred at room temperature for 30 min before Na_2SO_4 (0.30 mg) was added to the mixture and stirring was continued for an additional 30 min. A Büchner funnel was charged with Celite to a depth of 1 cm, and the resulting reaction mixture was filtered through this pad of filter aid, which was rinsed with 2 x 5 cm^3 of ethyl acetate. The resulting purple filtrate was concentrated under vacuum and chromatographed using silica gel.

4-Methoxyphenylboronic acid → **Intermediate 8** (1.62 mmol scale), 272.5 mg, 81%

3,4-Dimethoxyphenylboronic acid → **Intermediate 9** (1.38 mmol scale), 312.5 mg, 94%

2,3,4-Trimethoxyphenylboronic acid → **Intermediate 10** (1.62 mmol scale), 401.0 mg, 91%

4-Methoxyphenylboronic acid → **Intermediate 28** (1.38 mmol scale), 275.0 mg, 63%

3,4-Dimethoxyphenylboronic acid → **Intermediate 29** (1.38 mmol scale), 321.4 mg, 67%

2,3,4-Trimethoxyphenylboronic acid → **Intermediate 30** (1.38 mmol scale), 175.0 mg, 34%

4.4.2.2 General procedure D: Reductive amination using sodium triacetoxyborohydride

Mono-, bi- or tri-methoxy-biphenyl-4-carbaldehyde (0.41 mmol), amines (0.05 cm^3, 0.45 mmol) and 2 cm^3 MeOH were added to a 20 cm^3 sealed glass vial. The reaction was allowed to stir at room temperature for 16h. After monitoring by TLC, imine formation was confirmed and sodium triacetoxyborohydride (114 mg, 0.54 mmol) was added to the reaction mixture. The resulting reaction was left on the shaker for an additional 24h before it was quenched by adding 3.5 cm^3 saturated $NaHCO_3$ followed by extraction with EtOAc. The resulting reaction extracts were combined and chromatographed.

Intermediate ***8*** (272.5 mg, 81%)

Compound P18 (0.38mmols scale), 100.1mg, 89%

Compound P19 (0.29mmols scale), 91.4mg, 88%

Compound P20 (0.47mmols scale), 114.7mg, 66%

Intermediate ***9*** (312.3 mg, 94%)

Compound P11 (0.41mmols scale), 36.5mg, 27%

Compound P12 (0.41mmols scale), 46.0mg, 29%

Compound P13 (0.33 mmols scale), 125.3 mg, 95%

Compound P14 (0.41mmols scale), 72.5mg, 35%

*Intermediate **10*** (401 mg, 91%)

Compound P15 (0.37mmols scale), 109.6mg, 83%

Compound P16 (0.37mmols scale), 113.0mg, 73%

Compound P17 (0.23mmols scale), 61.3mg, 63%

*Intermediate **28*** (275 mg, 63%) → **Compound 31** (0.16mmols scale), 25.1mg, 39%

*Intermediate **29*** (321 mg, 67%) → **Compound 32** (0.26mmols scale), 40.8mg, 36%

*Intermediate **30*** (175 mg, 34%) → **Compound 33** (0.24mmols scale), 60.1mg, 58%

Table 4.4.1-A. Synthesized compounds and intermediates from reaction scheme 4-A.

Compd	Ar	R	Solvent	% yield
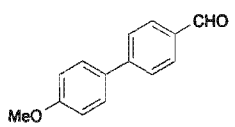 **II (I8)**	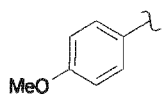	-	-	80
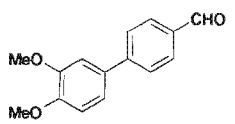 **II (I9)**	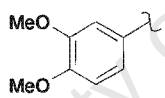	-	-	94
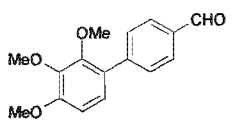 **II (I10)**	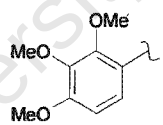	-	-	91
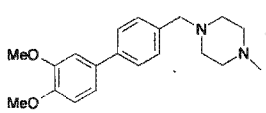 **III (P11)**	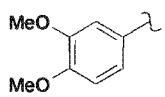	Me	MeOH	23
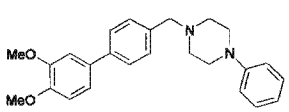 **III (P12)**	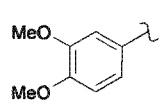	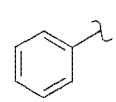	MeOH	27
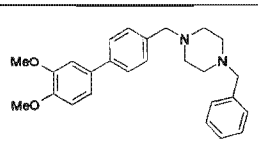 **III (P13)**	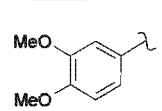	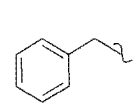	CH_2Cl_2	95
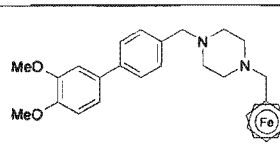 **III (P14)**	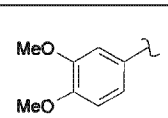	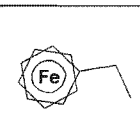	MeOH	35

Table 4.4.1-A. (Continued) Synthesized compounds and intermediates from reaction scheme 4-A.

Compd	Ar	R	Solvent	% yield
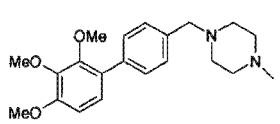 **III (P15)**	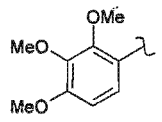	Me	CH_2Cl_2	83
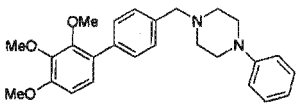 **III (P16)**	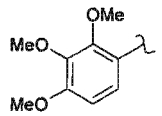	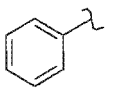	CH_2Cl_2	79
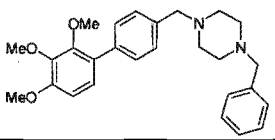 **III (P17)**	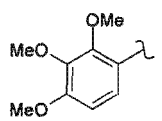	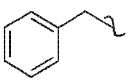	CH_2Cl_2	63
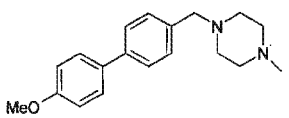 **III (P18)**	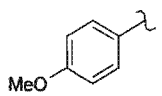	Me	CH_2Cl_2	89
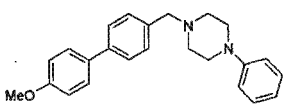 **III (P19)**	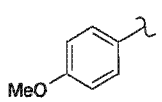	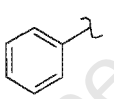	CH_2Cl_2	86
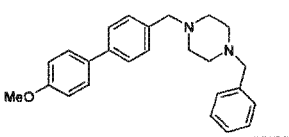 **III (P20)**	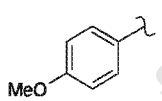	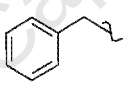	CH_2Cl_2	66

Amino alcohols (**P23-P25**) (Fig. 4.4.1-B) were synthesized in three steps, Scheme 4-B. Firstly, the starting material 4-bromophenol **IV** was alkylated with an epoxide in the presence of sodium hydride, as a base, followed by Suzuki coupling and piperazine amine alkylation reactions (epoxide ring opening) to afford the polyamine products **P23-P25**. The first alkylation reaction was completed with ease using epichlorohydrin to give a 96% yield of **V**. However, the Suzuki coupling of the epoxide was not very successful, yielding only 22% of the biarylepoxide **VI**. This could be due to some of the epoxide intermediate may have hydrolysed in the presence of the water used in the aqueous Suzuki protocol. The process of epoxide hydrolysis or ring opening would compete with the Suzuki cross coupling reaction. Purified **VI** then underwent a second alkylation reaction with piperazines to give the final products **VII** (31-47%). In contrast, a 70% yield of **P26** was produced from the alkylation of *N*-methylpiperazine with commercially available phenylbenzyl bromide.

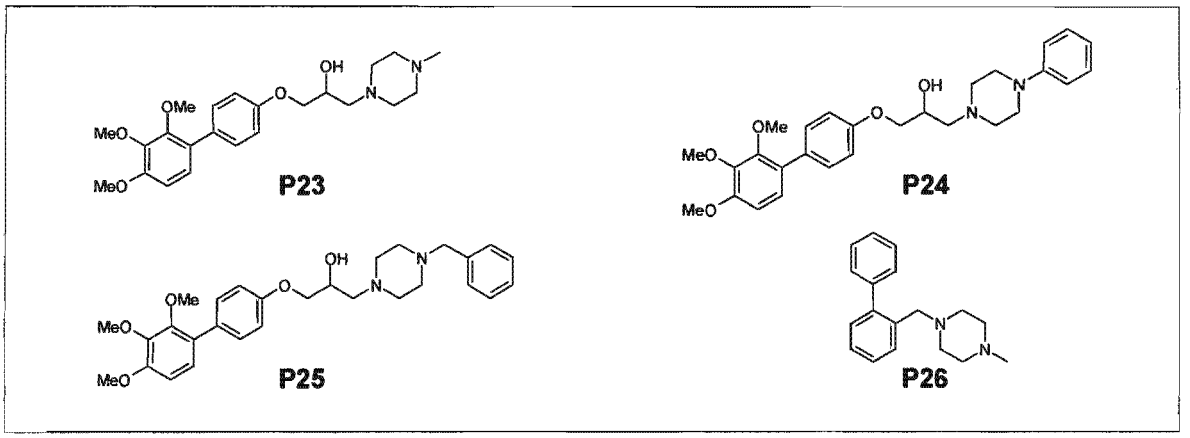

Figure 4.4.1-B. Target compounds for scheme 4-B.

B.

(i)

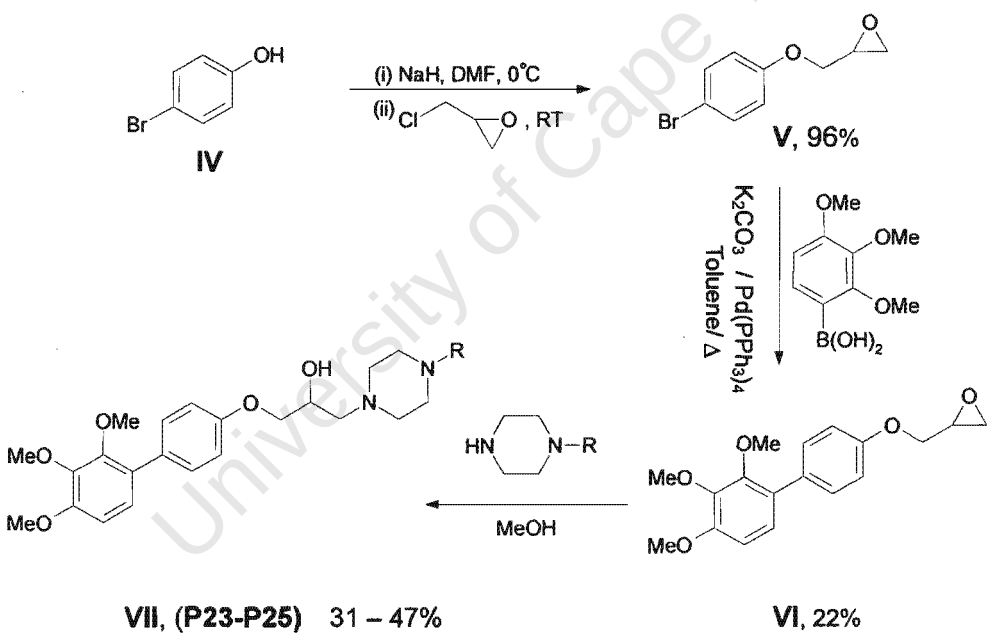

(ii)

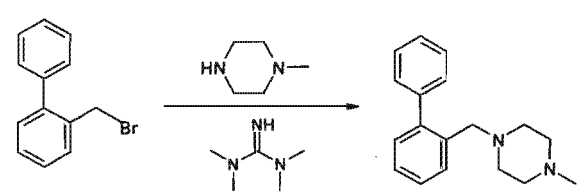

P26, 70%

Scheme 4-B. Synthesis of biphenyl compounds.

4.4.3 Synthesis of biphenylamines P23-P26

Synthesis of the biphenylamines **P23-P25** involved the generation of epoxide intermediates **I21** and **I22**. The epoxide intermediate **I21** was produced from a nucleophilic substitution reaction of the 4-bromophenol with epichlorohydrin. This was followed by Suzuki coupling on **I21** to give the biphenyl epoxide intermediate **I22**. Lastly, the desired polyamines were produced by epoxide ring opening.

4.4.3.1 Alkylation of bromophenol

4-Bromophenol (2.0 g, 11.52 mmol) was dissolved in 56 cm^3 of DMF in a 250 cm^3 round-bottomed flask at 0°C. Upon dissolution, sodium hydride (0.42 g, 17.34 mmol) was added to the flask with stirring at 0°C for 10 min. Epichlorohydrin (1.36 cm^3, 17.34 mmol) was then added to the reaction mixture over 3 min at 0°C. The resulting suspension was allowed to warm to 25 °C and left stirring for 18h. The reaction was monitored by TLC R_f (EtOAc-hexane, 20:80) 0.20; 110 cm^3 distilled water was used to quench the reaction, followed by extraction with EtOAc (2 x 110 cm^3). The yellowish oil-like organic phase was dried over Na_2SO_4 and concentrated under reduced pressure. This first step of alkylation was thus completed and gave 96% of the epoxide intermediate **21**.

4.4.3.2 Suzuki cross coupling

Intermediate **I21** (1.32 g, 5.76 mmol) then underwent the Suzuki reaction with 2,3,4-trimethoxyphenylboronic acid (2.44 g, 11.53 mmol) in dry toluene. To this suspension, the base of K_2CO_3 (2.36 g, 17.29mmol) was added under inert environment and stirred at 25 °C for 20 min. Tetrakis(triphenylphosphine)palladium(0) (0.20 g, 0.17 mmol) was then introduced as the catalyst while the reaction temperature was brought up to 88-92 °C, and the reaction mixture was refluxed for 3h before diluting with EtOAc (80 cm^3). The crude product was then washed sequentially with saturated $NaHCO_3$ (1 x 115 cm^3), distilled water (1 x 115 cm^3), 10% citric acid (1 x 115 cm^3), distilled water (1 x 115 cm^3) and lastly saturated brine (1 x 115 cm^3). The resulting organic phase was then collected, dried over $MgSO_4$, concentrated under reduced pressure and purified by column chromatography (SiO_2, EtOAc-hexane, 20:80) to yield the **I22** (401 mg, 22%).

4.4.3.3 General procedure E: Ring opening of epoxide intermediate I22

The epoxide intermediate **22** (150 mg, 0.59 mmol) (Scheme 4-B) was dissolved in 5 cm^3 MeOH together with amines (0.70 mmol) in a 20 cm^3 sealed glass vial. The resulting reaction mixture was left stirring at 25 °C for 4h before filtering and washing with MeOH. The mother liquor was concentrated and chromatographed.

Compound P23 (0.59mmols scale), 76.2mg, 31%

Compound P24 (0.59mmols scale), 132.7mg, 47%

Compound P25 (0.59mmols scale), 95.9mg, 33%

Compound P26 (1.0 mmols scale), 187mg, 70%

Table 4.4.1-B. Synthesized compounds from reaction scheme 4-B.

Compd	R	Solvent	% yield
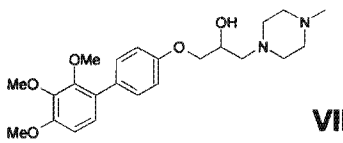 **VII (P23)**	Me	MeOH	31
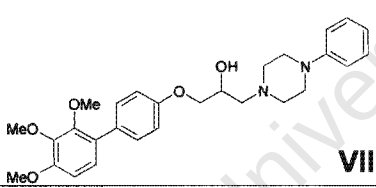 **VII (P24)**	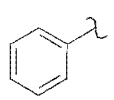	MeOH	47
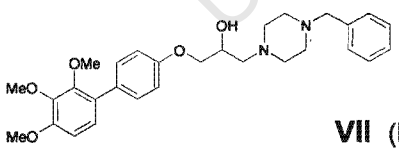 **VII (P25)**	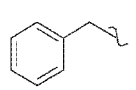	MeOH	33
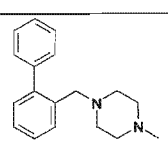 **(P26)**	Me	MeOH	70

Similarly, the starting material 4-hydroxybenzaldehyde **VIII** underwent alkylation to form the intermediate **IX** before Suzuki coupling took place to afford **X** in reaction scheme 4-C. Reductive amination of the biaryl intermediate aldehyde **X** completed the synthesis of products **XI** (36-58%).

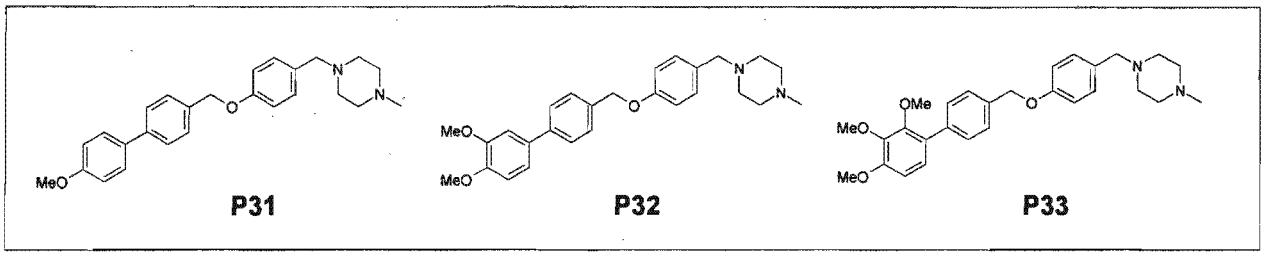

Figure 4.4.1-C. Target compounds for scheme 4-C.

C.

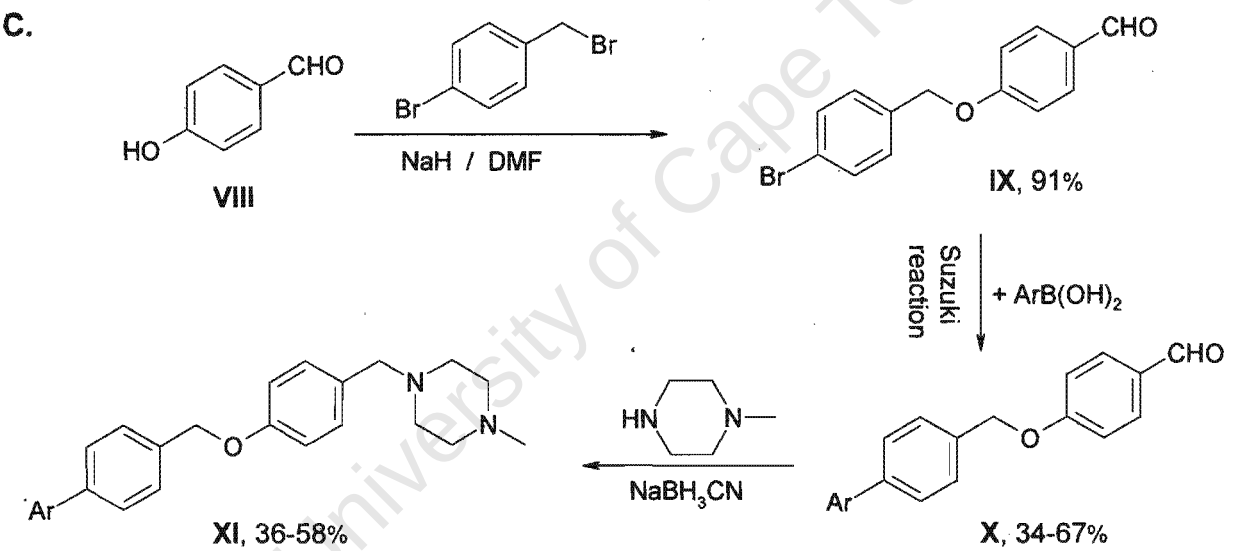

Scheme 4-C. Synthesis of biphenyl compounds.

4.4.4 Synthesis of biphenylamines P31-P33

Synthesis of the biphenylamines **P31-P33** involved 3 reaction steps. First, an alkylation reaction took place to 4-hydroxybenzaldehyde to give **I27**, followed by Suzuki couplings with different boronic acids to produce the corresponding biphenyl intermediates **I28-I30**. The desired products **P31-P33** were produced from the reductive amination of intermediate aldehydes **I28-I30**.

4.4.4.1 Alkylation of 4-bromobenzylbromide

4-Bromobenzylbromide (2.23 g, 8.94 mmol) was added to a stirred solution of powdered anhydrous sodium hydride (0.27 g, 11.1 mmol) and 4-hydroxybenzaldehyde (1.04 g, 8.52 mmol) in DMF (25 cm^3) at 0°C under an inert atmosphere. The resulting light yellow suspension was allowed to warm to 25 °C and stirred for an additional 18h. The reaction was then diluted with water (500 cm^3) and the yellow precipitate was collected by filtration and subsequent washing with water. Further drying under vacuum afforded the aldehyde **I27** (2.25 g, 91%); R_f (MeOH-CH_2Cl_2, 5:95) 0.23.

Table 4.4.1-C. Synthesized compounds and intermediates from reaction scheme 4-C.

Compd	Ar	Solvent	% yield
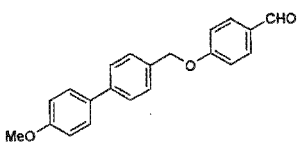 **X (I28)**	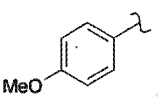	-	63
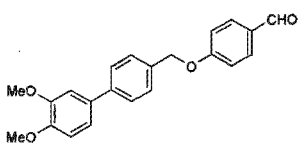 **X (I29)**	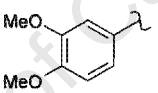	-	67
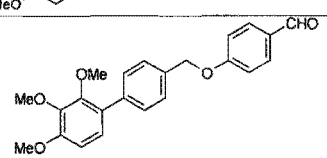 **X (I30)**	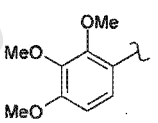	-	34
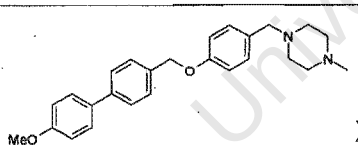 **XI (P31)**	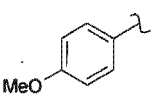	MeOH	39
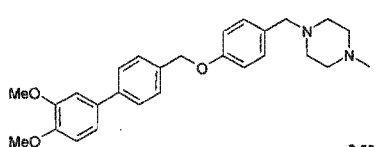 **XI (P32)**	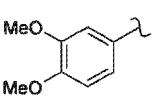	MeOH	36
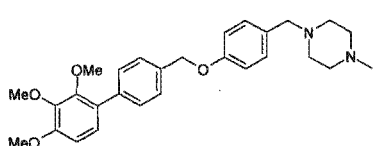 **XI (P33)**	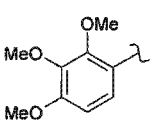	MeOH	58

All the synthesized compounds possess biphenyl derivatives possessing *ortho* and *para* substituents. The small library of synthesized compounds and the structural variations of the amines were evaluated *in vitro*. This led to a few generalizations on the structure-activity relationships for potential lead development (Chapter 5 and 6).

4.5 Characterization of synthesized compounds

The novel products (Table 4.5) were characterized by infrared spectroscopy (IR), ^{1}H, ^{13}C NMR, mass spectrometry and microanalysis. The uncorrected melting points were also recorded. The formulae, molecular weights, melting points, microanalysis and IR data and the respective % yields are reported in Table 4.5. IR gives the information about the functional groups present in the compound's structure. For example, the –OH group of alcohols absorbs strongly at 3200-3600 cm^{-1}; N-H group of amines at 3300-3500 cm^{-1}; C-N group of amines at 1180-1360cm^{-1}. The ^{1}H and ^{13}C NMR show the proton and carbon absorption peaks, whose relative positions, reflecting their differences in environments of protons and carbons, can give the detailed molecular information about molecular structure. For example, the characteristic ^{1}H signals for the biaryls are at δ 7-7.5 ppm and $-CH_3$ at δ 2-3 ppm. The characteristic ^{13}C signals of aromatic C=C are at δ 100-150 ppm. The ^{1}H, ^{13}C NMR, and mass spectra of the synthesized compounds can be found in Appendix 1.

Table 4.5. Summary of chemical formula, molecular weight, melting points, clogP and IR data of the intermediates and products.

Compound	Formulae	Molecular Weight (g/mol)	Melting point (°C)	cLogP	IR (NaCl) (cm^{-1})
I1	$C_{14}H_{12}O_2$	212.2468	-	-	-
I2	$C_{15}H_{14}O_3$	242.2726	-	-	-
I3	$C_{20}H_{16}O_2$	288.3444	-	-	-
P4	$C_{18}H_{30}N_2O_2$	306.4430	-	3.89	1136.2, 1345.8, 1662.9, 3402.3
P5	$C_{19}H_{26}N_2O$	298.4225	-	3.86	1136.2, 1345.8, 3402.3
P6	$C_{20}H_{28}N_2O_2$	328.4485	-	3.78	1136.2, 1345.8, 3402.3
P7	$C_{25}H_{30}N_2O$	347.5185	-	5.45	1136.2, 1345.8, 3402.3
I8	$C_{14}H_{12}O_2$	212.2468	-	3.37	-
I9	$C_{15}H_{14}O_3$	242.2726	-	3.07	-
I10	$C_{16}H_{16}O_4$	272.2984	-	2.13	-
P11	$C_{20}H_{28}N_2O_2$	326.4327	96 – 98	3.88	1148.3, 1347.5
P12	$C_{25}H_{28}N_2O_2$	388.5012	120 – 123	4.86	1148.3, 1347.5
P13	$C_{26}H_{30}N_2O_2$	402.5287	105 – 108	5.72	1148.3, 1347.5
P14	$C_{30}H_{36}N_2O_2Fe$	512.4641	110 – 112	-	1136.1, 1372.2
P15	$C_{21}H_{28}N_2O_3$	536.4586	-	2.96	1148.3, 1347.5
P16	$C_{26}H_{30}N_2O_3$	418.5280	65 – 68	3.94	1148.3, 1347.5

I = intermediates
P = products.
CLogP (VPL) = 4.47.

Table 4.5. (Continued) Summary of chemical formula, molecular weight, melting points, clogP and IR data of the intermediates and products.

Compound	Formula	Molecular Weight (g/mol)	Melting point (°C)	cLogP	IR (NaCl) (cm^{-1})
P17	$C_{27}H_{32}N_2O_3$	432.5546	-	4.80	1148.3, 1347.5
P18	$C_{19}H_{24}N_2O$	296.4076	106 – 108	4.14	1148.3, 1347.5
P19	$C_{24}H_{26}N_2O$	358.4760	123 – 127	5.12	1148.3, 1347.5
P20	$C_{25}H_{28}N_2O$	372.5026	117 – 120	5.98	1148.3, 1347.5
I21	$C_9H_9O_2Br$	229.0706	-	-	-
I22	$C_{18}H_{20}O_5$	316.3484	-	-	-
P23	$C_{23}H_{32}N_2O_5$	416.5106	103 – 106	1.03	756.4, 1053.4, 1217.9, 3406.1
P24	$C_{28}H_{34}N_2O_5$	478.5800	105 – 108	3.32	759.1, 1051.5, 1217.8, 3414.6
P25	$C_{29}H_{36}N_2O_5$	492.6138	76 – 79	4.24	758.9, 1051.2, 1217.8, 3409.2
P26	$C_{18}H_{22}N_2$	266.3807	56 – 58	4.04	1217.8
I27	$C_{14}H_{11}O_2Br$	291.1399	-	4.41	-
I28	$C_{21}H_{18}O_3$	318.3658	-	5.35	-
I29	$C_{22}H_{20}O_4$	348.3918	-	5.09	-
I30	$C_{23}H_{22}O_5$	378.4178	-	4.17	-
P31	$C_{26}H_{30}N_2O_2$	402.5344	127 – 130	5.83	1148.3, 1347.5
P32	$C_{27}H_{32}N_2O_3$	432.5546	112 – 114	5.56	1148.3, 1347.5
P33	$C_{28}H_{34}N_2O_4$	462.5806	68 – 70	4.65	1148.3, 1347.5

I = intermediates.
P = products.
CLogP (VPL) = 4.47.

4.5.1 Chemical synthesis during hit development

4.5.1.1 Synthesis of intermediate I1- I3 (Scheme 1)

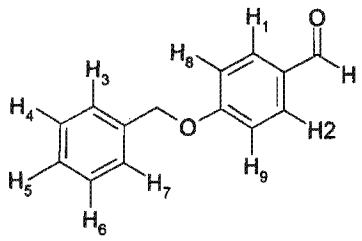

I1

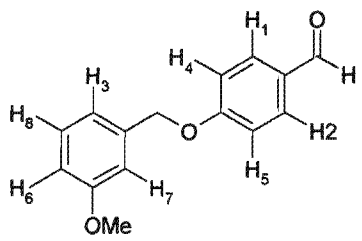

I2

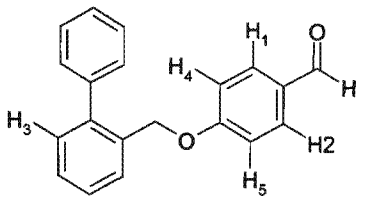

I3

***4-Benzyloxybenzaldehyde* I1**

The conditions employed for the preparation of this compound were those described in General Method A. Column chromatography (SiO_2, EtOAc-hexane, 10:90) afforded the intermediate **1** $C_{14}H_{12}O_2$ (64 mg, 43%); R_f (EtOAc-hexane, 10:90) 0.22; δ_H(200 MHz; $CDCl_3$) 9.89 (1H, s, -CHO), 7.85 (2H, d, *J* 8.7, H_1 and H_2), 7.42-7.21 (5H, m, H_3, H_4, H_5, H_6 and H_7), 6.92 (2H, d, *J* 8.7, H_8 and H_9) and 5.10 (2H, s, Ar-CH_2-O-).

4-(3-*Methoxy-benzyloxy*)-*benzaldehyde* I2

The conditions employed for the preparation of this compound were those described in General Method A. Column chromatography (SiO_2, EtOAc-hexane, 30:70) afforded the intermediate **2** $C_{15}H_{14}O_3$ (139 mg, 77%); R_f (EtOAc-hexane, 30:70) 0.35; δ_H(200 MHz; $CDCl_3$) 9.89 (1H, s, -CHO), 7.85 (2H, d, *J* 8.7, H_1 and H_2), 7.32 (1H, dd, *J* 8.7 and 2.4, H_3), 7.10-6.98 (4H, m, H_4, H_5, H_6 and H_7), 6.91 (H, t, *J* 8.7, H_8), 5.13 (2H, s, Ar-CH_2-O-) and 3.83 (3H, s, -OCH_3).

4-(*Biphenyl-2-ylmethoxy*)-*benzaldehyde* I3

The conditions employed for the preparation of this compound were those described in General Method A. Column chromatography (SiO_2, EtOAc-hexane, 30:70) afforded the intermediate **3** $C_{20}H_{16}O_2$ (144 mg, 82%); R_f (EtOAc-hexane, 30:70) 0.43; δ_H(200 MHz; $CDCl_3$) 9.87 (1H, s, -CHO), 7.78 (2H, d, *J* 8.7, H_1 and H_2), 7.65-7.61 (1H, m, H_3), 7.44-7.39 (8H, m, aromatic), 6.95 (2H, d, *J* 8.7, H_4 and H_5) and 5.03 (2H, s, Ar-CH_2-O-).

4.5.1.2 Synthesis of product P4-P7 (Scheme 1)

***N'*-[2-*Methoxy*-4-(3-*methyl*-*but*-2-*enyloxy*)-*benzyl*]-*N,N*-*dimethyl*-*propan*-1,3-*diamine* P4**

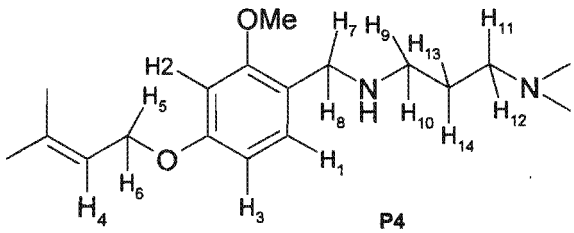

P4

The conditions employed for the preparation of this compound were those described in General Method B. Simple filtration with MeOH gave the product **P4** (76.2mg, 94%) as a yellowish oil; R_f (MeOH-CH_2Cl_2, 10:90) 0.22; δ_H(300 MHz; $CDCl_3$) 7.12 (1H, d, *J* 8.0, H_1), 6.47-6.40 (2H, m, H_2 and H_3), 5.48 (1H, t, *J* 7.5, H_4), 4.48 (2H, d, *J* 8.0, H_5 and H_6), 3.79 (3H, s, -OCH_3), 3.70 (2H, s, -Ar-CH_2-N-, H_7 and H_8), 2.63 (2H, t, *J* 7.5, H_9 and H_{10}), 2.30 (2H, t, *J* 7.5, H_{11} and H_{12}), 2.20 (3H, s, -N-CH_3), 2.15 (3H, s, –N-CH_3), 1.79 (3H, s, *CH_3*-CH-CH_3), 1.74 (3H, s, CH_3-CH-*CH_3*) and 1.64 (2H, quintet, *J* 7.5, H_{13} and H_{14}); δ_C(75 MHz; $CDCl_3$)130.6 (2C), 119.6 (2C), 104.6 (2C), 99.3 (2C), 64.8, 58.2, 55.3, 48.5, 47.5, 45.4, 30.8, 27.2, 25.8 and 18.1; EIMS *m/z* (50 eV) 306 $[M]^+$, 220 $[C_{13}H_{18}NO_2]^+$, 205 $[C_{13}H_{17}O_2]^+$, 85 $[C_5H_9O]^+$, 30 $[CH_2O]^+$. MS found: M^+, 306. $C_{18}H_{30}N_2O_2$ requires *M*, 306.4430.

***N'*-(4-*Benzyloxy*-*benzyl*)-*N,N*-*dimethyl*-*propan*-1,3-*diamine* P5**

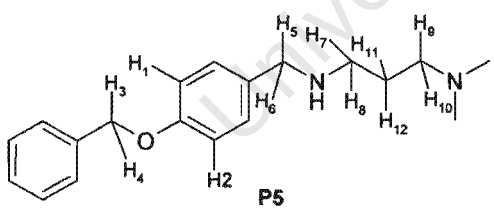

P5

The conditions employed for the preparation of this compound were those described in General Method B. Simple filtration with MeOH gave **P5** (81.4mg, 90%) as a yellowish oil; R_f (MeOH-CH_2Cl_2, 10:90) 0.22; δ_H(300 MHz; $CDCl_3$) 7.46-7.21 (7H, m, aromatic), 6.93 (2H, d, *J* 8.7, H_1 and H_2), 5.05 (2H, s, H_3 and H_4), 3.72 (2H, s, H_5 and H_6), 2.65 (2H, t, *J* 7.5, H_7 and H_8), 2.31 (2H, t, *J* 7.5, H_9 and H_{10}), 2.23 (3H, s, -N-CH_3), 2.21 (3H, s, –N-CH_3) and 1.72 (2H, quintet, *J* 7.5, H_{11} and H_{12}); δ_C(75 MHz; $CDCl_3$) 157.8, 137.1, 133.0, 129.2 (2C), 128.5, 128.0, 127.9 (2C), 127.4, 114.9, 114.8, 70.1, 58.0, 53.4, 47.8, 45.5 (2C), 28.1; EIMS *m/z* (50 eV) 298 $[M]^+$, 212 $[C_{14}H_{14}NO]^+$, 197 $[C_{14}H_{13}O]^+$, 107 $[C_7H_7O]^+$, 30 $[CH_2O]^+$. MS found: M^+, 298. $C_{19}H_{26}N_2O$ requires *M*, 298.4225.

***N'*-[4-(3-*Methoxy-benzyloxy*)-*benzyl*]-*N,N*-*dimethyl-propane*-1,3-*diamine* P6**

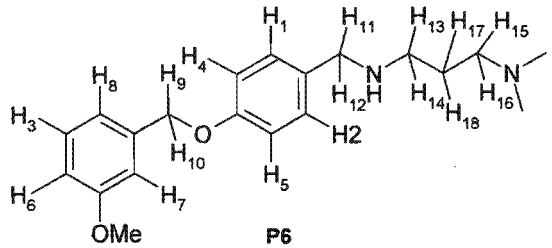

P6

The conditions employed for the preparation of this compound were those described in General Method B. Simple filtration with MeOH gave **P6** (178mg, quantitative yield) as a yellowish oil; R_f (MeOH-CH_2Cl_2, 10:90) 0.20; δ_H(300 MHz; $CDCl_3$) 7.32-7.21 (3H, m, H_1, H_2 and H_3), 7.03-6.91 (4H, m, H_4, H_5, H_6 and H_7), 6.95 (1H, dd, *J* 3.0 and 9.0, H_8), 5.02 (2H, s, H_9 and H_{10}), 3.81 (3H, s, -OCH_3), 3.76 (2H, s, H_{11} and H_{12}), 2.73 (2H, t, *J* 7.5, H_{13} and H_{14}), 2.37 (2H, t, *J* 7.5, H_{15} and H_{16}), 2.25 (3H, s, -N-CH_3), 2.23 (3H, s, –N-CH_3) and 1.74 (2H, quintet, *J* 7.5, H_{17} and H_{18}); δ_C(75 MHz; $CDCl_3$) 159.9, 158.0, 138.6, 131.5, 129.6, 129.5, 128.5, 119.6, 114.9 (2C), 113.5, 112.9, 69.9, 58.0, 55.2, 52.7, 47.4, 45.1 (2C), 26.6; EIMS *m/z* (50 eV) 328 $[M]^+$, 242 $[C_{15}H_{16}NO_2]^+$, 227 $[C_{15}H_{15}O_2]^+$, 121 $[C_8H_9O]^+$, 107 $[C_7H_7O]^+$, 30 $[CH_2O]^+$. MS found: M^+, 328. $C_{20}H_{28}N_2O_2$ requires *M*, 328.4485.

***N'*-[4-(*Biphenyl-2-ylmethoxy*)-*benzyl*]-*N,N*-*dimethyl-propane*-1,3-*diamine* P7**

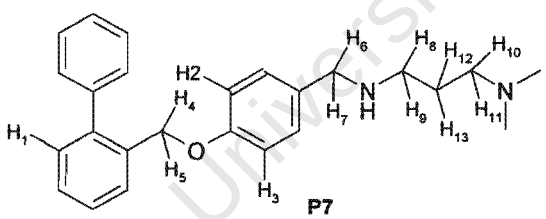

P7

The conditions employed for the preparation of this compound were those described in General Method B. Simple filtration with MeOH gave **P7** (139 mg, 97%) as a yellowish oil; R_f (MeOH-CH_2Cl_2, 10:90) 0.38; δ_H(300 MHz; $CDCl_3$) 7.61-7.58 (1H, m, H_1), 7.39-7.20 (10H, m, aromatic), 6.79 (2H, d, *J* 9.0, H_3 and H_4), 4.89 (2H, s, H_4 and H_5), 3.73 (2H, s, H_6 and H_7), 2.67 (2H, t, *J* 7.5, H_8 and H_9), 2.39 (2H, t, *J* 7.5, H_{10} and H_{11}), 2.26 (3H, s, -N-CH_3), 2.25 (3H, s, –N-CH_3) and 1.73 (2H, quintet, *J* 7.5, H_{12} and H_{13}); δ_C(75 MHz; $CDCl_3$) 157.8, 141.8, 140.5, 134.1, 130.0, 129.5 (2C), 129.2, 129.1, 128.2, 128.0, 127.6 (2C), 127.3 (3C), 114.8 (2C), 68.1, 57.7, 53.0, 47.3, 45.2 (2C), 27.1; EIMS *m/z* (50 eV) 374 $[M]^+$, 288 $[C_{20}H_{18}NO]^+$, 167 $[C_{13}H_{11}]^+$, 29 $[C_2H_5]^+$. MS found: M^+, 374. $C_{25}H_{30}N_2O$ requires *M*, 374.5185.

4.5.2 Chemical synthesis for hit modification

4.5.2.1 Synthesis of intermediate I8-I10 (Scheme 4-A)

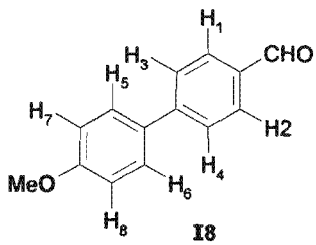

I8

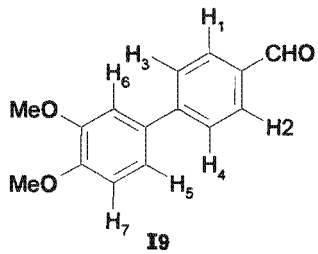

I9

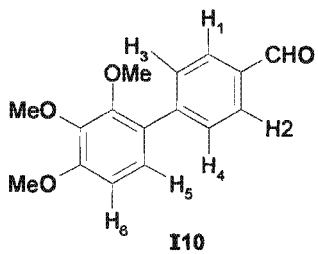

I10

***4'-Methoxy-biphenyl-4-carbaldehyde* I8**

The conditions employed for the preparation of this compound were those described in General Method C. Column chromatography (SiO_2, EtOAc-hexane, 20:80) afforded the aldehyde **I8** (272.5 mg, 80%) as yellow plates; R_f (EtOAc-hexane, 20:80) 0.40; δ_H(300 MHz; $CDCl_3$) 10.04 (1H, s, -CHO), 7.93 (2H, d, *J* 8.4, H_1 and H_2), 7.72 (2H, d, *J* 8.4, H_3 and H_4), 7.60 (2H, d, *J* 9.3, H_5 and H_6), 7.01 (2H, d, *J* 9.3, H_7 and H_8) and 3.87 (1H, s, $-OCH_3$). (Found: C, 78.86; H, 5.77. $C_{14}H_{12}O_2 \cdot 0.1H_2O$ requires C, 78.56; H, 5.70%).

3,4'-*Dimethoxy-biphenyl-4-carbaldehyde* I9

The conditions employed for the preparation of this compound were those described in General Method C. Column chromatography (SiO_2, EtOAc-hexane, 15:85) afforded the aldehyde **I9** (312.3 mg, 94%) as white cubes; R_f (EtOAc-hexane, 15:85) 0.30; δ_H(300 MHz; $CDCl_3$) 10.04 (1H, s, -CHO), 7.93 (2H, d, *J* 8.4, H_1 and H_2), 7.72 (2H, d, *J* 8.4, H_3 and H_4), 7.15-6.96 (3H, m, H_5, H_6 and H_7), 3.97 (3H, s, $-OCH_3$) and 3.94 (3H, s, $-OCH_3$) (Found: C, 73.93; H, 5.68. $C_{15}H_{14}O_3$ requires C, 74.36; H, 5.82%).

2',3',4'-*Trimethoxy-biphenyl-4-carbaldehyde* I10

The conditions employed for the preparation of this compound were those described in General Method C. Column chromatography (SiO_2, EtOAc-hexane, 20:80) afforded the aldehyde **I10**(401 mg, 91%) as yellowish-brown needles; R_f (EtOAc-hexane, 15:85) 0.25; δ_H(400 MHz; $CDCl_3$) 10.04 (1H, s, -CHO), 7.93 (2H, d, *J* 8.4, H_1 and H_2), 7.72 (2H, d, *J* 8.4, H_3 and H_4), 7.07 (1H, d, *J* 8.4, H_5), 6.78 (1H, d, *J* 8.4, H_6), 3.94 (3H, s, $-OCH_3$), 3.92 (3H, s, $-OCH_3$), and 3.69 (3H, s, $-OCH_3$) (Found: C, 70.74; H, 5.88. $C_{16}H_{16}O_4$ requires C, 70.57; H, 5.92%).

4.5.2.2 Synthesis of product P11-P20

1-(3',4'-*Dimethoxy-biphenyl-4-ylmethyl*)-4-*methyl-piperazine* P11

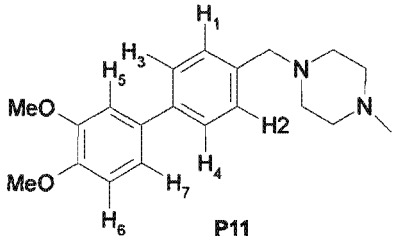

P11

The conditions employed for the preparation of this compound were those described in General Method D. Column chromatography (SiO_2, EtOAc-hexane, 60:40) gave the biaryl piperazine **P11** (36.5mg, 27%) as yellow needles; m.p. 96-98 °C; R_f (EtOAc-hexane, 60:40) 0.42; δ_H(300 MHz; $CDCl_3$) 7.45 (2H, d, *J* 8.4, H_1 and H_2), 7.37 (2H, d, *J* 8.4, H_3 and H_4), 7.12-7.10 (2H, m, H_5 and H_6), 6.94 (1H, d, *J* 8.7, H_7), 3.94 (3H, s, -OCH_3), 3.92 (3H, s, –OCH_3), 3.54 (2H, s, Ar-CH_2-N-), 2.47 (8H, broad s, 4 x –N-CH_2-) and 2.29 (3H, s, -N-CH_3); δ_C(100 MHz; $CDCl_3$) 149.2, 148.6, 139.9, 136.8, 134.1, 129.6 (2C), 126.6 (2C), 119.3, 111.6, 110.5, 62.7, 56.0 (2C), 55.1 (2C), 53.0 (2C) and 46.0; LC-MS found: M^+, 327.05. $C_{20}H_{26}N_2O_2$ requires *M*, 327.068. (Found: C, 71.94; H, 8.17; N, 8.54. $C_{20}H_{26}N_2O_2 \cdot 0.4H_2O$ requires C, 72.00; H, 7.98; N, 8.40%).

1-(3',4'-*Dimethoxy-biphenyl-4-ylmethyl*)-4-*phenyl-piperazine* P12

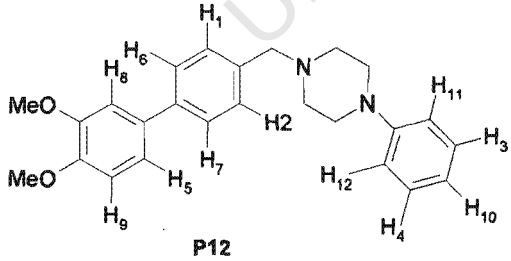

P12

The conditions employed for the preparation of this cornpound were those described in General Method D. Column chromatography (SiO_2, EtOAc-hexane, 60:40) gave the triaryl piperazine **P12** (46 mg, 29%) as yellow needles; m.p. 120-123 °C; R_f (EtOAc-hexane, 30:70) 0.20; δ_H(400 MHz; $CDCl_3$) 7.54 (2H, d, *J* 8.0, H_1 and H_2), 7.41 (2H, t, *J* 8.0, H_3 and H_4), 7.27-7.24 (3H, m, H_5, H_6 and H_7), 7.08-7.05 (2H, m, H_8 and H_9), 6.98-6.91 (3H, m, H_{10}, H_{11} and H_{12}), 3.95 (3H, s, -OCH_3), 3.92 (3H, s, –OCH_3), 3.63 (2H,

s, Ar-CH_2-N-), 3.24-3.21 (4H, m, 2x -*CH_2*-N-CH_2) and 2.69-2.66 (4H, m, 2x -CH_2-N-*CH_2*-); δ_C(100 MHz; $CDCl_3$) 149.6 (3C), 139.0, 136.8, 134.2, 129.6 (2C), 129.1 (3C), 126.7 (2C), 119.5, 116.0, 111.8 (2C), 110.5, 62.7, 56.0 (2C), 53.1 (2C) and 49.1 (2C); LC-MS found: M^+, 389.13. $C_{25}H_{28}N_2O_2$ requires M, 389.118. (Found: C, 77.32; H, 6.94; N, 7.61. $C_{25}H_{28}N_2O_2$ requires C, 77.29; H, 7.26; N, 7.21%).

1-*Benzyl*-4-(3',4'-*dimethoxy-biphenyl*-4-*ylmethyl*)-*piperazine* P13

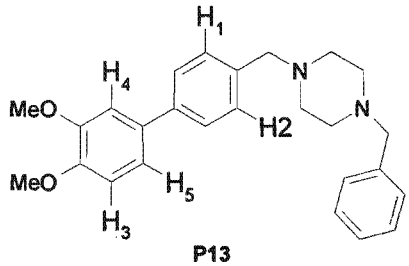

P13

The conditions employed for the preparation of this compound were those described in General Method D. Column chromatography (SiO_2, EtOAc-hexane, 60:40) gave the triaryl piperazine **P13** (125.3 mg, 94.5%) yellowish-brown plates; m.p. 105-108 °C; R_f (EtOAc-hexane, 60:40) 0.28; δ_H(300 MHz; $CDCl_3$) 7.49 (2H, d, *J* 8.4, H_1 and H_2), 7.37-7.30 (7H, m, aromatic), 7.11-7.09 (2H, m, H_3 and H_4), 6.94 (1H, d, *J* 8.4, H_5), 3.94 (3H, s, -OCH_3), 3.92 (3H, s, –OCH_3), 3.55 (2H, s, Ar-CH_2-N-), 3.53 (2H, s, Ar-CH_2-N-) and 2.51 (8H, broad s, 4 x –N-CH_2-); δ_C(100 MHz; $CDCl_3$) 149.5 (2C), 139.0, 137.0, 134.2, 129.7 (3C), 129.3 (2C), 128.2 (2C), 126.6 (3C), 119.5, 111.8, 110.5, 62.7 (2C), 56.0 (2C) and 53.0 (4C); LC-MS found: M^+, 403.13. $C_{26}H_{30}N_2O_2$ requires *M*, 402.504. (Found: C, 71.50; H, 5.88; N, 6.74. $C_{26}H_{30}N_2O_2 \cdot 1.9H_2O$ requires C, 71.48 H, 7.79; N, 6.41%).

Ferrocene compound P14

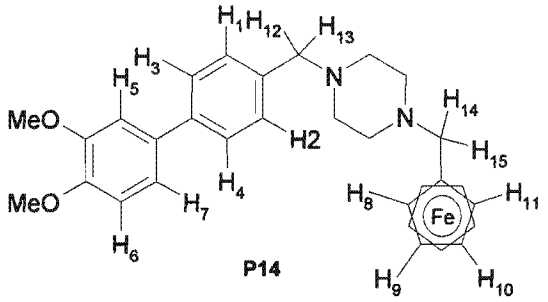

P14

The conditions employed for the preparation of this compound were those described in General Method D. Column chromatography (SiO_2, EtOAc-hexane, 60:40) gave the organometallic compound **P14** (73.2 mg, 35%) as orange plates; m.p. 110-112 °C; R_f (EtOAc-Hex, 30:70) 0.40; δ_H(300 MHz; $CDCl_3$) 7.50 (2H, d, *J* 9.0, H_1 and H_2), 7.35 (2H, d, *J* 9.0, H_3 and H_4), 7.17-7.10 (2H, m, H_5 and H_6), 6.93 (1H, d, *J* 9.0, H_7), 4.18 (4H, s, H_8, H_9, H_{10} and H_{11}), 4.10 (5H, s, C_5H_5), 3.94 (3H, s, -OCH_3), 3.92 (3H, s, –OCH_3), 3.51 (2H, s, H_{12} and H_{13}), 3.40 (2H, s, H_{14} and H_{15}) and 2.49 (8H, broad s, 4 x –NCH_2); δ_C(100 MHz; $CDCl_3$) 148.7, 139.9, 136.7, 134.4, 129.6 (9C), 126.6 (4C), 119.4, 111.8, 111.0, 70.3, 68.5, 68.0 (2C), 63.1 (2C), 58.7, 56.1, 52.9, and 52.5; LC-MS found: M^+, 511.09. $C_{30}H_{34}N_2O_2Fe$ requires *M*, 511.065. (Found: C, 70.59; H, 6.71; N, 5.49. $C_{30}H_{36}N_2O_2Fe$ requires C, 70.90; H, 6.71; N, 5.24%).

***1-Methyl-4-(2',3',4'-trimethoxy-biphenyl-4-ylmethyl)-piperazine* P15**

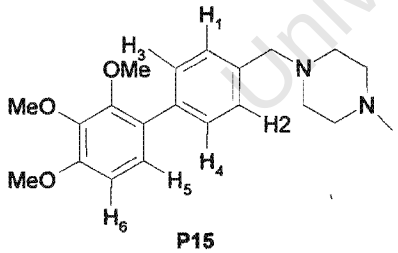

P15

The conditions employed for the preparation of this compound were those described in General Method D. Column chromatography (SiO_2, EtOAC-hexane, 50:50) gave the biaryl piperazine **P15** (109.6 mg, 83%) as yellow oil; R_f (EtOAc-hexane, 30:70) 0.25; δ_H(300 MHz; $CDCl_3$) 7.44 (2H, d, *J* 8.4, H_1 and H_2), 7.34 (2H, d, *J* 8.4, H_3 and H_4), 7.02 (1H, d, *J* 8.4, H_5), 6.73 (1H, d, *J* 8.4, H_6), 3.92 (3H, s, -OCH_3), 3.89 (3H, s, -OCH_3), 3.67 (3H, s, –OCH_3), 3.54 (2H, s, Ar-CH_2-N-), 2.51 (8H, broad s, 4 x –N-CH_2-) and 2.29 (3H, s, -N-CH_3); δ_C(100 MHz; $CDCl_3$) 153.1, 151.4, 142.6, 137.0, 136.5, 129.0, 128.9, 128.6

(2C), 124.8 (2C), 107.5, 62.8, 61.0 (2C), 56.1 (3C), 53.1 (2C) and 46.0; LC-MS found: M^+, 357.14. $C_{21}H_{28}N_2O_3$ requires *M*, 357.062. (Found: C, 70.45; H, 7.88; N, 7.76. $C_{21}H_{28}N_2O_3$ requires C, 70.76; H, 7.92; N, 7.86%).

1-*Phenyl*-4-(2',3',4'-*trimethoxy-biphenyl*-4-*ylmethyl*)-*piperazine* P16

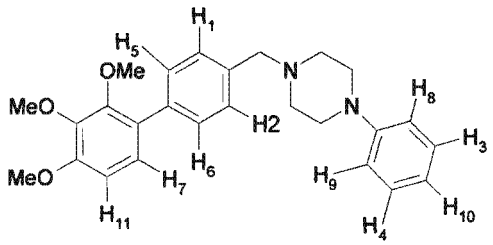

P16

The conditions employed for the preparation of this compound were those described in General Method D. Column chromatography (SiO_2, EtOAc-hexane 30:70) gave the triaryl piperazine **P16** (113.0 mg, 73%) yellow cubes; m.p. 65-68 °C; R_f (EtOAc-hexane, 30:70) 0.32; δ_H(400 MHz; $CDCl_3$) 7.48 (2H, d, *J* 8.4, H_1 and H_2), 7.38 (2H, d, *J* 8.4, H_3 and H_4), 7.28 (2H, d, *J* 8.4, H_5 and H_6), 7.04 (1H, d, *J* 8.4, H_7), 6.95 (2H, d, *J* 8.4, H_8 and H_9), 6.87 (1H, t, *J* 7.5, H_{10}), 6.74 (1H, d, *J* 8.4, H_{11}), 3.93 (3H, s, -OCH_3), 3.90 (3H, s, -OCH_3), 3.70 (3H, s, –OCH_3), 3.61 (2H, s, Ar-CH_2-N-), 3.25-3.20 (4H, m, 2 x *CH_2*-N-CH_2-) and 2.65-2.61 (4H, m, 2 x -CH_2-N-*CH_2*-); δ_C(100 MHz; $CDCl_3$) 153.1, 151.4, 142.6, 137.0, 136.5 (2C), 129.3 (2C), 129.2 (2C), 125.0 (2C), 119.8 (2C), 116.3 (3C), 107.7, 63.0, 61.0 (2C), 56.3 (2C), 53.4 and 49.4 (2C); LC-MS found: M^+, 419.10. $C_{26}H_{30}N_2O_3$ requires *M*, 419.112. (Found: C, 74.52; H, 7.27; N, 6.37. $C_{26}H_{30}N_2O_3$ requires C, 74.61; H, 7.22; N, 6.69%).

1-*Benzyl*-4-(2',3',4'-*trimethoxy-biphenyl*-4-*ylmethyl*)-*piperazine* P17

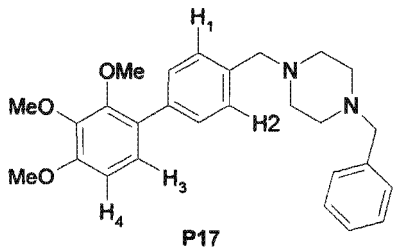

P17

The conditions employed for the preparation of this compound were those described in General Method D. Column chromatography (SiO_2, EtOAc-hexane 60:40) afforded the

triaryl piperazine **P17** (61.3 mg, 63%) as orange oil; R_f (EtOAc-hexane, 60:40) 0.30; δ_H(300 MHz; $CDCl_3$) 7.43 (2H, d, *J* 9.0, H_1 and H_2), 7.31-7.30 (7H, m, aromatic), 7.02 (1H, d, *J* 9.0, H_3), 6.72 (1H, d, *J* 9.0, H_4), 3.92 (3H, s, -OCH_3), 3.89 (3H, s, -OCH_3), 3.67 (3H, s, –OCH_3), 3.55 (2H, s, Ar-CH_2-N-), 3.53 (2H, s, Ar-CH_2-N-), and 2.52 (8H, broad s, 4 x -N-CH_2-); δ_C(100 MHz; $CDCl_3$) 153.1, 151.4, 143.6, 137.0, 136.5 (2C), 129.2 (2C), 129.0 (2C), 128.2 (2C), 127.0 (3C), 124.7, 115.5, 107.6, 63.1, 62.8, 60.9 (3C), 56.1 (2C) and 53.1 (2C); LC-MS found M^+, 433.10. $C_{27}H_{32}N_2O_3$ requires *M*, 433.142. (Found: C, 72.68; H, 6.93; N, 6.28%. $C_{27}H_{32}N_2O_3 \cdot 0.8H_2O$ requires C, 72.55; H, 7.57; N, 6.27%).

1-(4'-*Methoxy-biphenyl-4-yl-methyl*)-4-*methyl-piperazine* P18

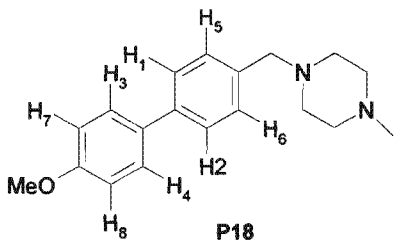

P18

The conditions employed for the preparation of this compound were those described in General Method D. Column chromatography (SiO_2, EtOAc-hexane, 50:50) afforded the biaryl piperazine **P18** (100.1 mg, 89%) as yellow plates; m.p. 106-108 °C; R_f (EtOAc-hexane, 50:50) 0.15; δ_H(300 MHz; $CDCl_3$) 7.53-7.7.48 (4H, m, H_1, H_2, H_3 and H_4), 7.36 (2H, d, *J* 8.7, H_5 and H_6), 6.97 (2H, d, *J* 8.7, H_7 and H_8), 3.84 (3H, s, -OCH_3), 3.54 (2H, s, Ar-CH_2-N-), 2.62 (8H, broad s, 4 x -N-CH_2-) and 2.29 (3H, s, -N-CH_3); δ_C(100 MHz; $CDCl_3$) 159.1, 139.6, 136.6, 133.6, 129.6 (2C), 128.0 (2C), 126.5 (2C), 114.2 (2C), 62.7, 55.3, 55.2, 53.1 (3C) and 46.0; LC-MS found: M^+, 297.04. $C_{19}H_{24}N_2O$ requires *M*, 297.074. (Found: C, 76.96; H, 8.37; N, 9.25. $C_{19}H_{24}N_2O$ requires C, 76.99; H, 8.16; N, 9.45%).

1-(4'-*Methoxy-biphenyl-4-ylmethyl*)-4-*phenyl-piperazine* P19

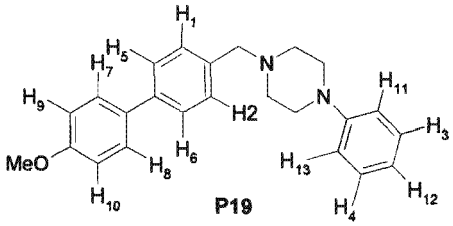

P19

The conditions employed for the preparation of this compound were those described in General Method D. Column chromatography (SiO_2, EtOAc-hexane, 30:70) afforded the triaryl piperazine **P19** (91.4 mg, 88%) as orange crystals; m.p. 123-127 °C; R_f (EtOAc-hexane, 30:70) 0.45; δ_H(400 MHz; $CDCl_3$) 7.55-7.51 (4H, m, H_1, H_2, H_3 and H_4), 7.40 (2H, d, *J* 8.4, H_5 and H_6), 7.29-7.23 (2H, m, H_7 and H_8), 7.00-6.91 (5H, m, H_9, H_{10}, H_{11}, H_{12} and H_{13}), 3.86 (3H, s, -OCH_3), 3.61 (2H, s, Ar-CH_2-N-), 3.24-3.21 (4H, m, 2 x -*CH_2*-N-CH_2-) and 2.67-2.64 (4H, m, 2 x -CH_2-N-*CH_2*); δ_C(100 MHz; $CDCl_3$) 159.1, 151.4, 139.7, 136.4, 133.5, 129.6 (2C), 129.1 (2C), 128.0 (2C), 126.6 (2C), 119.6,116.1 (2C), 114.2 (2C), 62.7, 55.3 (2C), 53.1 and 49.2 (2C); LC-MS found: M^+, 359.06. $C_{24}H_{26}N_2O$ requires *M*, 359.124. (Found: C, 77.53; H, 7.31; N, 6.20. $C_{24}H_{26}N_2O{\cdot}0.7H_2O$ requires C, 77.67; H, 7.43; N, 7.55%).

1-*Benzyl*-4-(4'-*methoxy-biphenyl-4-ylmethyl*)-*piperazine* P20

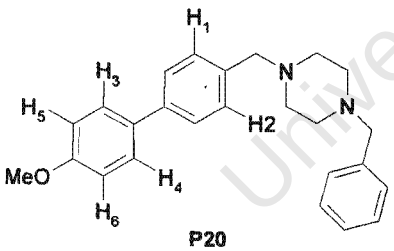

P20

The conditions employed for the preparation of this compound were those described in General Method D. Column chromatography (SiO_2, EtOAC-hexane, 60:40) gave the triaryl piperazine **P20** (114.7 mg, 66%) as yellow needles; m.p. 117-120 °C; R_f (EtOAc-hexane, 60:40) 0.27; δ_H(300 MHz; $CDCl_3$) 7.53-7.48 (4H, m, H_1, H_2, H_3, and H_4), 7.36-7.30 (7H, m, aromatic), 6.97 (2H, d, *J* 9.0, H_5 and H_6), 3.85 (3H, s, -OCH_3), 3.54 (2H, s, Ar-CH_2-N-), 3.51 (2H, s, Ar-CH_2-N-) and 2.50 (8H, broad s, 4 x –N-CH_2-); δ_C(100 MHz; $CDCl_3$) 159.1, 139.6, 138.2, 136.6, 133.6, 132.2, 132.0, 129.6, 129.2, 128.6, 128.4, 128.2, 128.0, 127.0 (2C), 126.5, 114.2 (2C), 63.1,62.7, 55.3 (3C) and 53.1 (2C); LC-MS found: M^+, 373.15. $C_{25}H_{28}N_2O$ requires *M*, 373.154. (Found: C, 79.41; H, 7.20; N, 6.54. $C_{25}H_{28}N_2O{\cdot}0.3H_2O$ requires C, 79.46; H, 7.62; N, 7.41%).

4.5.2.3 Synthesis of product P23-P26

1-(4-*Methyl-piperazin*-1-*yl*)-3-(2',3',4'-*trimethoxy-biphenyl*-4-*yloxy-propan*-2-*ol* P23

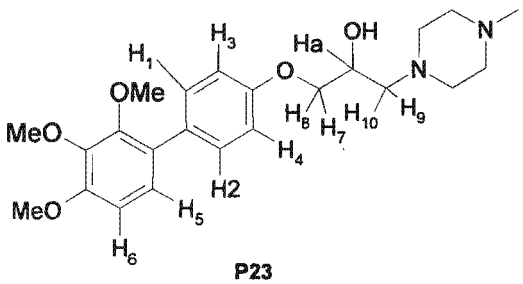

P23

The conditions employed for the preparation of this compound were those described in General Method E. Column chromatography (SiO_2, MeOH-CH_2Cl_2, 10:90) afforded the biaryl piperazine **P23** (76.2 mg, 31%) orange cubes; m.p. 103-106 °C; R_f(MeOH-CH_2Cl_2, 10:90) 0.21; δ_H(400 MHz; $CDCl_3$) 7.42 (2H, d, *J* 8.0, H_1 and H_2), 7.01-6.95 (3H, m, H_3, H_4 and H_5), 6.72 (1H, d, *J* 8.0, H_6), 4.11 (1H, quintet, *J* 7.5, Ha), 4.02 (2H, d, *J* 8.0, H_7 and H_8), 3.92 (3H, s, -OCH_3), 3.88 (3H, s, -OCH_3), 3.65 (3H, s, –OCH_3), 2.58-2.56 (2H, m, H_9 and H_{10}), 2.46 (8H, broad s, 4 x –N-CH_2-) and 2.29 (3H, s, -N-CH_3); δ_C(100 MHz; $CDCl_3$) 158.8, 153.5, 152.1, 142.6, 131.3, 130.4, 129.2, 128.2, 124.7, 114.5 (2C), 107.8, 70.6, 65.9, 61.0, 60.7, 56.3 (2C), 55.4, 53.6 (2C) and 46.2 and 29.9; LC-MS found: M^+, 417.05. $C_{23}H_{32}N_2O_5$ requires *M*, 417.050. (Found: C, 64.96; H, 8.64; N, 5.31. $C_{23}H_{32}N_2O_5 \cdot 0.5H_2O$ requires C, 64.92; H, 7.81; N, 6.58%).

1-(4-*Phenyl-piperazin*-1-*yl*)-3-(2',3',4'-*trimethoxy-biphenyl*-4-*yloxy*)-*propan*-2-*ol* P24

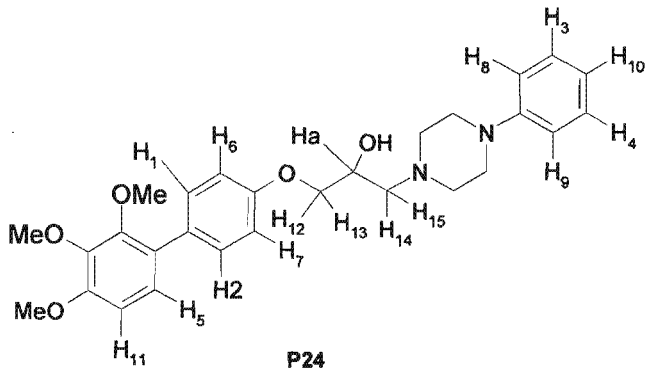

P24

The conditions employed for the preparation of this compound were those described in General Method E. Column chromatography (SiO_2, MeOH-CH_2Cl_2, 5:95) afforded the triaryl piperazine **24** (76.2 mg, 47%) as white needles; m.p. 105-108 °C; R_f (5% MeOH-CH_2Cl_2) 0.37; δ_H(400 MHz; $CDCl_3$) 7.43 (2H, d, *J* 8.0, H_1 and H_2), 7.27-7.23 (3H, m, H_3, H_4 and H_5), 7.01-6.92 (4H, m, H_6, H_7, H_8 and H_9), 6.89-6.85 (1H, m, H_{10}), 6.74 (1H, d, *J* 8.0, H_{11}), 4.18 (1H, quintet, *J* 7.5, Ha), 4.03 (2H, d, *J* 8.0, H_{12} and H_{13}), 3.93 (3H, s, -OCH_3), 3.89 (3H, s, -OCH_3), 3.66 (3H, s, –OCH_3), 3.24-3.20 (4H, m, 2 x -CH_2-N-CH_2-), 2.90-2.84 (2H, m, H_{14} and H_{15}) and 2.66-2.62 (4H, m, 2 x CH_2-N-CH_2-); δ_C(100 MHz; $CDCl_3$) 158.0, 153.2, 152.1, 131.3, 130.4, 129.4 (2C), 128.2 (3C), 124.8, 120.1, 116.4 (3C), 114.5 (2C), 107.8, 70.6, 66.0, 61.2, 61.0, 60.9, 56.3 (2C), 53.6, 49.5 and 29.9; LC-MS found M^+, 479.10. $C_{28}H_{34}N_2O_5$ requires *M*, 479.100. (Found: C, 70.62; H, 7.72; N, 5.42. $C_{28}H_{34}N_2O_5$ requires C, 70.27; H, 7.16; N, 5.85%).

1-(4-*Benzyl-piperazin*-1-*yl*)-3-(2',3',4'-*trimethoxy-biphenyl*-4-*yloxy*)-*propan*-2-*ol* P25

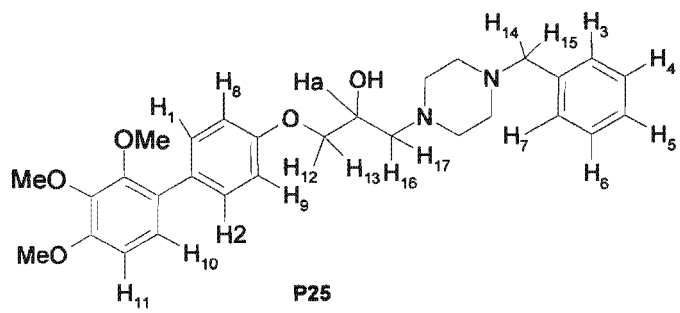

P25

The conditions employed for the preparation of this compound were those described in General Method E. Column chromatography (SiO_2, MeOH-CH_2Cl_2, 5%) afforded the triaryl piperazine **P25** (95.9mg, 33%) as yellow needles; m.p. 76-79 °C; R_f (5% MeOH/CH_2Cl_2) 0.29; δ_H(400 MHz; $CDCl_3$) 7.41 (2H, d, *J* 8.0, H_1 and H_2), 7.32-7.29 (5H,

m, H_3, H_4, H_5, H_6 and H_7),7.00-6.94 (3H, m, H_8, H_9 and H_{10}), 6.70 (1H, d, *J* 8.0, H_{11}), 4.13 (1H, quintet, *J* 7.5, Ha), 4.02 (2H, d, *J* 8.0, H_{12} and H_{13}), 3.92 (3H, s, -OCH_3), 3.89 (3H, s, -OCH_3), 3.65 (3H, s, –OCH_3), 3.51 (2H, s, H_{14} and H_{15}), 2.73 (2H, m, H_{16} and H_{17}) and 2.51 (8H, broad s, 4 x –N-CH_2-); δ_C(100 MHz; $CDCl_3$) 158.0, 152.6, 151.8, 138.5, 131.2, 130.4, 129.4 (2C), 128.4 (5C), 127.3, 124.8, 114.5 (2C), 107.8, 70.6, 65.8, 63.2, 61.2, 61.0, 60.7, 56.3 (2C), 53.6, 53.3 and 29.9; LC-MS found: M^+, 493.16. $C_{29}H_{36}N_2O_5$ requires *M*, 493.130. (Found: C, 69.37; H, 7.51; N, 5.49. $C_{29}H_{36}N_2O_5$·0.5H_2O requires C, 69.44; H, 7.43; N, 5.58%).

1-*Biphenyl-2-ylmethyl-4-methyl-piperazine* P26

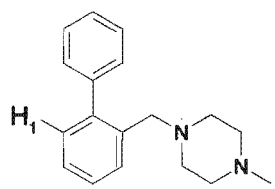

P26

N-Methylpiperazine (0.11 cm^3, 1.0 mmol) and 2-phenylbenzyl bromide (0.22 cm^3, 1.2 mmol) were dissolved in a minimum amount of dry toluene in a 25 cm^3 round-bottomed flask. After stirring at 25 °C under a N_2 purge for 10 min, the water soluble base 1,1,3,3-tetramethylguanidine (1.0 cm^3, 8.0 mmol) was added to the reaction mixture which was brought to reflux. 18h Later, the resulting reaction mixture was removed and extracted with EtOAc and distilled water. The organic phase was collected and chromatographed (SiO_2, MeOH-CH_2Cl_2, 15:85) yield the biphenyl piperazine **P26** (187 mg, 70%) as yellow cubes; m.p. 56-58 °C; R_f(15% MeOH-CH_2Cl_2) 0.42; δ_H(400 MHz; $CDCl_3$) 7.50 (1H, d, *J* 8.8, H_1), 7.34-7.22 (8H, m, aromatic), 3.42 (2H, s, Ar-CH_2-N-), 2.43 (8H, broad s, 4 x –N-CH_2-) and 2.29 (3H, s, -N-CH_3); δ_C(100 MHz; $CDCl_3$) 130.1, 130.0, 129.4 (2C), 127.8 (2C), 127.0 (4C), 126.8 (2C), 59.6 (2C), 55.0 (2C), 52.3 and 45.7; LC-MS found: M^+, 267.08. $C_{18}H_{22}N_2$ requires *M*, 267.080. (Found: C, 72.44; H, 8.29; N, 8.93. $C_{18}H_{22}N_2$·1.8H_2O requires C, 72.32; H, 8.62; N, 9.37%).

4.5.2.4 Synthesis of intermediate 27-30 (Scheme 4-C)

4-(4-*Bromo-benzyloxy*)-*benzaldehyde* I27

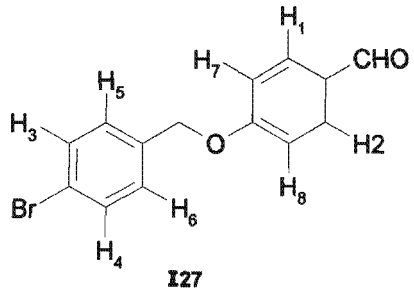

I27

4-Bromobenzaldehyde (2.23 g, 8.94 mmol) was added to a stirred solution of powdered anhydrous sodium hydride (0.27 g, 11.1 mmol) and 4-hydroxybenzaldehyde (1.04 g, 8.52 mmol) in DMF (25 cm^3) at 0°C under an inert atmosphere. The resulting light yellow suspension was allowed to warm to 25 °C and stirred for an additional 18h. The reaction was then diluted with water (500 cm^3) and the yellow precipitate was collected by filtration and subsequent washing with water. Further drying under vacuum afforded the aldehyde **I27** (2.25 g, 91%) as yellow cubes; R_f (MeOH-CH_2Cl_2, 5:95) 0.23; δ_H(400 MHz; $CDCl_3$) 9.89 (1H, s, -CHO), 7.84 (2H, d, *J* 8.8, H_1 and H_2), 7.53 (2H, d, *J* 8.8, H_3 and H_4), 7.23 (2H, d, *J* 8.8, H_5 and H_6), 7.05 (2H, d, *J* 8.8, H_7 and H_8) and 5.10 (2H, s, Ar-CH_2-) (Found: C, 57.72; H, 3.60. $C_{14}H_{11}O_2Br$ requires C, 57.76; H, 3.81%).

4-(4'-*Methoxy-biphenyl*-4-*ylmethoxy*)-*benzaldehyde* I28

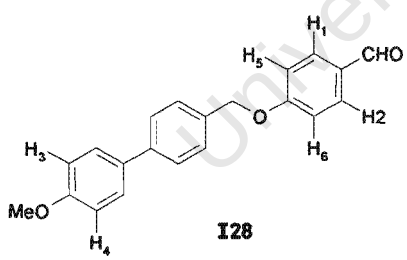

I28

The conditions employed for the preparation of this compound were those described in General Method C. The product was recrystalized using ethyl acetate. The pure white needles were separated from the yellow impurities to yield the aldehyde **I28** (275 mg, 63%); R_f (EtOAc-hexane, 10:90) 0.27; δ_H(400 MHz; $CDCl_3$) 9.90 (1H, s, -CHO), 7.86 (2H, d, *J* 8.7, H_1 and H_2), 7.60-7.46 (6H, m, aromatic), 7.11 (2H, d, *J* 8.7, H_3 and H_4), 6.99 (2H, d, *J* 8.7, H_5 and H_6), 5.18 (1H, s, Ar-CH_2-O-) and 3.85 (3H, s, -OCH_3) (Found: C, 77.76; H, 5.72. $C_{21}H_{18}O_3 \cdot 0.3H_2O$ requires C, 77.90; H, 5.79%).

4-(3',4'-*Dimethoxy-biphenyl-4-ylmethoxy)-benzaldehyde* I29

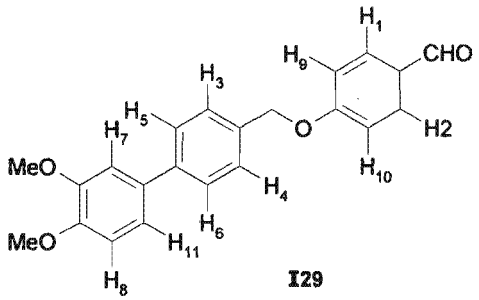

I29

The conditions employed for the preparation of this compound were those described in General Method C. The aldehyde **I29** was chromatographed (SiO_2, EtOAc-hexane, 15:85) as white cubes (321.4 mg, 67%); R_f (EtOAc-hexane, 15:85) 0.19; δ_H(400 MHz; $CDCl_3$) 9.94 (1H, s, -CHO), 7.84 (2H, d, *J* 8.8, H_1 and H_2), 7.61 (2H, d, *J* 8.8, H_3 and H_4), 7.44 (2H, d, *J* 8.8, H_5 and H_6), 7.16-7.10 (4H, m, H_7, H_8, H_9 and H_{10}), 6.97 (1H, d, *J* 8.8, H_{11}), 5.20 (2H, s, Ar-CH_2-O-) and 3.95 (3H, s, -OCH_3), 3.93 (3H, s, –OCH_3) (Found: C, 75.54; H, 5.64. $C_{22}H_{20}O_4 \cdot 0.1H_2O$ requires C, 75.46; H, 5.81%).

4-(2',3',4'-*Trimethoxy-biphenyl-4-ylmethoxy)-benzaldehyde* I30

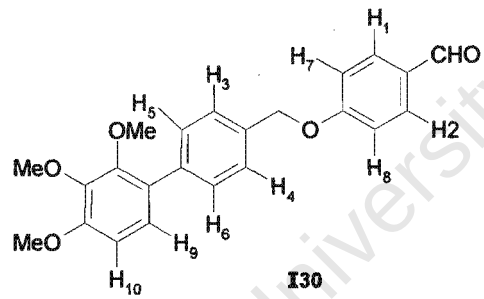

I30

The conditions employed for the preparation of this compound were those described in General Method C. The benzaldehyde **I30** was purified by chromatography (SiO_2, EtOAc-hexane, 15:85) as yellow cubes (175 mg, 34%) R_f (EtOAc-Hex, 15:85) 0.30; δ_H(400 MHz; $CDCl_3$) 9.94 (1H, s, -CHO), 7.85 (2H, d, *J* 8.8, H_1 and H_2), 7.55 (2H, d, *J* 8.8, H_3 and H_4), 7.47 (2H, d, *J* 8.8, H_5 and H_6), 7.11 (2H, d, *J* 8.8, H_7 and H_8), 7.02 (1H, d, *J* 8.8, H_9), 6.86 (1H, d, *J* 8.8, H_{10}), 5.20 (2H, s, Ar-CH_2-O) and 3.93 (3H, s, -OCH_3), 3.90 (3H, s, -OCH_3), 3.70 (3H, s, –OCH_3) (Found: C, 72.90; H, 5.79. $C_{23}H_{22}O_5$ requires C, 73.00; H, 5.86%).

4.5.2.5 Synthesis of product P31-P33

1-[4-(4'-*Methoxy-biphenyl-4-ylmethoxy*)-*benzyl*]-4-*methyl-piperazine* P31

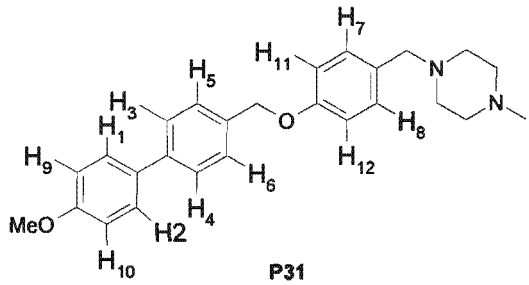

P31

The conditions employed for the preparation of this compound were those described in General Method D. Column chromatography (SiO_2, MeOH-CH_2Cl_2, 5:95) afforded the triaryl piperazine **P31** (25.1 mg, 39%) as yellow needles; m.p. 127-130 °C; R_f (5% MeOH-CH_2Cl_2) 0.30; δ_H(400 MHz; $CDCl_3$) 7.59-7.46 (6H, m, H_1, H_2, H_3, H_4, H_5 and H_6), 7.23 (2H, d, *J* 8.8, H_7 and H_8), 6.99-6.93 (4H, m, H_9, H_{10}, H_{11} and H_{12}), 5.10 (2H, s, Ar-CH_2-O-), 3.85 (3H, s, -OCH_3), 3.47 (2H, s, Ar-CH_2-N-), 2.46 (8H, broad s, 4 x -N-CH_2-) and 2.28 (3H, s, N-CH_3); δ_C(100 MHz; $CDCl_3$) 159.3, 158.0, 140.6, 135.5, 133.4, 130.5, 130.4, 128.1 (3C), 128.0 (2C), 126.9 (4C), 114.6, 114.3, 69.9, 62.4, 55.3 (2C), 55.1, 53.0 (2C) and 46.0; LC-MS found: M^+, 403.10. $C_{26}H_{30}N_2O_2$ requires *M*, 403.148. (Found: C, 72.48; H, 7.74; N, 6.07. $C_{26}H_{30}N_2O_2 \cdot 1.6H_2O$ requires C, 72.38; H, 7.75; N, 6.49%).

1-[4-(3',4'-*Dimethoxy-biphenyl-4-ylmethoxy*)-*benzyl*]-4-*methoxy-piperazine* P32

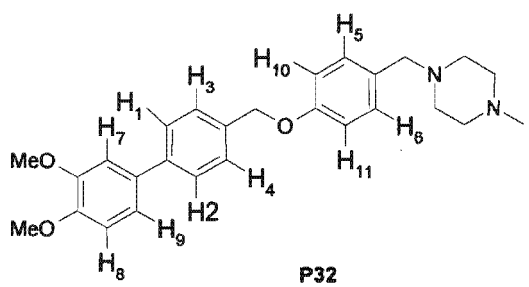

P32

The conditions employed for the preparation of this compound were those described in General Method D. Column chromatography (SiO_2, MeOH-CH_2Cl_2, 5:95) afforded the triaryl piperazine **P32** (40.8 mg, 36%) as white cubes; m.p. 112-114 °C; R_f (5% MeOH-CH_2Cl_2) 0.33; δ_H(400 MHz; $CDCl_3$) 7.58 (2H, d, *J* 8.8, H_1 and H_2), 7.49 (2H, d, *J*

8.8, H_3 and H_4), 7.23 (2H, d, *J* 8.8, H_5 and H_6), 7.15-7.10 (2H, m, H_7 and H_8), 6.96-6.94 (3H, m, H_9, H_{10} and H_{11}), 5.10 (2H, s, Ar-CH_2-O-), 3.94 (3H, s, -OCH_3), 3.92 (3H, s, –OCH_3), 3.46 (2H, s, Ar-CH_2-N-), 2.44 (8H, broad s, 4 x –N-CH_2-) and 2.27 (3H, s, -N-CH_3); δ_C(100 MHz; $CDCl_3$) 158.0, 149.2, 148.8, 140.8, 135.7, 133.9, 130.6, 130.4, 128.0 (2C), 127.0 (3C), 119.4, 114.5 (2C), 111.6, 110.5, 69.8, 62.4, 56.0 (2C), 55.1 (2C), 53.4, 53.0 and 46.0; LC-MS found: M^+, 433.10. $C_{27}H_{32}N_2O_3$ requires *M*, 433.142. (Found: C, 72.28; H, 6.72; N, 5.83. $C_{27}H_{32}N_2O_3 \cdot 0.9H_2O$ requires C, 72.26; H, 7.58; N, 6.24%).

1-*Methyl*-4-[4-(2',3',4'-*trimethoxy-biphenyl*-4-*ylmethoxy*)-*benzyl*-*piperazine* P33

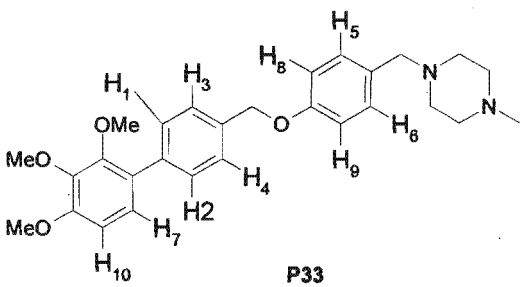

P33

The conditions employed for the preparation of this compound were those described in General Method D. Column chromatography (SiO_2, MeOH-CH_2Cl_2, 5:95) afforded the triaryl piperazine **P33** (60 mg, 58%) as yellowish needles; m.p. 68-70 °C; R_f (5% MeOH-CH_2Cl_2) 0.20; δ_H(300 MHz; $CDCl_3$) 7.52 (2H, d, *J* 8.8, H_1 and H_2), 7.46 (2H, d, *J* 8.8, H_3 and H_4), 7.24 (2H, d, *J* 8.8, H_5 and H_6), 7.01 (1H, d, *J* 8.8, H_7), 7.96 (2H, d, *J* 8.8, H_8 and H_9), 6.75 (1H, d, *J* 8.8, H_{10}), 5.08 (2H, s, Ar-CH_2-O-), 3.93 (3H, s, -OCH_3), 3.90 (3H, s, -OCH_3), 3.68 (3H, s, –OCH_3), 3.45 (2H, s, Ar-CH_2-N-), 2.44 (8H, broad s, 4 x –N-CH_2-) and 2.28 (3H, s, -N-CH_3); δ_C(100 MHz; $CDCl_3$) 158.1, 153.2, 142.6, 138.0, 135.5, 130.5, 130.4, 129.3, 128.3 (2C), 127.3 (3C), 124.8, 114.6 (2C), 111.8, 107.6, 70.0, 62.4, 61.0 (2C), 56.1 (2C), 55.1, 53.0 (2C) and 46.0; LC-MS found: M^+, 463.12. $C_{28}H_{34}N_2O_4$ requires *M*, 463.136. (Found: C, 70.10; H, 6.64; N, 5.32. $C_{28}H_{34}N_2O_4 \cdot 0.9H_2O$ requires C, 70.23; H, 7.47; N, 5.85%).

Chapter 5

Hit development: biological evaluation

5. *In Vitro* Screening against *P. falciparum*

5.1 Introduction

Drug resistance in malaria has been defined as "ability of a parasite strain to survive and/or to multiply despite the administration and absorption of a drug given in doses equal to or higher than those usually recommended but within the limits of tolerance of the subject." (WHO, 1965, 1973; Bruce-Chwatt *et al.,* 1981). However, the term CQ resistance could be misleading. It has been considered as an *in vitro* phenotype; the ability of malaria parasites to survive CQ at a therapeutic serum concentration *in vivo* and even the outcome of a clinical CQ therapy (Wellems and Plowe, 2001). CQ resistance throughout the *in vitro* investigation in this research is therefore defined to have two distinguishing features: (1) the ability of the parasites to survive and/or multiply at 0.1 μM (33 ng/ml) of CQ based on standard conditions of continuous culture and (2) the characteristic of chemosensitization by verapamil present at 1.0 μM.

The characteristic features of classical resistance modulators include the ability to modulate CQ resistance when used in combination with CQ. However, the factor limiting achievement of effective concentrations is the intrinsic side-effects. In the search for a hit compound as the basis of a CQ resistance reverser, a small group of rationally designed compounds generated were studied *in vitro* against *P. falciparum*. The intrinsic antiplasmodial activity, resistance reversal effect, effect in CQ accumulation as well as cytotoxic screening are reported and discussed in this chapter.

5.2 Hit development

In the early stage of drug discovery, it is essential to discover hits, which are prototype compounds possessing desired pharmacological activities, before any chemical modifications to improve their clinical features into lead molecules and ultimately fulfil the criteria for a pre-clinical candidate (see Table 2.1 – Rational drug design, P32). On the basis of known structure-activity relationship studies for MDR reversal agents, and inspection of the chemical structures of known chemosensitizers in malaria, a small number of compounds was designed and synthesized for preliminary exploratory biological studies in *P. falciparum* (Fig. 5.2).

According to known SAR in malaria MDR chemosensitizers, a hydrophobic moiety is important for good resistance reversal effects in CQ resistant parasites (see 2.2.2.1. SAR in chemosensitizers). In connection with the known SAR studies, the synthesized compounds possess different extended hydrophobic chemical features in their respective structures. Compound **P4** differs from the others with only one aromatic ring in its structure while the others contain at least two aromatic ring systems. The introduction of a methoxy group at position 3 on one of the hydrophobic rings of compound **P5** distinguishes compound **P6** from **P5**. In the structure of compound **P7**, a privileged biphenyl substructure was introduced.

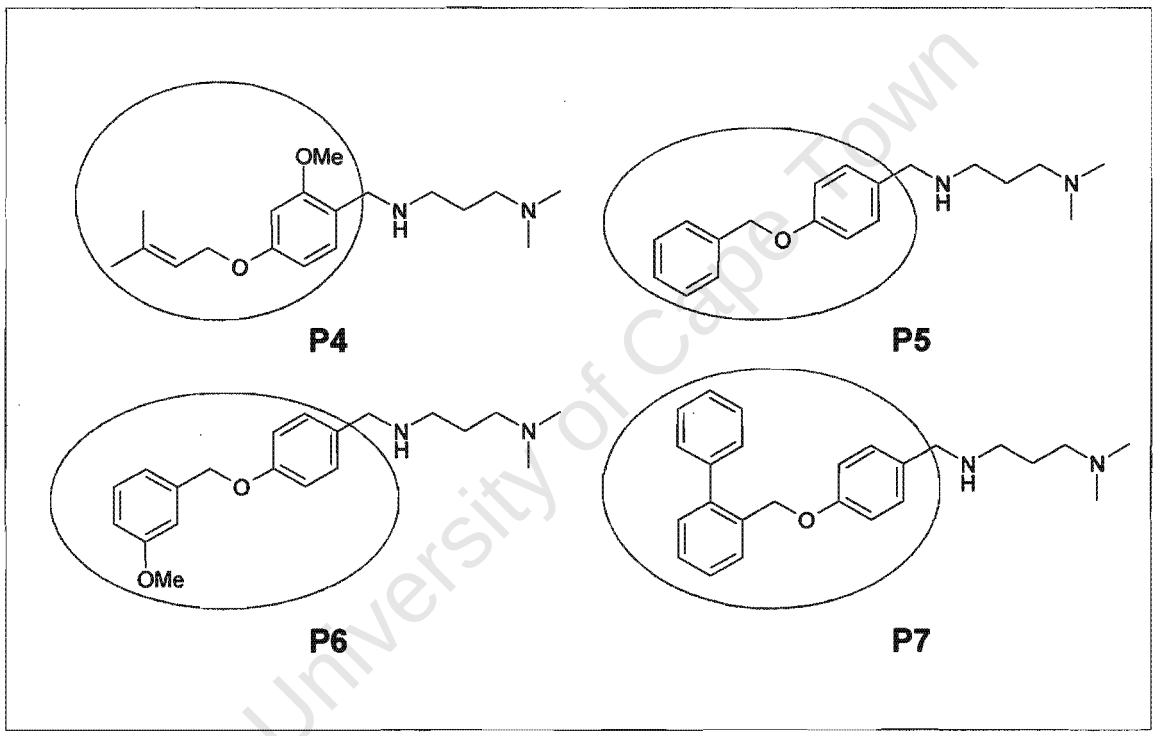

Figure 5.2. Chemical structures of potential hits.

The objective of this exploratory study was three-fold: (i) to extend and/or confirm the known structure-activity relationships of previously identified chemosensitizers in malaria with respect to the chemoreversal diamino propane pharmacophore hypothesis (Rasonaivo *et al.*, 2004), (ii) to confirm our hypothesis that two basic nitrogens in the side chain (reminiscent of a polyamine backbone) will give rise to concentration-dependent dual acting antimalarial and resistance reversal agents and, (iii) to test our hypothesis that a privileged biphenyl scaffold can form a basis for a novel class of chemosensitizers in malaria.

5.3 Results and discussions

5.3.1 Antiplasmodial activity

The K1 and RSA11 strains of *P. falciparum* are more resistant to CQ than the sensitive strain, D10 (Appendix 2, Fig. 5.3.1-A(a), Fig. 5.3.1-B(a) and Fig. 5.3.1-C(a)). The intrinsic antiplasmodial activities of the synthesized potential CQ resistance reversing agents alone were studied on the South African CQ^R strain RSA11. For comparative purposes, the activities were also assessed in K1. The pLDH assay was carried out and the results were analysed as parasite percentage viability versus logarithm of the drug concentration in μM. Fig. 5.3.1-B and Fig. 5.3.1-C (Appendix 2) show the results obtained. The degree of intrinsic antiplasmodial activity was measured by the 50% inhibitory concentrations (IC_{50}) at which 50% of the parasites were killed (Table 5.3.1). In addition to the IC_{50} values, the resistance index ($R_I = IC_{50}^{K1 \text{ or } RSA11} / IC_{50}^{D10}$) which gives an indication of the relative activity of the compounds in a drug resistant and sensitive strain of *P. falciparum*, is reported. For new compounds, this gives an indication of whether or not the compound will be active against CQ^R strains. i.e. the lower the R_I value, the better.

The small series of compounds synthesized all showed marked antiplasmodial activity against CQ-sensitive and resistant strains of falciparum malaria (Table 5.3.1). Since the synthesized compounds are structurally unrelated to CQ, comparisons were made within this series of compounds produced, in which a lower activity in **P4** was observed (IC_{50} > 2μM while the others exhibited IC_{50} < 2μM). This may be explained by the poly-aromatic substructure present in compounds **P5**, **P6** and **P7**. All the compounds exhibited substantially lower antimalarial activity against the CQ sensitive strain, D10 when compared to CQ. However, the intrinsic activity of **P7** was comparable to CQ in the CQ resistant strain K1 (**CQ:** IC_{50}^{K1}=0.196 μM; **P7:** IC_{50}^{K1}=0.148 μM), even though it was 3 times less active than CQ in the RSA11 strain (**CQ:** IC_{50}^{RSA11}=0.181 μM; **P7:** IC_{50}^{RSA11}=0.600 μM). Although the number of compounds synthesized for exploratory studies is very small, the superior activity of compound **P7** relative to the others may be due to the presence of the privileged biphenyl motif with a tendency to bind to various proteinaceous surfaces.

Table 5.3.1. *In vitro* antiplsmodial activity[a]

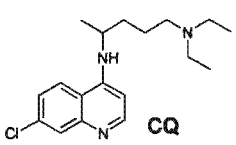

CQ

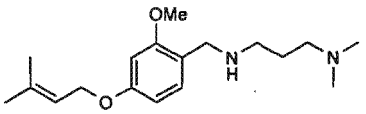

P4

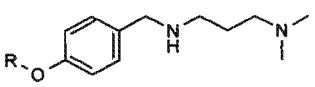

P5,P6,P7

Compd	R	IC_{50}^{D10}	IC_{50}^{K1}	R_I^{K1}	IC_{50}^{RSA11}	R_I^{RSA11}	clogP
CQ	—	0.024	0.196	8.17	0.181	7.54	5.06
P4	—	2.45	2.29	0.93	2.57	1.05	3.88
P5	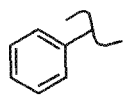	1.10	1.58	1.43	1.86	1.69	3.86
P6	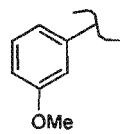	0.977	0.830	0.85	1.32	1.35	3.78
P7	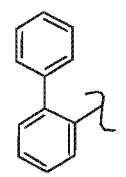	0.174	0.148	0.85	0.600	3.45	5.45

[a]Results are expressed as mean IC_{50} (μM) of three independent experiments performed in duplicate.

In terms of the relative activity of the compounds in different strains of *P. falciparum*, compound **P4** was equally active against CQ^S and CQ^R strains (R_I^{K1}=0.93; R_I^{RSA11}=1.05). Compound **P5** was slightly less active in the CQ resistant strains while **P6** (R_I^{K1}=0.85; R_I^{RSA11}=1.35) and **P7** (R_I^{K1}=0.85; R_I^{RSA11}=3.45) showed better activity against K1 than RSA11. This suggests that the hydrophobic structural feature incorporating substituents (methoxy group or another lipophilic aromatic ring) on the aromatic ring may improve their antiplasmodial activity against the K1 strain of malaria parasites as the more lipophilic compound, **P7**, (high clogP value) may be able to readily cross the parasite membrane and accumulate via pH trapping within the acidic parasite food vacuole.

5.3.2 Resistance reversal effects

All the concentrations selected for combination studies in CQ^R K1 and RSA11 isolates were derived from Fig. 5.3.1-B and Fig. 5.3.1-C (Appendix 2), respectively. Concentrations were chosen which were sub-lethal to the parasite cultures, in order to be able to distinguish the resistance reversal from the antimalarial effect (Table 5.3.1). The concentration chosen for the compounds was 0.03 μM, which is much lower than any of the intrinsic antiplasmodial IC_{50} values of the compounds tested. The CQ resistance reversing effects of the single drug combined with CQ on the resistant strains of K1 and RSA11 are illustrated in Fig. 5.3.2-A and Fig. 5.3.2-B, respectively. A dose-response curve of CQ alone serves as a control of the experiment (shown in black). The result of combination of CQ with each single compound is illustrated in colour. A shift of the curve to the left of the CQ dose-response curve indicates resistance reversal activity. Any shifts to the right of the CQ curve would suggest an antagonistic effect to the action of CQ.

As can be seen in Fig. 5.3.2-A, a slight shift of the CQ+compound curve to the left of the CQ alone on K1 strain was observed. This indicates weak resistance reversal effects on CQ action for all synthesized compounds. On RSA11 (Fig. 5.3.2-B), curves of **CQ+P4** and **CQ+P5** showed possible antagonistic effects while **CQ+P6** demonstrated no significant resistance reversal effects. As with data obtained on K1, **P7** showed little resistance reversal effects on RSA11. The control curve of CQ+VPL shows significant resistance reversal for both resistant strains (Fig. 5.3.2-A(2) and Fig. 5.3.2-B(2)).

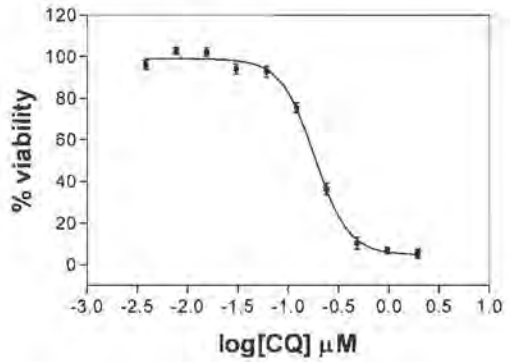

A-(1). Intrinsic antimalarial effect of CQ on K1

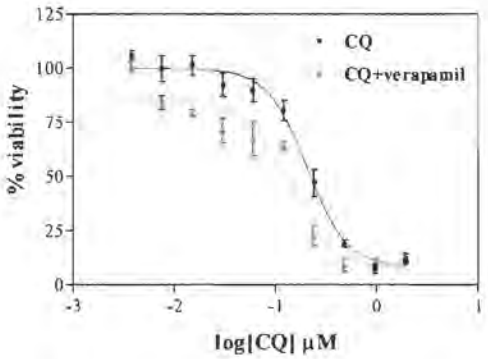

A-(2). Resistance reversal effect of Verapamil on K1

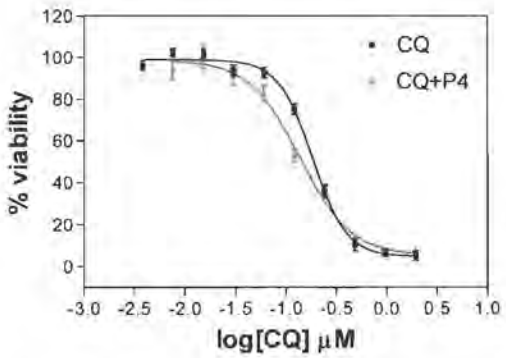

A-(3). Resistance reversal effect of **P4** on K1

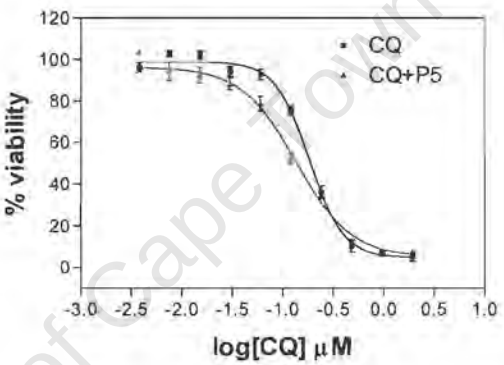

A-(4). Resistance reversal effect of **P5** on K1

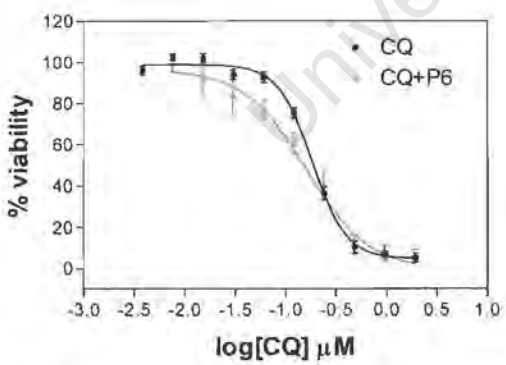

A-(5). Resistance reversal effect of **P6** on K1

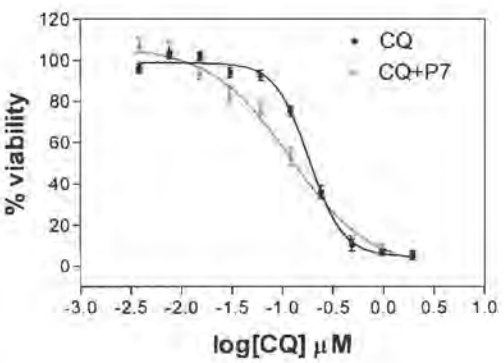

A-(6). Resistance reversal effect of **P7** on K1

Figure 5.3.2-A. Resistance reversal activity of a single drug plus CQ on CQ^R strain of K1.

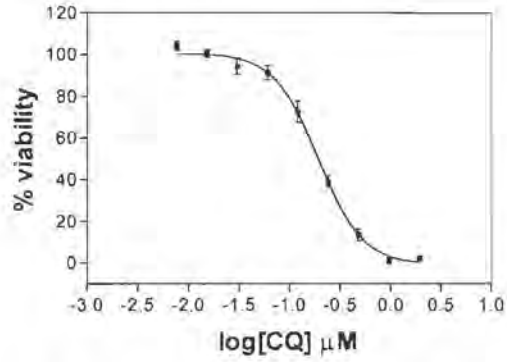

B-(1). Intrinsic antimalarial effect of CQ on RSA11

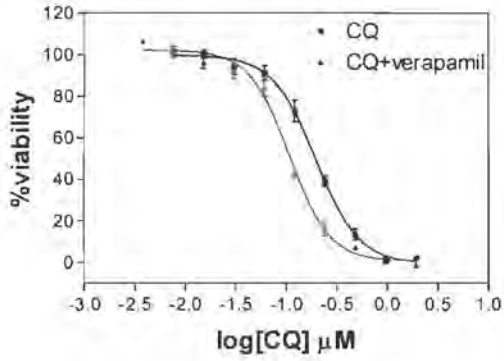

B-(2) Resistance reversal effect of Verapamil on RSA11

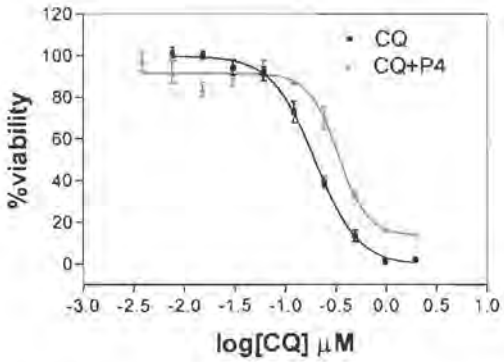

B-(3). Resistance reversal effect of **P4** on RSA11

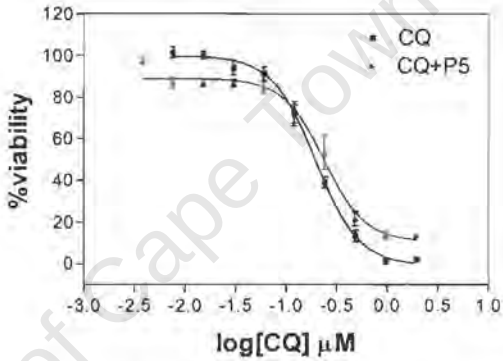

B-(4). Resistance reversal effect of **P5** on RSA11

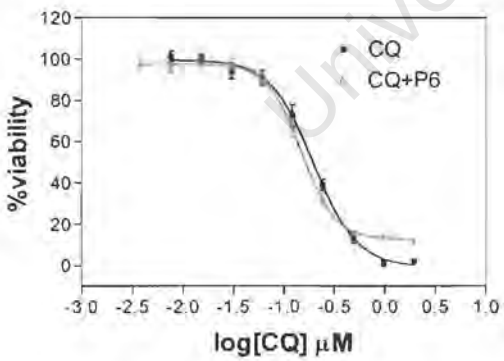

B-(5). Resistance reversal effect of **P6** on RSA11

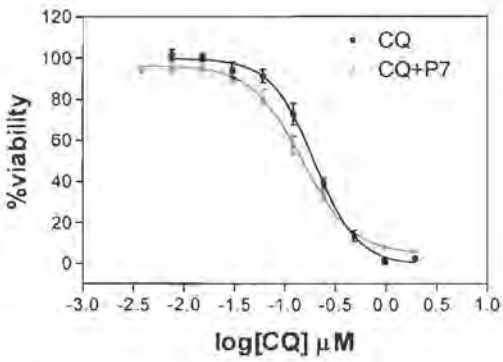

B-(6). Resistance reversal effect of **P7** on RSA11

Figure 5.3.2-B. Resistance reversal activity of a single drug plus CQ on CQ^R strain of RSA11.

For convenience, the IC_{50} values of the synthesized compounds in combination with CQ in this study as well as the Response Modification Index (RMI) outlines, which indicate the susceptibility of the sensitive strain and resistant strains to CQ alone and in combination with a single drug, can also be found in Table 5.3.2.1.

The RMI is defined as

$$R.M.I. = IC_{50}\,(z^*)/\,IC_{50}\,(z)$$

where

$IC_{50}(z^*)$ = IC_{50} of the combination of a particular drug with CQ

$IC_{50}(z)$ = IC_{50} of CQ alone

If the index < 1, a synergistic effect and/or potentiation are/is suggested. Otherwise, an antagonistic result (RMI > 1) and an unbiased result (RMI = 1) are stated.

Table 5.3.2.1. Resistance reversal effect.

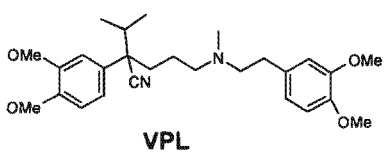

VPL

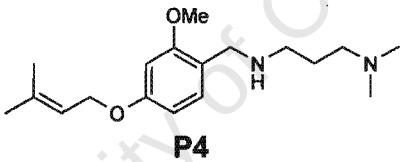

P4

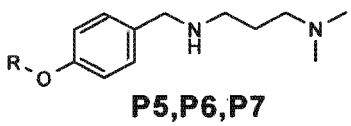

P5,P6,P7

Compd	R	IC_{50}^{K1}	RMI_{K1}	IC_{50}^{RSA11}	RMI_{RSA11}
CQ	—	0.196	—	0.181	—
CQ+VPL	—	0.126	**0.42**	0.109	**0.60**
CQ+P4	—	0.144	**0.73**	0.335	**1.85**
CQ+P5	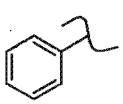	0.141	**0.72**	0.234	**1.29**
CQ+P6	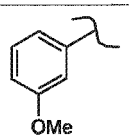	0.148	**0.76**	0.162	**0.90**
CQ+P7	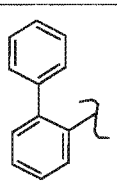	0.132	**0.67**	0.148	**0.82**

In this exercise, all the compounds synthesized were found to be less potent resistance reversers than VPL. However, the marked antiplasmodial activity and moderate resistance reversal effect of compound **P7** on both CQ^R strains are noteworthy. The RMI indices in Table 5.3.2.1 confirm the dose-response relationship of the compounds tested.

For resistance reversal effects, VPL showed the most potent CQ resistance reversing activity among the drugs tested as its CQ+VPL dose-response curve shifts to the left of the CQ curve in both CQ^R strains of K1 and RSA11 (Fig. 5.3.2). This was confirmed with the resistance modification indexes which indicate good reversing activity when RMI <1 (RMI_{K1}= 0.42 and RMI_{RSA11}= 0.60). All synthesized compounds showed moderate resistance modulating properties in the K1 isolate whereas compound **P7** demonstrated the best resistance reversal effect in both CQ^R strains (RMI_{K1}=0.67 and RMI_{RSA11}=0.82). Compound **P4** was shown to be the least potent resistance reverser although it exhibited the least intrinsic toxicity. When the alkyl chain was substituted with an aromatic ring (**P4** vs **P5**), the intrinsic antiplasmodial activity as well as the resistance reversal effect were improved, suggesting the importance of an aromatic hydrophobic moiety. Furthermore, when an additional methoxy group was attached to the substituted aromatic ring (compound **P5** vs **P6**), further enhancement in resistance reversing properties was observed in addition to increased antiplasmodial activity. Lastly, the effect of the biphenyl substructure in compound **P7** was evident since compound **P7**, the analogue of **P4**, showed significant chemosensitization as well as antimalarial effects. A tentative hypothesis is proposed that the poly–aromatic structural element is probably the pharmacophore that is responsible for interacting with proteins involved in the resistance mechanism. In addition, one possibility for the moderate chemosensitizing activities observed with the drugs investigated in this study could be that the chosen sub-lethal concentration of 0.03μM was minimal. It is expected that the higher concentrations of these drugs would produce greater chemosensitization and antiplasmodial activity against CQ resistant *P. falciparum*. However, it would not be possible to distinguish the antiplasmodial activity from resistance reversal effects at higher concentrations of the compounds due to the dual acting properties of the compounds.

5.3.3 Tritiated CQ accumulation with combinations of compounds

Substantial literature on the accumulation of CQ by falciparum infected erythrocytes has shown that the cytotoxic effect of CQ is due to the increased uptake of CQ within malaria parasites. In CQ^R parasites, an effective chemosensitizer leads to a potentiation of CQ uptake within the malaria-infected red blood cells. In efforts to establish a possible mechanism underlying resistance reversal effects of the novel products, radio-labelled CQ was used in this accumulation assay. CQ^S strain D10 standardized this assay as results reveal no potentiation effect against all the drugs tested in this strain (Fig.5.3.3-A).

The results presented in combination studies were validated in accumulation experiments. Typical resistance reversal agents are characterized by increased CQ accumulation in addition to the shift in the CQ curve. The concentrations of potential resistance reversers selected for the combination experiments were non-toxic to *P. falciparum* and derived from Fig. 5.3.1-A, -B and -C. The results are presented in Fig. 5.3.3 as fold increase versus the CQ combination with different compounds at various concentrations. The parasitized red blood cell served as a control. Fold increase in uptake refers to the ratio of radio-labelled ^{3}H-CQ counts of the combination to the ^{3}H-CQ control. The data for all three strains tested are expressed below as three independent experiments performed in triplicate.

In D10, none of the tested compounds significantly increased CQ uptake when compared to the control of parasitized red blood cell (pRBC) at all the concentrations tested. This confirms the prediction that there are no significant differences in CQ accumulation among all the compounds tested in the CQ sensitive clone.

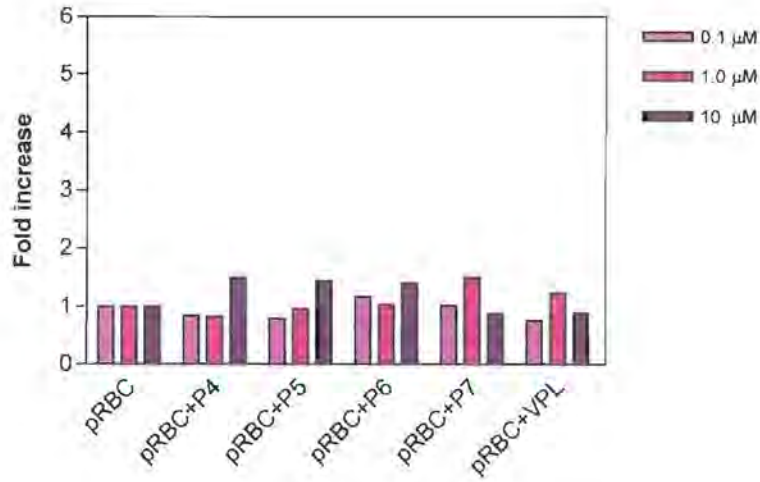

Figure 5.3.3-(A). Fold increase in ^{3}H-CQ uptake with combinations of drugs at different concentrations used on CQ^{S}, D10.

Against the CQ^{R} strain, K1, the compounds potentiated CQ uptake to an extent of 3 to 6 fold with the control, **VPL** exhibiting a 6 fold increase in CQ uptake at a drug concentration of 0.1 μM in the same assay (Fig. 5.3.3-B). At a higher drug concentration of 1.0 μM, compound **P7** showed an improved 8–fold increase in CQ uptake. In addition, the investigation at a concentration of 10 μM (100 times more than the lowest concentration of 0.1 μM tested) showed no further enhancement of CQ accumulation among all the drugs tested; this suggested that there is a saturation point in ^{3}H-CQ uptake. This may be due to toxic effects as a result of the high concentration of the compounds used (approximately 100 times their IC_{50}). Similarly, no significant difference in CQ resistance reversal activity was found for all the drugs tested at a concentration of 0.1 μM in RSA11. However, at a concentration of 1 μM, compound **P7** revealed a marked activity in potentiating CQ uptake which was 4-fold higher than **VPL** (2-fold). No significant CQ potentiation was observed for any of the compounds at 10 μM.

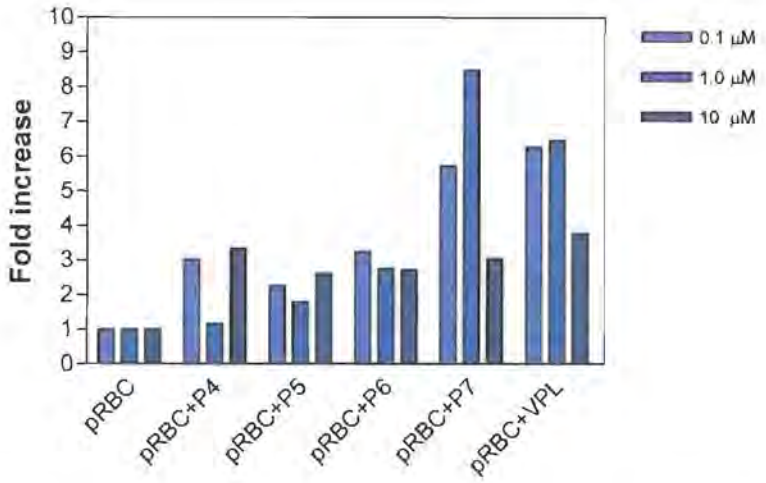

Figure 5.3.3-(B). Fold increase in ^{3}H-CQ uptake with combinations of drugs at different concentrations used on CQ^{R}, K1.

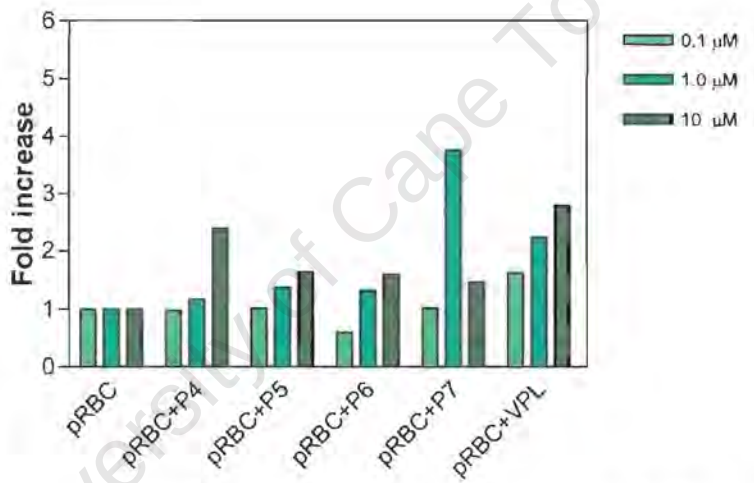

Fig. 5.3.3-(C). Fold increase in ^{3}H-CQ uptake with combinations of drugs at different concentrations used on CQ^{R}, RSA11.

When the compounds are compared within CQ^{R} strains, clearly compound **P7** is the most probable candidate as a resistance reversal agent among all the synthesized compounds. This compound not only exhibited weak to moderate intrinsic antimalarial activity (Table 5.3.1), which is ideal for a chemosensitizer, but also enhanced CQ action in a resistance reversal experiment (Table 5.3.2.1), a result confirmed in CQ accumulation experiments (Fig. 5.3.3). Additionally, it is noteworthy that compound **P7** was shown to possess the highest antimalarial activity of all the compounds tested and it even has better activity than CQ against CQ^{R} K1 strain.

5.3.4 Cytotoxicity screening

Despite the establishment of *in vitro* analyses against the infectious parasite cultures, it is also crucial to substantiate the cytotoxicity of a drug used at its therapeutic concentration. Cytotoxicity screening *in vitro* was achieved by the use of Chinese Hamster Ovarian (CHO) cells in MTT assays. Positive controls of daunomycin as well as the novel products synthesized were investigated. In this assessment, the same concentration range chosen to test resistance reversal assays was used on mammalian cells. The results are presented as percentage of viable CHO cells versus the logarithm of particular drug concentration in μM shown in Fig. 5.3.4.

The IC_{50} value of the standard, daunomycin, was 3.25±0.39 μM in CHO cell lines (Fig. 5.3.4-A). Compounds **P4**, **P5**and **P6** were shown to be non-toxic against the same cell line with 100% cell viability even at the highest concentration of 100 μg/ml (Fig. 5.3.4-B,-C and -D). Compound **P7** demonstrated a cytotoxic effect at a concentration of 125.89±3.15 μM which nevertheless was much higher than its antimalarial IC_{50} value (< 5 μM) among the *P. falciparum* parasites tested (Fig. 5.3.4-E). This indicates that compound **P7** is selectively cytotoxic for *P. falciparum*. Therefore, compound **P7** may be regarded as the hit molecule warranting further modifications and investigations as a potential lead compound.

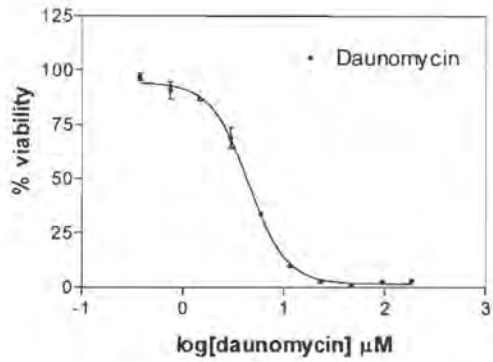

A. Cytotoxicity effect of daunomycin on CHO

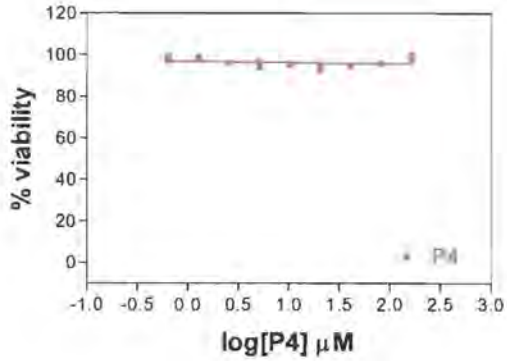

B. Cytotoxicity effect of of **P4** on CHO

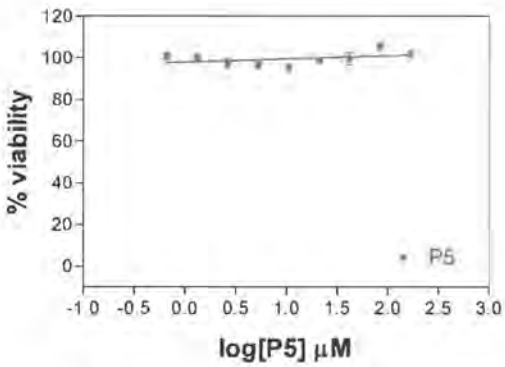

C. Cytotoxicity effect of **P5** on CHO

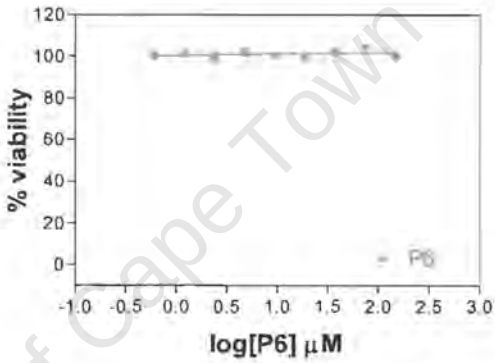

D. Cytotoxicity effect of of **P6** on CHO

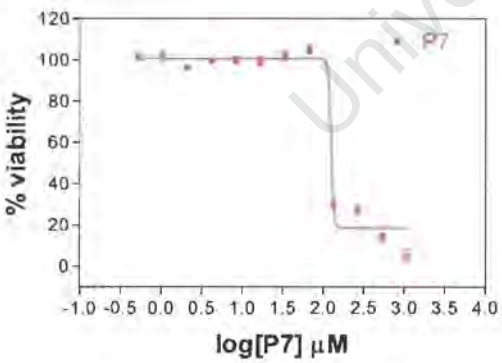

E. Cytotoxicity effect of **P7** on CHO

Figure 5.3.4. Cytotoxicity measurement of various compounds on CHO.

5.3.5 Further investigation of compound P7 using isobologram analysis

In order to understand the interaction of compound **P7** with CQ, a modified isobologram analysis protocol from Chawira and Warhurst (1987) was employed. Isobologram analysis (Section 3.2.3.2) involves graphic representation using fixed ratios of predetermined concentrations to determine the interactions of two different chemotherapeutic agents (see introduction). If the effect is synergistic, the parasite viability values at the fixed ratios for both CQ and **P7** are illustrated below the line and antagonism is indicated by values above the line.

In assessing the clinical potential of a combination of CQ with compound **P7**, the isobologram method was used (Fig. 5.3.5). An additive effect was observed against both CQ^S and CQ^R strains when CQ and **P7** were used at their corresponding IC_{50} concentrations (Fig. 5.3.5-A). This suggests that compound **P7** and CQ did not compete for the same binding site and there were no drug interactions. In addition, a more detailed assessment was made in a CQ^R strain by mixing the cocktails of CQ at its IC_{50} and IC_{25} concentrations with the toxic dose of **P7**. Both studies showed synergistic effects against RSA11. This indicated that there could be a drug interaction at the pharmacological site of action in falciparum malaria. In an attempt to realise a potential clinical combination, the IC_1 and IC_{10} of both CQ and **P7** were combined and examined (Fig. 5.3.5-C). However, both combinations demonstrated no better than an antagonistic effect, suggesting that compound **P7** and CQ interacted with each other to compete for the same binding site in the RSA11 isolate. To sum up, the isobologram analyses revealed that the best combination of CQ and compound **P7** is at their corresponding 50% inhibitory concentration.

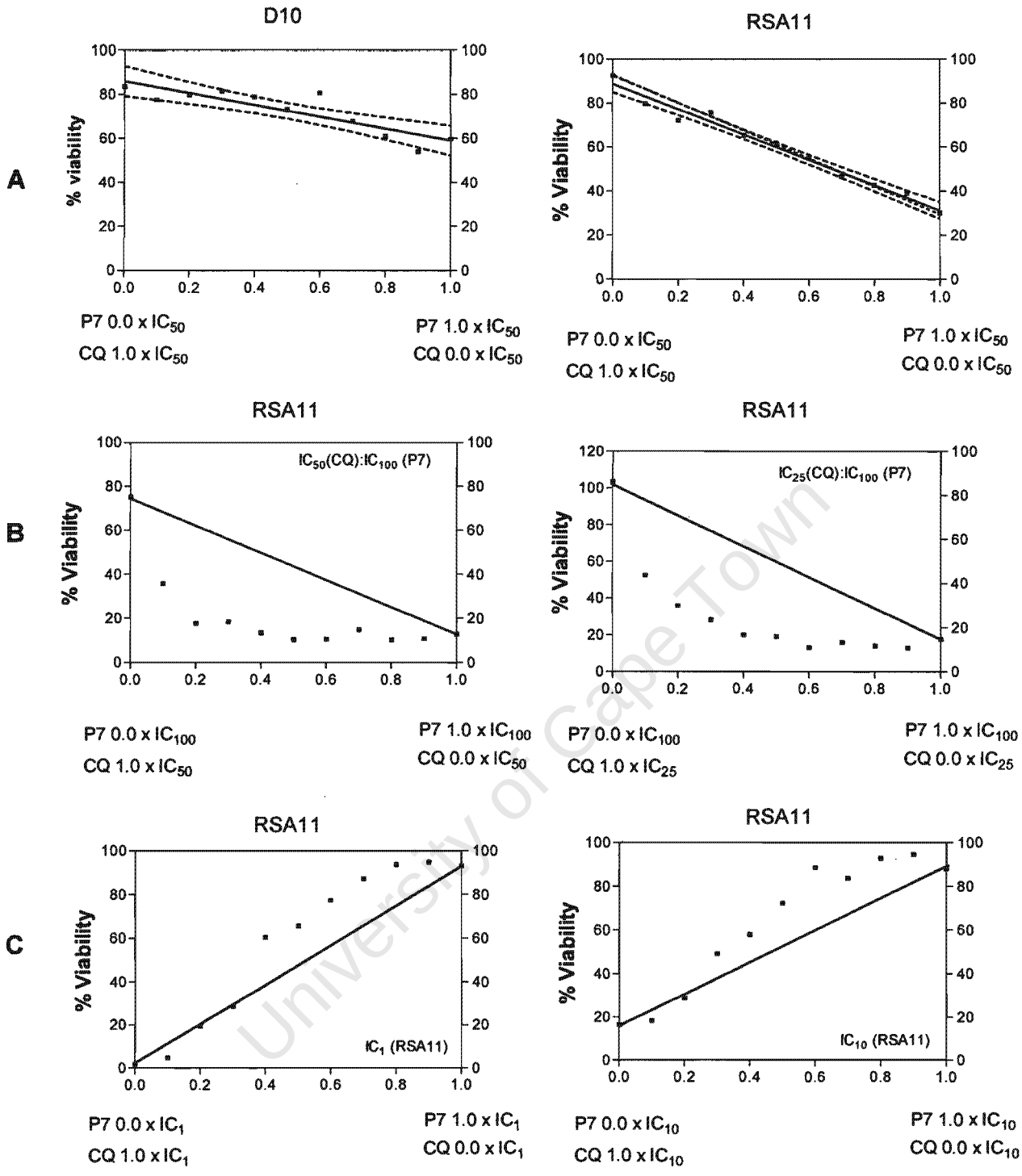

Fig. 5.3.5

A. Additive effect illustrated by the combinations of CQ and **P7** at their predetermined IC_{50} (straight line) against D10 and RSA11 with 95% confidence interval shown in dashed lines.

B. Synergistic effect shown by combinations of different ratios of CQ with **P7** at its toxic concentration on RSA11.

C. Antagonism effect demonstrated by the points above the joint line with the combinations of CQ and **P7** at fixed ratios of IC_1 and IC_{10}, respectively on RSA11.

Comparing the antiplasmodial activities of compound **P7** and amodiaquine (AQ), which is relatively active against CQ resistant parasites despite its structural analogy to CQ, the structural similarities observed are a tertiary nitrogen atom and the aromatic structural features. In addition, the major difference between CQ and AQ is the extra phenolic group that AQ contains. Collectively, this suggests that the highest antiplasmodial activity **P7** possesses among the compounds tested may be due to the tricyclic hydrophobic chemical feature. The importance of the 4-amino-7-chloroquinoline moiety in binding to the haem may account for the superior antiplasmodial activity of CQ and AQ relative to compound **P7**. The tricyclic moiety of **P7** may be involved in binding to haem, albeit presumably weakly, which may account for the superior antiplasmodial activity of **P7** relative to the other synthesized compounds. Possible binding to haem of compound **P7** may be enhanced by further structure-activity relationship studies focusing on the nature and relative position (relative to the side chain) of the tricyclic (or even bicyclic) moiety.

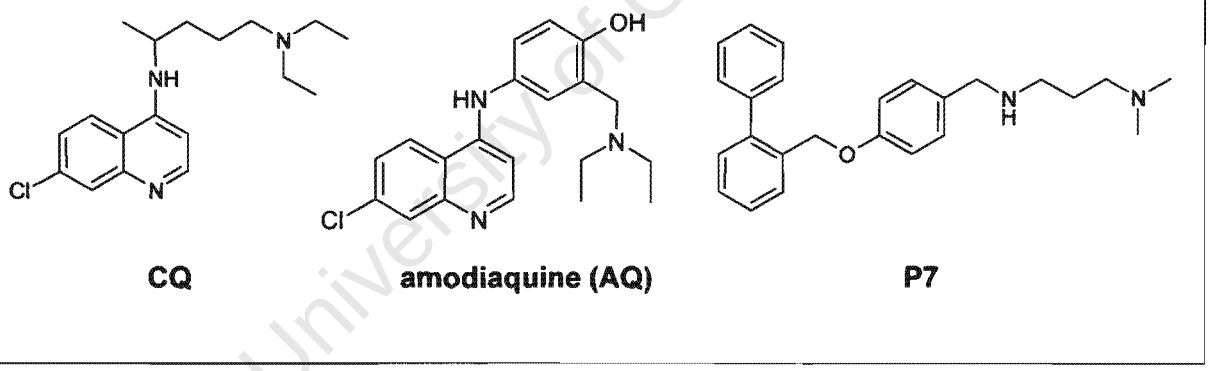

CQ **amodiaquine (AQ)** **P7**

5.4 Conclusion

This study demonstrated that novel exploratory compounds synthesized all possess intrinsic (albeit weak to modest) antiplasmodial activity against CQ-sensitive and –resistant *P. falciparum* parasites. Further, *in vitro* studies of resistance reversal in *P. falciparum* and cytotoxicity on mammalian cells showed that compound **P7** exhibited the greatest potential as a dual-acting antimalarial agent and CQ-resistance reverser. From a therapeutic point of view, it is infact an advantage to develop dual-acting antimalarial agents as drugs showing both antimalarial and CQ potentiating activity would be

Chapter 6

Screening of a small library of compounds

6. Screening of a small library of compounds

6.1 Introduction

In light of the identification of a privileged biphenyl substructure as a potential chemoreversal pharmacophore, a first generation small library of compounds was generated around the basic structure of this potential pharmacophore. This initial SAR library focused on replacing the flexible alkyl chain with a piperazinyl moiety, Fig. 6.1. In search of potential lead compounds, the biological activity of the novel products will be studied and discussed in this chapter. The assessment of *in vitro* antiplasmodial activity, resistance reversing effect, validation of CQ accumulation and selective cytotoxicity are also reported.

In chapter 5, compound **P7** was identified as being a worthwhile candidate for future investigation. In this chapter, a small library of novel products are developed based on the compound **P7** as well as chemical features known to be exhibited in existing antimalarial and/or resistance reversers. The objective was to attempt to improve selective cytotoxicity against *P. falciparum* and/or resistance reversal activity from the hit. *In vitro* screenings for antiplasmodial activity, resistance reversing effects, cytotoxicity, as well as careful inspections of their structures are investigated. The structure-activity relationships to be revealed are of interest in order to better understand which substructural features of the molecule are responsible for the antimalarial activity and which for the resistance reversal.

While this work was in progress, a series of dibenzosuberane-based amino alcohol piperazines were described as chemosensitizers active *in vivo* (Osa *et al.*, 2003). Coupled with the identification of compound **P7** during preliminary studies, this prompted the design of a preliminary SAR library. In addition, the methoxy substituent was chosen on the basis of known SAR, which point to the importance of a hydrophobic moiety, a protonatable nitrogen and the presence of Lewis basic sites for effective chemosensitization of resistant *P. falciparum* strains to CQ.

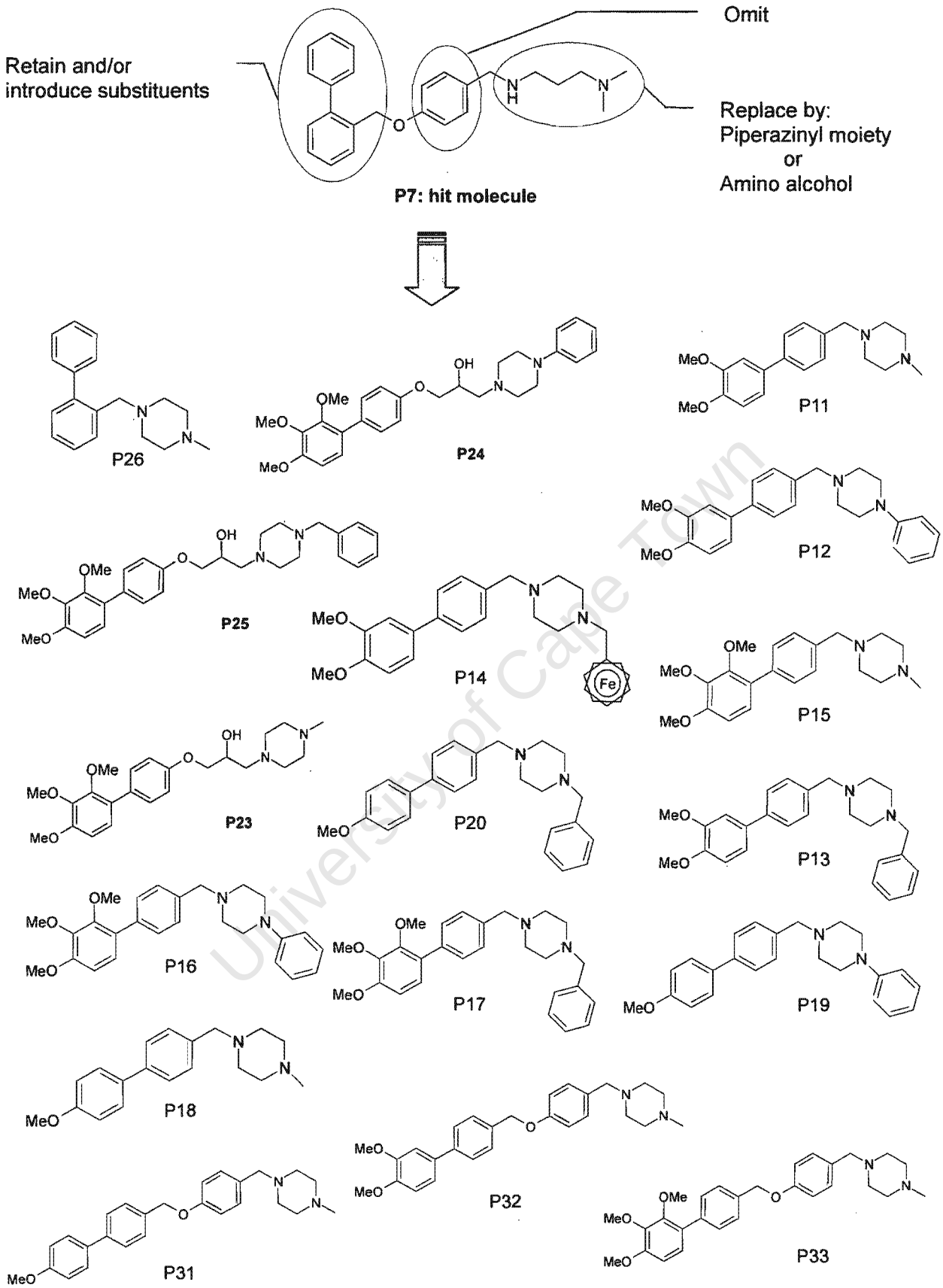

Figure 6.1. Preliminary structure-activity relationship library.

6.2 Results

6.2.1 *In vitro* antiplasmodial activity and cytotoxicity screening of modified compounds (Phase II)

The details of the synthesis and structural elucidation of the novel compounds are recorded in chapter 4.

The small library of compounds produced were firstly examined *in vitro* for intrinsic antimalarial activity against a CQ-sensitive strain, D10, and two CQ-resistant strains, K1 and RSA11, for comparison purposes. The results of dose-response curves for each strain are shown in Appendix 3 (Fig. 6.2.1.1 – Fig 6.2.1.3) and the corresponding IC_{50} values as well as their chemical structures are listed in Table 6.2.1 and summarized in Fig. 6.2.2.4-A. The resistance index (R_I), which is used to evaluate whether novel antimalarials are potential agents against CQ resistant parasites, are also listed in the table and discussed in section 6.3.1.

To measure cell chemosensitivity and selectivity of the modified compounds, concurrent cytotoxic analyses were conducted in a Chinese Hamster Ovarian cell line. Cell growth inhibition was monitored for the entire class of compounds (Fig. 6.2.1.4). However, no attempt was made to determine the IC_{50} (CHO) at concentrations in excess of $100\mu gml^{-1}$ as non-specific toxicity is often shown at such high concentrations. The IC_{50} (CHO) can also be found in Table 6.2.1 for comparison purposes.

The synthesized compounds displayed a range of antiplasmodial activity against *P. falciparum* strains, D10 (CQ-sensitive), K1 and RSA11 (CQ-resistant). Compound **P14**, **P17**, **P25**, **P26**, **P31**, **P32** and **P33** possess the greatest antiplasmodial activity against CQ^R parasites with the analogue **P26** exhibiting a reduced activity towards D10, but greater activity against K1 and RSA11. In addition, all the novel products were shown to have a wide safety margin against mammalian cells.

6.2.2 *In vitro* resistance reversal effect in *P. falciparum*

The *in vitro* dose-response curves of the combination studies were conducted against D10, K1 and RSA11 in a similar manner to the dose-response curve experiments (Section 3.2.3.1) and the subsequent results are shown in Appendix 3 (Fig. 6.2.2.1, Fig. 6.2.2.2 and Fig. 6.2.2.3). The concentration for each potential resistance modulator used for the combination study was derived from Fig. 6.2.1.1, 6.2.1.2 and 6.2.1.3 (Appendix 3) for D10, K1 and RSA11, respectively. A sub-lethal concentration of 1μM was selected for most of the compounds in this experiment against both CQ-sensitive and -resistant malaria cell cultures. A concentration of 0.25 μM was chosen for **P14** and **P26** which were toxic to the parasites at a concentration of 1.0 μM.

For comparison purposes, the corresponding IC_{50} values for each compound alone and in combination with CQ are summarised in **Table 6.2.1**. In addition to the 50% inhibitory concentration (IC_{50}), the resistance modification index (RMI = $IC_{50\ (CQ + drug)}$/ $IC_{50\ (CQ\ alone)}$) (Section 5.3.2), which as mentioned before gives an indication of the relative activity of the compound in the CQ-resistant isolates of falciparum malaria, are also recorded. Together with the tested candidates, the standard and the positive control of CQ and verapamil can also be found in the table.

The 50% inhibitory concentration of CQ plus single compound in D10, K1 and RSA11 are summarized in Fig. 6.2.2.4-B (shown in histograms). For comparative purposes, the RMI for K1 and RSA11 isolates are also illustrated in connected purple and red lines, respectively.

Table 6.2.1 *In vitro* antiplasmodial activity and resistance reversal effect of each drug alone and in combination with CQ (Phase II) in D10, K1 and RSA11.

Compound	Antimalarial activity IC_{50} (µM)					Resistance reversal activity IC_{50} (µM)					IC_{50} (µM)
	D10	K1	RSA11	R_I K1	R_I RSA11	D10	K1	RSA11	RMI K1	RMI RSA11	CHO
CQ 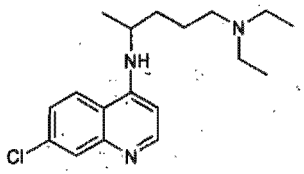	0.024 ± 0.004	0.196 ± 0.047	0.181 ± 0.045	—	—	—	—	—	—	—	ND
Verapamil 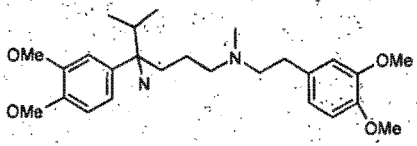	ND	ND	ND	—	—	ND	0.126 ± 0.042	0.109 ± 0.033	0.64	0.60	ND
Product 11 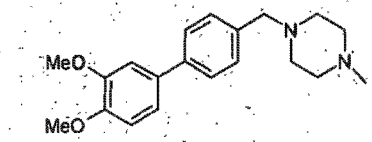	17.54 ± 4.11	10.30 ± 2.91	11.55 ± 1.54	0.59	0.66	0.021 ± 0.004	0.188 ± 0.031	0.136 ± 0.022	0.96	0.75	> 100
Product 12 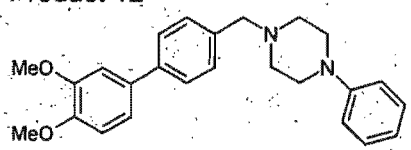	22.13 ± 4.69	19.65 ± 4.04	18.51 ± 2.62	0.89	0.84	0.019 ± 0.003	0.193 ± 0.031	0.140 ± 0.018	0.98	0.77	> 100

For D10, K1 and RSA11, the data are expressed as the mean IC_{50} ± SD (µM) of three independent experiments each performed in duplicate.
For CHO cells, the data are expressed as the mean IC_{50} ± SD (µM) of three independent experiments each performed in triplicate.
$R_I = IC_{50}^{K1 \text{ or } RSA11} / IC_{50}^{D10}$
RMI = IC_{50} (CQ + drug) / IC_{50} (CQ alone).

Table 6.2.1 (Continued) *In vitro* antiplasmodial activity and resistance reversal effect of each drug alone and in combination with CQ (Phase II) in D10, K1 and RSA11.

Compound	Antimalarial activity IC_{50} (μM)					Resistance reversal activity IC_{50} (μM)					IC_{50} (μM)
	D10	K1	RSA11	R_I K1	R_I RSA11	D10	K1	RSA11	RMI K1	RMI RSA11	CHO
Product 13 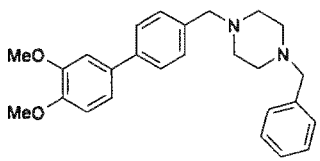	6.36 ± 2.20	15.46 ± 3.48	4.98 ± 1.22	2.43	0.78	0.019 ± 0.004	0.241 ± 0.040	0.218 ± 0.054	1.23	1.20	Non-toxic
Product 14 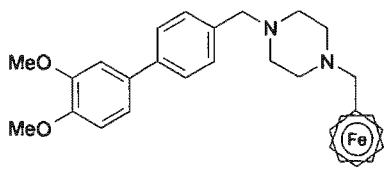	0.73 ± 0.14	1.49 ± 0.84	0.75 ± 0.28	2.04	1.03	0.036 ± 0.007	0.162 ± 0.075	0.096 ± 0.045	0.83	0.53	> 100 (173.78)
Product 15 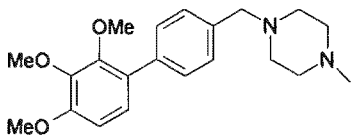	30.63± 1.53	9.90 ± 1.38	10.32 ± 1.81	0.32	0.34	0.020 ± 0.003	0.165 ± 0.035	0.146 ± 0.030	0.84	0.80	> 100
Product 16 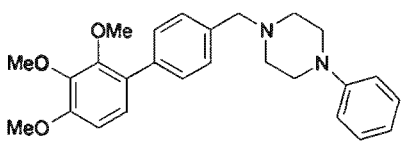	7.69 ± 1.53	19.50 ± 1.50	8.31 ± 1.13	2.54	1.08	0.021 ± 0.005	0.208 ± 0.055	0.107 ± 0.016	1.06	0.59	Non-toxic

For D10, K1 and RSA11, the data are expressed as the mean IC_{50} ± SD (μM) of three independent experiments each performed in duplicate.
For CHO cells, the data are expressed as the mean IC_{50} ± SD (μM) of three independent experiments each performed in triplicate.
$R_I = IC_{50}^{K1 \text{ or } RSA11} / IC_{50}^{D10}$
RMI = IC_{50} (CQ + drug) / IC_{50} (CQ alone).

Table 6.2.1 (Continued) *In vitro* antiplasmodial activity and resistance reversal effect of each drug alone and in combination with CQ (Phase II) in D10, K1 and RSA11.

Compound	Antimalarial activity IC_{50} (μM)					Resistance reversal activity IC_{50} (μM)					IC_{50} (μM)
	D10	K1	RSA11	R_I K1	R_I RSA11	D10	K1	RSA11	RMI K1	RMI RSA11	CHO
Product 17 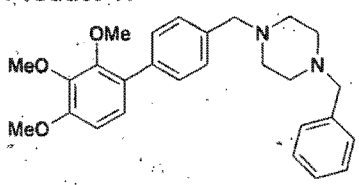	4.54 ± 1.35	1.98 ± 0.62	2.93 ± 1.07	0.44	0.65	0.019 ± 0.003	0.186 ± 0.051	0.143 ± 0.023	0.95	0.79	> 100 (134.90)
Product 18 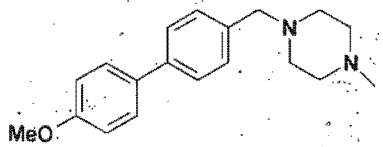	16.88 ± 3.36	19.64 ± 4.19	11.49 ± 2.58	1.18	0.68	0.023 ± 0.006	0.183 ± 0.030	0.149 ± 0.041	0.93	0.82	> 100
Product 19 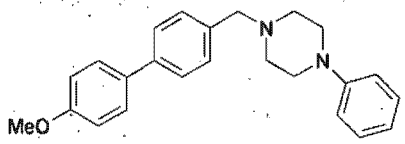	8.26 ± 1.71	16.90 ± 4.21	9.35 ± 2.40	2.05	1.13	0.033 ± 0.007	0.205 ± 0.060	0.106 ± 0.023	1.04	0.58	> 100 (128.82)
Product 20 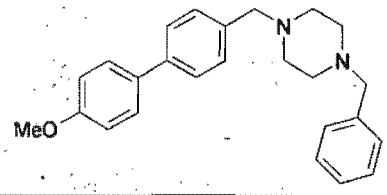	8.17 ± 1.82	25.95 ± 1.58	7.70 ± 1.16	3.18	0.94	0.019 ± 0.004	0.235 ± 0.055	0.153 ± 0.026	1.20	0.84	Non-toxic

For D10, K1 and RSA11, the data are expressed as the mean IC_{50} ± SD (μM) of three independent experiments each performed in duplicate.
For CHO cells, the data are expressed as the mean IC_{50} ± SD (μM) of three independent experiments each performed in triplicate.
$R_I = IC_{50}^{K1 \text{ or } RSA11} / IC_{50}^{D10}$
RMI = IC_{50} (CQ + drug) / IC_{50} (CQ alone).

Table 6.2.1 (Continued) *In vitro* antiplasmodial activity and resistance reversal effect of each drug alone and in combination with CQ (Phase II) in D10, K1 and RSA11.

Compound	Antimalarial activity IC_{50} (μM)					Resistance reversal activity IC_{50} (μM)					IC_{50} (μM)
	D10	K1	RSA11	R_I K1	R_I RSA11	D10	K1	RSA11	RMI K1	RMI RSA11	CHO
Product 23 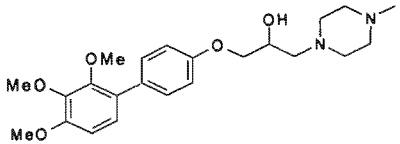	23.40 ± 4.04	8.84 ± 1.56	11.42 ± 1.66	0.38	0.49	0.022 ± 0.002	0.162 ± 0.035	0.122 ± 0.026	0.83	0.67	> 100
Product 24 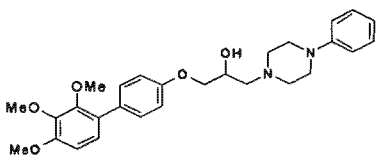	14.07 ± 2.34	5.46 ± 1.05	5.43 ± 1.07	0.39	0.39	0.013 ± 0.003	0.212 ± 0.066	0.137 ± 0.034	1.08	0.77	> 100
Product 25 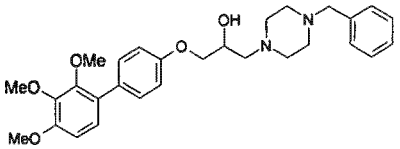	9.56 ± 1.48	2.02 ± 0.74	3.37 ± 1.11	0.21	0.35	0.022 ± 0.005	0.225 ± 0.040	0.137 ± 0.029	1.15	0.76	> 100
Product 26 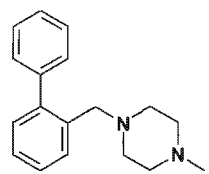	51.40 ± 1.82	0.60 ± 0.06	0.42 ± 0.17	0.01	0.01	0.021 ± 0.003	0.165 ± 0.037	0.091 ± 0.014	0.84	0.50	> 100

For D10, K1 and RSA11, the data are expressed as the mean IC_{50} ± SD (μM) of three independent experiments each performed in duplicate.
For CHO cells, the data are expressed as the mean IC_{50} ± SD (μM) of three independent experiments each performed in triplicate.
$R_I = IC_{50}^{K1 \text{ or } RSA11} / IC_{50}^{D10}$
RMI = IC_{50} (CQ + drug) / IC_{50} (CQ alone).

Table 6.2.1 (Continued) *In vitro* antiplasmodial activity and resistance reversal effect of each drug alone and in combination with CQ (Phase II) in D10, K1 and RSA11.

Compound	Antimalarial activity IC_{50} (µM)					Resistance reversal activity IC_{50} (µM)					IC_{50} (µM)
	D10	K1	RSA11	R_I K1	R_I RSA11	D10	K1	RSA11	RMI K1	RMI RSA11	CHO
Product 31 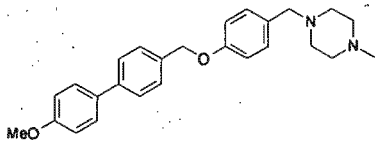	3.17 ± 1.72	4.14 ± 1.91	4.32 ± 1.36	1.31	1.36	0.017 ± 0.002	0.226 ± 0.059	0.137 ± 0.018	1.15	0.77	9.97±2.36
Product 32 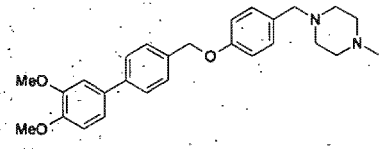	3.69 ± 0.17	4.14 ± 1.44	4.26 ± 1.65	1.12	1.15	0.017 ± 0.006	0.182 ± 0.068	0.056 ± 0.026	0.93	0.31	> 100 (173.78)
Product 33 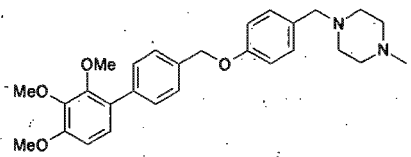	7.24 ± 1.46	6.18 ± 1.58	5.10 ± 1.61	0.85	0.70	0.022 ± 0.004	0.173 ± 0.030	0.149 ± 0.024	0.88	0.82	> 100 (131.82)

For D10, K1 and RSA11, the data are expressed as the mean IC_{50} ± SD (µM) of three independent experiments each performed in duplicate.
For CHO cells, the data are expressed as the mean IC_{50} ± SD (µM) of three independent experiments each performed in triplicate.
$R_I = IC_{50}^{K1 \text{ or } RSA11} / IC_{50}^{D10}$
RMI = IC_{50} (CQ + drug) / IC_{50} (CQ alone).

A

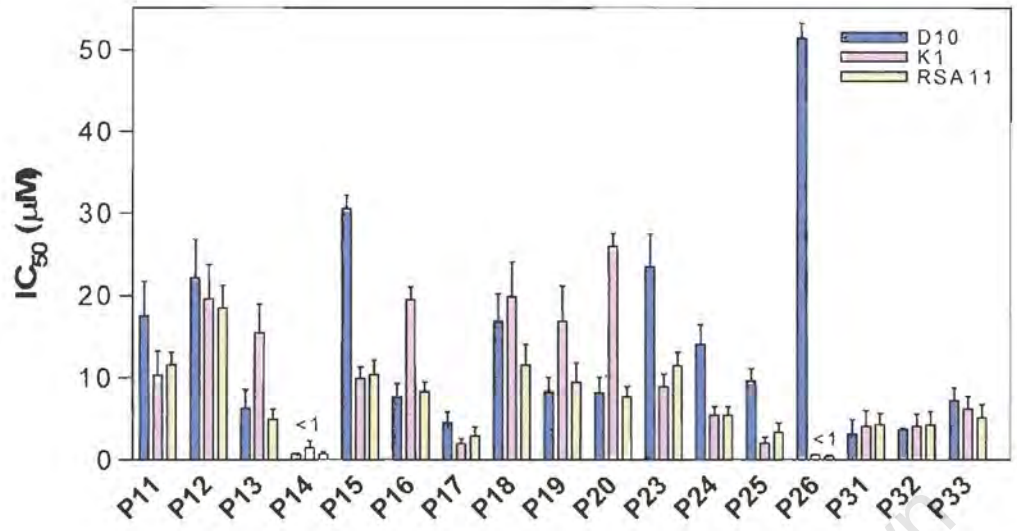

B

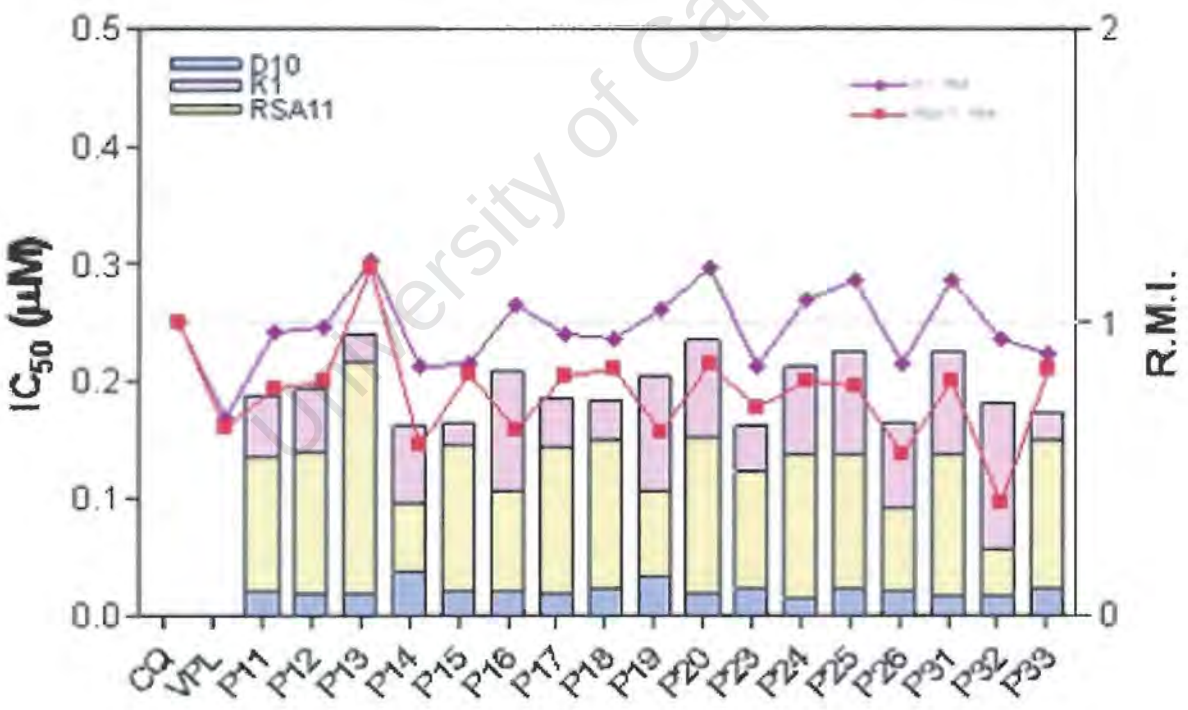

Figure 6.2.2.4.

A. Summary of the IC_{50} values of the synthesized compounds against D10, K1 and RSA11.

B. Summary of the IC_{50} of CQ plus each synthesized compound and the resistance modification index (R.M.I.) of the tested compounds against D10, K1 and RSA11.

6.2.3 Enhancement of radioactive CQ accumulation

Incorporation of radiolabeled CQ, ^{3}H-CQ, was used as the measured parameter of the response of the parasites to the drug in this study. For comparative purposes, stimulation of CQ accumulation by the range of compounds, tested at both 5 μM and 50 μM is summarized in Fig. 6.3.3.1.

Verapamil has been shown to increase CQ accumulation by 3 ~ 5 fold within CQ^{R} clones (Martin *et al.*, 1987; Adovelande *et al.*, 1998). In our hands, verapamil also reversed CQ resistance by enhancing CQ uptake within the parasites by 3 ~ 6 fold at concentrations of 5 μM and 50μM. Moreover, the potentiation ability of verapamil was found to reach a saturation point when 50 μM was tested which suggests that it is toxic to the parasites at this concentration so that no further enhancement of CQ accumulation could be shown.

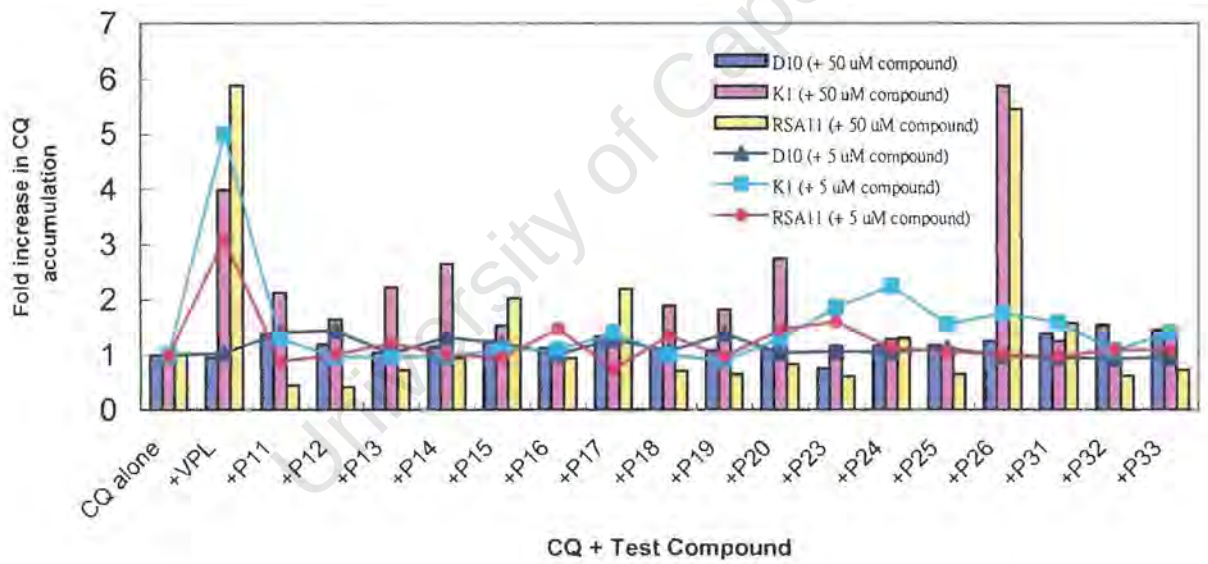

Figure 6.3.3.1. Summary of the fold increase in CQ accumulation against CQ plus single compound at 5 μM and 50 μM in D10, K1 and RSA11 of *P falciparum*.

As illustrated in Fig. 6.2.2.4-B (connected red line), all the synthesized compounds, except **P13**, showed improved CQ resistance reversing ability as their resistance modification indexes (RMI) lay below 1. In addition, the ability of the compounds to stimulate CQ accumulation in the CQ^{R} strain RSA11 was studied. The control, CQ-sensitive D10 strain, showed no increase in CQ accumulation when CQ was

combined with each single compound in accumulation measurements. A concentration of 5 μM was chosen as the lowest concentration for the envisaged investigations.

Despite the CQ+verapamil combination exhibiting a more pronounced effect at the 5 μM level, none of the compounds induced any marked increase in CQ accumulation within resistant parasites (Fig. 6.3.3.1, connected lines). However, when a 10-times higher concentration was used, compounds **P15** and **P17** showed a 2-fold increment in CQ uptake while compound **P26** enhanced CQ accumulation 5- and 6-fold in RSA11 (yellow bar) and K1 (pink bar), respectively.

It is well described that CQ resistant strains accumulate less CQ than their drug-sensitive counterparts (Fitch, 1970). Potential CQ resistance reverser **P26** was regarded as the classical resistance modulator as it potentiated CQ accumulation within resistant parasites and also showed significant reversal activity. Nevertheless, several structurally related compounds (**P16**, **P19**, **P23**, and **P32**) showed marked resistance reversal effects, compound **P32** in particular, without stimulating CQ uptake within the resistant parasites. It is reasonable to hypothesize that there may be another category of CQ resistance modulators, which reverse CQ resistance without potentiating CQ uptake (Chibale *et al.,* 2003). At present, the actual CQ resistance mechanism is still not known and the exact mechanism for the reduced CQ uptake by resistant strains is unclear. However, the mutated PfCRT transmembrane protein uncovered as the determinant of reversible CQ resistance by Fidock and his colleagues (Fidock *et al.,* 2000) will hopefully lead to a better understanding of CQ resistance. Further work could be done to establish whether the synthesized compounds interact with the PfCRT protein.

6.3 Discussion

6.3.1 *In vitro* antiplasmodial activity, cytotoxicity screening and resistance reversal of the synthesized compounds

From the library of synthesized compounds, compound **P14** was shown to possess the greatest antiplasmodial activity *in vitro*. It exhibited strong intrinsic antimalarial activity in D10 (IC_{50} = 0.73 μM), K1 (IC_{50} = 1.49 μM) and RSA11 (IC_{50} = 0.75 μM). Against RSA11

the activity was comparable to CQ (Table 6.2.1). Compound **P26** was found to be more effective against CQ resistant *P. falciparum* than the sensitive D10 (IC_{50}^{K1} = 0.60 μM, IC_{50}^{RSA11} = 0.42 μM). Nevertheless, compounds **P14** and **P26** are less potent compared to **P7**, the hit compound previously identified (IC_{50}^{D10} = 0.174 μM, IC_{50}^{K1} = 0.148 μM, IC_{50}^{RSA11} = 0.600 μM). Thus, all of the intrinsic activities of the modified products were improved.

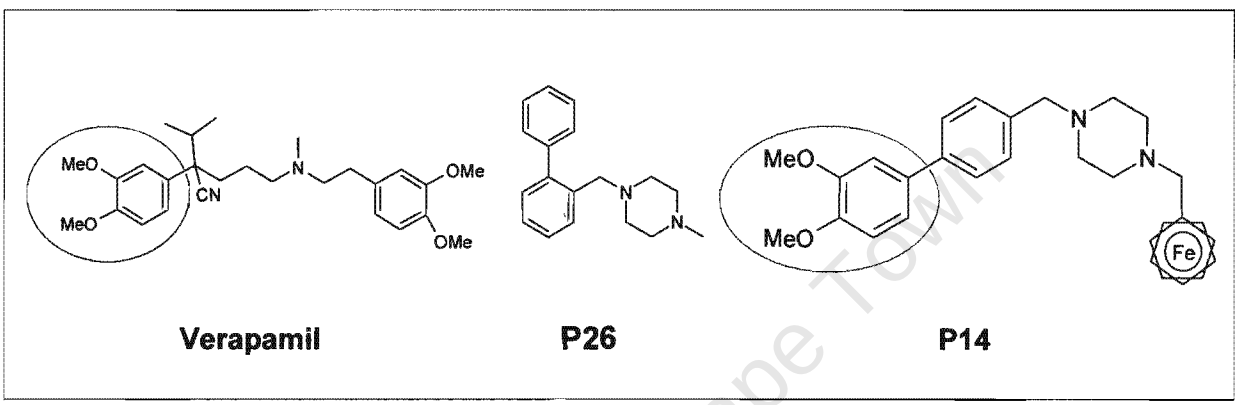

Figure 6.4.1.1. Chemical structures of verapamil, compound **P14** and **P26**.

In order to establish which structural features are important for antiplasmodial and/or CQ resistance reversal activity, **P26** the simplest compound, incorporating a potential pharmacophoric biaryl motif and a piperazinyl substructure, was designed and synthesized. The piperazinyl moiety was incorporated based upon its presence in previously disclosed CQ resistance reversal agents (Osa *et al.*, 2003). Compound **P26** was found to be approximately 100 times more potent in K1 and RSA11 than in D10 as an antiplasmodial agent (R_I^{K1}=R_I^{RSA11}=0.01). This behaviour of compound **P26** is reminiscent of aryl methanols exemplified by mefloquine which are substantially more active in K1 than in D10. The structural dissimilarity between **P26** and mefloquine warrants further investigation into the mechanism of action of **P26** especially in view of its very limited cytotoxicity towards mammalian cells (IC_{50}^{CHO} > 100 μM).

Furthermore, the general finding for most compounds that the resistance reversing ability is more pronounced against African CQ resistant strain RSA11 than against the K1 clone was also observed in compound **P26** (RMI_{RSA11} = 0.50; RMI_{K1} = 0.84). In summary, the beneficial selective cytotoxicity was retained in **P26** after the hit modifications, in which the alkyl amino side chain in **P7** was substituted with a piperazinyl substructure. Moreover, the alteration of piperazinyl substitution improved the intrinsic antimalarial activity for potential chemosensitizers as well as retaining the reversal properties of the lead.

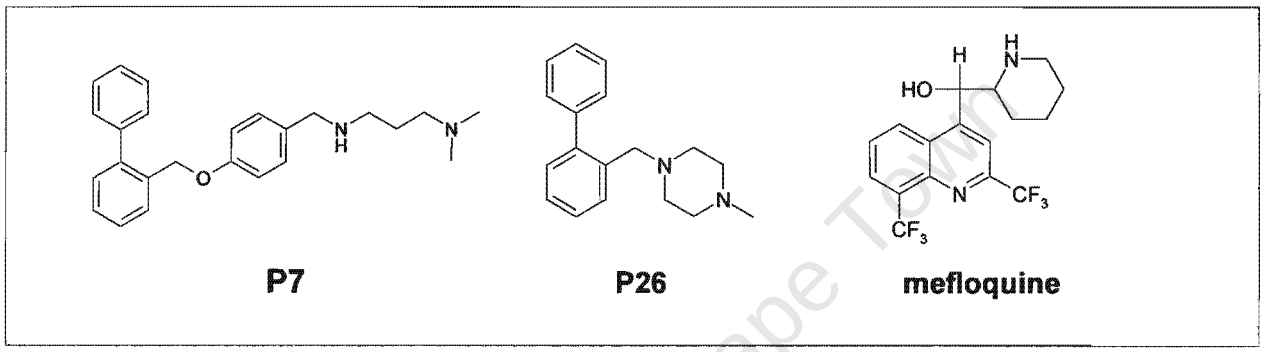

Figure 6.4.1.2. Chemical structures of hit compound **P7**, compound **P26** and mefloquine.

Ferrocene is an organometallic complex, which has a sandwich structure with the Fe atom sandwiched between two five-membered rings. It has a high hydrophobicity and low toxicity *in vivo*, which makes it very attractive for drug design (Biot, 2004). In view of this, CQ and the hydrophobic and cytotoxic ferrocene were incorporated into organometallic chloroquine analogues (Biot *et al.*, 1997). One of the organometallic analogues, ferroquine, was investigated extensively and showed high antimalarial activity *in vitro* as well as *in vivo* in mice infected with *P.* berghei *N.* and *P. yoelii NS* (Fig. 6.4.1.3) (Biot *et al.*, 1997). Ferroquine was believed to be able to diffuse across the parasite membranes freely since it has a high lipophilicity as well as providing an additional anchoring point suitable for hydrophobic interactions with haematin. In line with this, Pradines *et al.*, 2001 described such an organometallic chloroquine analogue as a possible promising alternative prophylactic agent to combat CQ resistant malaria.

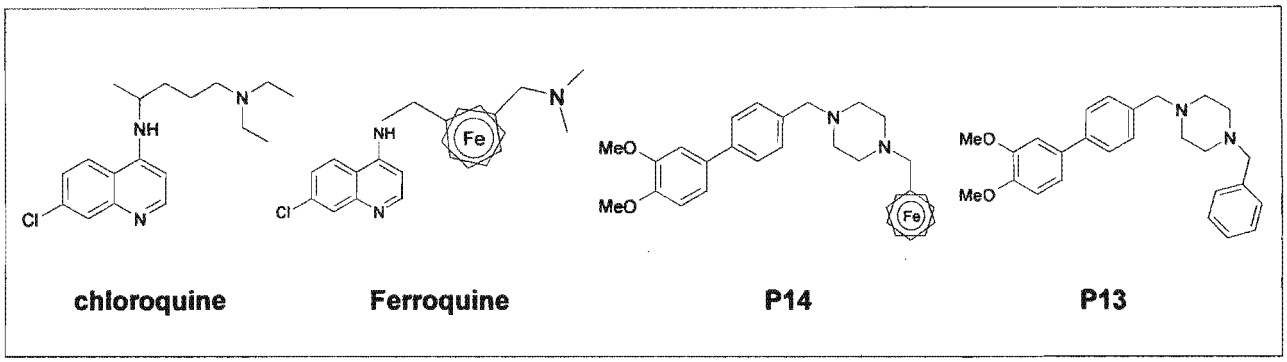

Figure 6.4.1.3. Structures of chloroquine and organometallic chloroquine.

In light of this, a potential ferrocene containing resistance modulator, **P14**, was synthesized for direct comparison with compound **P13**. This was with a view to exploring any potential beneficial effects of the ferrocenyl moiety. Like ferroquine, compound **P14** showed antiplasmodial activity not only towards CQ susceptible *falciparum*, but also to CQ resistant malaria parasites (IC_{50}^{D10}= 0.73 μM; IC_{50}^{K1}= 1.49 μM; IC_{50}^{RSA11}= 0.75 μM), however, it was less active in K1 (R_I^{K1}= 2.04). In addition, this compound also exhibits a high resistance reversal effect on RSA11 (RMI = 0.53) similar to that of verapamil (RMI = 0.60). It is noteworthy that in addition to the concentration-dependent dual (antiplasmodial and chemosensitization) activity of **P14**, this compound was found to be non-cytotoxic towards the mammalian CHO cell line at a concentration of 100 μg/ml. The partial structural similarity between verapamil and **P14** with respect to the 3, 4-dimethoxyphenyl substructure is also noteworthy. In comparison with its analogue **P13**, compound **P14** showed superior antiplasmodial activities against both CQ^S and CQ^R strains tested (for **P14:** $IC_{50}^{D10, K1 \text{ and } RSA11}$ < 1.5 μM vs. **P13:** $IC_{50}^{D10, K1 \text{ and } RSA11}$ > 5 μM). In line with this, when the ferrocenyl moiety was replaced with a hydrophobic aromatic ring system, compound **P13** displayed an interesting superior activity against RSA11 (R_I^{P13}=0.78 vs R_I^{P14}=1.03) than that of **P14**. In addition to its antiplasmodial property, compound **P14** was shown to possess better resistance reversal activities than its analogue **P13**. This suggests that the ferrocenyl moiety may play an important role, possibly as a hydrophobic and/or lipophilic group, in the dual acting properties against CQ resistant malaria (Fig. 6.4.1.3).

When compared to **P26**, compound **P14** had a greater intrinsic antiplasmodial activity (IC_{50}^{D10} = 0.73 μM, IC_{50}^{K1} = 1.49 μM, IC_{50}^{RSA11} = 0.75) although **P26** was potent in both CQ^R strains (IC_{50}^{D10} = 51.40 μM, IC_{50}^{K1} = 0.60 μM, IC_{50}^{RSA11} = 0.42). In terms of resistance reversal effects, **P26** showed a slightly better activity profile in RSA11 while both compounds possessed a higher degree of chemosensitization than verapamil in this African strain as well as retaining selective cytotoxicity. Based upon this preliminary data, the biphenyl motif and a terminal tertiary amine nitrogen are proposed to play an important role in restoring CQ sensitivity within this series of compounds. The ferrocenyl substituent seems to play a role in aspects of antiplasmodial activity. The lipophilicity of the compound may be a possible factor (Section 6.4.3). However, the role of dimethoxyphenyl substructure was further investigated along with the nature of the piperazinyl unit, section 6.4.2.

6.3.2 Substructural features: methoxy and piperazinyl moieties

As previously mentioned in this thesis (Section 2.2.2.1), previous SAR studies have pointed out the importance of Lewis basic sites on the aromatic hydrophobic unit for effective chemosensitization. This is exemplified by the 3,4-dimethoxyphenyl moiety in verapamil. In this regard, we wished to initially study the influence of the number of methoxy groups on chemosensitization.

Given the importance of a protonatable nitrogen in chemosensitization of resistant malaria parasites, we also wished to study the effect of the nature and number of such nitrogens. Accordingly, *N*-methylpiperazine, phenylpiperazine and benzylpiperazine were selected for preliminary studies (Fig. 6.4.2.1). The products modified from *N*-methylpiperazine and benzylpiperazine both contain two protonatable basic nitrogens. The phenylpiperazine products contain one protonatable nitrogen since the (aniline) nitrogen attached directly to the phenyl ring is less basic due to conjugation of the lone pair of electrons into the aromatic ring.

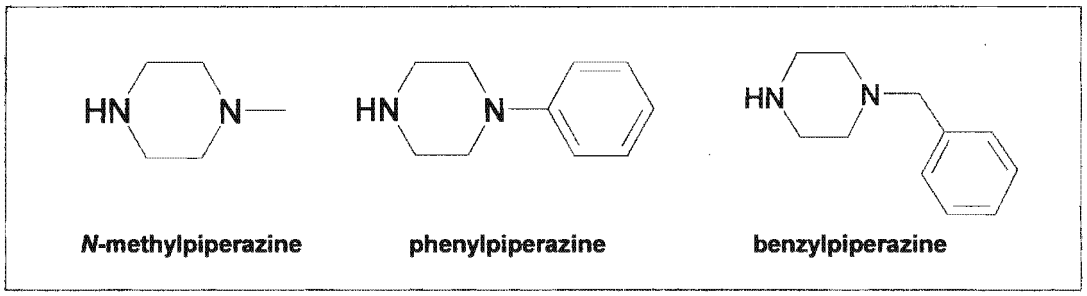

Figure 6.4.2.1. Chemical structures of commercially available piperazines studied.

We also wished to explore the effect of the β-amino alcohol moiety in compounds **P23**, **P24**, and **P25** since this moiety is antimalarial pharmacophore as found in mefloquine. In addition, it is also present in some MDR reversal agents in cancer (Avendaño and Menéndez, 2002). Accordingly, compounds have been grouped on the basis of the aforementioned considerations, Fig. 6.4.2.2.

Among these three closely related chemical analogues in group A, **P11** exhibited the strongest antiplasmodial activity overall (IC_{50}^{D10} = 17.54 μM, IC_{50}^{K1} = 10.03 μM, IC_{50}^{RSA11} = 11.55 μM). In terms of relative activity against CQ resistant malaria, both compounds **P11** and **P12** (R_I < 1) were more active compared to the benzypiperazinyl derivative **P13** (R_I > 1). The concentration dependent dual activity of **P11** and **P12** (RMI_{RSA11} = 0.75) are similar. Both compounds improved their resistance modification index (RMI) to less than 1 in K1. On the other hand, **P13** showed a slightly greater intrinsic antimalarial activity with reduced resistance reversal effect (RMI > 1 for both CQ resistant strains). These data suggest that the benzylpiperazinyl substructure in product **P13** may be more important in antiplasmodial activity than in CQ resistance reversal.

With a view to establishing the effect of the number of methoxy groups in the aromatic ring on both the antiplasmodial and resistance reversal properties, group B and C compounds were targeted.

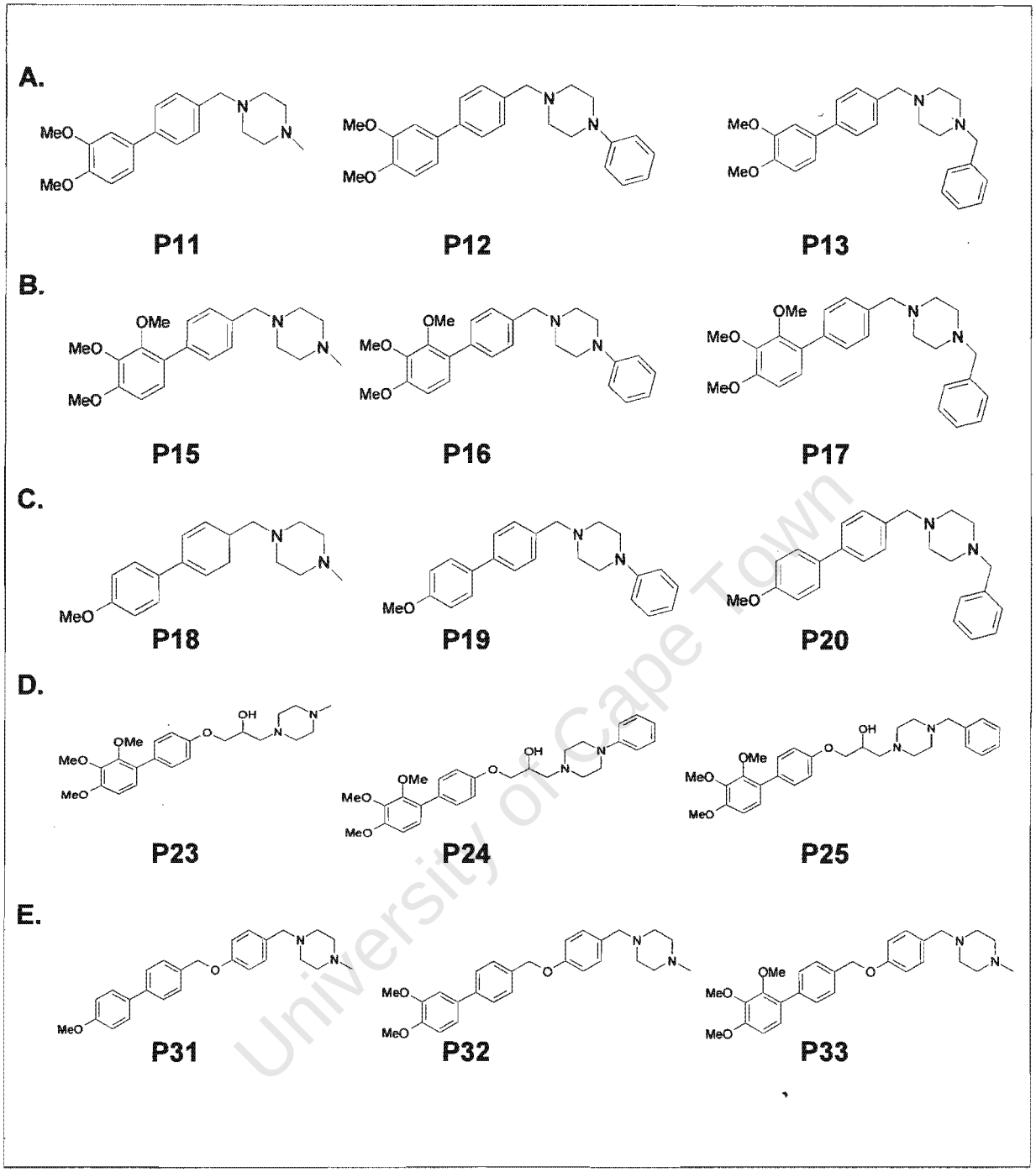

Figure 6.4.2.2. Chemical structures of closely related analogues.

A. Dimethoxybiphenyl scaffold with *N*-methyl-, phenyl- and benzyl- piperazinyl.

B. Trimethoxybiphenyl scaffold with *N*-methyl-, phenyl- and benzyl- piperazinyl.

C. Monomethoxybiphenyl scaffold with *N*-methyl-, phenyl- and benzyl- piperazinyl.

D. Trimethoxybiphenyl β-alcohol scaffold with *N*-methyl-, phenyl- and benzyl-piperazinyl.

E. Extended *N*-methylpiperazinyl side chain with mono-, di- and Tri-methoxybiphenyl substructure.

When compared within group **B**, compound **P17** was expected to exhibit the strongest antiplasmodial activity as it contains the benzylpiperazinyl substructure present in **P13**. In addition, its resistance reversal effect was moderate without much improvement compared to the analogues in group **A**. *N*-methylpiperazine substituted analogue, **P15**, demonstrated approximately 3-times greater antimalarial activity against the CQ resistant isolates than against sensitive D10 (R_I^{K1} = 0.32; R_I^{RSA11} = 0.34) whereas **P16** displayed similar antiplasmodial activity towards CQ-sensitive and -resistant strains (IC_{50}^{D10} = 7.69 μM; IC_5^{RSA11} = 8.31 μM). Comparing compounds **P11** and **P15**, the additional methoxy group in position 2 of **P15** showed no significant differences in either antiplasmodial or chemoreversal activity against *P. falcipaurm* though it demonstrated a better activity against CQ resistant parasites (R_I^{P15} ~ 0.3 vs R_I^{P11} ~ 0.6). Additionally, the comparison between **P12** and **P16** revealed that the extra methoxy group found in the structure of **P16** enhanced the antiplasmodial activity to *ca* 2.5 fold in D10 and (IC_{50}^{P12}=22.13 μM vs. IC_{50}^{P16}=7.69 μM) and RSA11 (IC_{50}^{P12}=18.51 μM vs. IC_{50}^{P16}=8.31μM).

In parallel, compound **P17**, which contains the trimethoxybiphenyl moiety, showed greater antiplasmodial as well as chemoreversal activity when compared to analogue **P13** (**P17:** $IC_{50}^{D10, K1, RSA11}$ < 5μM vs. **P13:** $IC_{50}^{D10, K1, RSA11}$ > 5μM; **P17:** $RMI_{K1/RSA11}$ < 1 vs. **P13:** $RMI_{K1/RSA11}$ > 1). Compound **P16**, in particular, demonstrated significant CQ resistance reversing effect (RMI_{RSA11} = 0.59) which is comparable to that of verapamil (RMI = 0.60), though, it was not as successful in K1. Careful inspection of the structures may lead to a tentative hypothesis of a basic chemosensitizing pharmacophore comprising of a biphenyl fragment with a possible link to an arylpiperazinyl substructure, especially for restoring CQ sensitivity in RSA11. This hypothesis may be strain-dependent and needs to be tested further in a broader range of resistant strains.

The antiplasmodial activities of the chemical analogues in group **C** were not distinctively different from each other and showed lower activities towards CQ resistant parasites (R_I > 1). However, it is noteworthy that **P19** exhibited a remarkable resistance reversing ability in the African strain (RMI_{RSA11} = 0.58) while **P18** (RMI_{RSA11} = 0.82) and **P20** (RMI_{RSA11} = 0.84) showed moderate CQ resistance reversal activity. This observation is

consistent with earlier findings with compound **P12** (RMI_{RSA11} = 0.77) and **P16** (RMI_{RSA11} = 0.59) since **P12**, **P16** and **P19** all contain the phenylpiperazinyl structural moiety.

Comparing compounds from groups **A**, **B** and **C**, the trimethoxybiphenyl-based compounds were the strongest antiplasmodial agents while group **C** compounds, which possess only one methoxy group showed the least antiplasmodial activity. These data suggest that the greater number of methoxy groups these compounds possess, the more potent antiplasmodial agents they are. Compound **P17** (trimethoxybiphenyl–benzylpiperazinyl) exhibited the strongest antiplasmodial activity amongst the series of compounds against falciparum D10, K1 and RSA11. In terms of further development of more effective antiplasmodial agents within this series of compounds, the trimethoxybiphenyl and benzylpiperazinyl substructural motifs could form a basis.

On the other hand, the phenylpiperazine modified compounds, **P12**, **P16** and **P19** displayed substantial resistance reversal effects when compared with *N*-methylpiperazine and benzylpiperazine derivatives. While the comparative degrees of chemosensitization against mono-, di, and tri-methoxybiphenyl building templates were not determined, these results suggest that the phenylpiperazinyl moiety may be an important substructure in these CQ resistance modulators since modified analogues containing this moiety possess insignificant intrinsic antiplasmodial activity, which is a requirement for an ideal chemosensitiser. Furthermore, these chemically modified compounds in general all showed reduced antiplasmodial activity of which only the phenylpiperazine substituted derivatives revealed comparative degrees of chemosensitization when compared with **P26** and **P14**. Nevertheless, all the novel compounds in groups **A** – **C** demonstrated a large therapeutic margin of safety on the mammalian cells of CHO.

6.3.2.1 Substitutions with longer side chain

In order to improve the potential of initially synthesized antiplasmodial agents and/or resistance reversers against CQ resistant parasites, further chemical modifications were made to produce two small classes of analogues with extended side chains. In one class,

group **D**, the well recognized amino alcohol antiplasmodial pharmacophore was incorporated in order to enhance antiplasmodial activity.

Within group **D**, **P25**, as expected displayed the best antimalarial activity against both CQ-sensitive and -resistant strains of falciparum as its structure included the trimethoxybiphenyl and benzylpiperazinyl substructural motifs described previously. In addition, the indicator (R_I) for potential novel antimalarials against CQ resistant malaria is well below 1 for all compounds in group D, this suggests that the β-alcohol amino group may be an important functional group for antimalarial agents particularly against CQ-resistant malaria. However, the amino alcohol analogue **P24** (modified with phenylpiperazine) did not display the predicted high resistance reversal activity. Instead the *N*-methylpiperazine modified alcohol derivative (**P23**) was the most potent resistance reverser (RMI_{SA11} = 0.67).

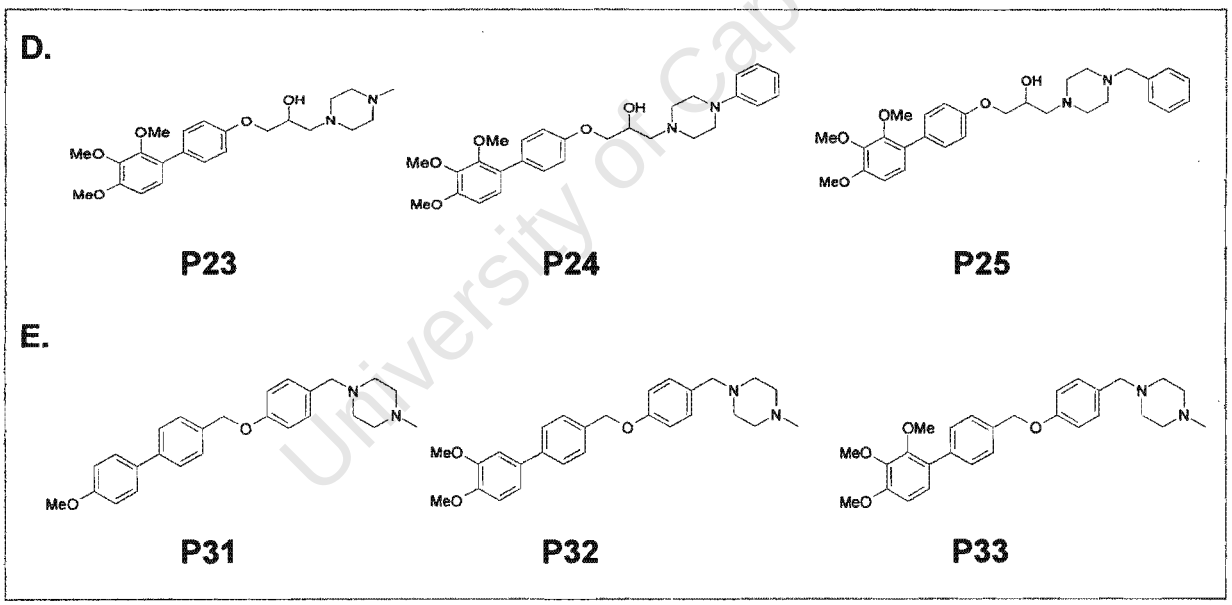

Figure 6.4.2.2. Chemical structures of closely related analogues.

D. Trimethoxybiphenyl amino alcohol scaffold with *N*-methyl-, phenyl- and benzyl-piperazine.
E. Extended *N*-methylpiperazine side chain with mono-, di- and Tri-methoxybiphenyl substructure.

More diverse analogues of the identified biphenyl pharmacophore with mono-, di- and tri-methoxy functional groups in addition to different piperazines were incorporated to form group **E** compounds **P31**, **P32** and **P33**. Out of the compounds in this group, a shorter side chain and relatively smaller derivatives were constructed. This small series

of analogues all produced improvement as antimalarials against CQ-sensitive and –resistant *P. falciparum* (IC_{50} < 8 μM). However, in terms of selective cytotoxicity, analogue **P31** (IC_{50}^{CHO} = 9.97±2.36 μM) exhibited high cytotoxicity towards a mammalian cell line. Future development of compound **P31** as a potential antimalarial agent will need to focus on reducing this cytotoxicity.

It is noteworthy that amongst all the compounds synthesized in this study, derivative **P32** in particular showed a marked resistance reversal effect (RMI_{RSA11} = 0.31) while possessing antiplasmodial activity and, more importantly, a non-cytotoxic effect in a mammalian cell line. The weak intrinsic antimalarial effect found in **P32** could be beneficial when it is used in combination with CQ since it restored CQ sensitivity in resistant cell lines. It could also function as an antimalarial (albeit weak), provided there is a large therapeutic safety margin.

Since CQ's mode of action and the mechanism of CQ resistance still remain controversial at present, it is unclear why the dimethoxy derivative **P32**, is approximately 3-times more active as a CQ resistance reverser than its analogues, **P31** and **P33**. Coincidentally, one of the most successful resistance modulators in cancer therapy, verapamil, also consists of a dimethoxyphenyl substructural motif. Nonetheless, the important roles played by the bicyclic privileged biphenyl and phenylpiperazinyl substructural motifs in chemosensitization were established. In terms of further development of resistance reversers, attempts could be made to explore chemical analogues with reduced molecular weight which incorporate the biaryl and phenylpiperazinyl substructural motifs.

6.3.3 Lipophilicity SAR

In order to correlate the general properties of lipophilicity (hydrophobicity) to the structural analogues in antiplasmodial and/or chemoreversal activity, the measured and calculated partition coefficient, logP, is used. It is an indicator of the tendency of water to exclude the non-polar groups or molecules in an aqueous environment. Moreover, logP is known to correlate to compounds that contain one aliphatic tertiary amine whereas the calculation programs, ClogP, is used to estimate compounds with a piperazine in the

aliphatic chains (Wiese and Pajeva, 2001). For comparison purposes, the clogP values of corresponding compounds are tabulated in Table 6.4.3.

Table 6.4.3. The clogP values for the library of compounds.

	clogP			Antimalarial activity	Reversal activity
A	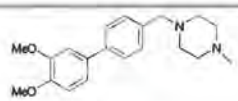 **P11** 3.88	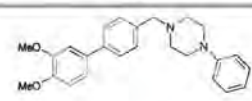 **P12** 4.86	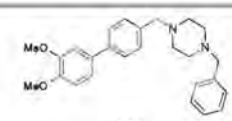 **P13** 5.72	P11: + P12: + P13: ++	P11: ++ P12: ++ P13: ++
B	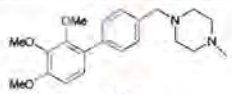 **P15** 2.96	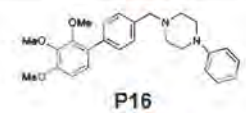 **P16** 3.94	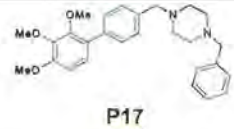 **P17** 4.80	P15: + P16: + P17: ++	P15: ++ P16: +++ P17: ++
C	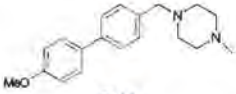 **P18** 4.14	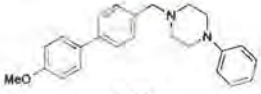 **P19** 5.12	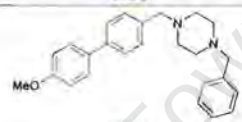 **P20** 5.98	P18: + P19: ++ P20: ++	P18: + P19: +++ P20: ++
D	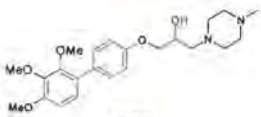 **P23** 1.03	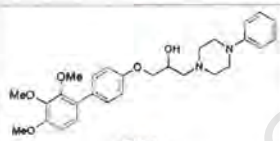 **P24** 3.32	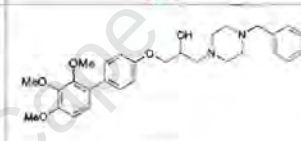 **P25** 4.24	P23: + P24: ++ P25: ++	P23: ++ P24: ++ P25: ++
E	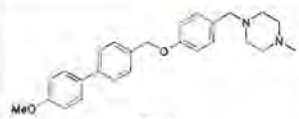 **P31** 5.83	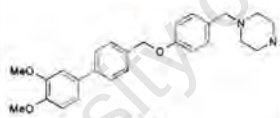 **P32** 5.56	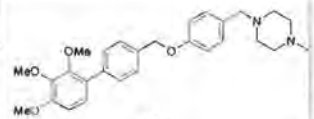 **P33** 4.65	P31: ++ P32: ++ P33: ++	P31: ++ P32: +++ P33: ++

ClogP(21)=4.04
+: weak; ++: moderate, +++: good

It was found that there was a small increase in antimalarial activity (from weak to moderate) with an increase of lipophilicity (from left to right) for the compounds in group **A-D**. In terms chemoreversal effects, no clear trend of relationships with lipophilicity was observed. Compounds **P13**, **P19**, **P20**, **P31** and **P32** possess clogP values of greater than 5, which does not fulfil the 'Lipinski's rule of 5' (Section 2.1.1) and showed poor to moderate activities in antiplasmodial activities. In contrast, these compounds possessing high clogP values showed moderate to good chemosensitization of CQ-resistant parasites. This suggests that these compounds may interact hydrophobically with the DV integral membrane proteins and replace the lost positive charge of PfCRT; this causes the protonated CQ to be trapped inside the parasitic DV, leading to parasite death like

verapamil as suggested by Sidu, Warhurst and their colleagues (Sidhu *et al.*, 2002; Warhurst, 2003). These data concluded that lipophilicity is an important parameter for antiplasmodial activity as well as resistance reversal.

In analysing structure-activity relationships from the series of compounds, several generalizations can be made as follows:

(i) Addition of a benzylpiperazinyl unit to the biarylamino building block enhanced antiplasmodial activity, which was particularly enhanced when a ferrocenyl substructure in the piperazine nucleus was included,

(ii) An increase in the number of methoxy substituents on the biaryl scaffold was accompanied by an increase in antiplasmodial activity,

(iii) Incorporation of a phenylpiperazinyl substructural feature resulted in elevated resistance reversal effects,

(iv) The shorter distance between the biaryl scaffold and amino functional group produced enhanced antiplasmodial activity and CQ resistance reversing ability,

(v) The more hydrophobic the compound, the better antiplasmodial and chemoreversal activities they possess.

To sum up the hit optimization process, organometallic compound **P14** was the most active antiplasmodial agent against both CQ-sensitive and –resistant clones of falciparum infected parasites, while **P26** was selectively more potent in resistant strains. On the other hand, in terms of chemosensitization, all the new compounds showed effective resistance reversal in the African CQ^R strain RSA11, with **P32** being the most potent. Moreover, 95% of the novel compounds synthesized showed little cytotoxicity, which is crucial in the later stage of drug discovery and development. A careful inspection of the chemical structures of these modified compounds from lead **P7** led to a tentative proposal that a combination of two privileged bicyclic structures, biphenyl and arylpiperazinyl moieties, is the chemoreversal pharmacophore in this series of compounds. One could therefore postulate from this that compounds **P14**, **P26** and **P32** hold the greatest potential for further development as promising potential lead compounds.

6.4 Conclusion

In this study, novel compounds synthesized on the basis of known structure-activity relationships studies were evaluated *in vitro* for antiplasmodial activity, CQ resistance reversal, cytotoxicity and in CQ accumulation assays. All of them showed no cross resistance with CQ (the susceptibility to the compounds tested was not accompanied by an increase in CQ resistance level) and were within a wide therapeutic safety margin except **P31**, which possessed high cytotoxicity against the CHO cell line. In terms of antiplasmodial activity, compounds **P26** and **P14** were shown to exhibit the greatest potential as the most promising antimalarials and warrant further investigation for lead generalization and optimization. It is noteworthy that although these compounds possess relatively high antiplasmodial activity to be ideal chemosensitizers, it may be an advantage as a dual acting (antiplasmodial and chemoreversal) drug from a therapeutic point of view (Chibale *et al.,* 2003). In addition, **P26** displayed classical resistance reversal activity while **P32**, which showed the greatest potential as a CQ resistance modulator, showed no significant stimulation of CQ retention in resistant *P. falciparum*. From the empirical data of the small library of compounds, tentative structure-activity relationships revealed that benzylpiperazine analogues displayed high antiplasmodial activity while phenylpiperazine substituted derivatives demonstrated enhanced CQ resistant reversal effects. In terms of CQ resistance modulators, an additional class of resistance modulators which showed effective resistance reversal activity without promoting increased uptake of CQ within CQ resistant malaria parasites was proposed.

Chapter 7

Drug interactions with ABC transporters in yeast

7.1 Introduction

One of the strategies used by microbes, parasites and tumor cells to evade chemotherapy is to overexpress broadly specific transporter proteins to extrude drugs out of the cells (Kolaczkowski *et al.,* 1998). As a result, membrane transport phenomena have been implicated in the evolution of drug resistance in both prokaryotic (bacterial) and eukaryotic systems (yeasts, human tumor cells and intracellular parasites such as *P. falciparum*). In an effort to expand our understanding of the mechanism of action and resistance associated with CQ, *Saccharomyces cerevisiae* was used as a model eukaryotic system in this study.

The partial reversal of CQ resistance by verapamil suggests that CQ resistance phenotype may be based on verapamil-sensitive components mediated by the ABC transporter protein *Pf*MDR1 and/or other verapamil-insensitive components (Klokouzas *et al.,* 2003). This led to a hypothesis that ABC transporters may be acting alongside other proteins to bring about the drug resistance. In addition, it was proposed that verapamil interact hydrophobically with CQ transporter protein(s) in malaria to restore CQ to sensitivity (Sidhu *et al.,* 2002; Warhurst *et al.,* 2002). The objective of this study was to investigate the specific transport in the membrane proteins of yeast *S. cerevisiae in vitro* to obtain more insight into the function and substrate specificity of the series of compounds synthesized.

Drug interactions with transporter proteins can have a direct and/or adverse effect on the therapeutic safety and efficacy of many important drugs (Mizuno *et al.,* 2003). This may be due to competitive substrate interactions at the transporter binding site. It is thus of interest to investigate whether the series of potential CQ chemosensitizers are substrates for the ABC transporter proteins in efforts to investigate the drug resistance and/or reversal phenomenon. To obtain detailed information about the individual differences, two isogenic strains of *S. cerevisiae* of YOR1 and YCF1 were used in the study. The ABC transporters of YOR1 and YCF1 were found to localize to the yeast outer membrane and digestive vacuolar membrane, respectively. YOR1 is involved in the detoxification of a wide range of organic anions containing carbonyl groups while YCF1

plays an important role in vacuolar detoxification of heavy metals. In addition, the *Pf*MDR1 transporter, which also localizes to the digestive vacuolar membrane of malaria parasites, has been proposed to be associated with the drug resistance process (Reed *et al.,* 2000). With the functional and localization similarities of the ABC transporters in yeast (YCF1) and in malaria (*Pf*MDR1), the potentially important information derived from the drug interaction with the yeast ABC transporter, YCF1, may provide information into the function of related eukaryotic transporter proteins in malaria.

7.2 Results and discussion

7.2.1 Solid medium assay

The yeast oligomycine resistance protein, Yor1p, is known for its ability to confer oligomycine resistance. The mutant strains AD1, AD1-3 and Super Yor with the corresponding wild type, US50-18C, were chosen to establish this technique (Decottignies *et al.,* 1998). AD1 contains the deletion of *yor1* gene and AD1-3 contains not only the deletion of *yor1* gene but also other transporter genes. Super Yor is the overexpressed *yor1* strain.

Traditionally, the drug inhibition test has been performed on solid medium assay (Chapter 3.4.1) and the growth of yeast cells is inspected manually and physically (Fig. 7.2.1-A). Various dilutions of test compounds were applied to the agar plates and an analysis of colonies grown was then performed (Table 7.2.1; Fig. 7.2.1B). This assay was established in our laboratory.

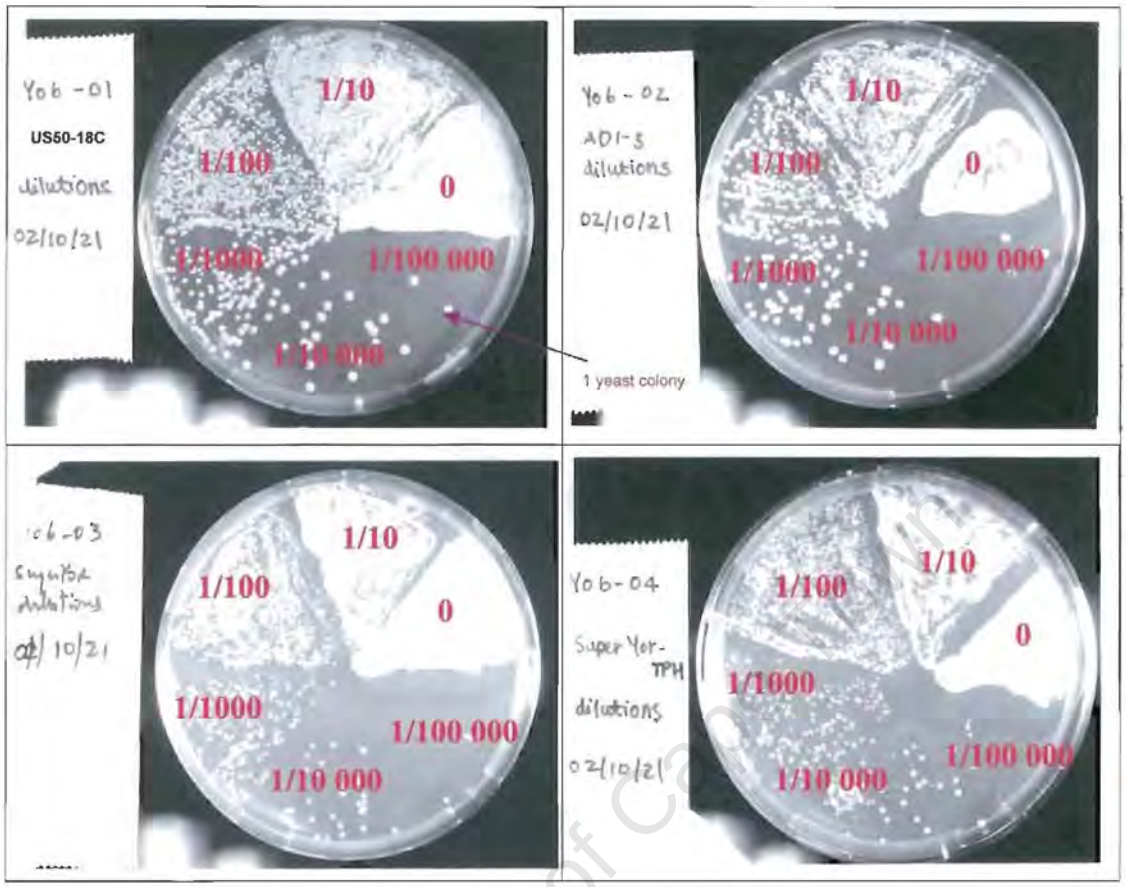

Figure. 7.2.1-A. Various dilutions of different clones of yeasts developed on solid YPD-agar medium assay.

Table 7.2.1. Analysis of different yeast clones grown against different concentrations of oligomycines.

S. cerevisiae	[oligomycine] μg/ml				
	0.00	**0.05**	**0.50**	**5.00**	**50.00**
US50-18C	5,0	5,7	6,0	0,0	0,0
AD1	2,3	2,7	0,0	0,0	0,0
AD1-3	1,0	1,7	0,0	0,0	0,0
Super Yor	4,0	9,0	4,7	3,0	3,3

The number of yeast clones is in arbitrary units.

US50-18C is the wild type strain. AD1: Δ*yor1*. AD1-3: Δ*yor1*, Δ*snq2* and Δ*pdr5*. Super Yor: overexpression of yor1.

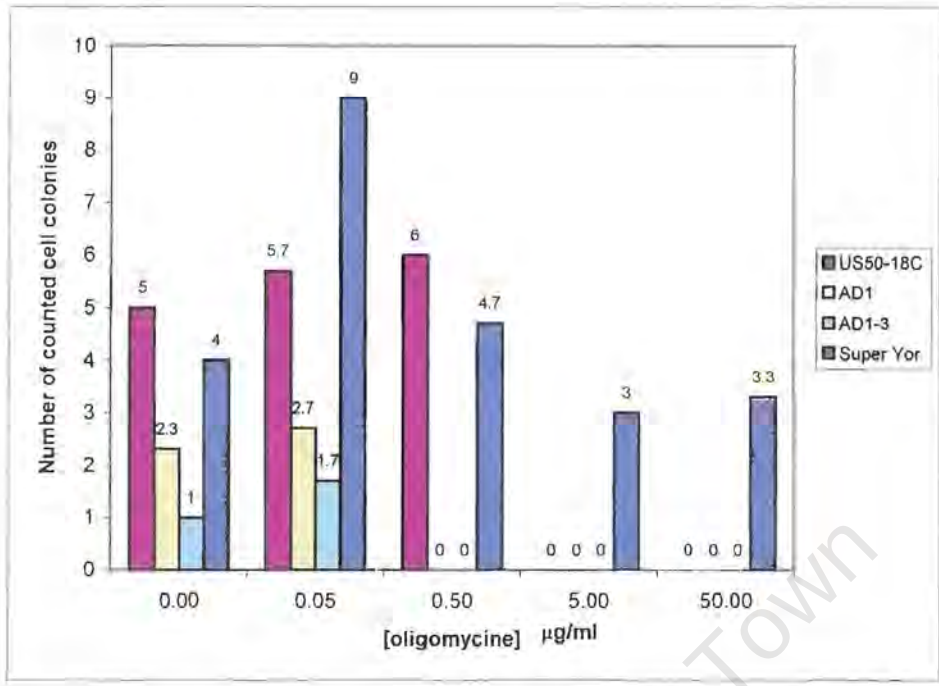

Figure 7.2.1-B. Illustration of oligomycines response against different yeast clones.

The results showed that the wild type (WT) strain, US50-18C (purple bar), was able to survive oligomycine pressure at a concentration of 0.5 µg/ml while the overexpressed *yor1* mutant Super Yor strain (blue bar) was able to survive at the highest concentration of 50 µg/ml tested (Fig. 7.2.1-B). The isogenic mutant AD1 (yellow bar), which lacks only the Yor1p transporter protein, and the mutant AD1-3 (green bar) bearing deletions in *yor1*, *snq2* and *pdr5* showed their limited tolerance to oligomycine even at a low concentration of 0.05 µg/ml. These data show that the Yor1p is responsible for the oligomycine resistance.

7.2.2 Liquid culture assay

In an attempt to investigate substrate specificity of transport proteins in this study, the traditional sensitivity test was adapted for screening using 96-well microtitre plates (Chapter 3.4.2). Several *S. cerevisiae* cell lines were used of which the YOR1p was initially used as a standard protein for the assay.

This liquid culture assay (LCA) was successfully established and developed on the basis of the traditional solid medium assay. It was achieved through a series of data computations (Fig. 7.2.2-A, B, C and D) (Details in Section 3.4.2). Results from the LCA were consistent with earlier findings (Decottignies *et al.*, 1998). A summary of dose-response curves of oligomycine against different *S. cerevisiae* used is also reported (Table 7.2.2; Fig. 7.2.2-E).

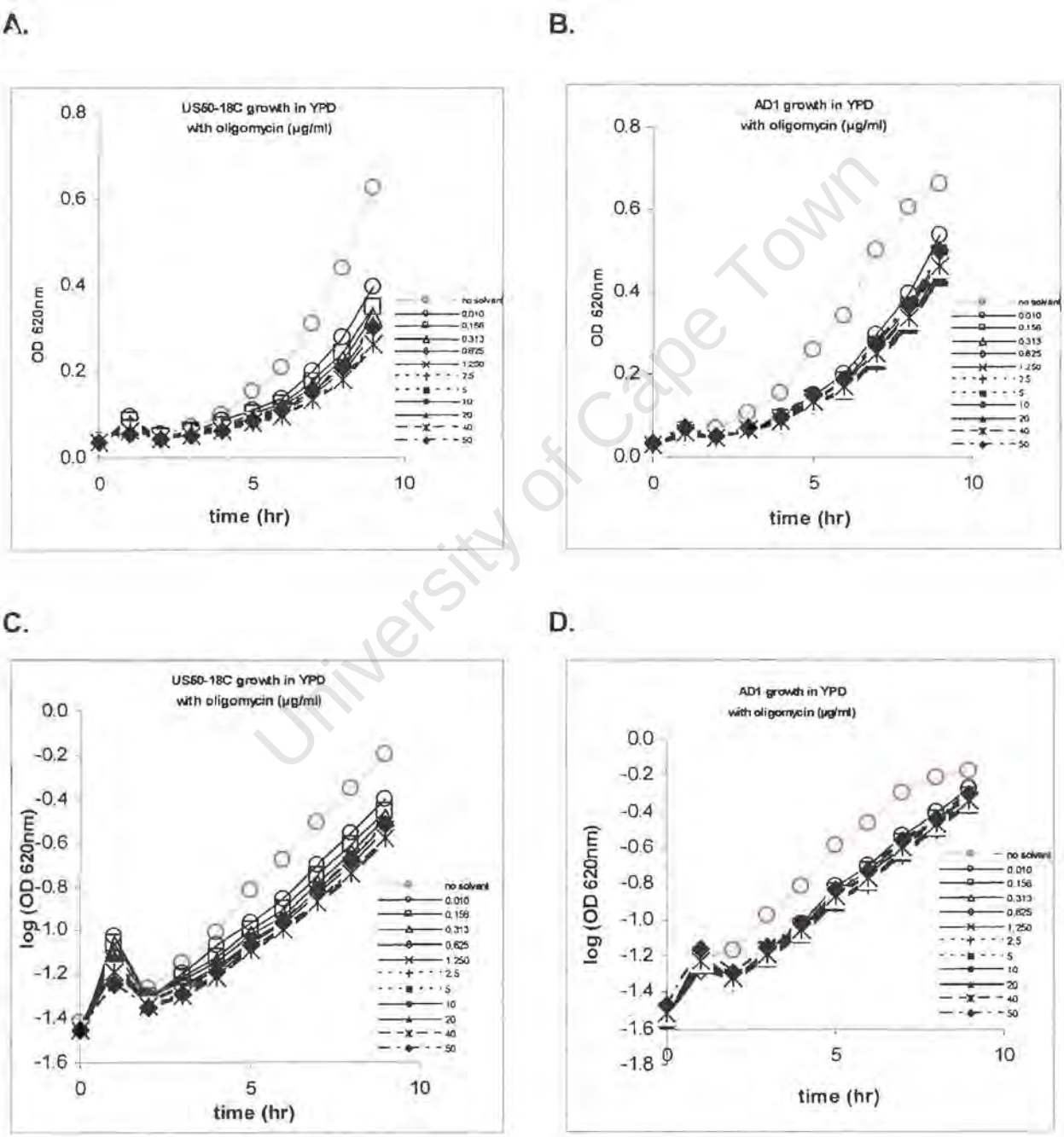

Fig. 7.2.2.
A. **Wild type (US50-18C)** growth: graph of Optical Density (OD_{620}) vs. time (hr).
B. **AD1** growth: graph of Optical Density (OD_{620}) vs. time (hr).
C. **Wild type (US50-18C):** graph of growth rate vs. time (hr).
D. **AD1** graph of growth rate vs. time (hr).

The growth inhibition curves for the WT (US50-18C) and AD1 strains in various concentrations of oligomycine are shown in Fig. 7.2.2-A and -C while the growth rates for both strains are shown in Fig. 7.2.2-B and –D, in which both strains showed similar susceptibility to oligomycine. Results in this study confirm that growth of AD1 was not inhibited by oligomycine (Fig. 7.2.2) (Decottignies *et al.*, 1998; Kolaczkowski *et al.*, 1998). This finding was consistent with that observed in the traditional solid medium assay (Fig. 7.2.1).

In addition, the LCA results were confirmed in a cytotoxicity assay using single and multiple gene mutations in the ABC transporters. Of the *S. cerevisiae* strains tested, those with Δ*yor1* deletion (AD1, AD1-3, AD1,2,4-7) (section 3.4) were shown to regain oligomycine sensitivity in Fig. 7.2.2-E and summarized in Table 7.2.2.

E.

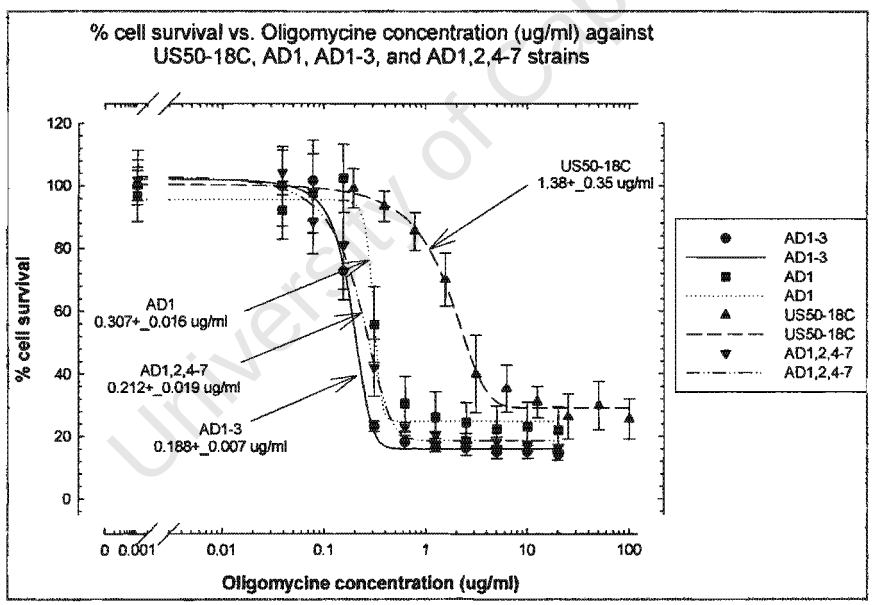

US50-18C is the wild type strain. AD1: Δ*yor1*. AD1-3: Δ*yor1*, Δ*snq2* and Δ*pdr5*.
AD1,2,4-7: Δ*yor1*, Δ*snq2*, Δ*pdr10*, Δ*pdr11*, Δ*ycf1*, Δ*pdr3*

Figure 7.2.2-E. A summary of dose-response curves of oligomycine against *S. cerevisiae*.

The resistance factor, R_f, is an indicator to identify the relative activity of the drugs to the drug sensitive and/or drug resistant strains. $R_f = IC_{50}^{resistant}/IC_{50}^{sensitive}$. Therefore, if $R_f > 1$, the more resistant the yeast strain is to the drug. The resistance factors of the strains tested in Fig. 7.2.2-E are indicated in Table 7.2.2.

Table 7.2.2. The IC_{50} values of oligomycine against several *S. cerevisiae*.

Strains	IC_{50} (µg/ml)	Resistance Factor (R_f)
US50-18C	1.38 ± 0.35	5.86
AD1	0.31 ± 0.02	≅ 1
AD1-3	0.19 ±0.01	≅ 1
AD1,2,4-7	0.21 ± 0.02	≅ 1

R_f = IC_{50} (strains)/ IC_{50} (AD1)
AD1= corresponding wild type yeast strain with *YOR1* gene deletion.
AD1-3 and AD1,2,4-7 = corresponding wild type yeast strain with *YOR1* and other major transporter protein gene deletions.

As can be seen, the US50-18C (WT), which is the only strain possessing the *yor1* gene, was the most resistant to oligomycine among the strains tested (IC_{50} = 1.38 µM.). When the AD1,2,4-7 strain, bearing more transporter gene deletions, was compared to AD1, the *Δyor1* gene strain, both showed similar degrees of susceptibility to oligomycine as well as AD1-3 ($R_f^{AD1} \cong R_f^{AD1-3} \cong R_f^{AD1,2,4-7} \cong 1$). The results confirm that YOR1p is the major ABC transporter protein for oligomycine. The LCA results are consistent with those obtained from the solid medium assay: YOR1p ABC transporter protein conferred oligomycine resistance. A 6-fold increase in oligomycine tolerance in US50-18C, which contains the Yor1p transporter protein, was shown. The newly developed LCA was thus capable of demonstrating the functional property of YOR1p for the purpose of this study. LCA is much more efficient than the classical solid medium assay and it is comparable to the cytotoxicity assay as it possesses the advantage of taking into consideration the average duration of cell proliferation with respect to the single point evaluation in a cytotoxicity test.

The series of novel compounds were investigated in the membrane protein, YOR1p, and vacuolar membrane protein, YCF1p, for substrate specificities using LCA. Results obtained against YOR1p were comparable to those of YCF1p. Since the *PfMDR1* gene product of PfPgh-1 was found to locate to the malaria vacuolar membrane, results obtained from YCF1p were discussed for comparison purposes.

7.2.3 Transport activity of YCF1p

Prior to investigating novel compounds using the LCA, a positive control of Cd^{2+} was tested. A control using the WT was performed and illustrated in Fig. 7.2.3-A, -B and C while the YCF1 strain are shown in Fig. 7.2.3-D, -E and –F, respectively. The growth curves of the WT and YCF1 displayed similar growth patterns (Fig. 7.2.3-A vs –D) as well as the growth rate ($logOD_{620}$ vs time) (Fig. 7.2.3-B vs –E). When the growth rate was compared with Cd^{2+} (Fig. 7.2.3-C vs –F), IC_{50} values for WT and YCF1 are determined as 100.4±3.7 μM and 26.7±2.2 μM, respectively, which are consistent with literature findings that YCF1 is responsible for the Cd^{2+} response (Vido et al., 2001).

The synthesized compounds showed consistent non-inhibition effect on both YCF1 and its corresponding WT strain throughout the library of compounds generated. Results for the most promising lead compound **P26** as potential effective chemosensitizer are shown below and compared with verapamil (Fig. 7.2.3-G to J).

The well-known resistance modulator, VPL, showed a minor inhibition effect on growth in the transporters of the WT yeast cells (Fig. 7.2.3-G). However, the responsible transporter was shown not to be YCF1p since it showed no growth inhibition in YCF1 against most of the concentrations used (Fig. 7.2.3-H). YCF1p was clearly not involved in the flux of the synthesized compounds as the representative data of compound **P26** revealed similar growth patterns in both WT and YCF1 (Fig. 7.2.3-I, -J). The highest concentration of 100 μg/ml of compound **P26** used showed a small degree of inhibition against YCF1, which may be due to its toxicity at this level (shown in dark blue curve in Fig. 7.2.3-J). Thus both **P26** and VPL appear not to be the substrates for the yeast transport protein of YCF1.

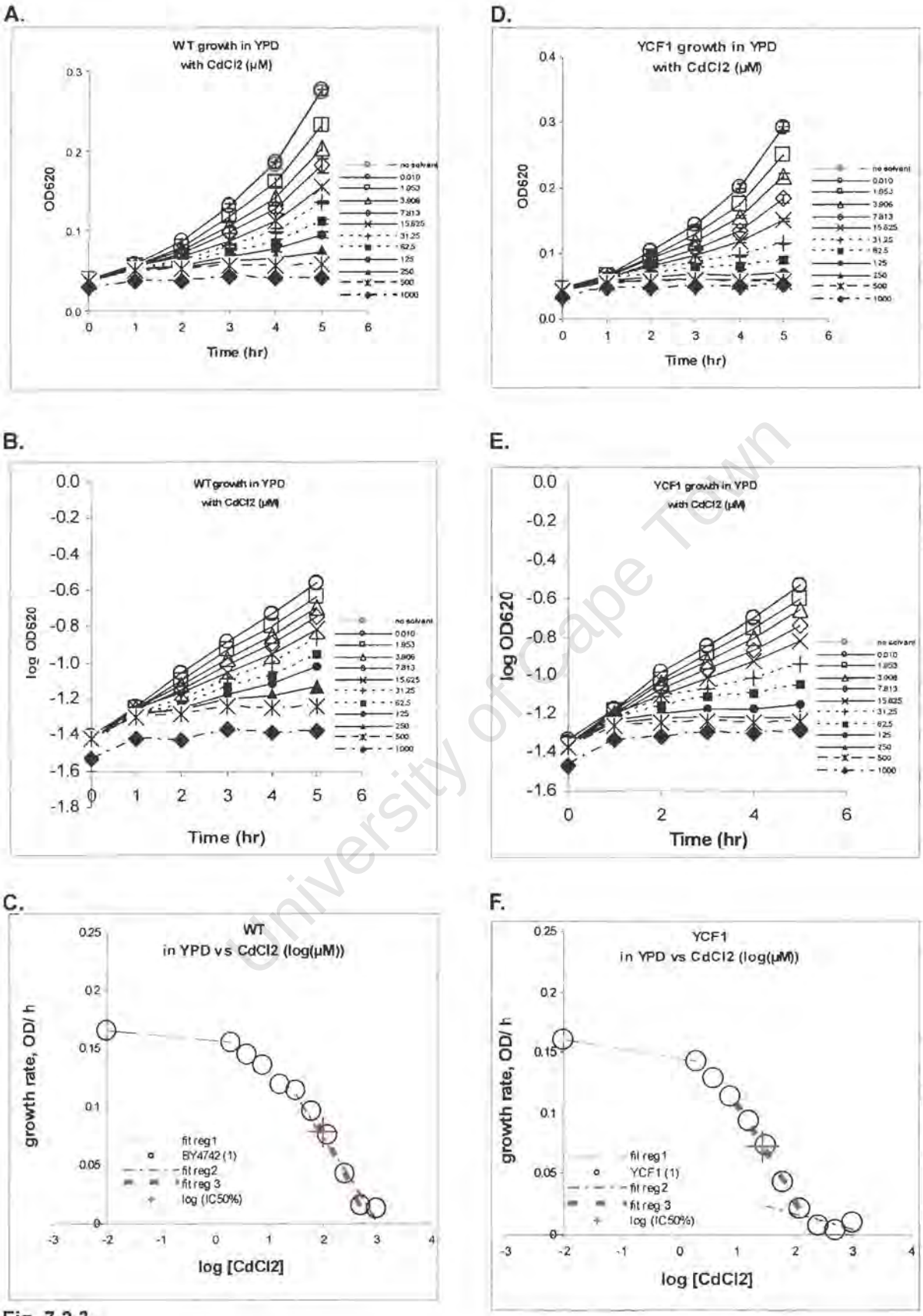

Fig. 7.2.3.

A. **WT** growth vs. time (hr).
B. **WT** growth rate vs. time (hr).
C. **WT** growth rate vs. log[Cd^{2+}] µM.
D. **YCF1** growth vs. time (hr).
E. **YCF1** growth rate vs. time (hr).
F. **YCF1** growth rate vs. log[Cd^{2+}] µM

G.

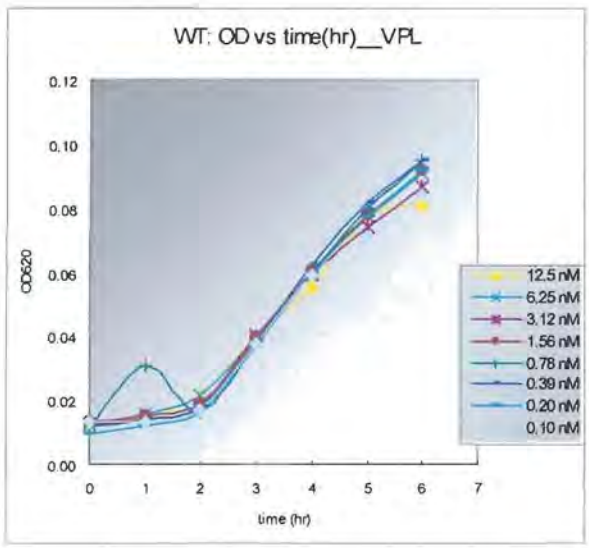

H.

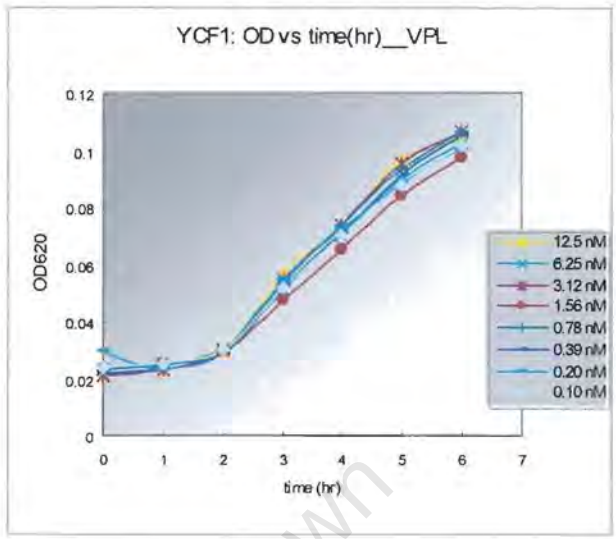

I.

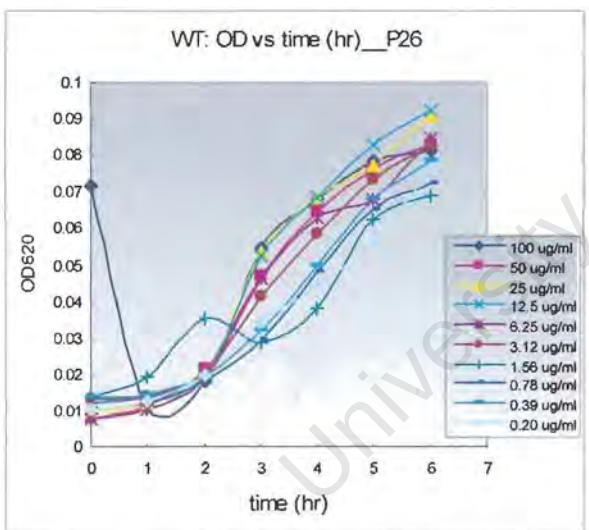

J.

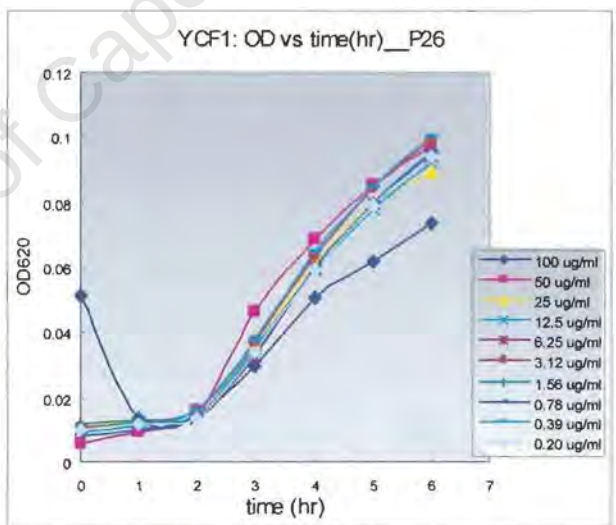

Figure 7.2.3. (Continued)

G. VPL response in WT: cell growth vs. time (hr).
H. VPL response in YCF1: cell growth vs. time (hr).
I. Compound **P26** response in WT: cell growth vs. time (hr).
J. Compound **P26** response in YCF1: cell growth vs. time (hr).

The fact that YCF1p localizes to the membrane of the digestive vacuole suggests similarity to that of P-glycoprotein homologue 1 in malaria and the PfCRT transporter protein. Although the transporter assessments were performed indirectly on the yeast

transporter proteins, it has shown that VPL and the related compounds which contain the hydrophobic biphenyl moiety and the basic piperazinyl substructural feature are not the substrates for YCF1. Thus no drug-protein interaction with this ABC transporter was suggested. It has been proposed that VPL interacts hydrophobically with the receptors to restore CQ sensitivity in CQ resistant malaria parasites although there is no direct evidence that VPL binds to the ABC transporter protein, Pgph-1, and/or to the PfCRT, which does not belong to the ABC family (Sidhu *et al.,* 2002; Warhurst *et al.,* 2002). However, this study showed no hydrophobic interaction between verapamil (and the synthesized analogues) and YCF1. Further work on these compounds can be performed against the identified CQ resistance determinant, PfCRT and/or PfPgh1, to show if these compounds enhance CQ to sensitivity when used in combination with CQ in CQ resistant parasites.

7.3 Conclusion

Drug targeting is one effective approach to optimize the pharmacological profiles of drug candidates using transporter functions. *To our knowledge, this is the first time studies on the effect of antimalarial resistance reversers on drug transporters in yeasts have been attempted*. Even though this drug transporter study did not shed light on the CQ resistance mechanism, the effort reveals a possible means to study the structure and function of yeast or malaria transporter proteins.

Chapter 8

Research summary and future investigations

8.1 Research summary

Malaria is one of the world's most important infectious diseases and causes severe morbidity and mortality in tropical and sub-tropical regions of the world. Even today, the amazing adaptive qualities of the mosquito vector, *Anopheles*, combine with travel, trade and natural events to cause serious health and socioeconomic problems particularly in the poorest countries among the underprivileged populations. The worsening problems of drug and insecticide resistance as well as the limited number of antimalarials and effective antimalarial drug regimens have contributed to the increasing prevalence of malaria and the difficulties in providing adequate disease management. At present, since malaria control and treatment rely profoundly on chemotherapeutic agents, it is imperative to rapidly put in place strategic plans for the discovery and development of novel antimalarials and/or other alternatives to challenge the ever-increasing drug resistance phenomenon. An alternative strategy to overcome the malaria burden is drug combination. The pioneering work with multi-drug resistance in tumor cells has shown the possibility to reverse anticancer agent resistance by using a combination of chemosensitizers. The pressing need for new alternative, new resistance chemosensitizers in combinations with CQ was investigated in light of the work in cancer.

By combining the power of biology and medicinal chemistry, a small series of CQ resistance reversal agents were rationally designed based on known structure-activity relationship studies. The compounds were synthesized in high yields and *N'*-[4-(*biphenyl*-2-*ylmethoxy*)-*benzyl*]-*N,N-dimethyl-propane*-1,3-*diamine* (**P7**) showed the greatest potential as a dual-acting antimalarial agent (IC_{50} < 0.6 μM) and CQ-resistance reverser (RMI_{K1}=0.67; RMI_{RSA11}=0.82) *in vitro*. The potential pharmacophore of the identified hit compound, **P7**, was tentatively proposed as the biphenyl moiety in the initial exploratory process of the drug discovery and development.

In light of the *in vitro* activity of **P7**, a library of analogous compounds focusing on replacing the flexible alkyl side chain with a piperazinyl moiety was successfully synthesized and evaluated for *in vitro* antiplasmodial activity, resistance reversal effect,

cytotoxicity as well as their effect on tritiated CQ accumulation. Among the 17 novel compounds, the organometallic ferrocenyl compound (**P14**) and 1-*biphenyl*-2-*ylmethyl*-4-*methyl-piperazine* (**P26**) displayed the greatest potential as the most promising antimalarials (IC_{50} < 1 μM) and warrant further investigation for lead generation and optimization. In terms of resistance reversal effect, **P26** showed the characteristic of a classical resistance reversal agent (RMI_{RSA11}=0.50) while 1-[4-(3',4'-*dimethoxy-biphenyl*-4-*ylmethoxy*)-*benzyl*]-4- *methoxy-piperazine* (**P32**) displayed the greatest potential as a CQ resistance modulator (RMI_{RSA11}=0.31). An additional class of resistance modulators which showed effective resistance reversal activity without potentiating CQ uptake within CQ-resistant *P. falciparum* was identified. In addition, a number of generalizations were made based on the structure-activity relationships from the library of compounds. It is noteworthy that although **P26** displayed relative high antiplasmodial activity to be an ideal chemosensitizer, it may be an advantage for such compounds to act as both antiplasmodial and chemoreversal agents (Chibale *et al.*, 2003).

Furthermore, since drug targeting is an effective approach to optimizing the pharmacological profiles of drug candidates using transporter functions, substrate specificity on yeast transporter proteins was studied. In this study, studies on the effect of antimalarial resistance reversers on drug transporters in yeast have been attempted for the first time. Although the screen did not shed light on the CQ resistance mechanism, the effort has provided a possible means to study the structure and function of yeast or malaria transporter proteins.

The objective of this thesis was to use known structure-activity relationships of chemosensitizers to rationally design, synthesize and optimize a library of novel compounds to meet the basic *in vitro* requirements in the initial exploratory stage of drug discovery and development, and ultimately fulfill the criteria for a pre-clinical candidate. This study focused on drug discovery and optimization of the antiplasmodial and chemoreversal activity of a library of compounds. The information gained from the development of hits into potential lead molecules could provide a basis for further structure-activity relationship trends for novel CQ-resistance chemosensitizers.

8.2 Future investigations

Although a library of biphenyl-based compounds was synthesized, a multitude of chemical modifications could potentially be made. Different substitution patterns of the biphenyl moiety would provide vast chemical diversity. This optimization process may identify more promising leads and ultimately more suitable drug candidate(s) for drug development.

In addition, evaluation of these novel compounds for their clinical characteristics *in vivo* would also play an essential role in drug development. However, the ideal animal model for displaying the precise pharmacodynamic and pharmacokinetic properties for human malaria is not yet available. Regardless, all mammalian *Plasmodium* species share comparable life cycles and are sensitive to the same drugs and their diversity is similar to that observed in human *Plasmodium.* As a result the murine models, such as *P. berghei*, have become more and more widely used (Sherman *et al.,* 1998). Careful time course studies correlating the host response with the environmental changes during development would provide valuable information about the *in vivo* intrinsic toxicity, antimalarial and/or chemoreversal activity, pharmacokinetic and pharmacodynamic profiles. The active metabolites of the compounds could also be investigated by radioactive labeling during drug metabolism studies *in vivo*.

With the substrate specificity study established, further work on these compounds could be performed against the identified transporter protein, PfCRT. The information may shed light on the mechanism of CQ's action as well as CQ resistance mechanism such that it may serve as a platform to evade the scourge of malaria.

Bibliography

Adovelande, J., Delèze, J. and Schrével, J. (1998). Synergy between two calcium channel blockers, verapamil and fantofarone (SR33557), in reversing chloroquine resistance in *Plasmodium falciparum*. *Biochem. Pharmacol.* **55:** 433-440.

Aldieri, E., Atragene, D., Bergandi, L., Riganti, C., Costamagna, C., Bosia, A. and Ghigo, D. (2003). Artemisinin inhibits inducible nitric oxide synthase and nuclear factor NF-kB activation. *FEBS Letters* **552:** 141-144.

Alibert, S., Santelli-Rouvier, C., Pradines, B., Houdoin, C., Parzy, D., Karolak-Wojciechowska, J. and Barbe, J. (2002). Synthesis and effects on chloroquine susceptibility in Plasmodium falciparum of a series of new dihydroanthracene derivatives. *J. Med. Chem.* **45:** 3195-3209.

Avendaño, C. and Menéndez, J. C. (2002). Inhibitors of Multidrug Resistance to Antitumor Agents. *J. Med. Chem.* **9:**159-193.

Batra, S., Srivastava, P., Roy, K., Pandey, V. C. and Bhaduri, A. P. (2000). A new class of potential chloroquine-resistance reversal agents for Plasmodia: synthesis and biological evaluation of 1-(3'-diethylaminopropyl)-3-(substituted phenylmethylene)pyrrolidines. *J. Med. Chem.* **43:** 3428-3433.

Bauer, B. E., Wolfger, H. and Kuchler, K. (1999). Inventory and function of yeast ABC proteins: about sex, stress, pleiotropic drug and heavy metal resistance. *Biochimica et Biophysica Acta* **1461:** 217-236.

Biot, C., Glorian, G., Maciejewski, L. A. and Brocard, J. S. (1997). Synthesis and antimalarial activity *in vitro* and *in vivo* of a new ferrocene-chloroquine analogue. *J. Med. Chem.* **40**, 3715-3718.

Biot, C. (2004). Ferroquine: A new weapon in the fight against malaria. *Current Medicinal Chemistry - Anti-Infective Agents* **3:** 135-147.

Bitonti, A. J., Sjoerdsma, A., McCann, P. P., Kyle, D. E., Oduola, A. M. J., Rossan, R. N., Milhous, W. K. and Davidson, D. E. (1988). Reversal of chloroquine resistance in malaria parasite *Plasmodium falciparum* by desipramine. *Science* **242:** 1301-1303.

Bray, P. G., Howells, R. E. and Ward, S. A. (1992). Vacuolar acidification and CQ sensitivity in *Plasmodium falciparum*. *Biochem. Pharmacol.* **43:** 1219-1227.

Bray, P. G. and Ward, S. A. (1998). A comparison of the phenomenology and genetics of multidrug resistance in cancer cells and quinoline resistance in *Plasmodium falciparum*. *Pharmacol. Ther.* **77:** 1-28.

Bruce-Chwatt, L. J. (1981). Chemotherapy of malaria, second edition (ed. Bruce-Chwatt, L. J.). WHO, Geneva.

Burckhardt, G. and Wolff, N. A. (2000). Structure of renal organic anion and cation transporters. *Am. J. Physiol. Renal Physiol.* **278:** F853-F866.

Chawira, A. N. and Warhurst, D. C. (1987). The effect of artemisinin combined with standard antimalarials against chloroquine-sensitive and chloroquine-resistant strains of *Plasmodium falciparum in vitro. Journal of Tropical medicine and Hygiene* **90:** 1-8.

Chibale, K. (2002). A chemical approach towards understanding the mechanism and reversal of drug resistance in Plasmodium falciparum: Is it viable? IUBMB *Life* **53:** 249-252.

Chibale, K., Visser, M., van Schalkwyk, D., Smith, P. J., Saravanamuthu, A. and Fairlamb, A. H. (2003). Exploring the potential of xanthene derivatives as trypanothione reductase inhibitors and chloroquine potentiating agents. *Tetrahedron* **59:** 2289-2296.

Chou, A. C., Chevli, R. and Fitch, C. D. (1980). Ferriprotoporphyrin IX fultills the criteria for identification as chloroquine receptor of malaria parasites. *Biochem.* **19:** 1543-1549.

Ciak, J. and Hahn, F. (1966). Chloroquine: mode of action. *Science* **151:** 347-349.

Ciach, M., Zong, K., Kain, K. and Crandall, I. (2003). Reversal of mefloquine and quinine resistance in *Plasmodium falciparum* with NP30. Antimicrobial agents and chemotherapy **47(8):** 2393-2396.

Clarkson, C. (2002). Isolation and characterization of two antiplasmodial diterpenes from *Harpagophytum procumbens (*devil's claw) and chemical modification of a related analogue. University of Cape Town, South Africa. Unpublished PhD thesis.

Cui, Z., Hirata, D., Tsuchiya, E., Osada, H. and Miyakawa, T. (1996). The multidrug resistance-associated protein (MRP) subfamily (Yrs/Yor1) of *Saccharomyces cerevisiae* is important for the tolerance to a broad range of organic anions. *J. Biol. Chem.* **271:** 14712-14716.

De, D., Byers, L. D. and Krogstad, D. J. (1997). Antimalarials: synthesis of 4-aminoquinolines that circumvent drug resistance in malaria. *J. Heterocycl. Chem.* **34:** 315-320.

Decottignies, A., Grant, A. M., Nichols, J. W., de Wet, H., McIntosh, D. B. and Goffeau, A. (1998). ATPase and multidrug transport activities of the overexpressed yeast ABV protein Yor1p. *J. Biological Chem.* **273:** 12612-12622.

Deharo, E., Barkan, D., Krugliak, M., Golenser, J. and Ginsburg, H. (2003). Potentiation of the antimalarial action of chloroquine in rodent malaria by drugs known to reduce cellular glutathione levels. *Biochem. Pharmacol.* **66:** 809-817.

Department of Health. (March 2003). Guidelines for the prevention of malaria in South Africa. The National Department of Health, Pretoria.

Dieckmann-Schuppert, A., Bamberger, U. and Schwarz, R. T. (1993). Chloroquine resistance in *Plasmodium falciparum* is not reversed by BIBW-22, a compound reversing the multidrug resistance phenotype in mammalian cancer cells. *Biochem. Pharmacol.* **46:** 1421-1424.

Dorn, A., Stoffel, R., Matile, H, Bubendorf, A. and Ridley, R. G. (1995). Malarial haemozoin/β-haematin supports haem polymerization in the absence of protein. *Nature* **374:** 269-271.

Dorn, A., Vippagunta, S. R., Matile, H., Jaquet, C., Vennerstrom, J. and Ridley, R. G. (1998). An assessment of drug-haematin binding as a mechanism for inhibition of haematin polymerization by quinoline antimalarials. *Biochem. Pharmacol.* **55:** 727-736.

Duraisingh, M. T., Roper, C., Walliker, D. and Warhurst, D. C. (2000). Increased sensitivity to the antimalarials mefloquine and artemisinin is conferred by mutations in the *pfmdr1* gene of *Plasmodium falciparum*. *Mol. Microbiol.* **36(4):** 955-961.

Dzekunov, S. M., Ursos, L. M. B. and Roepe, P. D. (2000). Digestive vacuolar pH of intact intraerythrocytic *P. falciparum* either sensitive or resistant to chloroquine. *Mol. Biochem. Parasitol.* **110:** 107-124.

Eckstein-Ludwig, U., Webb, R. L., van Goethem, I. D. A., East, J. M., Lee, A. G., Kimura, M., O'Neill, P. M., Bray, P. G., Ward, S. A. and Krishna, S. (2003). Artemisinins target the SERCA of *Plasmodium falciparum*. *Nature* **424:** 957-961.

Egan, T., J., Ross, D. C. and Adams, P. A. (1994). Quinoline antimalarial drugs inhibit spontaneous formation of β-haematin (malaria pigment). *FEBS Lett.* **352:** 54-57.

Egan, T. J. (2001). Structure-function relationships in chloroquine and related 4-aminoquinoline antimalarials. *Mini. Rev. Med. Chem.* **1:** 113-123.

Erlanson, D. A., McDowell, R. S. and O'Brien, T. (2004). Fragment-based drug discovery. *J. Med. Chem.* **47:** 3463-3482.

Evans, B. E., Rittle, K. E., Bock, M. G., DiPardo, R. M., Freidinger, R. M., Whitter, W. L., Lundell, G. F., Veber, D. F., Anderson, P. S., Chang, R. S., Lotti, V. J., Cerino, D. J., Chen, T. B., Kling, P. J., Kunkel, K. A., Springer, J. P. and Hirshfield, J. J. (1988). Methods for drug discovery: development of potent, selective, orally effective cholecytokinin antagonists. *J. Med. Chem.* **31:** 2235-2246.

Fattori, D. (2004). Molecular recognition: the fragment approach in lead generation. *Drug Discovery Today* **9**, 229-239.

Ferrari, V. and Cutler, D. J. (1991). Simulation of kinetic data on the influx and efflux of chloroquine by erythrocytes infected with *Plasmodium falciparum*: evidence for a drug-importer in chloroquine-sensitive strains. *Biochem. Pharmacol.* **42:** 167-169.

Ferté, J., Kühnel, J-M., Chapuis, G., Rolland, Y., Lewin, G. and Schwaller, M. A. (1999). Flavonoid-related modulators of multidrug resistance: synthesis, pharmacological activity and structure-activity relationships. *J. Med. Chem.* **42:** 478-489.

Fitch, C. D. (1970). *Plasmodium falciparum* in owl monkeys: drug resistance and chloroquine binding capacity. *Science* **169**, 289-298.

Fitch, C. D., Chevli, H. S., Banyal, G., Phillips, G., Pfaller, M. A., and Krogstad, D. J. (1982). Lysis of *Plasmodium falciparum* by ferriprotoporphyrin IX and a chloroquine-ferriprotoporphyrin IX complex. *Antimicrob. Agents chemother.* **21:** 819-822.

Fidock, D. A., Nomura, T., Talley, A. K., Cooper, R. A., Dzekunov, S. M., Ferdig, M. T., Ursos, L. M. B., Sidhu, A. S., Naude, B., Deitsch, K. W., Su, X., Wootton, J. C., Roepe, P. D. and Wellems, T. E. (2000). Mutations in the *P. falciparum* digestive vacuole transmembrane protein PfCRT and evidence for their role in chloroquine resistance. *Molecular Cell* **6:** 861-871.

Fidock, D. A., Rosenthal, P. J., Croft, S. L., Brun, R. and Nwaka, S. (2004). Antimalarial drug discovery: efficacy models for compounds screening. *Nature Rev. Drug Discovery* **3:** 509-520.

Foley, M. and Tilley, L. (1997). Quinoline antimalarials: mechanisms of action and resistance. *International Journal for Parasitology* **27:** 231-240.

Foote, S. J., Kyle, D. E., Martin, R. K., Oduola, A. M. J., Korsyth, K., Kemp, D. J. and Cowman, A. F. (1990). Several alleles of the multidrug-resistance gene are closely linked to chloroquine resistance in *Plasmodium falciparum. Nature* **345:** 255-258.

Ford, J. M. (1996). Experimental reversal of P-glycoprotein-mediated multidrug resistance by pharmacological chemosensitizers. *Eur. J. Cancer* **32A(6):**991-1001.

Francis, S., Sullivan, D. and Goldberg, D. (1997). Haemoglobin metabolism in the malaria parasite *Plasmodium falciparum. Annu. Rev. Microbiol.* **51:** 97-123.

Gardner, M. J., Hall, N., Fung, E., White, O., Berriman, M., Hyman, R. W., Carlton, J. M., Pain, A., Nelson, K. E., Bowman, S., Paulsen, I. T., James, K., Eisen, J. A., Rutherford, K., Salzberg, S. L., Craig, A., Kyes, S., Chan, M. S., Nene, V., Shallom, S. J., Suh, B., Peterson, J., Angiuoli, S., Pertea, M., Allen, J., Selengut, J., Haft, D., Mather, M. W., Vaidya, A. B., Martin, D. M., Fairlamb, A. H., Fraunholz, M. J., Roos, D. S., Ralph, S. A., McFadden, G. I., Cummings, L. M., Subramanian, G. M., Mungall, C., Venter, J. C., Carucci, D. J., Hoffman, S. L., Newbold, C., Davis, R. W., Fraser, C. M. and Barrell, B. (2002). Genome sequence of the human malaria parasite *Plasmodium falciparum. Nature* **419:** 498-511.

Gerena, L. Bass, G. T., SR, Kyle, D. E., Oduola, A. M. J., Milhous, W. K. and Martin, R. K. (1992). Fluoxetine hydrochloride enhances in vitro susceptibility to chloroquine in resistant *Plasmodium falciparum. Antimicrob. Agents chemother.* **36(12):** 2761-2765.

Ginsburg, H., Famin, O., Zhang, J. and Drugliak, M. (1998). Inhibition of glutathione-dependant degradation of haem by chloroquine and amodiaquine as a possible basis for their antimalarial mode of action. *Biochem. Pharmacol.* **56:** 1305-1313.

Goldberg, D. E. and Slater, A. F. G. (1992). The pathway of haemoglobin degradation in malaria parasites. *Parasitol. Today* **8:** 280-283.

Goldberg, D. E., Slater, A. F. G., Cerami, A. and Henderson, G. B. (1990). Haemoglobin degradation in the malaria parasites *Plasmodium falciparum*: An ordered process in a unique organelle. *Proc. Natl. Acad. Sci. USA.* **87:** 2931-2935.

Guan, J., Kyle, D. E., Gerena, L., Zhang, Q., Milhous, W. K. and Lin, A. J. (2002). Design, synthesis, and evaluation of new chemosensitizers in multi-drug-resistant *Plasmodium falciparum. J. Med. Chem.* **45:** 2741-2748.

Gupta, S., Thapar, M. M., Mariga, S. T., Wernsdorfer, W. H. and Bjorkman, A. (2002). *Plasmodium falciparum: in vitro* interactions of artemisinin with amodiaquine, pyronaridine, and chloroquine. *Exp. Parasitol.* **100:** 28-35.

Hajduck, P. J., Bures, M., Praestgaard, J. and Fesik, W. (2000). Privileged molecules for protein binding identified from NMR-based screening. *J. Med. Chem.* **43:** 3443-3447.

Hann, M. M., Lesch, A. R. and Harper, G. J. (2001). Molecular complexity and its impact on the probability of finding leads for drug discovery. *J. Chem. Inf. Comput. Sci.* **41:** 856-864.

Hawley, S. R., Bray, P. G., Mungthin, M., Atkinson, J. D. O'Neill, P. M., and Ward, S. A. (1998). Relationship between Antimalarial Drug Activity, Accumulation, and Inhibition of Heme Polymerization in *Plasmodium falciparum in Virto. Antimicro. Agents. Chemother.* **42:** 682-686.

Hider, R. C., and Liu, Z. (1997). The treatment of malaria with iron chelators. *Journal of Pharmacy and Pharmacology* **49**, 59-64.

Holt, R. A., Subramanian, G. M., Halpern, A., Sutton, G. G., Charlab, R., Nusskern, D. R., Wincker, P., Clark, A. G., Ribeiro, J. M., Wides, R., Salzberg, S. L., Loftus, B., Yandell, M., Majoros, W. H., Rusch, D. B., Lai, Z., Kraft, C. L., Abril, J. F., Anthouard, V., Arensburger, P., Atkinson, P. W., Baden, H., de Berardinis, V., Baldwin, D., Benes, V., Biedler, J., Blass, C., Bolanos, R., Boscus, D., Barnstead, M., Cai, S., Center, A., Chaturverdi, K., Christophides, G. K., Chrystal, M. A., Clamp, M., Cravchik, A., Curwen, V., Dana, A., Delcher, A., Dew, I., Evens, C. A., Flanigan, M., Grunshober-Freimoser, A., Friedli, L., Gu, Z., Guan, P., Guigo, R., Hillenmeyer, M. E., Hladun, S. L., Hogan, J. R., Hong, Y. S., Hoover, J., Jaillon, O., Ke, Z., Kodira, C., Kokoza, E., Koutsos, A., Letunic, I., Levitsky, A., Liang, Y., Lin. J. J., Lobo, N. F., Lopez, J. R., Malek, J. A., McIntosh, T. C., Meister, S., Miller, J., Mobarry, C., Mongin, E., Murphy, S. D., O'Brochta, D. A., Pfannkoch, C., Qi, R., Regier, M. A., Remington, K., Shao, H., Sharakhova, M. V., Sitter, C. D., Shetty, J., Smith, T. J., Strong, R., Sun, J., Thomasova, D., Ton, L. Q., Topalis, P., Tu, Z., Unger, M. F., Walenz, B., Wang, A., Wang, J., Wang, M., Wang, X., Woodford, K. J., Wortman, J. R., Wu, M., Yao, A., Zdobnov, E. M., Zhang, H., Zhao, Q., Zhao, S., Zhu, S. C., Zhimulev, I., Coluzzi, M., della Torre, A., Roth, C. W., Louis, C., Kalush,

F., Mural, R. J., Myers, E. W., Adams, M. D., Smith, H. O., Broder, S., Gardner, M. J., Fraser, C. M., Birney, E., Bork, P., Brey, P. T., Venter, J. C., Weissenbach, J., Kafatos, F. C., Collins, F. H. and Hoffman, S. L. (2002).The genome sequence of the malaria mosquito Anopheles gambiae. *Science* **298:** 129-149.

Horton, D. A., Bourne, G. T. and Smythe, M. L. (2003). The combinatorial synthesis of bicyclic privileged structures or privileged substructures. *Chem. Rev.* **103:** 893-930.

Hoshen, M. B., Na-Bangchang, K., Stein, W. D. and Ginsgurg, H. (2000). Mathematical modeling of the chemotherapy of *Plasmodium falciparum* malaria with artesunate: postulation of 'dormancy', a partial cytostatic effect of the drug, and its implication for treatment regimens. *Parasitol.* **121:** 237-246.

Hussain, R. F., Nouri, A. M. E. and Oliver, R. T. D. (1993). A new approach for measurement of cytotoxicity using colorimetric assay. *J. Immunol. Methods* **160(1):** 89-96.

Hwang, M., Ahn, C. H., Pine, P. S., Yin, J. J., Hryeyna, C. A., Light, T. and Aszalos, A. (1996). Effect of combination of suboptimal concentrations of P-glycoprotein blockers on the proliferation of MDR1 gene expressing cells. *Int. J. cancer* **65:** 389-397.

Hyde, J. E. (2002). Mechanism of resistance of *Plasmodium falciparum* to antimalarial drugs. *Microbes and Infection* **4:** 165-174.

Inselburg, J. (1985). Induction and isolation of artemisinine-resistant mutants of *Plasmodium falciparum. Am. Soc. Trop. Med. Hyg.* **34:** 417-418.

Kaldor, S. W., Siegel, M. S., Fritz, J. E., Dressman, B. A. and Hahn, P. C. (1996). Use of solid supported nucleophiles and electrophiles for the purification of non-peptide small molecule library. *Tetrahedron Letters* **37**(40): 7193-7196.

Katzmann, D. J., Epping, E. A. and Moye-Rowley, W. S. (1999). Mutational disruption of plasma membrane trafficking of *Saccharomyces cerevisiae* Yor1p, a homologue of mammalian multidrug resistance protein. *Mol. Cell Biol.* **19:** 2998-3009.

Kirby, G. C. (1996). Medicinal plants and the control of parasites. *Transactions of the Royal Society of Tropical Medicine and Hygiene* **90:** 605-609.

Kirschning, A., Monenschein, H. and Wittenberg, R. (2001). Functionalized polymer-emerging versatile tools for solution-phase chemistry and automated parallel synthesis. *Angew. Chem. Int. Ed.* **40:** 650-679.

Klokouzas, A., Shahi, S., Hladky, S. B., Barrand, M. A. and van Veen H. W. (2003). ABC transporters and drug resistance in parasitic protozoa. *International Journal of Antimicrobial agents* **22:** 301-317.

Kolaczkowski, M., Kolaczkowska, A., Luczynski, J., Witek, S and Goffeau, A. (1998). *In vitro* characterization of the drug response profile of the major ABC transporters and other components of the yeast pleiotropic drug resistance network. *Microbial Drug Resistance* **4:**143-158.

Krogstad, D. J., Gluzman, I. Y., Kyle, D. E., Oduola, A. M. J., Martin, S. K., Milhous, W. K. and Schlesinger, P. H. (1987). Efflux of chloroquine from *Plasmodium falciparum*: mechanism of chloroquine resistance. *Science* **235:** 1283-1285.

Krogstad, D. J. (1996). Malaria as a re-emerging disease. *Epidemiol. Rev.* **18:** 77-79.

Krogstad, D. J., Schlesinger, P. H. and Gluzman, I. Y. (1992). The specificity of chloroquine. *Parasitol. Today* **8:** 183-184.

Kyle, D. E., Oduola, A. M. J., Martin, S. K. and Milhous, W. K. (1990). Trans. Soc. Trop. Med. Hyg. 84: 874-

Lambros, C. and Vanderberg, J. P. (1979). Synchronization of *Plasmodium falciparum* erythrocytic stages in culture. *Journal of Parasitology* **65(3):** 410-420.

Landgraf, B., Kollaritsch, H., Wiedermann, G. and Wernsdorer, W. H. (1994). *Plasmodium falciparum*: susceptibility *in vitro* and *in vivo* to chloroquine and sulfadoxine-pyrimethamine in Ghanaian schoolchildren. *Trans. R. Soc. Trop. Med. Hyg.* **88:** 440-442.

Lee, G., Dallas, S., Hong, M. and Bendayan, R. (2001). Drug transporters in the central nervous system: brain barriers and brain parenchyma considerations. *Pharmacol. Rev.* **53:** 569-586.

Li, Z. S., Lu, Y. P., Zhen, R. G., Szczypka, M., Thiele, D. and Rea, P. A. (1997). A new pathway for vacuolar cadmium sequestration in *Saccharomyces cerevisiae*: YCF1-catalysed transport of bis(glutathionato)cadmium. *Biochemistry* **94:** 42-47.

Lipinski, C. A., Lombardo, F., Dominy, B. W. and Feeney, P. J. (1997). Experimental and computational approaches to estimate solubility and permeability in drug discovery and development settings. *Adv. Drug Deliv. Rev.* **23:** 3-25.

Makler, M. T., Ries, J. M., Williams, J. A., Bancroft, J. E., Piper, R. C., Gibbins, B. L. and Hinrichs, D. J. (1993). Parasite lactate dehydrogenase as an assay for *Plasmodium falciparum* drug sensitivity. *American Journal of Tropical Medicine and Hygiene* **48** (6): 739-741.

Martin, K. M., Oduola, A. M. J. and Milhous, W. K. (1987). Reversal of chloroquine resistance in *Plasmodium falciparum* by verapamil. *Science* **235:** 899-901.

Martiney, J. A., Cerami, A. and Slater, A. F. G. (1995). Verapamil reversal of chloquoquine resistance in malaria parasite *Plasmodium falciparum* is specific for resistant parasites and independent of the weak base effect. *J. Biol. Chem.* **270:** 22393-22398.

Meshnick, S. R., Taylor, T. E. and Kamchonwongpaisan, S. (1996). Artemisinin and the antimalarial endoperoxides: From herbal remedy to targeted chemotherapy. *Microbiol. Rev.* **60:** 301-315.

Mizuno, N., Niwa, T., Yotsumoto, Y. and Sugiyama, Y. (2003). Impact of drug transporter studies on drug discovery and development. *Pharmacol. Rev.* **55:** 425-461.

Mosmann, T. (1983). Rapid colorimetric assay for cellular growth and survival: Application to proliferation and cytotoxic assays. *J. Immunol. Methods.* **65:** 55-63.

Nwaka, S. and Ridley, R. G. (2003). Virtual drug discovery and development for neglected diseases through public–private partnership. *Nature Rev. Drug Discovery* **2:** 919-928.

O'Brien, F. L. and Hahn, F. E. (1965). Chloroquine structural requirements for binding to deoxyribonucleic acid and antimalarial activity. *Antimicrob. Agents Chemother.* **5:** 315-320.

Olliaro, P. L., Haynes, R. K., Meunier, B. and Yuthavong, Y. (2001). Possible modes of action of artemisinin-type compounds. *Trends Parasitol.* **17:** 122-126.

Orjih, A. U., Ryerse, J. S. and Fitch, C. D. (1994). Hemoglobin catabolism and the killing of intraerythrocytic *Plasmodium falciparum* by chloroquine. *Experimenta.* **50:** 34-38.

Osa, Y., Kobayashi, S., Sato, Y., Suzuki, Y., Takino, K., Takeuchi, T., Miyata, Y., Sakaguchi, M. and Takayanagi, H. (2003). Structural properties of dibenzosuberanylpiperazine derivatives for efficient reversal of chloroquine resistance in *Plasmodium chabaudi. J. Med. Chem.* **46:** 1948-1956.

Pasvol, G. (1995). Clinical infectious diseases: Malaria (ed. Pasvol, G.) Volume 2/Number 2. W. B. Saunders Company Ltd, Cambridge, London, UK.

Patchett, A. A. (2002). 2002 Alfred Burger Award address in medicinal chemistry. Natural products and design: interrelated approaches in drug discovery. *J Med. Chem.* **45:** 5609-5616.

Pradines, B., Fusai, T., Daries, W., Laloge, V., Rogier, C., Millet, P., Panconi, E., Kombila, M. and Parzy, D. (2001). Ferrocene-chloroquine analogues as antimalarial agents: *in virto* activity of ferrochloroquine against 103 Gabonese isolates of *Plasmodium falciparum*. *Journal of Antimicrobial Chemotherapy* **48**, 179-184.

Rasoanaivo, P., Ratsimamanga-Urverg, S. and Frappier, F. (1996). Reversing agents in the treatment of drug-resistant malaria. *Current medicinal chemistry* **3:** 1-10.

Rasoanaivo, P., Ramanitrahasimbola, D., Rakotonandrasana, O. L. and Ratsimamanga, S. (2004). Biodiversity, traditional medicine and resistance modulators. Submitted.

Raynes, K. J., Bray. P. G., Ward, S. A. (1999). Altered binding of chloroquine to ferriprotoporphyrin IX is the basis for chloroquine resistance. *Drug Resistance Update* **2:** 97-103.

Reed, M. B., Saliba, K. J., Caruana, S. R., Kirk, K. and Cowman, A. (2000). Pgh1 modulates sensitivity and resistance to multiple antimalarials in *Plasmodium falciparum*. *Nature* **403:** 906-909.

Ridley, R. G. (2002). Medical need, scientific opportunity and the drive for antimalarial drugs. *Nature* **415:** 686-693.

Ridley, R. G. (2003). To kill a parasite. *Nature* **424:** 887-889.

Riordan, J. R., Deuchars, K., Kartner, N., Alon, N., Trent, J. and Ling, V. (1985). Amplification of P-glycoprotein genes in multidrug-resistant mammalian cell lines. *Nature* **316:** 817-819.

Rishton, G. M. (2003). Non lead-likeness and lead-likeness in biochemical screening. *Drug Discovery Today* **8**, 86-96.

Roll Back Malaria. Malaria in South Africa. http://www.malaria.org.za/Malaria_Risk/Update/update.html (accessed 21 July 2004)

Rosenthal, P. J. and Meshnick, S. R. (1996). Hemoglobin catabolism and iron utilization by malaria parasites. *Mol. Biochem. Parasitol.* **83:** 131-139.

Rosenthal, P. J. (2003). Antimalarial drug discovery: old and new approaches. *The Journal of Experimental Biology* **206:** 3735:3744.

Sanchez, C. P., Wünsch, S. and Lanzer, M. (1997). Identification of chloroquine importer in *Plasmodium falciparum*: differences in import kinetics are genetically linked with chloroquine resistance phenotype. *J. Biol. Chem.* **272:** 2652-2658.

Sanchez, C., Stein, W. and Lanzer, M. (2003). Trans stimulation provides evidence for a drug efflux carrier as the mechanism of chloroquine resistance in *Plasmodium falciparum*. *Biochemistry* **42:** 9383-9394.

Sidhu, A. B. S., Verdier-Pinard, D. and Fidock, D. A. (2002). Chloroquine resistance in *Plasmodium falciparum* malaria parasites conferred by *pfcrt* mutations. *Science* **298:** 210-213.

Smith, A. G. (2000). How toxic is DDT? *Lancet* **356:** 267-268.

Schmatz, D. and Schaffer, J. (1991). Antiparasite agents. *Annu. Rep. Med. Chem.* **26:** 161-170.

Sherman, I. W. (1998). Malaria – Parasite Biology, Pathogenesis and Protection (ed. Sherman, I. W.) American Society for Microbiology, Washington DC.

Shuker, S. B., Hajduk, P. J., Meadows, R. P. and Fesik, S. W. (1996). Discovering high-affinity ligands for proteins: SAR by NMR. *Science* **274:** 1531-1534.

Sieuwerts, A. M., Klijn, J. G. M., Peters, H. A. and Foekens, J. A. (1995). The MTT Tetrazolium Salt Assay Scrutinized: how to use this assay reliably to measure metabolic activity of cell cultures *in vitro* for the assessment of growth characteristics, IC_{50}-values and cell survival. *Eur. J. Clin. Chem. Clin. Biochem.* 33: 813-823,

Slater, A. F. G. and Cerami, A. (1992). Inhibition by chloroquine of a novel haem polymerase enzyme activity in malaria trophozoites. *Nature* **335:** 167-169.

Sowunmi, A., Oduola, A. M. J., Ogundahunsi, O. A. T., Falade, C. O., Gbotosho, G. O. and Salako, L. A. (1997). Enhanced efficacy of chloroquine-chlopheniramine combination in acute uncomplicated falciparum malaria in children. *Trans. Royal Soc. Trop. Med. Hyg.* **91:** 63-67.

Spring, D. R., Krishnan, S., Blackwell, H. E. and Schreiber, S. L. (2001). Diversity-oriented synthesis of biaryl-containing medium rings using a one bead/one stock solution plateform. *J. Am. Chem. Soc.* **124(7):** 1354-1363.

Stanforth, S. P. (1997). Catalytic cross-coupling reactions in biaryl synthesis. *Tetrahedron* **54:** 263-303.

Su, X-z., Carucci, D. J. and Wellems, T. E. (1997). Complex polymorphisms in a ~330 kDa protein are linked to chloroquine-resistant *P. falciparum* in Southeast Asia and Africa. *Cell* **91:** 593-603.

Sullivan, D. J., Jr, Gluzman, L. Y. and Goldberg, D. E. (1996a). Plasmodium hemozoin formation mediated by histidine-rich proteins. *Science* **271:** 219-222.

Sullivan, D. J., Jr, Gluzman, L. Y. Russel, D. G. and Goldberg, D. E. (1996b). On the molecular mechanism of chloroquine's antimalarial action. *Proc. Natl. Acad. Sci. USA.* **93:** 11865-11870.

Suzuki, T., Fukazawa, N., San-nohe, K., Sato, W., Yano, O and Tsuruo, T. (1997). Structure-activity relationship of newly synthesized quinoline derivatives for reversal of multidrug resistance in cancer. *J. Med. Chem.* **40:** 2047-2052.

Teague, S. J., Davis, A. M., Leeson, P. D. and Oprea, T. (1999). The design of lead-like combinatorial libraries. *Angew chem., Int. Ed. Engl.* **38:** 3743-3748.

Terret, N. K., Gardner, M., Gordon, D. W., Kobylecki, R. J. and Steele, J. (1995). Combinatorial synthesis – the design of compound libraries and their application to drug discovery. *Tetrahedron* **51(30):** 8135-8173.

Trager, W. and Jensen, J. B. (1978). Cultivation of malarial parasites. *Nature* **273:** 621-622.

Trigalo, F., Joyeau, R., Pham, V. C., Youté, J. J., Rasoanaivo, P. and Frappier, F. (2004). Synthesis of modulators of chloroquine resistance in *Plasmodium falciparum*: analogues of malagashanine from strychnobrasiline. *Tetrahedron* **65:** 5471-5474.

van Schalkwyk, D. A., Walden, J. C. and Smith, P. J. (2001). Reversal of chloroquine resistance in *Plasmodium falciparum* using combinations of chemosensitizers. *Antimicrob. Agents chemother.* **45:** 3171-3174.

Vido, K., Daniel, S., Lagniel, G., Lopez, S., Toledano, M. B. and Labarre, J. (2001). A proteome analysis of the cadmium response in *Saccharomyces cerevisiae. J. Biological Chem.* **276:** 8469-8474.

Wang, P., Read, M., Sims, P. F. G. and Hyde, J. E. (1997). Sulfadoxine resistance in the human malaria parasite *Plasmodium falciparum* is determined by mutations in dihydropteroate synthetase and an additional factor associated with folate utilization. *Mol. Microbiol.* **23:** 979-986.

Ward, S. A., Bray, P. G. and Hawley, S. R. (1997). Quinoline resistance mechanisms in *Plasmodium falciparum*: the debate goes on. *Parasitology* **114:** S125-S136.

Warhurst, D. C., Craig, J. C. and Adagu, I. S. (2002). Lysosomes and drug resistance in malaria. *The Lancet* **360:** 1527-1529.

Warhurst, D. C. (2003). Polymorphism in the *Plasmodium falciparum* chloroquine-resistance transporter protein links verapamil enhancement of chloroquine sensitivity with the clinical efficacy of amodiaquine. *Malaria Journal* **2:** 31-42.

Wellems, T. E., Walker-Jonah, A. and Panton, L. J. (1991). Genetic mapping of the chloroquine-resistant locus on *Plasmodium falciparum chromosome 7. Proc. Natl. Acad. Sci. USA* **88:** 3382-3386.

Wellems, T. E. *Plasmodium* chloroquine resistance and the search for a replacement antimalarial drug. *Science* **298:**124-126.

WHO, World Health Organisation Fact Sheet No. 94. WHO information. (2004). http://www.rbm.who.int/cmc_upload/0/000/015/372/RBMInfosheet_1.html (accessed 21 July 2004)

Wiese, M. and Pajeva, I. K. (2001). Structure-activity relationships of multidrug resistance reversers. *Current Medicinal Chemistry* **8:** 685-713.

Wolfe, M. S., and Cordero, J. F. (1985). Safety of chloroquine in chemosupression of malaria during pregnancy. *Br. Med. J. (Clin. Res.)* **290:** 1466-1467.

Wootton, J. C., Feng, X., Ferdig, M. T., Cooper, R. A., Mu, J., Baruch, D. I., Magill, A. J. and Su, X-z. (2002). Genetic diversity and chloroquine selective sweeps in *Plasmodium falciparum. Nature* **418:** 320-323.

Xu, W., Mohan, R. and Morrissey, M. M. (1997). Polymer supported bases in combinatorial chemistry: synthesis of aryl ethers from phenols and alkyl halides and aryl halides. *Tetrahedron Letters* **38**(42): 7337-7340.

Wünsch, S., Sanchez, C. P., Gekle, M., Grosse-Wortmann, L., Wiesner, J. and Lanzer, M. (1998). Differential stimulation of the Na^+/H^+ exchanger determines chloroquine uptake in *Plasmodium falciparum. J. Cell Biol.* **140:** 335-345.

Yayon, A., Cabantchik, Z. I. and Ginsburg, H. (1984). Identification of the acidic compartment of *Plasmodium falciparum* infected human erythrocytes as the target of the antimalarial drug chloroquine. *The EMBO Journal* **3**(11): 2695-2700.

Yamey, G. (2004). Roll Back Malaria: a failing global health campaign. Only increased donor support for malaria control can save it. *BMJ* **328:** 1086-1087.

Zhang, H, Howard, E. M. and Roepe, P. D. (2002). Analysis of the antimalarial drug resistance protein Pfcrt in yeast. *J. Biol. Chem.* **277:** 49767-49775.

Zarchin, S., Krugliak, M. and Ginsburg. (1986). Digestion of the host erythrocyte by malarial parasites is the primary target for quinoline-containing antimalarials. *Biochem. Pharmacol.* **35:** 2435-2442.

http://www.gmap.net/oxford/image/ malaria_2002.jpg

http://images.encarta.msn.com/xrefmedia/aencmed/targets/illus/ilt/T073615A.gif

Appendix 1

Compound P4

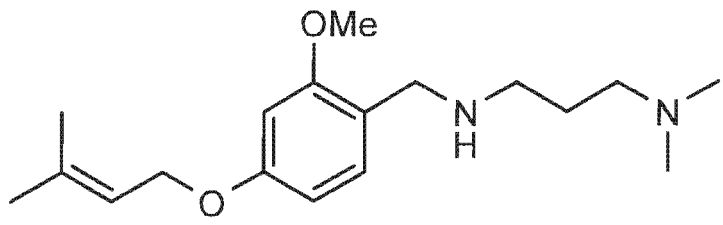

Compound P4

IUPAC

N'-[2-*Methoxy*-4-(3-*methyl*-*but*-2-*enyloxy*)-*benzyl*]-*N,N*-*dimethyl*-*propan*-1,3-*diamine*

List of spectra:

- ^{1}H NMR (300MHz, $CDCl_3$)
- ^{13}C NMR (100MHz, $CDCl_3$)
- Mass spectrum

P4

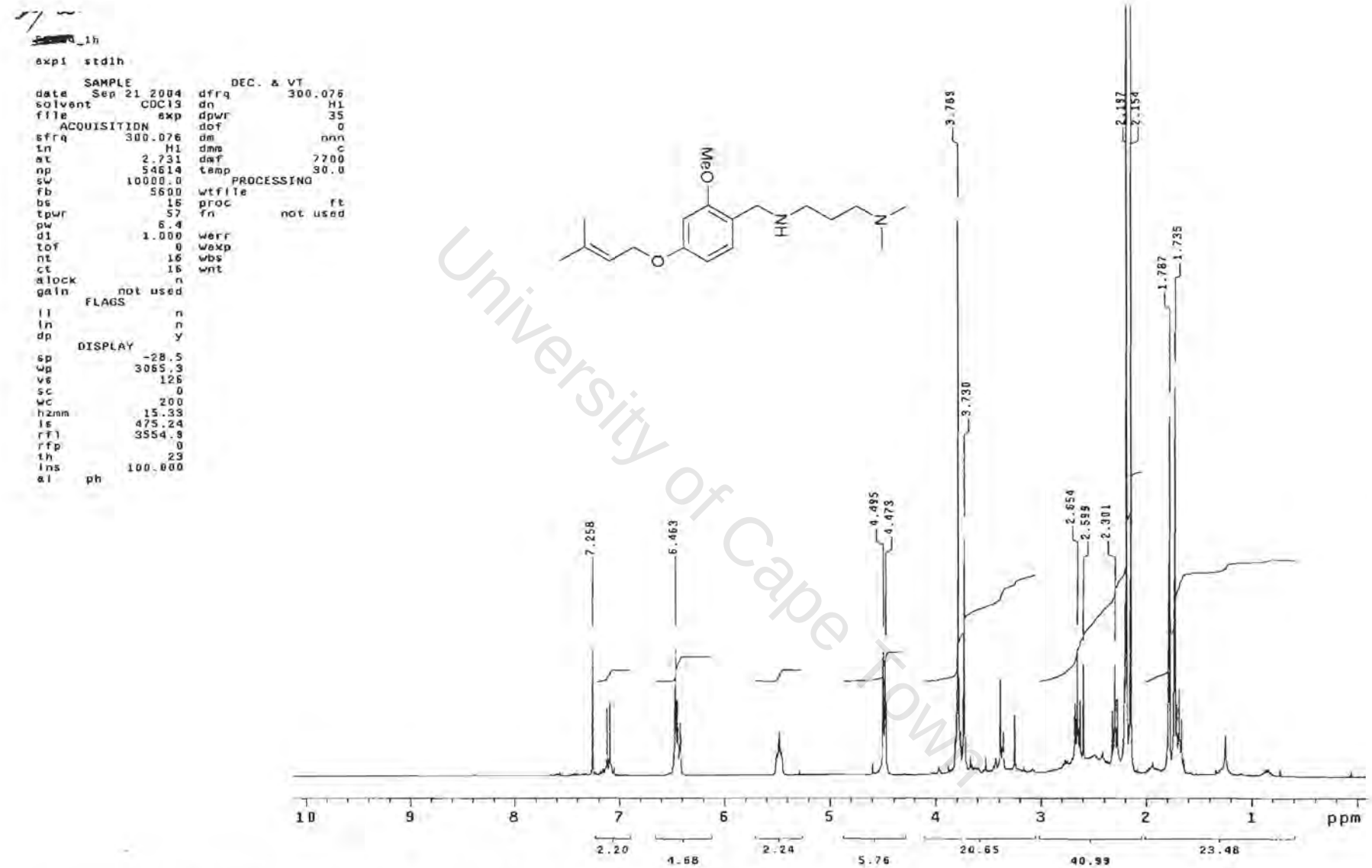

Figure 4.1.1. ^{1}H NMR spectrum of compound **P4** in $CDCl_3$, 300 MHz

P4

```
SY-2_13C

Pulse Sequence: s2pul
 Solvent: CDCl3
 Temp. 30.0 C / 303.1 K
Mercury-300BB  "kudu300"

 Pulse 63.9 degrees
 Acq. time 1.815 sec
 Width 18761.7 Hz
 1630 repetitions
OBSERVE  C13,  75.4537290 MHz
DECOUPLE  H1, 300.0756915 MHz
 Power 35 dB
 continuously on
 WALTZ-16 modulated
DATA PROCESSING
 Line broadening 0.5 Hz
FT size 131072
Total time 4 hr, 48 min, 4 sec
```

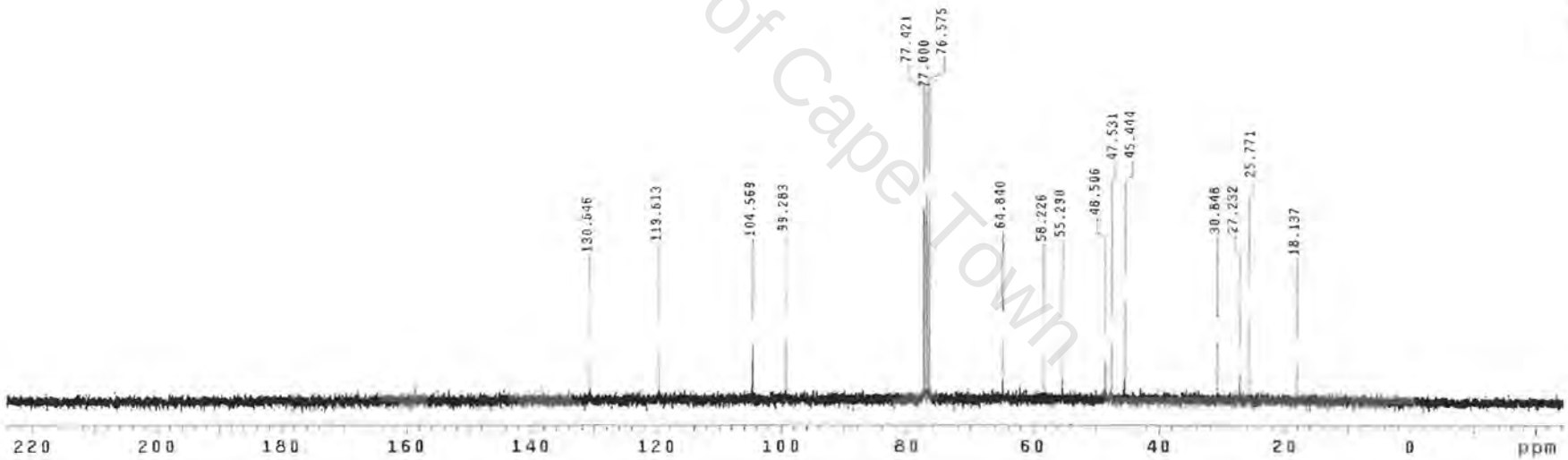

Figure 4.1.2. ^{13}C NMR spectrum of compound **P4** in $CDCl_3$, 75 MHz

P4

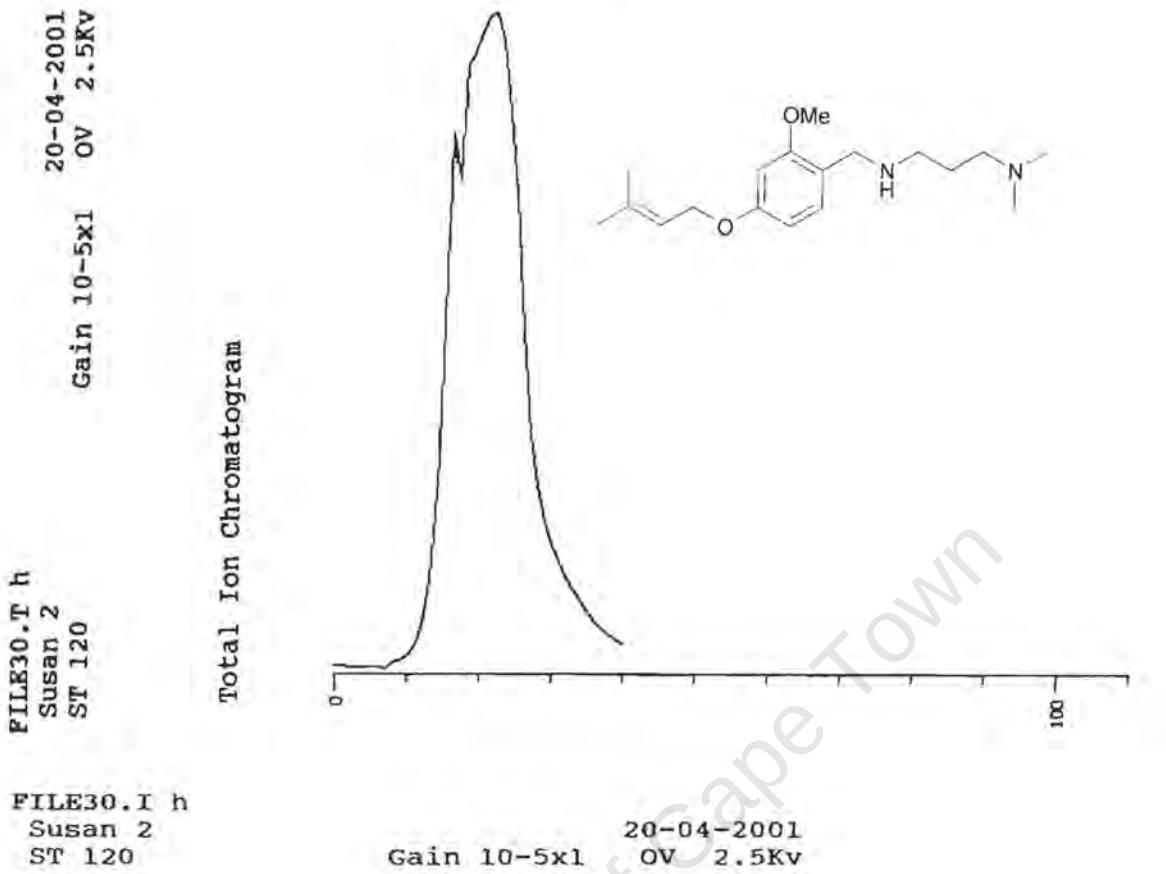

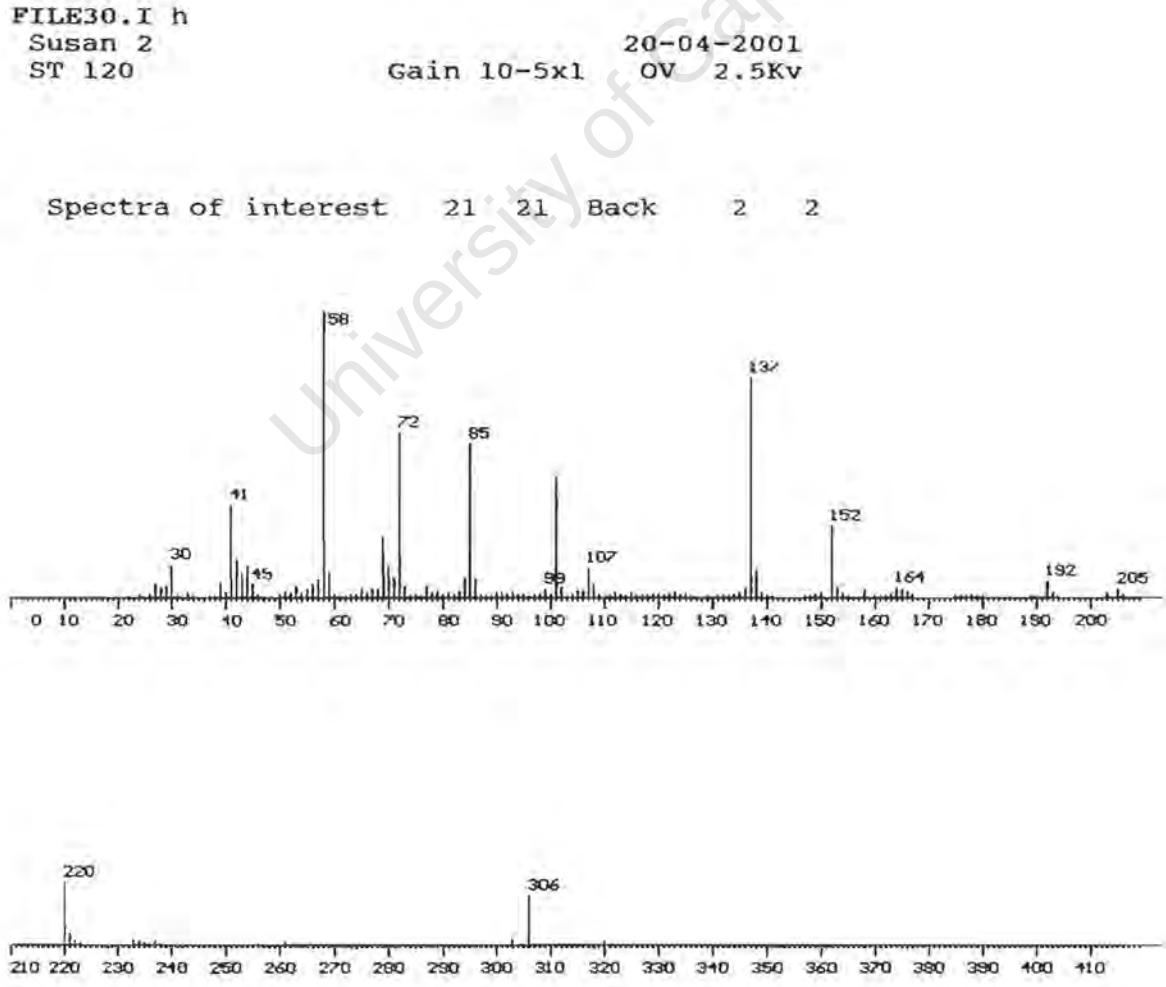

Figure 4.1.3. Mass spectrum of compound **P4**.

Compound P5

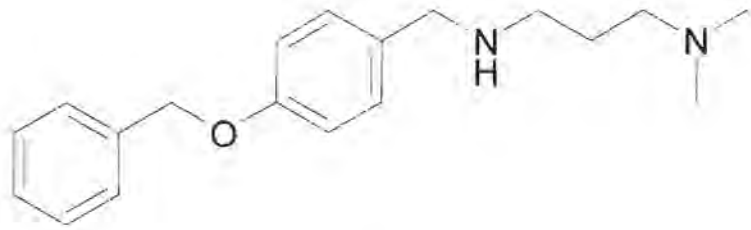

Compound P5

IUPAC

N'-(4-Benzyloxy-benzyl)-N,N-dimethyl-propan-1,3-diamine

List of spectra:

- ^{1}H NMR (300MHz, $CDCl_3$)
- ^{13}C NMR (100MHz, $CDCl_3$)
- Mass spectrum

P5

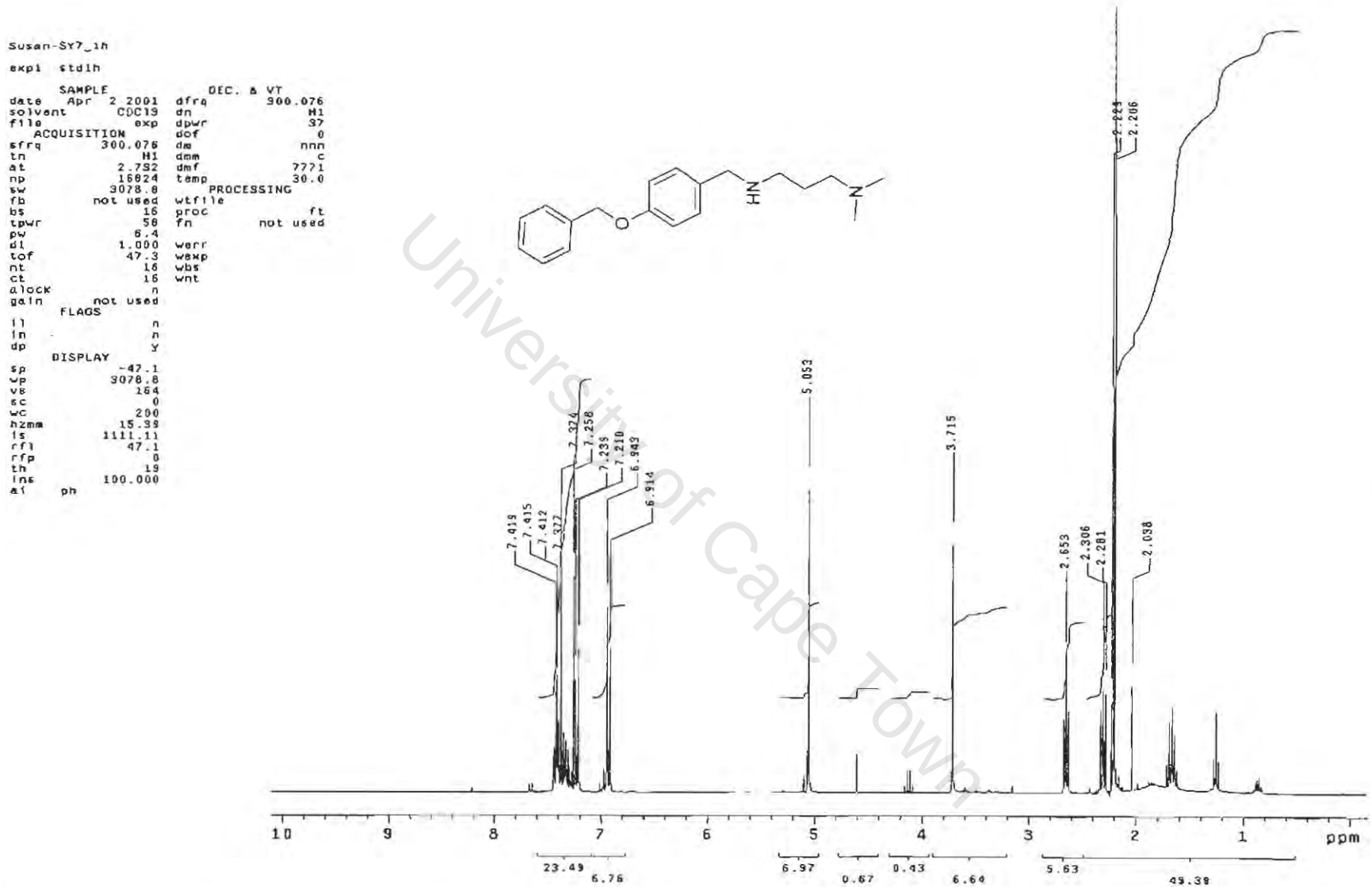

Figure 4.1.4. ^{1}H NMR spectrum of compound **P5** in $CDCl_3$, 300 MHz

P5

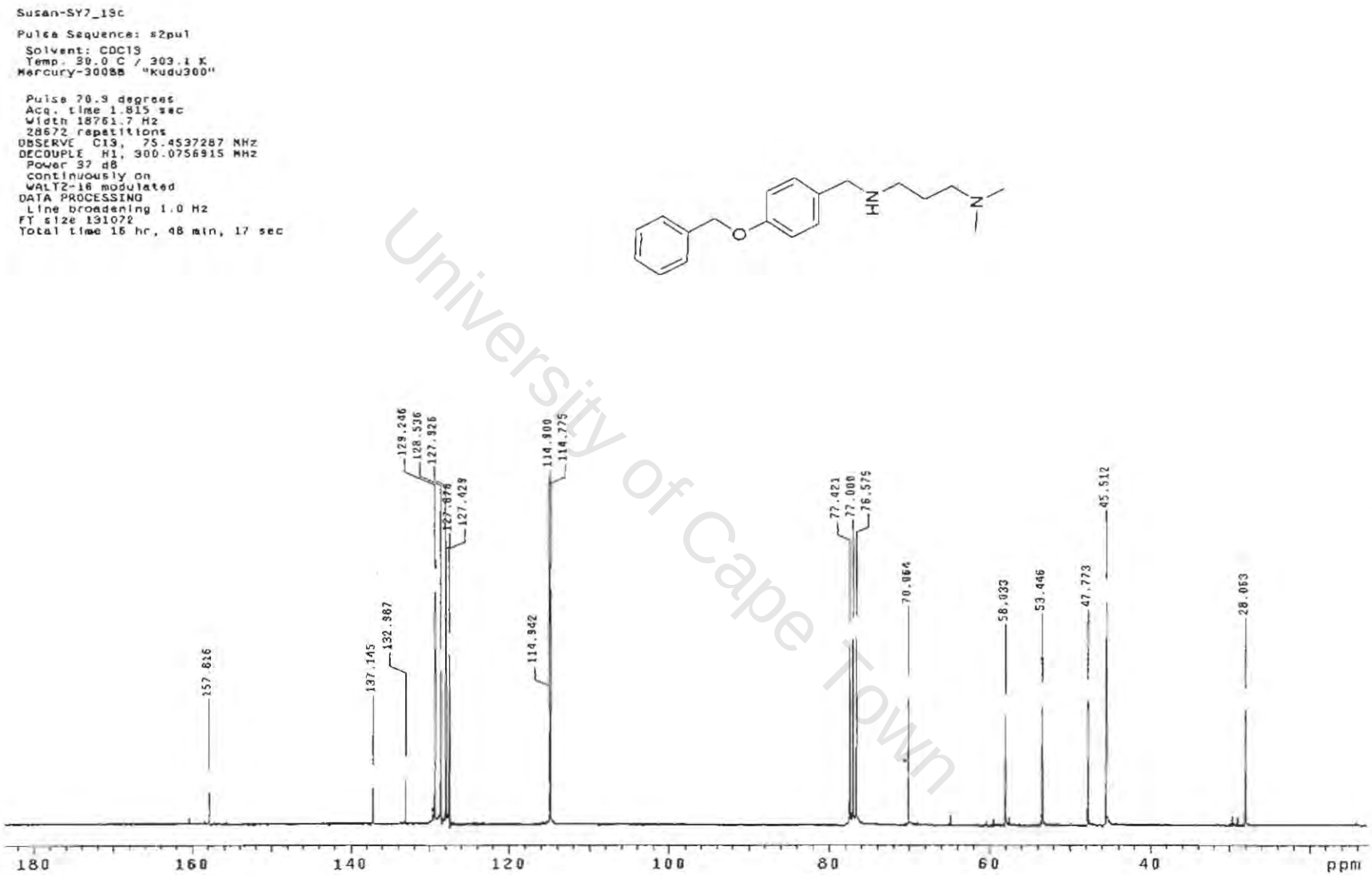

Figure 4.1.5. ^{13}C NMR spectrum of compound **P5** in $CDCl_3$, 75 MHz

P5

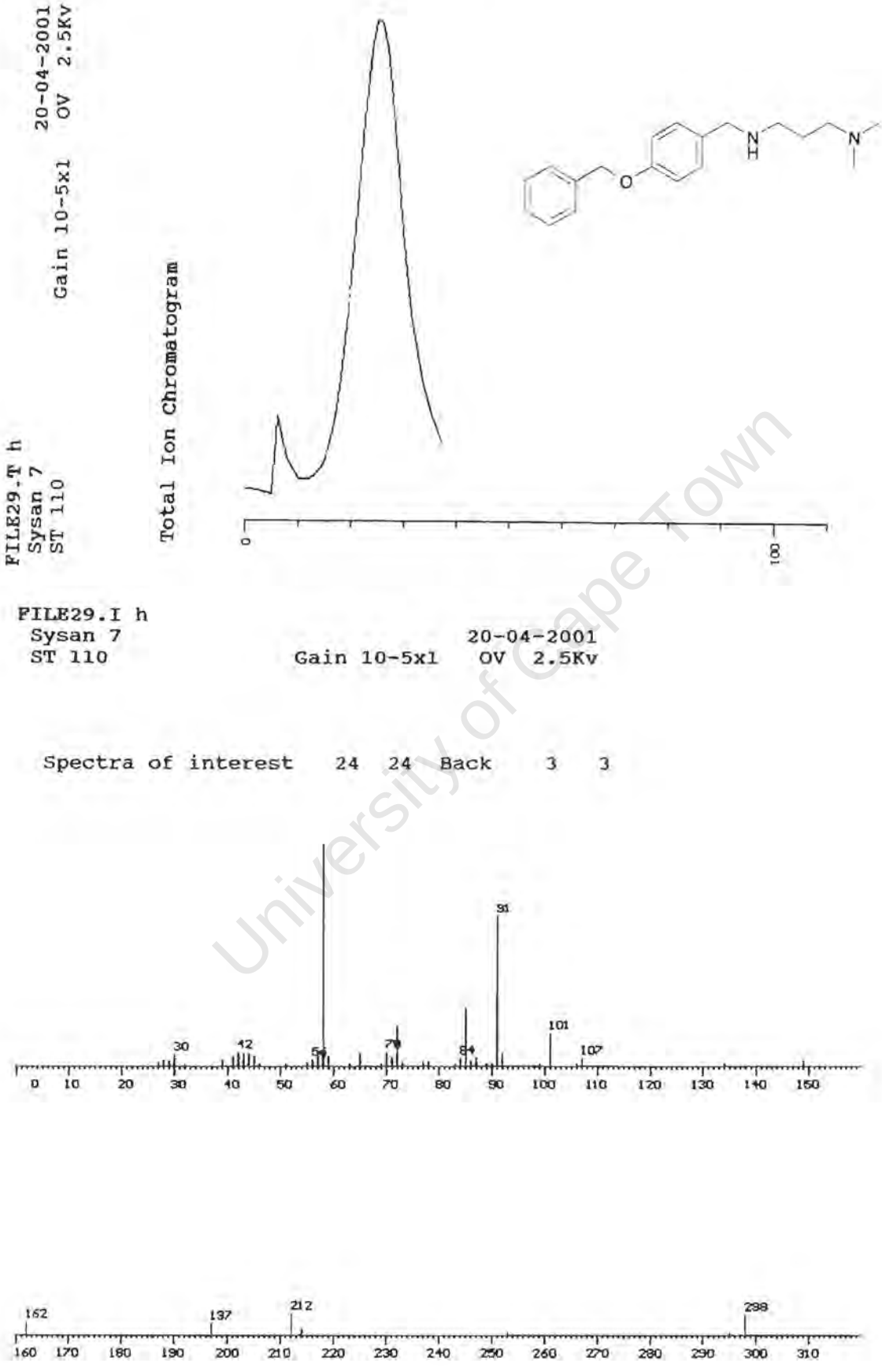

Figure 4.1.6. Mass spectrum of compound **P5**.

Compound P6

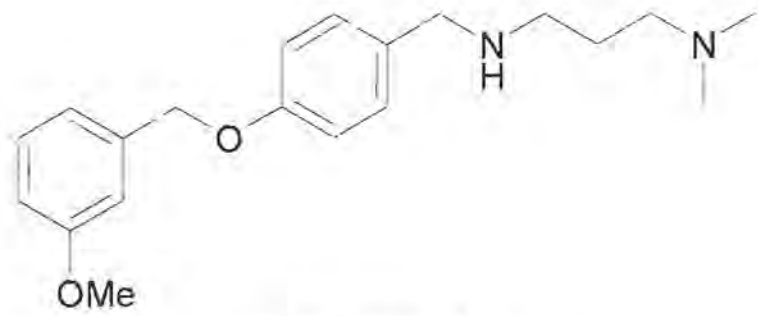

Compound P6

IUPAC

N'-[4-(3-*Methoxy-benzyloxy*)-*benzyl*]-*N*,*N*-*dimethyl*-*propane*-1,3-*diamine*

List of spectra:

- ^{1}H NMR (300MHz, $CDCl_3$)
- ^{13}C NMR (100MHz, $CDCl_3$)
- Mass spectrum

P6

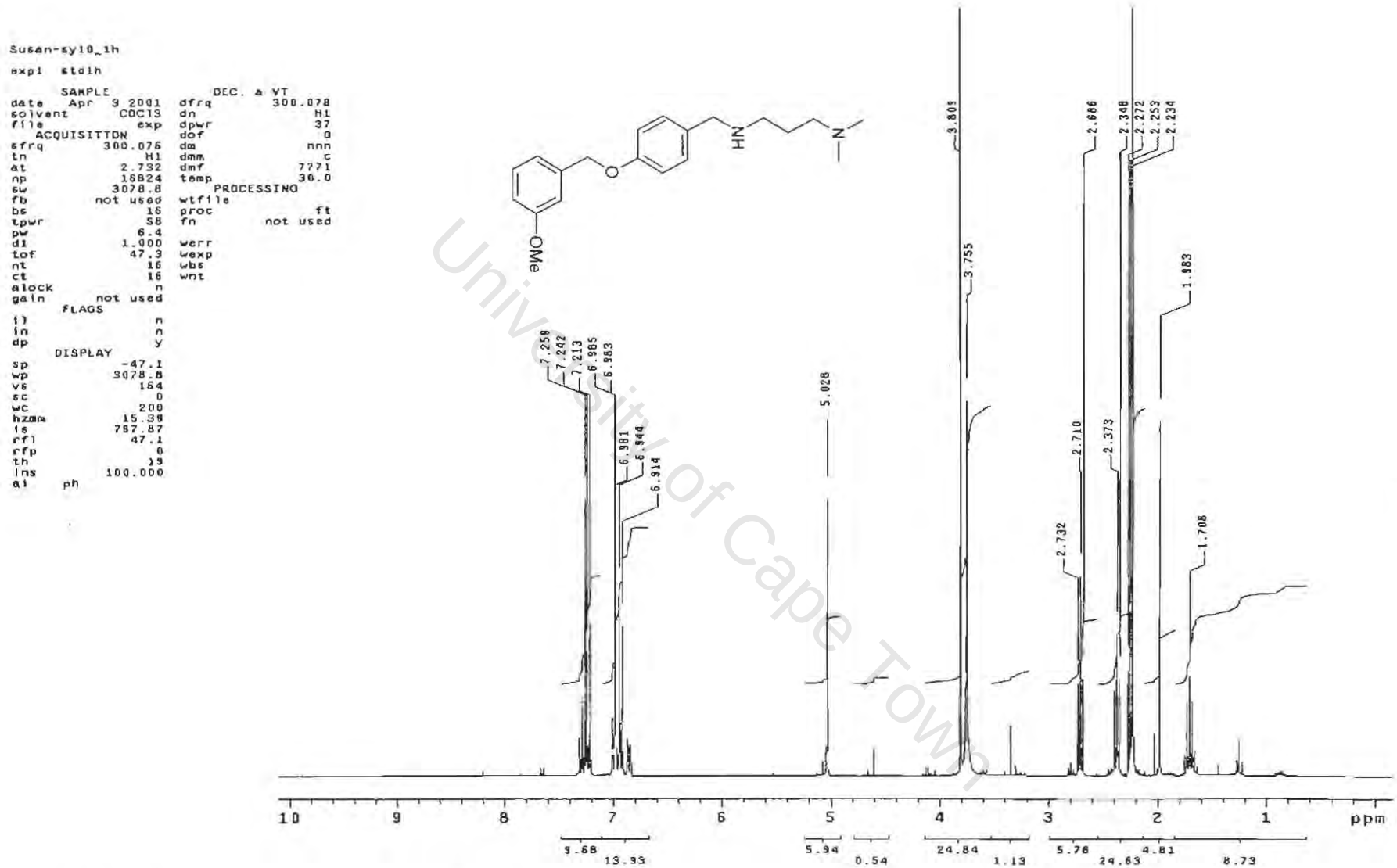

Figure 4.1.7. ^{1}C NMR spectrum of compound **P6** in $CDCl_3$, 300 MHz

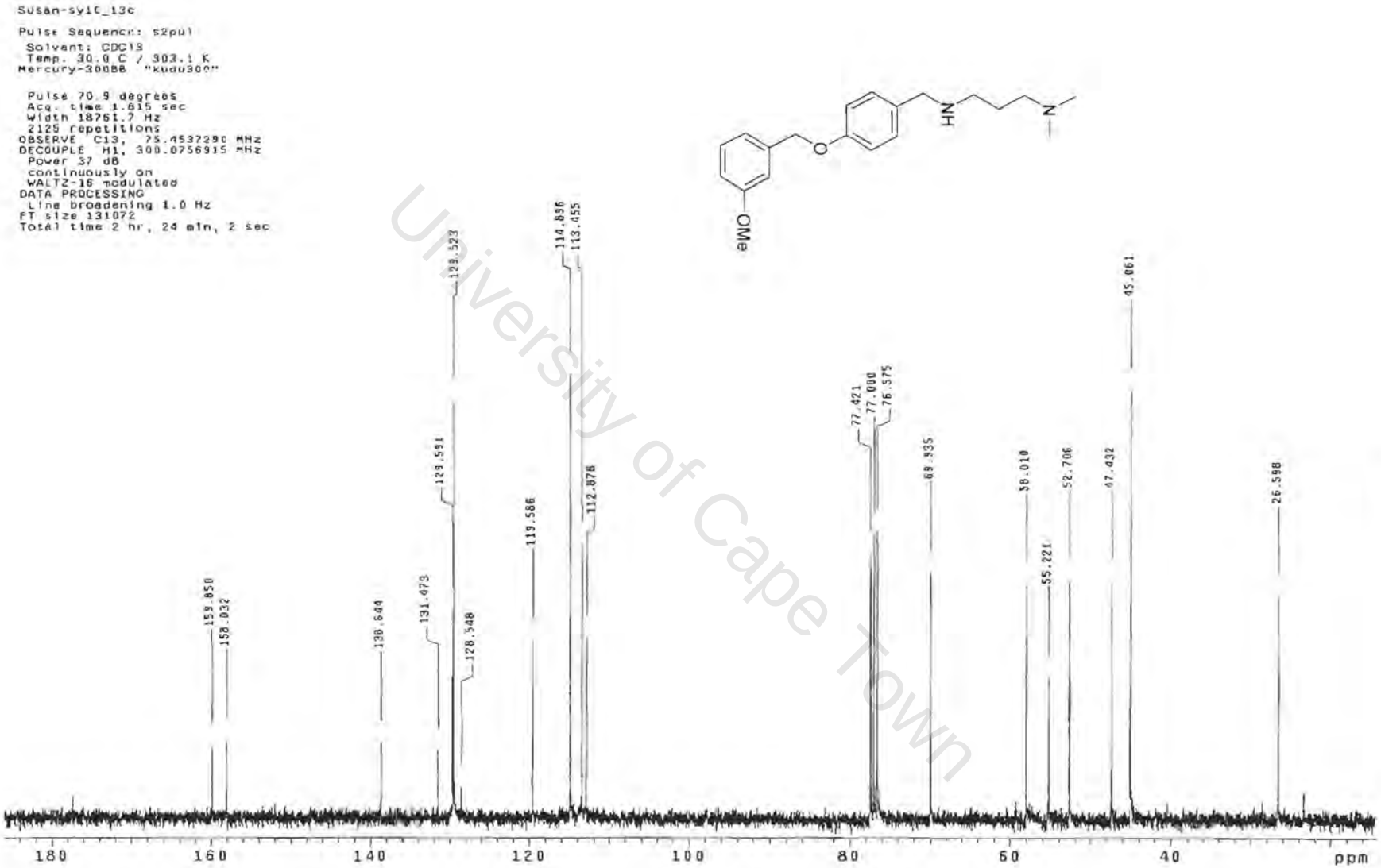

Figure 4.1.8. ^{13}C NMR spectrum of compound **P6** in $CDCl_3$, 75 MHz

P6

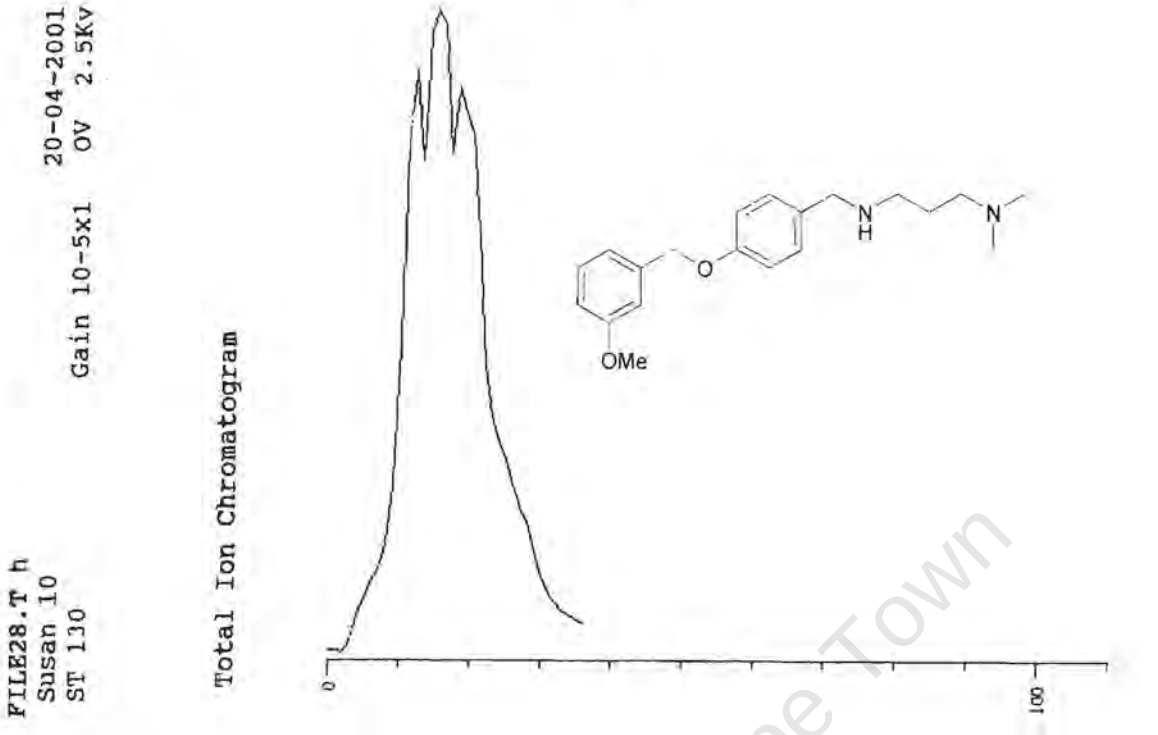

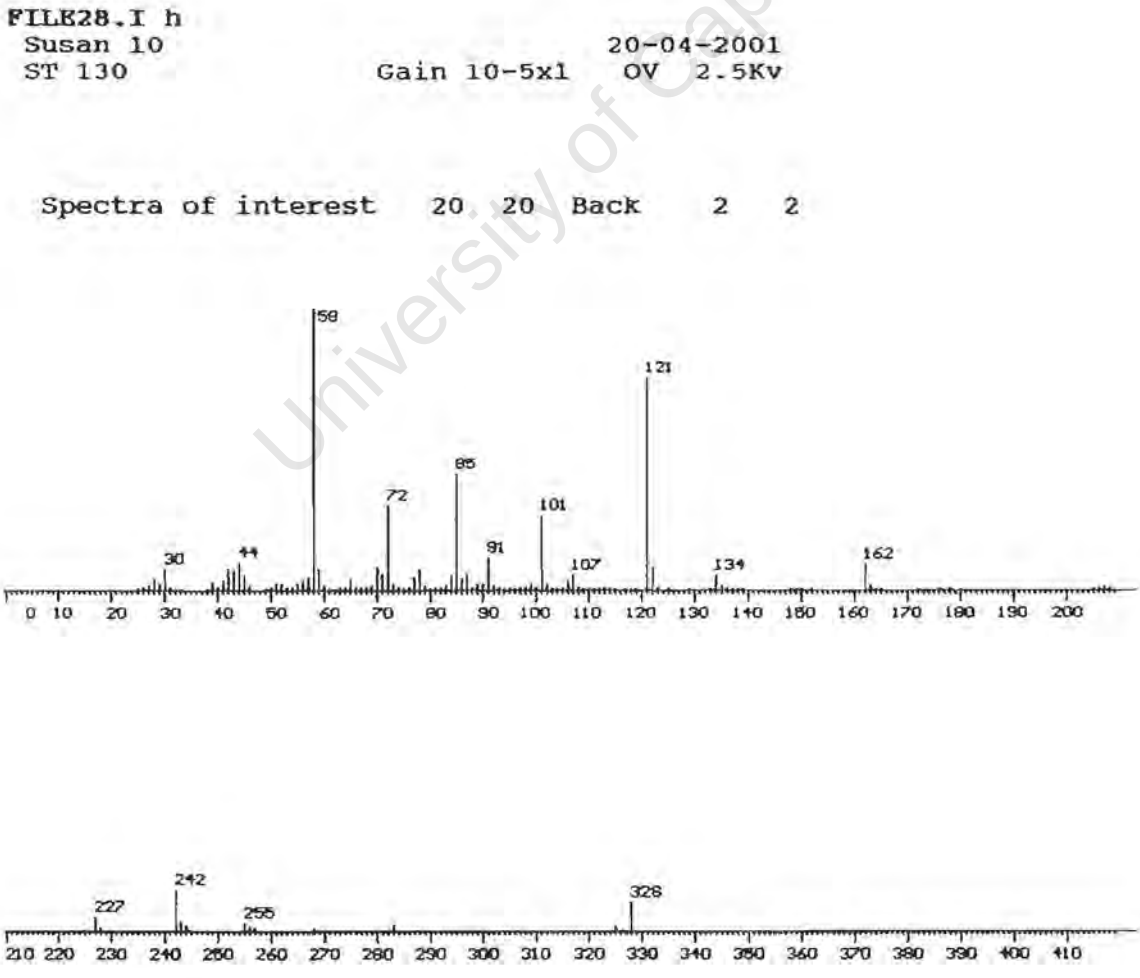

Figure 4.1.9. Mass spectrum of compound **P6**.

Compound P7

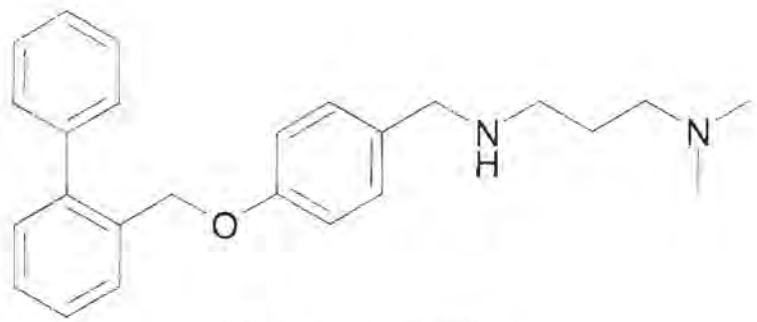

Compound P7

IUPAC

N'-[4-(*Biphenyl*-2-*ylmethoxy*)-*benzyl*]-*N,N-dimethyl-propane*-1,3-*diamine*

List of spectra:

- ^{1}H NMR (300MHz, $CDCl_3$)
- ^{13}C NMR (100MHz, $CDCl_3$)
- Mass spectrum

P7

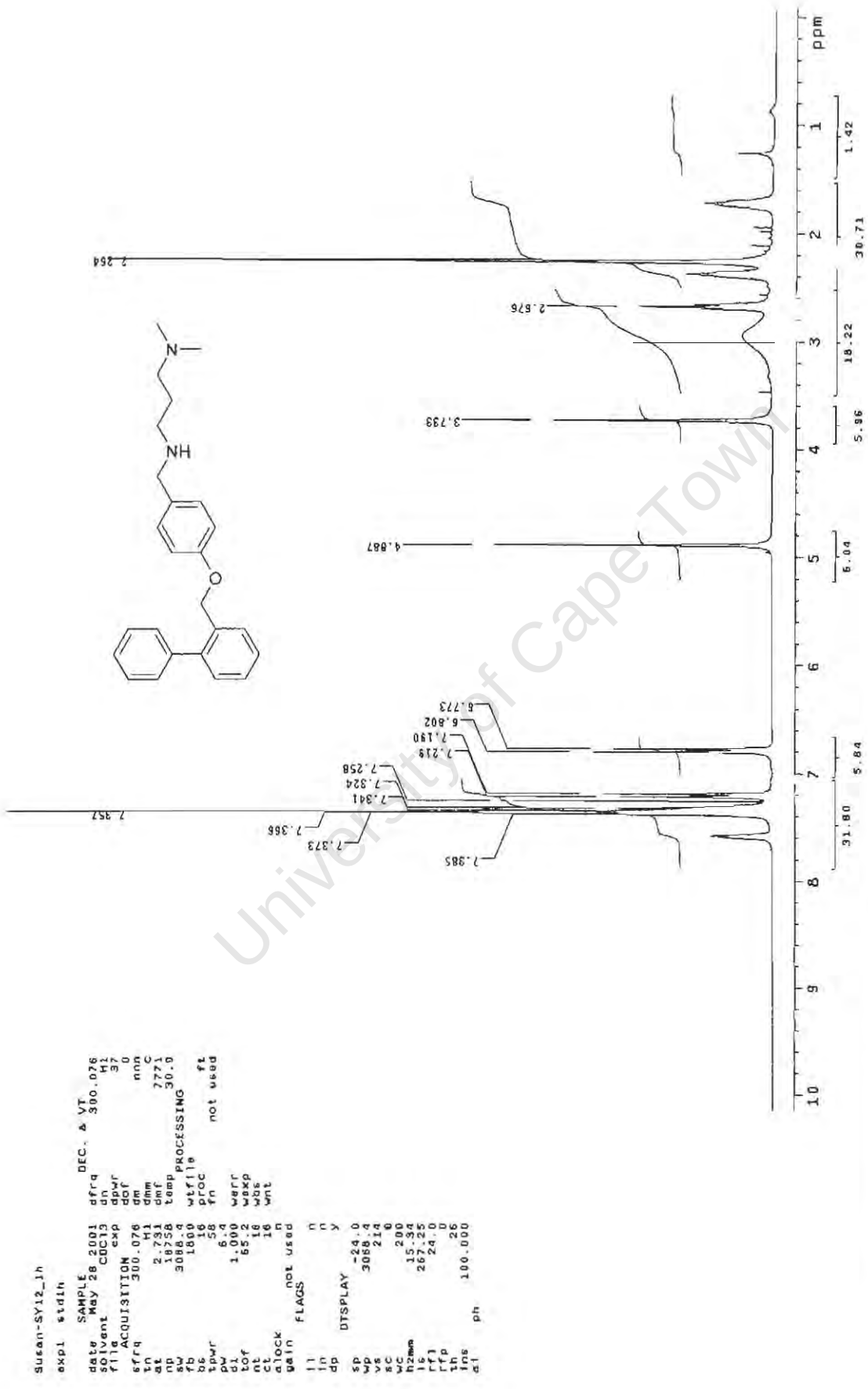

Figure 4.1.10. ^{1}H NMR spectrum of compound **P7** in $CDCl_3$, 300 MHz

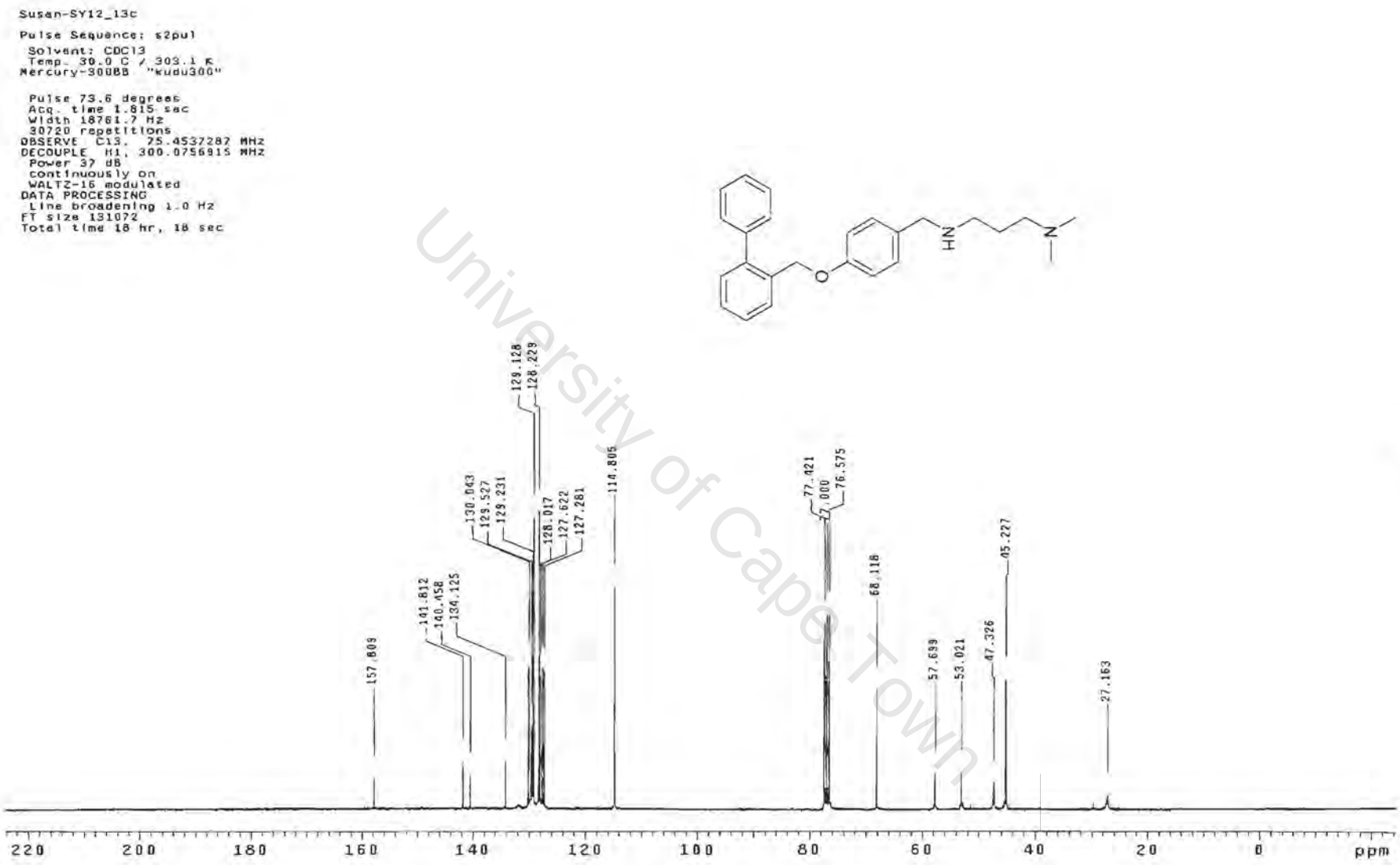

Figure 4.1.11. ^{13}C NMR spectrum of compound **P7** in $CDCl_3$, 75 MHz

P7

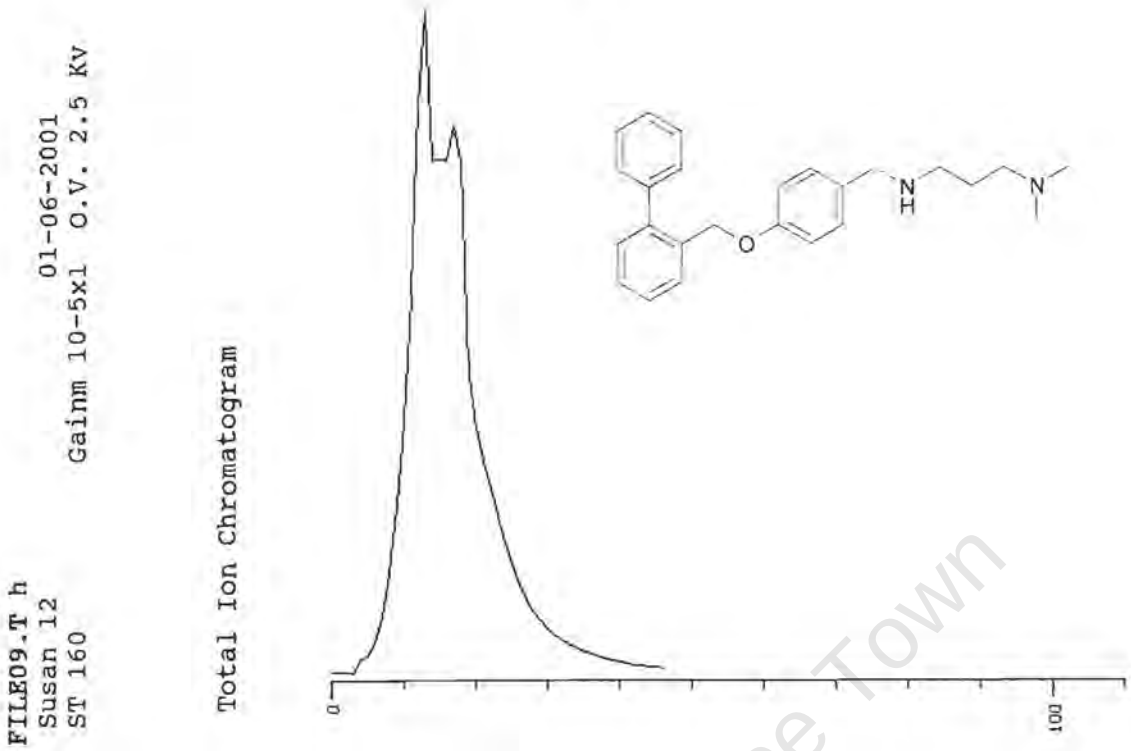

FILE09.I h
Susan 12
ST 160
01-06-2001
Gainm 10-5x1 O.V. 2.5 Kv

Spectra of interest 27 27 Back 1 1

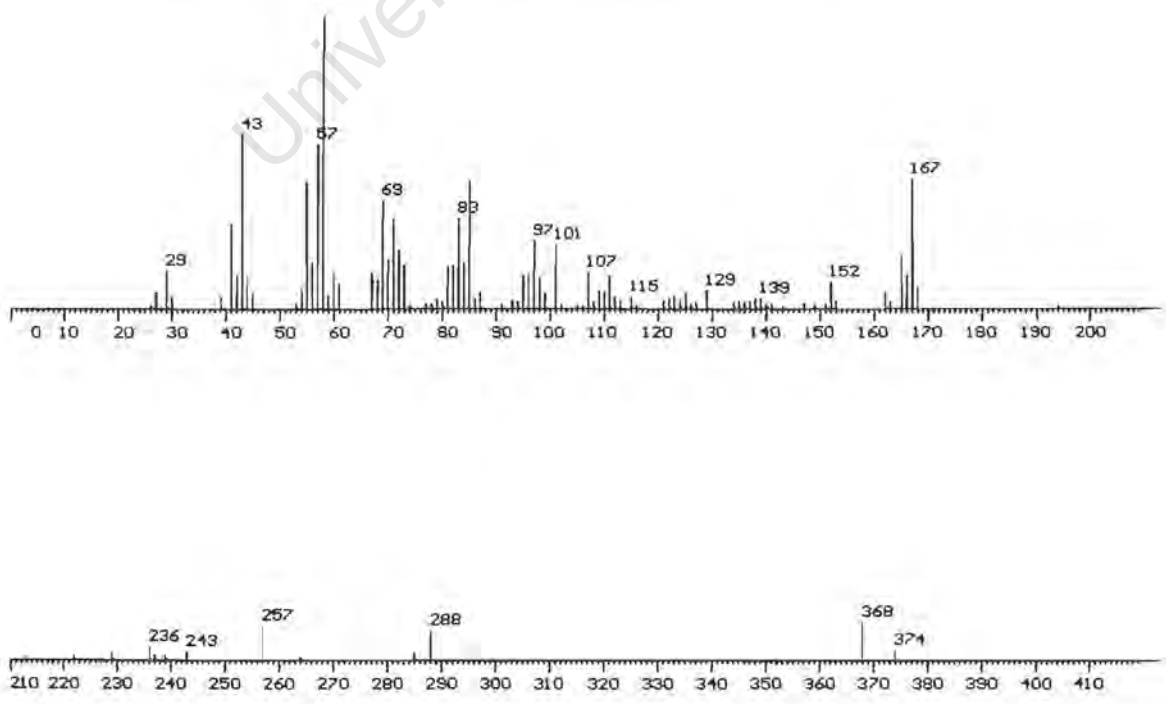

Figure 4.1.12. Mass spectrum of compound **P7**.

I8

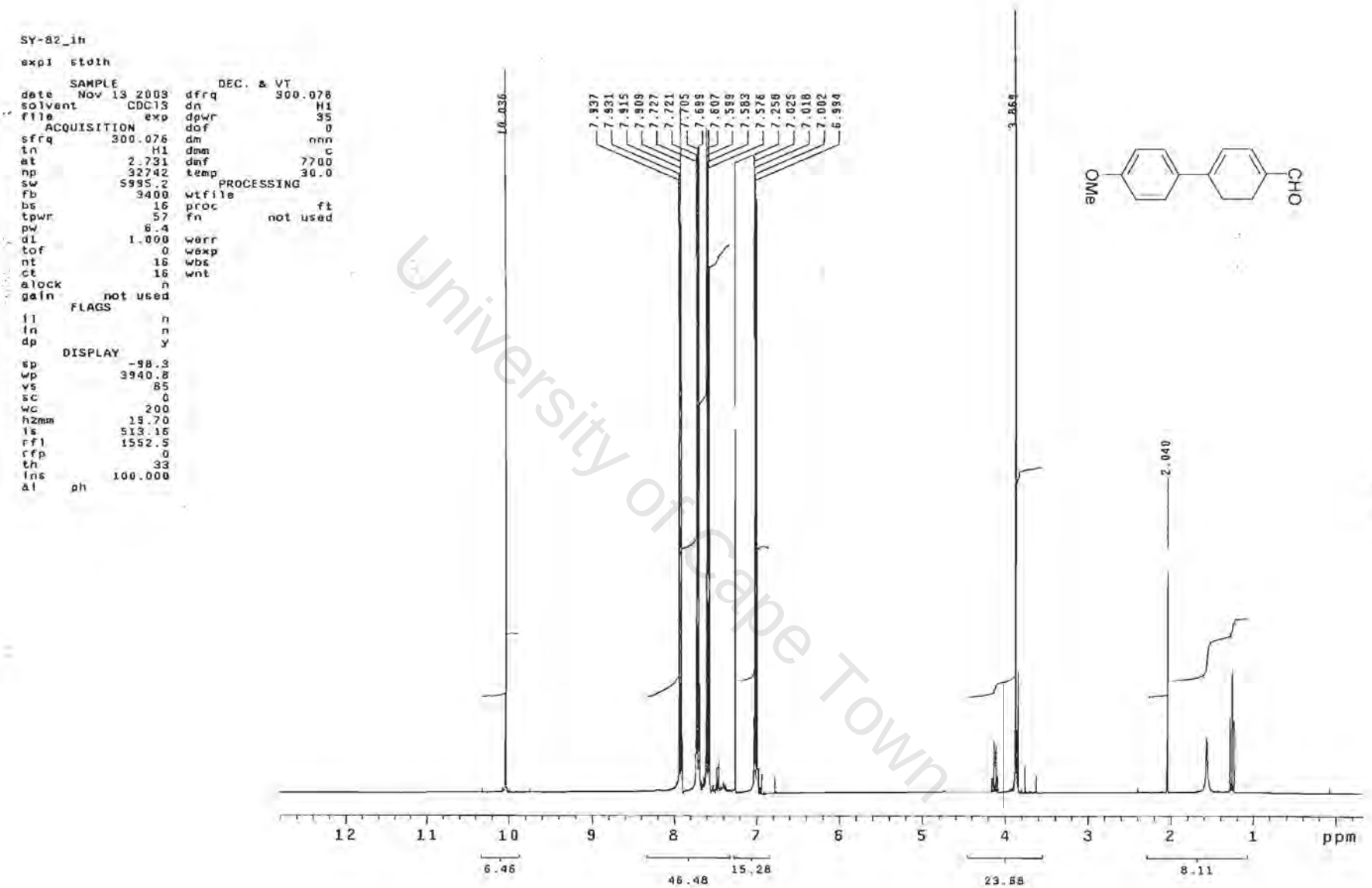

Figure A.4.1.1. ^{1}H NMR spectrum of intermediate **8** in $CDCl_3$, 300 MHz

I9

```
Susan-SY-55_1h

exp1  std1h

      SAMPLE                DEC. & VT
date    Oct  1 2003   dfrq        300.076
solvent      CDCl3    dn              H1
file           exp    dpwr            35
   ACQUISITION        dof              0
sfrq       300.076    dm             nnn
tn              H1    dmm              c
at           2.731    daf           7700
np           32742    temp          30.0
sw          5995.2       PROCESSING
fb            3400    wtfile
bs              16    proc            ft
tpwr            57    fn         not used
pw             6.4
dl           1.000    werr
tof              0    wexp
nt              16    wbs
ct              16    wnt
alock            n
gain       not used
      FLAGS
fl               n
in               n
dp               y
     DISPLAY
sp          -87.7
wp         3709.9
vs             27
sc              0
wc            200
hzmm        18.55
is          500.00
rfl         1552.5
rfp             0
th             20
ins         100.000
al     ph
```

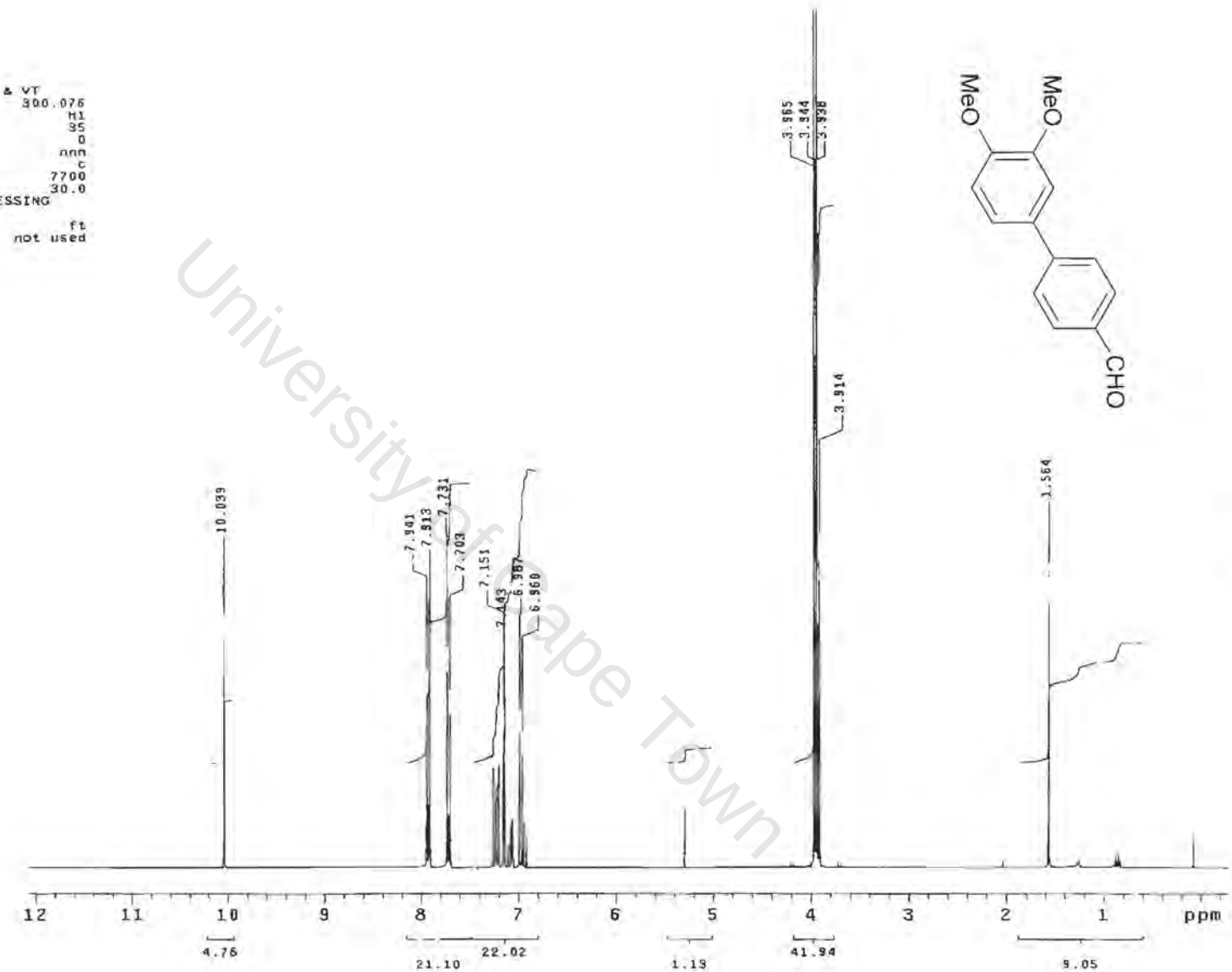

Figure A 4.1.2. ^{13}H NMR spectrum of intermediate **9** in $CDCl_3$, 300 MHz

I10

```
SY 81 in CDCl3
400 MHz 1H Spectrum (552)
Susan

exp4  std1h

       SAMPLE                  DEC. & VT
date    Nov 19 2003   dfrq          999.951
solvent       CDCl3   dn                H1
file            exp   dpwr              38
   ACQUISITION        dof                0
sfrq         399.851   dm               nnn
tn                H1   dmm                c
at             3.702   dmf            11450
np             44416   dseq
sw            5988.8   dres            1.0
fb         not used    homo              n
bs                16   temp           21.0
tpwr              58      PROCESSING
pw               2.0   wtfile
d1                 0   proc              ft
tof                0   fn         not used
nt                12   math               f
ct                12
alock              n   werr
gain              20   wexp
       FLAGS           wbs
il                 n   wnt
in                 n
dp                 y
hs                nn
     DISPLAY
sp            -147.0
wp            4814.5
vs               160
sc                 0
wc               200
hzmm           24.07
is            5798.37
rfl            574.0
rfp                0
th                 68
ins           100.000
nm     ph
```

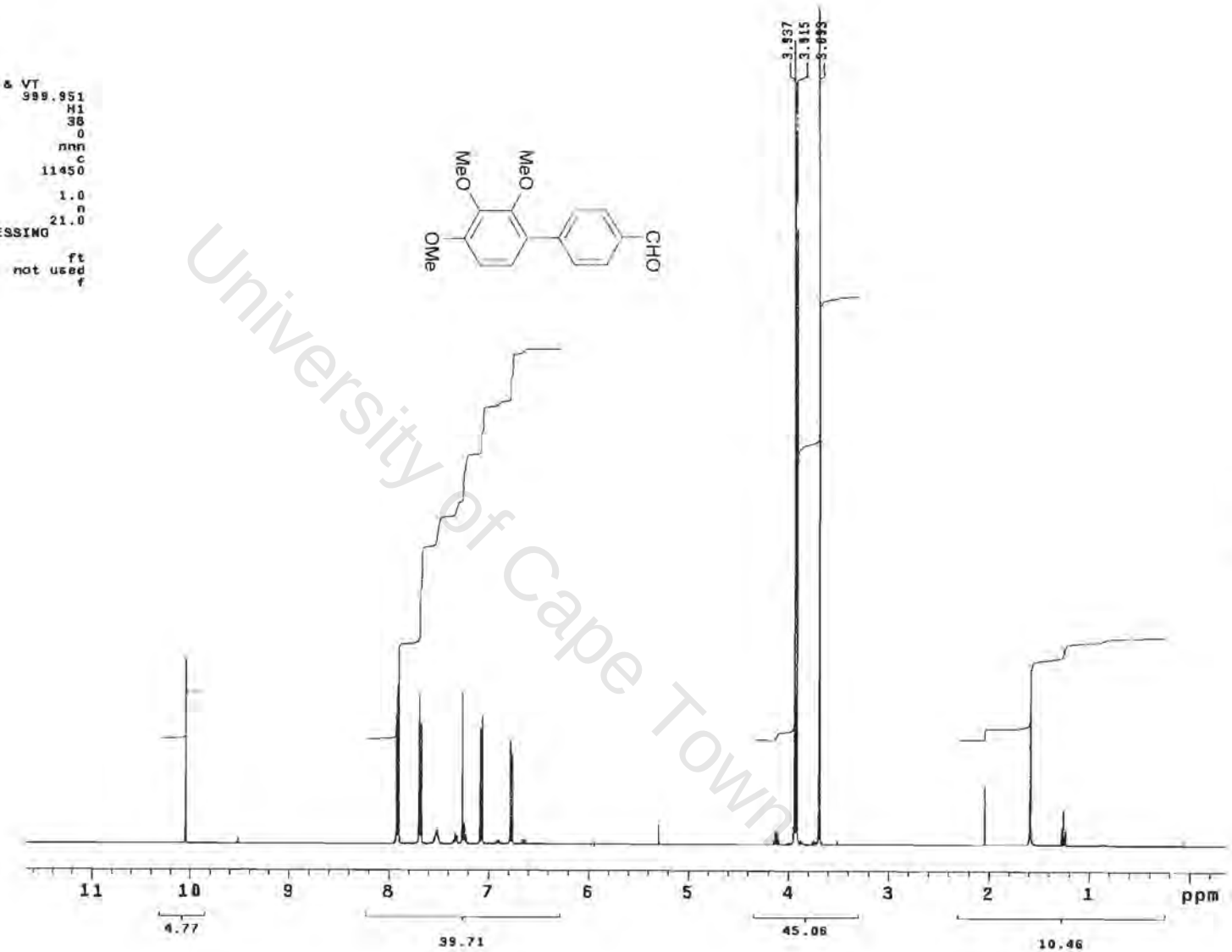

Figure A.4.1.3. ^{1}H NMR spectrum of intermediate **10** in $CDCl_3$, 300 MHz

Compound P11

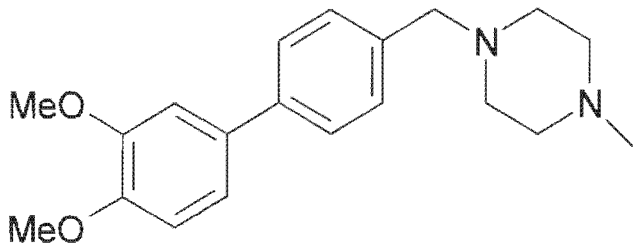

Compound P11

IUPAC

1-(3',4'-*Dimethoxy-biphenyl*-4-*ylmethyl*)-4-*methyl-piperazine*

List of spectra:

- ^{1}H NMR (300MHz, $CDCl_3$)
- ^{13}C NMR (100MHz, $CDCl_3$)
- Mass spectra

P11

```
Susan-SY61_1h

expl  stdth

        SAMPLE                    DEC. & VT
date    Oct 17 2003     dfrq          300.076
solvent       CDCl3     dn                Hl
file            exp     dpwr              35
   ACQUISITION          dof               0
sfrq        300.078     dm                nnn
tn               Hl     dmm               c
at             2.731     dmf            7700
np             32742     temp           30.0
sw            5995.2          PROCESSING
fb             3400     wtfile
bs               18     proc              ft
tpwr             57     fn          not used
pw              6.4
d1              1.000    werr
tof                0    wexp
nt                16    wbs
ct                18    wnt
alock              n
gain        not used
        FLAGS
ll                 n
in                 n
dp                 y
      DISPLAY
sp             -95.3
wp           3166.8
vs              108
sc                0
wc              200
hzmm          15.83
is            500.00
rfl          1552.5
rfp               0
th                20
ins           100.000
al      ph
```

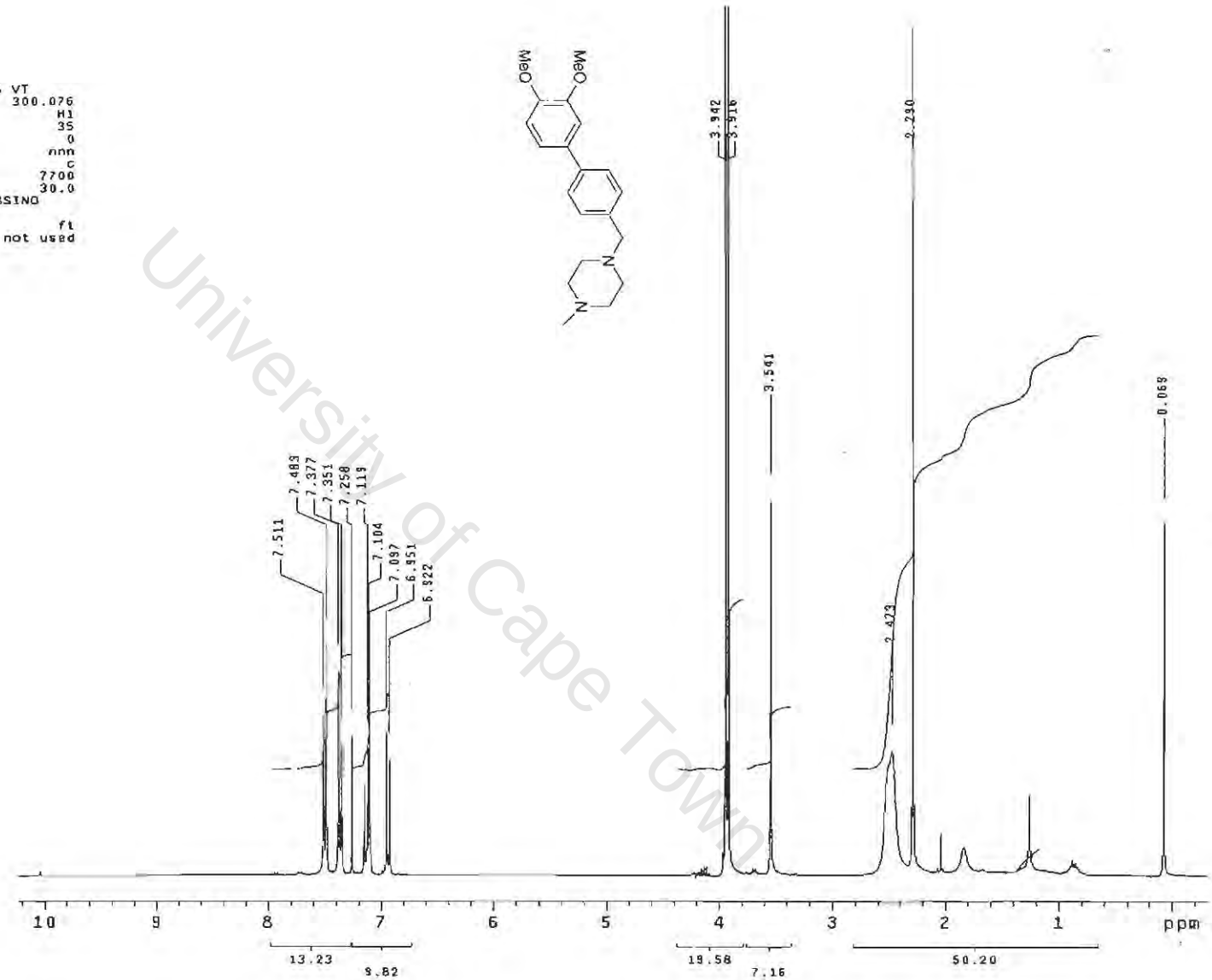

Figure A.4.1.4. ^{1}H NMR spectrum of compound **P11** in $CDCl_3$, 300 MHz

P11

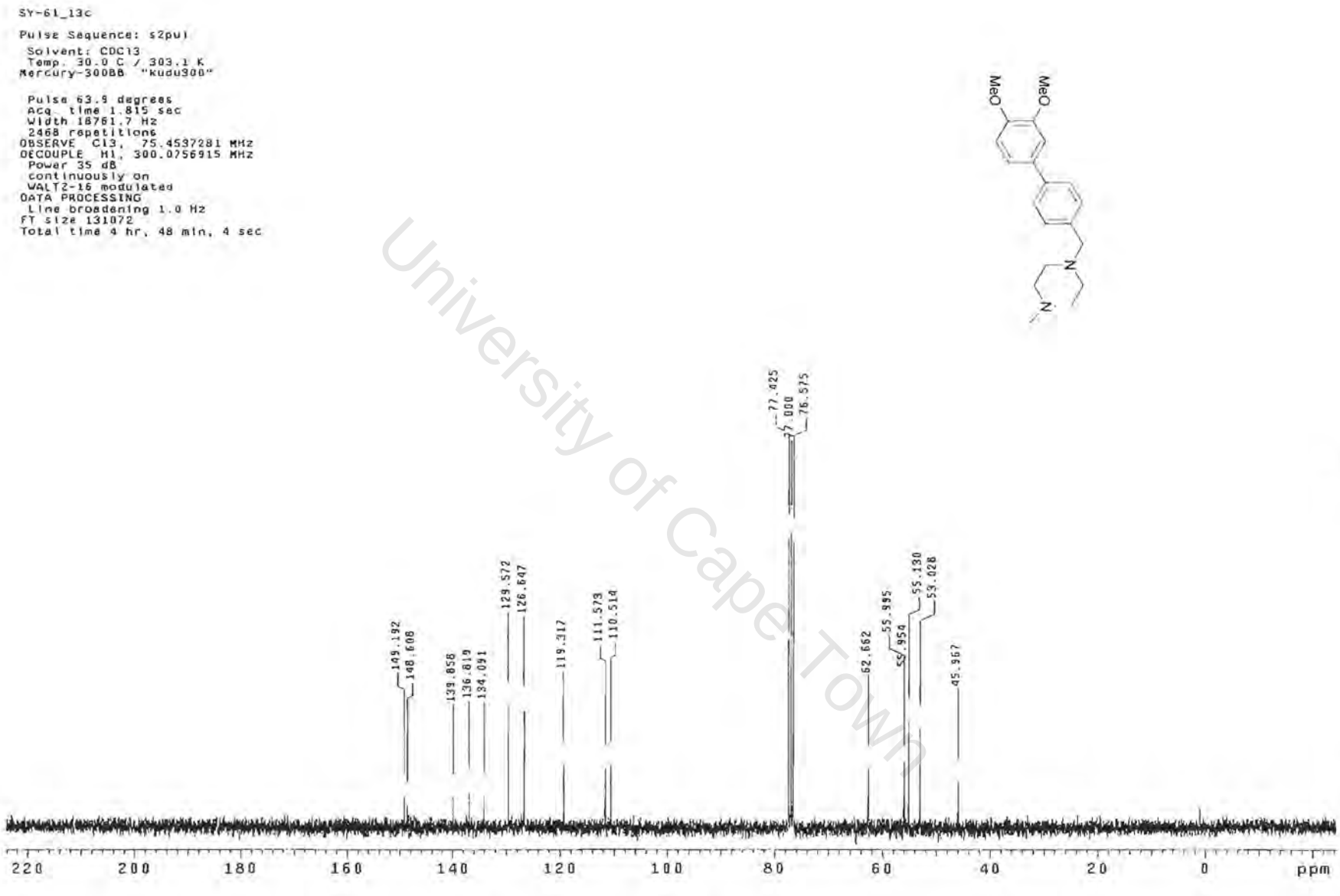

Figure A.4.1.5. ^{13}C NMR spectrum of compound **P11** in $CDCl_3$, 100 MHz

P11

Printing Time: 09:49:36 AM
Printing Date: Thursday, October 07, 2004

*Installation

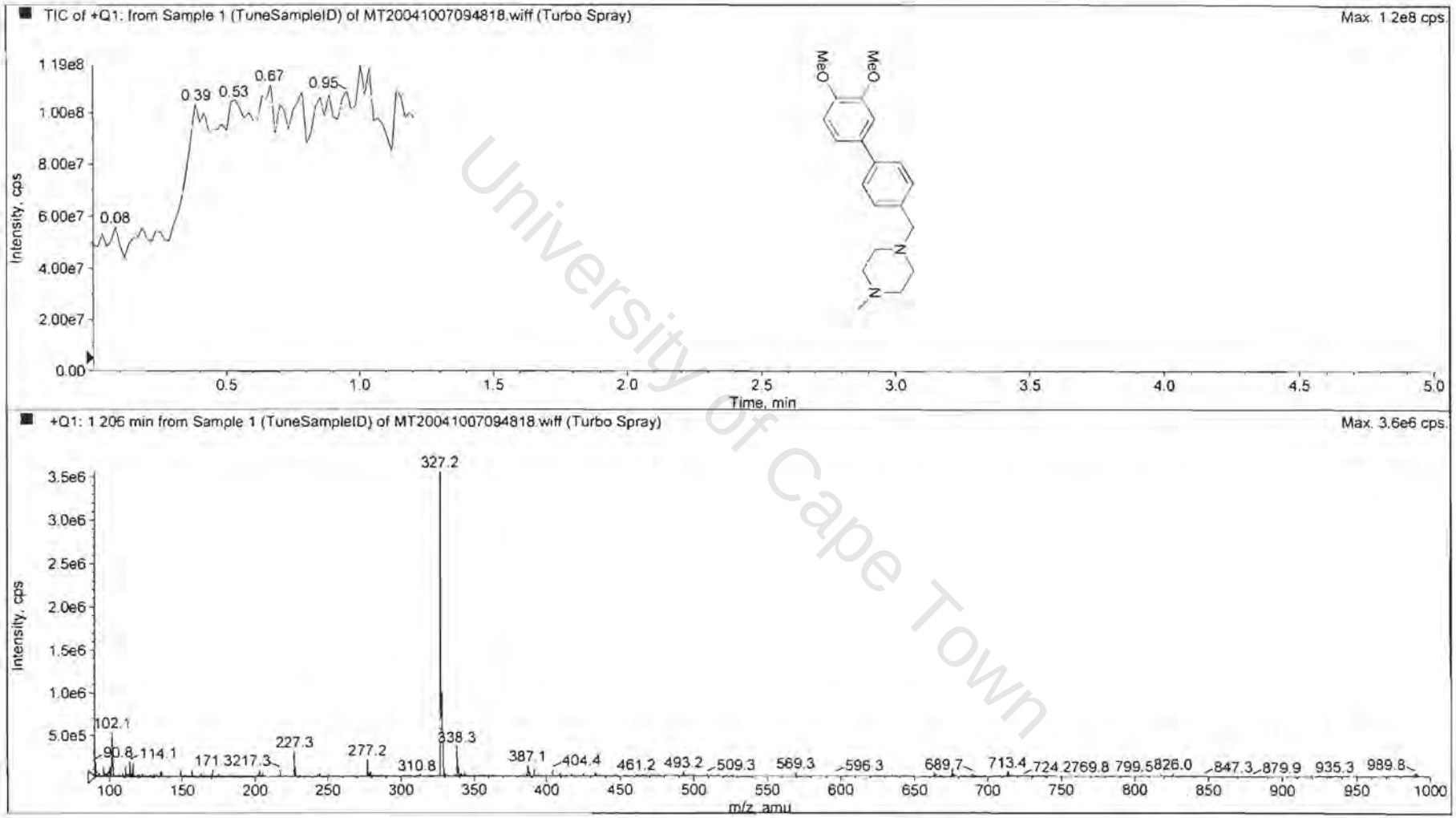

Page 1 of 1

Figure A.4.1.6.1. Mass spectrum of compound **P11**.

P11

Printing Time: 09:53:21 AM
Printing Date: Thursday, October 07, 2004

*Installation

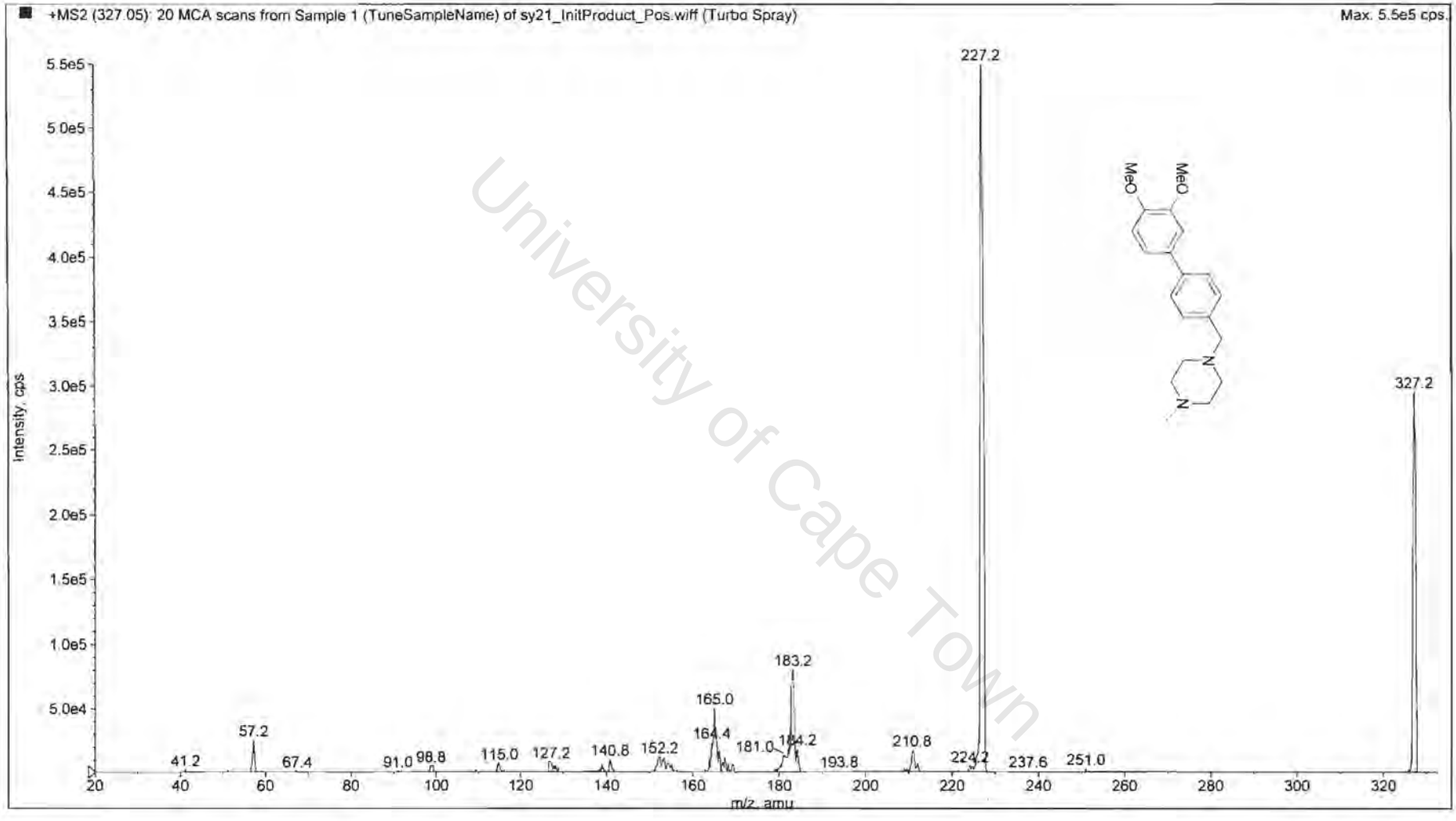

Page 1 of 1

Figure A.4.1.6.2. Mass spectrum of compound **P11**.

Compound P12

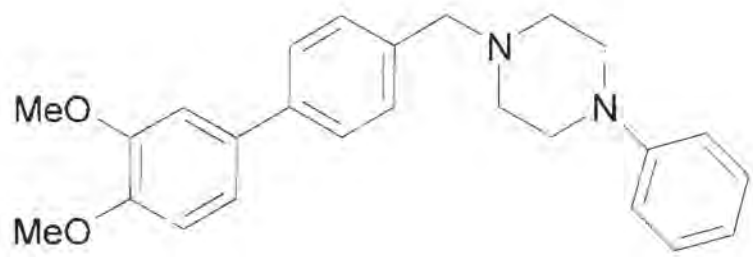

Compound P12

IUPAC

1-(3',4'-*Dimethoxy-biphenyl*-4-*ylmethyl*)-4-*phenyl-piperazine*

List of spectra:

- ^{1}H NMR (400MHz, $CDCl_3$)
- ^{13}C NMR (100MHz, $CDCl_3$)
- Mass spectra

P12

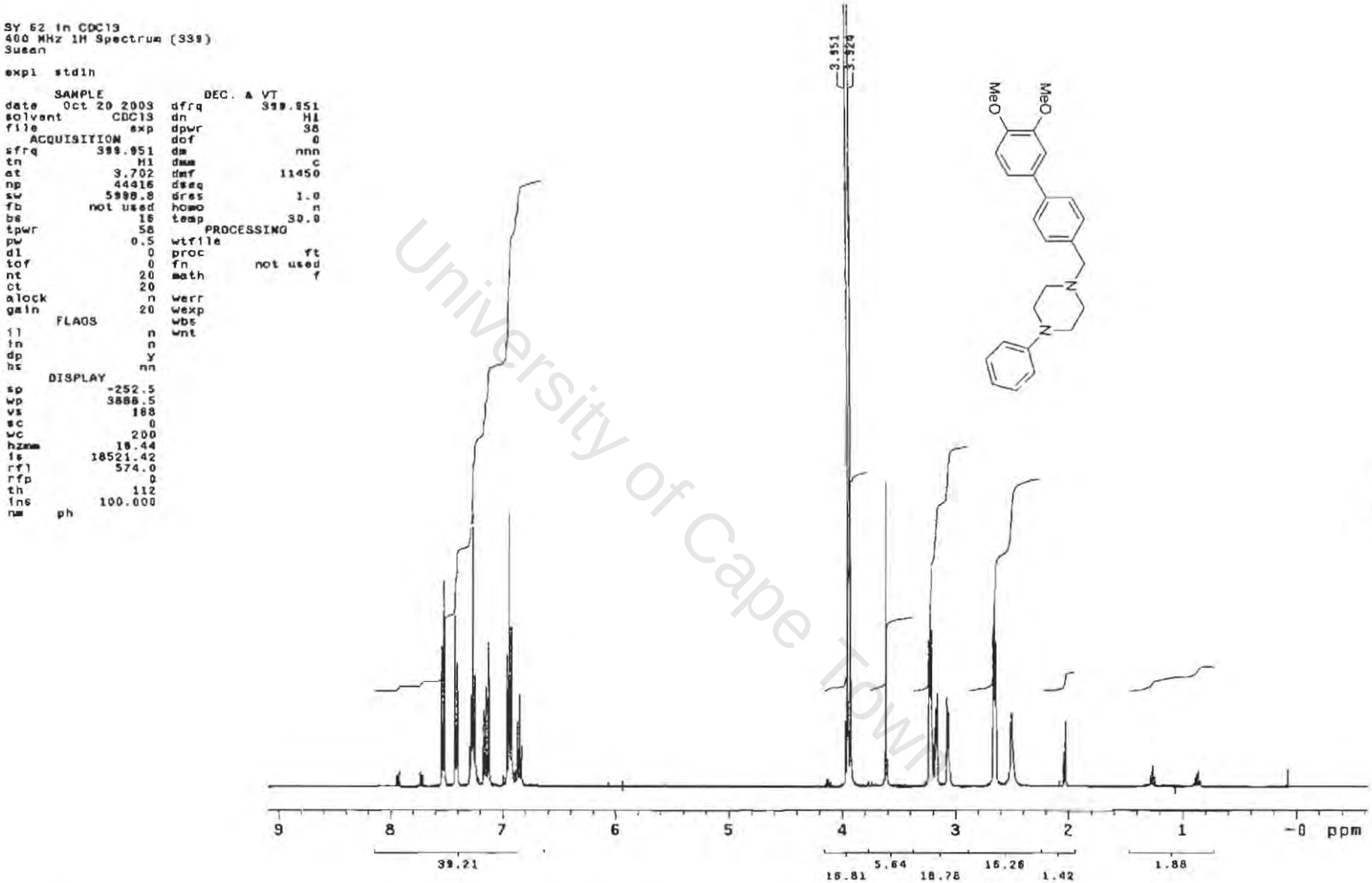

Figure A.4.1.7. ^{1}H spectrum of compound **P12** in $CDCl_3$, 400 MHz

P12

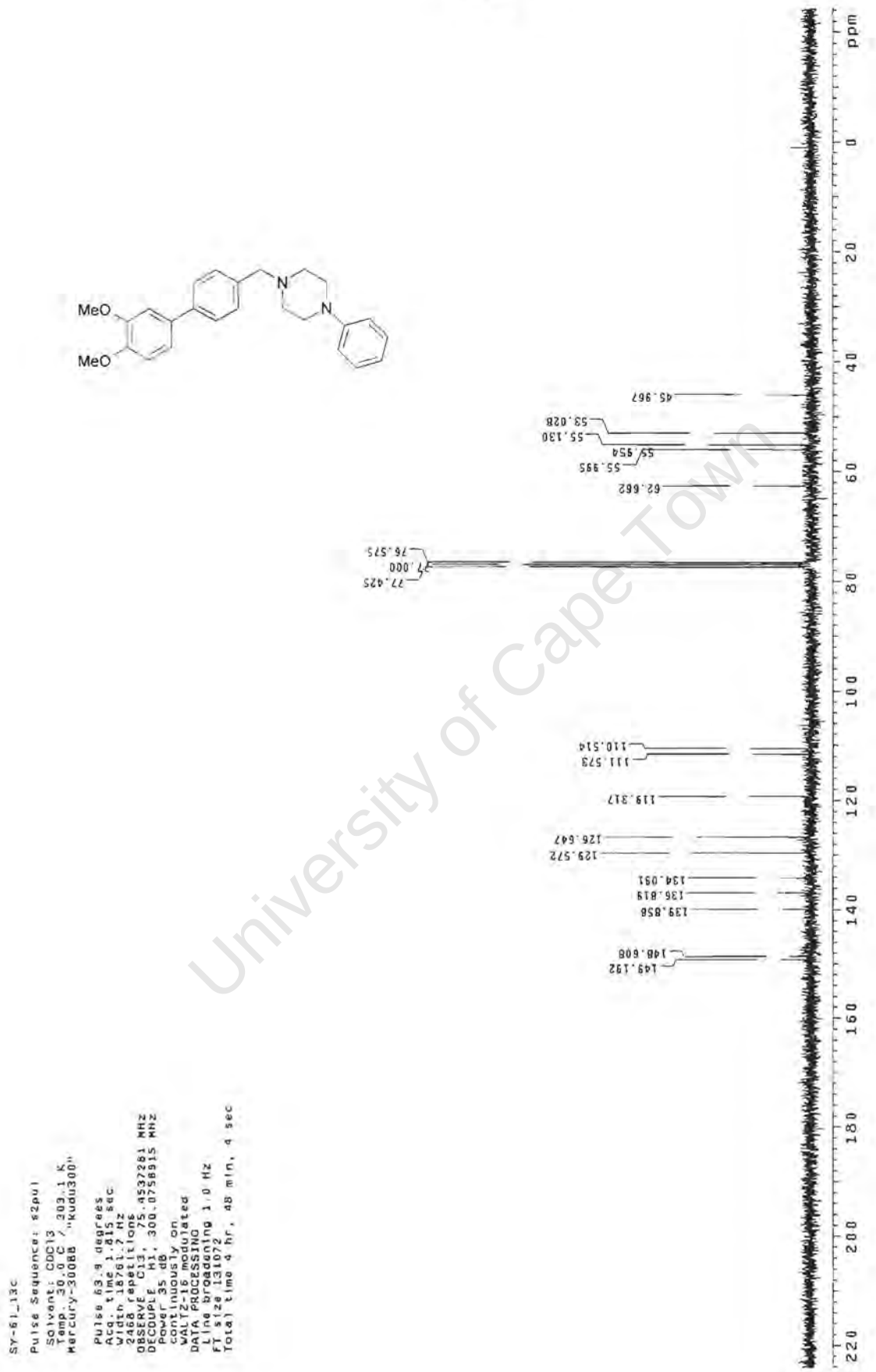

SY-61_13C
Pulse Sequence: s2pul
Solvent: CDCl3
Temp.: 30.0 C / 303.1 K
Mercury-300BB "kudu300"

Pulse 63.9 degrees
Acq. time 1.815 sec
Width 18761.2 Hz
2468 repetitions
OBSERVE C13, 75.4537281 MHz
DECOUPLE H1, 300.0758915 MHz
Power 35 dB
continuously on
WALTZ-16 modulated
DATA PROCESSING
Line broadening 1.0 Hz
FT size 131072
Total time 4 hr, 48 min, 4 sec

Figure A.4.1.8. ^{13}C NMR spectrum of compound **P12** in $CDCl_3$, 100 MHz

P12

Printing Time: 10:12:45 AM
Printing Date: Friday, October 08, 2004

*Installation

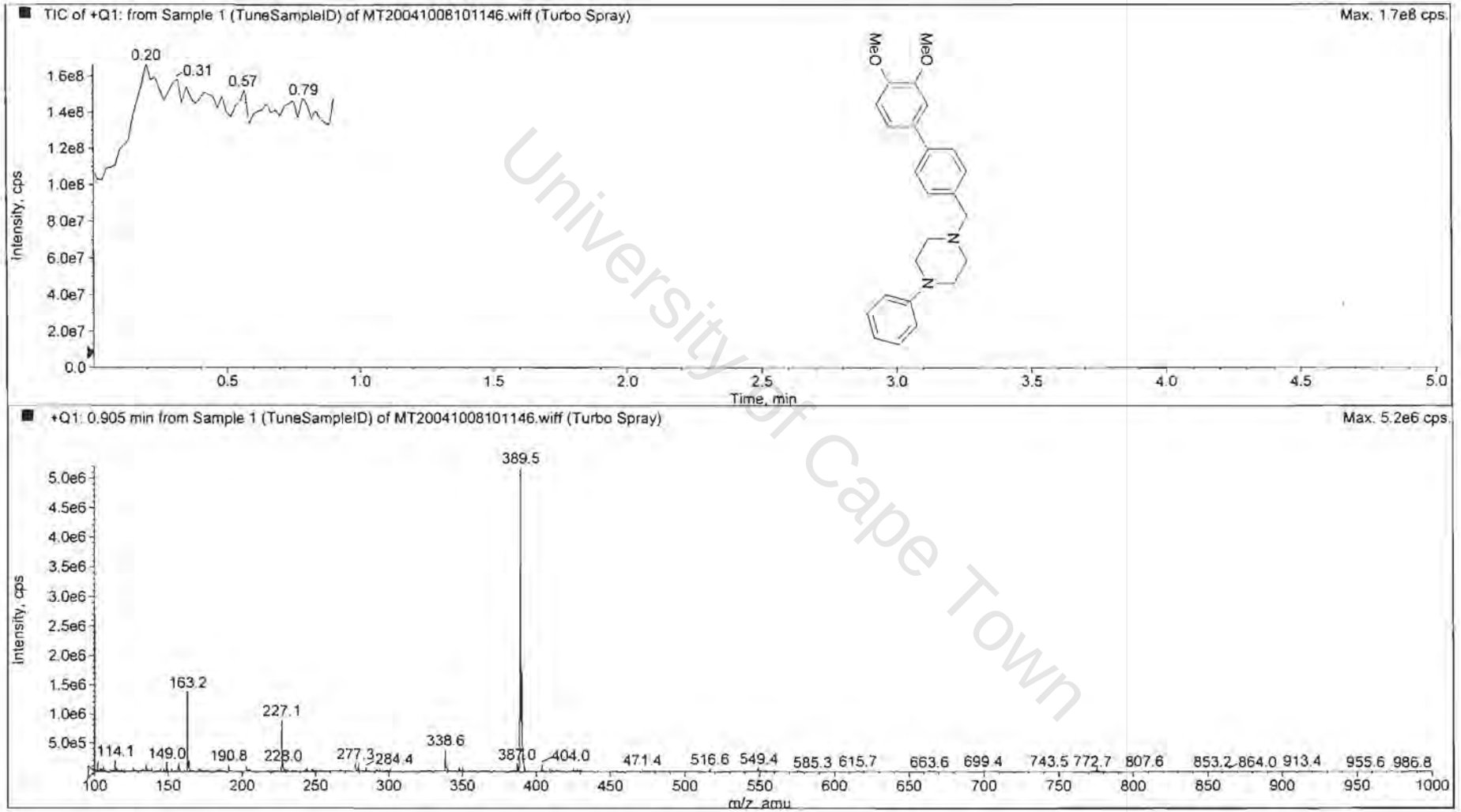

Page 1 of 1

Figure A.4.1.9.1. Mass spectrum of compound **P12**.

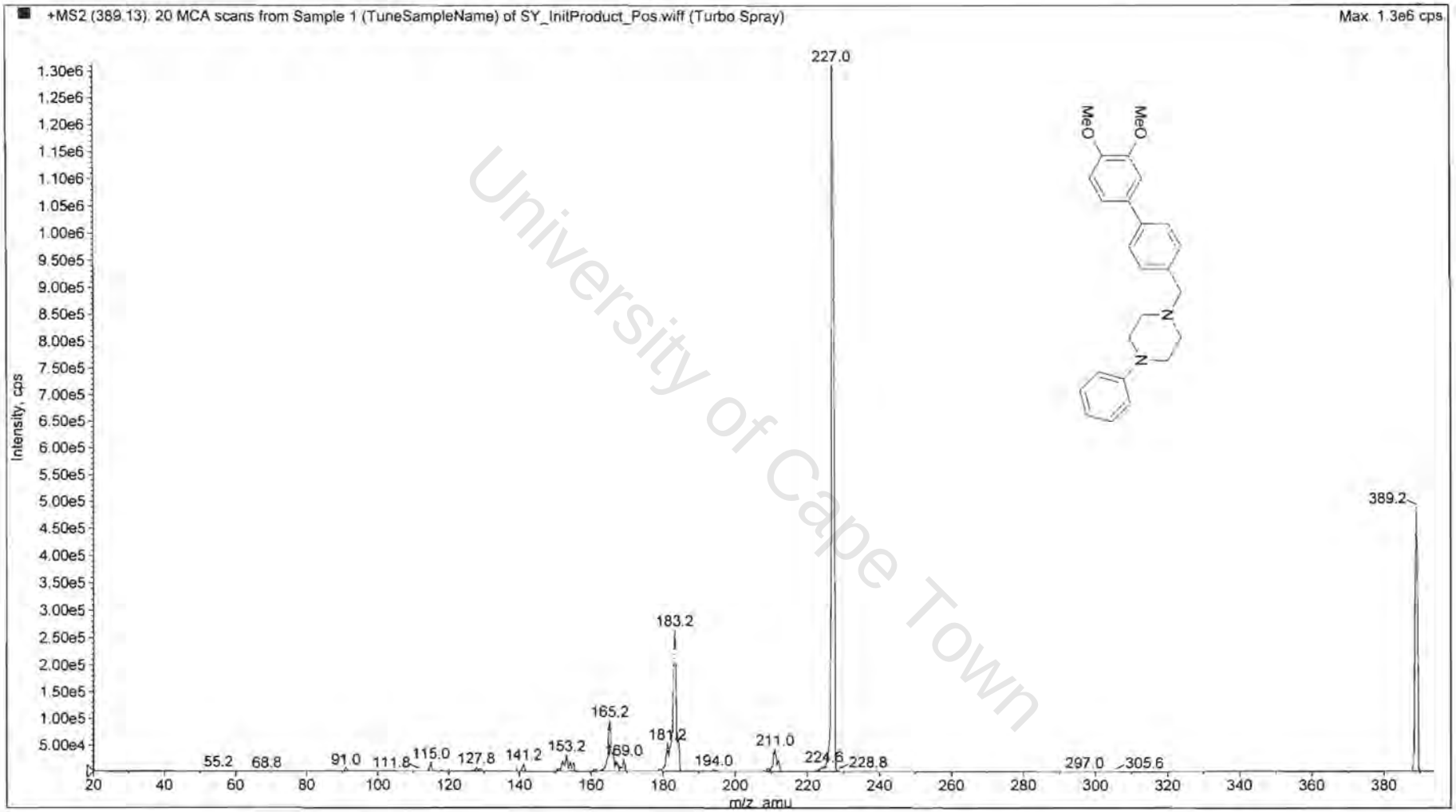

Figure A.4.1.9.2. Mass spectrum of compound **P12**.

Compound P13

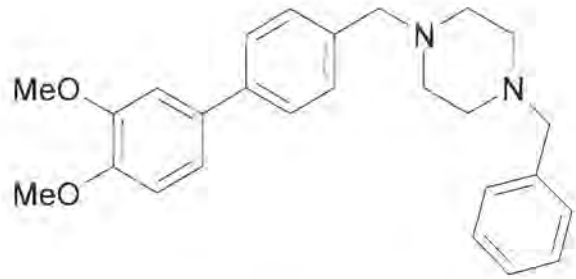

Compound P13

IUPAC

1-*Benzyl*-4-(3',4'-*dimethoxy-biphenyl*-4-*ylmethyl*)-*piperazine*

List of spectra:

- ^{1}H NMR (300MHz, $CDCl_3$)
- ^{13}C NMR (100MHz, $CDCl_3$)
- Mass spectra

P13

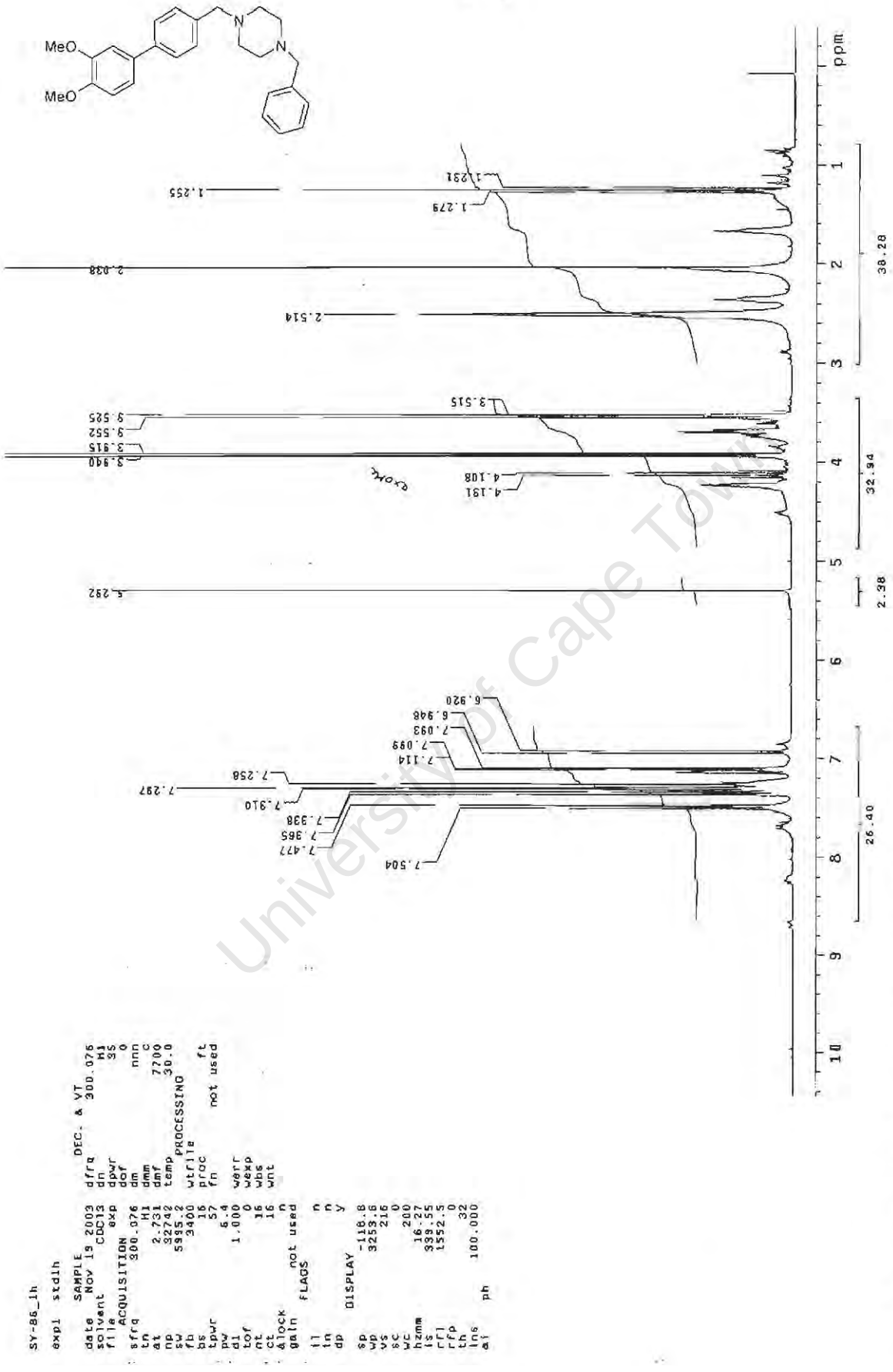

Figure A.4.1.10. ^{1}H NMR spectrum of compound **P13** in $CDCl_3$, 400 MHz

P13

Figure A.4.1.11. ^{13}C NMR spectrum of compound **P13** in $CDCl_3$, 100 MHz

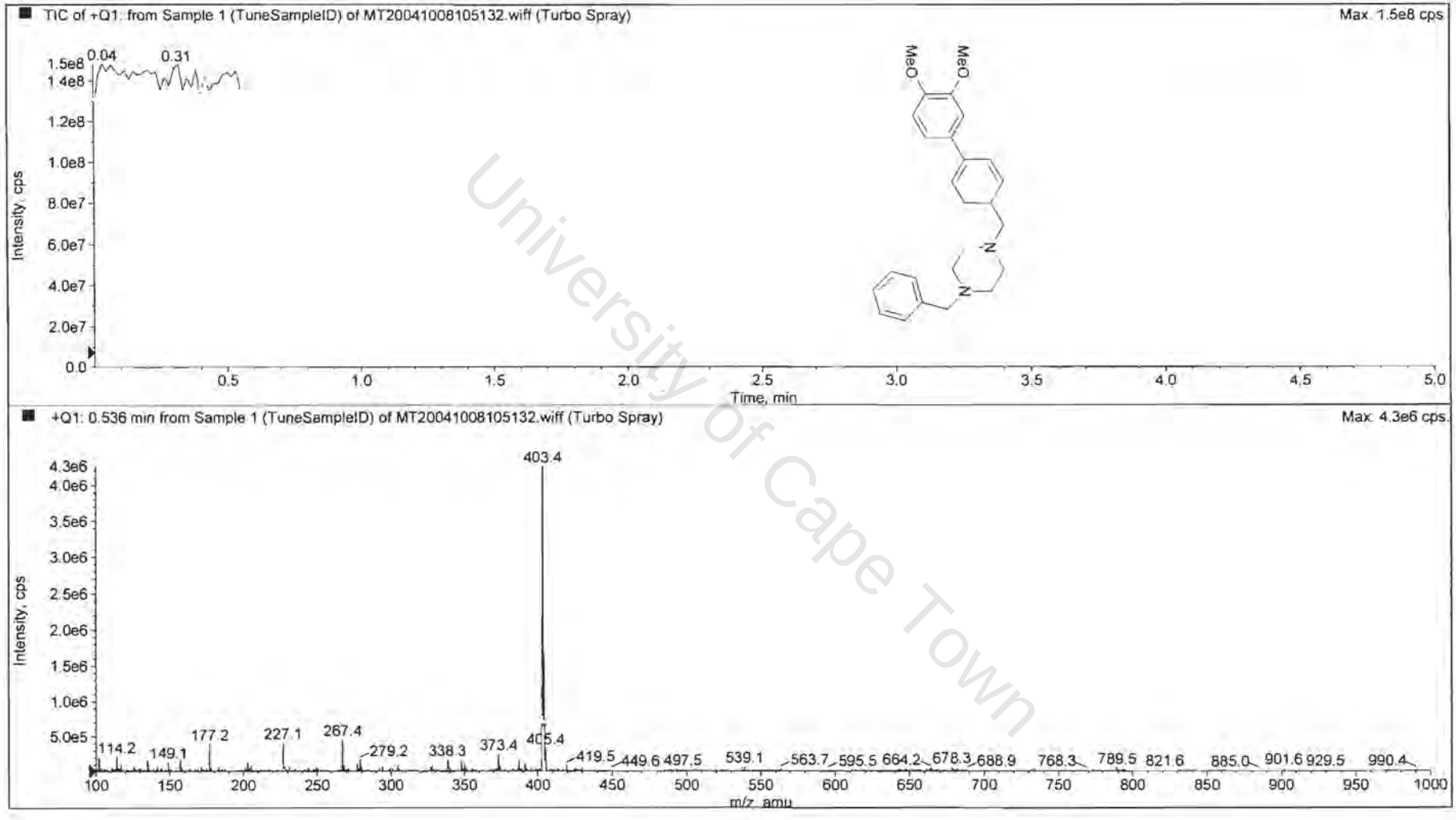

Figure A.4.1.12.1. Mass spectrum of compound **P13**.

P13

Printing Time: 10:56:19 AM
Printing Date: Friday, October 08, 2004

"Installation

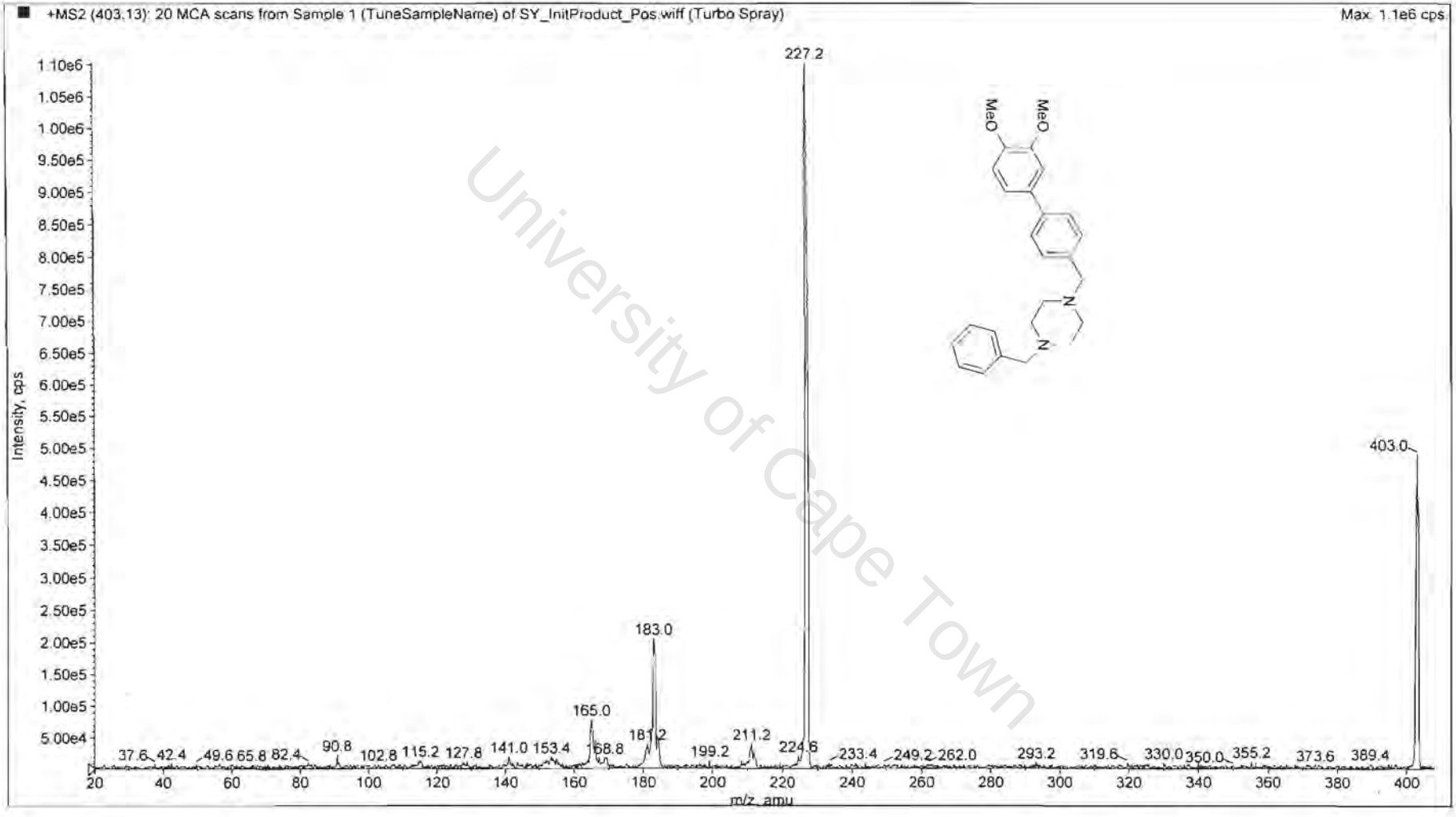

Page 1 of 1

Figure A.4.1.12.2. Mass spectrum of compound **P13**.

Compound P14

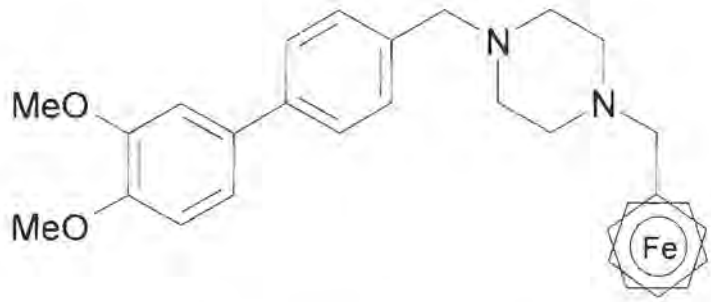

Compound P14

List of spectra:

- ^{1}H NMR (300MHz, $CDCl_3$)
- ^{13}C NMR (100MHz, $CDCl_3$)
- Mass spectra

P14

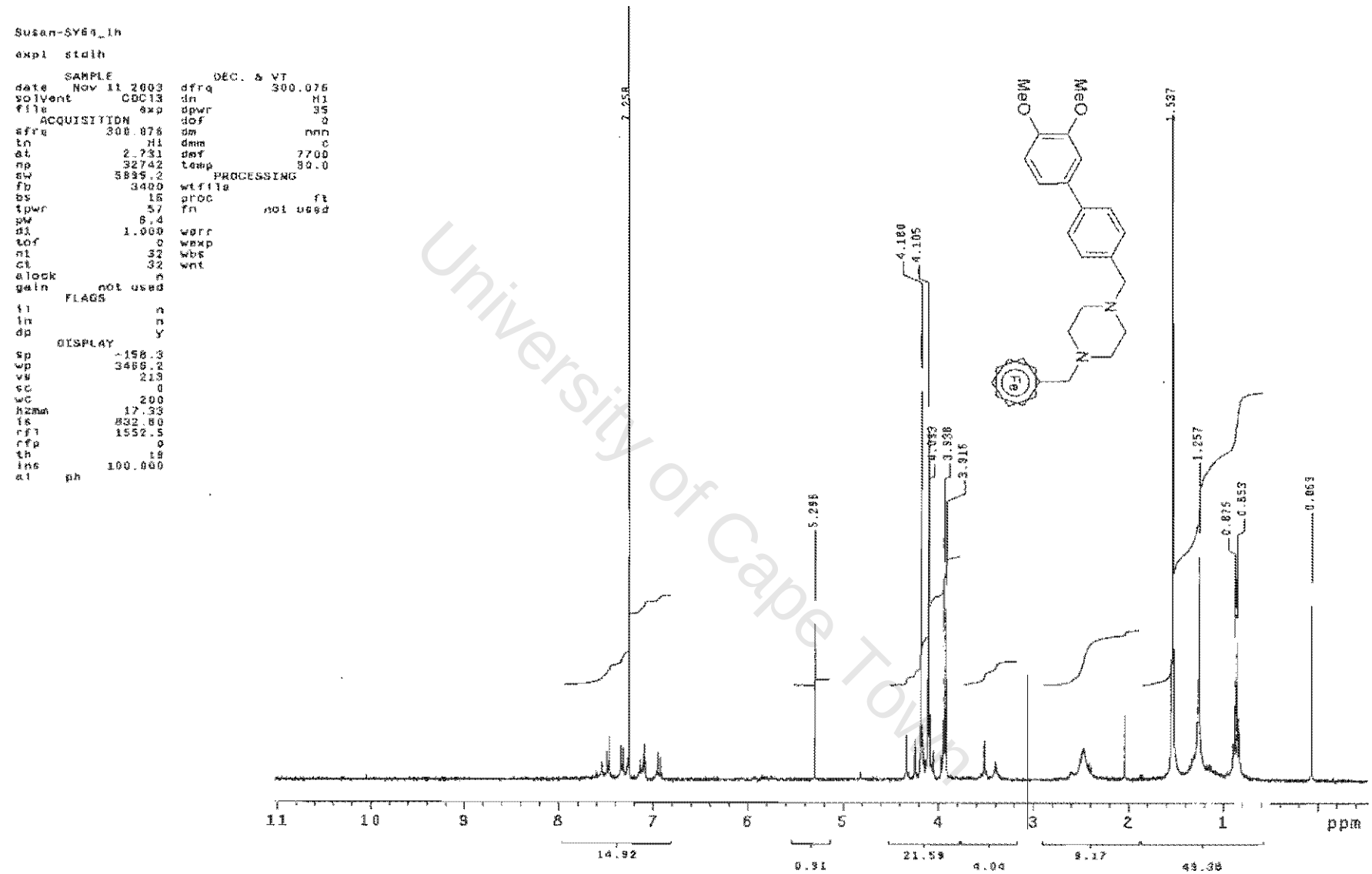

Figure A.4.1.13. ^{1}H NMR spectrum of compound **P14** in $CDCl_3$, 300 MHz.

P14

Figure A.4.1.14. ^{13}C NMR spectrum of compound **P14** in $CDCl_3$, 100 MHz

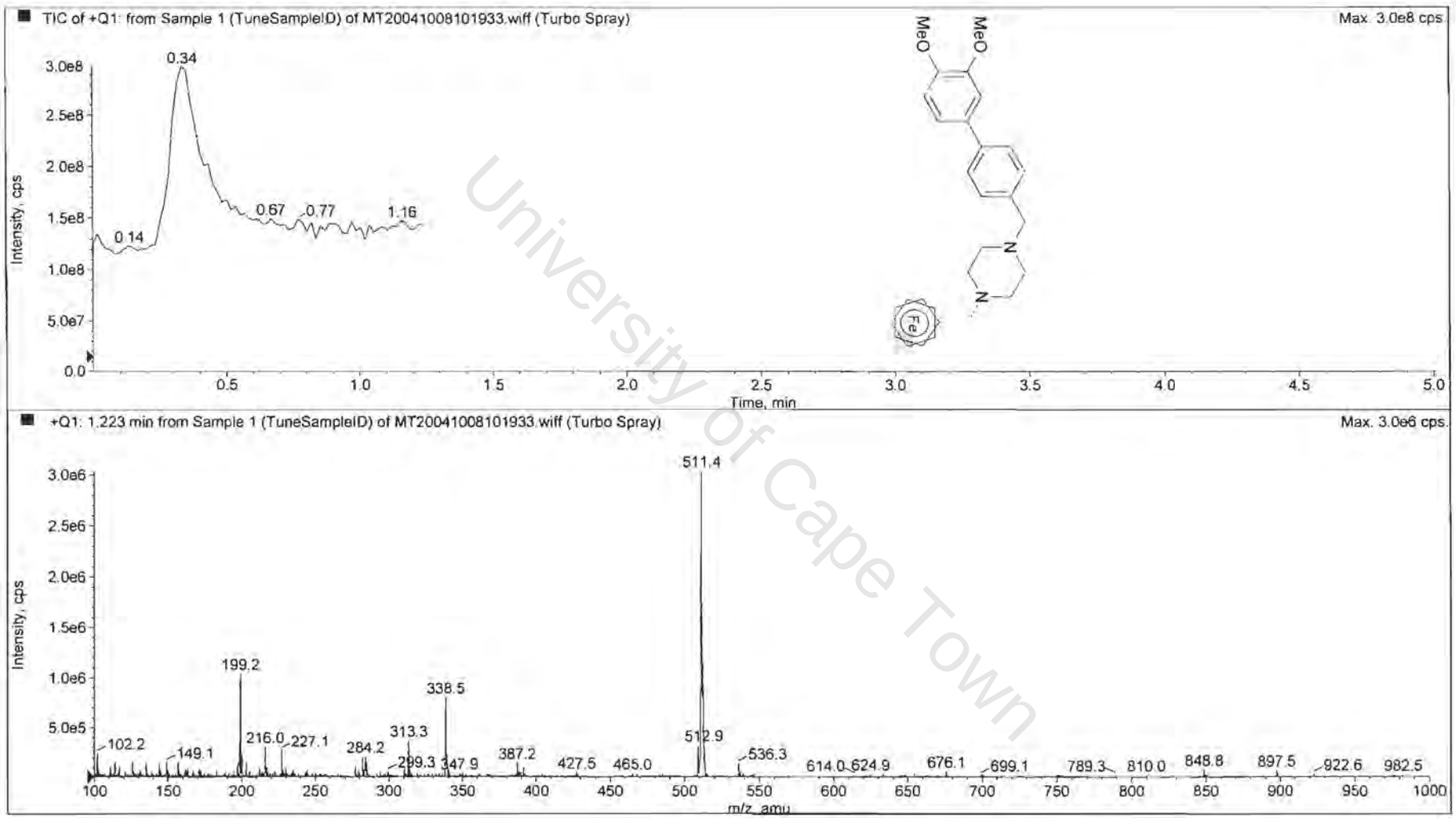

Figure A.4.1.15.1. Mass spectrum of compound **P14**.

P14

Printing Time: 10:26:19 AM
Printing Date: Friday, October 08, 2004

*Installation

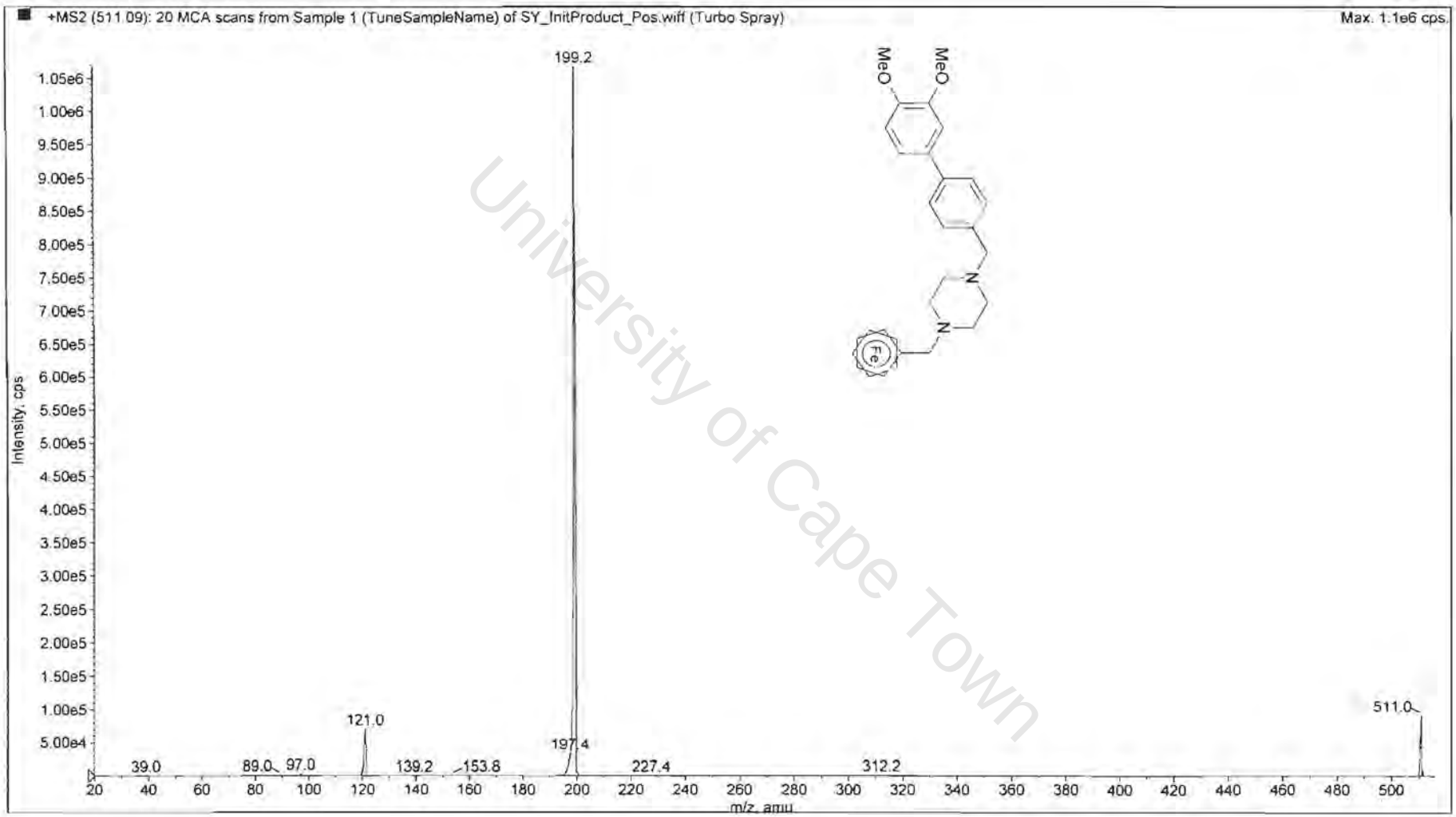

Page 1 of 1

Figure A.4.1.15.2. Mass spectrum of compound **P14**.

Compound P15

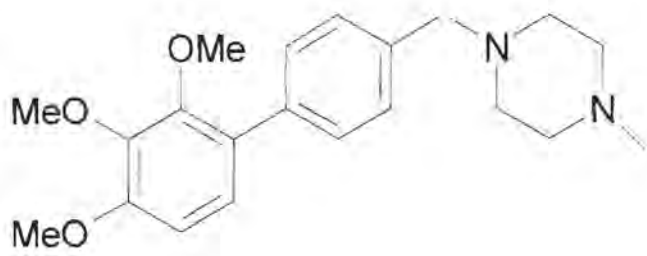

Compound P15

IUPAC

1-*Methyl*-4-(2',3',4'-*trimethoxy-biphenyl*-4-*ylmethyl*)-*piperazine*

List of spectra:

- ^{1}H NMR (300MHz, $CDCl_3$)
- ^{13}C NMR (100MHz, $CDCl_3$)
- Mass spectra

P15

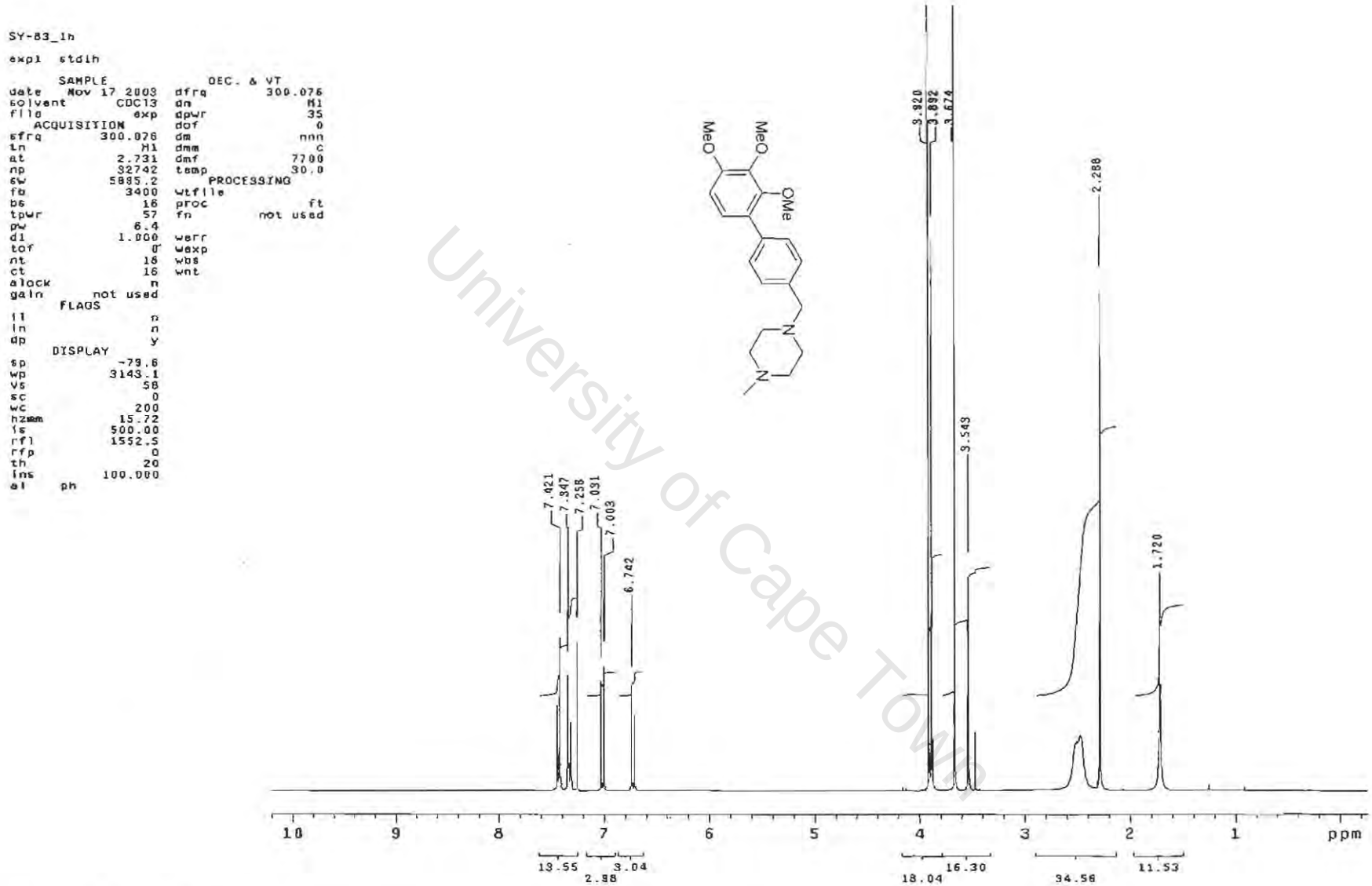

Figure A.4.1.16. ^{1}H NMR spectrum of compound **P15** in $CDCl_3$, 300 MHz

P15

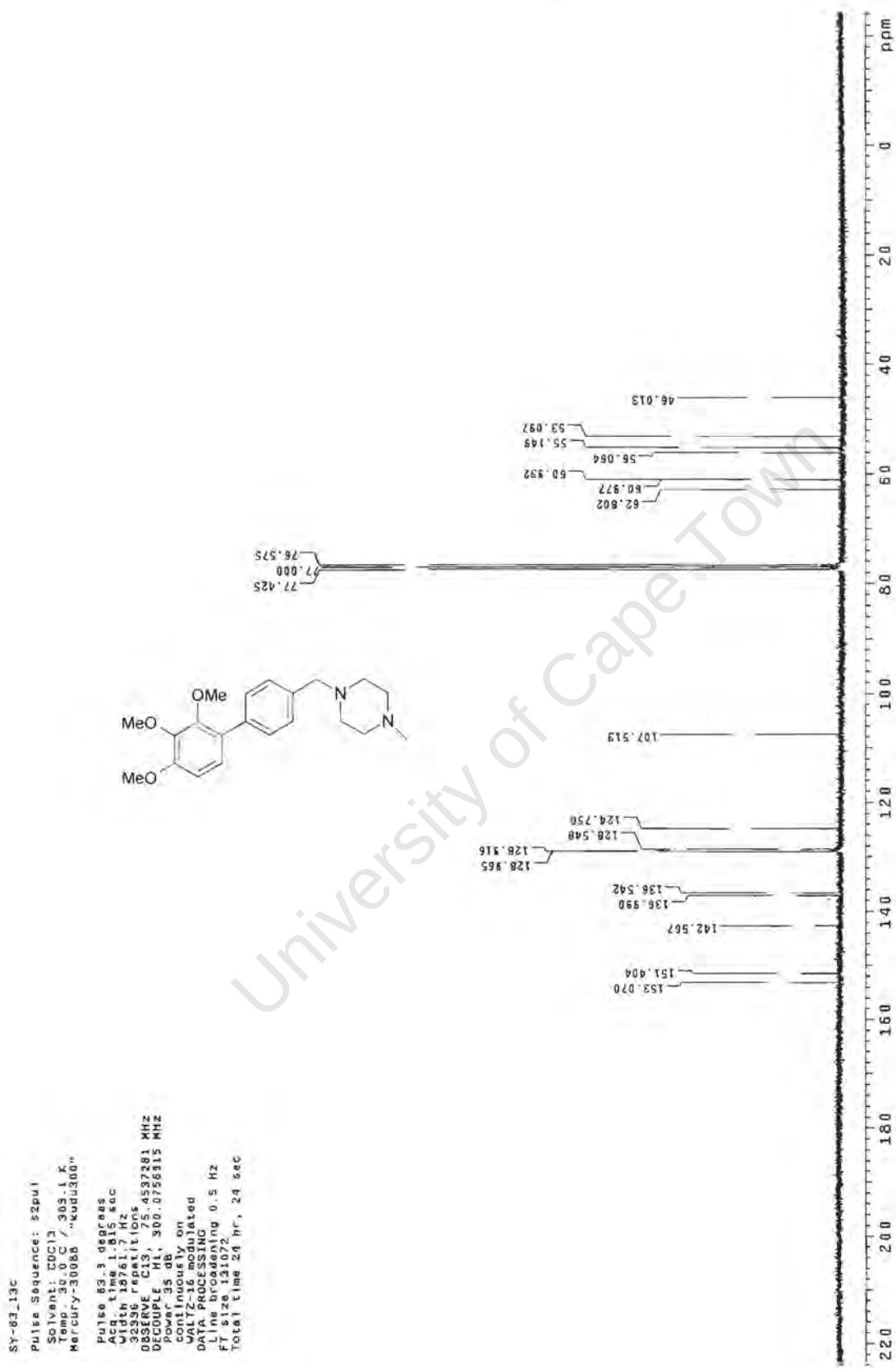

Figure A.4.1.17. ^{13}C NMR spectrum of compound **P15** in $CDCl_3$, 100 MHz.

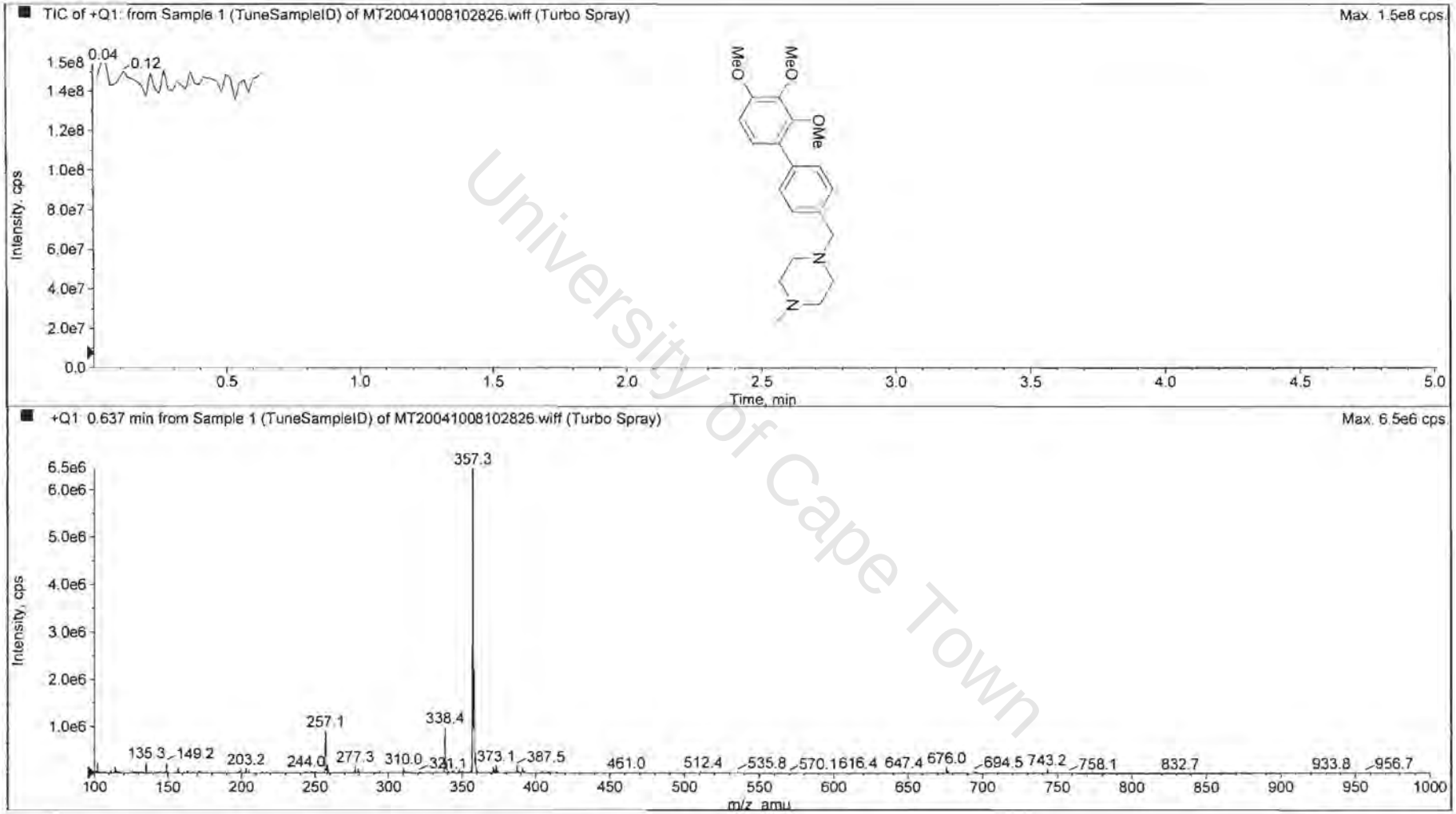

Figure A.4.1.18.1. Mass spectrum of compound **P15**.

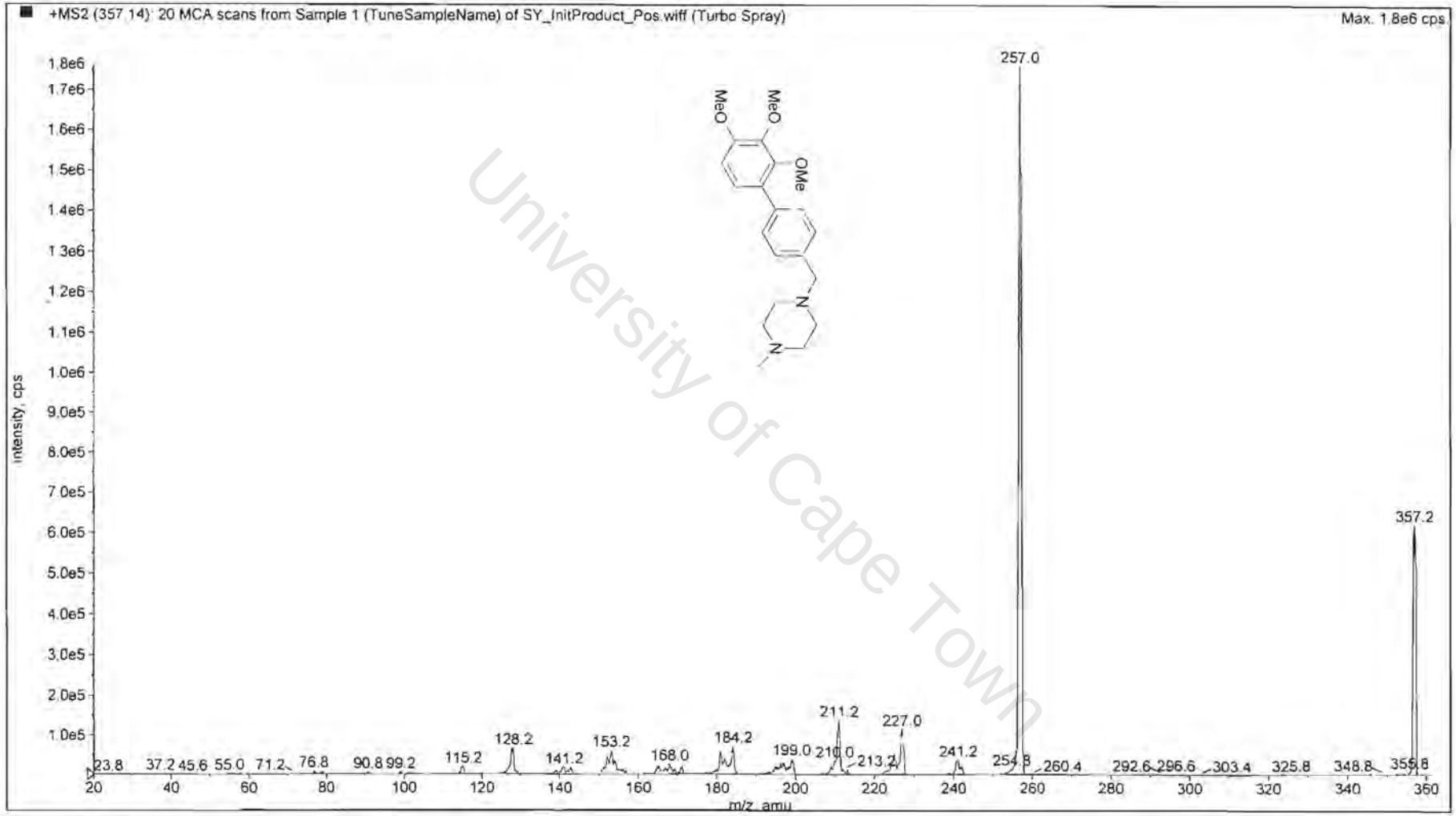

Figure A.4.1.18.2. Mass spectrum of compound **P15**.

Compound P16

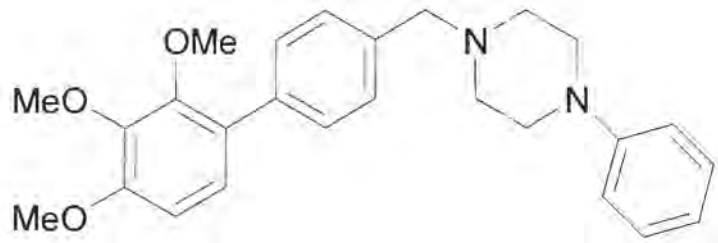

Compound P16

IUPAC

1-*Phenyl*-4-(2',3',4'-*trimethoxy-biphenyl*-4-*ylmethyl*)-*piperazine*

List of spectra:

- ^{1}H NMR (400MHz, $CDCl_3$)
- ^{13}C NMR (100MHz, $CDCl_3$)
- Mass spectra

P16

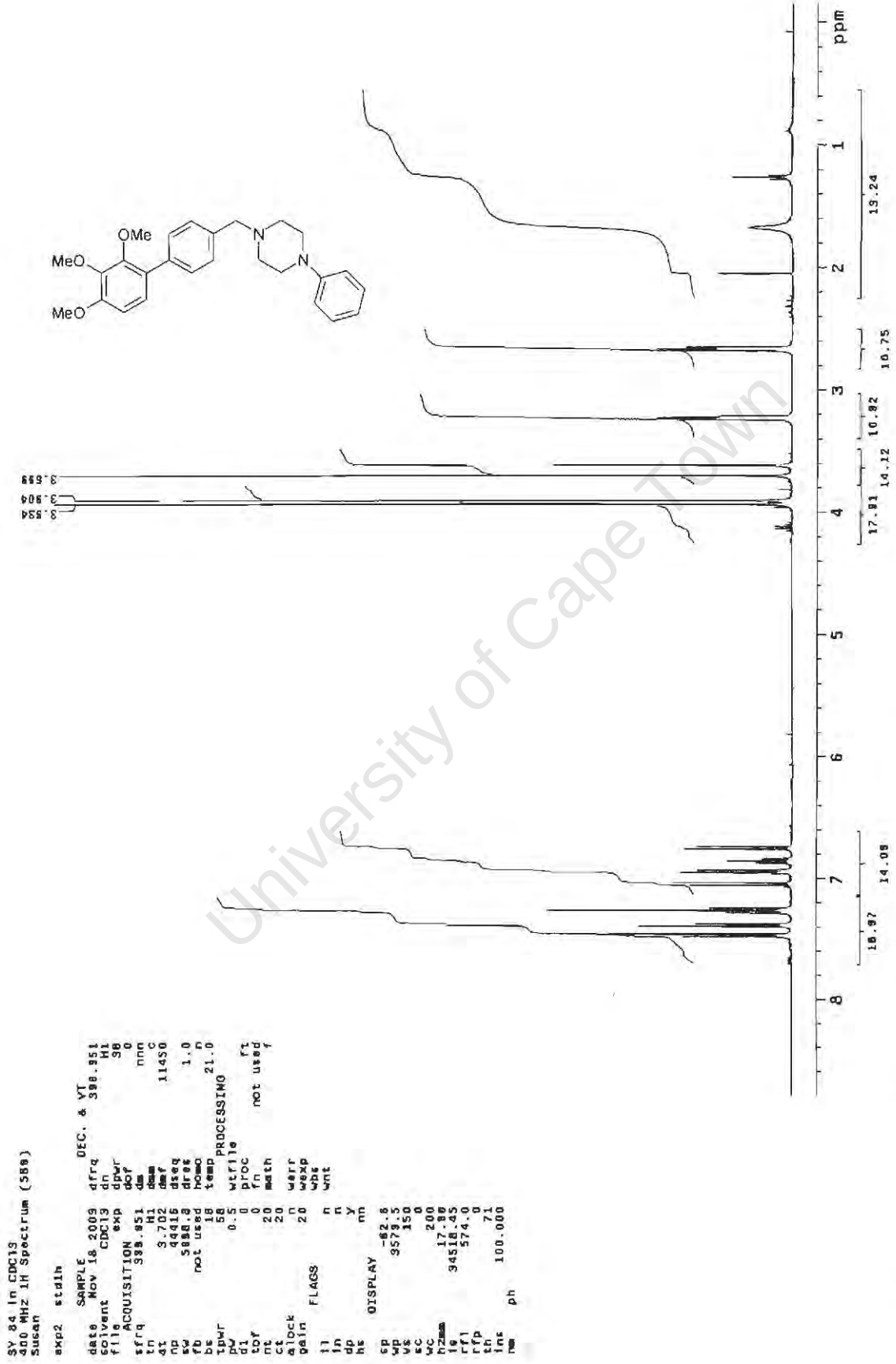

Figure A.4.1.19. ^{1}H NMR spectrum of compound **P16** in $CDCl_3$, 400 MHz.

P16

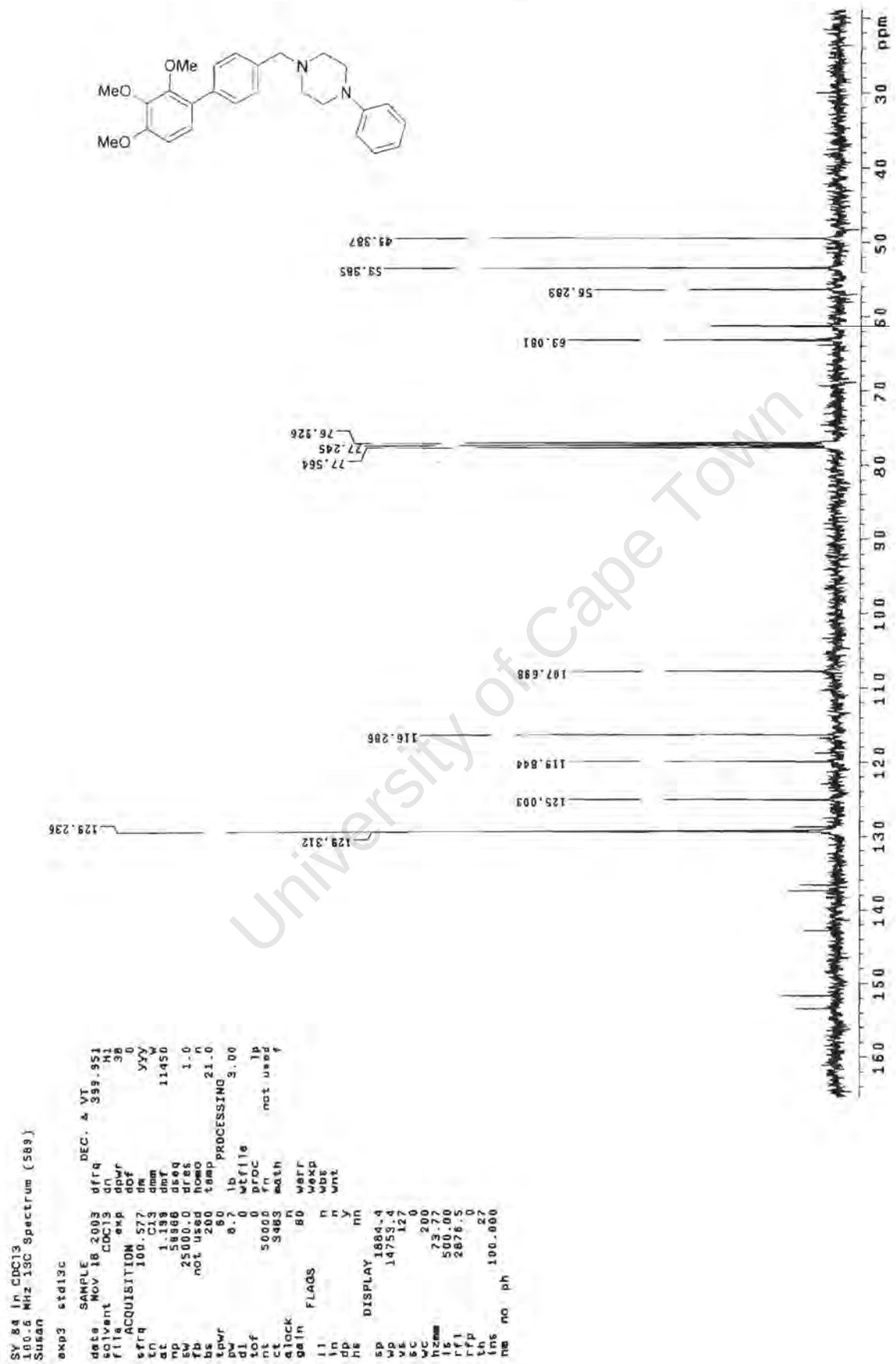

Figure A.4.1.20. ^{13}C NMR spectrum of compound **P16** in $CDCl_3$, 100 MHz.

P16

Printing Time: 10:36:09 AM
Printing Date: Friday, October 08, 2004

*Installation

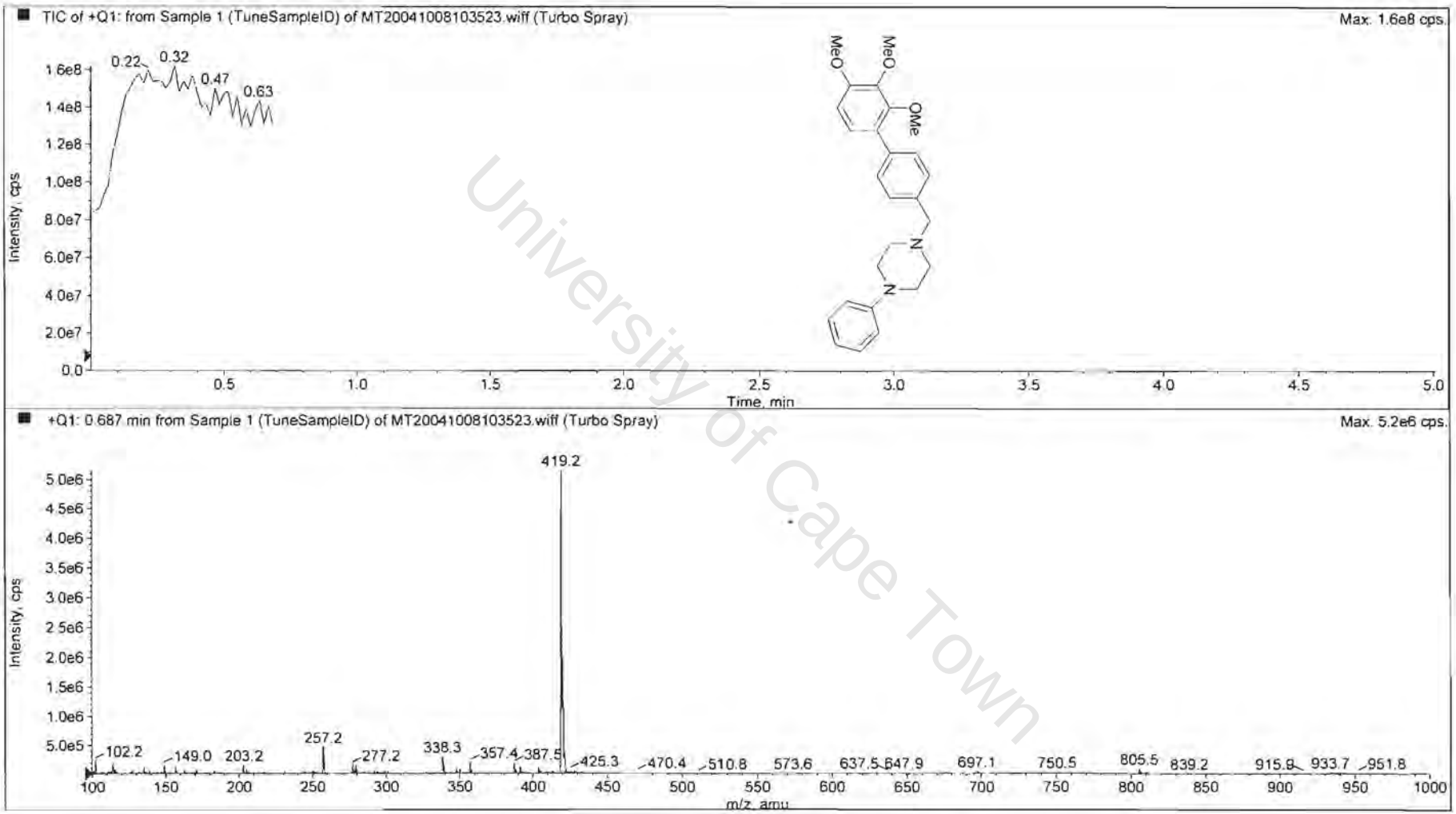

Page 1 of 1

Figure A.4.1.21.1. Mass spectrum of compound **P16**.

Printing Time: 10:40:33 AM
Printing Date: Friday, October 08, 2004

*Installation

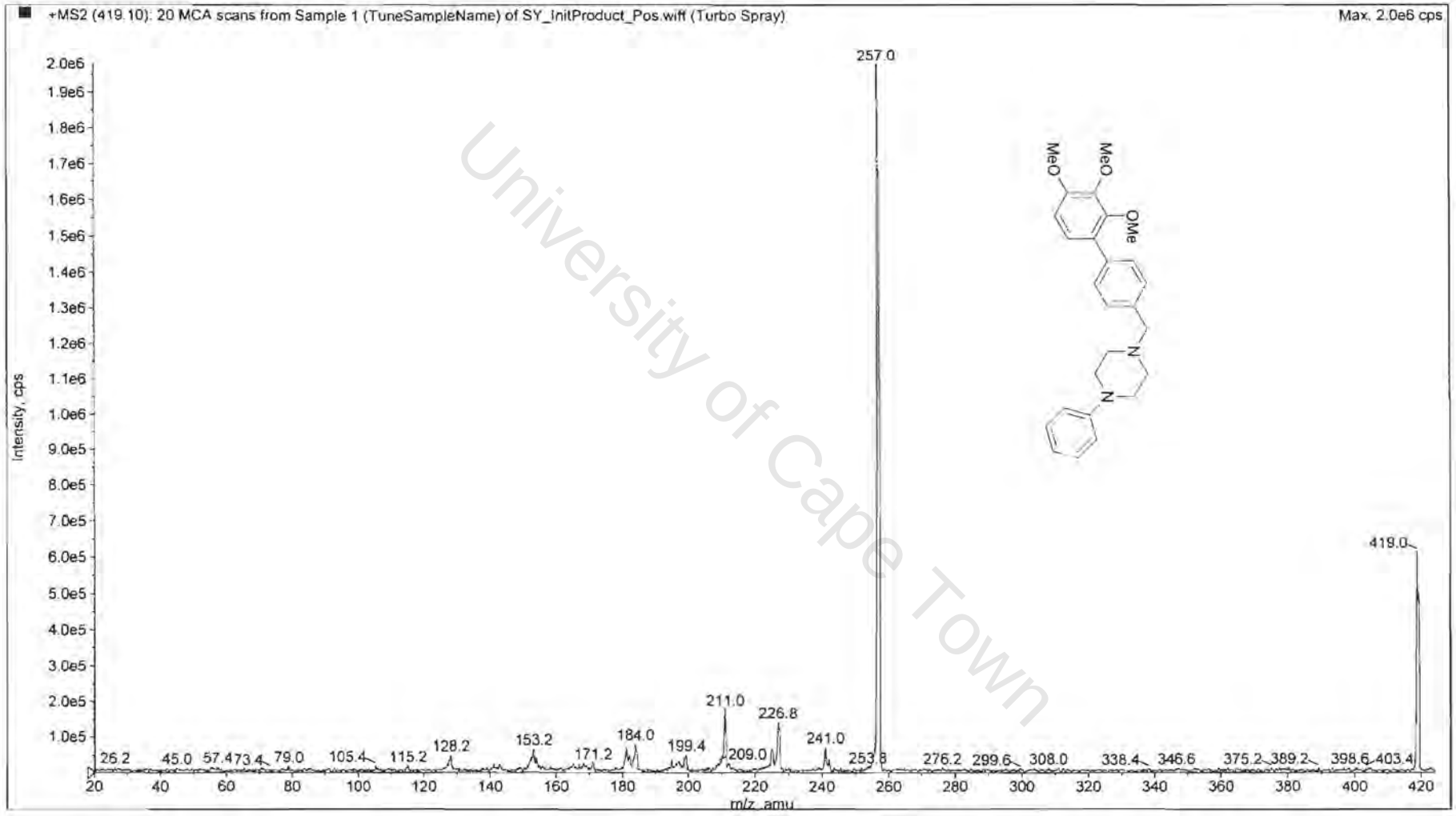

Page 1 of 1

Figure A.4.1.21.2. Mass spectrum of compound **P16**.

Compound P17

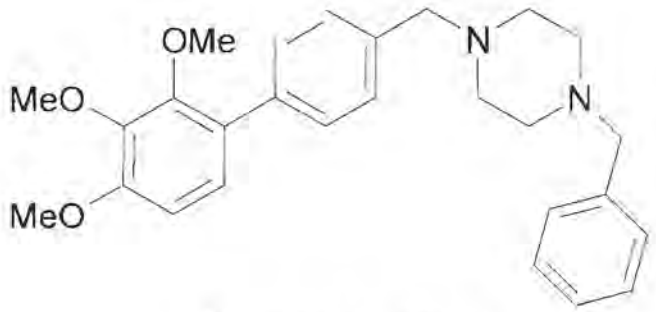

Compound P17

IUPAC

1-*Benzyl*-4-(2',3',4'-*trimethoxy-biphenyl*-4-*ylmethyl*)-*piperazine*

List of spectra:

- ^{1}H NMR (300MHz, $CDCl_3$)
- ^{13}C NMR (100MHz, $CDCl_3$)
- Mass spectra

P17

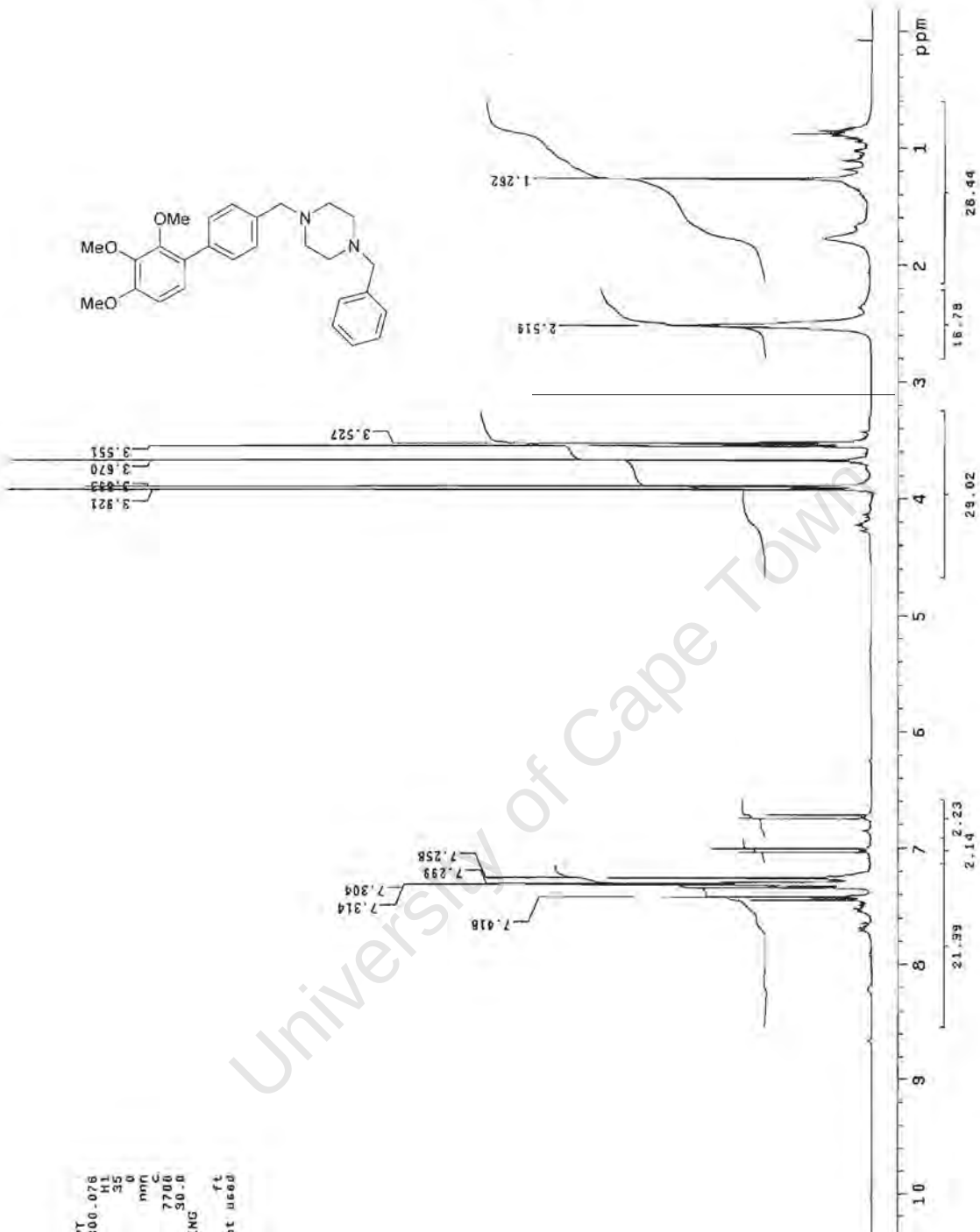

Figure A.4.1.22. ^{1}H NMR spectrum of compound **P17** in $CDCl_3$, 300 MHz.

P17

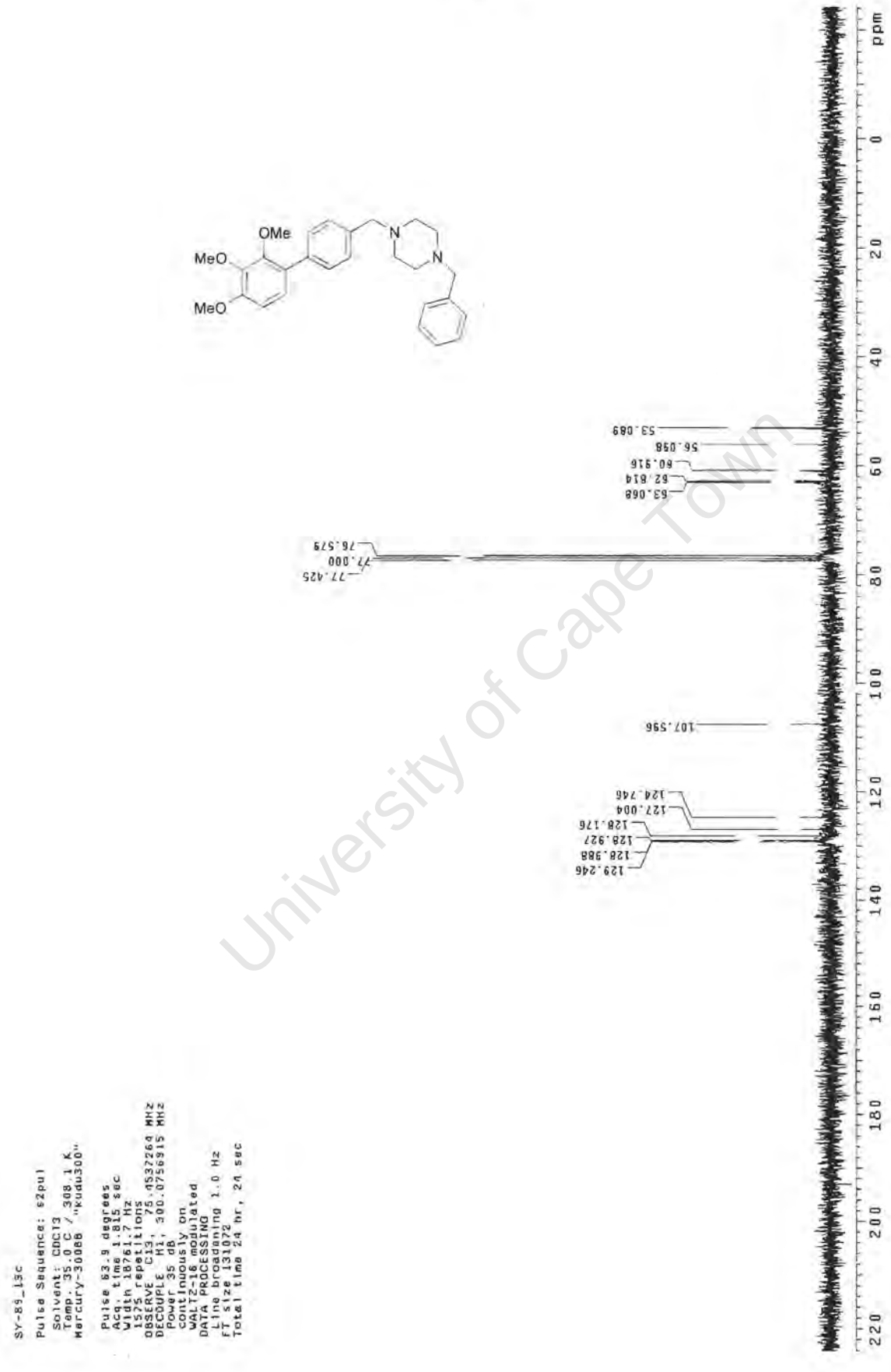

Figure A.4.1.23. ^{13}C NMR spectrum of compound **P17** in $CDCl_3$, 100 MHz.

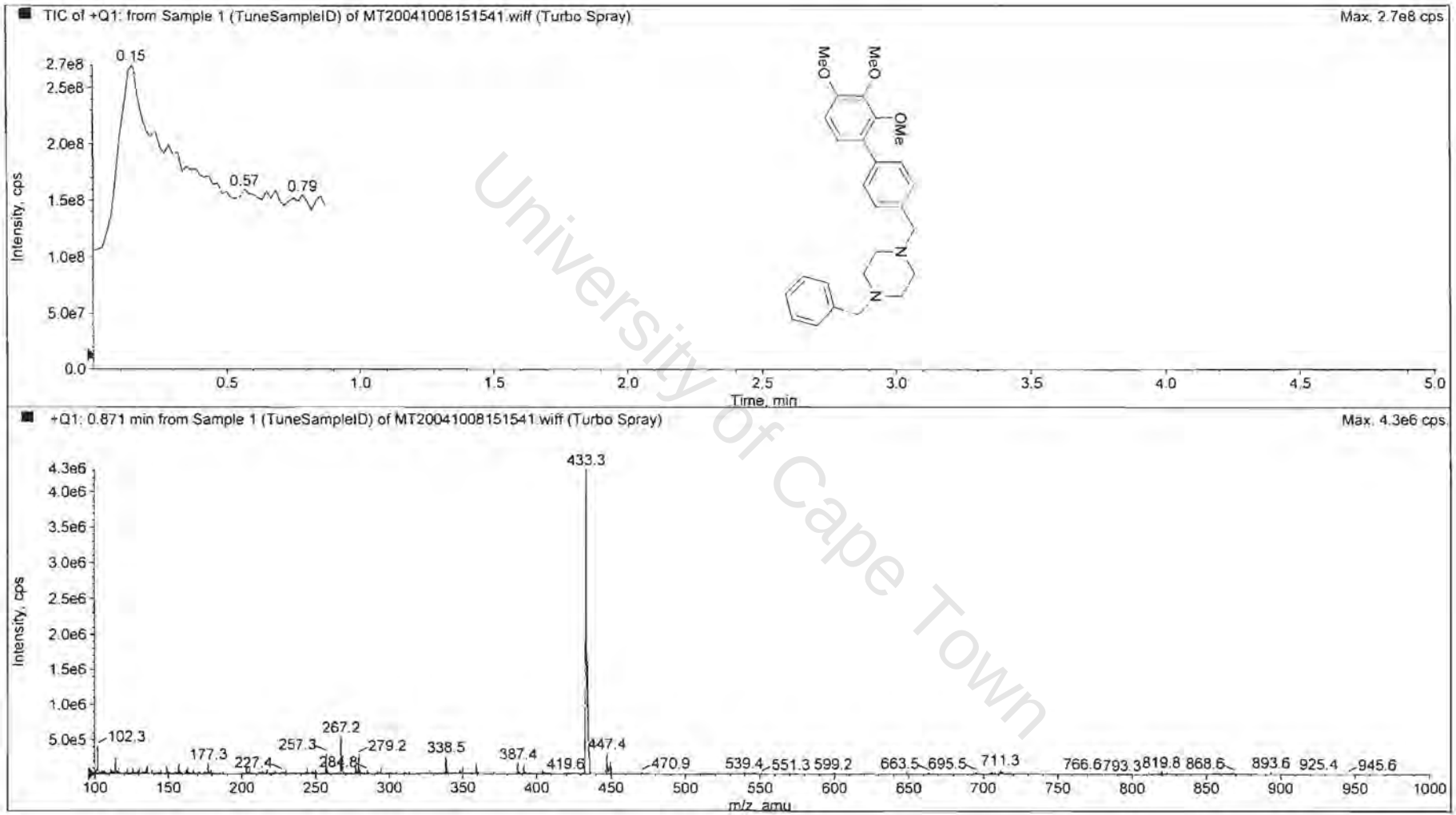

Figure A.4.1.24.1. Mass spectrum of compound **P17**.

Printing Time: 03:21:00 PM
Printing Date: Friday, October 08, 2004

*Installation

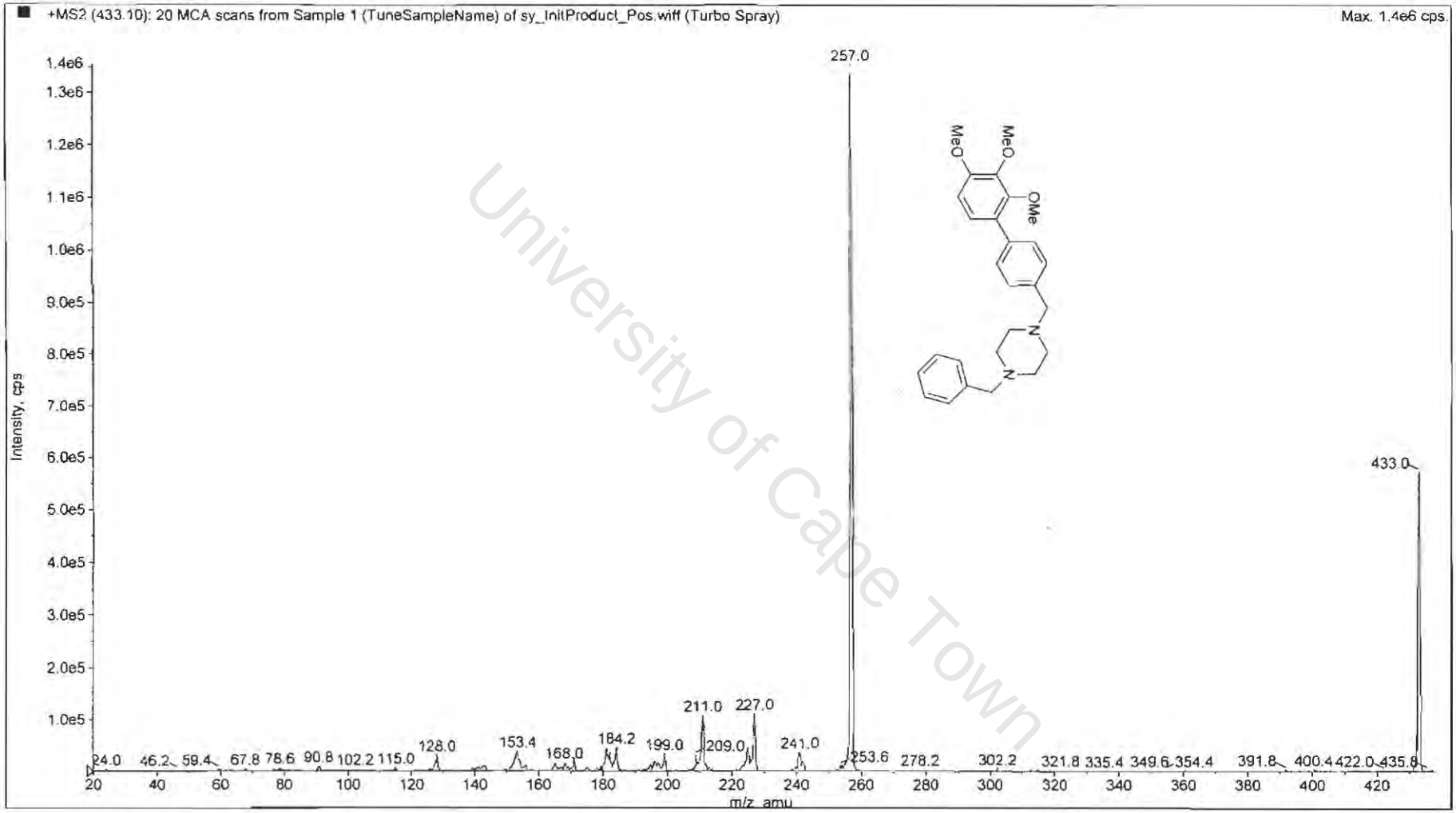

Page 1 of 1

Figure A.4.1.24.2. Mass spectrum of compound **P17**.

Compound P18

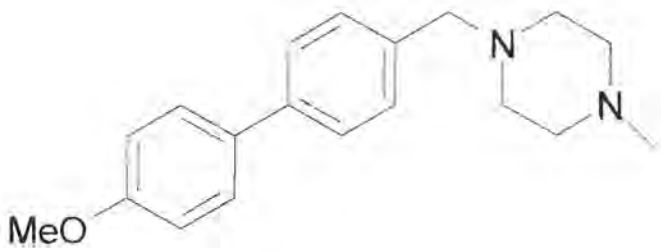

Compound P18

IUPAC

1-(4'-*Methoxy-biphenyl-4-yl-methyl*)-4-*methyl-piperazine*

List of spectra:

- ^{1}H NMR (300MHz, $CDCl_3$)
- ^{13}C NMR (100MHz, $CDCl_3$)
- Mass spectra

```
SY-87_1h

expl  std1h

        SAMPLE
date    Nov 20 2003
solvent       CDCl3
file            exp
    ACQUISITION
sfrq        300.076
tn              H1
at            2.731
np            32742
sw           5995.2
fb             3400
bs               16
tpwr             57
pw              6.4
d1            1.000
tof               0
nt               16
ct               16
alock             n
gain       not used
       FLAGS
il                n
in                n
dp                y
      DISPLAY
sp           -71.6
wp          3109.9
vs               87
sc                0
wc              200
hzmm          15.52
is           599.24
rfl          1552.5
rfp               0
th               18
ins          100.000
al     ph

        DEC. & vT
dfrq        300.076
dn               H1
dpwr             35
dof               0
dm              nnn
dmm               c
dmf            7700
temp           30.0
    PROCESSING
wtfile
proc             ft
fn         not used

werr
wexp
wbs
wnt
```

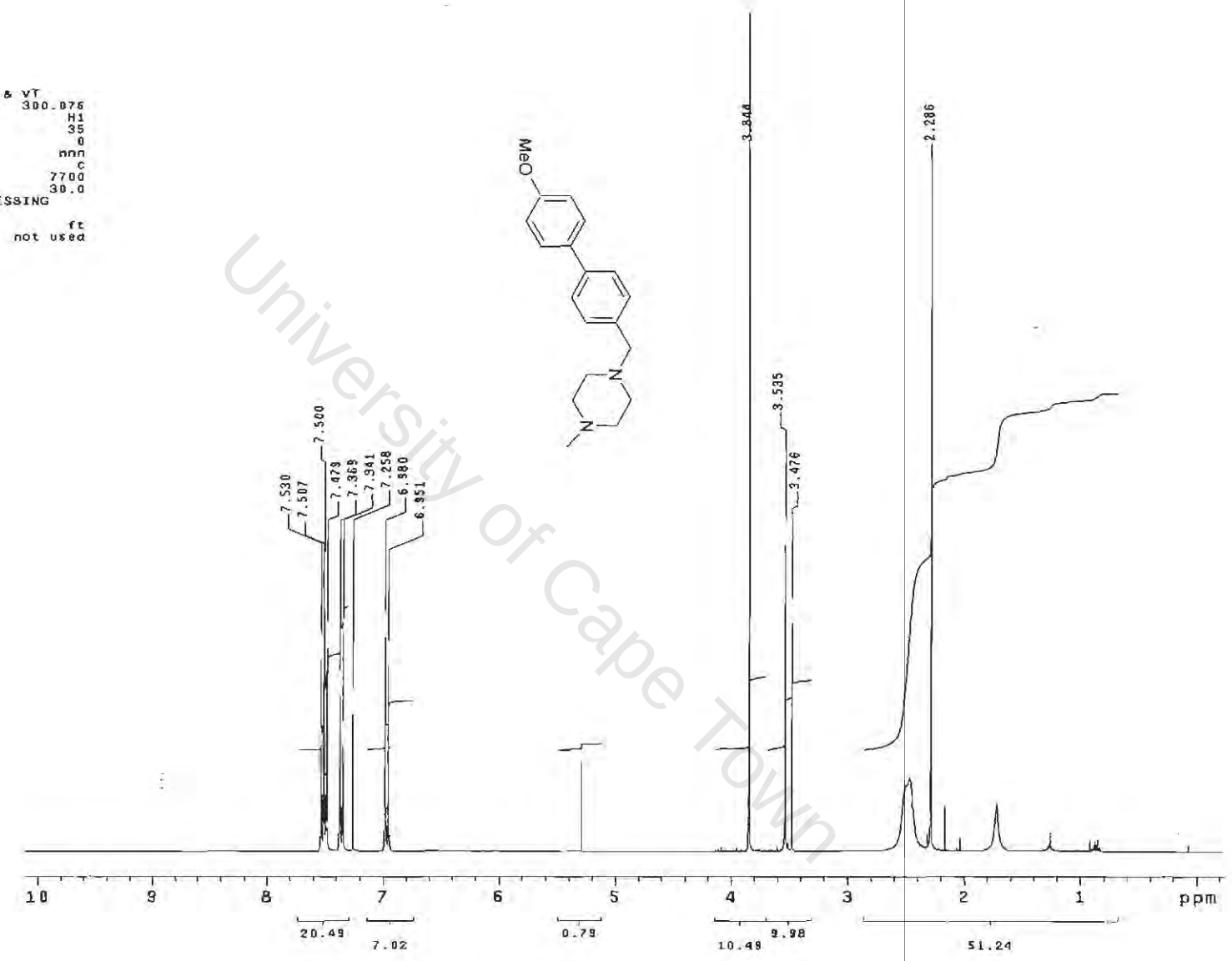

Figure A.4.1.25. ^{1}H NMR spectrum of compound **P18** in $CDCl_3$, 300 MHz.

P18

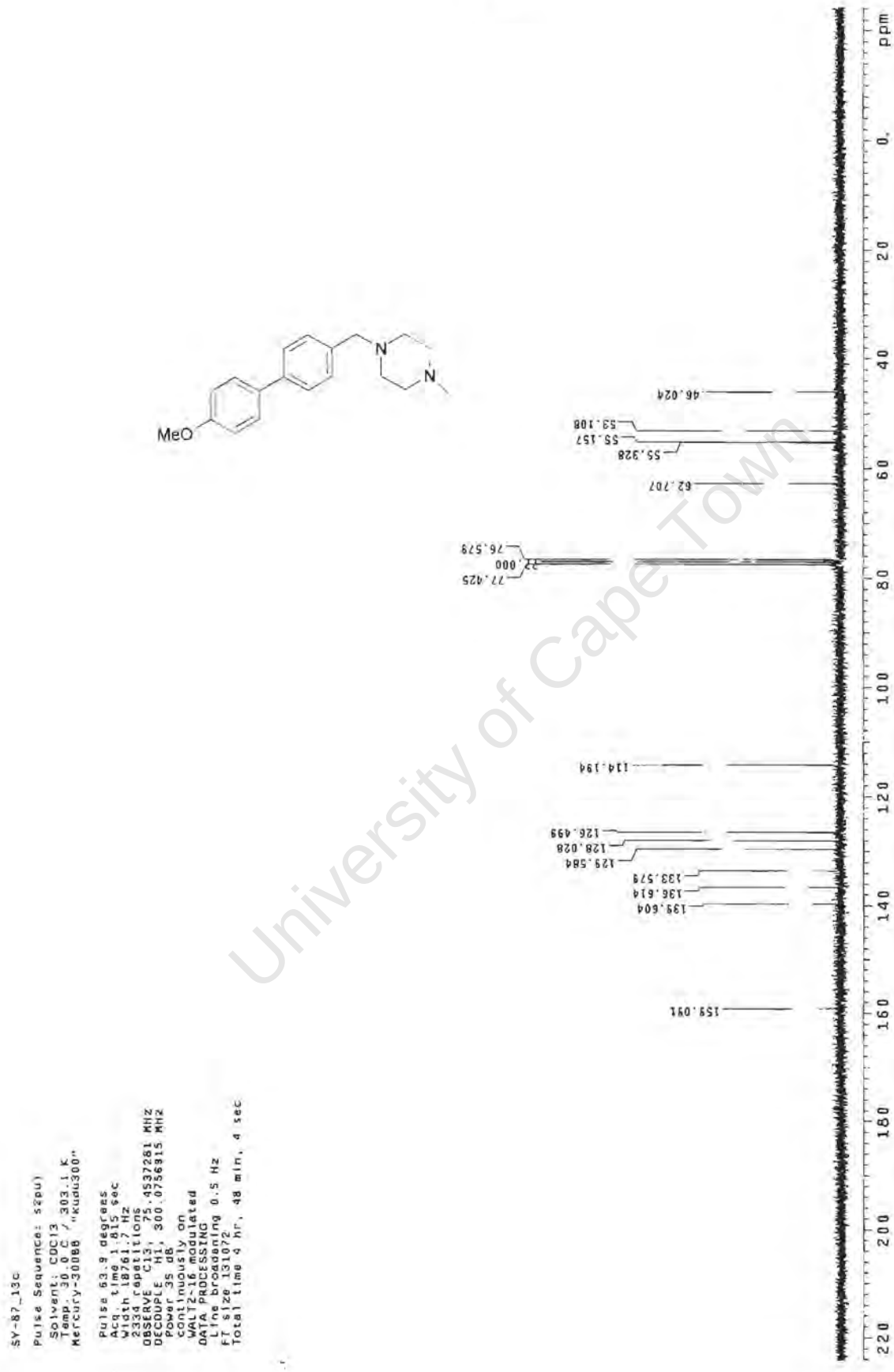

Figure A.4.1.26. ^{13}C NMR spectrum of compound **P18** in $CDCl_3$, 100 MHz.

Printing Time: 02:57.48 PM
Printing Date: Friday, October 08, 2004

*Installation

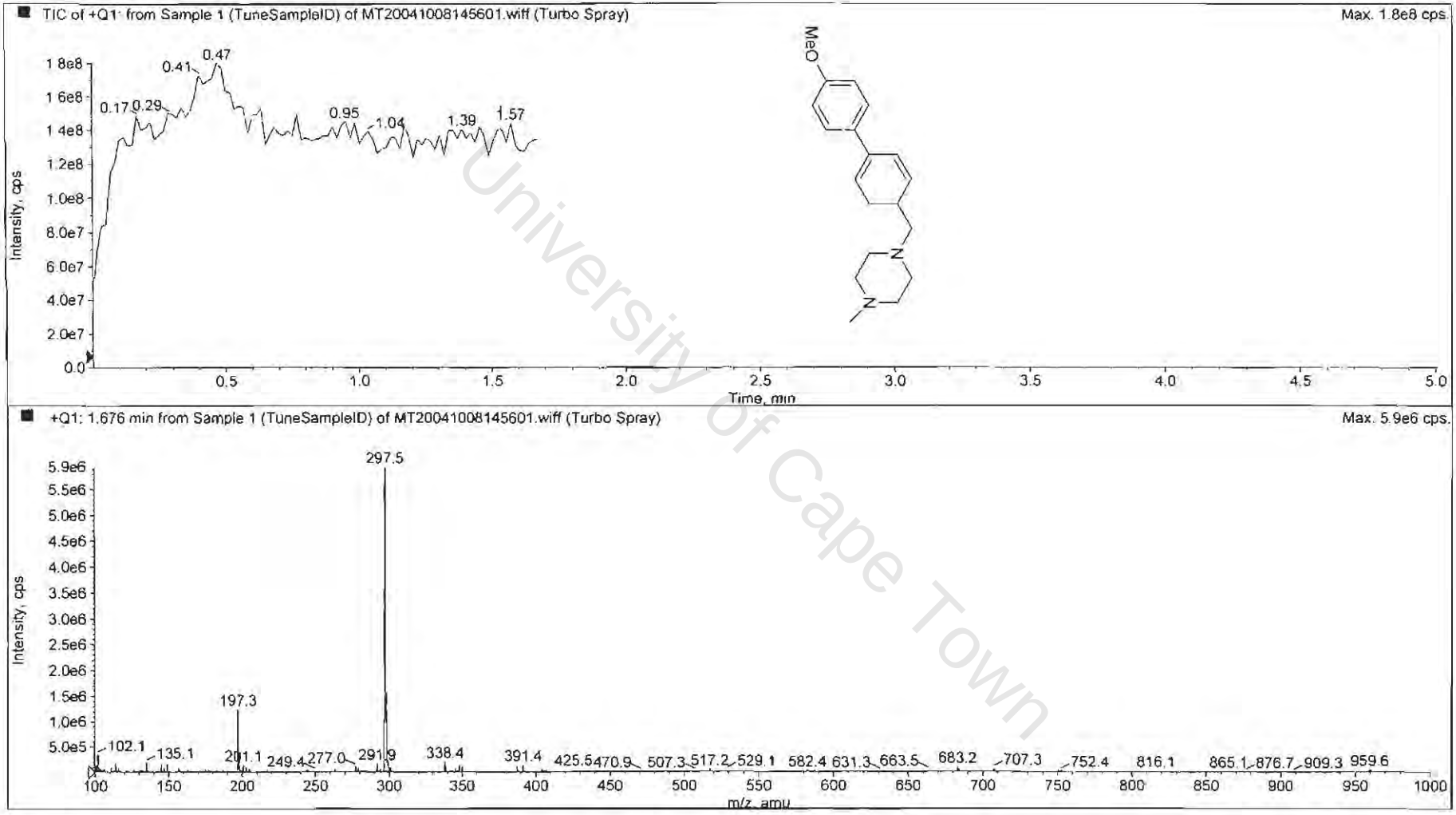

Page 1 of 1

Figure A.4.1.27.1. Mass spectrum of compound **P18**.

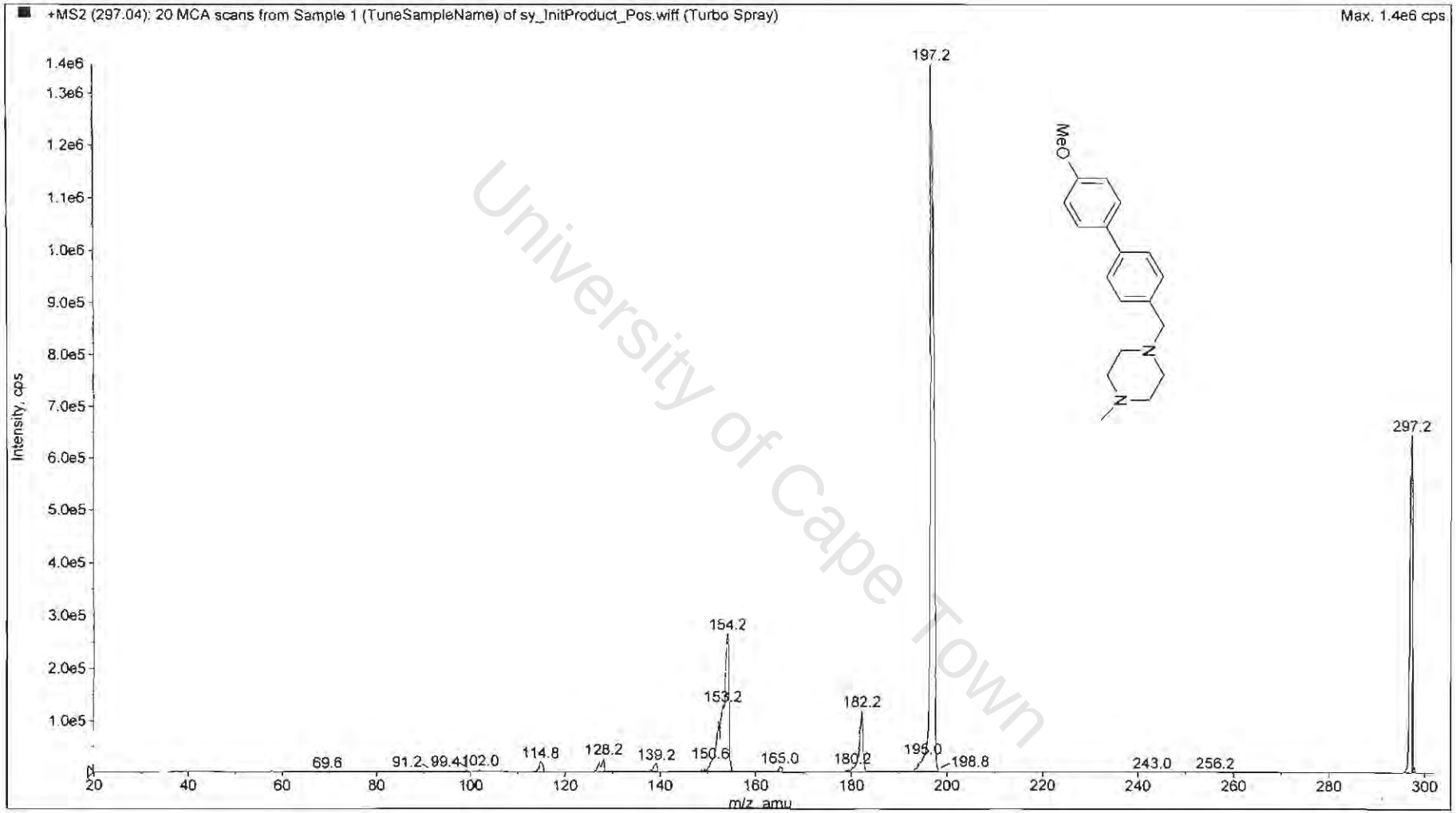

Figure A.4.1.27.2. Mass spectrum of compound **P18**.

Compound P19

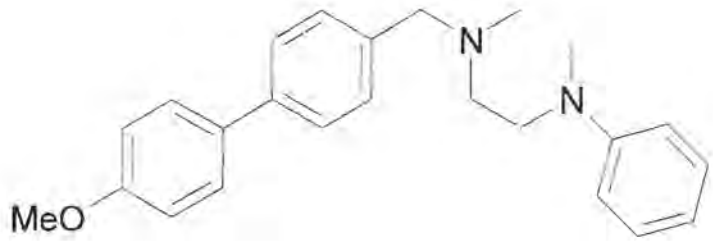

Compound P19

IUPAC

1-(4'-*Methoxy-biphenyl-4-ylmethyl*)-4-*phenyl-piperazine*

List of spectra:

- ^{1}H NMR (400MHz, $CDCl_3$)
- ^{13}C NMR (100MHz, $CDCl_3$)
- Mass spectra

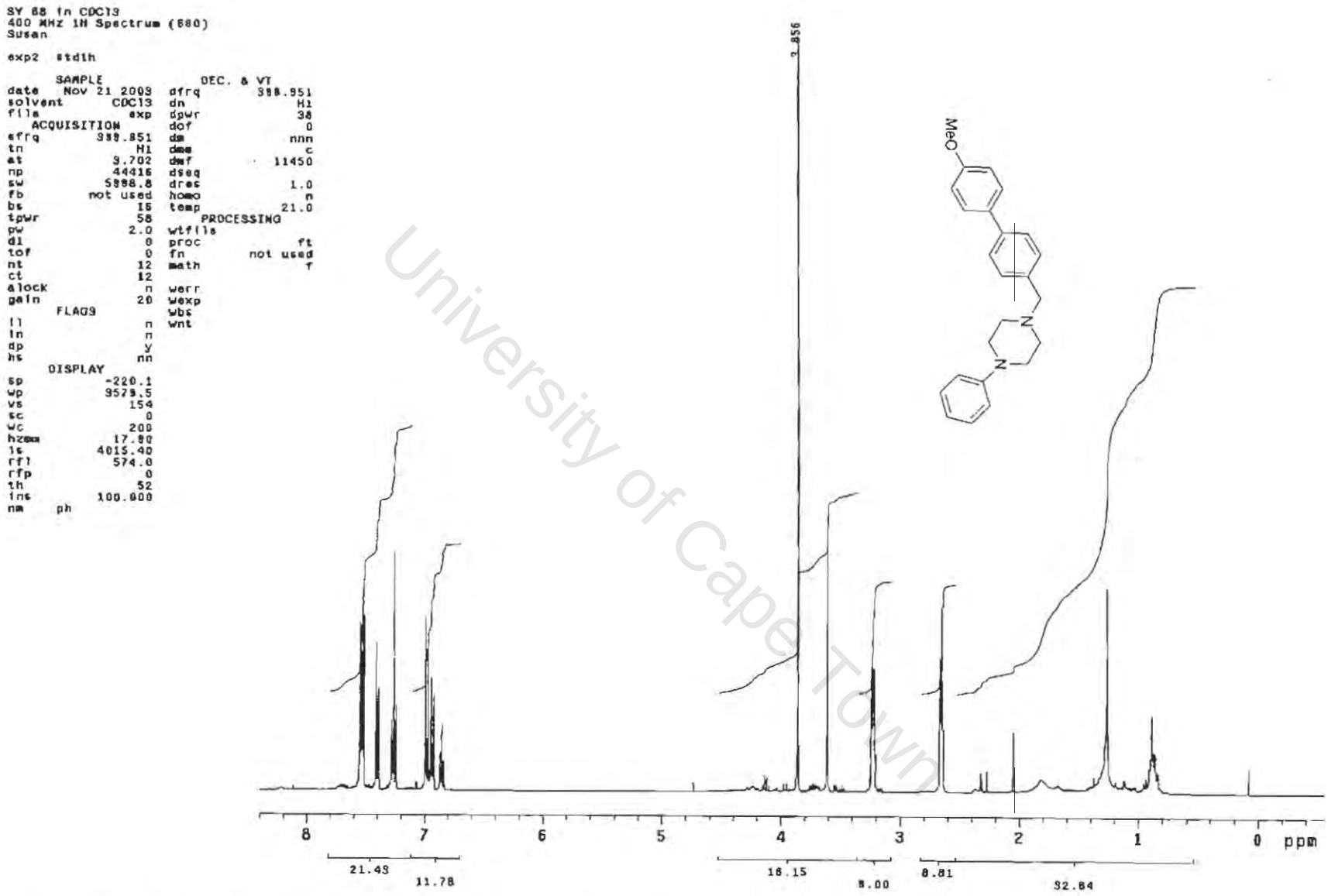

Figure A.4.1.28. ^{1}H NMR spectrum of compound **P19** in $CDCl_3$, 400 MHz.

P19

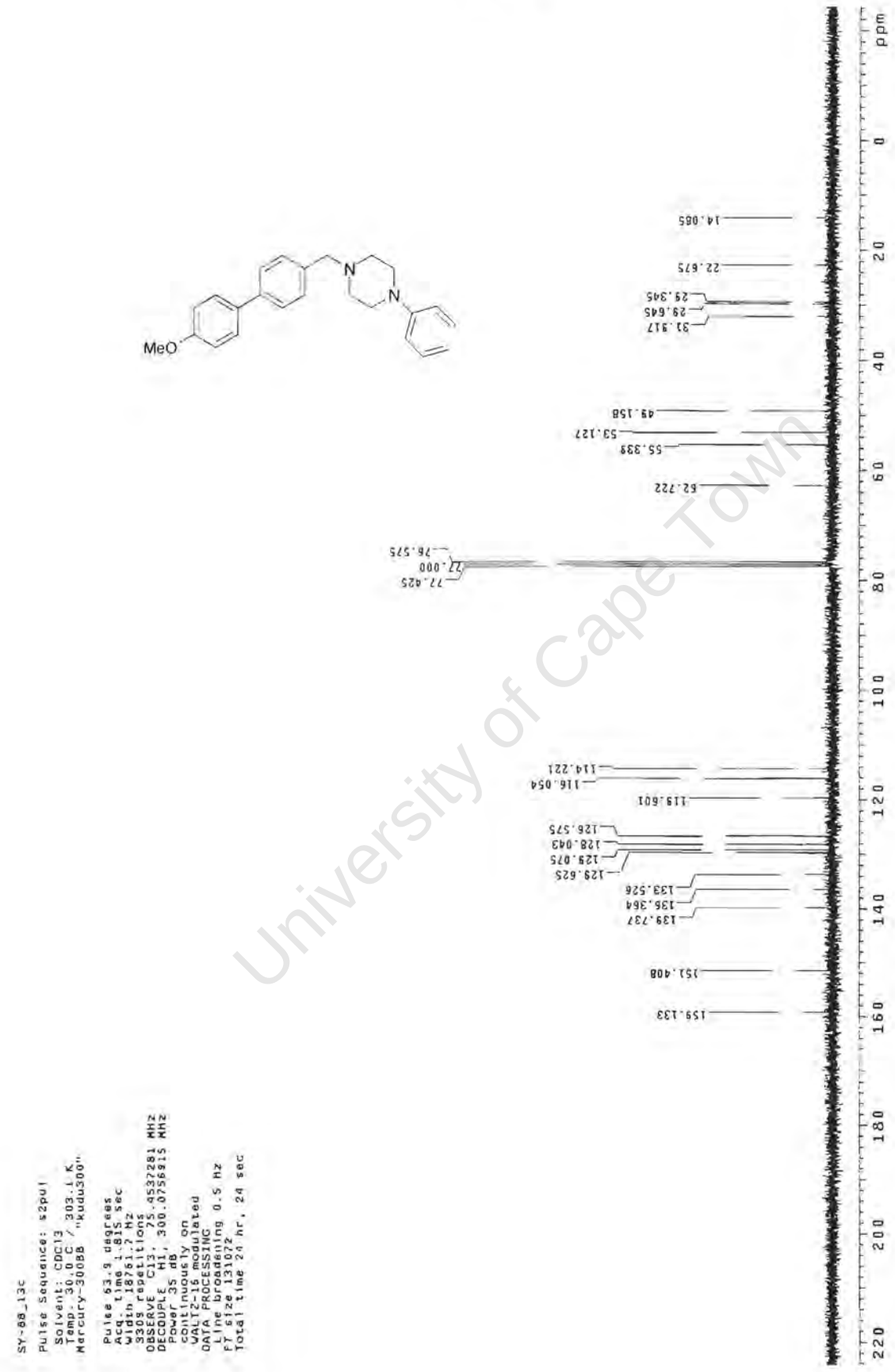

Figure A.4.1.29. ^{13}C NMR spectrum of compound **P19** in $CDCl_3$, 100 MHz.

Printing Time: 03:05:15 PM
Printing Date: Friday, October 08, 2004

*Installation

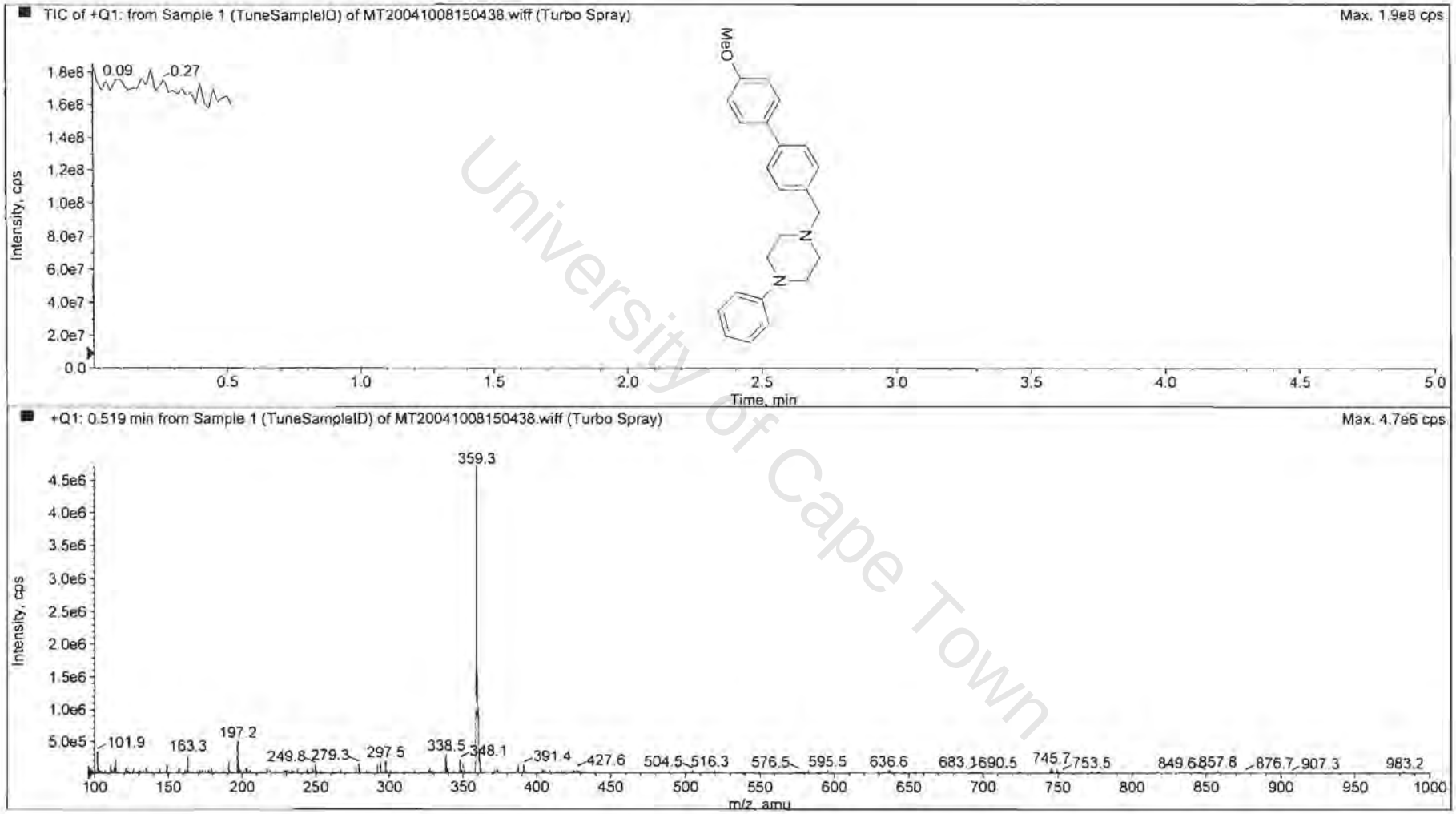

Page 1 of 1

Figure A.4.1.30.1. Mass spectrum of compound **P19**.

Printing Time: 03:09:23 PM
Printing Date: Friday, October 08, 2004

*Installation

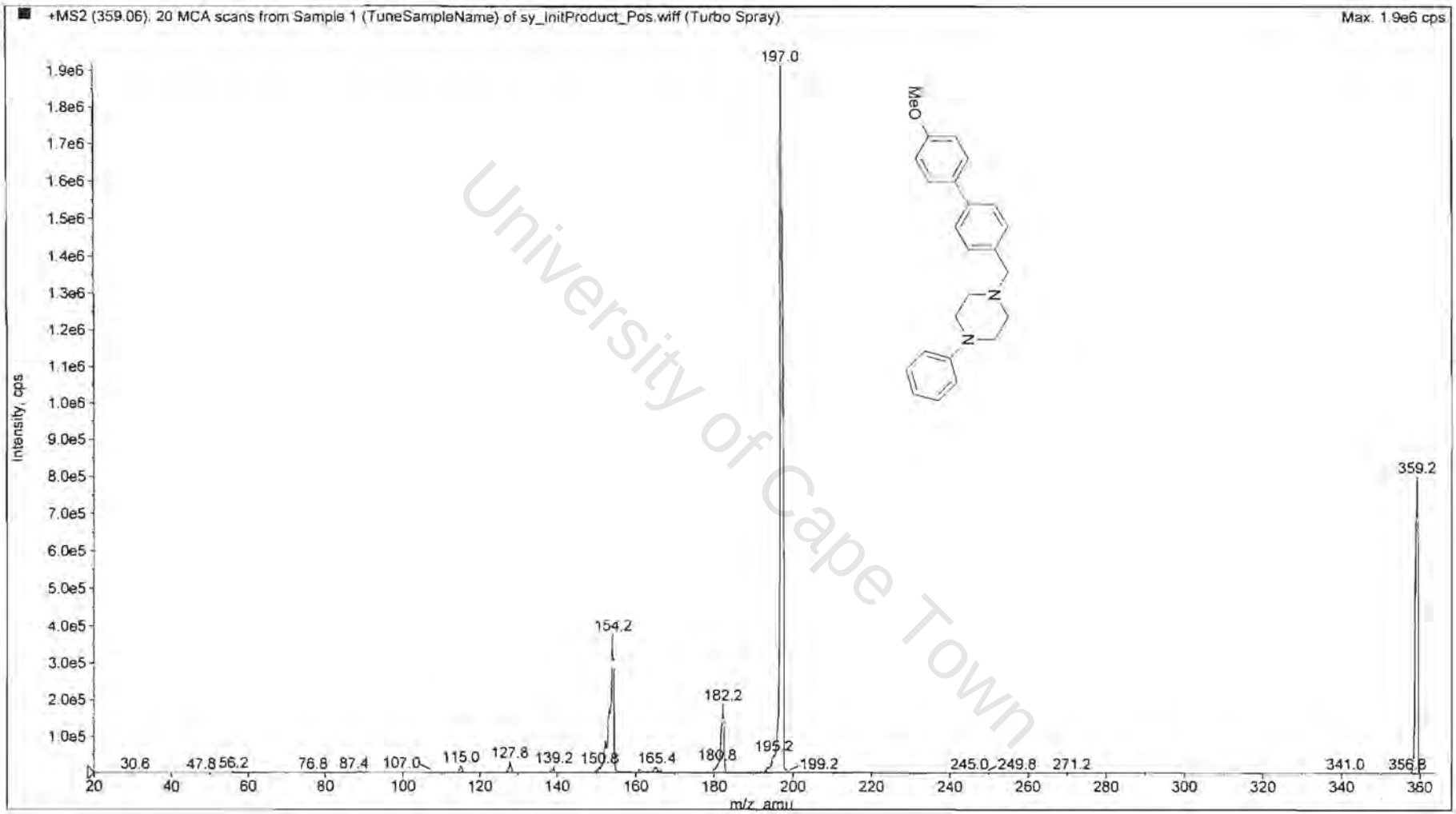

Page 1 of 1

Figure A.4.1.30.2. Mass spectrum of compound **P19**.

Compound P20

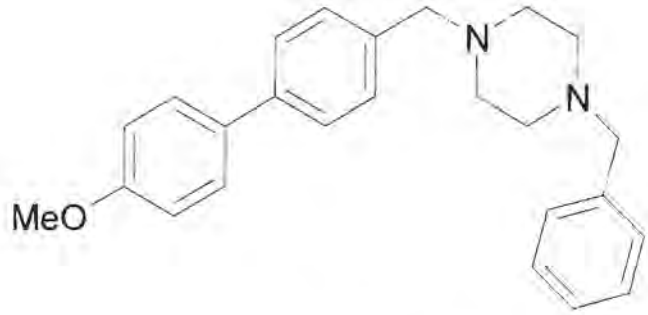

Compound P20

IUPAC

1-*Benzyl*-4-(4'-*methoxy-biphenyl*-4-*ylmethyl*)-*piperazine*

List of spectra:

- ^{1}H NMR (300MHz, $CDCl_3$)
- ^{13}C NMR (100MHz, $CDCl_3$)
- Mass spectra

P20

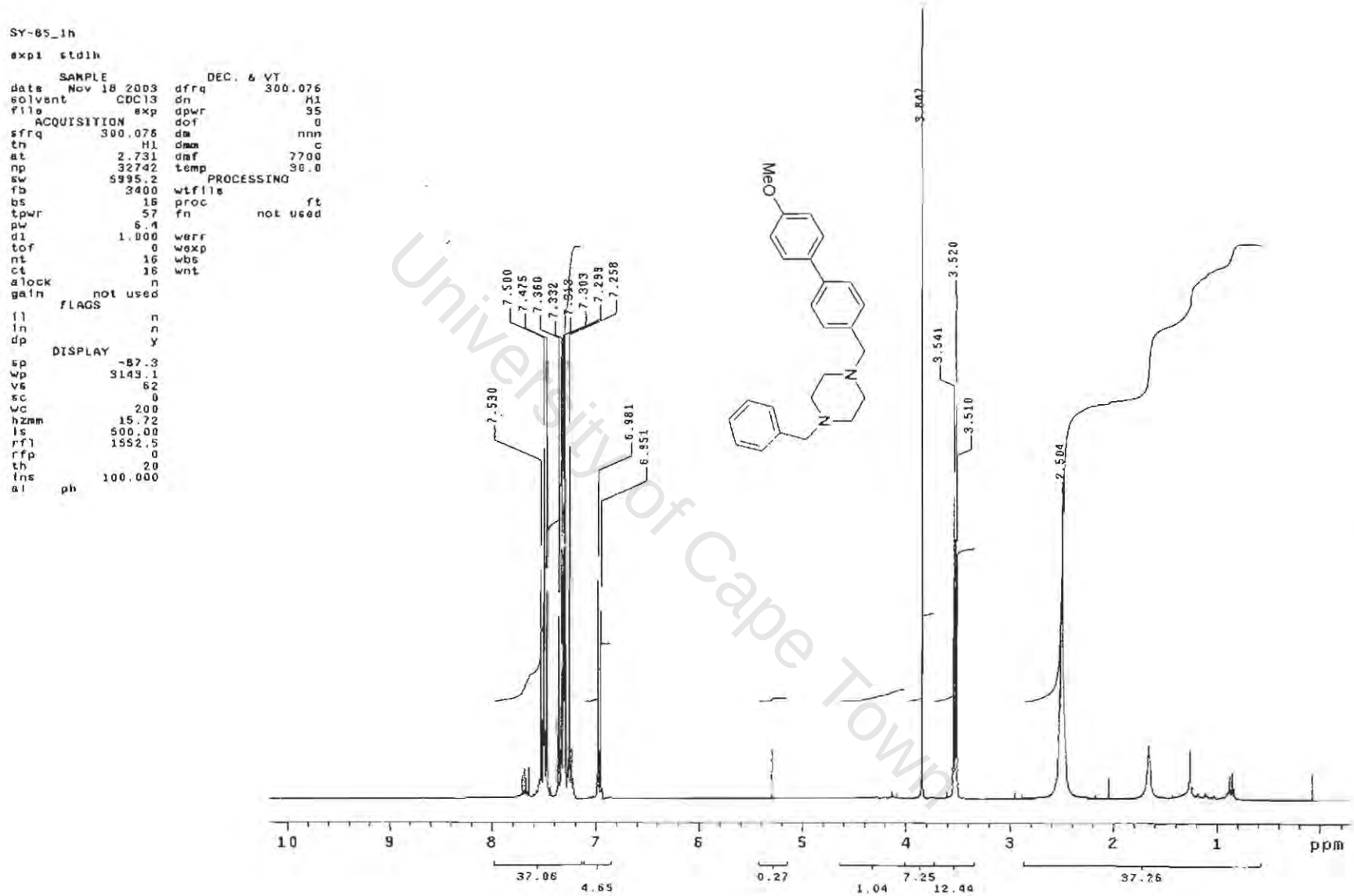

Figure A.4.1.31. ^{1}H NMR spectrum of compound **P20** in $CDCl_3$, 300 MHz.

P20

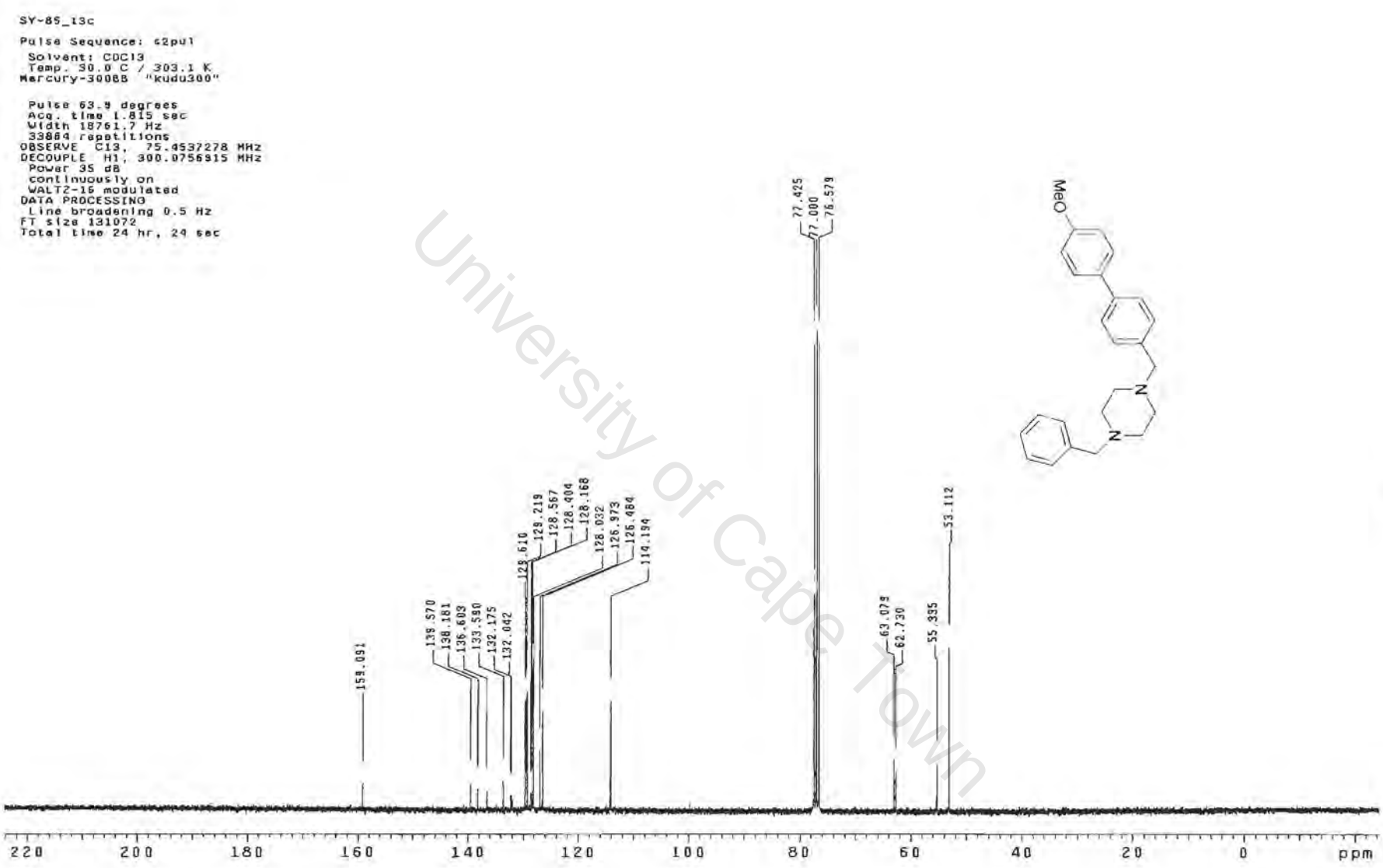

Figure A.4.1.32. ^{13}C NMR spectrum of compound **P20** in $CDCl_3$, 100 MHz.

P20

Printing Time: 10:45:09 AM
Printing Date: Friday, October 08, 2004

*Installation

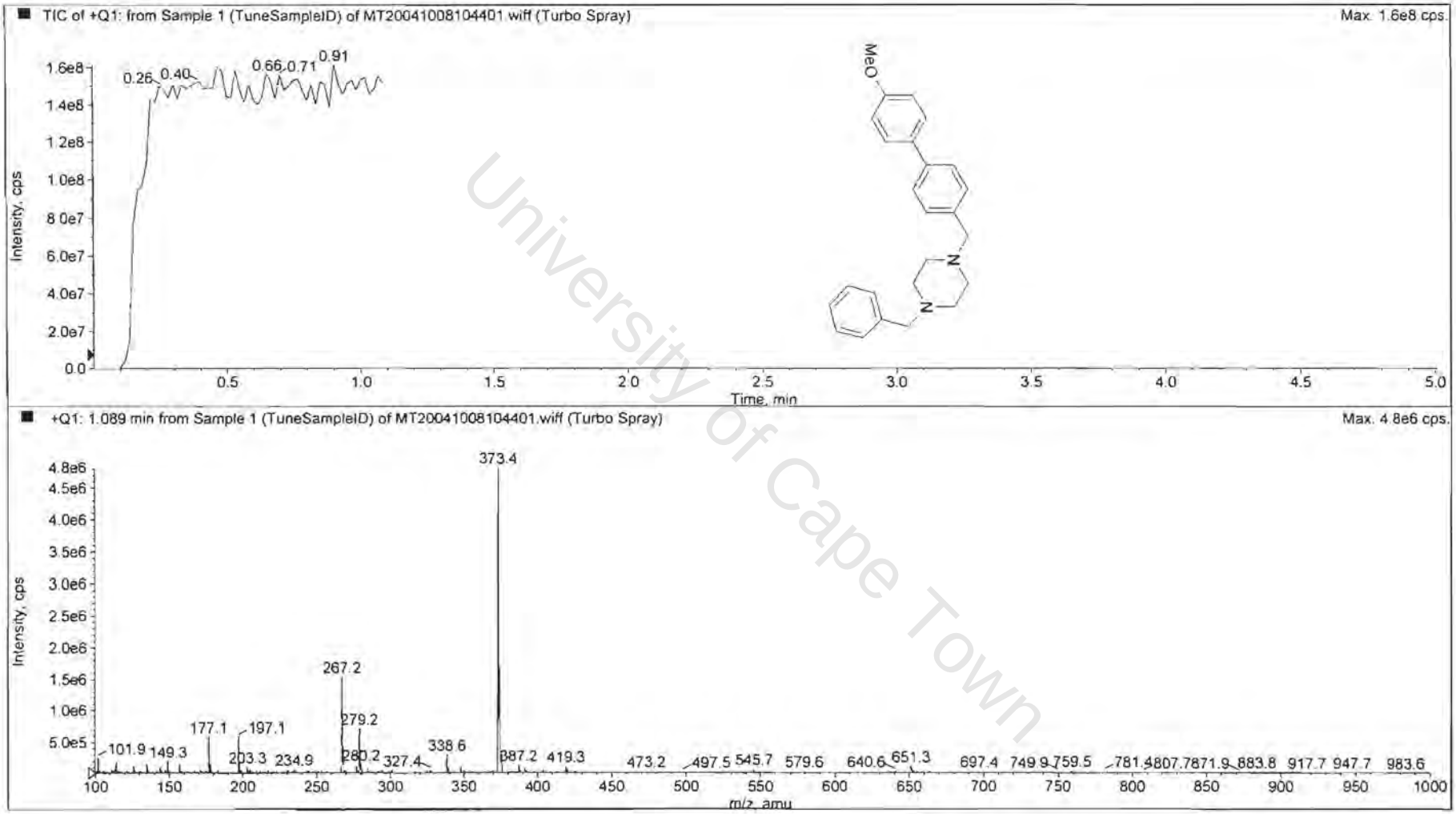

Page 1 of 1

Figure A.4.1.33.1. Mass spectrum of compound **P20**.

P20

Printing Time: 10:49:29 AM
Printing Date: Friday, October 08, 2004

*Installation

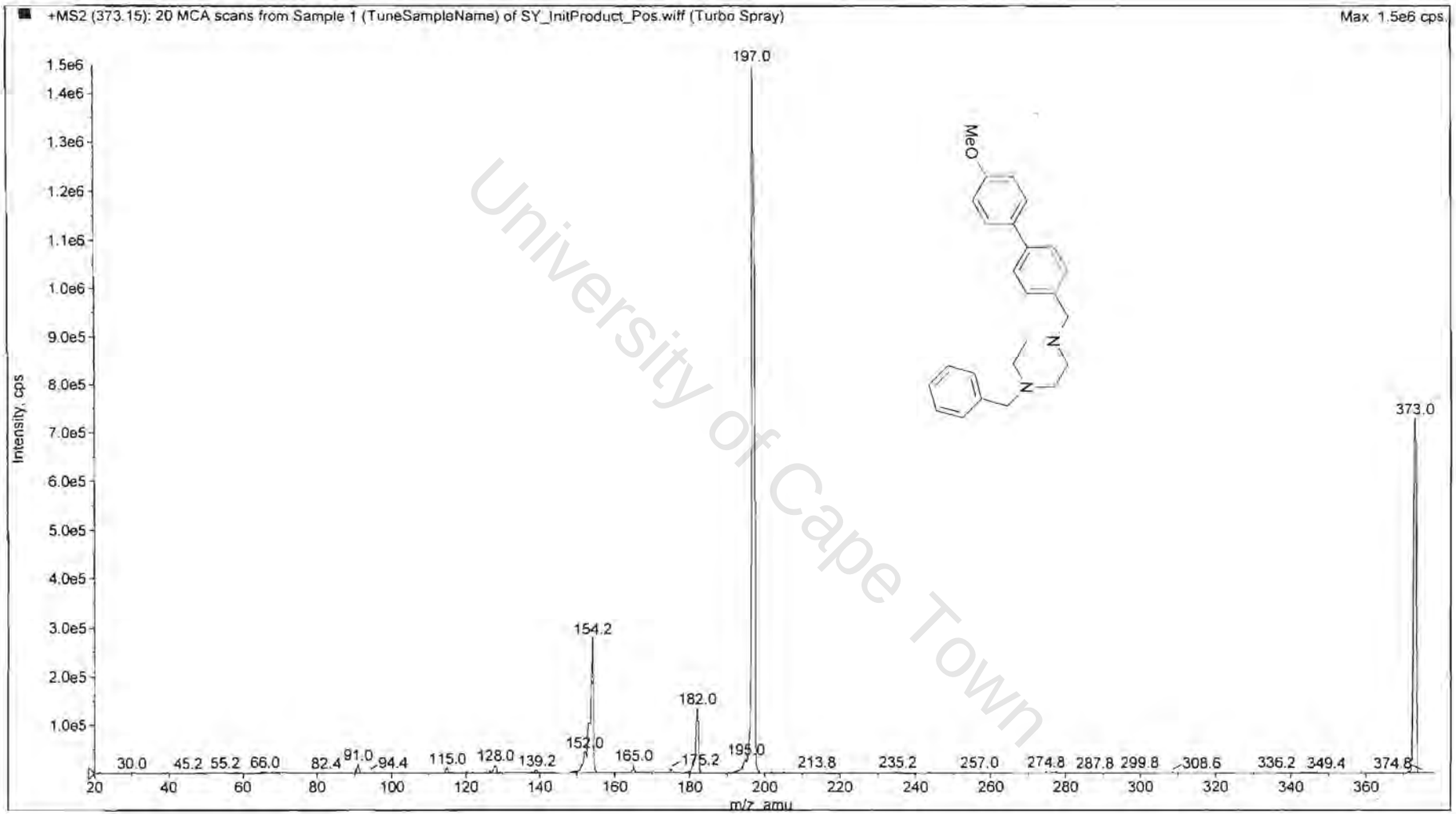

Page 1 of 1

Figure A.4.1.33.2. Mass spectrum of compound **P20**.

Compound P23

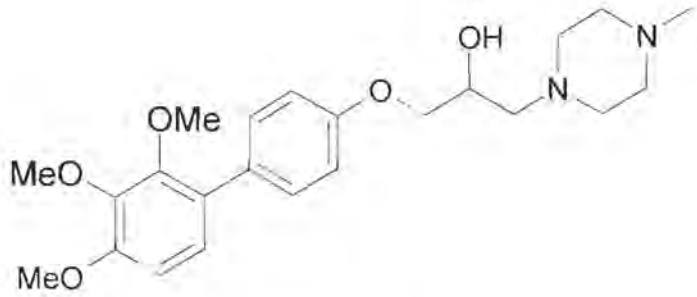

Compound P23

IUPAC

1-(4-*Methyl-piperazin*-1-*yl*)-3-(2',3',4'-*trimethoxy-biphenyl*-4-*yloxy-propan*-2-*ol*

List of spectra:

- ^{1}H NMR (400MHz, $CDCl_3$)
- ^{13}C NMR (100MHz, $CDCl_3$)
- Mass spectra

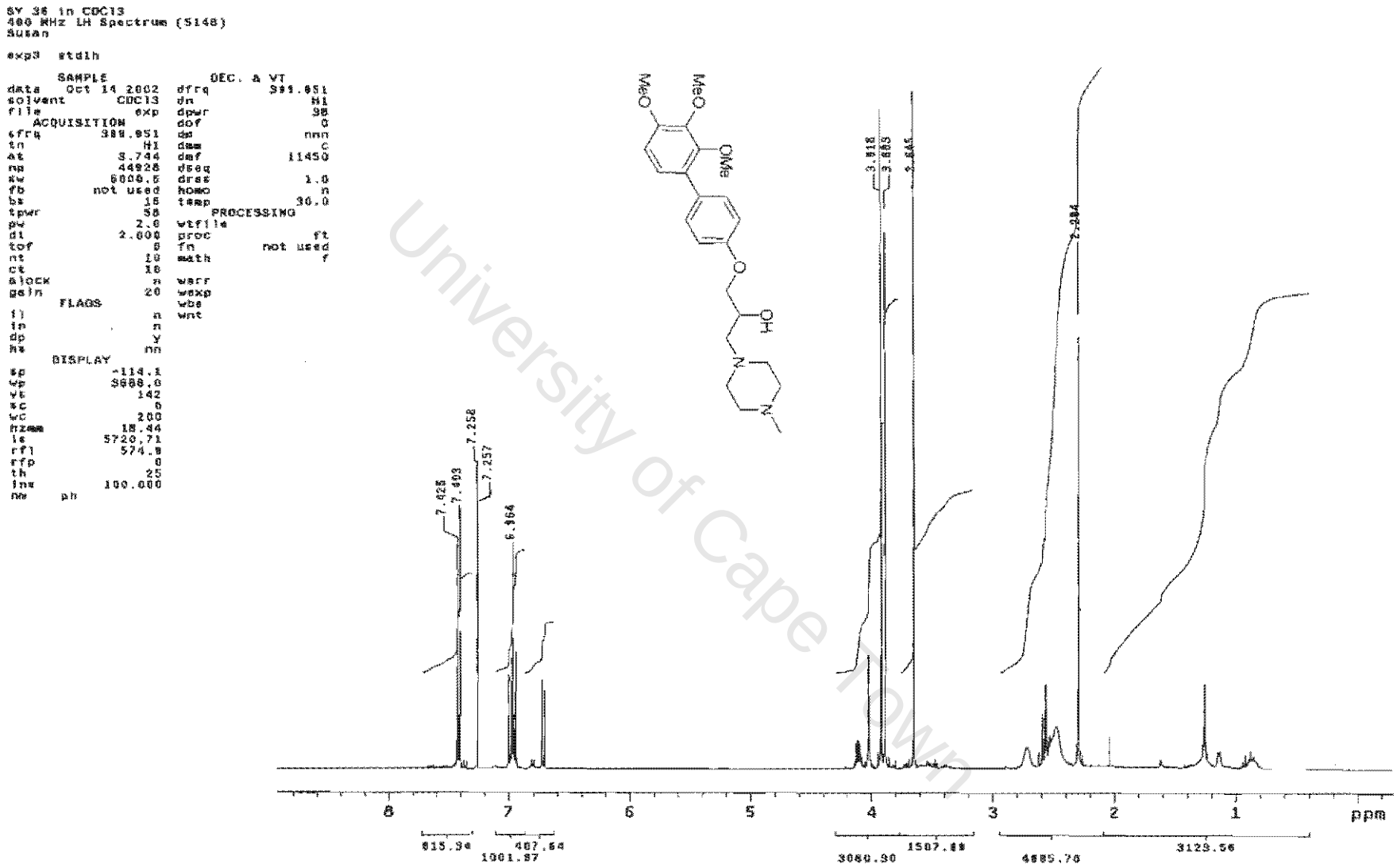

Figure B.4.1.1. ^{1}H NMR spectrum of compound **P23** in $CDCl_3$, 400 MHz.

```
SY 96 in CDCl3
100.6 MHz 13C Spectrum (5148)
Susan

exp4  std13c

        SAMPLE                  DEC. & VT
date    Oct 14 2002   dfrq          399.551
solvent       CDCl3   dn                H1
file            exp   dpwr              43
    ACQUISITION       dof                0
sfrq        100.577   dm               yyy
tn              C13   dmm                W
at            1.188   dmf            11450
np             55868   dseq
sw          25000.0   dres             1.0
fb        not used    homo               n
bs              200   temp            30.0
tpwr             60       PROCESSING
pw              8.7   lb               3.00
d1                0   wtfile
tof               0   proc               lp
nt           200000   fn           not used
ct             2856   math               f
alock             s
gain             50   werr
        FLAGS         wexp
il                n   wbs
in                n   wnt
dp                y
hs               nn
      DISPLAY
sp           1632.6
wp          15761.3
vs             7186
sc                0
wc              200
hzmm          78.81
is           500.00
rfl          2876.5
rfp               0
th               36
ins          100.000
al  no  ph
```


Figure B.4.1.2. ^{13}C NMR spectrum of compound **P23** in $CDCl_3$, 100 MHz.

Printing Time: 09:43:28 AM
Printing Date: Thursday, October 07, 2004
*Installation

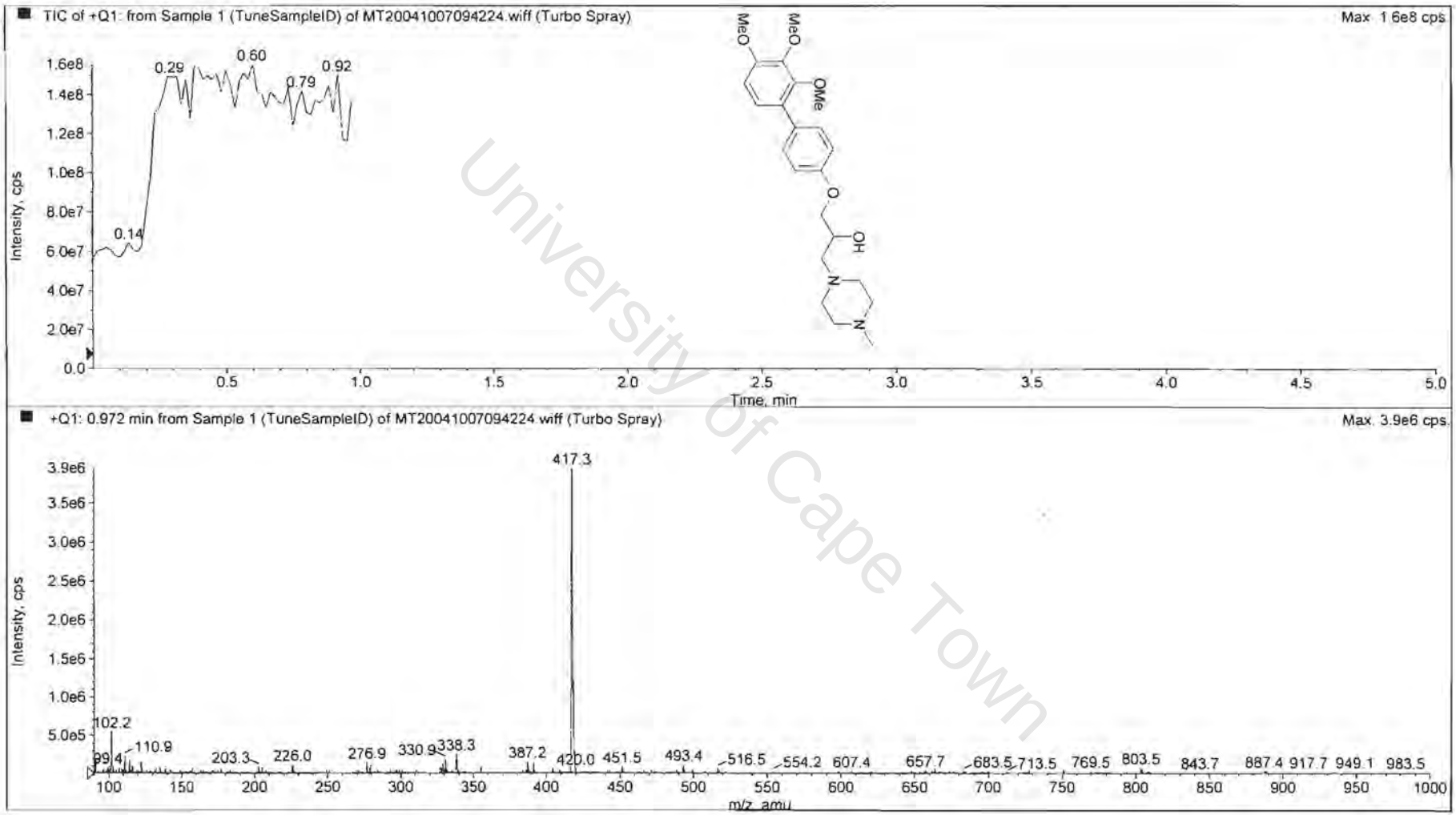

Page 1 of 1

Figure B.4.1.3.1. Mass spectrum of compound **P23**.

Printing Time: 09:46:42 AM
Printing Date: Thursday, October 07, 2004
*Installation

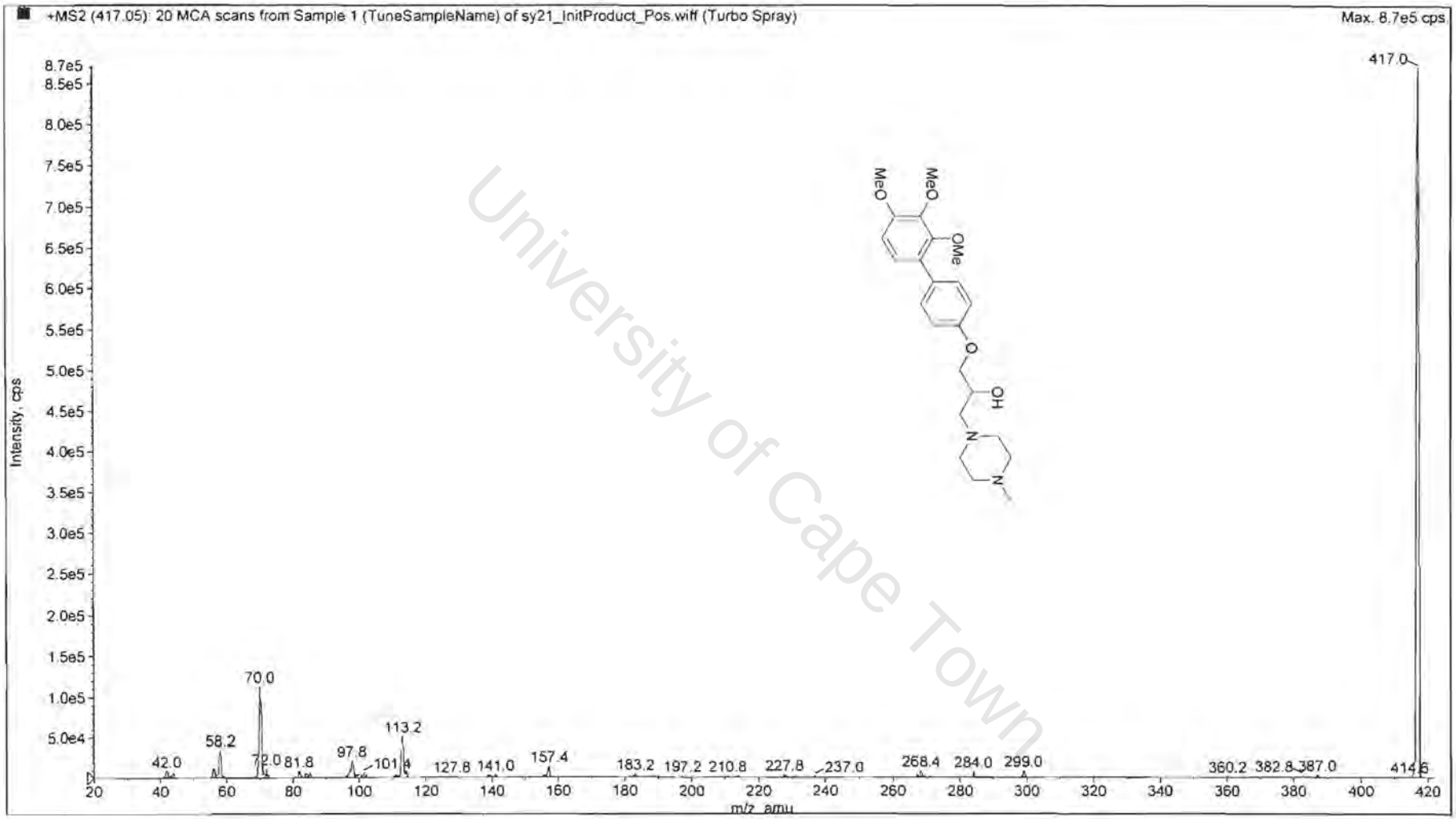

Page 1 of 1

Figure B.4.1.3.2. Mass spectrum of compound **P23**.

Compound P24

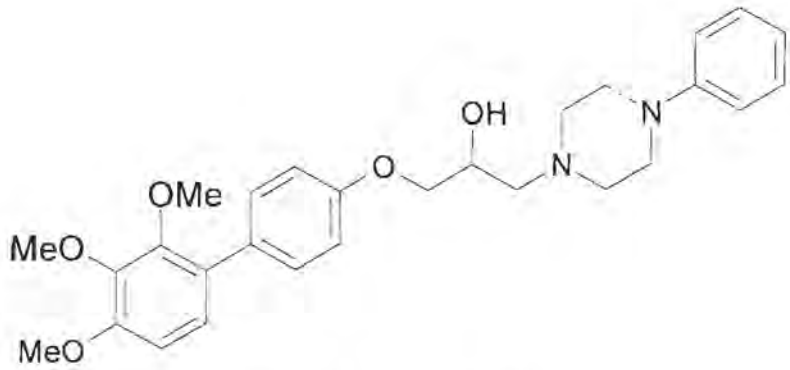

Compound P24

IUPAC

1-(4-*Phenyl-piperazin*-1-*yl*)-3-(2',3',4'-*trimethoxy-biphenyl*-4-*yloxy*)-*propan*-2-*ol*

List of spectra:

- ^{1}H NMR (400MHz, $CDCl_3$)
- ^{13}C NMR (100MHz, $CDCl_3$)
- Mass spectra

P24

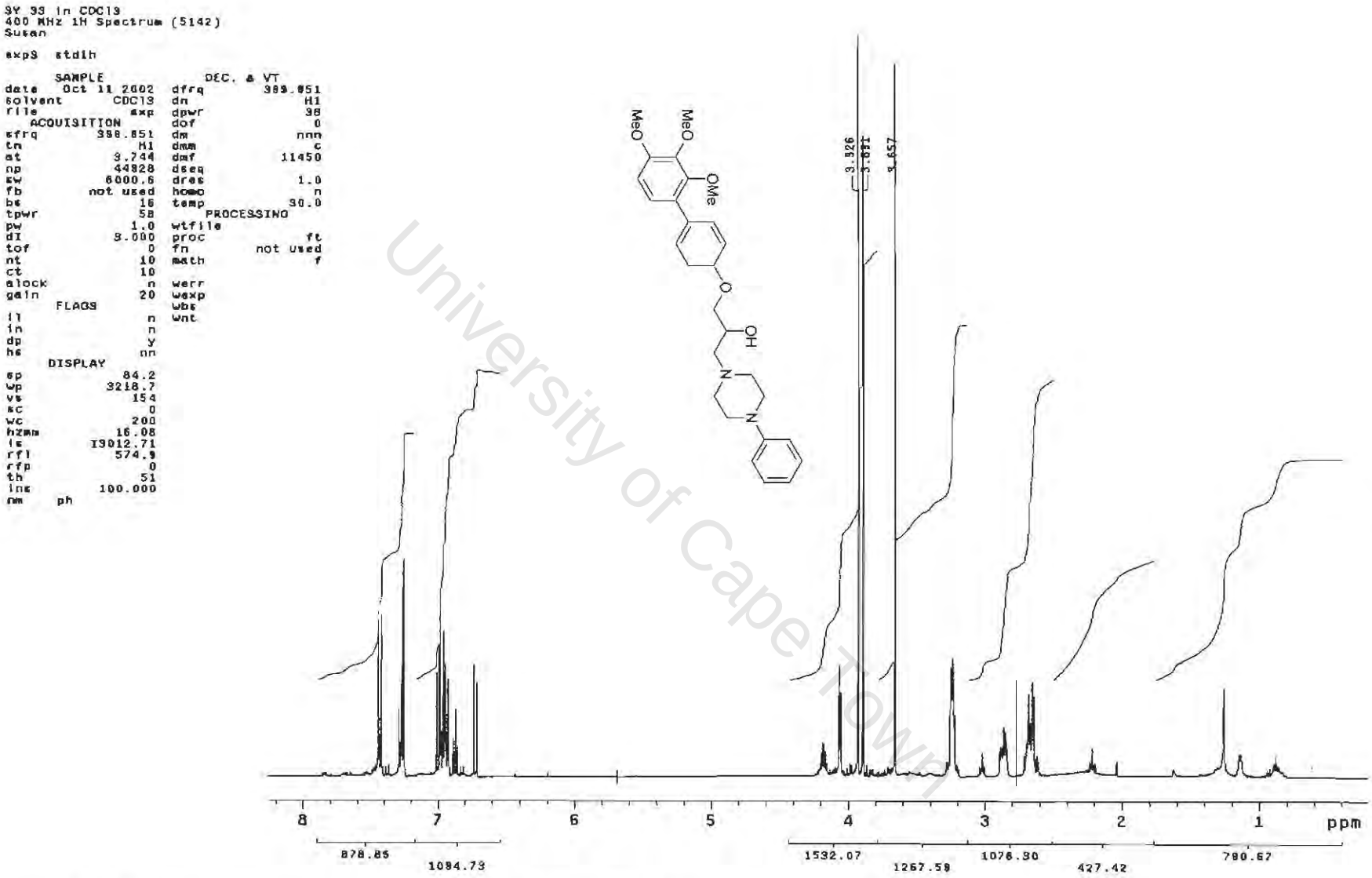

Figure B.4.1.4. ^{1}H NMR spectrum of compound **P24** in $CDCl_3$, 400 MHz.

Figure B.4.1.5. ^{13}C NMR spectrum of compound **P24** in $CDCl_3$, 100 MHz.

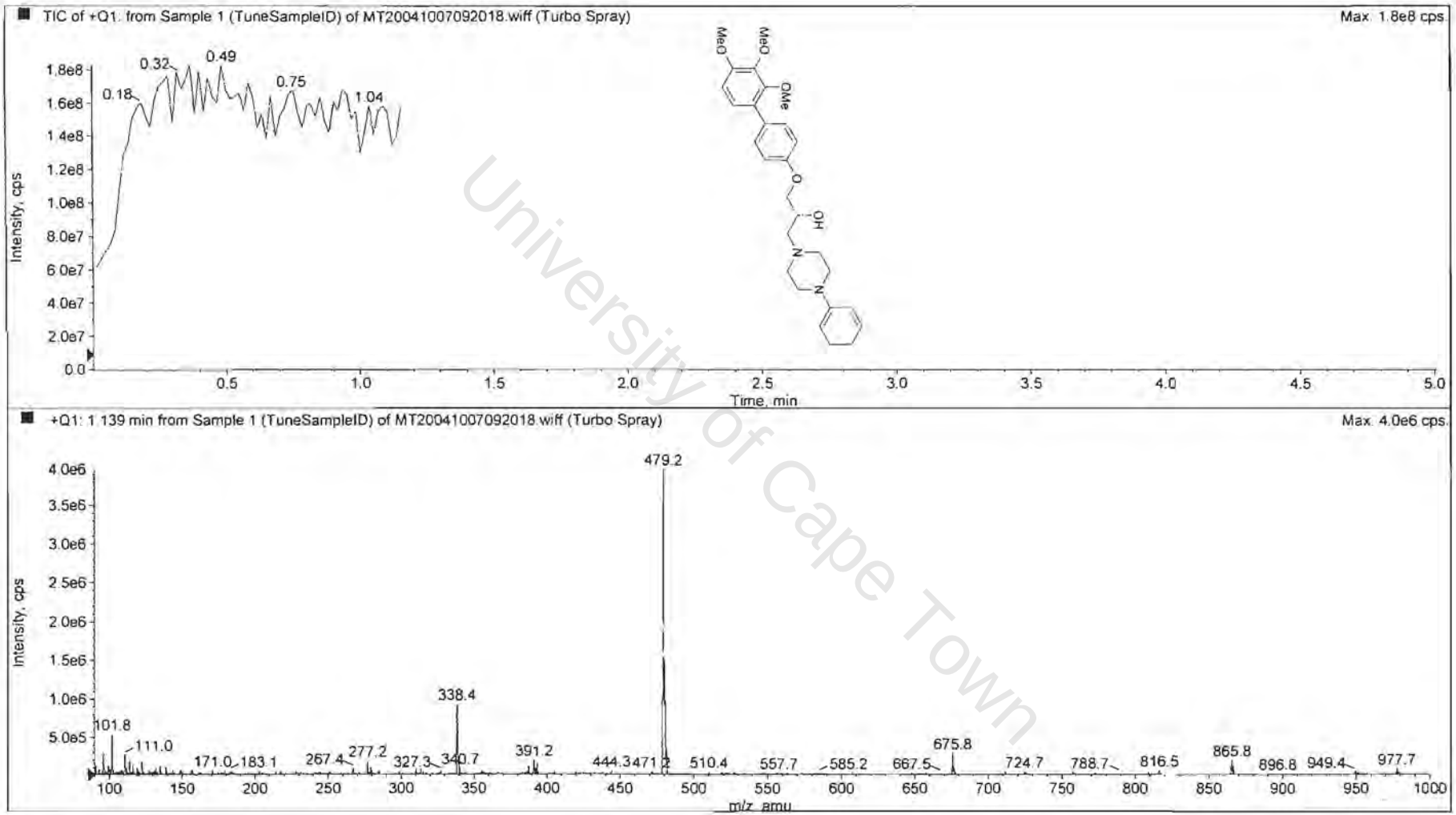

Page 1 of 1

Figure B.4.1.6.1. Mass spectrum of compound **P24**.

Printing Time: 09:26:02 AM *Installation
Printing Date: Thursday, October 07, 2004

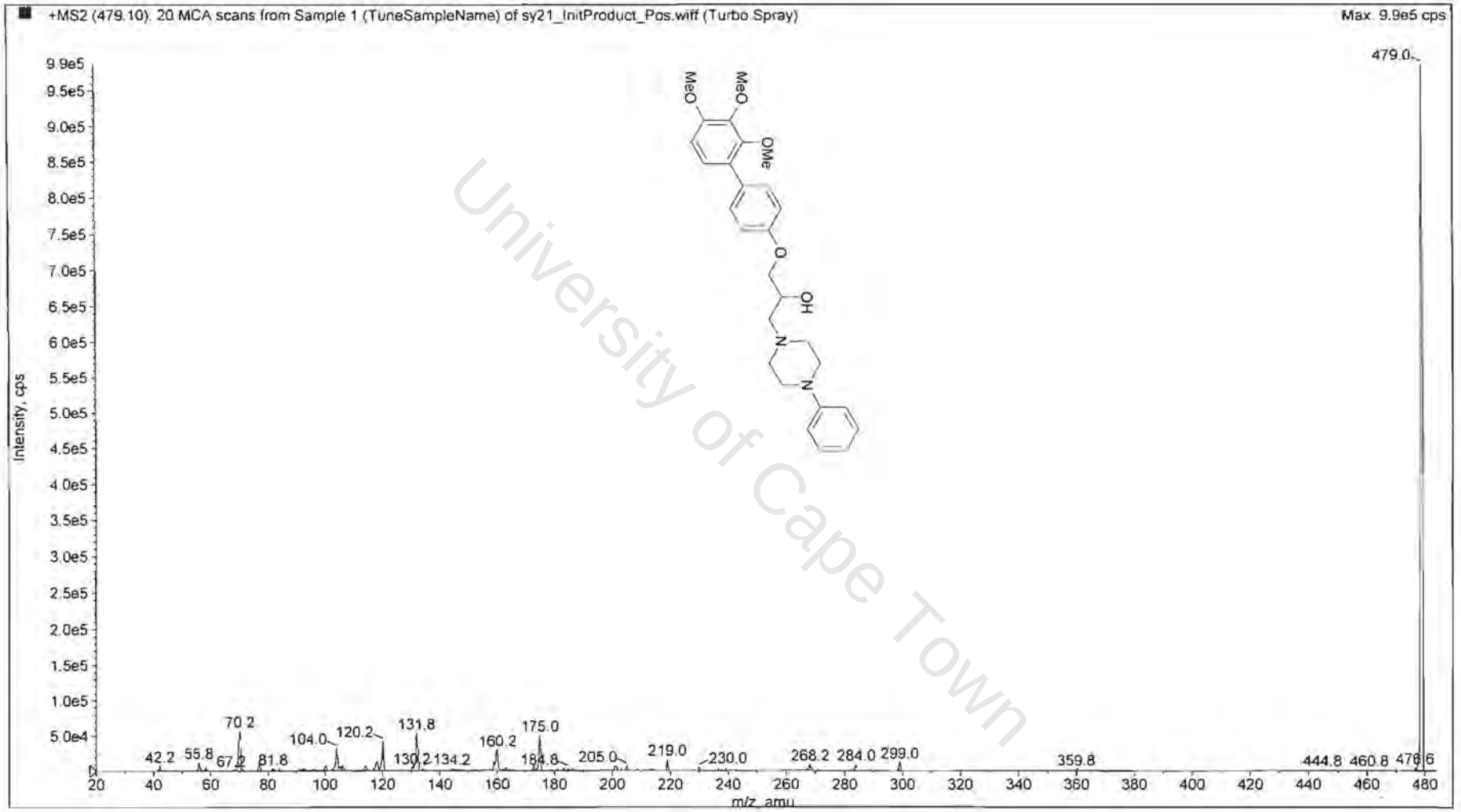

Page 1 of 1

Figure B.4.1.6.2. Mass spectrum of compound **P24**.

Compound P25

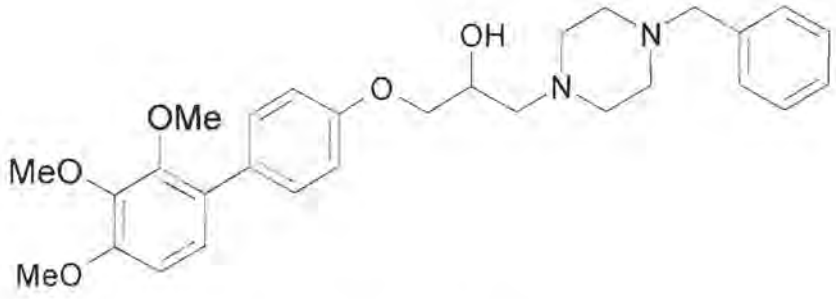

Compound P25

IUPAC

1-(4-*Benzyl-piperazin*-1-*yl*)-3-(2',3',4'-*trimethoxy-biphenyl*-4-*yloxy*)-*propan*-2-*ol*

List of spectra:

- ^{1}H NMR (400MHz, $CDCl_3$)
- ^{13}C NMR (100MHz, $CDCl_3$)
- Mass spectra

P25

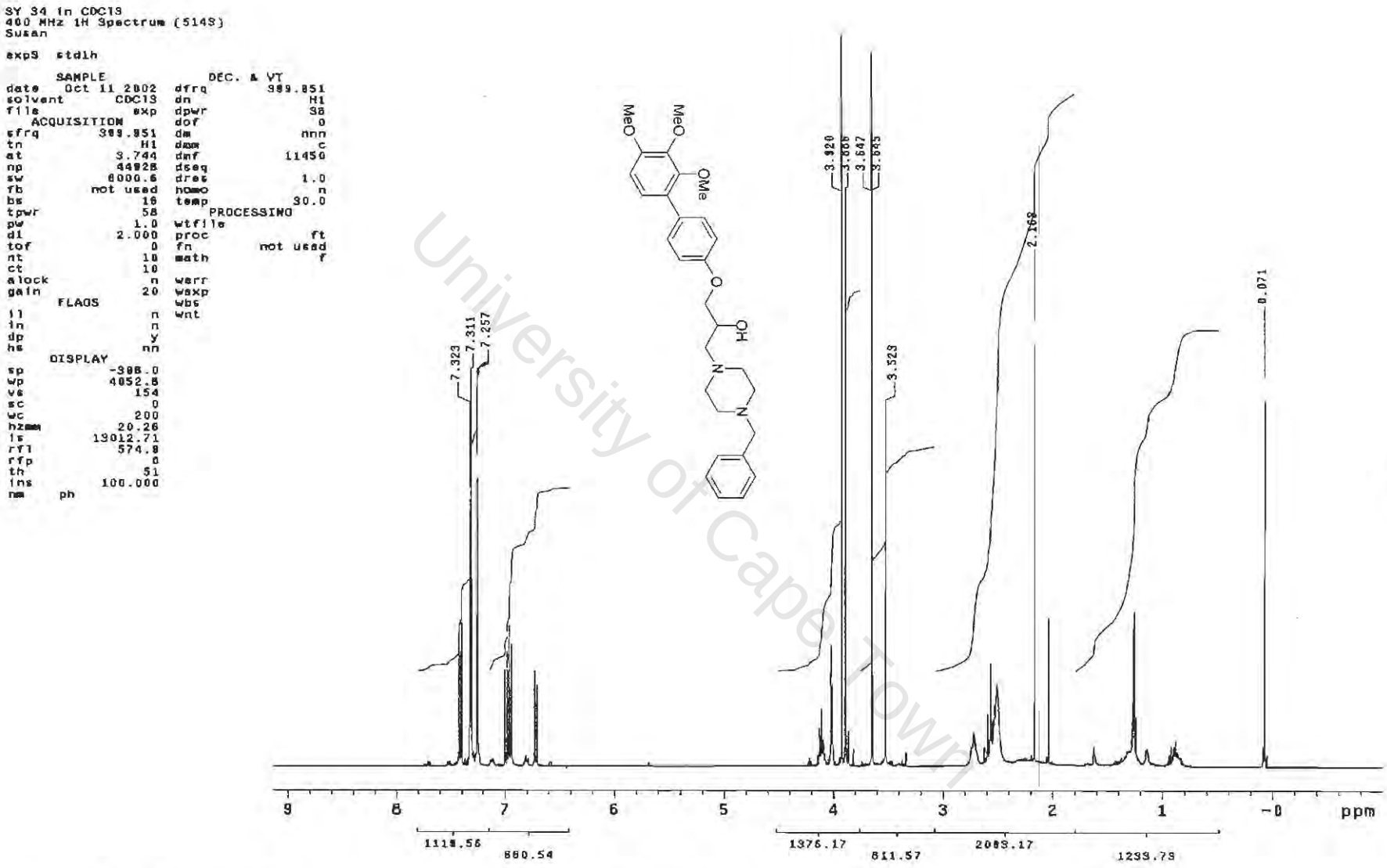

Figure B.4.1.7. ^{1}H NMR spectrum of compound **P25** in $CDCl_3$, 400 MHz.

P25

Figure B.4.1.8. ^{13}C NMR spectrum of compound **P25** in $CDCl_3$, 100 MHz.

Printing Time: 09:36:59 AM
Printing Date: Thursday, October 07, 2004

*Installation

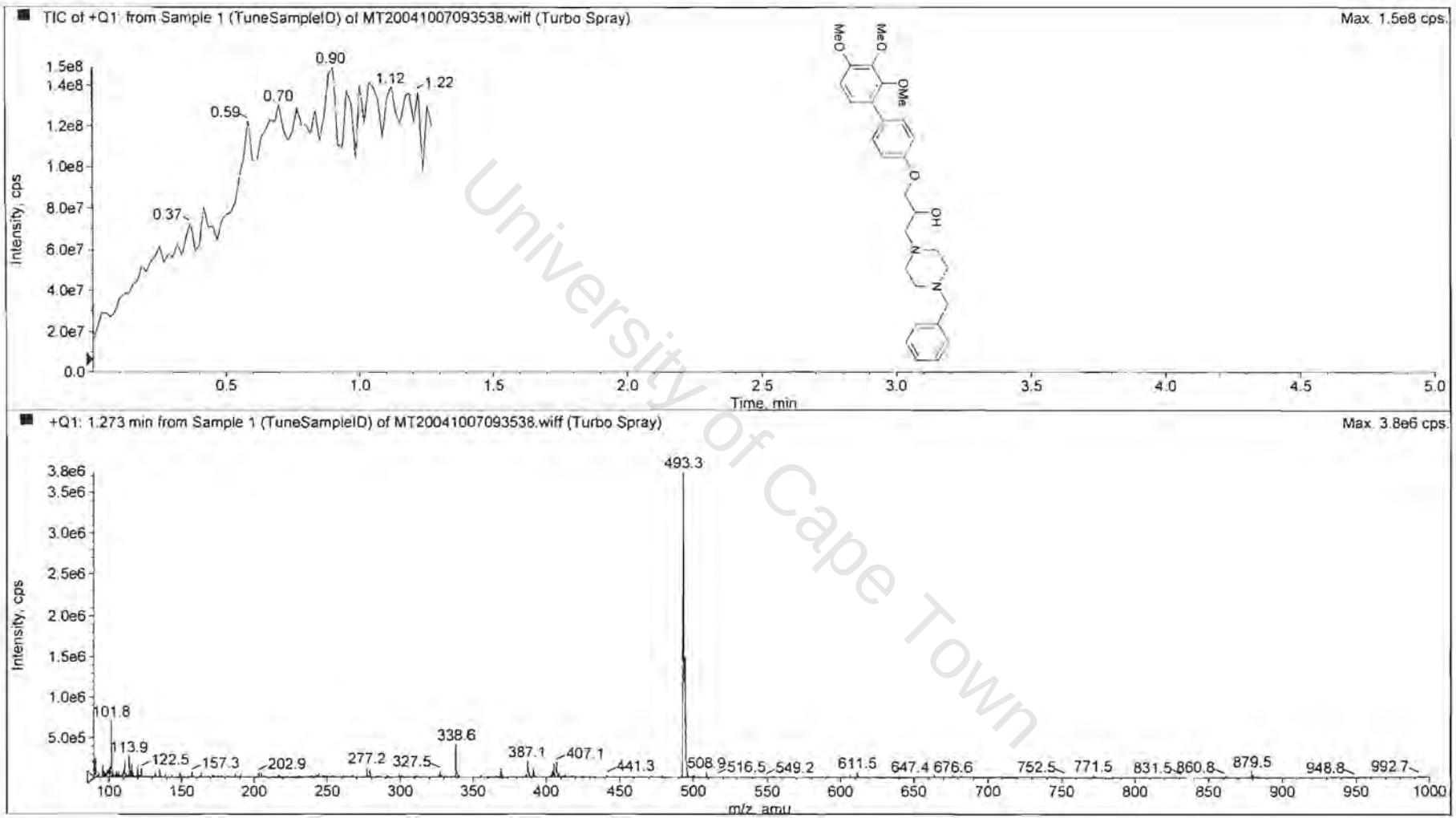

Page 1 of 1

Figure B.4.1.9.1. Mass spectrum of compound **P25**

Printing Time: 09:40:39 AM
Printing Date: Thursday, October 07, 2004

*Installation

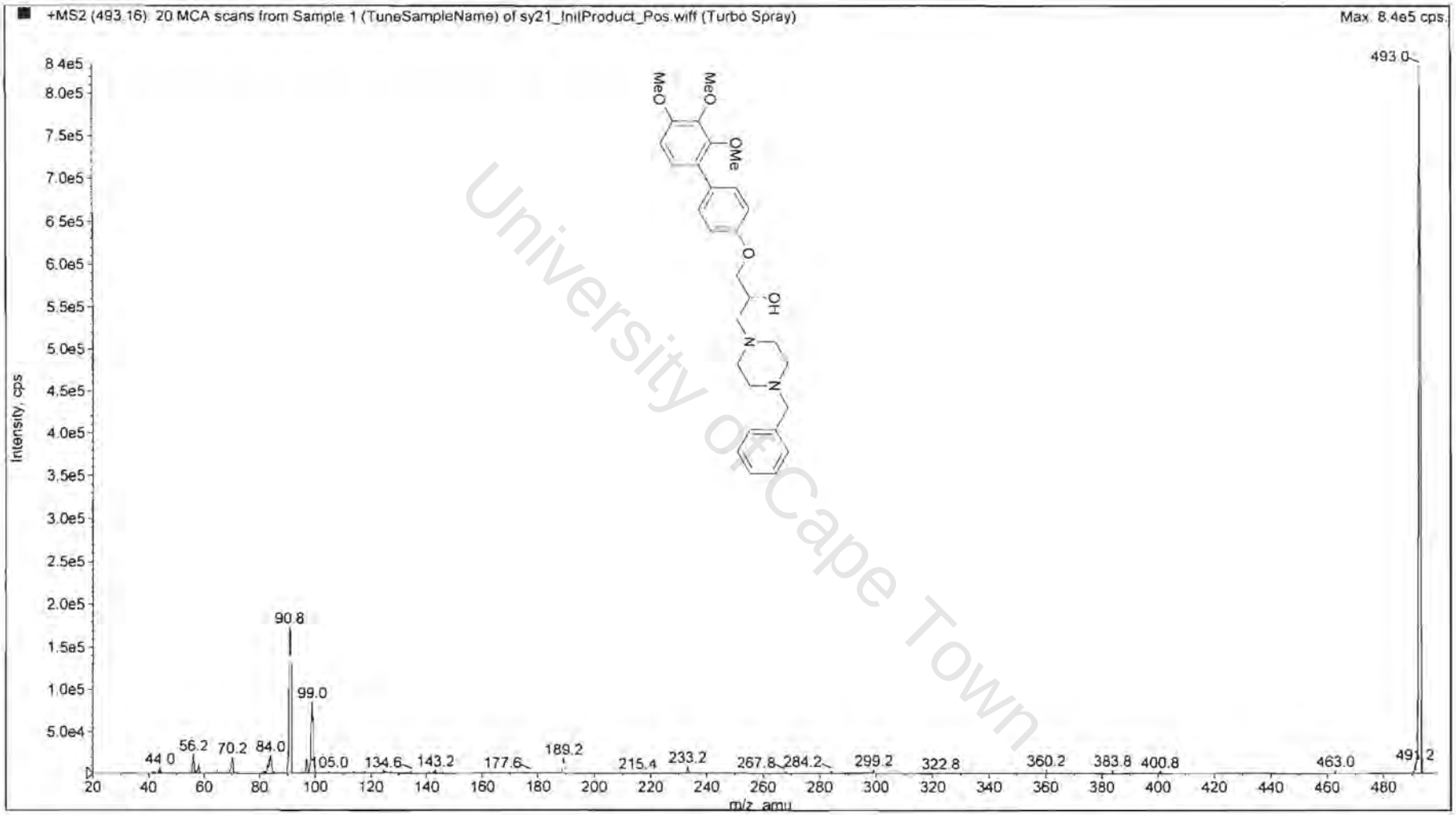

Page 1 of 1

Figure B.4.1.9.2. Mass spectrum of compound **P25**.

Compound P26

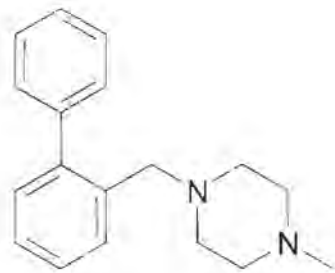

Compound P26

IUPAC

1-Biphenyl-2-ylmethyl-4-methyl-piperazine

List of spectra:

- ^{1}H NMR (400MHz, $CDCl_3$)
- ^{13}C NMR (100MHz, $CDCl_3$)
- Mass spectra

P26

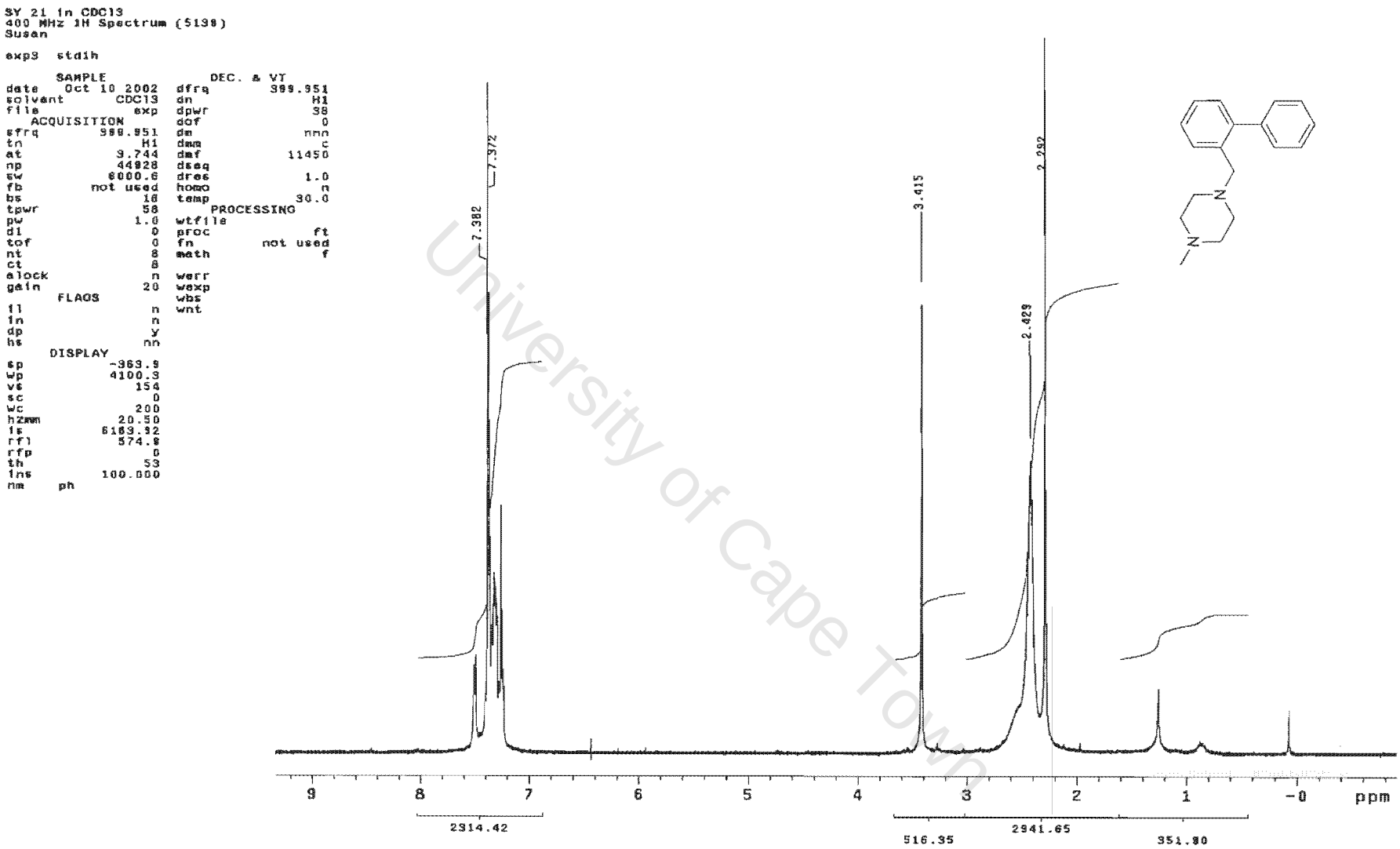

Figure B.4.1.10. ^{1}H NMR spectrum of compound **P26** in $CDCl_3$, 400 MHz

```
SY 21 in CDCl3
100.6 MHz 13C Spectrum (5139)
Susan

exp4  std13c

       SAMPLE                    DEC. & VT
date      Oct 10 2002   dfrq          399.951
solvent       CDCl3     dn                H1
file            exp     dpwr              48
    ACQUISITION         dof                0
sfrq        100.577     dm               yyy
tn              C13     dmm                w
at            1.188     dmf            11450
np            58968     dseq
sw         25000.0      dres             1.0
fb         not used     homo               n
bs              200     temp            30.0
tpwr             60         PROCESSING
pw              8.7     lb               4.00
dl               0      wtfile
tof              0      proc               lp
nt          200000      fn         not used
ct             997      math               f
alock              s
gain              60     werr
       FLAGS            wexp
ft                 n     wbs
in                 n     wnt
dp                 y
hs                nn
      DISPLAY
sp           2234.4
wp          13101.6
vs              104
sc                0
wc              200
hzmm          85.51
is            500.00
rfl           2904.2
rfp               0
th                35
ins          100.000
nm  no  ph
```

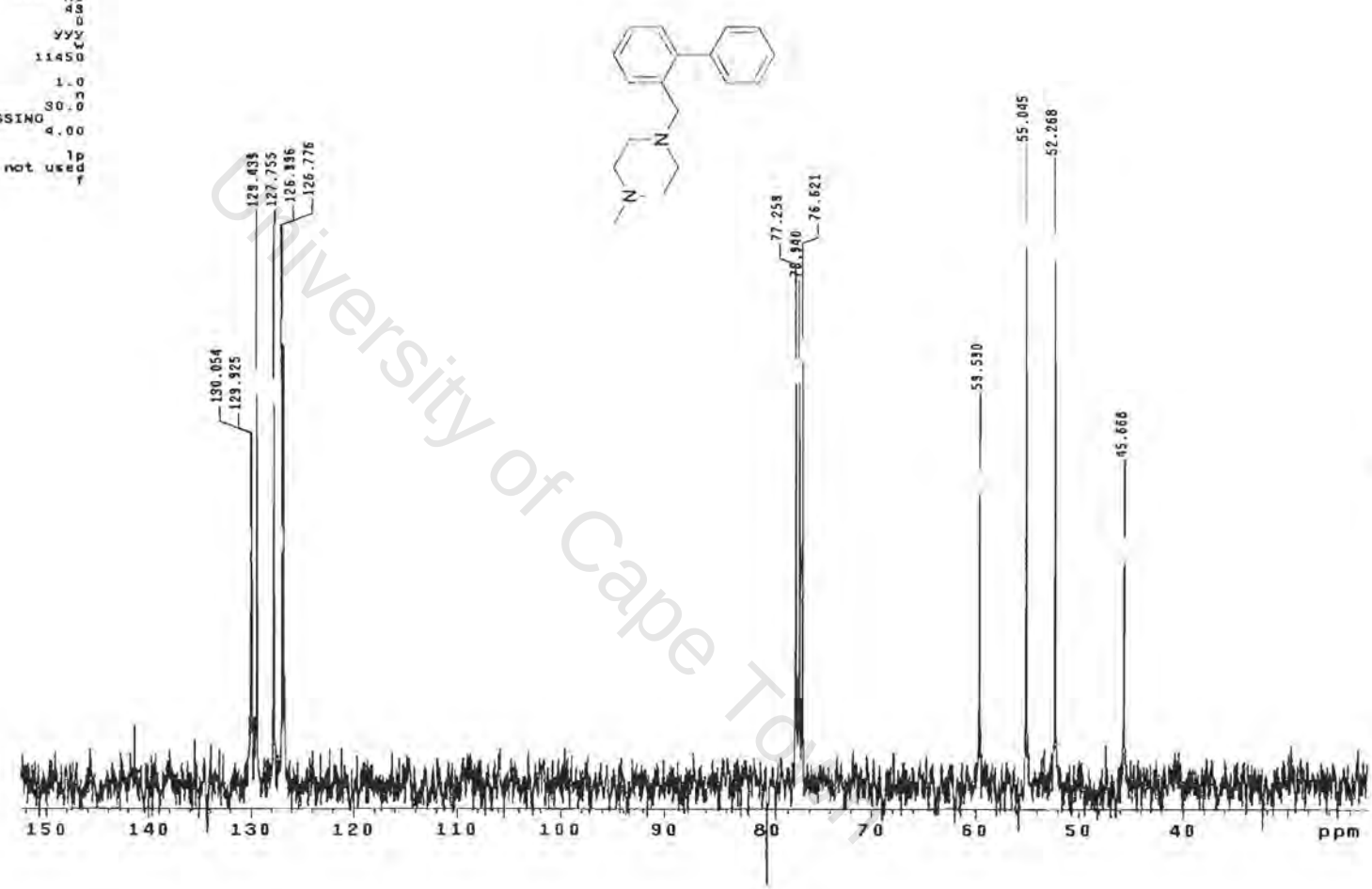

Figure B.4.1.11. ^{13}C NMR spectrum of compound **P26** in $CDCl_3$, 100 MHz

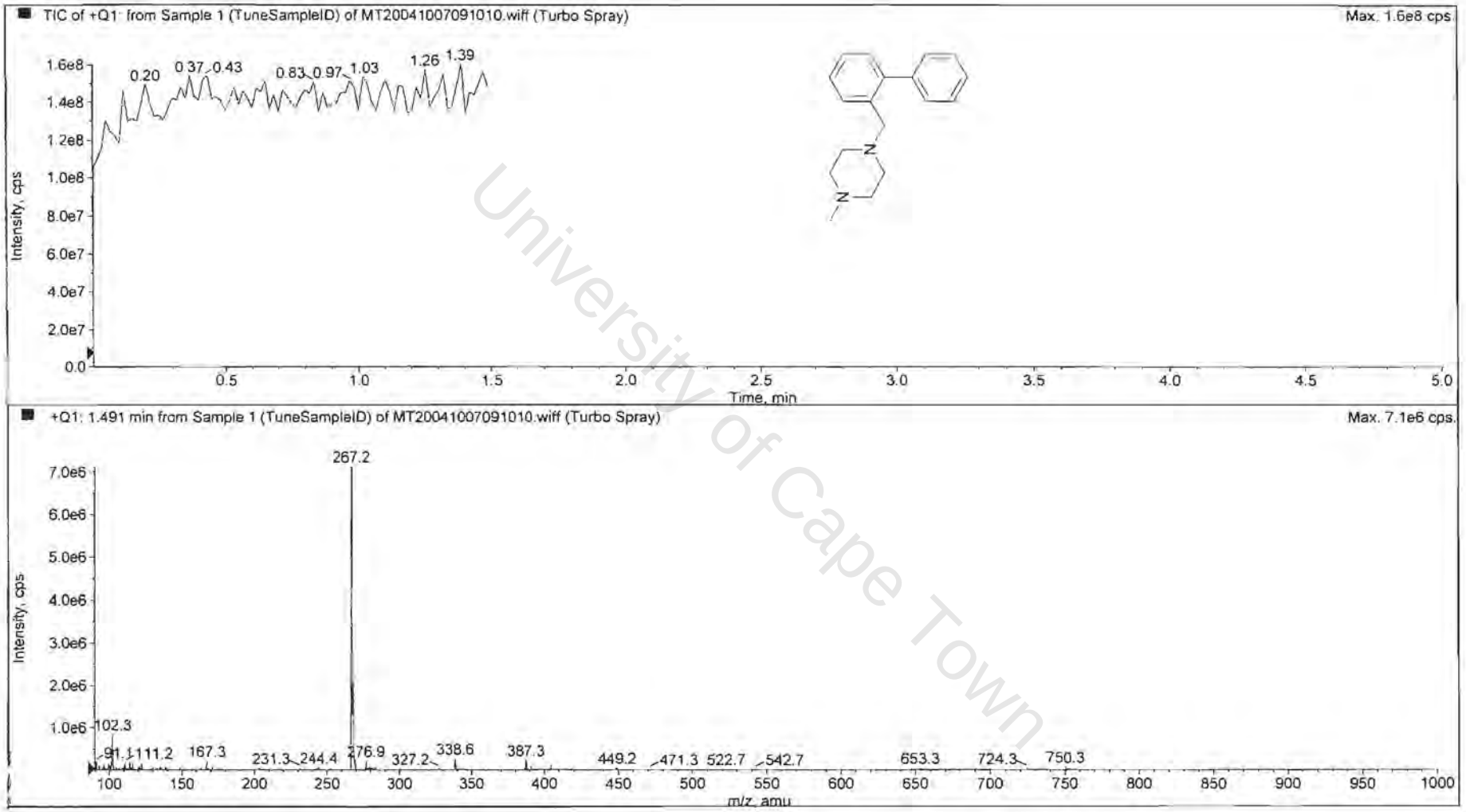

Figure B.4.1.12.1. Mass spectrum of compound **P26**.

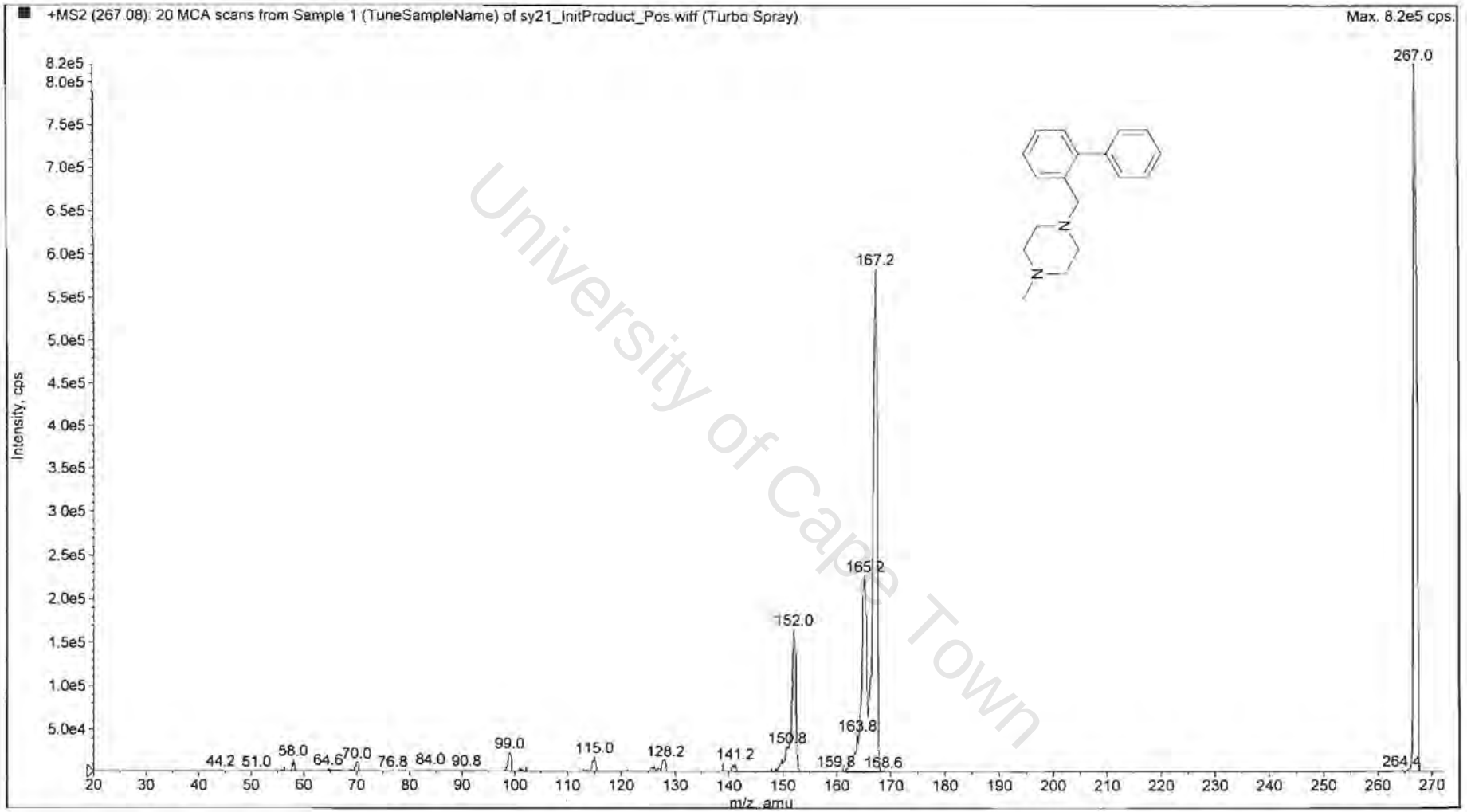

Figure B.4.1.12.2. Mass spectrum of compound **P26**.

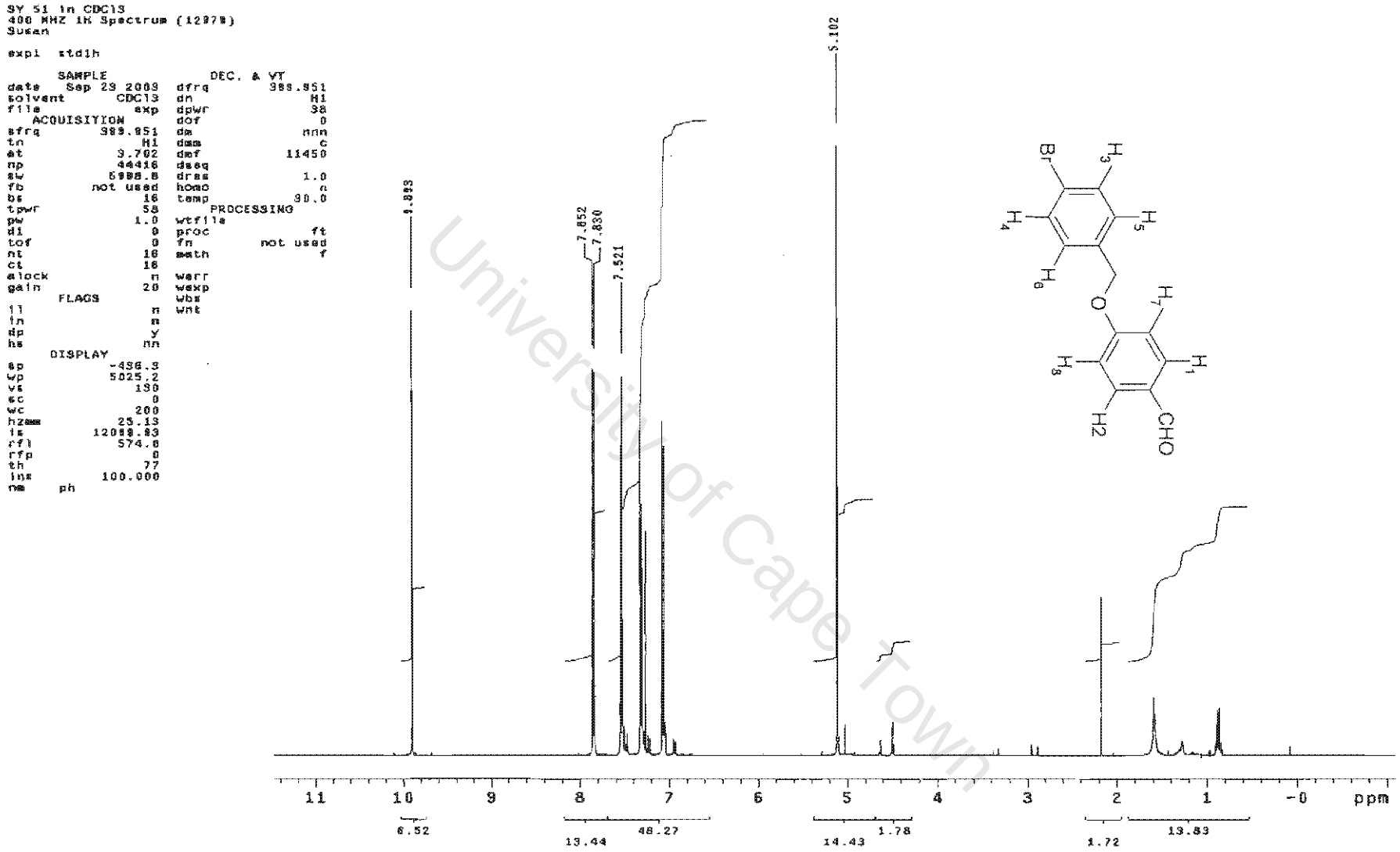

Figure C.4.1.1. ^{1}H NMR spectrum of intermediate **27** in $CDCl_3$, 300 MHz.

I28

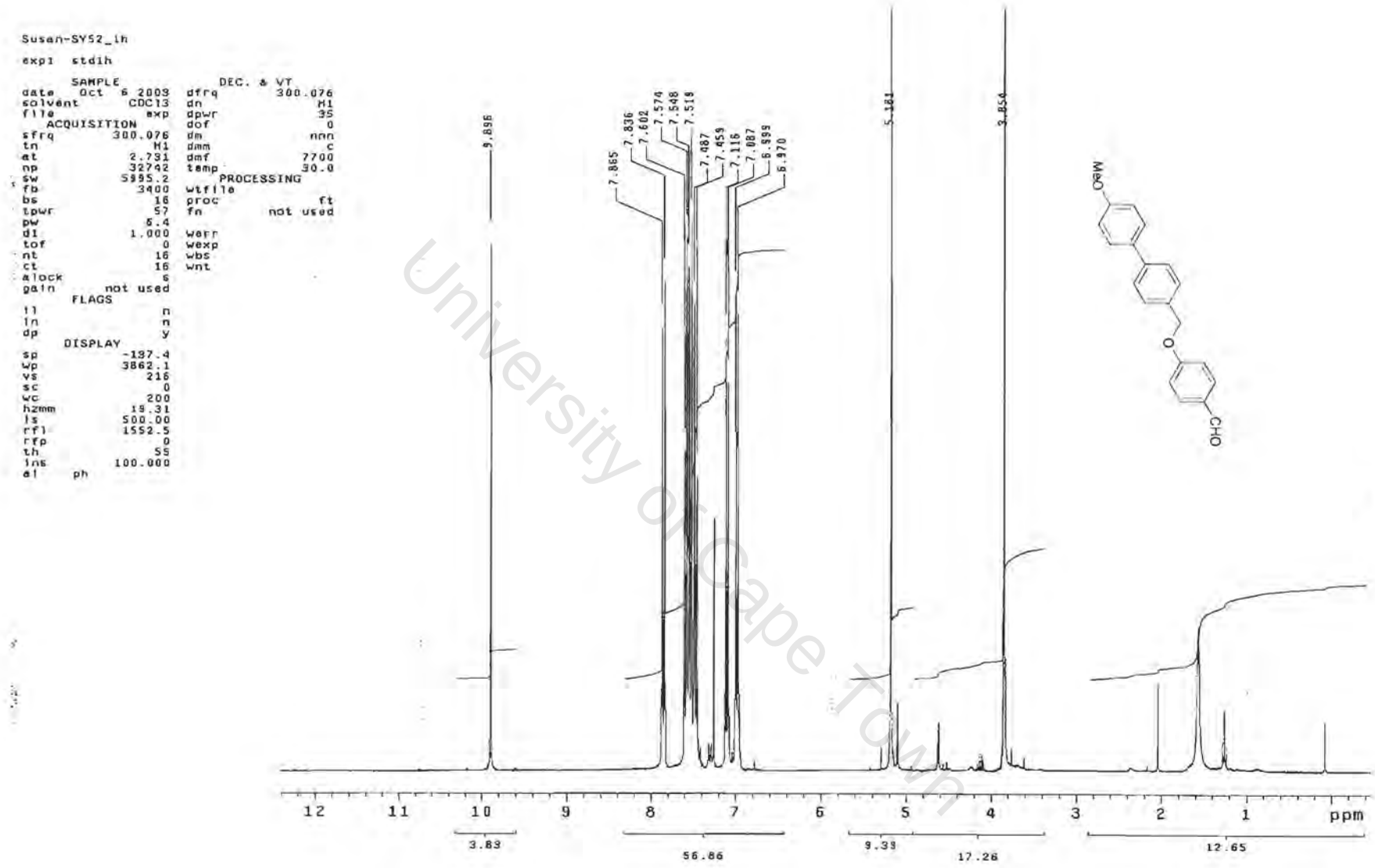

Figure C.4.1.2. ^{13}C NMR spectrum of intermediate **28** in $CDCl_3$, 300 MHz.

I29

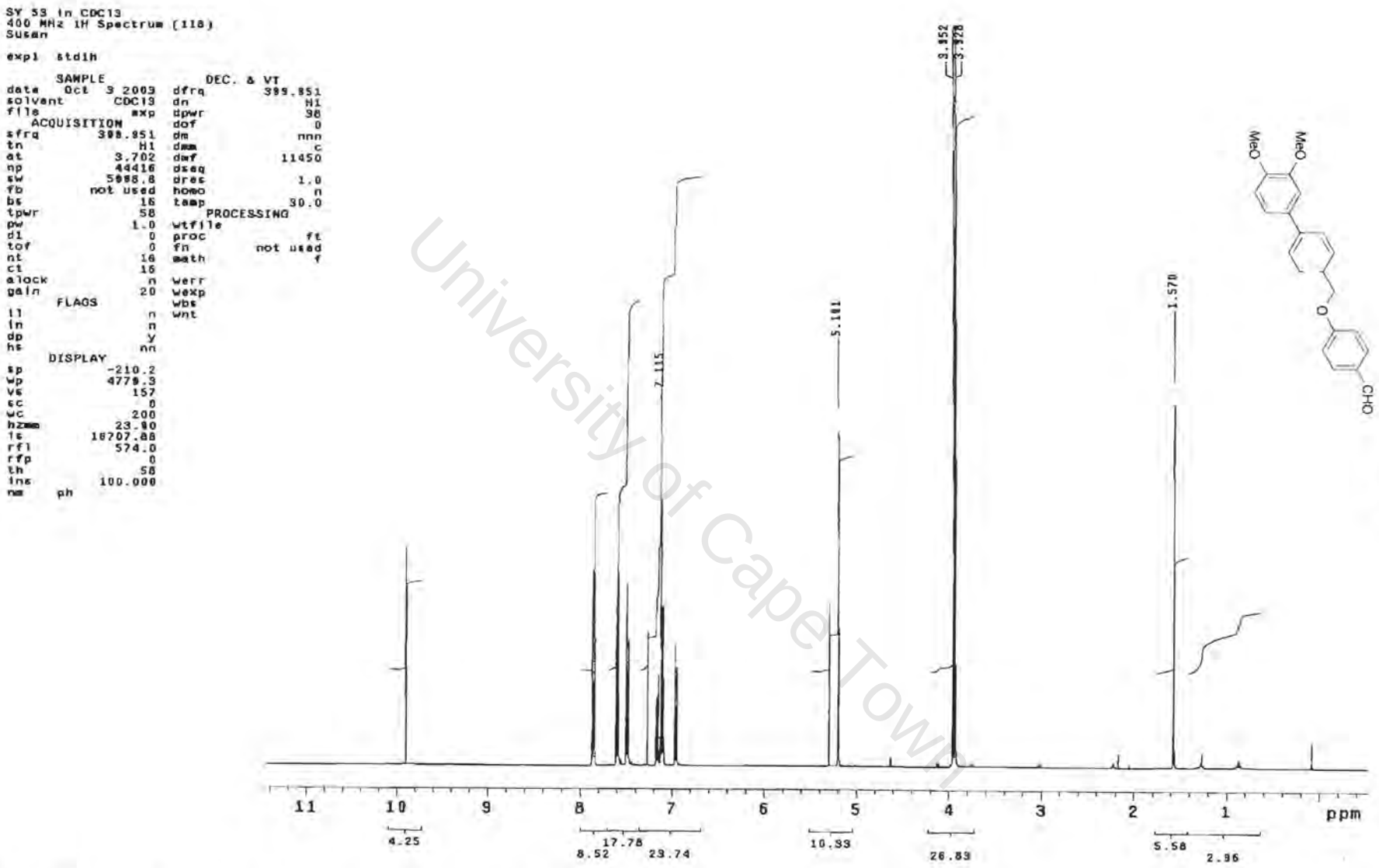

Figure C.4.1.3. ^{1}H NMR spectrum of intermediate **29** in $CDCl_3$, 300 MHz.

I30

```
SY 54 in CDCl3
400 MHz 1H Spectrum (103)
Susan

exp1  std1h

        SAMPLE                DEC. & VT
date    Oct  2 2003  dfrq          399.951
solvent       CDCl3  dn                H1
file            exp  dpwr              38
   ACQUISITION       dof                0
sfrq        399.951  dm               nnn
tn               H1  dmm                c
at             3.704  dmf            11450
np             55552  dseq
SW          7499.1    dres             1.0
fb        not used    homo               n
bs               16   temp            30.0
tpwr             58        PROCESSING
pw              8.5   wtfile
d1                0   proc              ft
tof               0   fn          not used
nt               16   math               f
ct               16
alock             n   werr
gain             20   wexp
      FLAGS           wbs
il                n   wnt
in                n
dp                y
hs               nn
     DISPLAY
sp           -174.8
wp           4733.7
vs              325
sc                0
wc              200
hzmm          23.67
is          25825.94
rfl           1324.1
rfp               0
th              105
ins          100.000
nm    ph
```


Figure C.4.1.4. ^{1}H NMR spectrum of intermediate **30** in $CDCl_3$, 300 MHz.

Compound P31

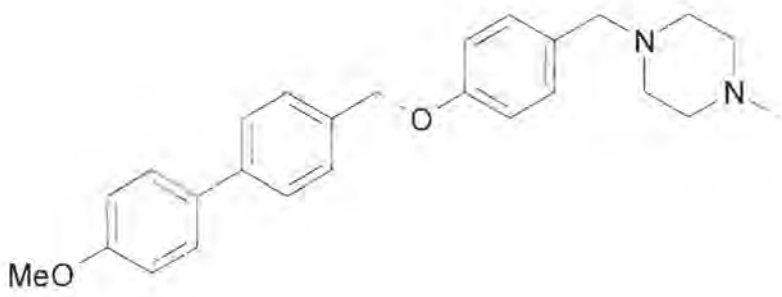

Compound P31

IUPAC

1-[4-(4'-*Methoxy-biphenyl-4-ylmethoxy)-benzyl*]-4-*methyl-piperazine*

List of spectra:

- ^{1}H NMR (400MHz, $CDCl_3$)
- ^{13}C NMR (100MHz, $CDCl_3$)
- Mass spectra

P31

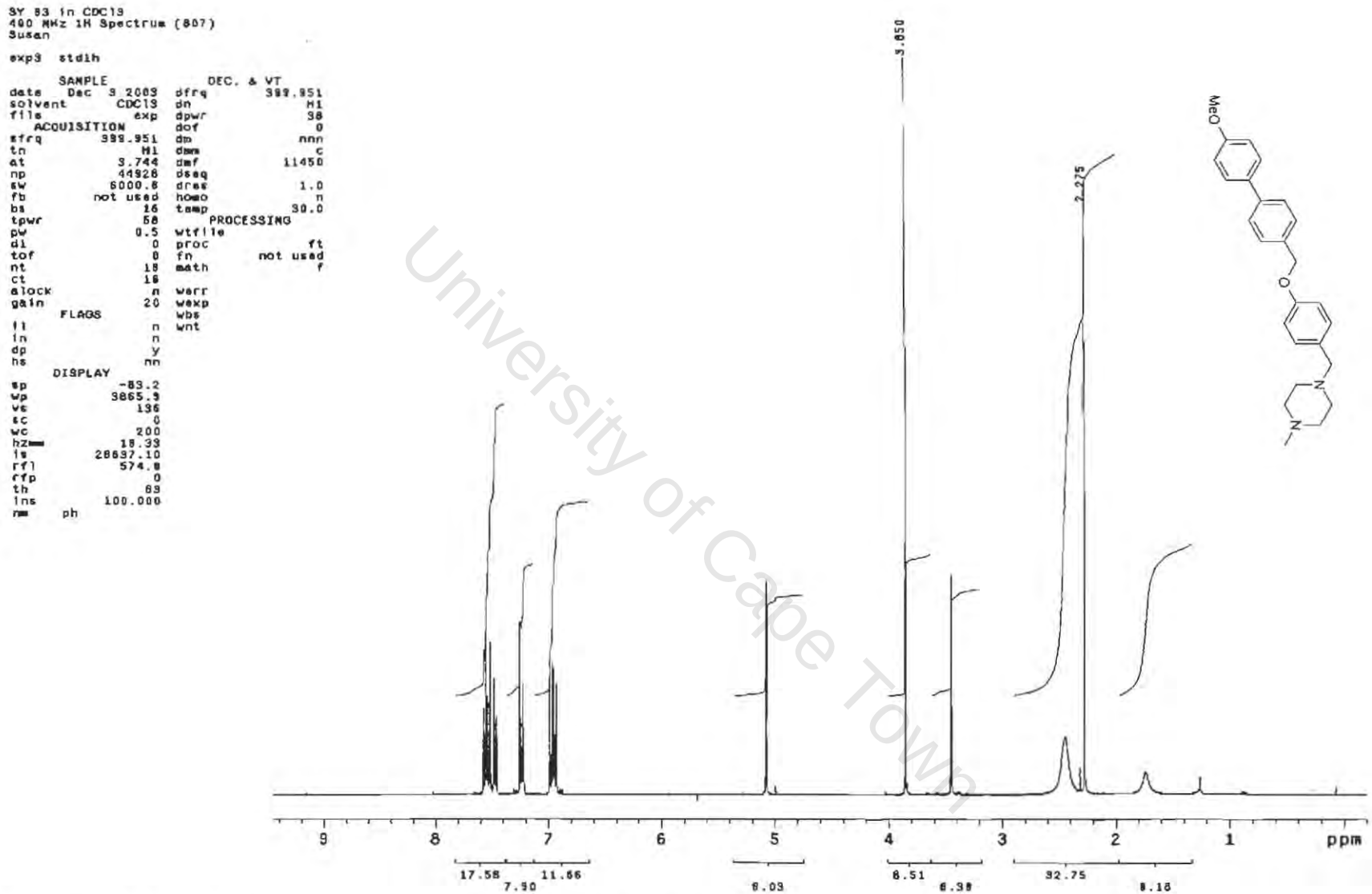

Figure C.4.1.5. ^{1}H NMR spectrum of compound **P31** in $CDCl_3$, 400 MHz.

P31

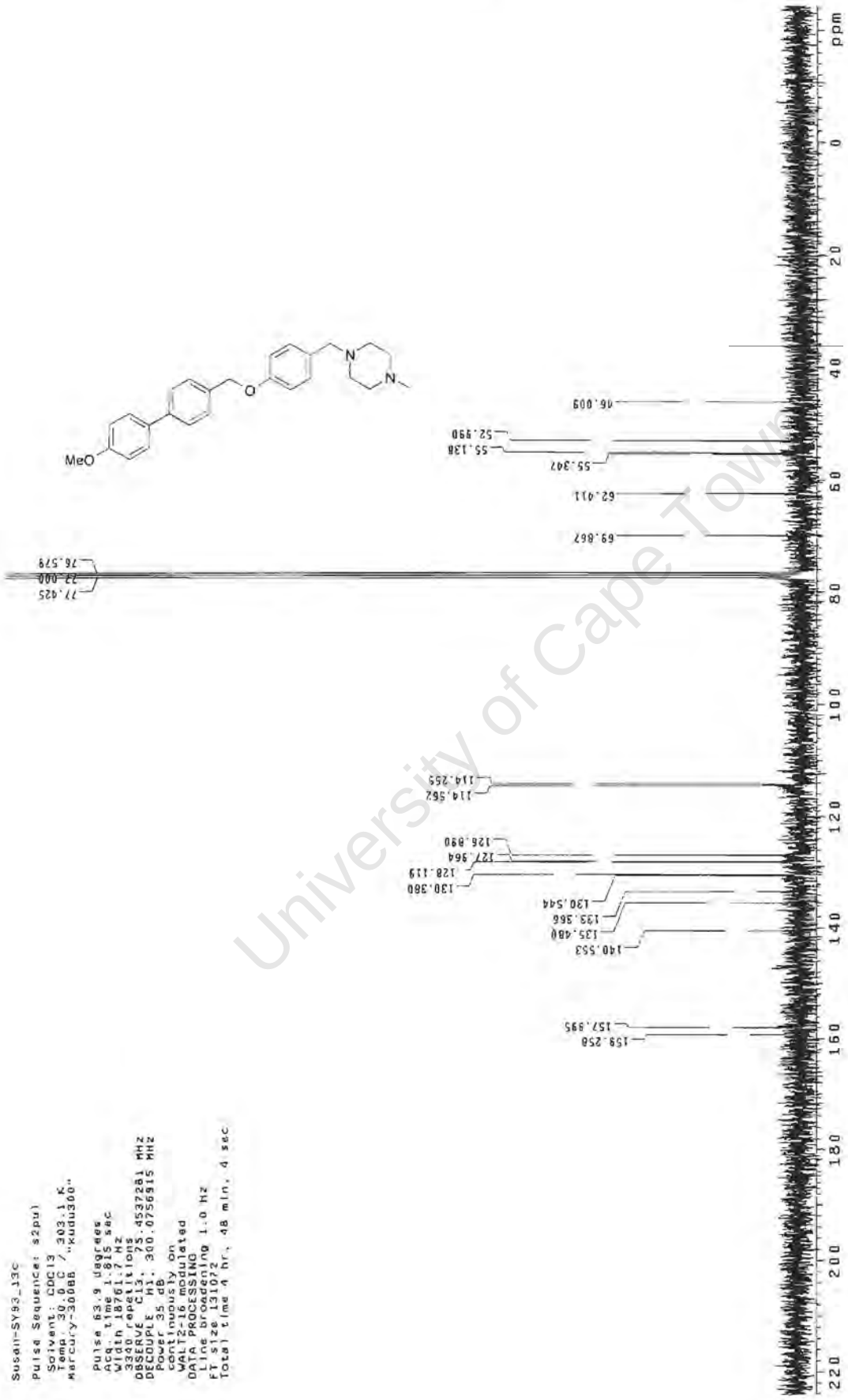

Figure C.4.1.6. ^{13}C NMR spectrum of compound **P31** in $CDCl_3$, 100 MHz.

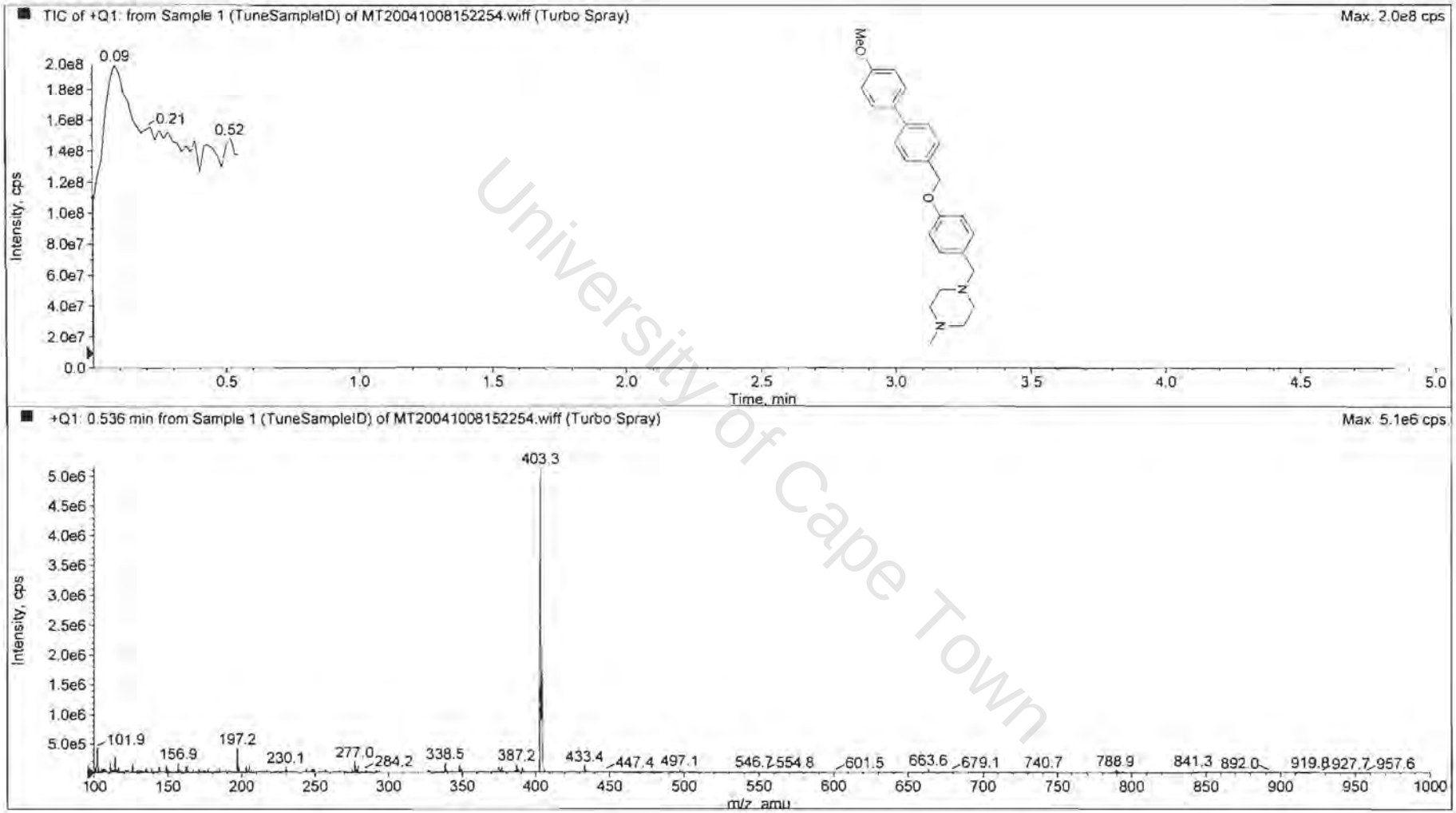

Figure C.4.1.7.1. Mass spectrum of compound **P31**.

P31

Printing Time: 03:30:43 PM
Printing Date: Friday, October 08, 2004

*Installation

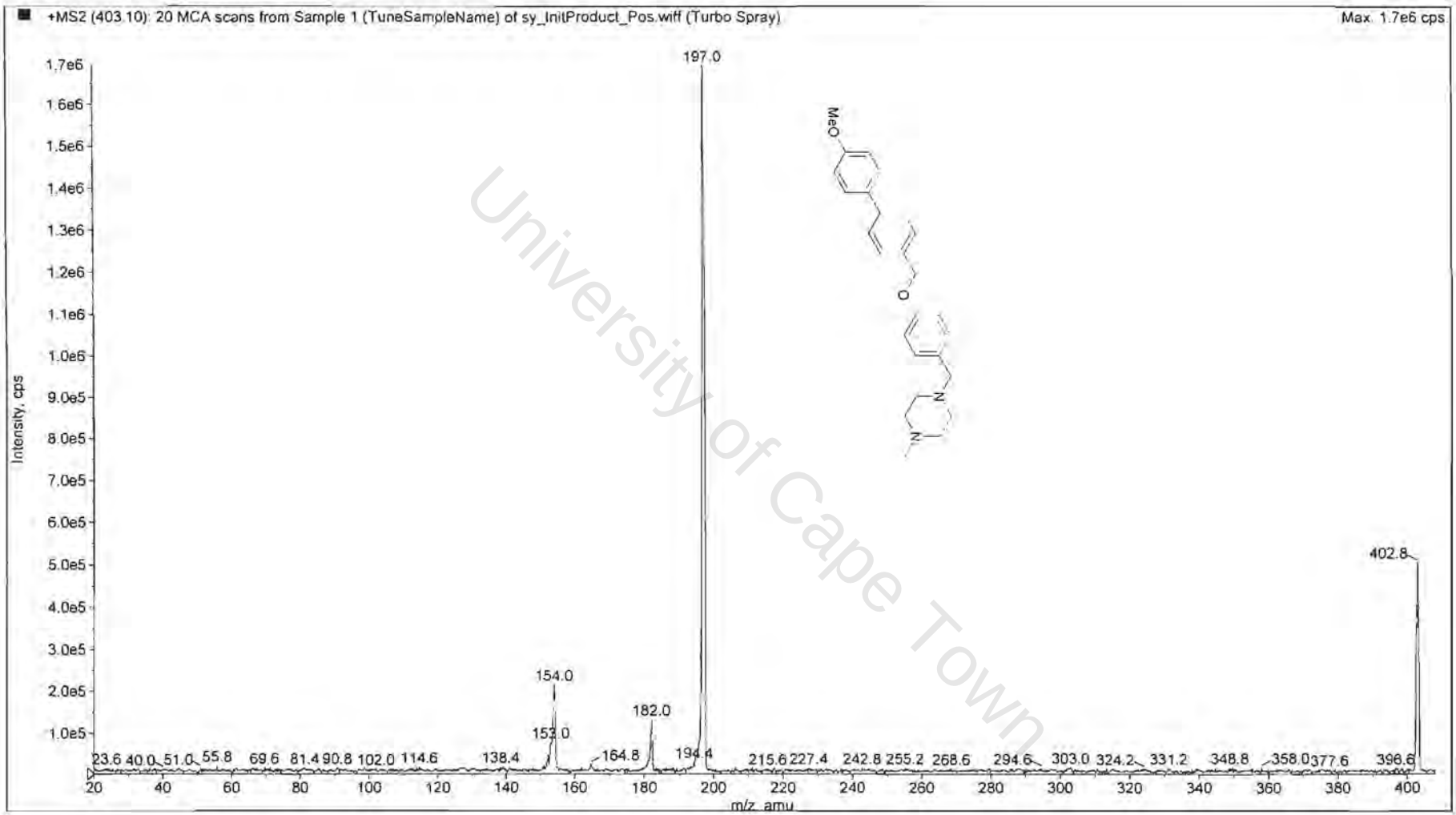

Page 1 of 1

Figure C.4.1.7.2. Mass spectrum of compound **P31**.

Compound P32

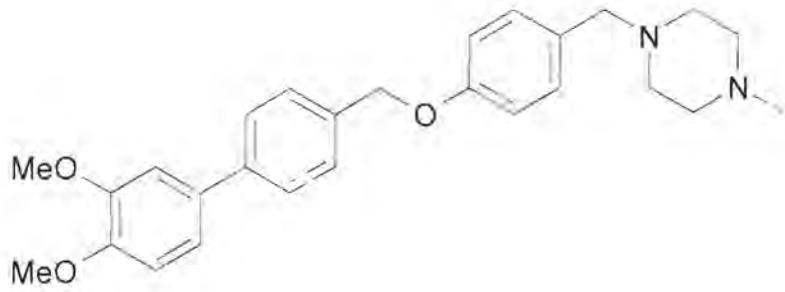

Compound P32

IUPAC

1-[4-(3',4'-*Dimethoxy-biphenyl-4-ylmethoxy*)-*benzyl*]-4-*methoxy-piperazine*

List of spectra:

- ^{1}H NMR (400MHz, $CDCl_3$)
- ^{13}C NMR (100MHz, $CDCl_3$)
- Mass spectra

P32

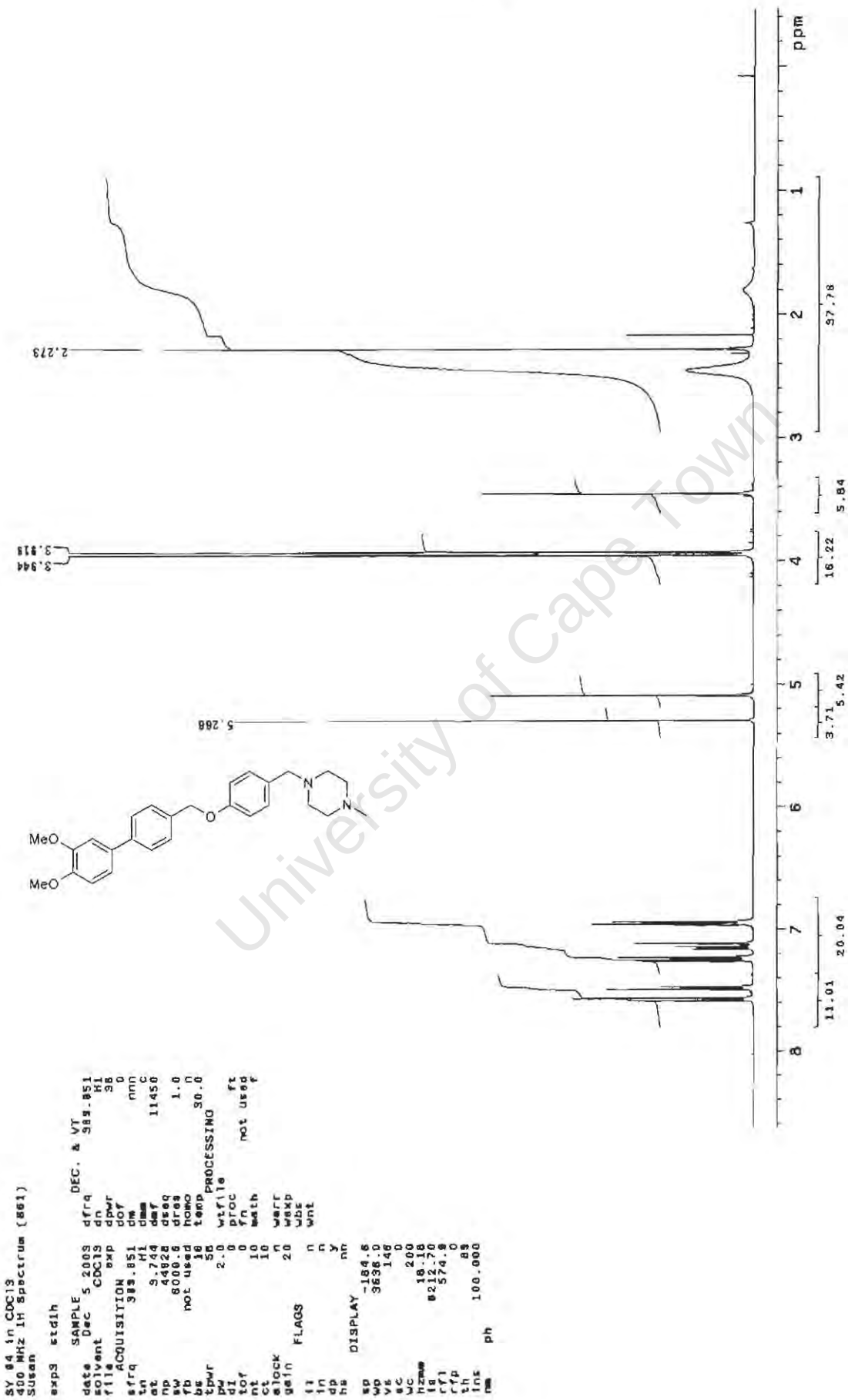

Figure C.4.1.8. ^{1}H NMR spectrum of compound **P32** in $CDCl_3$, 400 MHz.

P32

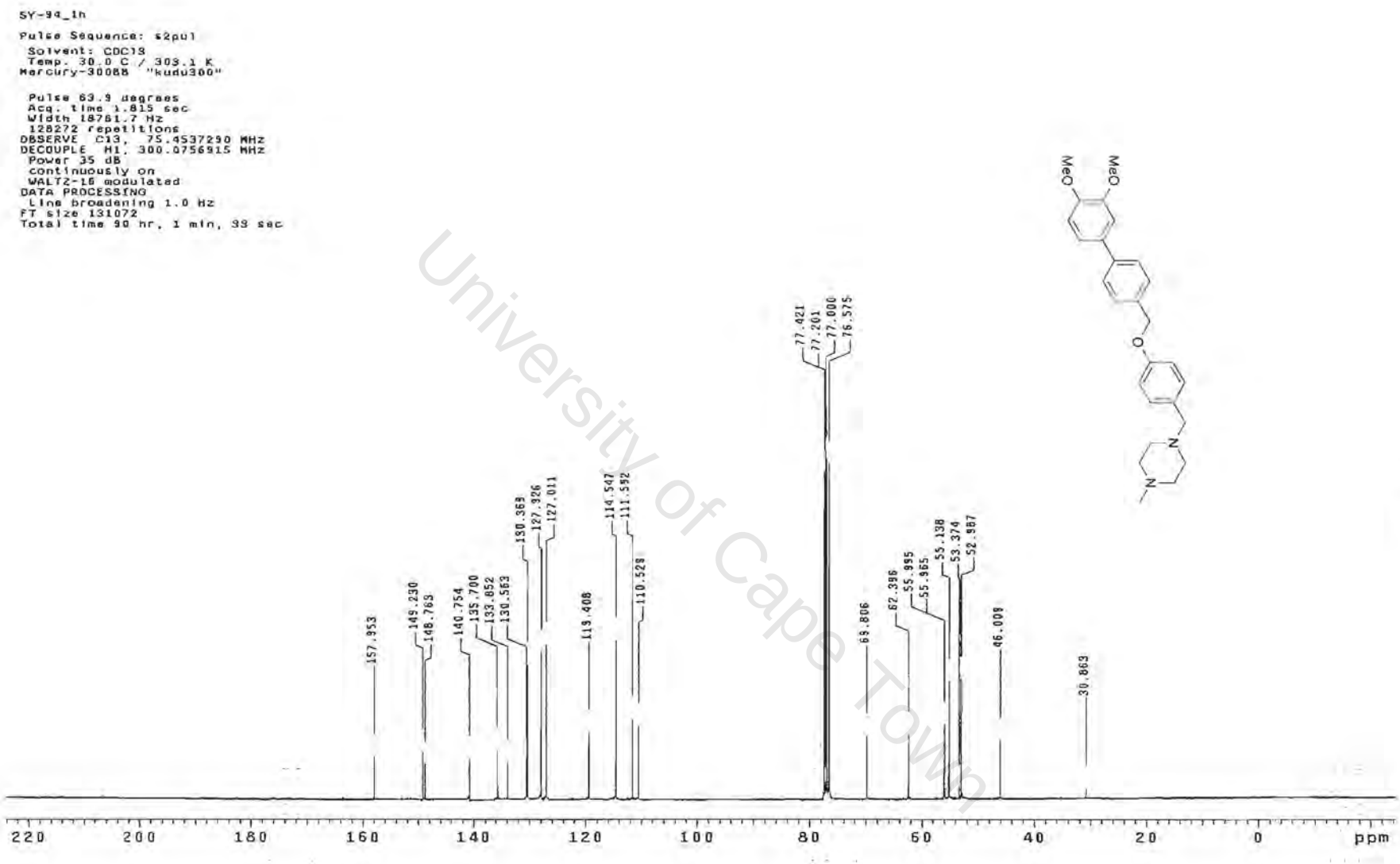

Figure C.4.1.9. ^{13}C NMR spectrum of compound **P32** in $CDCl_3$, 100 MHz.

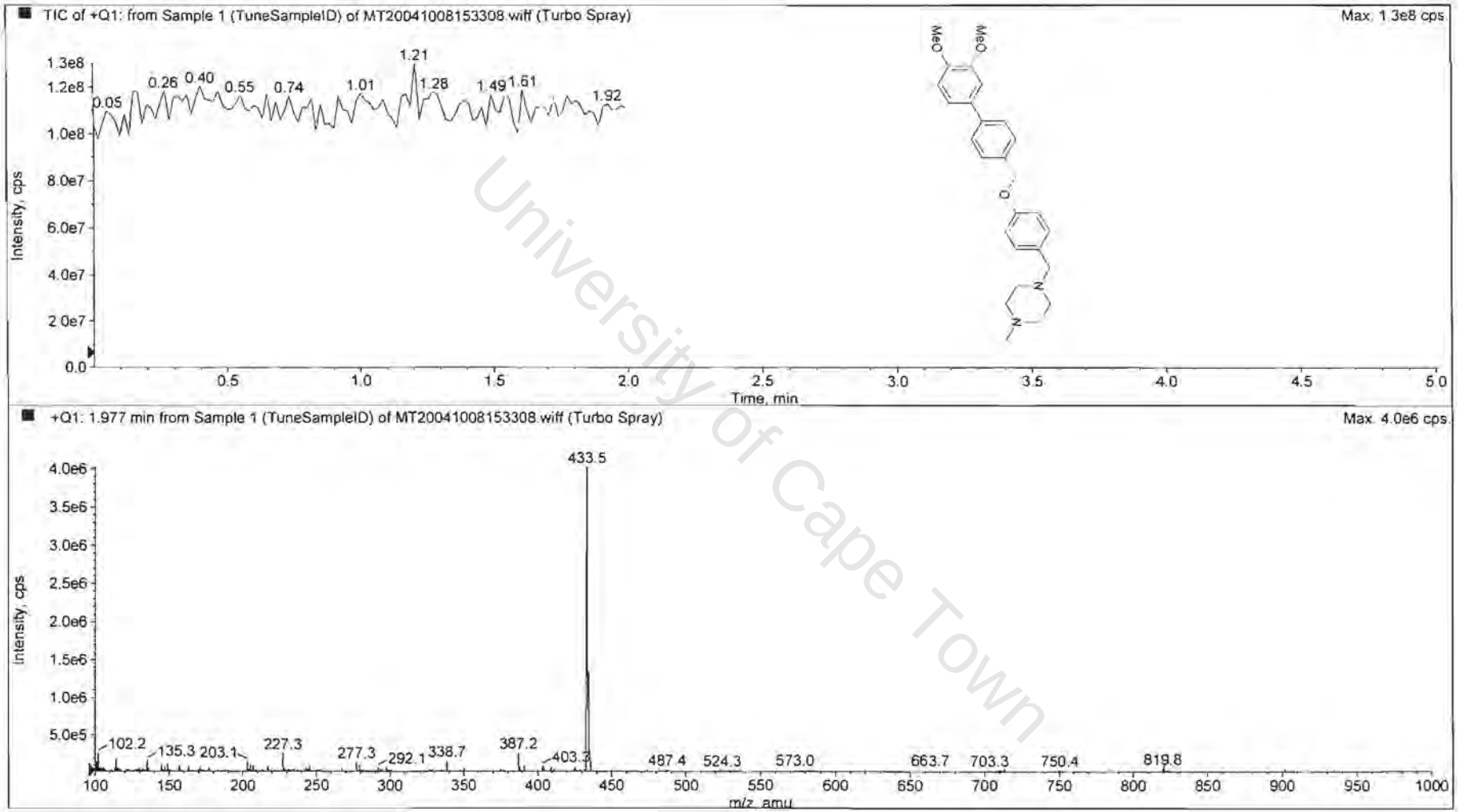

Figure C.4.1.10.1. Mass spectrum of compound **P32**.

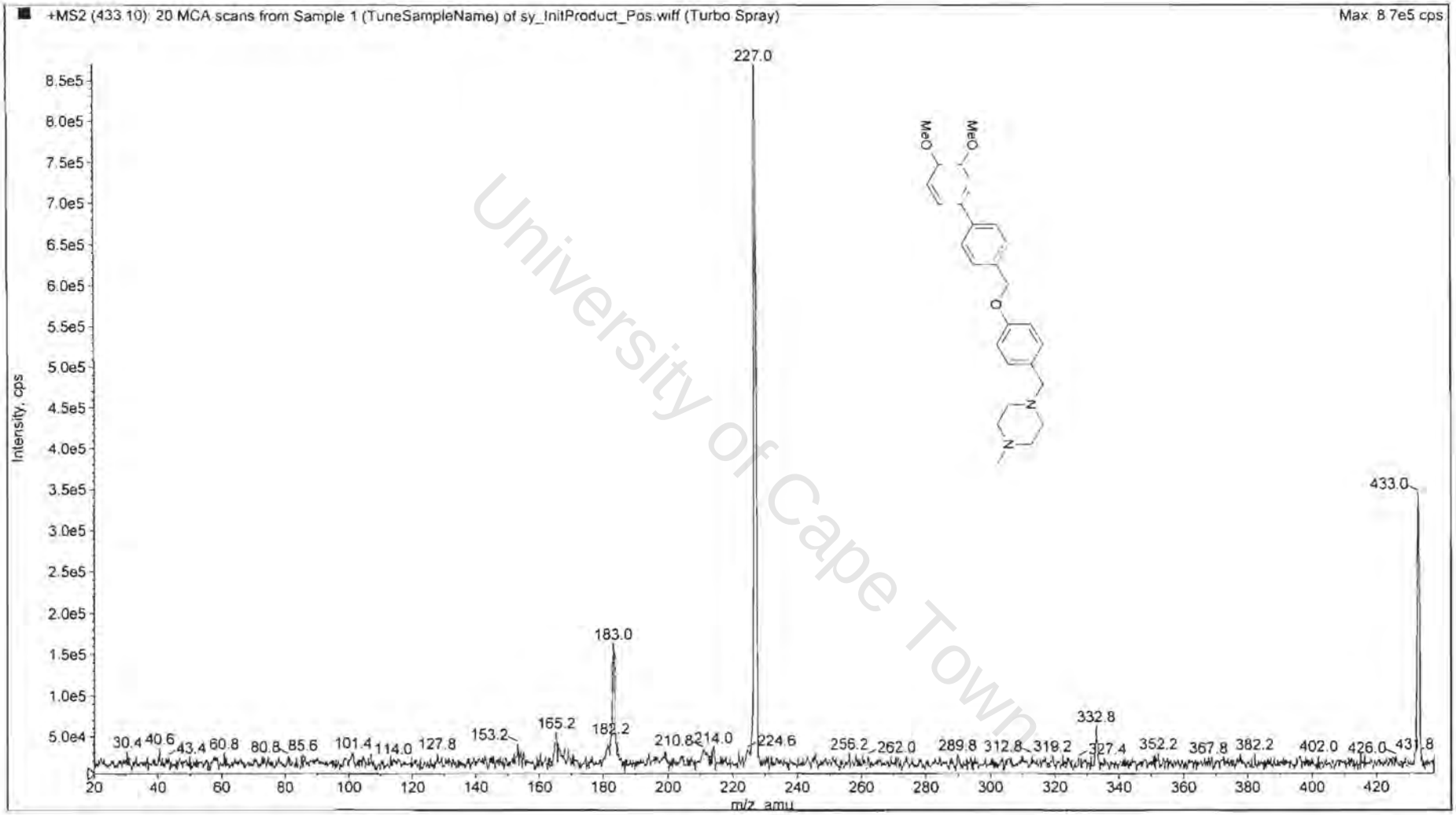

Figure C.4.1.10.2. Mass spectrum of compound **P32**.

Compound P33

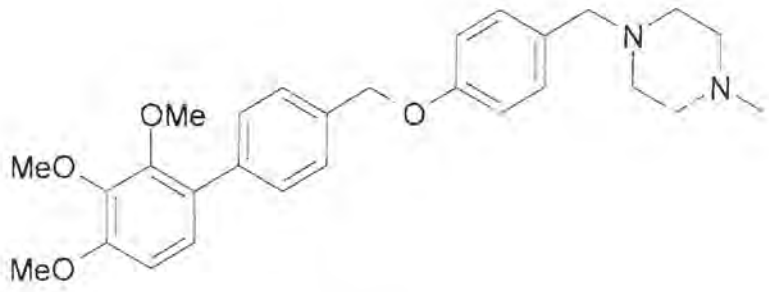

Compound P33

IUPAC

1-*Methyl*-4-[4-(2',3',4'-*trimethoxy-biphenyl*-4-*ylmethoxy*)-*benzyl-piperazine*

List of spectra:

- ^{1}H NMR (400MHz, $CDCl_3$)
- ^{13}C NMR (100MHz, $CDCl_3$)
- Mass spectra

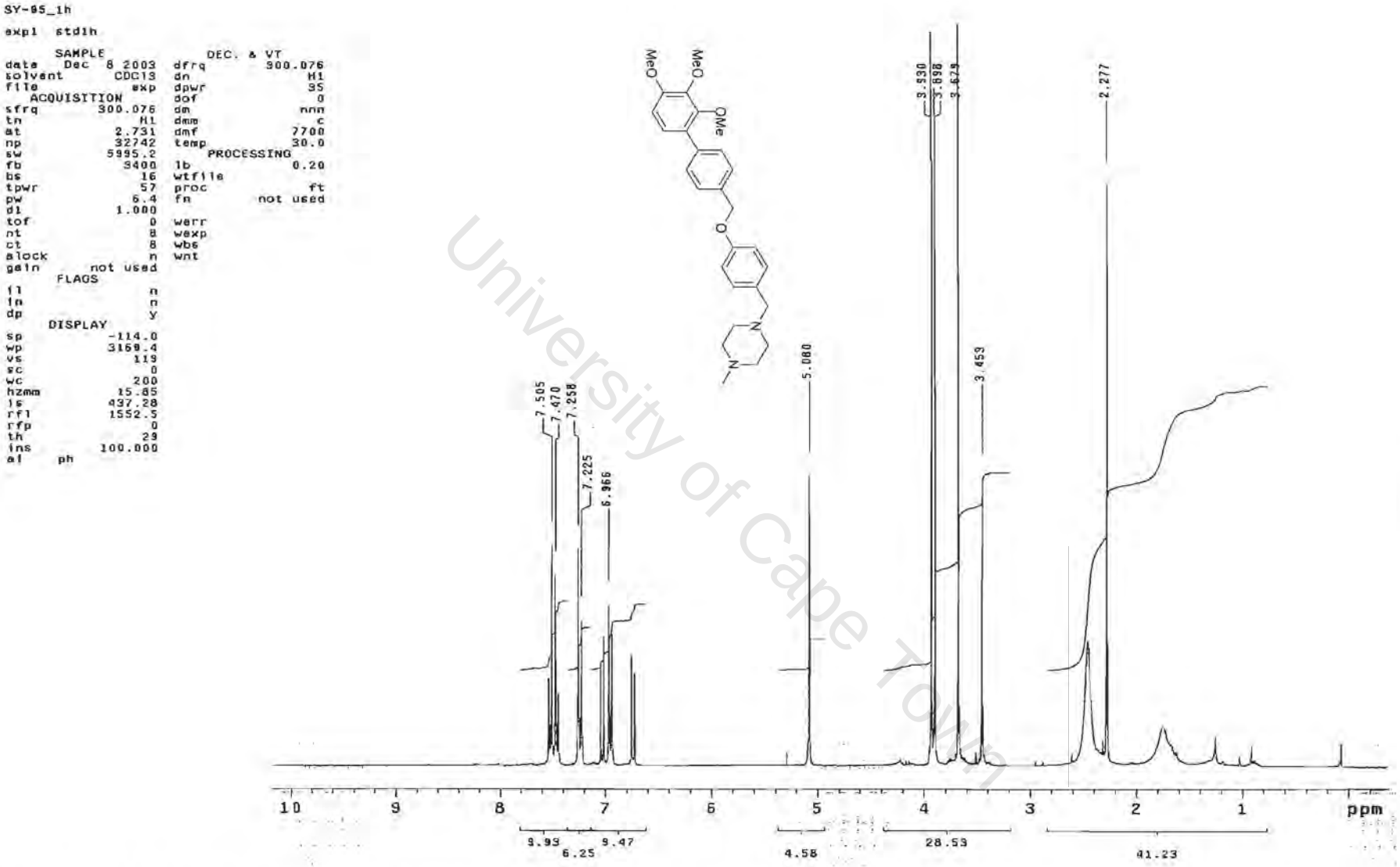

Figure C.4.1.11. ^{1}H NMR spectrum of compound **P33** in $CDCl_3$, 400 MHz.

P33

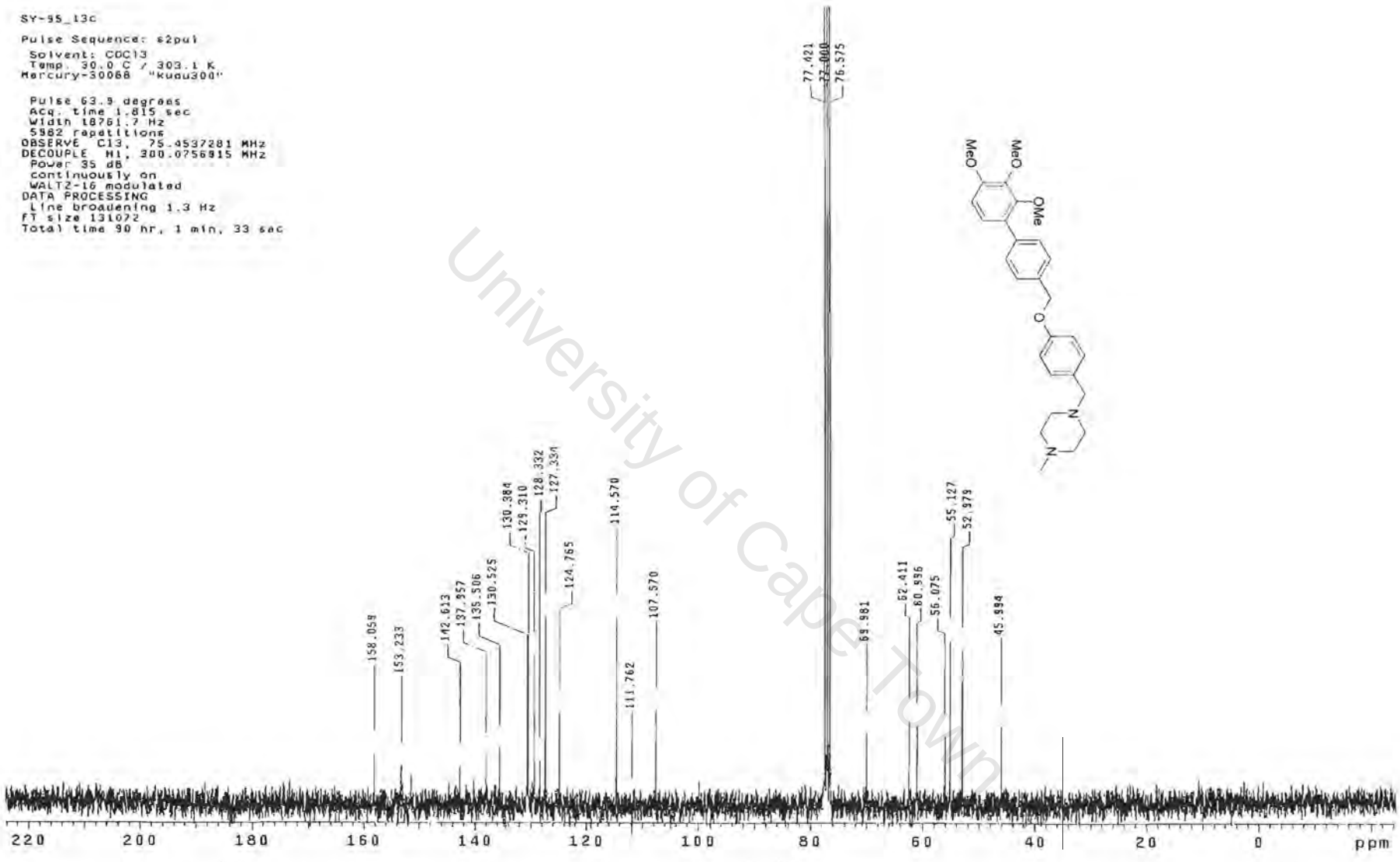

Figure C.4.1.12. ^{13}C NMR spectrum of compound **P33** in $CDCl_3$, 100 MHz.

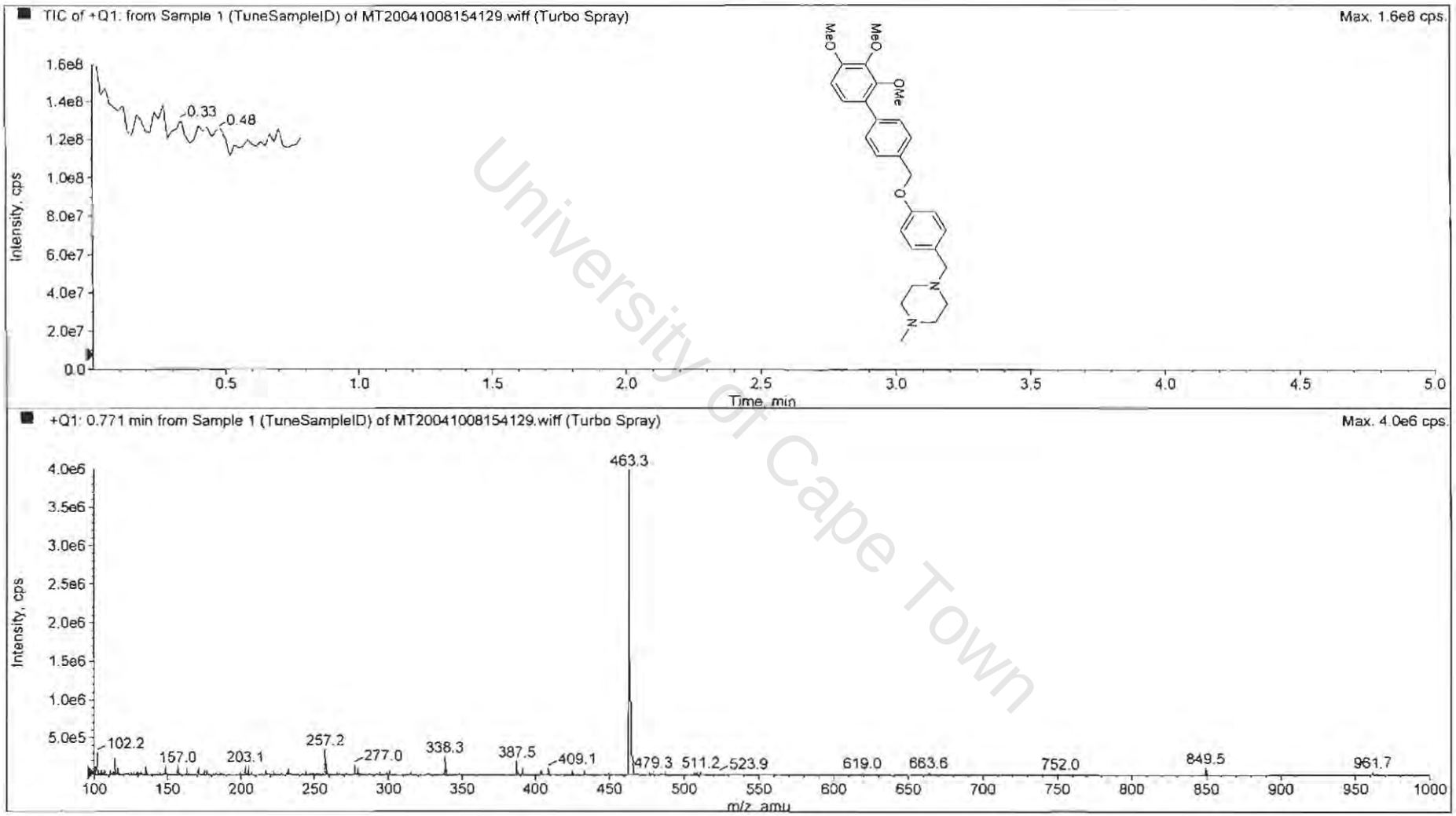

Figure C.4.1.13.1. Mass spectrum of compound **P33**.

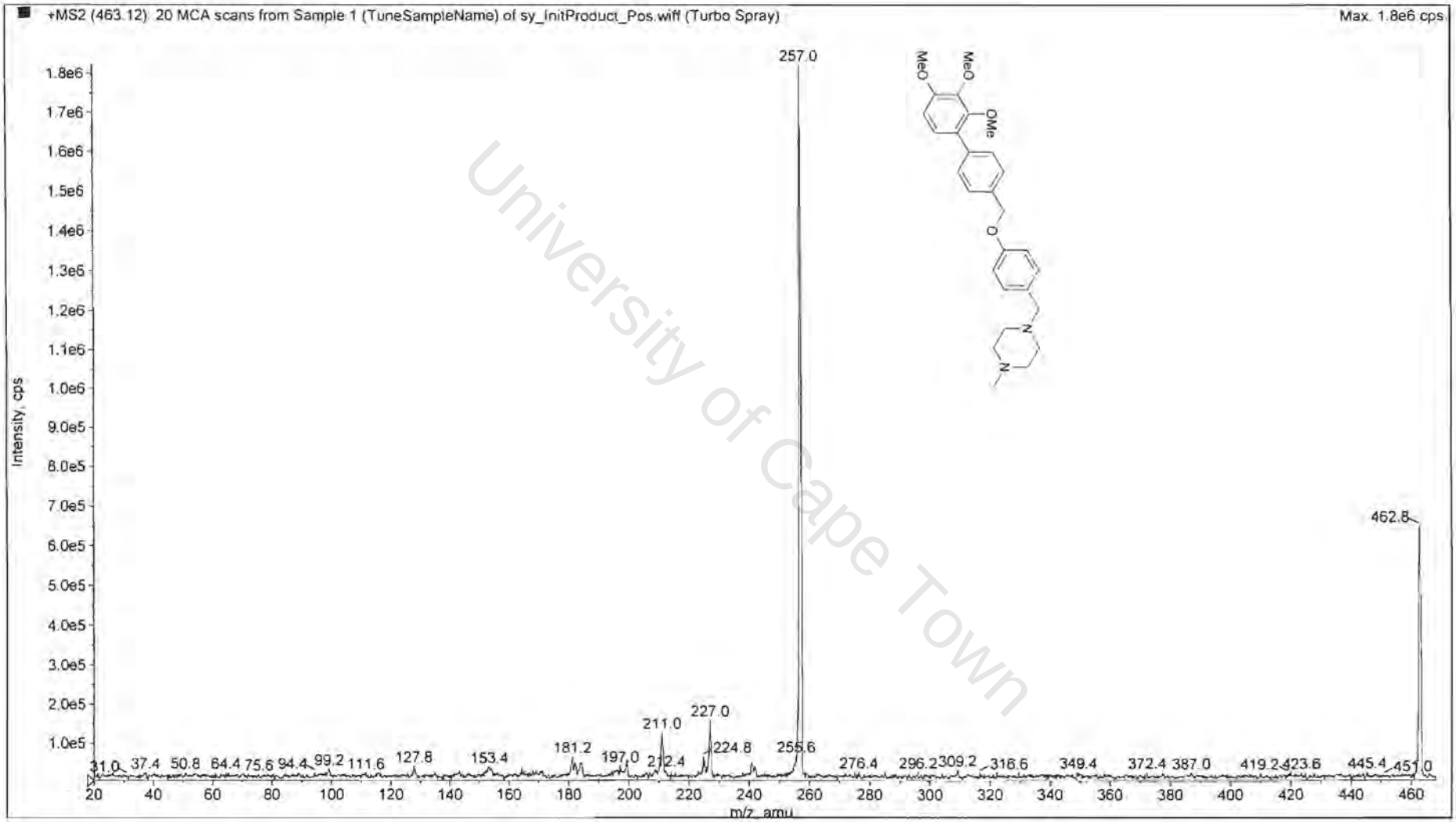

Figure C.4.1.13.2. Mass spectrum of compound **P33**.

Appendix 2

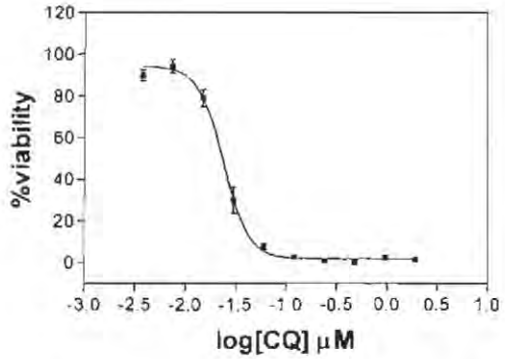

A-(a). Intrinsic antimalarial effect of CQ on D10

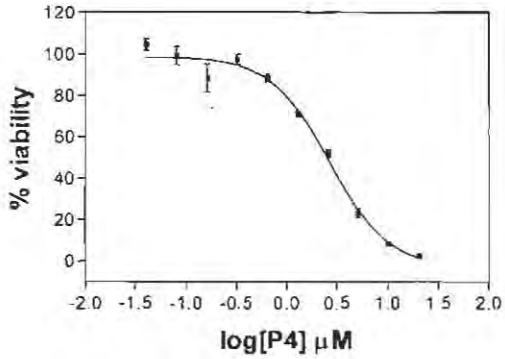

A-(b). Intrinsic antimalarial effect of P4 on D10

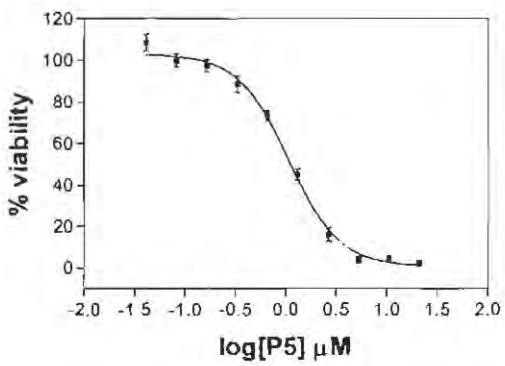

A-(c). Intrinsic antimalarial effect of P5 on D10

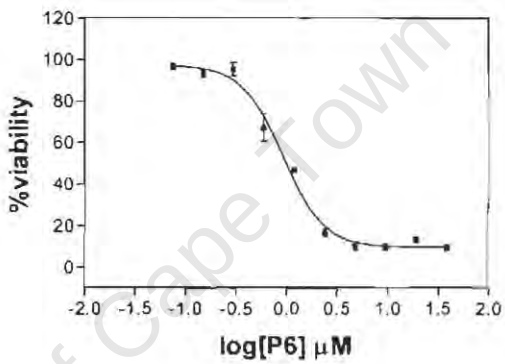

A-(d). Intrinsic antimalarial effect of P6 on D10

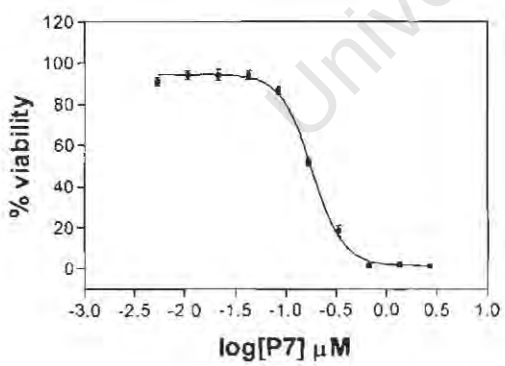

A-(e). Intrinsic antimalarial effect of P7 on D10

Figure 5.3.1-A. Intrinsic antimalarial activity of various drugs on CQ^S strain of D10.

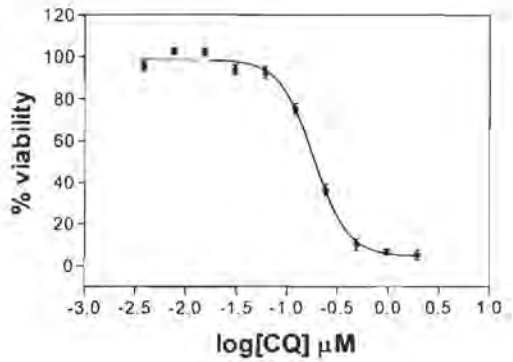

B-(a). Intrinsic antimalarial effect of CQ on K1

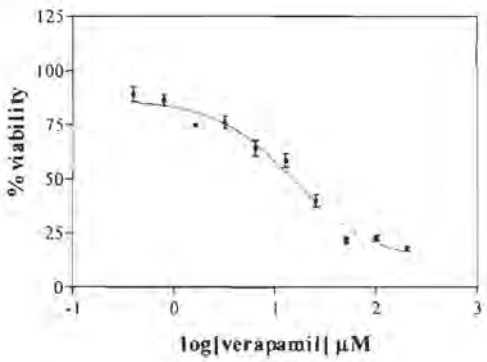

B-(b). Intrinsic antimalarial effect of Verapamil on K1

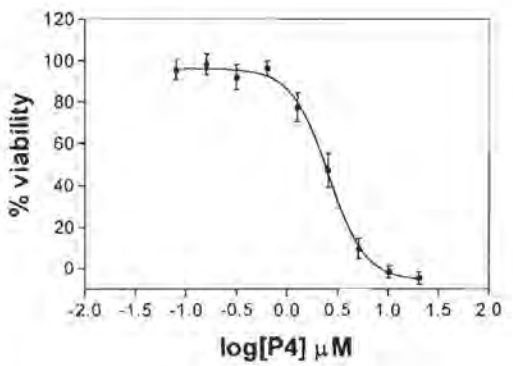

B-(c). Intrinsic antimalarial effect of P4 on K1

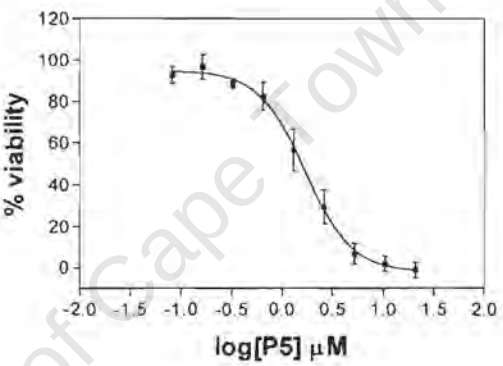

B-(d). Intrinsic antimalarial effect of P5 on K1

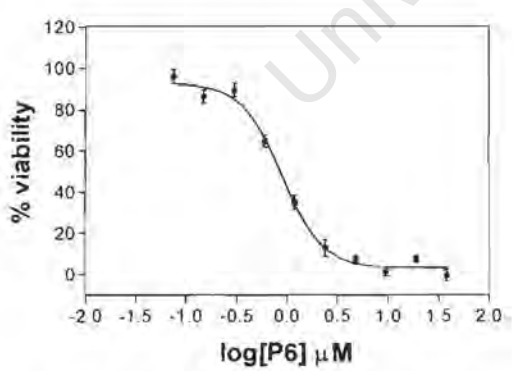

B-(e). Intrinsic antimalarial effect of P6 on K1

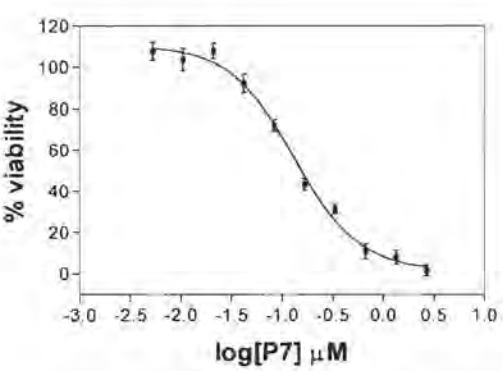

B-(f). Intrinsic antimalarial effect of P7 on K1

Figure 5.3.1-B. Intrinsic antimalarial activity of various drugs on CQ^R strain of K1.

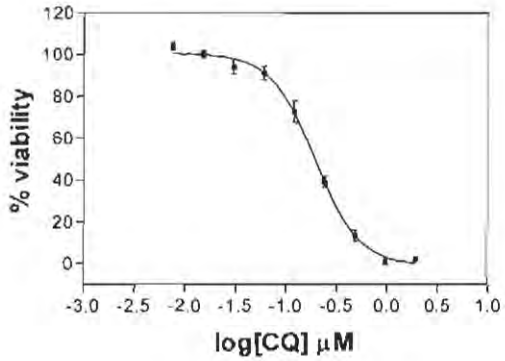

C-(a). Intrinsic antimalarial effect of CQ on RSA11

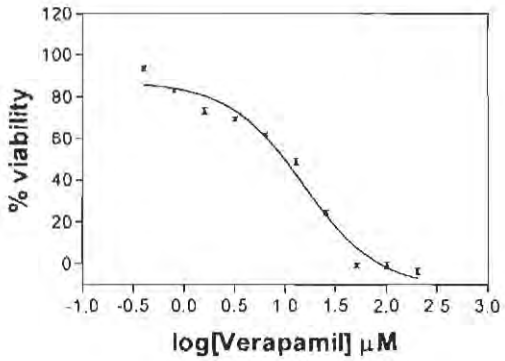

C-(b). Intrinsic antimalarial effect of Verapamil on RSA11

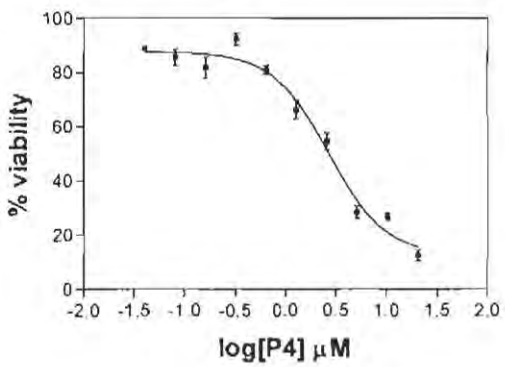

C-(c). Intrinsic antimalarial effect of P4 on RSA11

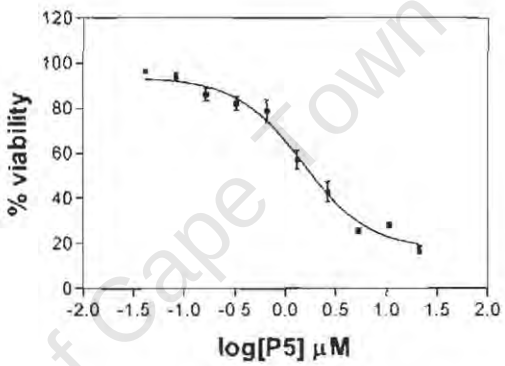

C-(d). Intrinsic antimalarial effect of P5 on RSA11

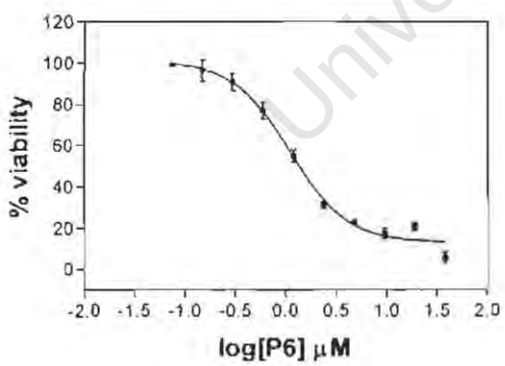

C-(e). Intrinsic antimalarial effect of P6 on RSA11

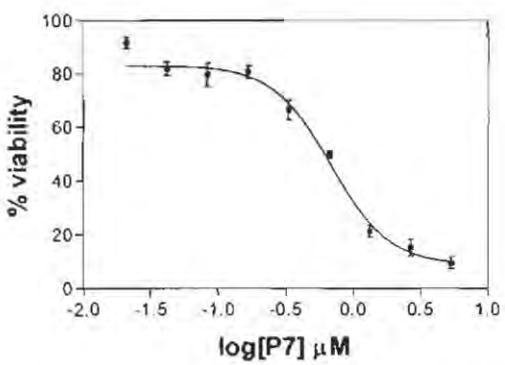

C-(f). Intrinsic antimalarial effect of P7 on RSA11

Figure 5.3.1-C. Intrinsic antimalarial activity of various drugs on CQ^R strain of RSA11.

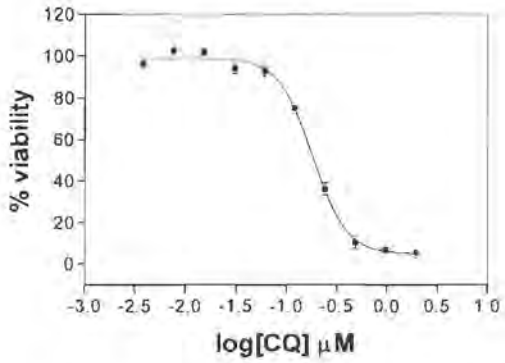

A-(1). Intrinsic antimalarial effect of CQ on K1

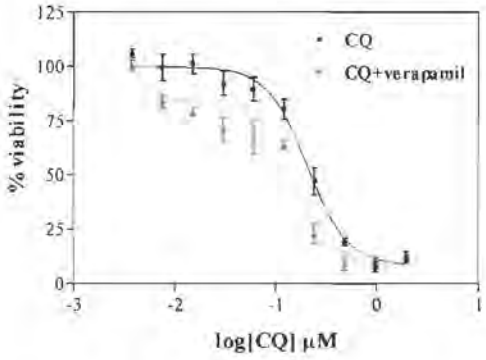

A-(2). Resistance reversal effect of Verapamil on K1

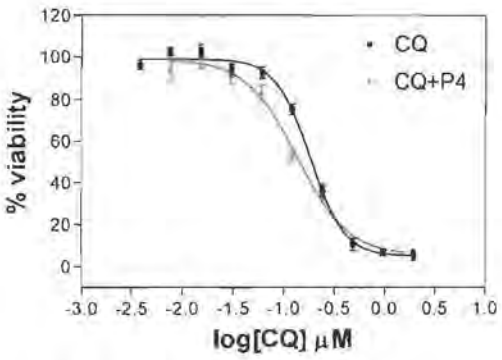

A-(3). Resistance reversal effect of P4 on K1

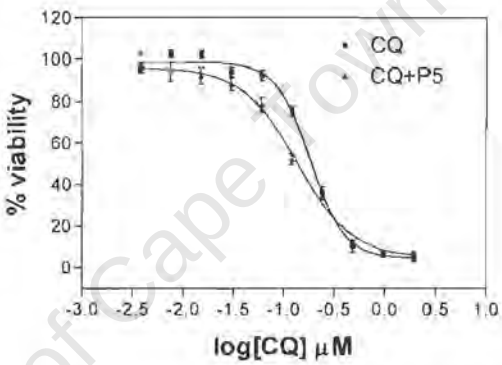

A-(4). Resistance reversal effect of P5 on K1

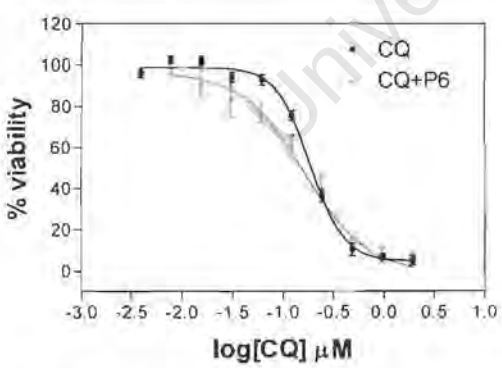

A-(5). Resistance reversal effect of P6 on K1

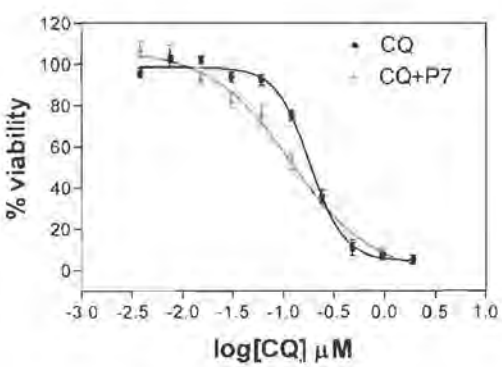

A-(6). Resistance reversal effect of P7 on K1

Figure 5.3.2-A. Resistance reversal activity of a single drug plus CQ on CQ^R strain of K1.

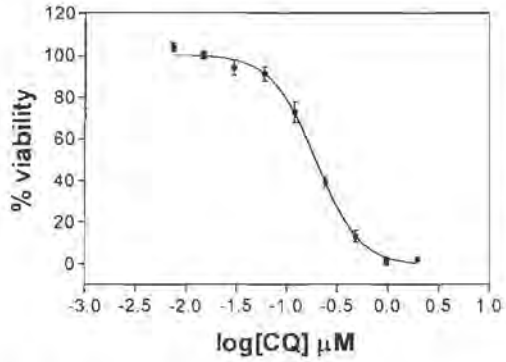

B-(1). Intrinsic antimalarial effect of CQ on RSA11

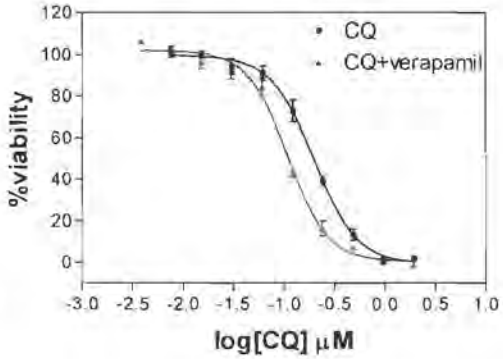

B-(2) Resistance reversal effect of Verapamil on RSA11

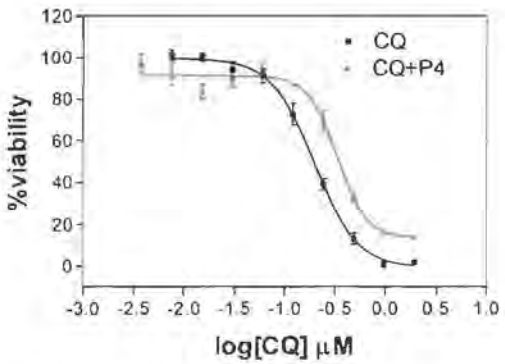

B-(3). Resistance reversal effect of P4 on RSA11

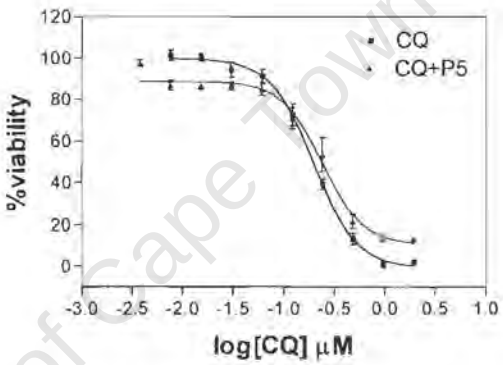

B-(4). Resistance reversal effect of P5 on RSA11

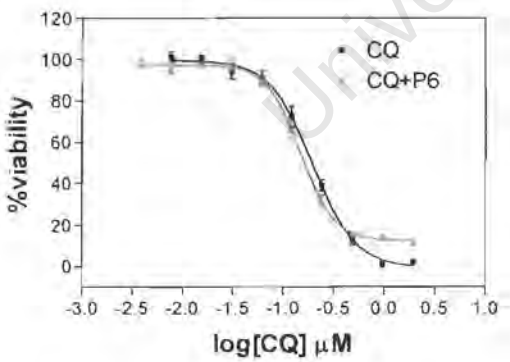

B-(5). Resistance reversal effect of P6 on RSA11

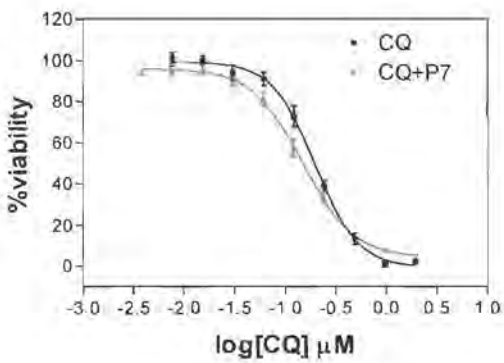

B-(6). Resistance reversal effect of P7 on RSA11

Figure 5.3.2-B. Resistance reversal activity of a single drug plus CQ on CQ^R strain of RSA11.

Appendix 3

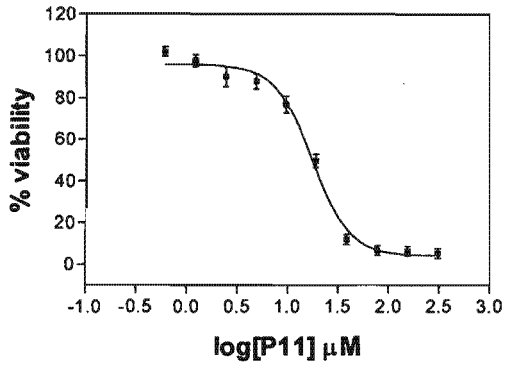

Fig. 6.2.1.1.1. Intrinsic antimalarial effect of P11 on D10

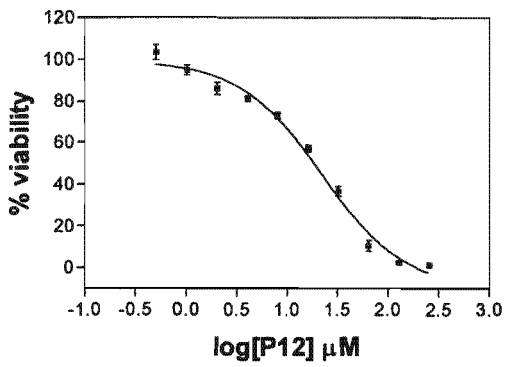

Fig. 6.2.1.1.2. Intrinsic antimalarial effect of P12 on D10

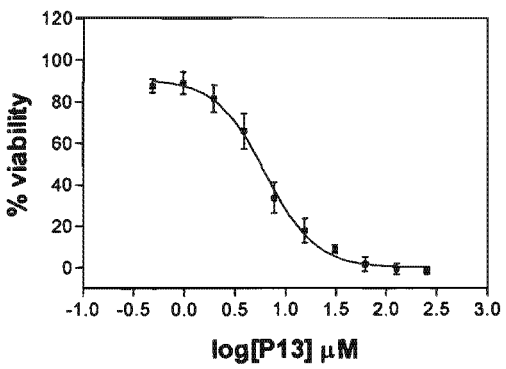

Fig. 6.2.1.1.3. Intrinsic antimalarial effect of P13 on D10

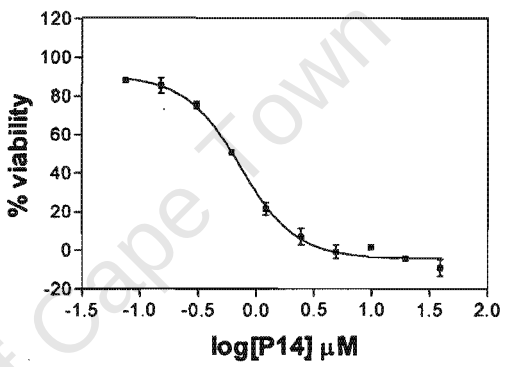

Fig. 6.2.1.1.4. Intrinsic antimalarial effect of P14 on D10

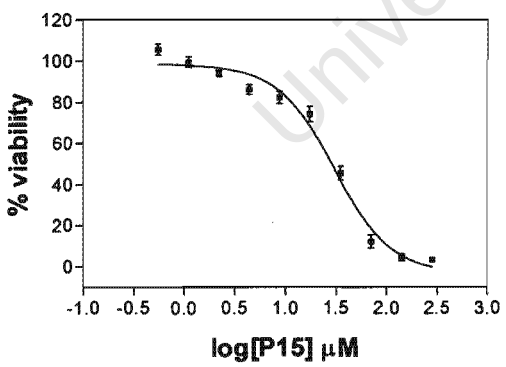

Fig. 6.2.1.1.5. Intrinsic antimalarial effect of P15 on D10

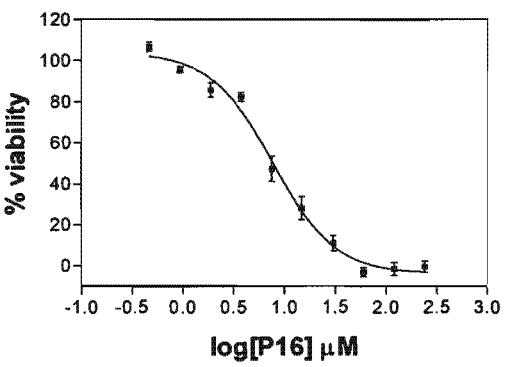

Fig. 6.2.1.1.6. Intrinsic antimalarial effect of P16 on D10

Figure 6.2.1.1. Intrinsic antimalarial activity of various drugs on CQ^S strain of D10.

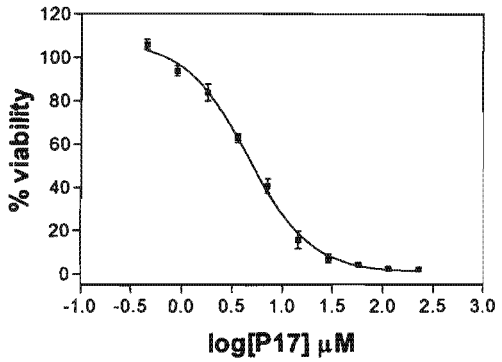

Fig. 6.2.1.1.7. Intrinsic antimalarial effect of P17 on D10

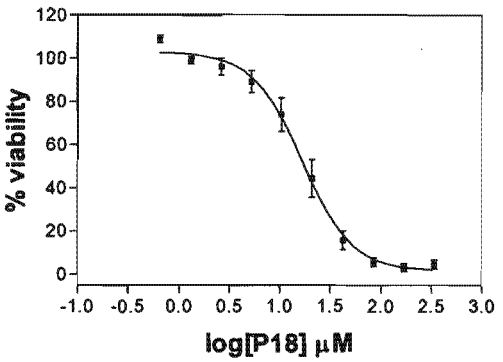

Fig. 6.2.1.1.8. Intrinsic antimalarial effect of P18 on D10

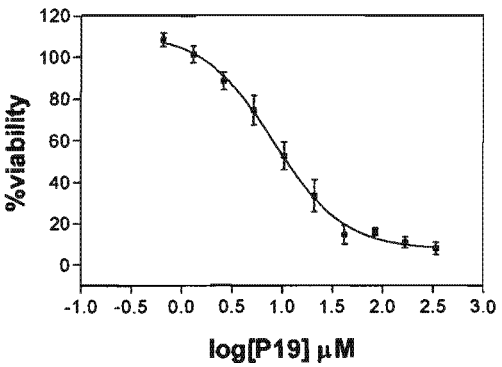

Fig. 6.2.1.1.9. Intrinsic antimalarial effect of P19 on D10

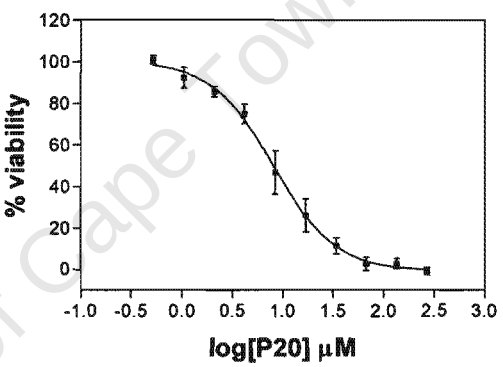

Fig. 6.2.1.1.10. Intrinsic antimalarial effect of P20 on D10

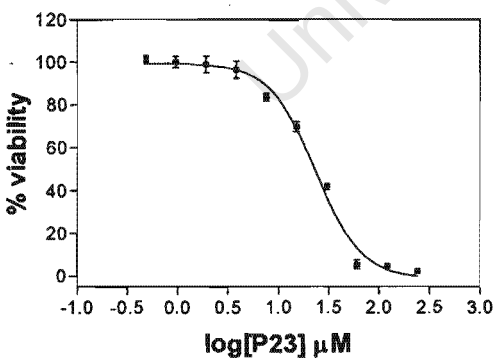

Fig. 6.2.1.1.11. Intrinsic antimalarial effect of P23 on D10

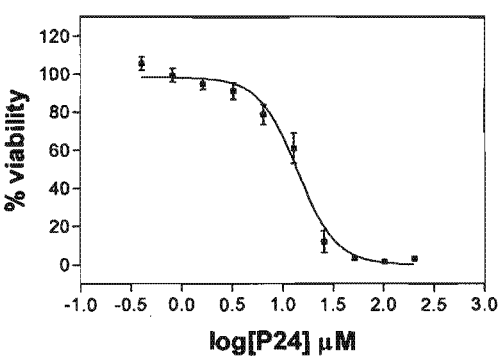

Fig. 6.2.1.1.12. Intrinsic antimalarial effect of P24 on D10

Figure 6.2.1.1. (Continued) Intrinsic antimalarial activity of various drugs on CQ^S strain of D10

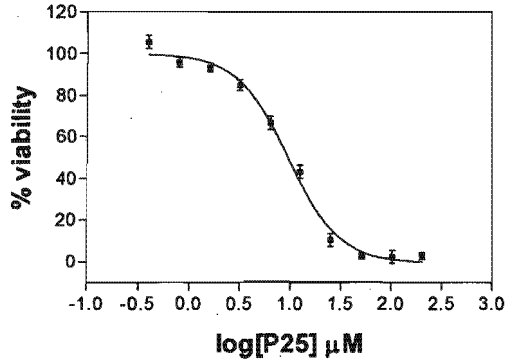

Fig. 6.2.1.1.13. Intrinsic antimalarial effect of P25 on D10

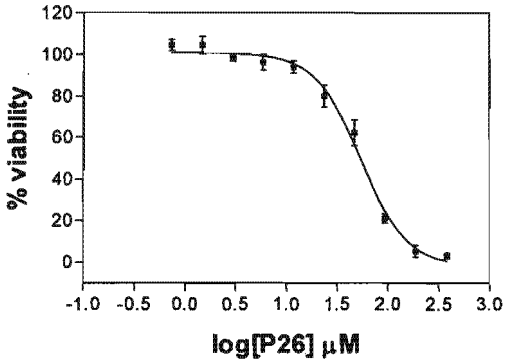

Fig. 6.2.1.1.14. Intrinsic antimalarial effect of P26 on D10

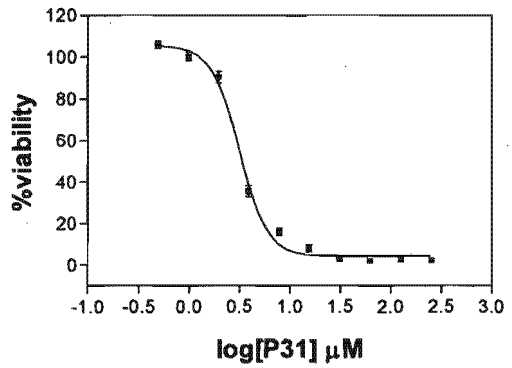

Fig. 6.2.1.1.15. Intrinsic antimalarial effect of P31 on D10

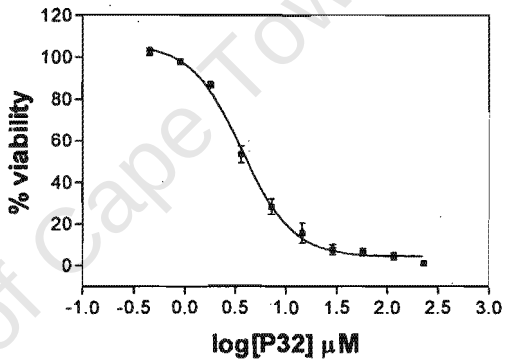

Fig.6.2.1.1.16. Intrinsic antimalarial effect of P32 on D10

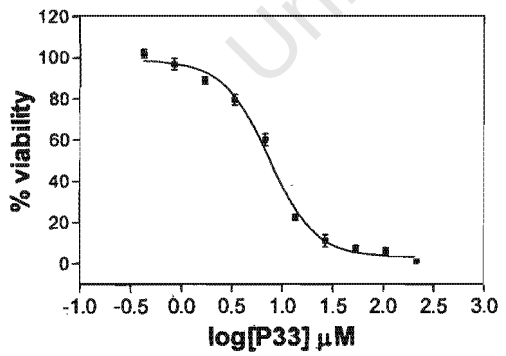

Fig. 6.2.1.1.17. Intrinsic antimalarial effect of P33 on D10

Figure 6.2.1.1. (Continued) Intrinsic antimalarial activity of various drugs on CQ^S strain of D10.

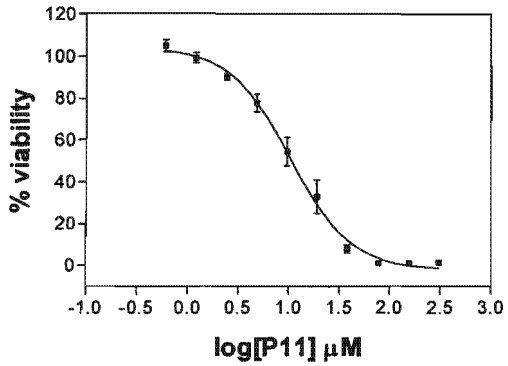

Fig. 6.2.1.2.1. Intrinsic antimalarial effect of P11 on K1

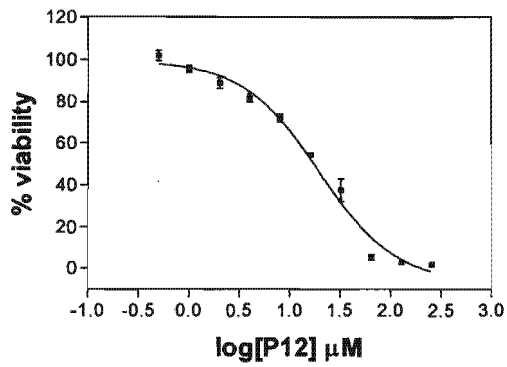

Fig. 6.2.1.2.2. Intrinsic antimalarial effect of P12 on K1

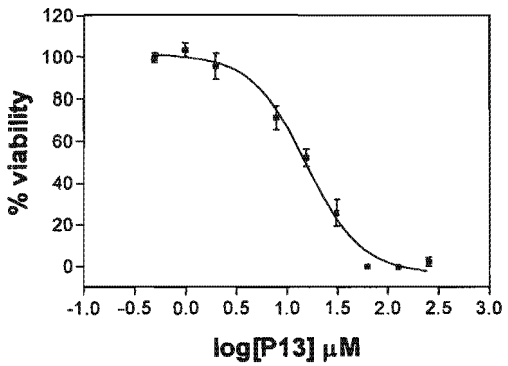

Fig. 6.2.1.2.3. Intrinsic antimalarial effect of P13 on K1

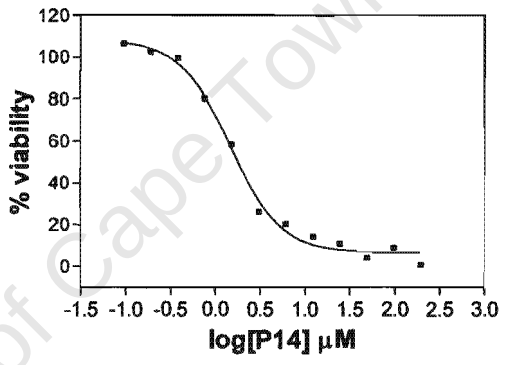

Fig. 6.2.1.2.4. Intrinsic antimalarial effect of P14 on K1

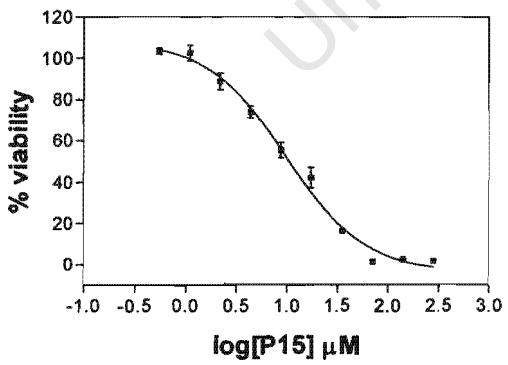

Fig. 6.2.1.2.5. Intrinsic antimalarial effect of P15 on K1

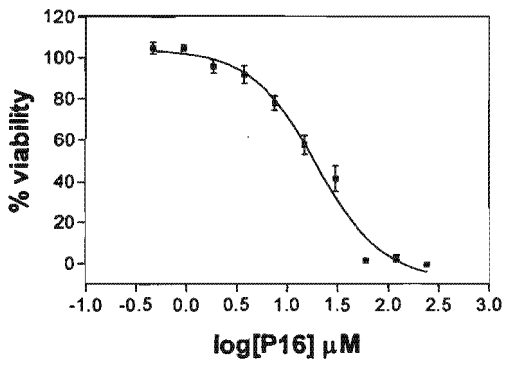

Fig. 6.2.1.2.6. Intrinsic antimalarial effect of P16 on K1

Figure 6.2.1.2. Intrinsic antimalarial activity of various drugs on CQ^R strain of K1.

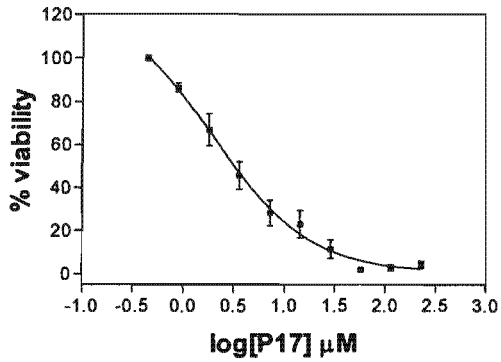

Fig. 6.2.1.2.7. Intrinsic antimalarial effect of P17 on K1

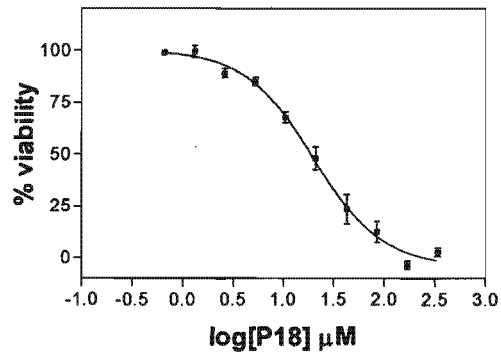

Fig. 6.2.1.2.8. Intrinsic antimalarial effect of P18 on K1

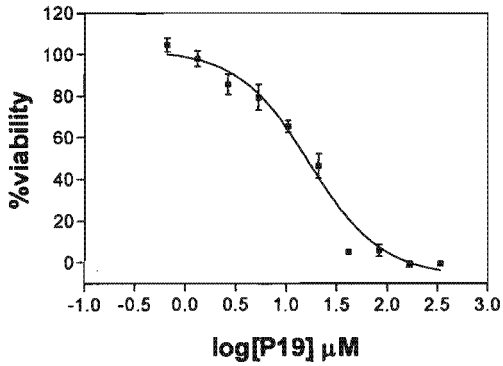

Fig. 6.2.1.2.9. Intrinsic antimalarial effect of P19 on K1

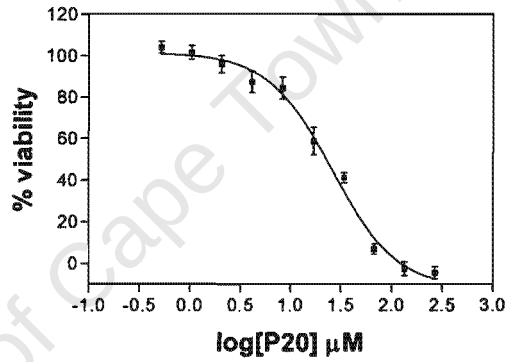

Fig. 6.2.1.2.10. Intrinsic antimalarial effect of P20 on K1

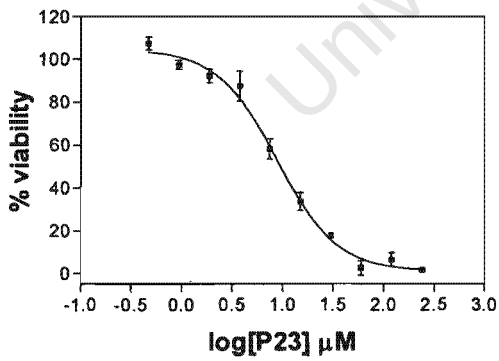

Fig. 6.2.1.2.11. Intrinsic antimalarial effect of P23 on K1

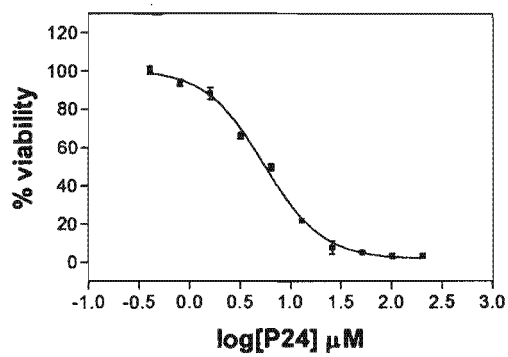

Fig. 6.2.1.2.12. Intrinsic antimalarial effect of P24 on K1

Figure 6.2.1.2. (Continued) Intrinsic antimalarial activity of various drugs on CQ^R strain of K1.

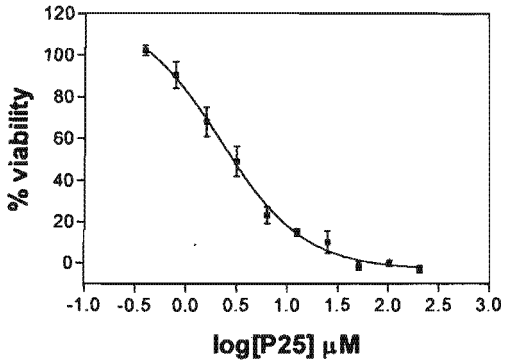

Fig. 6.2.1.2.13. Intrinsic antimalarial effect of P25 on K1

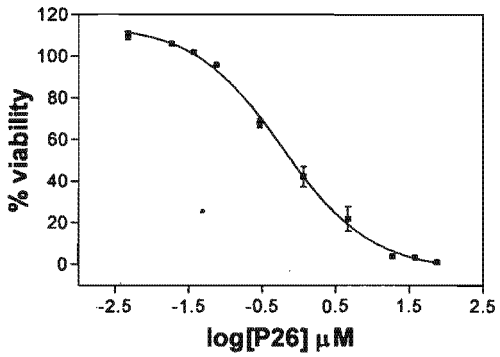

Fig. 6.2.1.2.14. Intrinsic antimalarial effect of P26 on K1

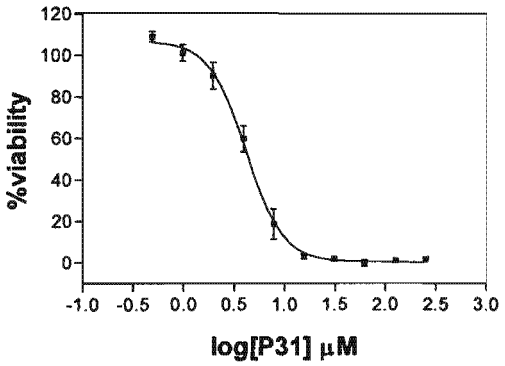

Fig. 6.2.1.2.15. Intrinsic antimalarial effect of P31 on K1

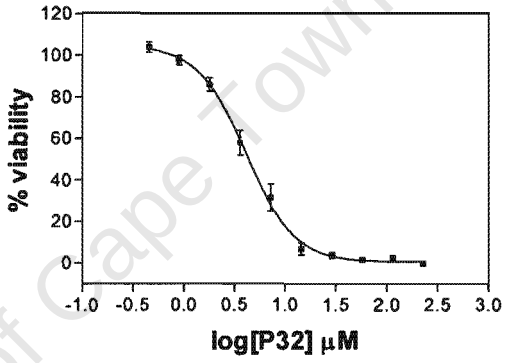

Fig. 6.2.1.2.16. Intrinsic antimalarial effect of P32 on K1

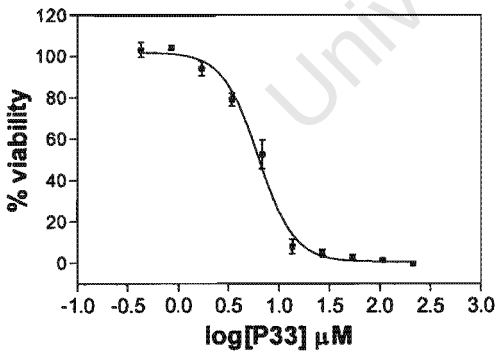

Fig. 6.2.1.2.17. Intrinsic antimalarial effect of P33 on K1

Figure 6.2.1.2. (Continued) Intrinsic antimalarial activity of various drugs on CQ^R strain of K1.

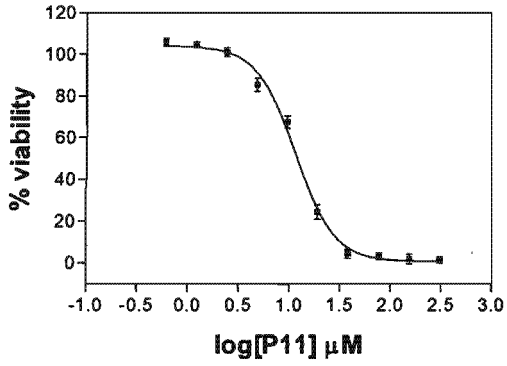

Fig. 6.2.1.3.1. Intrinsic antimalarial effect of P11 on RSA11

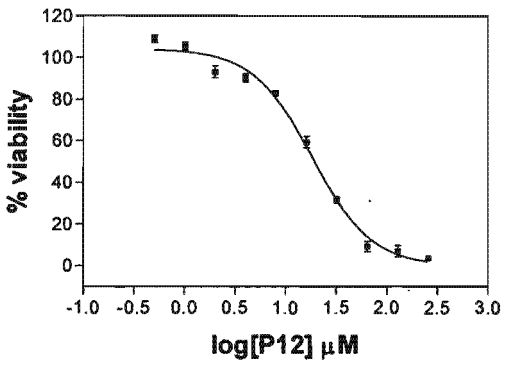

Fig.6.2.1.3.2. Intrinsic antimalarial effect of P12 on RSA11

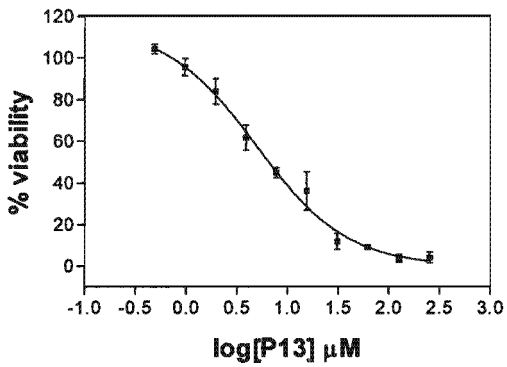

Fig. 6.2.1.3.3. Intrinsic antimalarial effect of P13 on RSA11

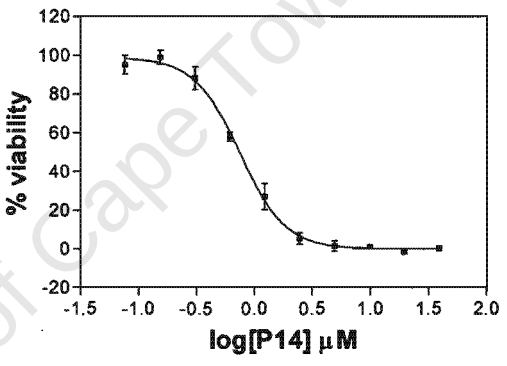

Fig.6.2.1.3.4. Intrinsic antimalarial effect of P14 on RSA11

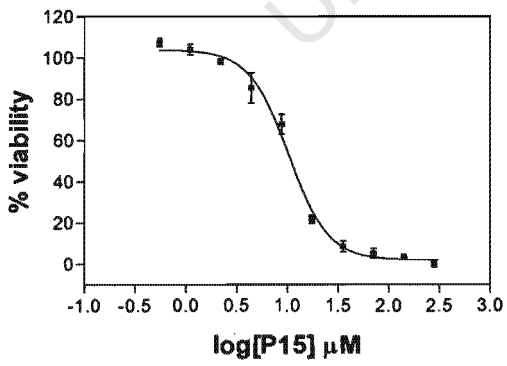

Fig. 6.2.1.3.5. Intrinsic antimalarial effect of P15 on RSA11

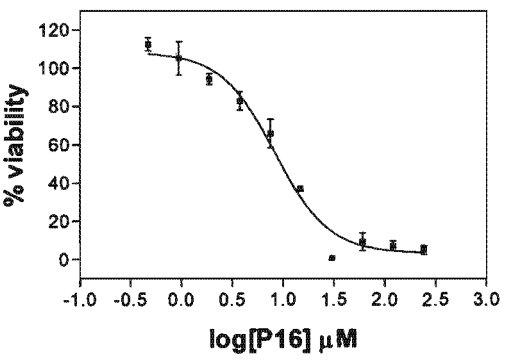

Fig.6.2.1.3.6. Intrinsic antimalarial effect of P16 on RSA11

Figure 6.2.1.3. Intrinsic antimalarial activity of various drugs on CQ^R strain of RSA11.

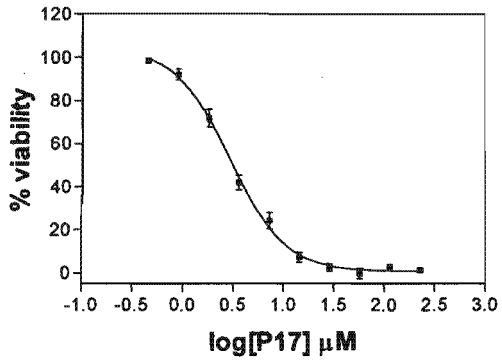

Fig. 6.2.1.3.7. Intrinsic antimalarial effect of P17 on RSA11

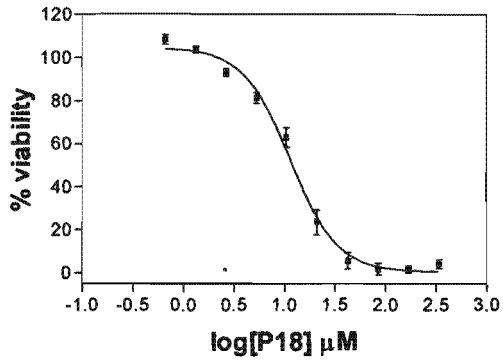

Fig. 6.2.1.3.8. Intrinsic antimalarial effect of P18 on RSA11

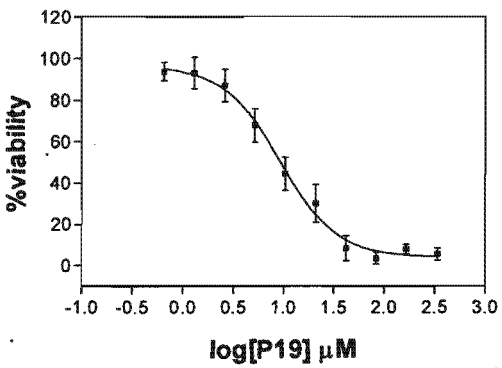

Fig. 6.2.1.3.9. Intrinsic antimalarial effect of P19 on RSA11

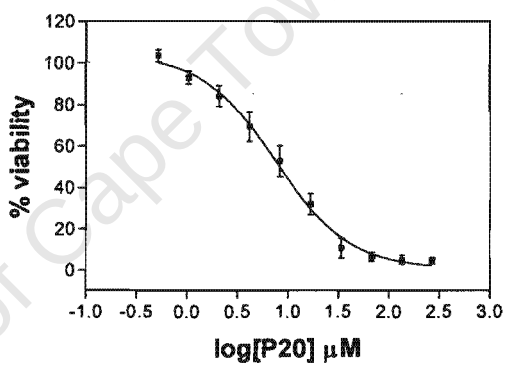

Fig. 6.2.1.3.10. Intrinsic antimalarial effect of P20 on RSA11

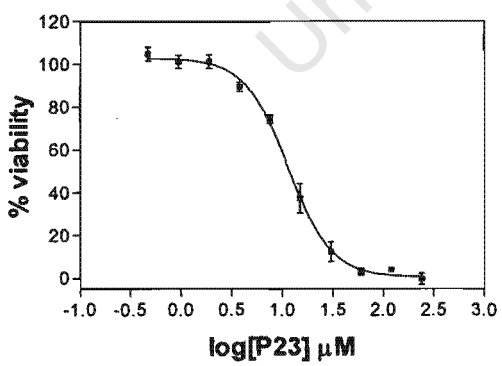

Fig. 6.2.1.3.11. Intrinsic antimalarial effect of P23 on RSA11

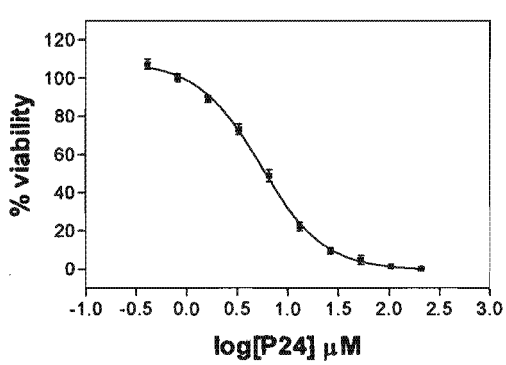

Fig. 6.2.1.3.12. Intrinsic antimalarial effect of P24 on RSA11

Figure 6.2.1.3. (Continued) Intrinsic antimalarial activity of various drugs on CQ^R strain of RSA11.

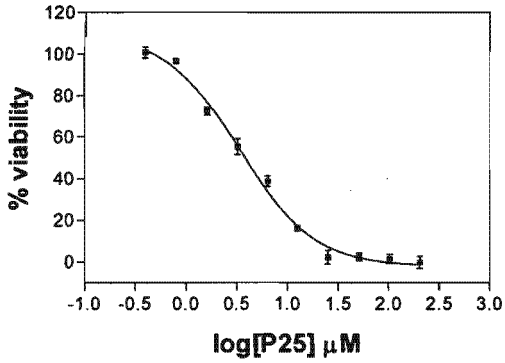

Fig. 6.2.1.3.13. Intrinsic antimalarial effect of P25 on RSA11

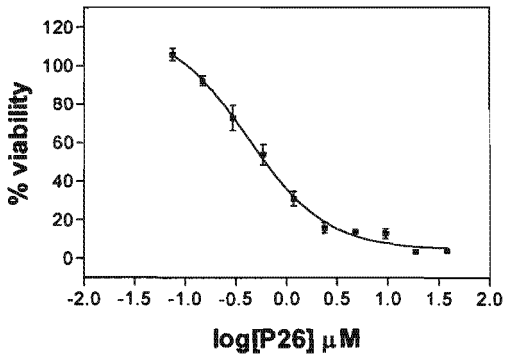

Fig. 6.2.1.3.14. Intrinsic antimalarial effect of P26 on RSA11

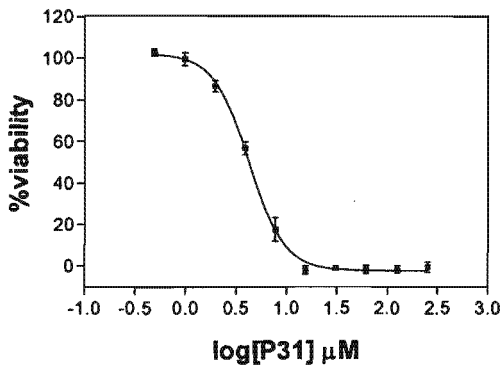

Fig. 6.2.1.3.15. Intrinsic antimalarial effect of P31 on RSA11

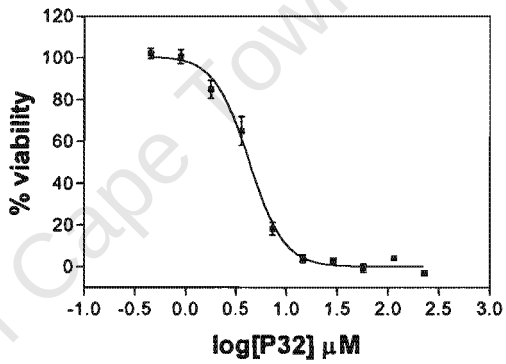

Fig. 6.2.1.3.16. Intrinsic antimalarial effect of P32 on RSA11

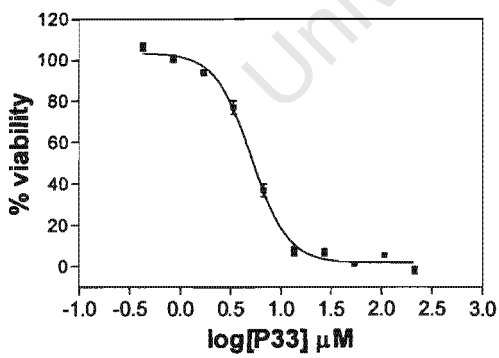

Fig. 6.2.1.3.17. Intrinsic antimalarial effect of P33 on RSA11

Figure 6.2.1.3. (Continued) Intrinsic antimalarial activity of various drugs on CQ^R strain of RSA11.

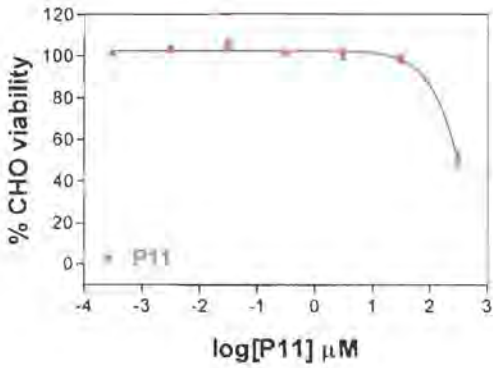

Fig. 6.2.1.4.1. Cytotoxicity effect of P11 on CHO

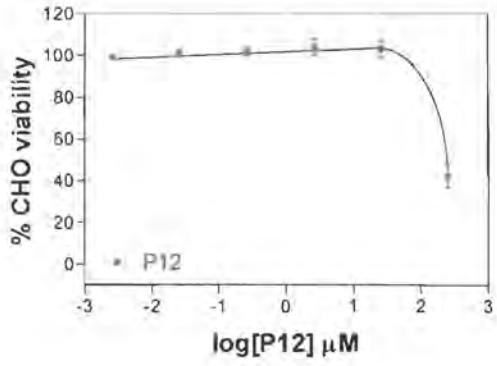

Fig. 6.2.1.4.2. Cytotoxicity effect of P12 on CHO

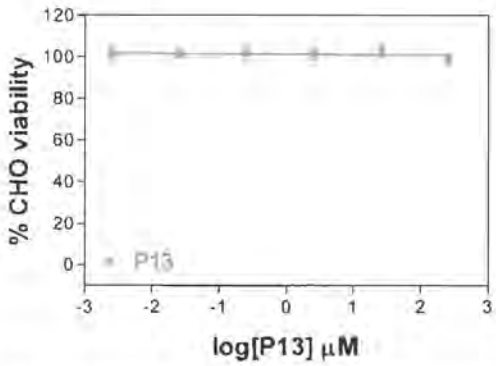

Fig. 6.2.1.4.3. Cytotoxicity effect of P13 on CHO

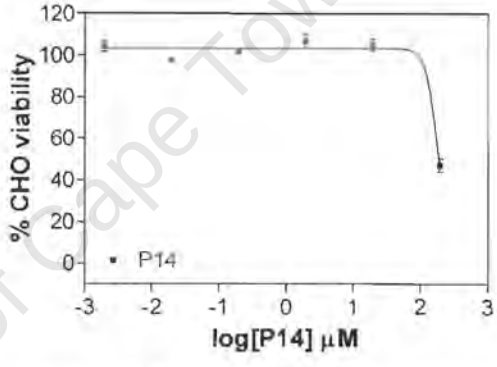

Fig. 6.2.1.4.4. Cytotoxicity effect of P14 on CHO

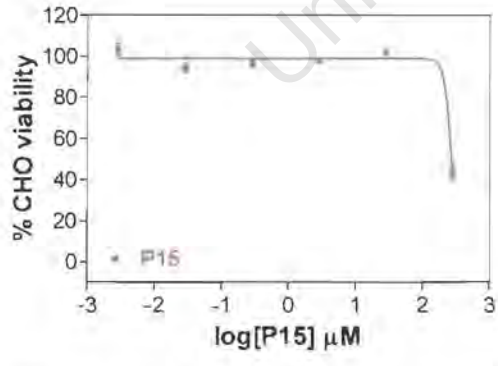

Fig. 6.2.1.4.5. Cytotoxicity effect of P15 on CHO

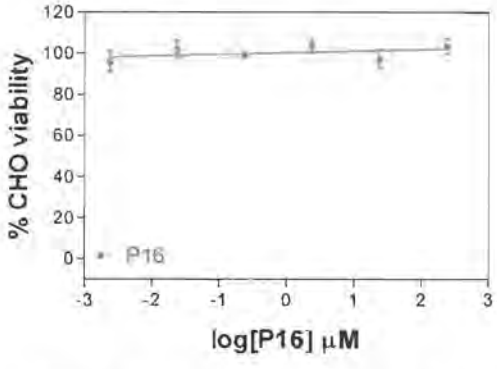

Fig. 6.2.1.4.6. Cytotoxicity effect of P16 on CHO

Figure 6.2.1.4. Dose-response curves of various compounds against Chinese hamster ovarian cells (CHO).

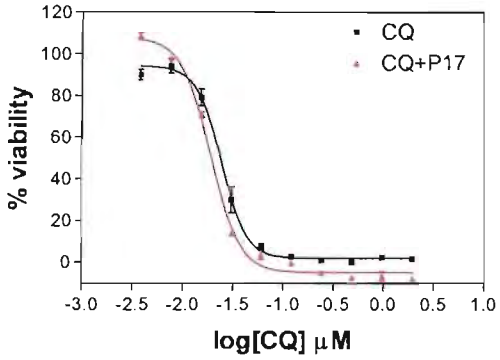

Fig. 6.2.2.1.7. Resistance reversal effect of P17 on D10

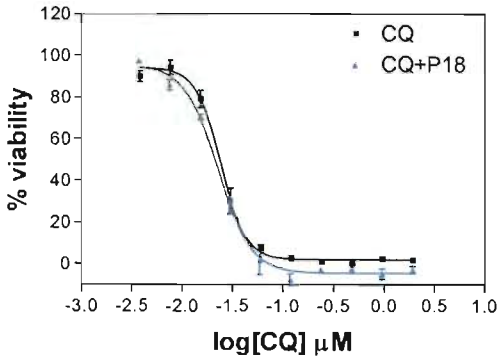

Fig.6.2.2.1.8. Resistance reversal effect of P18 on D10

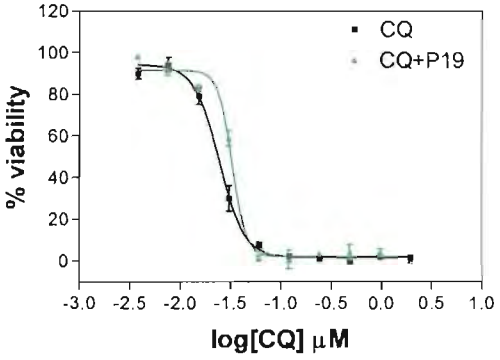

Fig. 6.2.2.1.9. Resistance reversal effect of P19 on D10

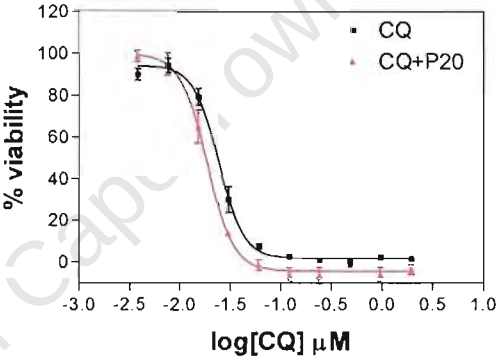

Fig.6.2.2.1.10. Resistance reversal effect of P20 on D10

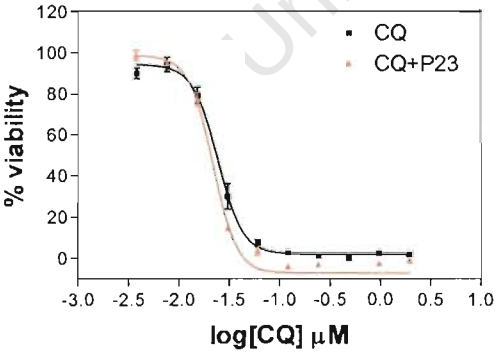

Fig. 6.2.2.1.11. Resistance reversal effect of P23 on D10

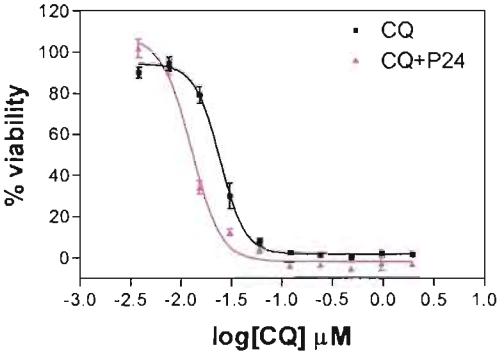

Fig.6.2.2.1.12. Resistance reversal effect of P24 on D10

Figure 6.2.2.1. (Continued) Resistance reversal effect of a single drug plus CQ on CQ^S strain of D10. Each point represents the mean of 3 independent experiments each performed in duplicate.

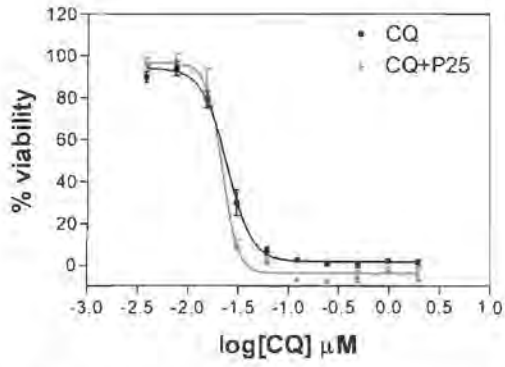

Fig. 6.2.2.1.13. Resistance reversal effect of P25 on D10

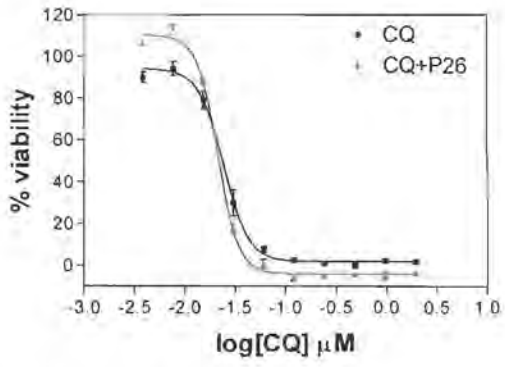

Fig.6.2.2.1.14. Resistance reversal effect of P26 on D10

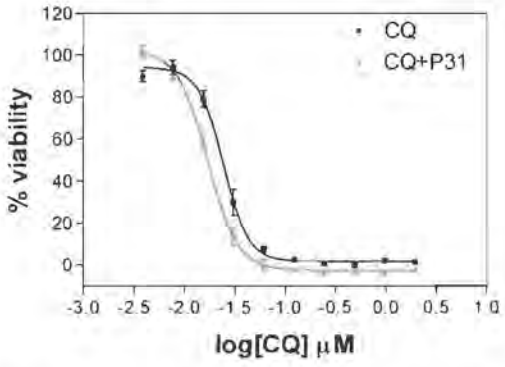

Fig. 6.3.2.1.15. Resistance reversal effect of P31 on D10

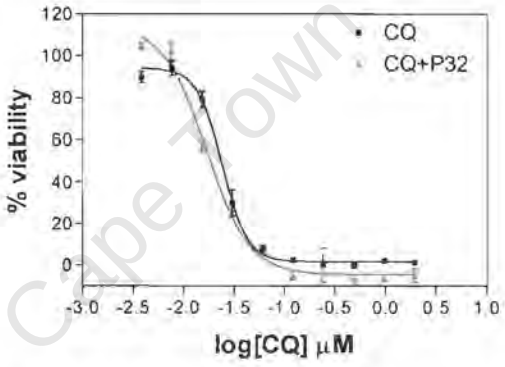

Fig. 6.3.2.1.16. Resistance reversal effect of P32 on D10

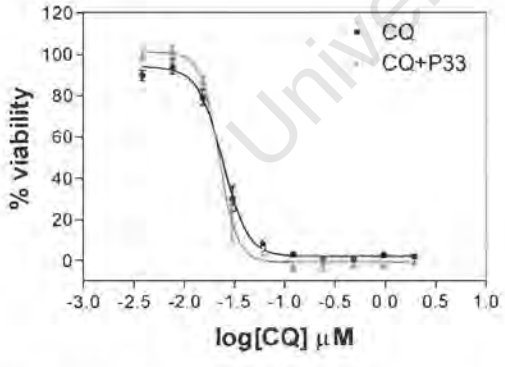

Fig. 6.3.2.1.17. Resistance reversal effect of P33 on D10

Figure 6.2.2.1. (Continued) Resistance reversal effect of a single drug plus CQ on CQ^S strain of D10. Each point represents the mean of 3 independent experiments each performed in duplicate.